
MICROALGAE AS FACTORY OF HIGH VALUE BIOPRODUCTS

Paola Imbimbo

Dottorato in Biotecnologie – XXII ciclo

Università di Napoli Federico II



Dottorato in Biotecnologie – XXII ciclo

Università di Napoli Federico II



MICROALGAE AS FACTORY OF HIGH VALUE BIOPRODUCTS

Paola Imbimbo

Dottorando: Paola Imbimbo

Relatore: Prof.ssa Daria Maria Monti

Coordinatore: Prof. Marco Moracci

Settore Scientifico Disciplinare: BIO/10

INDEX

RIASSUNTO.....	1
SUMMARY.....	7
1 Introduction.....	9
1.1 Microalgae and biotechnological applications.....	11
1.2 Circular economy, green chemistry and microalgal biorefinery.....	11
1.3 High-value bio-products from microalgae.....	12
1.4 <i>Galdieria phlegrea</i>	17
1.5 The Aim of the thesis.....	19
1.6 References.....	20
2 A cascade extraction of active phycocyanin and fatty acids <i>Galdieria phlegrea</i>	25
2.1 Introduction.....	28
2.2 Materials and methods.....	29
2.3 Results.....	33
2.4 Discussion.....	43
2.5 References.....	44
3 Green compressed fluid technologies to extract antioxidants and lipids from <i>Galdieria phlegrea</i> in a biorefinery approach.....	49
3.1 Introduction.....	52
3.2 Materials and methods.....	53
3.3 Results and Discussion	59
3.4 Conclusions.....	70
3.5 References.....	72
4 A thermophilic C-phycocyanin with unprecedented biophysical and biochemical properties.....	75
4.1 Introduction.....	78
4.2 Materials and methods.....	79
4.3 Results and Discussion.....	83
4.4 Conclusions.....	102
4.5 References.....	103
5 General discussion.....	109
5.1 Results.....	114
APPENDIX.....	116

RIASSUNTO

I cambiamenti climatici, il riscaldamento globale e l'aumento della popolazione rappresentano i principali problemi dei nostri giorni. Tali problemi stanno portando all'inevitabile esaurimento delle risorse naturali. Negli ultimi anni, l'Unione Europea e altre organizzazioni internazionali hanno incentivato il passaggio dall'economia lineare a quella circolare. Quest'ultima rappresenta un modello di produzione e consumo volto ad un prolungato riutilizzo e riciclo dei materiali e dei prodotti esistenti. Ciò contribuirà ad allungare il "ciclo vitale" dei prodotti, minimizzando, così, la produzione dei rifiuti. Questo modello di economia promuove lo sviluppo sostenibile tenendo presente l'impatto economico, ambientale, tecnologico e sociale. L'economia circolare abbraccia i principi della chimica verde, il cui obiettivo è quello di promuovere un migliore utilizzo delle risorse, la riduzione dei rifiuti e un utilizzo più intelligente dell'energia. L'idea di utilizzare rifiuti e prodotti naturali come risorse e lo sviluppo di una piattaforma integrata in grado di produrre diversi bioprodotto a partire da una singola biomassa, prende vita con il concetto della bioraffineria. Infatti, le bioraffinerie sono state identificate come una idea promettente per sviluppare industrie basate sulle biomasse. In tale contesto si è sviluppato l'uso delle microalghe come materia prima alternativa e sostenibile. Le microalghe sono considerate delle vere e proprie fabbriche in quanto sono in grado di effettuare la fotosintesi convertendo la CO₂ in glucosio e rilasciando ossigeno come prodotto di scarto. Esse rappresentano una enorme riserva di proteine, lipidi, zuccheri e molecole ad alto valore che possono essere usate per l'uomo o come mangime. Le microalghe presentano diversi vantaggi: sono organismi con cicli di crescita brevi e, a differenza di molte piante stagionali, possono essere coltivate tutto l'anno. Non necessitano di terreni agricoli o di acqua pulita e, di conseguenza, non sottraggono spazi altrimenti destinati all'agricoltura. Poiché alcune specie sono ricche in lipidi, le microalghe sono state ampiamente studiate nel passato come alternativa ai carburanti di prima generazione. Negli ultimi anni, diversi governi e investitori privati hanno puntato sulla produzione di biocarburanti di terza generazione a partire da microalghe. Tuttavia, questa iniziativa si è rivelata fallimentare a causa degli elevati costi di produzione e di raccolta. Inoltre, la conversione degli oli estratti in biocarburanti rappresenta uno dei motivi alla base di un mancato sviluppo su larga scala e dell'incompleta commercializzazione delle microalghe. È stato stimato che, per competere con il prezzo dei carburanti attualmente in

commercio, il costo dei biocarburanti di terza generazione dovrebbe essere ridotto di 10 volte.

Un altro collo di bottiglia che inibisce il pieno sfruttamento delle microalghe nella produzione su larga scala è il controllo dei parametri di crescita e il problema delle contaminazioni. Le microalghe generalmente possono essere coltivate in stagni aperti o in fotobioreattori. Mentre i fotobioreattori sono sistemi chiusi che consentono di controllare i parametri di coltivazione e di ottenere una produttività molto elevata, gli stagni aperti sono sistemi esterni non controllati con una produttività limitata. Nonostante i fotobioreattori risultino essere il metodo di coltivazione più efficiente, ad oggi, i sistemi a stagno aperto sono quelli ampiamente utilizzati su scala industriale. Il principale vantaggio dei sistemi aperti è dovuto al basso investimento iniziale, alla bassa richiesta di energia, ai bassi costi operativi e di manutenzione. In questo scenario, i microrganismi estremofili hanno destato molto interesse, in quanto hanno la capacità di vivere e svilupparsi in condizioni considerate ostili per la maggior parte dei microorganismi, come in presenza di elevate concentrazioni di metalli pesanti, ambienti acidofili (pH 1.0- 3.0) o ad alte temperature (>50°C). La capacità di crescere in condizioni così estreme limita il problema delle contaminazioni. Per questo motivo, le microalghe estremofile rappresentano i migliori candidati per la produzione su larga scala.

Negli ultimi decenni, le microalghe hanno suscitato interesse non solo per la produzione di biocarburanti, ma anche per la loro capacità di sintetizzare diverse molecole ad alto valore commerciale, come proteine, carotenoidi e acidi grassi polinsaturi che possono trovare applicazione non solo nell'industria alimentare e dei mangimi, ma anche nel settore cosmetico, nutraceutico e farmaceutico.

Per promuovere lo sviluppo delle industrie basate sulle alghe, è necessario sviluppare una piattaforma integrata, in grado di produrre più prodotti in cascata. A tal scopo, lo sviluppo di un sistema di bioraffineria e lo sviluppo di un'efficace strategia di coltivazione potrebbero ridurre i costi di produzione.

Attualmente, le tecnologie più utilizzate per estrarre diversi bioprodotto sono estrazioni convenzionali che prevedono l'utilizzo di solventi organici come cloroformio, acetone, metanolo e dietiletere. Le estrazioni convenzionali richiedono solitamente grandi quantità di solvente, tempi prolungati e vengono eseguite a partire dalla biomassa essiccata. Questi sono i motivi per cui la fase di estrazione rappresenta un altro svantaggio per lo sviluppo delle industrie basate sulle alghe. Di recente è aumentata la domanda da parte dei consumatori di prodotti naturali e sicuri la cui produzione non richiede l'utilizzo di solventi

tossici. Lo sviluppo di tecniche “verdi” per estrarre composti ad alto valore rappresenta un progresso significativo. Tali tecniche consentono di ottenere prodotti bioattivi riducendo o eliminando completamente i solventi tossici, minimizzando l'impatto ambientale. Inoltre, consentono di ridurre i tempi di estrazione e di migliorarne le rese, risultando vantaggiose anche in termini economici.

Lo scopo del presente progetto di dottorato è stato lo sviluppo di un processo in cascata, in accordo con il concetto di bioraffineria, al fine di ottenere tre prodotti ad alto valore. La microalga selezionata è stata *Galdieria phlegrea* (ceppo 009), un'alga rossa termoacidofila in grado di sintetizzare diverse molecole ad alto valore.

L'attenzione è stata inizialmente focalizzata sulla progettazione di un processo in scala di laboratorio per ottenere due diverse molecole a partire dalla biomassa umida di *G. phlegrea*: la ficocianina e gli acidi grassi polinsaturi. Innanzitutto, sono state estratte le proteine mediante una procedura ad alta pressione, quindi la ficocianina è stata isolata attraverso un singolo passaggio di purificazione ottenendo un grado di purezza molto elevato. È risaputo che le ficocianine sono dotate di attività antiossidante, per questo motivo è stata valutata la capacità della ficocianina di proteggere i cheratinociti umani immortalizzati dallo stress indotto dai raggi UVA. Successivamente l'attenzione è stata focalizzata sulla seconda classe di molecole da estrarre: i lipidi. A tale scopo, a partire dalla biomassa residua, i lipidi sono stati estratti mediante una tecnica convenzionale che prevede l'uso di cloroformio/metanolo. L'estratto ottenuto è stato poi frazionato per isolare gli acidi grassi polinsaturi. È stato interessante notare che a partire dalla biomassa rotta la quantità di acidi grassi polinsaturi isolati è risultata essere superiore a quella ottenuta dalla biomassa grezza (estrazione effettuata in parallelo), suggerendo così un efficiente modello preliminare di bioraffineria.

Per valorizzare ulteriormente la biomassa di *G. phlegrea*, il modello iniziale di bioraffineria messo a punto è stato integrato con i principi della chimica verde. Il nuovo modello proposto ha previsto tre fasi sequenziali, combinando un'estrazione convenzionale e due procedure innovative*:

1. Estrazione ad alta pressione per la ficocianina;
2. Estrazione con fluidi pressurizzati (PLE) per ottenere i carotenoidi;
3. Estrazione con fluidi supercritici (SFE) per ottenere i lipidi.

Rispetto alle estrazioni convenzionali, le estrazioni con i fluidi compressi hanno permesso di ottenere rese maggiori di carotenoidi e lipidi utilizzando solventi eco-sostenibili, sicuri ed economici. Inoltre, le estrazioni sono state effettuate in tempi più brevi e con un minore

consumo di solvente. La frazione contenente i carotenoidi è stata caratterizzata attraverso analisi HPLC, che hanno permesso di identificare β -carotene e zeaxantina quali principali pigmenti presenti nell'estratto. Inoltre, sono stati condotti diversi esperimenti su cheratinociti umani immortalizzati per verificare che la tecnica di estrazione utilizzata, il PLE, non avesse alterato la capacità antiossidante dei carotenoidi estratti. In particolare, è stata analizzata l'inibizione della produzione di ROS intracellulari dopo l'induzione dello stress ossidativo e l'attivazione del *pathway* di Nrf-2, proteina normalmente coinvolta nella risposta allo stress.

Infine, è stata effettuata una completa caratterizzazione biofisica e biochimica della ficocianina estratta e purificata. In particolare, è stata determinata la sequenza primaria della proteina e ne è stata valutata la stabilità termica e in funzione del pH. I risultati ottenuti hanno mostrato chiaramente che la ficocianina estratta da *G. phlegrea* è termoresistente in quanto è in grado di preservare la sua azione antiossidante anche in seguito a pastorizzazione termica. È stato dimostrato inoltre che la struttura della ficocianina è stabile in un intervallo di pH compreso tra 4.0 e 9.0, nonché ad alte temperature, con valori di $T_m > 80^\circ\text{C}$ tra pH 5.0 e 7.0. Infine, è stato dimostrato che la proteina possiede un'azione citotossica selettiva per le cellule tumorali.

In conclusione, con il presente progetto di dottorato è stato delineato un processo sostenibile in accordo con i principi della bioraffineria e della chimica verde, valorizzando la biomassa di *G. phlegrea*. La strategia proposta per il recupero in cascata di ficocianine, carotenoidi e acidi grassi polinsaturi potrebbe essere facilmente applicata a livello industriale. Considerando l'alto valore di mercato dei tre prodotti ottenuti, il modello messo a punto potrebbe contribuire ad aumentare le fonti di guadagno relative al processo, compensando così gli elevati costi di coltivazione e quelli a valle per la raccolta e il frazionamento della biomassa in differenti prodotti. Ciò potrebbe portare ad un bilancio economico positivo della bioraffineria basata sulle microalghe. Inoltre, lo sviluppo di un processo eco-sostenibile e sicuro potrebbe determinare il consenso da parte dell'opinione pubblica, ancora troppo restia all'utilizzo di prodotti ottenuti da microalghe.

Nonostante i prodotti biologici risultino essere di rilevanza strategica per molte aziende, sono ancora molti i problemi e le sfide da affrontare per giungere ad una piena industrializzazione e commercializzazione di tali prodotti. Attualmente in letteratura sono riportati molti studi sull'efficacia dei singoli passaggi che potrebbero

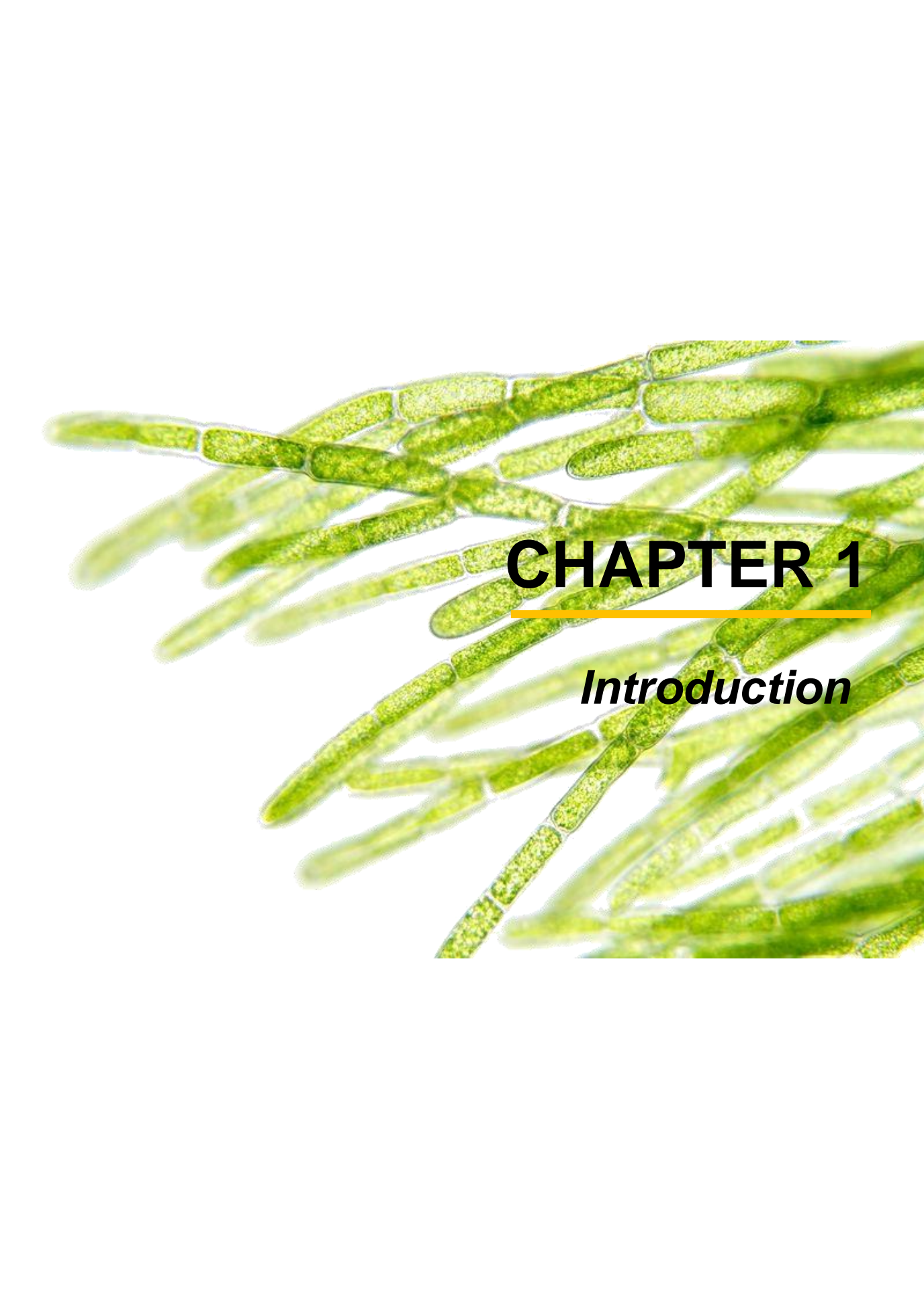
costituire una bioraffineria, tuttavia i tentativi di strutturare un intero processo sono ancora molto pochi. Un altro problema da non sottovalutare è la reticenza da parte delle aziende di conformarsi alle esigenze sociali e ambientali necessarie per ottenere l'accettazione pubblica. Studi recenti hanno dimostrato che i costi associati alle bioraffinerie convenzionali, rappresentano circa il 20-40% dei costi di un intero processo. Questi costi aumentano fino al 60% quando si parla di bioraffinerie basate sull'utilizzo di microalghe.

Per ridurre i costi, gli sforzi dovrebbero essere focalizzati sullo sviluppo di tecniche semplici che richiedono solo poche operazioni unitarie, tenendo però presente che le tecnologie sviluppate *ad hoc* per una singola operazione dovrebbero sempre essere affiancate da una attenta valutazione dell'impatto di queste sull'intero processo. Solo lo sviluppo di una piattaforma integrata in grado di valorizzare al massimo la biomassa delle microalghe favorirà la transizione dalla produzione in scala di laboratorio a quella su larga scala. Solo in questo modo le bioraffinerie basate sulle microalghe potrebbero diventare una solida realtà industriale.

*Gli esperimenti di estrazione con i fluidi compressi sono stati effettuati nel laboratorio della Prof.ssa Elena Ibañez, Istituto di ricerca in scienze alimentari (CIAL), Madrid, Spagna.

SUMMARY

The aim of this PhD thesis was the use of red thermo-acidophilic microalgae, *Galdieria phlegrea* (stain 009) to develop a biorefinery to obtain three different high value bio-products. First, a preliminary cascade approach has been designed to recover phycocyanin and lipids from the wet biomass of the microalga grown in autotrophic conditions. Extractions were performed in two sequential steps: a conventional high-pressure procedure to recover phycocyanins (PCs) and a solvent extraction to obtain fatty acids. PCs were isolated by a single purification step obtaining a high purity grade and they fully retained their antioxidant activity on a cell-based model. From the residual biomass, fatty acids were recovered, with a higher yield with respect to those obtained from the raw biomass. Then, a green approach was used to recover PCs, carotenoids and lipids in cascade. PC extraction was performed as mentioned above and the isolation was optimized by ultrafiltration. Carotenoids were obtained by a pressurized liquid extraction (PLE) on the residual biomass and finally lipids were extracted by supercritical fluid extraction (SFE). The used extraction procedures are green, fast, and cost-effective and allow to improve the extraction yield up to 40% for carotenoids and up to 12% for lipids in comparison with conventional extractions. The carotenoids extracted by PLE were tested as antioxidants, thus proving that the procedure employed for the extraction did not affect their bioactivity. Finally, a complete biophysical and biochemical characterization of purified phycocyanin was carried out. The results show that the protein is stable under different pHs and unfolds with an apparent melting temperature higher than 80°C within a pH range between 5.0-7.0. The protein also exerts interesting in cell antioxidant properties even after the pasteurization process, and is cytotoxic for cancer cells, whereas it is not toxic for non-malignant cells. In conclusion, in the present PhD thesis, a green biorefinery was set up, thus completely valorizing the biomass of *G. phlegrea*. The proposed approach to recover in a cascade approach PCs, carotenoids and PUFAs could be easily scaled up at industrial level. The obtained results could also contribute to increase the revenue streams of the process, thus compensating the large cultivation and downstream costs for biomass production. Furthermore, the development of a green process could also increase the social acceptance of industrial microalgal products.

A microscopic view of green algae filaments, showing multiple parallel chains of rectangular cells. The cells are filled with a granular green substance, likely chloroplasts, and are connected by thin cell walls. The filaments are arranged in a fan-like pattern, extending from the bottom right towards the top left.

CHAPTER 1

Introduction

1.1 Microalgae and biotechnological applications

Microalgae are very small plant-like microorganisms between 1-50 micrometers in diameter, without roots or leaves. They are prokaryotic or eukaryotic microorganisms that use solar energy and nutrients to convert carbon dioxide (CO₂) into biomass (Feron and Hendriks 2005). With respect to plants, microalgae are more competitive: they do not compete for arable lands, they can grow on seawater and on residual nutrients, they have higher areal productivity, thus accumulating larger amounts of valuable components within a short time (Chauton 2015).

Algae mitigate large amounts of carbon dioxide, as about 1.8 tons of CO₂ are consumed by one ton of microalgae (Kliphuis 2010). Depending on the cultivation system used, microalgae accumulate lipids, proteins or carbohydrates and for this reason they are emerging as potential feedstock for a number of different industrial sectors, such as food commodities, biofuels, bio-based chemicals, fine organics, bioplastics, pigments, cosmetics and pharmaceuticals (Posada 2016).

Microalgae cultures have been extensively studied in the last decades, particularly for biodiesel production (Mata, Martins, and Caetano 2010). However, the analysis of the large-scale productions points out that the technologies proposed to produce liquid fuels are still not self-sustainable from an economic point of view. The main disadvantages reside in the high production and transformation costs, high freshwater requirements for cultivation, and high acid value of microalgal oil in comparison with other biofuels feedstocks (González-Delgado and Kafarov 2011). Thus, the use of microalgae to obtain only biofuels does not seem to be economically feasible. For this reason, the obtainment of co-products is becoming essential for their commercial production (Axelsson 2012). Improving the extraction techniques or dedicating a percentage of the algal crop to the obtainment of high value products (e.g., with terrestrial agriculture) may help in closing the economic gap between petroleum and algae biofuels.

1.2 Circular economy, green chemistry and microalgal biorefinery

In 1987, the UN World Commission on Environment and Development defined sustainability as *“the development that meets the needs of the present without compromising the ability of future generations to meet their own needs”* (World Commission on Environment and Development Report). Demographic pressure and climate changes are heavily relying on the natural resources of planet

earth. This dramatic situation is fostering the necessity to favor sustainability over productivity. One of the key aspects of sustainable development is the reduction or even total elimination of wastes (Herrero and Ibañez 2018). Over the last decade the new concept of Circular Economy (CE) has gained attention (Ghisellini, Cialani, and Ulgiati 2016). The idea behind CE is the use of renewable materials as feedstock for fuels and chemicals, where all the by-products find feed or industrial applications and the wastes are completely degradable. This economy model promotes the sustainable development by keeping in mind the economic, environmental, technological and social impact. In this context, Green Chemistry embraces the effort to face the challenge related to sustainable development of the chemical industry (Song and Han 2015).

The concept of Green Chemistry was first formulated at the beginning of the '90s (Anastas and Eghbali 2010). Its innovation lied in the promotion of a better use of resources, a reduction of wastes and a more intelligent use of energy. The idea of utilizing wastes as well as natural products as resources and the development of an integrated platform able to produce different bio-products from biomasses, came to life with the biorefinery concept.

Biorefinery has been identified as the most promising concept for the creation of a biomass-based industry, since it overcomes linear processes of biomass transformation by using waste materials and increasing the obtainment of bio-products. Microalgae have a high potential to be used as starting material in the biorefinery process since they contain different metabolites of interest and are currently used to obtain many products (González-Delgado and Kafarov 2011). Indeed, the possibility to obtain different molecules from different microalgal components (lipids, proteins and carbohydrates) in a cascade approach would render these organisms a suitable starting point for the industrial development of a biorefinery (Soh 2014).

1.3 High-value bio-products from microalgae

Given their different nature, microalgae can produce a wide variety of nutrients and secondary metabolites that are beneficial for humans or animals. Valuable current or potential co-products include carotenoids, polyunsaturated fatty acids (PUFAs) and phycobiliproteins (Hannon 2010). Microalgae can synthesize many other unique molecules with commercial potential, such as toxins, vitamins, antibiotics, sterols, lectins, mycosporine-like amino acids, halogenated compounds and polyketides. In some instances, the expression of

molecules that improve crop protection may also have a pharmaceutical value. Several issues hinder the industrial exploitation of the cited high-value microalgal products (Spolaore 2006). On one hand, it is required to select operating conditions for microalgal culture that maximize the production of the all selected high-value products. On the other hand, the microalgal fractionation process should include procedures that allow extracting different products without any interference on their chemical and biological characteristics. However, one should keep in mind that different microalgal growth conditions may be required to isolate different high-value products. As an example, the production of lipids increases for cultures carried out at low light intensities and at low temperature, which is not compatible with antioxidant production. On the other hand, antioxidant production is enhanced by high-intensity irradiation and by N- and P-stress conditions, since it results in the generation of radical species in cells (Goiris 2015). Moreover, a serious concern about the cultivation of microalgae under stress conditions is the decrease or the arrest of growth rates and consequently the decrease of the total production and productivity (Markou and Nerantzis 2013).

1.3.1 Phycobiliproteins

Phycobiliproteins (PBPs) are brilliantly colored, highly fluorescent, water-soluble protein components of the photosynthetic light-harvesting antenna complexes of cyanobacteria (blue-green algae), red algae, and cryptomonads. These proteins are classified into two large groups based on their colors, the phycoerythrin group, red, and the phycocyanin one, blue. Phycocyanins include C-phycocyanin (C-PC), R-phycocyanin (R-PC), and allophycocyanin (A-PC) (Soni 2006). Phycobiliproteins are assembled into an organized cellular structure, namely, the phycobilisome that is attached in regular arrays to the external surface of the thylakoid membrane, which acts as major light harvesting pigments in cyanobacteria and red algae (Figure 1). Phycobilisomes consist of an allophycocyanin core surrounded by phycocyanin on the periphery. Phycocyanin is the major constituent, whereas allophycocyanin functions as the bridging pigment between phycobilisomes and the photosynthetic lamella (Eisele 2000). The phycobilisome allows the pigments to be geometrically arranged in a way that helps to optimize light capture and transfer of energy. All the phycobiliproteins absorb incident light directly, but, in addition, they participate in an energy transfer chain within the phycobilisome in a sequence: phycoerythrin → phycocyanin → allophycocyanin → chlorophyll-a. During last few decades, PBPs have been investigated

for their antioxidant activity. The demand for antioxidants is primarily driven by a growing demand for health and dietary supplements. Currently, natural antioxidants are expensive compared to synthetic antioxidants. Nevertheless, natural pigments are the most influential compounds in the overall revenue from the microalgal biomass (Ruiz 2016). This is very attractive since there is a growing consumer preference for food and cosmetic products enriched in “green” antioxidants.

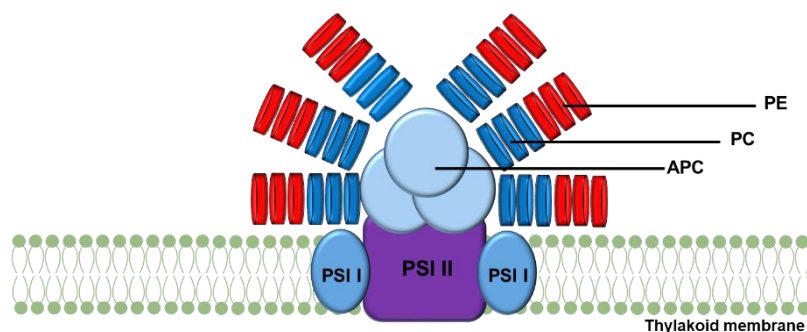


Figure 1. Graphic representation of phycobilisome. Phycobilisome consists of a central core with radiating rods. This core contains allophycocyanins (APC) that are the close to the photosystems (PSI) and promote the energy transfer during photosynthesis. Six rods are attached to the core. Each rod disk consists in hexamers of phycocyanin (PC) and phycoerythrin (PE) arranged to reflect the resonance energy transfer pathway: PE→PC→APC→PSI.

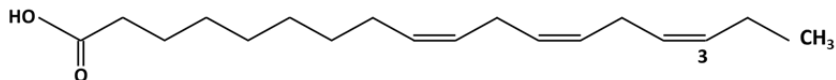
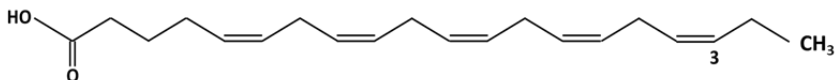
1.3.2 Poly-Unsaturated Fatty Acids (PUFA)

The main components of algal lipid fraction are represented by fatty acids (FA), waxes, sterols, hydrocarbons, ketones and pigments (Halim et al. 2011). Depending on the species, total lipids usually represent 20-50% in dry weight of the total biomass. Generally, fatty acids can be classified in two categories based on the polarity of the molecular head group: (i) neutral lipids and free fatty acids (FFA) and (ii) polar lipids or amphipathic lipids, which can be further subcategorized into phospholipids and glycolipids. Lipids synthesis and accumulation by microalgae depends on the species and is also affected by culture conditions, such as nutrient concentration, salinity, light intensity periods, temperature, pH and even the association with other microorganisms (Richmond A. 2004; Guschina and Harwood 2006). Omega-3 (ω -3) polyunsaturated fatty acids (PUFAs) (Figure 2) are a specific group of polyunsaturated fatty acids in which the first

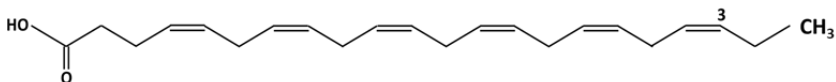
double bond is located between the third and fourth carbon atom counting from the methyl end of the fatty acid (Ryckebosch 2012), and it comprises: α -linolenic acid (ALA 18:3), eicosapentaenoic acid (EPA, 20:5), docosapentaenoic acid (22:5) and docosahexaenoic acid (DHA, 22:6) (Fraeye 2012). The long chain provides significant health benefits, particularly in reducing cardiac diseases such as arrhythmia, stroke and high blood pressure (Pulz and Gross 2004). Moreover, they have beneficial effects against depression, rheumatoid arthritis, asthma and can be used for treatment of inflammatory diseases, such as rheumatoid arthritis, Crohn's disease, ulcerative colitis, psoriasis, lupus and cystic fibrosis (Wen and Chen 2003; Sijtsma and De Swaaf 2004).

Among PUFA, the ω -6 are those in which the first double bond is located between the sixth and seventh carbon atom counting from the methyl end of the fatty acid and comprises γ -linolenic acid (GLA, 18:3 ω -6) and arachidonic acid (ARA, 20:6 ω -6), which have been shown to possess beneficial activities (Soni, Trivedi, and Madamwar 2008). As an example, in pregnant women, the adequate intake of EPA and DHA is crucial for healthy development of the fetal brain and ARA and DHA are required for normal growth and brain functional development, whereas EPA is considered essential for the regulation of some biological functions and prevention of arrhythmia, atherosclerosis, cardiovascular disease and cancer (Pulz and Gross 2004).

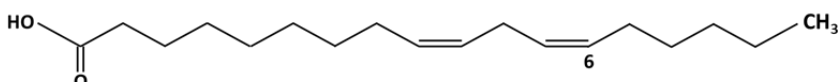
To date, fish oil is the major commercial source of polyunsaturated fatty acids, especially for the low production costs. Its quality depends on the fish species, the season/climate and geographical location of catching sites and food quality consumed by the fish. Noteworthy, in some cases, there is a contamination danger by lipid-soluble environmental pollutants (Ryckebosch 2012). Moreover, fish oil is not suitable for vegetarians, and its odor makes it unattractive for consumption. Nevertheless, fish oil is characterized by a higher amount of ω -3 (60% EPA+DHA) in comparison with microalgae-based oil, and for this reason, it remains the main commercial source of ω -3.

ω -3 α -Linolenic acid (ALA)

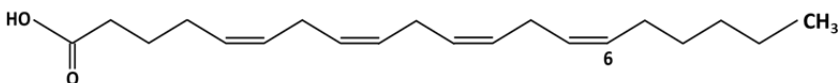
Eicosapentaenoic acid (EPA)



Docosahexaenoic acid (DHA)

 ω -6

Linoleic acid (LA)



Arachidonic acid (AA)

Figure 2. Molecular structure of common ω -3 and ω -6 polyunsaturated fatty acids. Polyunsaturated fatty acids have the first double binding in position 3 (ω -3) or in position 6 (ω -6). All double bindings are in cis formation. The ω -3 fatty acids include alpha-linolenic acid (ALA), eicosapentaenoic acid (EPA), and docosahexaenoic acid (DHA). The ω -6 include linoleic acid (LA) and arachidonic acid (AA).

1.3.3 Carotenoids

An important and well-known class of antioxidants from microalgae are carotenoids (Figure 3). They are lipophilic compounds, which represent a large group of biological chromophores with an absorption range between 400 and 550 nm, resulting in their yellow-orange color. Carotenoids can represent up to 14% of algal biomass. Most carotenoids share a common C40 backbone structure of isoprene unit (termed terpenoid), and are divided into two groups: carotenes, which are true hydrocarbons, and xanthophylls (Gong and Bassi 2016) which contain also oxygen atoms (Mulders 2014). They can be also

classified as primary (essential for survival) and secondary (by exposure to specific stimuli). Carotenoids play key roles in light harvesting and energy transfer during photosynthesis and in the protection of the photosynthetic apparatus against photooxidative damage (Ye, Jiang, and Wu 2008). Several studies have demonstrated that carotenoids contribute significantly to the total antioxidant capacity of microalgae (Takaichi 2011). Carotenoids have received increased attention during the last decade due to their intrinsic antioxidant activity and potential function in preventing adverse health conditions in humans. Noteworthy, carotenoids are able to quench singlet oxygen (1O_2) and free radicals responsible for cell damage. In medical science, carotenoids can help in preventing and treating many diseases, such as cancer, cardiovascular disease, diabetes and osteoporosis (Shaish 2006; Kohlmeier 1997; Rao and Rao 2007).

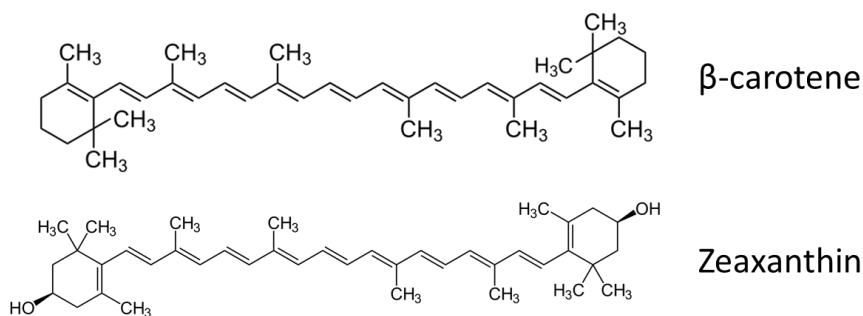


Figure 3. Molecular structure of carotenoids. β-carotene, with the molecular formula $C_{40}H_{56}$, belongs to the group of carotenoids consisting of isoprene units. It is the most abundant form of carotenoid and it is a precursor of the vitamin A. β-carotene is composed of two retinyl groups. Zeaxanthin, with molecular formula $C_{40}H_{56}O_2$, is a carotenoid xanthophyll. Zeaxanthin is an isomer of Lutein. The main difference between them is in the location of a double bond in one of the end rings. This difference gives Lutein three chiral centers whereas zeaxanthin has two.

1.4 *Galdieria phlegrea*

Galdieria phlegrea (Figure 4) is a red thermo-acidophilic microalga that belongs to Cyanidiales. The order of Cyanidiales is comprised of asexual, unicellular red algae characterized by a simple morphology. Cells have a spherical shape and possess a thick wall containing one plastid (i.e. chloroplast), 1-3 mitochondria, a nucleus, a

vacuole and storage products (Albertano 2000; Carfagna 2015; Ciniglia 2004; Graziani 2013; Pinto 2007).

They can live at low pH environments (0.2 - 4.0) and at medium to high temperature (up to 56°C) (Castenholz 2010). To date, these unicellular taxa are classified into three genera: *Cyanidium*, *Cyaniadidoschyzon* and *Galdieria* (Ciniglia 2004). Besides low pH and high temperature, *Galdieria* have several unique features, such as different mechanisms for metal tolerance; this allows cells to grow in toxic environments where other organisms cannot grow at all or can roughly do it (Nagasaka 2003; Yoshimura 1999).

Galdieria is able to grow auto-, mixo- and hetero-trophically on a wide range of carbon sources and different strains are able to maintain their photosynthetic apparatus when grown heterotrophically (Carfagna 2018).

The autotrophic cultivation of *Galdieria* has been studied for its ability to accumulate pigments, β -carotene, astaxanthin, zeaxanthin and phycocyanin, commonly used in food or in health applications. Moreover, the ability of *Galdieria* to be cultivated under conditions considered hostile for other microorganisms overcomes the problem of contaminations.

Galdieria phlegrea is a species collected for the first time in the Phlegrean Fields (Naples, Italy). This site is characterized by a crypto endolithic environment, a relatively dry condition and reduced light intensities (Ciniglia 2004). It has been demonstrated that *G. phlegrea* has developed an ameliorative strategy to adapt to extreme environments, such as the ability to express a complete data-set of genes required for urea hydrolysis, necessary as an alternative nitrogen source in N-limited environments (Qiu 2013).

G. phlegrea (strain 009), contains abundant reserves of organic sulphur as glutathione, even under S starvation, and more generally a particular setting of sulphur metabolism (Carfagna 2016). These characteristics could explain the outstanding thermo-resistance and thermo-induction of the C-PC synthesized by the strain 009.

For these unique extremophilic properties, the microalga *Galdieria phlegrea* (strain 009) has attracted interest for biotechnological applications.

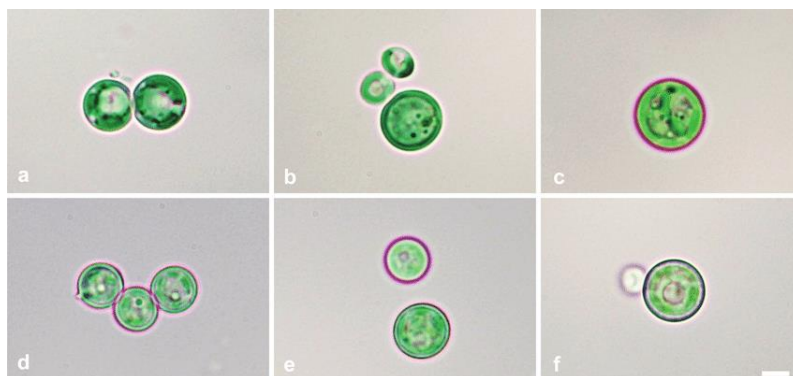


Figure 4. Comparison between the morphology of two *Galdieria* species: a-c, *G. sulphuraria*; d-f, *G. phlegrea* (Dovilè 2018).

1.5 The Aim of the thesis

The aim of this PhD thesis is the use of *Galdieria phlegrea* (strain 009) to obtain different high value bio-products subsequently. The idea is to develop a cascade extraction method according to the biorefinery concept, in order to obtain the three class of molecules starting from the one with the highest market value. The research activities are presented in three sections explained hereinafter.

1. Strain selection, optimization of growth conditions and preliminary process design.

The optimization of *G. phlegrea* (strain 009) growth conditions to obtain high levels of bioproducts was set-up. Then, by using a cascade approach, phycocyanin (PC) and lipids were obtained. PC was isolated by a single purification step from the wet biomass and lipids recovered from the residual biomass were characterized by gas chromatography analysis. Finally, PC antioxidant activity was validated on a cell-based model, using human immortalized keratinocytes. **(Chapter 2)**

2. Optimization of the biorefinery design.

Optimization of the isolation of PC was carried out. Then, the residual wet biomass was used to extract two different bioproducts in two sequential steps: carotenoids by using Pressurized Liquid Extraction (PLE) and lipids by Supercritical Fluid Extraction (SFE). The bioactivity of the extracted

carotenoids obtained by PLE was validated on a cell-based model, using human immortalized keratinocytes. **(Chapter 3)**

3. Biophysical and biochemical characterization of PC.

Primary sequence of PC was determined. Then, a study on the stability of the protein was carried out. In particular, the effects of pH and temperature variations on protein stability were evaluated. Moreover, cytotoxic activity of the protein and the antioxidant activity of PC after thermal pasteurization were evaluated. **(Chapter 4)**

1.6 References

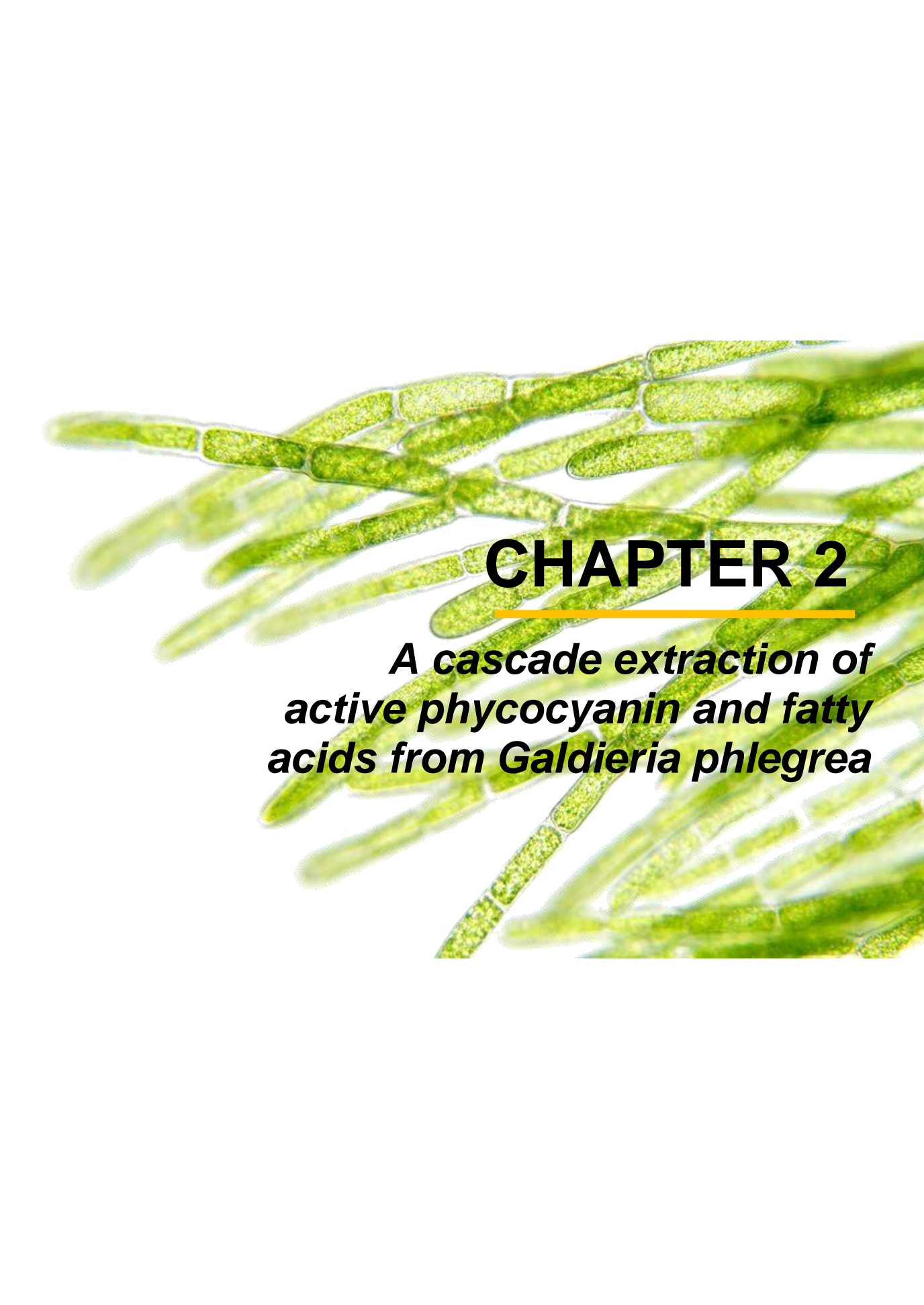
- Albertano, P., C. Ciniglia, G. Pinto, and A. Pollio. 2000. "The Taxonomic Position of *Cyanidium*, *Cyanidioschyzon* and *Galdieria*: An Update." *Hydrobiologia* 433 (1993): 137–43. <https://doi.org/10.1023/A:1004031123806>.
- Anastas, Paul, and Nicolas Eghbali. 2010. "Green Chemistry: Principles and Practice." *Chemical Society Reviews* 39 (1): 301–12. <https://doi.org/10.1039/b918763b>.
- Axelsson, Lisa, Maria Franzén, Madelene Ostwald, Göran Berndes, G. Lakshmi, and N. H. Ravindranath. 2012. "Perspective: *Jatropha* Cultivation in Southern India: Assessing Farmers' Experiences." *Biofuels, Bioproducts and Biorefining* 6 (3): 246–56. <https://doi.org/10.1002/bbb>.
- Carfagna, Simona, Claudia Bottone, Pia Rosa Cataletto, Milena Petriccione, Gabriele Pinto, Giovanna Salbitani, Vincenza Vona, Antonino Pollio, and Claudia Ciniglia. 2016. "Impact of Sulfur Starvation in Autotrophic and Heterotrophic Cultures of the Extremophilic Microalga *Galdieria Phlegrea* (Cyanidiophyceae)." *Plant and Cell Physiology* 57 (9): 1898–1898. <https://doi.org/10.1093/pcp/pcw112>.
- Carfagna, Simona, Viola Landi, Francesca Coraggio, Giovanna Salbitani, Vincenza Vona, Gabriele Pinto, Antonino Pollio, and Claudia Ciniglia. 2018. "Different Characteristics of C-Phycocyanin (C-PC) in Two Strains of the Extremophilic *Galdieria Phlegrea*." *Algal Research* 31: 406–12. <https://doi.org/10.1016/j.algal.2018.02.030>.
- Carfagna, Simona, Gaetana Napolitano, Daniela Barone, Gabriele Pinto, Antonino Pollio, and Paola Venditti. 2015. "Dietary Supplementation with the Microalga *Galdieria Sulphuraria* (Rhodophyta) Reduces Prolonged Exercise-Induced Oxidative Stress in Rat Tissues." *Oxidative Medicine and Cellular Longevity* 2015: 1–11. <https://doi.org/10.1155/2015/732090>.
- Castenholz. 2010. "A Fast Growing and Edible Red Marine Macroalga." *Red Algae in the Genomic Age* 13 (1952): 357–71. <https://doi.org/10.1007/978-90-481-3795-4>.
- Chauton, Matilde S., Kjell Inge Reitan, Niels Henrik Norsker, Ragnar Tveterås, and Hans T. Kleivdal. 2015. "A Techno-Economic Analysis of Industrial Production

- of Marine Microalgae as a Source of EPA and DHA-Rich Raw Material for Aquafeed: Research Challenges and Possibilities.” *Aquaculture* 436: 95–103. <https://doi.org/10.1016/j.aquaculture.2014.10.038>.
- Ciniglia, Claudia, Hwan Su Yoon, Antonino Pollio, Gabriele Pinto, and Debashish Bhattacharya. 2004. “Hidden Biodiversity of the Extremophilic Cyanidiales Red Algae.” *Molecular Ecology* 13 (7): 1827–38. <https://doi.org/10.1111/j.1365-294X.2004.02180.x>.
- Dovilė, B, N Linda, C Adam, K Filip, and J Jan. 2018. “Burning Coal Spoil Heaps as a New Habitat for the Extremophilic Red Alga *Galdieria Sulphuraria* Burning Coal Spoil Heaps as a New Habitat for the Extremophilic Red Alga *Galdieria Sulphuraria*.” *Fottea* 18 (October): 19–29. <https://doi.org/10.5507/fot.2017.015>.
- Eisele, Leslie E., Sasha H. Bakhru, Xuemei Liu, Robert MacColl, and Mercedes R. Edwards. 2000. “Studies on C-Phycocyanin from *Cyanidium Caldarium*, a Eukaryote at the Extremes of Habitat.” *Biochimica et Biophysica Acta - Bioenergetics* 1456 (2–3): 99–107. [https://doi.org/10.1016/S0005-2728\(99\)00110-3](https://doi.org/10.1016/S0005-2728(99)00110-3).
- Feron, P H M, and C A Hendriks. 2005. “CO 2 Capture Process Principles and Costs.” *Oil & Gas Science and Technology* 60 (3): 451–59.
- Fraeye, Ilse, Charlotte Bruneel, Charlotte Lemahieu, Johan Buyse, Koenraad Muylaert, and Imogen Foubert. 2012. “Dietary Enrichment of Eggs with Omega-3 Fatty Acids: A Review.” *Food Research International* 48 (2): 961–69. <https://doi.org/10.1016/j.foodres.2012.03.014>.
- Ghisellini, Patrizia, Catia Cialani, and Sergio Ulgiati. 2016. “A Review on Circular Economy: The Expected Transition to a Balanced Interplay of Environmental and Economic Systems.” *Journal of Cleaner Production* 114: 11–32. <https://doi.org/10.1016/j.jclepro.2015.09.007>.
- Goiris, Koen, Willem Van Colen, Isabel Wilches, Fabián León-tamariz, Luc De Cooman, and Koenraad Muylaert. 2015. “Impact of Nutrient Stress on Antioxidant Production in Three Species of Microalgae.” *Algal Research* 7: 51–57. <https://doi.org/10.1016/j.algal.2014.12.002>.
- Gong, Mengyue, and Amarjeet Bassi. 2016. “Carotenoids from Microalgae : A Review of Recent Developments.” *Biotechnology Advances* 34 (8): 1396–1412. <https://doi.org/10.1016/j.biotechadv.2016.10.005>.
- González-Delgado, Ángel-Darío, and Viatcheslav Kafarov. 2011. “Microalgae Based Biorefineries: Issues to Consider.” *Ciencia, Tecnología y Futuro* 4 (4): 5–22.
- Graziani, Giulia, Simona Schiavo, Maria Adalgisa Nicolai, Silvia Buono, Vincenzo Fogliano, Gabriele Pinto, and Antonino Pollio. 2013. “Microalgae as Human Food: Chemical and Nutritional Characteristics of the Thermo-Acidophilic Microalga *Galdieria Sulphuraria*.” *Food & Function*, no. November 2015: 144–52. <https://doi.org/10.1039/c2fo30198a>.
- Guschina, Irina A., and John L. Harwood. 2006. “Lipids and Lipid Metabolism in Eukaryotic Algae.” *Progress in Lipid Research* 45 (2): 160–86.

- <https://doi.org/10.1016/j.plipres.2006.01.001>.
- Halim, Ronald, Brendan Gladman, Michael K. Danquah, and Paul A. Webley. 2011. "Oil Extraction from Microalgae for Biodiesel Production." *Bioresource Technology* 102 (1): 178–85. <https://doi.org/10.1016/j.biortech.2010.06.136>.
- Hannon, Michael, Javier Gimpel, Miller Tran, Beth Rasala, and Stephen Mayfield. 2010. "Biofuels from Algae: Challenges and Potential." *Biofuels* 1 (5): 763–84. <https://doi.org/10.4155/bfs.10.44>.
- Herrero, Miguel, and Elena Ibañez. 2018. "Green Extraction Processes, Biorefineries and Sustainability: Recovery of High Added-Value Products from Natural Sources." *Journal of Supercritical Fluids* 134 (December 2017): 252–59. <https://doi.org/10.1016/j.supflu.2017.12.002>.
- Kliphuis, Anna M J, Lenneke De Winter, Carsten Vejrazka, Dirk E Martens, Marcel Janssen, and H Wijffels. 2010. "Photosynthetic Efficiency of *Chlorella Sorokiniana* in a Turbulently Mixed Short." *Biotechnology Journal* 26 (3): 687–96. https://doi.org/10.1002/btpr_379.
- Kohlmeier, Lenore, Jeremy D Kark, Enrique Gomez-gracia, Blaise C Martin, Susan E Steck, Alwine F M Kardinaal, Jetmund Ringstad, et al. 1997. "Lycopene and Myocardial Infarction Risk in the EURAMIC Study." *American Journal of Epidemiology* 146 (8): 618–26.
- Markou, Giorgos, and Elias Nerantzis. 2013. "Microalgae for High-Value Compounds and Biofuels Production: A Review with Focus on Cultivation under Stress Conditions." *Biotechnology Advances* 31 (8): 1532–42. <https://doi.org/10.1016/j.biotechadv.2013.07.011>.
- Mata, Teresa M., António A. Martins, and Nidia S. Caetano. 2010. "Microalgae for Biodiesel Production and Other Applications: A Review." *Renewable and Sustainable Energy Reviews* 14 (1): 217–32. <https://doi.org/10.1016/j.rser.2009.07.020>.
- Mulders, Kim L. M., Packo P Lamers, Dirk E Martens, and H Wijffels. 2014. "Phototrophic Pigment Production with Microalgae: Biological Constrains and Opportunities." *Journal of Phycology* 50 (2): 229–42. <https://doi.org/10.1111/jpy.12173>.
- Nagasaka, Seiji, Naoko K. Nishizawa, Tokuko Watanabe, Satoshi Mori, and Etsuro Yoshimura. 2003. "Evidence That Electron-Dense Bodies in *Cyanidium Caldarium* Have an Iron-Storage Role." *BioMetals* 16 (3): 465–70. <https://doi.org/10.1023/A:1022563600525>.
- Pinto, G. 2007. "Cyanidiophyceae." In *Algae and Cyanobacteria in Extreme Environments*, 387–97. https://doi.org/https://doi.org/10.1007/978-1-4020-6112-7_20.
- Posada, John A., Laura B. Brentner, Andrea Ramirez, and Martin K. Patel. 2016. "Conceptual Design of Sustainable Integrated Microalgae Biorefineries: Parametric Analysis of Energy Use, Greenhouse Gas Emissions and Techno-Economics." *Algal Research* 17: 113–31.

- <https://doi.org/10.1016/j.algal.2016.04.022>.
- Pulz, Otto, and Wolfgang Gross. 2004. "Valuable Products from Biotechnology of Microalgae." *Applied Microbiology and Biotechnology* 65 (6): 635–48. <https://doi.org/10.1007/s00253-004-1647-x>.
- Qiu, Huan, Dana C Price, Andreas P M Weber, Valérie Reeb, Eun Chan Yang, Jun Mo Lee, Su Yeon Kim, and Hwan Su Yoon. 2013. "Adaptation through Horizontal Gene Transfer in the Cryptoendolithic Red Alga *Galdieria Phlegrea*." *Current Biology* 23 (19): 865–66. <https://doi.org/10.1016/j.cub.2013.08.046>.
- Rao, A V, and L G Rao. 2007. "Carotenoids and Human Health." *Pharmacological Research* 55: 207–16. <https://doi.org/10.1016/j.phrs.2007.01.012>.
- Richmond A. 2004. *Handbook of Microalgal Culture. Handbook of Microalgal Culture: Applied Phycology and Biotechnology*. <https://doi.org/10.1002/9781118567166>.
- Ruiz, Jesús, Giuseppe Olivieri, Jeroen de Vree, Rouke Bosma, Philippe Willems, J. Hans Reith, Michel H. M. Eppink, et al. 2016. "Towards Industrial Products from Microalgae." *Energy Environ. Sci.* 24: 405–13. <https://doi.org/10.1039/C6EE01493C>.
- Ryckebosch, Eline, Charlotte Bruneel, Koenraad Muylaert, and Imogen Foubert. 2012. "Microalgae as an Alternative Source of Omega-3 Long Chain Polyunsaturated Fatty Acids." *Lipid Technology* 24 (6): 128–30. <https://doi.org/10.1002/lite.201200197>.
- Shaish, Aviv, Ayelet Harari, Lea Hananshvili, Hofit Cohen, Rafael Bitzur, Tamar Luvish, Esfir Ulman, et al. 2006. "Increases Plasma HDL-Cholesterol in Fibrate-Treated Patients" 189: 215–21. <https://doi.org/10.1016/j.atherosclerosis.2005.12.004>.
- Sijtsma, L., and M. E. De Swaaf. 2004. "Biotechnological Production and Applications of the ω -3 Polyunsaturated Fatty Acid Docosahexaenoic Acid." *Applied Microbiology and Biotechnology* 64 (2): 146–53. <https://doi.org/10.1007/s00253-003-1525-y>.
- Soh, Lindsay, Mahdokht Montazeri, Berat Z Haznedaroglu, Cuchulain Kelly, Jordan Peccia, Matthew J Eckelman, and Julie B Zimmerman. 2014. "Bioresource Technology Evaluating Microalgal Integrated Biorefinery Schemes: Empirical Controlled Growth Studies and Life Cycle Assessment." *Bioresource Technology* 151: 19–27. <https://doi.org/10.1016/j.biortech.2013.10.012>.
- Song, Jinliang, and Buxing Han. 2015. "Green Chemistry: A Tool for the Sustainable Development of The." *National Science Review* 2 (3): 255–56. <https://doi.org/10.1093/nsr/nwu076>.
- Soni, Badrish, Beena Kalavadia, Ujval Trivedi, and Datta Madamwar. 2006. "Extraction, Purification and Characterization of Phycocyanin from *Oscillatoria Quadripunctulata*-Isolated from the Rocky Shores of Bet-Dwarka, Gujarat, India." *Process Biochemistry* 41 (9): 2017–23. <https://doi.org/10.1016/j.procbio.2006.04.018>.

- Soni, Badrish, Ujjval Trivedi, and Datta Madamwar. 2008. "A Novel Method of Single Step Hydrophobic Interaction Chromatography for the Purification of Phycocyanin from *Phormidium Fragile* and Its Characterization for Antioxidant Property." *Bioresource Technology* 99 (1): 188–94. <https://doi.org/10.1016/j.biortech.2006.11.010>.
- Spolaore, Pauline, Claire Joannis-Cassan, Elie Duran, and Arsène Isambert. 2006. "Commercial Applications of Microalgae." *Journal of Bioscience and Bioengineering* 101 (2): 87–96. <https://doi.org/10.1263/jbb.101.87>.
- Takaichi, Shinichi. 2011. "Carotenoids in Algae : Distributions , Biosyntheses and Functions," 1101–18. <https://doi.org/10.3390/md9061101>.
- Wen, Zhi You, and Feng Chen. 2003. "Heterotrophic Production of Eicosapentaenoic Acid by Microalgae." *Biotechnology Advances* 21 (4): 273–94. [https://doi.org/10.1016/S0734-9750\(03\)00051-X](https://doi.org/10.1016/S0734-9750(03)00051-X).
- World Commission on Environment and Development Report, World Commission on Environment and Development Report, Our Common Future, Oxford University Press Oxford, 1987 ISBN 9780192820808.
- Ye, Z., Jiang, J.H., Wu, G.H.. 2008. "Biosynthesis and Regulation of Carotenoids in *Dunaliella* : Progresses and Prospects" 26: 352–60. <https://doi.org/10.1016/j.biotechadv.2008.03.004>.
- Yoshimura, Etsuro, Seiji Nagasaka, Yoshiyuki Sato, Kenichi Satake, and Satoshi Mori. 1999. "Extraordinary High Aluminium Tolerance of the Acidophilic Thermophilic Alga, *Cyanidium Caldarium*." *Soil Science and Plant Nutrition* 45 (3): 721–24. <https://doi.org/10.1080/00380768.1999.10415835>.

A microscopic image of Galdieria phlegrea, showing several long, thin, green filaments. Each filament is composed of a series of rectangular cells joined together. The cells have a granular, greenish-yellow interior, likely due to the presence of chlorophyll and other photosynthetic pigments. The filaments are arranged in a somewhat parallel but slightly overlapping manner, extending from the upper left towards the lower right of the frame.

CHAPTER 2

***A cascade extraction of
active phycocyanin and fatty
acids from Galdieria phlegrea***

Applied Microbiology and Biotechnology

(2019) 103: 9455–9464

<https://doi.org/10.1007/s00253-019-10154-0>**A cascade extraction of active phycocyanin and fatty acids from *Galdieria phlegrea*****Paola Imbimbo^a, Valeria Romanucci^a, Antonino Pollio^b, Carolina Fontanarosa^a, Angela Amoresano^a, Armando Zarrelli^a, Giuseppe Olivieri^{c,d*}, Daria Maria Monti^{a*}**

^a Department of Chemical Sciences, University of Naples Federico II, via Cinthia 4, 80126, Naples, Italy

^b Department of Biology, University of Naples Federico II, via Cinthia 4, 80126, Naples, Italy

^c Bioprocess Engineering Group, Wageningen University and Research, Droevendaalsesteeg 1, 6700AA, Wageningen, the Netherlands

^d Department of Chemical, Materials and Industrial Engineering, University of Naples Federico II, Piazzale Tecchio 80, 80125, Napoli, Italy

Abstract

The setup of an economic and sustainable method to increase the production and commercialization of products from microalgae, beyond niche markets, is a challenge. Here, a cascade approach has been designed to optimize the recovery of high valuable bioproducts starting from the wet biomass of *Galdieria phlegrea*. This unicellular thermo-acidophilic red alga can accumulate high-value compounds and can live under conditions considered hostile to most other species. Extractions were performed in two sequential steps: a conventional high-pressure procedure to recover phycocyanins and a solvent extraction to obtain fatty acids. Phycocyanins were purified to the highest purification grade reported so far and were active as antioxidants on a cell-based model. Fatty acids isolated from the residual biomass contained high amount of PUFAs, more than those recovered from the raw biomass. Thus, a simple, economic, and high effective procedure was set up to isolate phycocyanin at high purity levels and PUFAs.

2.1 Introduction

Microalgae can be rich suppliers of proteins and carbohydrates and, under stress conditions; they can accumulate large quantities of lipids. Therefore, microalgae have been claimed to be potential feedstock for a number of different industrial applications, such as food commodities, biofuels, bio-based chemicals, fine organics, bioplastics, pigments, cosmetics, and pharmaceuticals (Moody 2014; Posada 2016; Quinn and Davis 2015; Ruiz 2016; Tredici 2016). With respect to plants, microalgae possess several advantages: they do not need arable lands, they can grow on seawater and on residual nutrients from wastewater, and they possess higher areal productivity (Chauton 2015). However, the analysis of the large-scale production pointed out that the technologies proposed to obtain only one product are still not self-sustainable from an economic point of view (Leu and Boussiba 2014; Moody 2014; Quinn and Davis 2015; Ruiz 2016; Tredici 2016). The reasons rely on the following: (1) high cultivation costs, especially for cooling in case of adopting close photobioreactor technology, and (2) low profit per unit of biomass coming from a single specific product, especially in case of bulk commodities (food, feed, or fuel), which are characterized by low prices that can hardly compensate the production cost. An intermediate step is first required to promote investments and foster the commercialization of algae-based products: the exploitation of some high value products at production scale smaller than the large one needed for fuel and food (González-Delgado and Kafarov 2011). In that respect, among the cell components, hydrophilic antioxidants such as phycocyanins (PCs) (> 100 €/kg and > 100 M€/year) and lipids rich in polyunsaturated fatty acids (PUFAs) (> 10 €/kg and > 100 M€/year) are good candidates due to their high selling price (Ankush 2019; Ruiz 2016). Moreover, customers are frequently willing to pay a higher price for biobased products than for chemical-based products. Here, a cascade approach has been designed to get two classes of high-value molecules, starting from the same cultivation: phycocyanins and polyunsaturated fatty acids. PC is an antenna pigment, which increases the photosynthetic efficiency by collecting light energy at wavelengths, which chlorophylls do not absorb. PC is water soluble, very stable overtime at its physiological pH, and contains a chromophore prosthetic group. The latter is very fluorescent and is currently used in flow cytometry, immunological analysis, and in detection of reactive oxygen species. In addition, PC is a protein endowed with a strong antioxidant, hepato-protective, anti-inflammatory, neuro-protective, and anti-proliferative activity (Carfagna 2015; Fernández-Rojas 2014; Patel

2018; Romay 2003; Sonani 2017). However, it has to be considered that the use of PC in industry is still limited because of its sensitivity to high temperature and extreme pH, which reduce PC yields or may cause dissociation phenomena, leading to the bleach of the blue color (Manirafasha 2016; Mehta 2018). PUFAs are essential for human function, as they have anti-inflammatory, antioxidant, neuro-protective, and cardioprotective activities, but many of them (such as omega-3 and omega-6) have to be taken up through the diet (Cuellar-Bermudez 2015; Zárata 2017). Actually, they are obtained from fish oil (Salmonidae, Scombridae, and Clupeidae families), which is an unsustainable source both from an economic and environmental point of view (Patel 2019). Moreover, pollution of marine ecosystems, and the possibility that fishes accumulate mercury, led to an increased interest in alternative sustainable sources (Spolaore 2006). Marine microalgae are a source of commercial omega-3 PUFAs and they are the primary producers of basic fatty acids in marine food webs (Bergé and Barnathan 2005). PUFAs from algae also have the advantage of being suitable for vegetarian and vegan nutrition. In this context, the microalga *Galdieria phlegrea*, a unicellular thermo-acidophilic red alga, has gained our attention since it is rich in pigments and PUFAs. Additionally, its optimal growth condition is at pH 1.5 and at temperatures in the range 35–45°C (Carfagna 2015). This represents a great advantage as it will dramatically reduce the risk of contaminations in open ponds systems as well as the cooling cost in case of closed photobioreactors (Sakurai 2016). Here, we set up the optimal autotrophic growth condition for *G. phlegrea* (strain 009) and extracted and purified active PC. Then, by using a cascade approach, we extracted and purified lipids from the residual biomass. Finally, PC antioxidant activity was validated in an applicative environment, with a cell-based model, using human immortalized keratinocytes. This contribution provides a clear validation of the feasibility of a multiproduct biorefinery applied to *G. phlegrea* at lab-scale.

2.2 Material and methods

2.2.1 Microalgal strain and culture conditions

Galdieria phlegrea (strain 009) was provided from the Algal Collection of the University Federico II (ACUF, <http://www.acuf.net>). Pre-cultures of 50 mL were inoculated in Allen medium (Allen 1968) with pH 1.5 in bubble column photobioreactors, with a starting concentration of 8 O.D./mL for autotrophic condition and 14 O.D./mL for the mixotrophic condition. Cultures were performed at 37±1°C under

constant fluorescent light with an intensity of 200 PAR [$\mu\text{mol}/\text{m}^2/\text{s}$]. A gas-mixing device provided the desired carbon dioxide (CO_2) concentration to the photobioreactors, by mixing air and pure carbon dioxide from a pressurized vessel at the final flow rate of 3 vvm. In autotrophy conditions, no organic carbon source was supplemented to the medium, whereas organic carbon with 3% glycerol (final concentration) was supplemented during mixotrophy conditions. The algal growth was monitored daily by measuring the absorbance at 730 nm, which is related to the biomass concentration and is indicated by optical density (O.D.).

2.2.2 Cell concentration

The biomass of *G. phlegrea* was measured as O.D.. Analysis of the dry cell weight was carried out by weighing aliquots of culture. The O.D. values were converted into biomass concentration via an appropriate calibration between O.D. and dry cell weight. The conversion factor was 1 O.D./mL = 0.2 mg_{biomass}/mL for *G. phlegrea*.

2.2.3 Protein extraction and quantification.

The biomass was harvested by centrifugation at 1200 g for 30 min at room temperature and resuspended in 50 mM sodium acetate pH 5.5 (Wu 2016). Cells were disrupted by two consecutive cycles of French Press (each at 2 kbar). After centrifugation at 5000 g at 4°C for 30 min, proteins were recovered in the supernatant, whereas the residual biomass was used to extract lipids (as described below). Proteins were assayed by BCA Protein Assay Kit (Thermo Scientific).

2.2.4. Phycocyanin quantification and purification

The absorbance of crude extracts was measured at 615 and 652 nm to obtain phycocyanin concentration, according to the Bennett and Bogorad equation (Bennett and Bogorad, 1973):

$$C_{PC} \left(\frac{\text{mg}}{\text{mL}} \right) = \frac{[Abs_{615\text{nm}} - (0.474 \times Abs_{652\text{nm}})]}{5.34}$$

These wavelengths correspond to the maximum of absorption of phycocyanin (PC, 615 nm) and allophycocyanin (APC, 652 nm), respectively. The grade of purity of phycocyanin was calculated by measuring the ratio $A_{620\text{nm}}/A_{280\text{nm}}$. A single step purification was performed to recovery phycocyanin. A size-exclusion chromatography was performed by using a Sephadex G-75 fine equilibrated in 50 mM

sodium acetate pH 5.5. Fractions were collected and the absorbance at 280 and 620 nm was measured.

2.2.5 Lipid extraction, purification, and analysis

The residual biomass (i.e., after protein extraction) was dried at 60°C for 24 h. Lipids were selectively extracted by mixing CHCl₃-MeOH (2:1 v/v) with a Soxhlet extractor for 8 h. Then, the solution was dried under nitrogen flux to recover and weigh lipids. One milligram was placed into a 16 × 125 mm screw-cap Pyrex tube and 1 mL of hexane and 1 mL of BF₃ in MeOH (14%, wt/vol) were added. The tube was incubated in a 50°C water bath for 1 h with vigorous handshaking for 20 s every 30 min. Then, 1 mL of a saturated solution of NaHCO₃ and 2 mL of hexane were added and the tube was vortex-mixed. After centrifugation, the hexane layer containing the fatty acid methyl ester (FAME) was placed into a gas chromatography vial, capped, and stored at - 20°C until GC analysis. The organic layer containing FAMEs was collected, dried, dissolved in an appropriate volume of hexane (100 µL), and analyzed using a Shimadzu 2010 series GC FID (Shimadzu, Milano, Italy). The gas chromatograph was equipped with an SP52-60 capillary column (100 m × 0.25 mm i.d. × 0.20 µm film thickness) with a non-bonded, poly(bis-cyanopropyl siloxane) phase (Sigma-Aldrich, St Louis, MO, USA) and nitrogen as the carrier gas. Samples (1 µL) were introduced into the injector using an AOC-20i auto sampler (Shimadzu, Milano, Italy) heated to 250°C with a split ratio of 10:1. The initial temperature was 160°C with a 2 min hold, followed by a 6°C/min ramp to 200°C with a 2 min hold and finally followed by a 6°C/min ramp to 220°C with a 25 min hold. The following parameters were set during the experiments: detector temperature, 275°C; carrier gas: helium for chromatography at a pressure of 1.8 psi, auxiliary gas: hydrogen for chromatography at a pressure of 18 psi, air chromatography at a pressure of 22 psi; and sensitivity of the instrument, 4 to 16 times the minimum attenuation. In situ digestion and mass spectrometry analyses. Sample aliquots (30 µg) were submitted to electrophoresis on a 10% polyacrylamide gel (0.1% SDS, 25 mM Tris-HCl, 192 mM glycine, pH 8.3). Gel was stained with Coomassie Brilliant blue and the main gel lanes excised from the gel and destained prior to further processing. Briefly, gel slices were washed with three cycles of 0.1 M NH₄HCO₃ pH 8.0 and acetonitrile, followed by reduction (10 mM DTT; 100 mM NH₄HCO₃ 45 min, 56°C) and alkylation (55 mM IAM; 100 mM NH₄HCO₃, 30 min, RT). Gel slices were washed with three further cycles of 100 mM NH₄HCO₃ pH 8.0 and acetonitrile. Finally, gel plugs

were rehydrated in 40 mL sequencing grade modified trypsin (10 ng/μL trypsin; 10 mM NH₄HCO₃) and incubated overnight at 37°C. Peptides mixture was eluted, vacuum-dried, and resuspended in 0.1% formic acid for LC-MS/MS. Peptide samples were loaded onto a Michrom C18 Captrap to initially desalt samples and from there were introduced directly into a LTQ-Orbitrap MS (Thermo Fisher Scientific, Surrey, UK) via a fused silica C18 capillary column (Nikkyo Technos CO, Tokyo, Japan) and a nanoelectrospray ion source. The mobile phase comprised H₂O with 0.1% formic acid (buffer A) and 100% acetonitrile with 0.1% formic acid (buffer B). The gradient ranged from 5 to 30% buffer B in 95 min followed by 30 to 60% B in 15 min and a step gradient to 85% B for 5 min with a flow of 0.42 μL/min, finally a return to the initial conditions of 5% B. The FTMS full scan mass spectra (from 450 to 1600 m/z) were acquired with a resolution of $r = 60\ 000$. This was followed by data-dependent MS/MS fragmentation in centroid mode of the most intense ion from the survey scan using collision-induced dissociation in the linear ion trap: normalized collision energy 35%; activation Q 0.25; electrospray voltage 1.5 kV; capillary temperature 200°C; and isolation width 2.00. Singly charged ions were excluded from the MS/MS analysis and Xcalibur software version 2.1.0 SP1 build 1160 (Thermo Fisher Scientific, U.K.) was used for data acquisition. Raw data files were processed using MaxQuant. MS/MS spectra were searched against human protein in Uniprot database. Proteins identified by in-gel digestion proteomics, carbamydomethylation on cysteine and oxidation of methionine with acetylation of protein N-terminal were considered as dynamic and static post-translational modifications, respectively.

2.2.6 Cell culture and MTT assay

Human immortalized keratinocytes (HaCaT) were from Innoprot and were cultured in 10% fetal bovine serum in Dulbecco's modified Eagle's medium, in the presence of 1% antibiotics and 2 mM L-glutamine, in a 5% CO₂ humidified atmosphere at 37°C. Cells were seeded in 96-well plates at a density of 2×10^3 /well. Approximately 24 h after seeding, increasing concentrations of the crude extract or pure PC (0.1–1 mg/mL) were added to the cells for different length of time. At the end of each experimental point, cell viability was measured by the tetrazolium salt colorimetric assay (MTT), as described by Arciello *et al.* (Arciello 2011). Cell survival was expressed as the percentage of viable cells in the presence of the specific molecule compared with control cells (represented by the average obtained between untreated cells and cells supplemented with the highest concentration of buffer). Each

sample was tested in three independent analyses, each carried out in triplicates. Determination of intracellular ROS levels. The protective effect of crude extract and of pure PC (0.1 or 0.25 mg/mL), against oxidative stress, was measured by determining the intracellular reactive oxygen species (ROS) levels. The protocol used by Del Giudice *et al.* was followed (Del Giudice 2017), with some modifications. Briefly, cells were exposed for 2 h to the molecules under test and then irradiated by UVA light for 10 min (100 J/cm²). Fluorescence intensity of the fluorescent probe (2', 7'-dichlorofluorescein, DCF) was measured at an emission wavelength of 525 nm and an excitation wavelength of 488 nm using a Perkin-Elmer LS50 spectrofluorimeter. Emission spectra were acquired at a scanning speed of 300 nm/min, with 5 slit width for both excitation and emission. ROS production was expressed as percentage of DCF fluorescence intensity of the sample under test, compared with the untreated sample. Three independent experiments were carried out, each one with three determinations.

2.2.7 Statistical analyses

In all the experiments, samples were analyzed in triplicate. The results are presented as mean \pm SD) and compared by one-way ANOVA according to the Bonferroni's method (*post hoc*) using Graphpad Prism for Windows, version 6.01.

2.3 Results

2.3.1 Effect of carbon dioxide

To establish *G. phlegrea* optimal growth conditions, different concentrations of carbon dioxide were tested: 2, 5, and 20% (v/v). As *Galdieria* is the only alga, among Cyanidiales, that can grow autotrophically as well as mixotrophically and heterotrophically, using over 27 kinds of sugars and sugar alcohols (Gross and Schnarrenberger 1995), we compared autotrophy and mixotrophy conditions overtime. Figure 1A shows algal growth in autotrophic conditions, whereas Figure 1B is referred to mixotrophic conditions. CO₂ negatively affected algal growth in both the experimental conditions analyzed, as an increase of the pH value was observed (pH 3) and a concomitant decrease in the total biomass concentration was found. Accordingly, in the absence of CO₂, a significant increase in the algal growth (up to 3.4 g/L for autotrophic growth and 6 g/L for mixotrophic growth) was observed (Figure 1C, D). Thus, during mixotrophy (Figure 1D), the reached biomass concentration is almost

two-fold higher than during autotrophy (Figure 1C), suggesting mixotrophy as the best growth condition.

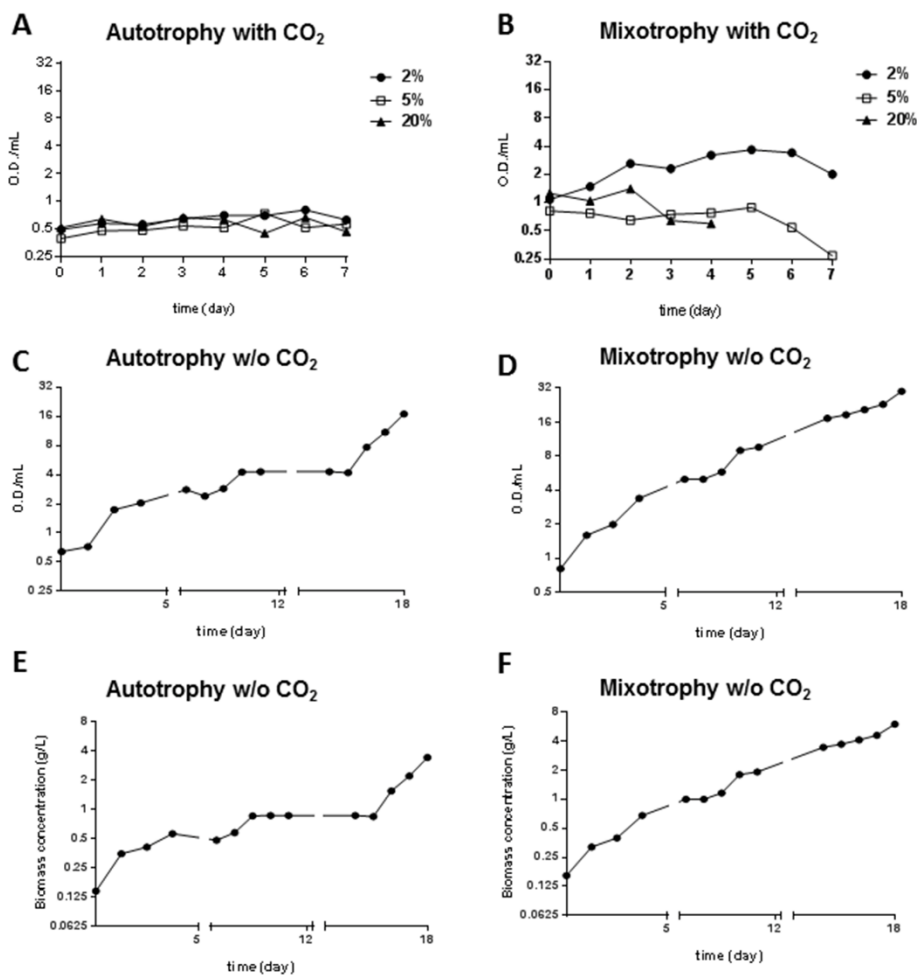


Figure 1: Growth of *Galdieria phlegrea* in photobioreactors. Cells were grown in the presence on increasing amount of CO₂, and O.D. was measured every day. Growth is expressed as a function of time. **A, C:** Cells grown in autotrophy. **B, D:** Cells grown in mixotrophy. **A, B:** Black circles, cells grown in the presence of 2%CO₂, empty circles, cells grown in the presence of 5% CO₂; black triangles, cells grown in the presence of 20% CO₂. **C, D:** *G. phlegrea* grown in the absence of CO₂, reported as biomass concentration.

2.3.2 Biorefinery process design

In the context of using microalgae in a biorefinery approach, an efficient model for the recovery and isolation of high-value products was designed. The strategy (Figure 2) was focused on the subsequent extraction of two class of molecules, phycocyanin and lipids, starting from phycocyanin, which has the highest market value.

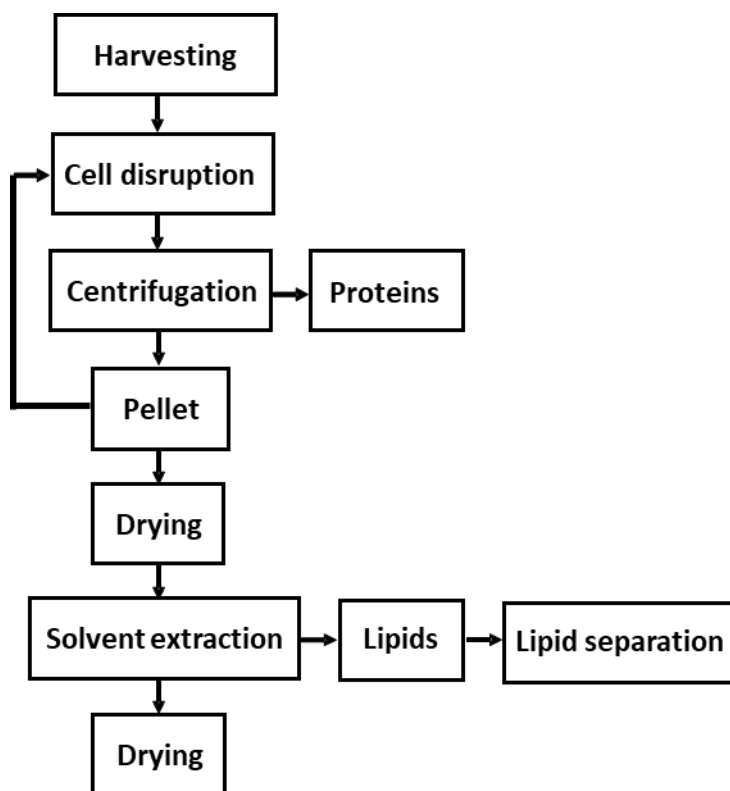


Figure 2: A schematic representation of the biorefinery strategy design.

2.3.3 Pigments extraction and purification

The harvested biomass was extracted by two cycles of French Press. Supernatants were analyzed by SDS-PAGE followed by Coomassie staining (Figure 3A) and revealed the presence of two major protein species, whose molecular weight corresponded to those of α - and β -subunits of PC. As PC is a blue colored protein, it is visible also in the absence of any coloration (Figure 3B), or after exposure to UV light (Figure 3C), taking advantage of its fluorescent nature. These results suggested that the two major protein species were PC.

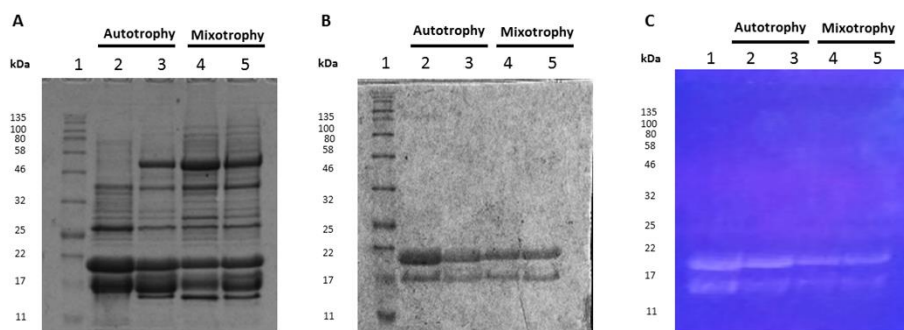


Figure 3: PC extraction from *Galdieria phlegrea* grown in autotrophic and mixotrophic conditions. SDS-PAGE analysis of samples after French Press extraction. Lane 1: molecular weight markers; lanes 2–3: soluble proteins after the 1st and 2nd cycle of extraction by French Press of biomass grown in autotrophy; lanes 4–5: soluble proteins after the 1st and 2nd cycle of extraction by French Press of biomass grown in mixotrophy. In all lanes, 30 μ g of total proteins was analyzed. **A:** SDS-PAGE stained by Blue Coomassie. **B:** Unstained gel. **C:** Gel exposed to UV light.

As shown in Table 1, total proteins and PC extracted by the French Press were very similar in both the analyzed conditions. Interestingly, even though the protein yield was not high, the ratio between PCs and total proteins was higher than 60%, with a relative purity grade of 3.

Table 1. Extraction yield of *Galdieria phlegrea* grown in autotrophic and mixotrophic conditions

	Total protein (mg)	Total PC (mg)	Protein yield (%)	PC yield (%)	PC/proteins (%)
Autotrophy	45±5	28±4	15±3	9±3	63
Mixotrophy	48±4	31±7	16±2	10±3	64

It has been reported that different purity grades indicate different applications of phycocyanin: (i) food grade if purity is ≤ 0.7 , (ii) reagent grade, when the ratio is between 0.7 and 3.9, and (iii) analytical grade if the ratio is ≥ 4.0 (Fernández-Rojas 2014). The isolation of phycocyanin was performed by a single step of purification, using a size-exclusion chromatography. SDS-PAGE analysis (Figure S1) showed the presence of few protein bands identified as phycocyanin by in situ digestion and mass spectrometry analyses, thus confirming the high purity level of the sample. Moreover, the purity grade reached was higher than 5 for autotrophy and higher than 2 for mixotrophy (Table 2). Thus, we decided to use the residual biomass from autotrophic growth to extract lipids. The PC was recovered with a rate of 179 mg/g cell mass of *G. phlegrea* through this protocol.

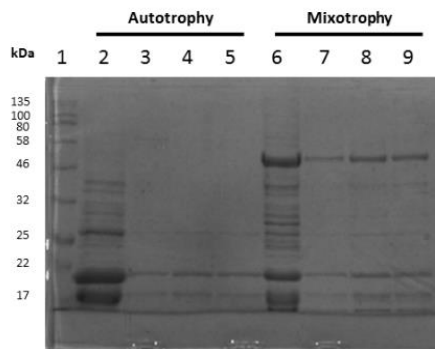


Figure S1: PC purification from *Galdieria phlegrea* extracts grown in autotrophic and mixotrophic conditions. SDS-PAGE analysis of samples after purification. Lane 1: molecular weight markers; lane 2: soluble proteins extracted by French Press grown in autotrophy (30 μg); lanes 3-5: samples eluted by the size-exclusion chromatography (5 μg); lane 6: soluble proteins extracted by French Press grown in mixotrophy (30 μg). Lanes 7-9: samples eluted by the size-exclusion chromatography (5 μg).

Table 2. Concentration and purity grade of PC after purification.

	PC concentration (mg/mL)	Purity grade (Abs₆₂₀ / Abs₂₇₈)
Autotrophy		
Crude extract	1.9±0.1	3
Fraction 2	0.119±0.003	5.02
Fraction 3	0.224±0.04	5.28
Fraction 4	0.216±0.09	5.01
Mixotrophy		
Crude extract	1.7±0.8	1.9
Fraction 2	0.126±0.03	2.8
Fraction 3	0.243±0.02	2.97
Fraction 4	0.272±0.08	2.76

2.3.4 Lipid extraction and purification

According to the circular economy strategy, we extracted lipids as the second class of molecules. The lipid extraction was performed on residual algal biomass after a drying step. In order to verify if lipids extraction could be affected by the previous French Press extraction, in a parallel experiment, lipids were extracted also from the raw dried biomass. As shown in Table 3, the yield of total lipids was 79% for the raw biomass and 21% for the disrupted biomass. The isolation of three different lipid classes was carried out by performing a solid phase extraction (SPE), and results are reported in Table 3. Then, a gas chromatography analysis was performed and the results are reported in Table 4. It is interesting to notice that polyunsaturated, monounsaturated, and saturated fatty acids were present, but a significant increase in PUFAs content was observed in the disrupted biomass, in comparison with the raw one, as reported in Figure 4. In particular, in the raw material, oleic (MUFA) and linoleic (PUFA) acids (3.72 and 2.00%, respectively) were mainly present, whereas, in the disrupted biomass, ω -3 eicosapentaenoic acid (EPA, 6.81%), the two ω -6 linoleic (LA, 9.61%) and arachidonic acids (AA, 9.00%), and the monounsaturated oleic acid (OA, 4.00%) were present, along with lower percentages of α -linoleic (ALA), γ -linoleic (GLA), dihomo- γ -linoleic (DGLA), and palmitoleic (POA) acids. As for the saturated fatty acids, about 90% were present in the raw material and only 60% in the disrupted biomass, with palmitic and stearic acids as the main species, in the ratio of 3 to 1 in both materials.

Table 3. Yields of total lipids. Mean yields are expressed as the percentage of the ratio between each algal compound and dried biomass.

	Lipid yield (%)	Neutral lipids (%)	Fatty acids (%)	Phospholipids (%)
Before French press	79±26	68±23	16±2	56±28
Post French press	21±3	33±2	17±1	41±3

Table 4. Gas chromatography analysis on samples before and after French Press. Polyunsaturated, monounsaturated and saturated fatty acids are reported as relative percentages.

PUFA		Before French press (%)	Post French press (%)
FATTY ACIDS			
18:3 (n-3)	α -Linoleic acid (ALA)	-	1.31 \pm 0.30
20:5 (n-3)	Eicosapentanoic acid (EPA)	-	6.81 \pm 1.50
22:5 (n-3)	Docosapentanoic-n3 acid (DPA)	0.17 \pm 0.04	0.41 \pm 0.10
18:2 (n-6)	Linoleic acid (LA)	2.00 \pm 0.24	9.61 \pm 1.11
18:3 (n-6)	γ -Linoleic acid (GLA)	-	3.30 \pm 0.40
20:3 (n-6)	Dihomo- γ -linoleic acid (DGLA)	0.23 \pm 0.05	2.40 \pm 10
20:4 (n-6)	Arachidonic acid (AA)	0.16 \pm 0.01	9.00 \pm 0.30
22:4 (n-6)	Docosatetraenoic acid (DTA)	-	0.20 \pm 0.01
MUFA			
16:1	Palmitoleic acid (POA)	0.42 \pm 0.01	1.20 \pm 0.20
18:1	Oleic acid (OA)	3.72 \pm 0.80	4.00 \pm 0.70
SFA			
16:0	Palmitic acid (PA)	69.0 \pm 3.3	45.1 \pm 3.0
18:0	Stearic acid (SA)	22.0 \pm 2.1	13.0 \pm 1.5

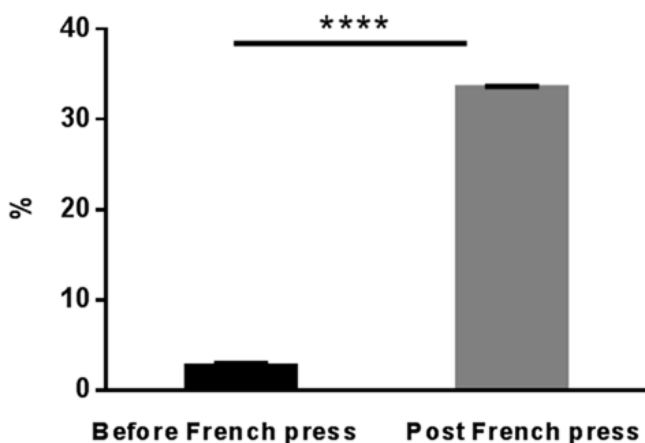


Figure 4: Percentage of total polyunsaturated fatty acids. The black bar refers to PUFA extracted from the raw biomass and the grey bar to PUFA extracted from the residual biomass after PC extraction. **** $p < 0.00005$ between the samples.

2.3.5. Phycocyanin characterization

It is known that PC is endowed with many biological functions, among which the antioxidant activity. In order to verify that the extraction procedures did not affect PC biological activity, we analyzed its ability as an antioxidant agent. First, we analyzed its biocompatibility on immortalized human keratinocytes (HaCaT). Thus, cells were incubated in the presence of increasing amount of PC (from 0.1 to 1 mg/mL) for different length of time (24–72 h). In a parallel experiment, the crude extract was analyzed as it is widely used to produce functional food or food additives (Chentir 2018). At the end of each incubation, cell viability was assessed by the MTT assay, and cell survival was expressed as the percentage of viable cells in the presence of PC or of the crude extract compared with that of untreated cells. Interestingly, no cytotoxic effect was observed when cells were incubated with pure phycocyanin (Figure 5A) under all the experimental conditions analyzed. On the other hand, when cells were incubated with the crude extract, a 50% reduction in cell viability was observed at the highest concentration after 72 h of incubation (Figure 5B). Once established the complete biocompatibility of purified PC, the protective effect on UVA-stressed HaCaT cells was evaluated. Keratinocytes were chosen as antioxidants should be able to protect the skin from UV-induced oxidative stress, as they are normally present in the outermost layer of

the skin. As a source of stress, we used a UVA lamp, commonly used in the nail products industry. Cells were treated with 0.1 mg/mL and 0.25 mg/mL of PC or the crude extract for 2 h, and then oxidative stress was induced by UVA irradiation (100 J/cm²) for 10min. At the end of the irradiation, H₂-DCFDA was added to measure intracellular ROS level. As shown in Figure 5C, UVA induced a significant increase in intracellular ROS levels (200%) with respect to untreated cells. Interestingly, cells treated with 0.25 mg/mL of the crude extract showed an increase of intracellular ROS levels in the absence of any treatment, and no protection after UVA treatment, thus suggesting that the crude extract acts as a source of stress per se. Noteworthy, cells treated with 0.25 mg/mL of pure phycocyanin did not show any alteration in ROS level (Figure 5D), and a significant protection against UVA-induced oxidative stress was observed when cells were treated with either 0.1 or 0.25 mg/mL of the purified PC.

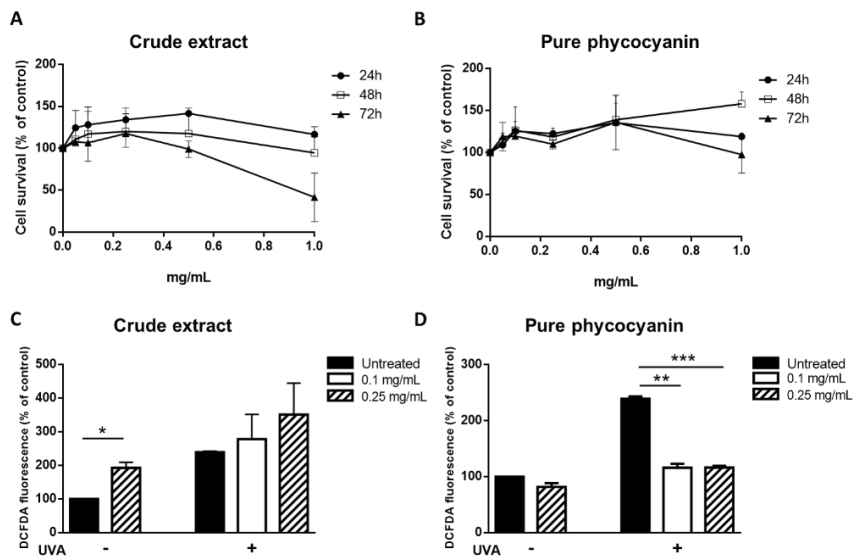


Figure 5. Effect of crude extract and pure phycocyanin on HaCaT cells. A, B: Dose-response curves of HaCaT cells after 24 h, 48 h and 72 h incubation with increasing concentrations of crude extract (A) or pure PC (B) (0.1-1 mg/mL). Cell viability was assessed by the MTT assay and reported as a function of extract concentration. Data shown are means \pm S.D. of three independent experiment. **C, D:** Cells were pre-incubated in the presence of 0.1 mg/mL and 0.25 mg/mL crude extract (C) or pure PC (D) for 2 h and then irradiated by UVA (100 J/cm²). Intracellular ROS levels were evaluated by DCFDA assay. Values are expressed as fold increase with respect to control (i.e. untreated) cells. Data shown are means \pm S.D. of three independent experiment. ** indicates $p < 0.005$, *** indicates $p < 0.0005$ with respect to UVA treated cells.

2.4 Discussion

In this study, we have shown a feasible design to obtain different high-value molecules starting from the wet biomass of *Galdieria phlegrea*. We first extracted proteins and phycocyanin, with a ratio between total phycocyanin and total proteins higher than 60%. This ratio is much higher than that previously reported by Carfagna and colleagues, who found that PC content was about 10% (Carfagna 2018). Moreover, the purity grade of PC in the raw extract was already 3, and became higher than 5 at the end of the single purification step. To the best of our knowledge, this is the first report on the purification of PC from *G. phlegrea* by a single step procedure and with such a high purity grade (Sonani 2016). It must be stressed out that the proposed procedure to isolate PC from *G. phlegrea* is an economical process, as it is obtained from wet biomass, in aqueous buffer and by using a size exclusion chromatography, which could be easily substituted by ultrafiltration in a scaling-up process. Thus, our procedure is economically sustainable and much “greener” than others, which usually use dried biomass or detergents and at least two purification steps (Sonani 2016). Moreover, PC isolated by this procedure is active as antioxidant molecule when tested on a cell-based model. UV radiations were used to test the antioxidant potential of the purified PC. Indeed, it is well known that UV radiations are considered one of the most harmful exogenous factors for the human skin, as, in addition to the development of erythema, ROS are produced. Particularly, in the last few years, UVA radiations have been used in the nail industry more and more often. A recent paper reported that two healthy women, middle-aged, with no personal or family history of skin cancer, developed squamous cell carcinoma on the dorsum of their hands. Both women reported previous exposure to UVA radiation for cosmetic nail treatment (Diffey 2012). This has prompted some concerns about the safety of this procedure (Diffey 2012). Interestingly, PC was able to counteract the negative effects induced by UVA radiation. PC antioxidant activity at 0.1 mg/ mL is in agreement with that one reported in vivo by Sonani and coworkers (Sonani 2017) who purified PC from *Synechococcus*, but with a lower purity grade, 4. Even though PC is widely considered as an antioxidant protein, nothing is reported in literature on its activity on stressed eukaryotic cells, but its activity is rather demonstrated only by in vitro assays, with some concerns from the scientific community (Charalampopoulos 2018). Moreover, starting from the residual biomass, we isolated polyunsaturated fatty acids. Interestingly, we found that the amount of isolated PUFAs from the

broken biomass (34%) was higher than that obtained from the raw biomass (2.5%), suggesting that the biorefinery procedure here described could be a good alternative to obtain PUFAs without using fish oil (about 25% PUFAs) (Miyaguti 2018). Among the several advantages of using PUFAs from microalgae, there is the absence of fishy taste, fishy smell, no risk of carcinogens accumulation, and the possibility to use “vegetarian,” “vegan,” or “organic” labels. Moreover, the world demand of PUFAs is increasing, as it is used for infants, nutritional supplements, and pharmaceuticals (Deschamps 2016). To date, microalgae are considered significant sources of PUFAs, as up to 30–70% of lipids in their cell dry weight is found (Breuer 2013; Chisti 2007; Sun 2018). It is well established that several factors can influence lipid accumulation, such as nitrogen and phosphorus starvation, pH, temperature, and light intensity (Hindersin 2014), leading to a 20% increase (Ramesh Kumar 2019). However, stress conditions imply extremely controlled systems and the possibility to obtain only lipids. In addition, stress conditions enhance the accumulation of intracellular triacylglycerol lipids which contain lower amount of PUFAs with respect to polar lipids, mainly located on the cell membrane (Breuer 2013). By using our procedure, PC and lipids can be easily and economically obtained in a cascade approach.

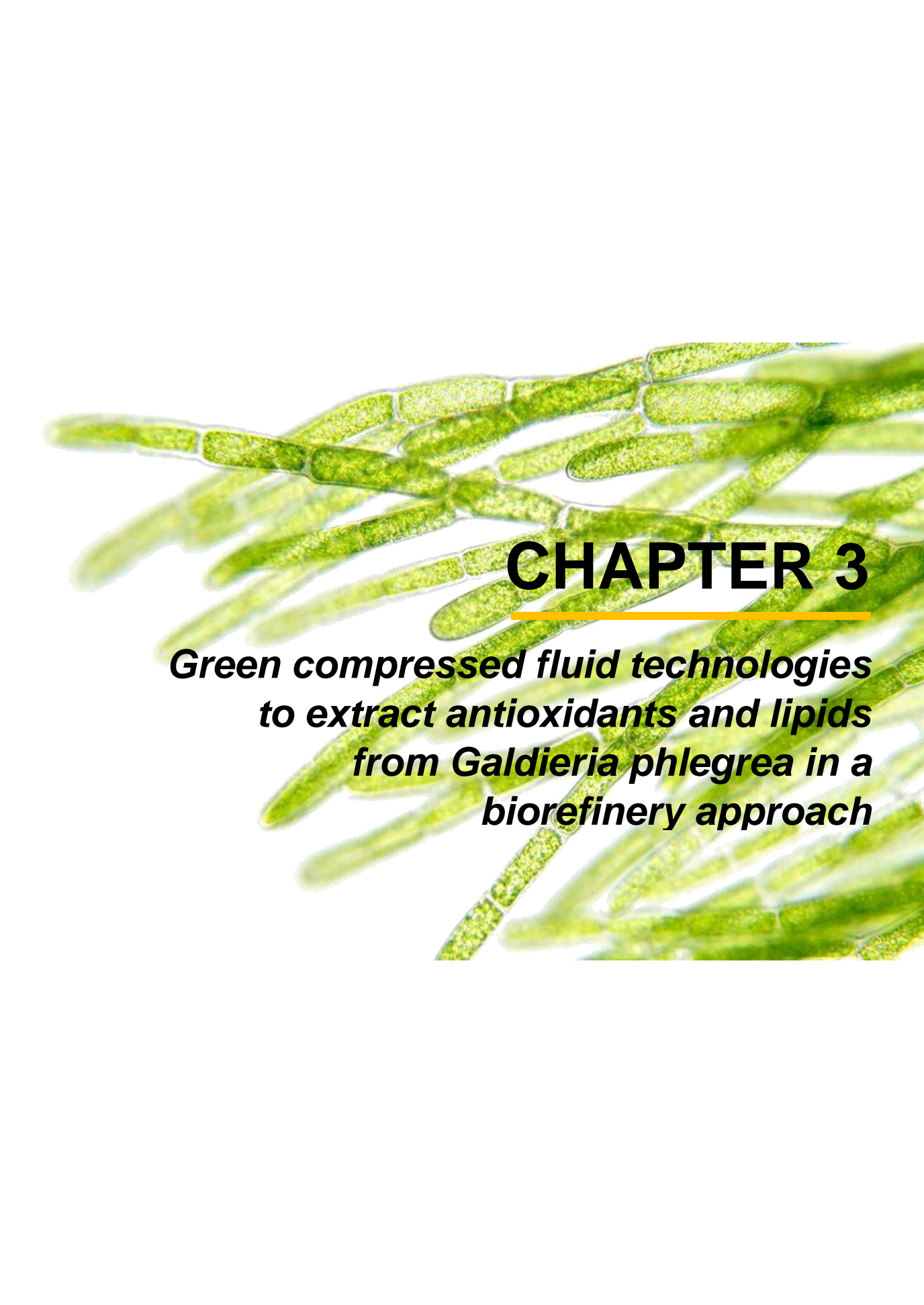
2.5 References

- Allen MM. (1968) Simple conditions for growth of unicellular blue-green algae on plates. *Journal of Phycology* 4:1–4.
- Ankush Nikam, 2019. Phycocyanin market growing at a value CAGR of 7.6% throughout the period of forecast 2018 – 2028 | *Daily chronicle*. March 7. URL <https://www.dailychronicle24.com/2019/03/07/ phycocyanin-market-growing-at-a-value-cagr-of-7-6-throughoutthe- period-of-forecast-2018-2028>.
- Arciello A, De Marco N, Del Giudice R, Guglielmi F, Pucci P, Relini A, Monti DM, Piccoli R (2011) Insights into the fate of the N-terminal amyloidogenic polypeptide of ApoA-I in cultured target cells. *Journal of Cellular and Molecular Medicine* 15:2652–2663.
- Bennett A., Bogorad L., 1973. Complementary chromatic adaptation in a filamentous blue-green alga. *The Journal of Cell Biology*. 58(2), 419-435.
- Bergé, J. P., & Barnathan, G. "Fatty acids from lipids of marine organisms: molecular biodiversity, roles as biomarkers, biologically active compounds, and economical aspects." *Marine biotechnology* 1. Springer, Berlin, Heidelberg, 2005. 49-125.

- Breuer, G., Evers, W. A., de Vree, J. H., Kleinegris, D. M., Martens, D. E., Wijffels, R. H., & Lamers, P. P. (2013). Analysis of fatty acid content and composition in microalgae. *Journal of Visualized Experiment*, 80: e50628.
- Carfagna S, Napolitano G, Barone D, Pinto G, Pollio A, Venditti P (2015) Dietary supplementation with the microalga *Galdieria sulphuraria* (Rhodophyta) reduces prolonged exercise-induced oxidative stress in rat tissues. *Oxidative Medicine and Cellular Longevity*. 2015:1–11.
- Carfagna S, Landi V, Coraggio F, Salbitani G, Vona V, Pinto G, Pollio A, Ciniglia C (2018) Different characteristics of C-phycocyanin (C-PC) in two strains of the extremophilic *Galdieria phlegrea*. *Algal Research* 31:406–412.
- Charalampopoulos D, Ismail AB, Birch GG, Elmore S, Alasalvar C, Shahidi F, Kilmartin P, Pegg R, Finglas P, Wrolstad R, Astley SB, van Camp J, Melton LD, Granato D, Zhou P, Miyashita K, Hidalgo FJ (2018) Antioxidant activity total phenolics and flavonoids contents: should we ban in vitro screening methods. *Food Chemistry* 264:471–475.
- Chauton MS, Reitan KI, Norsker NH, Tveterås R, Kleivdal HT (2015) A techno-economic analysis of industrial production of marine microalgae as a source of EPA and DHA-rich raw material for aquafeed: research challenges and possibilities. *Aquaculture* 436: 95–103.
- Chentir I, Hamdi M, Li S, Doumandji A, Markou G, Nasri M (2018) Stability, bio-functionality and bioactivity of crude phycocyanin from a two-phase cultured Saharian *Arthrospira* sp. strain. *Algal Research* 35:395–406.
- Chisti Y. (2007) Biodiesel from microalgae. *Biotechnology Advances* 25:294–306.
- Cuellar-Bermudez SP, Aguilar-Hernandez I, Cardenas-Chavez DL, Ornelas-Soto N, Romero-Ogawa MA, Parra-Saldivar R. (2015) Extraction and purification of high-value metabolites from microalgae: essential lipids, astaxanthin and phycobiliproteins. *Microbial Biotechnology* 8:190–209.
- Del Giudice, R., Petruk, G., Raiola, A., Barone, A., Monti, D.M., Rigano, M.M., 2017. Carotenoids in fresh and processed tomato (*Solanum lycopersicum*) fruits protect cells from oxidative stress injury. *Journal of the Science of Food Agriculture* 97(5), 1616-1623.
- Deschamps, N., 2016. Nutritional supplements in the U.S., 7th Edition. URL <https://www.prnewswire.com/news-releases/nutritionalsupplements-in-the-us-7th-edition-300469500.html>
- Diffey, B.L. (2012) The risk of squamous cell carcinoma in women from exposure to UVA lamps used in cosmetic nail treatment. *British Journal of Dermatology* 167:1175–1178.
- Fernández-Rojas B, Hernández-Juárez J, Pedraza-Chaverri J (2014) Nutraceutical properties of phycocyanin. *Journal of Functional Foods*. 11, 375-392.

- González-Delgado Á-D, Kafarov V (2011) Microalgae based biorefineries: issues to consider. *Ciencia, Tecnología y Futuro* 4:5–22.
- Gross W, Schnarrenberger C (1995) Heterotrophic growth of two strains of the acidothermophilic red alga *Galdieria sulphuraria*. *Plant Cell Physiol.*36:633–638
- Hindersin S, Leupold M, Kerner M, Hanelt D (2014) Key parameters for outdoor biomass production of *Scenedesmus obliquus* in solar tracked photobioreactors. *Journal of Applied Phycology* 26:2315–2325.
- Leu S, Boussiba S (2014) Advances in the production of high-value products by microalgae. *Industrial Biotechnology* 10:169–183.
- Manirafasha, E., Ndikubwimana, T., Zeng, X., Lu, Y., Jing, K., 2016. Phycobiliprotein: potential microalgae derived pharmaceutical and biological reagent. *Biochemical Engineering Journal* 109, 282-296.
- Mehta P, Singh D, Saxena R, Rani R, Gupta RP, Puri SK, Mathur AS (2018) High value coproducts from algae: an innovational way to deal with advance algal industry. *Waste to Wealth*: 343–363.
- da Silva Miyaguti, N. A., de Oliveira, S. C. P., & Gomes-Marcondes, M. C. C. (2018). Maternal nutritional supplementation with fish oil and/or leucine improves hepatic function and antioxidant defenses, and minimizes cachexia indexes in Walker-256 tumor-bearing rats offspring. *Nutrition Research*, 51, 29-39.
- Moody JW, McGinty CM, Quinn JC (2014) Global evaluation of biofuel potential from microalgae. *Proceedings of the National Academy of Sciences* 111:8691–8696.
- Patel HM, Rastogi RP, Trivedi U, Madamwar D (2018) Structural characterization and antioxidant potential of phycocyanin from the cyanobacterium *Geitlerinema* sp. H8DM. *Algal Research* 32:372–383.
- Patel A, Matsakas L, Hrůzová K, Rova U, Christakopoulos P (2019) Biosynthesis of nutraceutical fatty acids by the oleaginous marine microalgae *Phaeodactylum tricorutum* utilizing hydrolysates from organosolv-pretreated birch and spruce biomass. *Marine Drugs* 17:119.
- Posada JA, Brentner LB, Ramirez A, Patel MK (2016) Conceptual design of sustainable integrated microalgae biorefineries: parametric analysis of energy use, greenhouse gas emissions and techno-economics. *Algal Research* 17:113–131.
- Quinn JC, Davis R (2015) The potentials and challenges of algae based biofuels: a review of the techno-economic, life cycle, and resource assessment modeling. *Bioresource Technology* 184:444–452.

- Ramesh Kumar B, Deviram G, Mathimani T, Duc PA, Pugazhendhi A (2019) Microalgae as rich source of polyunsaturated fatty acids. *Biocatalysis and agricultural biotechnology*. 17:583–588.
- Romay C, González R, Ledón N, Ramirez D, Rimbau V (2003) C-phycocyanin: a biliprotein with antioxidant, anti-inflammatory and neuroprotective effects. *Current Protein and Peptide Science* 4:207–216.
- Ruiz J, Olivieri G, de Vree J, Bosma R, Willems P, Reith JH, Eppink MHM, Kleinegris DMM, Wijffels RH, Barbosa MJ (2016) Towards industrial products from microalgae. *Energy & Environmental Science*. 9:3036–3043.
- Sakurai T, Aoki M, Ju X, Ueda T, Nakamura Y, Fujiwara S, Umemura T, Tsuzuki M, Minoda A (2016) Profiling of lipid and glycogen accumulations under different growth conditions in the sulfotolerant red alga *Galdieria sulphuraria*. *Bioresour. Technol.* 200:861–866.
- Sonani RR (2016) Recent advances in production, purification and applications of phycobiliproteins. *World Journal of Biological Chemistry* 7:100.
- Sonani RR, Patel S, Bhastana B, Jakharia K, Chaubey MG, Singh NK, Madamwar D (2017) Purification and antioxidant activity of phycocyanin from *Synechococcus* sp. R42DM isolated from industrially polluted site. *Bioresour. Technol.* 245:325–331
- Spolaore P, Joannis-Cassan C, Duran E, Isambert A (2006) Commercial applications of microalgae. *Journal of Bioscience and Bioengineering* 101:87–96.
- Sun XM, Geng LJ, Ren LJ, Ji XJ, Hao N, Chen KQ, Huang H (2018) Influence of oxygen on the biosynthesis of polyunsaturated fatty acids in microalgae. *Bioresour. Technol.* 250, 868-876.
- Tredici MR, Rodolfi L, Biondi N, Bassi N, Sampietro G (2016) Techno-economic analysis of microalgal biomass production in a 1-ha Green Wall Panel (GWP®) plant. *Algal Research* 19:253–263.
- Wu HL, Wang GH, Xiang WZ, Li T, He H (2016) Stability and antioxidant activity of food-grade phycocyanin isolated from *Spirulina platensis*. *International Journal of Food Properties* 19:2349–2362.
- Zárate R, el Jaber-Vazdekis N, Tejera N, Pérez JA, Rodríguez C (2017) Significance of long chain polyunsaturated fatty acids in human health. *Clinical and Translational Medicine* 6(1), 25.

A microscopic image of Galdieria phlegrea, a green microalga. The image shows several long, cylindrical, multi-celled filaments. Each cell is roughly rectangular and contains a granular, greenish-yellow interior, likely representing chloroplasts and other organelles. The cells are arranged in parallel chains, with some filaments overlapping others. The background is white, making the green filaments stand out.

CHAPTER 3

***Green compressed fluid technologies
to extract antioxidants and lipids
from Galdieria phlegrea in a
biorefinery approach***

Green compressed fluid technologies to extract antioxidants and lipids from *Galdieria phlegrea* in a biorefinery approach

Paola Imbimbo^a, Monica Bueno^b, Luigi D'Elia^a, Antonino Pollio^c, Elena Ibañez^b, Giuseppe Olivieri^{d,e*}, Daria Maria Monti^{a*}

^a Department of Chemical Sciences, University of Naples Federico II, via Cinthia 4, 80126, Naples, Italy

^b Laboratory of Foodomics, Institute of Food Science Research, CIAL, CSIC, Nicolás Cabrera 9, 28049 Madrid, Spain

^c Department of Biology, University of Naples Federico II, via Cinthia 4, 80126, Naples, Italy

^d Bioprocess Engineering Group, Wageningen University and Research, Droevendaalsesteeg 1, 6700AA, Wageningen, the Netherlands

^e Department of Chemical, Materials and Industrial Engineering, University of Naples Federico II, Piazzale Tecchio 80, 80125, Napoli, Italy

Abstract

A green approach was used to recover, in a cascade approach, phycocyanins, carotenoids and lipids from *Galdieria phlegrea*. Phycocyanin extraction was performed by high-pressure homogenization and purified by ultrafiltration, whereas carotenoids were obtained by a pressurized liquid extraction and lipids by supercritical fluid extraction. The second step of this innovative, green and cost-effective procedure is able to improve the recovery of zeaxanthin and β -carotene up to 40%, without affecting the quality of compounds and avoiding the use of organic solvents and the drying processes. The isolated carotenoids were active as antioxidants, as clearly shown by their protective activity on a cell-based model. Lipid yield was increased by 12% with respect to traditional methods.

3.1 Introduction

Microalgae are a continuous and reliable source of safe natural and high value products, such as soluble proteins, polyunsaturated fatty acids (PUFA) and pigments. Phycocyanins (PCs) are blue colored, highly fluorescent and water-soluble proteins, synthesized in cyanobacteria and red algae. PCs, as the other phycobiliproteins, are antenna pigments able to improve the photosynthetic efficiency of microalgae. Because of their brilliant color, PCs are commonly used in cosmetic and food industry (Santiago-Santos, Ponce-Noyola, Olvera-Ramírez, Ortega-López, & Cañizares-Villanueva 2004). They are also endowed with therapeutic properties such as antioxidant, anti-inflammatory, hepato-protective and antitumoral activity (Basha 2008).

Among pigments, carotenoids function as accessory pigments in light-harvesting photosystem during photosynthesis (Jin & Melis 2003) and they are also important for their antioxidant function, as they deactivate free radicals, thus preventing cell damages. In the last decades, carotenoids have attracted great interest for their beneficial effect on human health. The demand of carotenoids is rapidly growing: the global carotenoid market was estimated to be ~1.24 billion USD in 2016, and is projected to increase to ~1.53 billion USD by 2021, at a compound annual growth rate (CAGR) of 3.78% from 2016 to 2021 (Sathasivam & Ki 2018). To date, commercially available carotenoids are generally synthetic, since they are more stable than natural ones. However, the emulsified preparations of synthetic carotenoids show high toxicity, carcinogenicity, and teratogenicity properties, thus generating criticism among health-conscious consumers (Nagarajan, Ramanan, Raghunandan, Galanakis, & Krishnamurthy 2017). Being microalgae good producers of many pigments, the extraction of carotenoids from these microorganisms would be very competitive in the market and would have a huge economic impact (Ambati 2019). Microalgae can accumulate also significant amount of lipids (from 1 to 70%) (Spolaore, Joannis-Cassan, Duran, & Isambert 2006), depending on the strain and the culture conditions (Pruvost, Van Vooren, Le Gouic, Couzinet-Mossion, & Legrand 2011).

Lipids can be employed as feedstock for nutraceutical, pharmaceutical, foods and biofuel industries. To date, bioenergy market has the lowest value. This is due to the fact that biogas, bioethanol and biodiesel have a selling price of 0.2 €/m³, 0.4 €/Kg, 0.5 €/L respectively, a price that still exceeds their high downstream process costs (20.5 €/m³, 33.34 €/kg, 25.56 g €/L respectively) (Barsanti & Gualtieri 2018). Thus, an improvement in efficient, cost-

effective and green extraction techniques to produce high-quality compounds is needed. In this context, microalgae are an excellent source of molecules endowed with biological activity. Noteworthy, the design of a suitable integrated biorefinery platform able to efficiently extract target compounds in a cascade approach, and in accordance with the green chemistry principles, is still a challenge. Among all the innovative techniques, compressed fluid extractions are considered the most competitive ones, since they may fulfill these criteria (Gallego, Bueno, & Herrero 2019).

In this context, pressurized liquid extraction (PLE) and supercritical fluid extraction (SFE) are the most widely employed as they are based on the use of the same system, so they would represent a process intensification. PLE and SFE are innovative techniques that use liquid solvents at elevated temperature and pressure to extract molecules. Moreover, the extraction performance are enhanced as compared to those techniques carried out at near room temperature and atmospheric pressure (Camel 2001; Gallego & Bueno 2019; Mubarak, Shaija, & Suchithra 2015).

In the present work, we set up a cascade approach to recover high value bioproducts from *Galdieria phlegrea*, a unicellular thermo-acidophilic red alga. The experimental strategy is reported in Figure 1. Starting from the previously established technique used to disrupt cells and extract PCs (Imbimbo 2019), an optimization of the isolation of PC was carried out. Then, the residual wet biomass was used to extract two different bioproducts in two sequential steps: carotenoids by using Pressurized Liquid Extraction (PLE) and finally lipids by Supercritical Fluid Extraction (SFE). The bioactivity of the extracted carotenoids obtained by PLE was validated on a cell-based model, using human immortalized keratinocytes, and compared to the bioactivity of the commercial molecules.

3.2 Material and methods

3.2.1 Reagents

HPLC-grade acetone and methanol were from VWR (Barcelona, Spain). Antibodies were from Cell Signal Technology (Danvers, MA, USA). All the other reagents and standards were from Sigma-Aldrich (Madrid, Spain).

3.2.2 Microalgal strain and culture conditions

Galdieria phlegrea (strain 009) was provided from the Algal Collection of the University Federico II (ACUF, <http://www.acuf.net>).

Cells were grown in autotrophic conditions in photobioreactors, as described in Imbimbo et al. (Imbimbo 2019)

3.2.3 Phycocyanin extraction and purification

After harvesting the biomass by centrifugation at 1200 *g* for 30 min at room temperature, cells were suspended in 50 mM sodium acetate pH 5.5 (Wu, Wang, Xiang, Li, & He 2016). Cell disruption was performed by high-pressure (French Press). Two consecutive cycles, each at 2 kbar, were performed to disrupt the biomass. Cell lysate was obtained by centrifugation at 5000 *g* at 4°C for 30 min and proteins were recovered in the supernatant, whereas the residual biomass was used for further extractions. To purify PC, two single step purification techniques were used in parallel: gel-filtration and ultrafiltration.

The size-exclusion chromatography was performed by using a Sephadex G-75 fine equilibrated in 50 mM sodium acetate pH 5.5. The ultrafiltration was performed by using 100 kDa molecular weight cut off membranes and the process was performed at room temperature. At the end of the purification, the permeate was discarded and the retentate collected. The grade of purity of phycocyanin was calculated by measuring the ratio $A_{620\text{nm}}/A_{280\text{nm}}$.

3.2.4 Storage of biomass

The residual wet biomass, after protein extraction, was stored at – 80°C. To avoid that the storage conditions would affect the results, extraction of carotenoids was performed after 72h.

3.2.5 Conventional carotenoids extraction

Carotenoids were extracted using the method of Reyes et al. (José, Reyes, Mendiola, & Iba 2014). Briefly, 200 mg of lyophilized biomass was mixed with 20 mL HPLC-grade acetone containing 0.1% (w/v) butylate hydroxytoluene (BHT) and the mixture was shaken for 24 h in a thermostatic shaker at 500 rpm and 20°C. Then, the sample was centrifuged at 4°C for 10 min at 5000 *g*. The supernatant was collected and the solvent removed under N₂ stream. The extracts were weighted and stored in the dark at -20°C.

3.2.6 Conventional lipid extraction

Total lipid extraction was performed according to the Axelsson and Gentili method (Axelsson & Gentili 2014). 25 mg of freeze-dried microalgae biomass were mixed with 8 mL of chloroform/methanol 2:1

(v/v). Then, 2 mL of NaCl 0.73% (w/v) were added and mixed again. The sample was centrifuge at 350 *g* for 5 min at room temperature, allowing the separation of the two phases. The lower layer was removed and collected. The solvent was removed under N₂ stream. The extracts were weighted and stored in the dark at -20°C.

3.2.7 Compressed Fluid Extraction processes

All high pressure extractions were performed in a homemade compressed fluid extractor coupled to a PU-2080 HPLC pump from Jasco (Tokyo, Japan). This equipment can be employed to carry out both PLE and SFE. To this purpose, 2 g of wet algal biomass (the equivalent of 200 mg of dried biomass) were mixed with silica gel of 150 Å (*S150*) pore size with particle size of 200-425 mesh. The required amount of this silica gel was added as adsorbent till obtain a static paste (José 2014). Silica prevents the paste draining in the equipment pipeline when loading in the extraction cell and improves the solute recovery (Reyes, Mendiola, Suárez-Alvarez, Ibañez, & Del Valle 2016). The mixture was added into a stainless-steel extraction cell sandwiched between glass wool to prevent clogging problems. Extraction were carried out in triplicate in two sequential steps, decreasing the polarity of the solvents, in order to exhaust the microalgae biomass relevant extractable compounds. Pressurized liquid extraction was performed at static extraction mode at 100 bar, 50°C for 30 min using pure ethanol as solvent. The extracts were collected in glass vials, dried under N₂ stream and then weighted and stored at -20°C in the dark. Subsequently, the residue of the previous extraction was used as raw material for the next step. Supercritical fluid extraction was carried out in the same apparatus, using CO₂ as solvent. The extraction was performed at 350 bar, 60°C for 100 min. CO₂ flow rate was set up at 5 mL/min. Pressure was controlled by using a back pressure regulator. The extracts were collected in glass vials, dried under N₂ stream and then weighted and stored at -20°C in the dark. A schematic representation of the used apparatus is reported in figure S1.

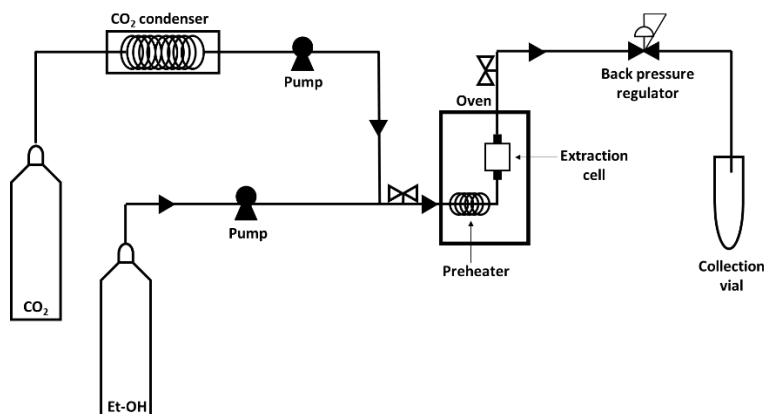


Figure S1: Compressed Fluid Extraction apparatus. The oven is equipped with a preheater and an extraction cell. Two pumps are connected to the extraction cell and a back pressure regulator connects the oven to the collection vial.

3.2.8 Total carotenoid determination

The total carotenoid content was determined spectrophotometrically as described by Gilbert-López *et al.* (Gilbert-López 2015). The lipophilic extracts were dissolved in pure methanol in a concentration ranging from 0.05 to 5 mg/mL. A standard calibration curve of β -carotene (from 5 to 200 $\mu\text{g/mL}$) was used to calculate the concentration of total carotenoids. The absorbance of samples was recorded at 470 nm. Total carotenoids content was expressed as the ration of mg of carotenoids and g of extract. Carotenoid yield was expressed as mg of carotenoids extracted per g of dry biomass. Analyses was carried out in triplicate.

3.2.9 Carotenoids characterization by HPLC-DAD-MS

Carotenoids were characterized by HPLC-DAD using the method described by Castro-Puyana *et al.* (Castro-Puyana 2013), with some modifications. HPLC analyses were performed using an Agilent 1100 series liquid chromatograph (Santa Clara, CA, USA) equipped with a diode-array detector, and using a YMC-C30 reversed-phase column (250 mm \times 4.6 mm inner diameter, 5 μm particle size; YMC Europe, Schermbeck, Germany) and a pre-column YMC-C30 (10 mm \times 4 mm i.d., 5 μm). The mobile phase was a mixture of methanol–MTBE–water (90:7:3, v/v/v) (solvent A) and methanol–MTBE (10:90, v/v) (solvent B). Carotenoids were eluted according to the following gradient: 0 min, 0% B; 20 min, 30% B; 35 min, 50% B; 45 min, 80% B;

50 min, 100% B; 60 min, 100% B; 62 min, 0% B. The flow rate was 0.8 mL/min while the injection volume was 10 μ L. The detection was performed at 280, 450 and 660 nm, although spectra from 240 to 770 nm were recorded using the DAD (peak width >0.1 min (2 s) and slit 4 nm). The instrument was controlled by LC Chem Station 3D Software Rev. B.04.03 from Agilent. Extracts were dissolved in pure methanol in a concentration ranging from 1 to 10 mg/mL to 10 and filtered through 0.45 μ m nylon filters before HPLC analysis. Each dilution was injected in triplicate. For calibration plots, different concentrations of zeaxanthin (from 3.9 to 62.5 μ g/mL) and of β -carotene (from 31.3 to 1000 μ g/mL) were analyzed in duplicate as described in Gallego (Gallego & Martínez 2019). The same instrument was directly coupled at the exit of the DAD to an Agilent ion trap 6320 mass spectrometer (Agilent Technologies) via an atmospheric pressure chemical ionization (APCI) interface. Analyses were conducted under positive ionization mode using the parameters described elsewhere (Gallego & Bueno 2019). This time extracts were dissolved in pure methanol in concentrations between 10 and 20 mg/mL and injected in duplicate. Automatic tandem mass spectrometry (MS/MS) analyses were also performed, fragmenting the two highest precursor ions.

3.2.10 ABTS assay

The antioxidant activity of the lipophilic extract was evaluated by ABTS assay (2,2'-Azinobis-[3-ethylbenzthiazoline-6-sulfonic acid]). The colorimetric assay is based on the reduction of the ABTS⁺ radical by the antioxidant molecules present in the sample. The radical is produced by the reaction of a 7 mM ABTS solution mixed with 2.45 mM of potassium persulfate conducted for 16 h at room temperature in the dark. The mixture is then diluted in deionized water to obtain an absorbance of 0.7 ± 0.02 at 734 nm. Lipophilic extract in different concentrations was allowed to react with ABTS for 7 min in the dark and the absorbance was measured at 734 nm again. Trolox (6-hydroxy-2,5,7,8-tetramethylchromane-2-carboxylic acid) was used as standard to obtain a calibration curve. Each extract was analyzed three times in triplicate.

3.2.11 Cell culture and cytotoxicity assay

Human immortalized keratinocytes (HaCaT) were from Innoprot (Biscay, Spain), whereas immortalized murine fibroblasts (BALB/c 3T3) were from ATCC (Manassas, Virginia). Cells were cultured in 10% fetal bovine serum in Dulbecco's modified Eagle's medium, in the presence

of 1% antibiotics and 2 mM L-glutamine, in a 5% CO₂ humidified atmosphere at 37°C. HaCaT cells were seeded in 96-well plates at a density of 2x10³ cell/well and BALB/c 3T3 at a density of 3x10³ cell/well. Approximately 24 h after seeding, increasing concentrations of lipophilic extract (from 10 to 100 µg/mL) were added to the cells for different length of time. At the end of each experimental point, cell viability was measured by the MTT assay, as described by Arciello *et al.* (Arciello 2011). Cell survival was expressed as the percentage of viable cells in the presence of the lipophilic extract compared to control cells (represented by the average obtained between untreated cells and cells supplemented with the highest concentration of buffer). Each sample was tested in three independent analyses, each carried out in triplicates.

3.2.12 DCFDA assay

The antioxidant effect of the lipophilic extract (50 µg/mL) was measured by determining the intracellular ROS levels. The protocol used by Del Giudice *et al.* was followed (Del Giudice 2017), with some modifications. Briefly, HaCaT cells were exposed for different length of time to the extract under test and then irradiated by UVA light for 10 min (100 J/cm²). Fluorescence intensity of the fluorescent probe (2',7'-dichlorofluorescein, DCF) was measured at an emission wavelength of 525 nm and an excitation wavelength of 488 nm using a Perkin-Elmer LS50 spectrofluorimeter (Shelton, CT, USA). Emission spectra were acquired at a scanning speed of 300 nm/min, with 5 slit width both for excitation and emission. ROS production was expressed as percentage of DCF fluorescence intensity of the sample under test, compared to the untreated sample. Three independent experiments were carried out, each one with three determinations.

3.2.13 Determination of lipid peroxidation levels

The levels of lipid peroxidation were determined by using the thiobarbituric acid reactive substances (TBARS) assay according to the protocol proposed by Petruk *et al.* (Petruk 2016). Briefly, HaCaT cells were pre-incubated for 15 and 30 min with lipophilic extract and then irradiated by UVA light for 10 min (100 J/cm²). Cells were detached by trypsin, centrifuged at 1000 *g* for 10 min and 5x10⁵ cells were resuspended in 0.67% thiobarbituric acid (TBA) and an equal volume of 20% trichloroacetic acid was added. Samples were then heated at 95°C for 30 min, incubated on ice for 10 min and centrifuged at 3000 *g* for 5 min, at 4°C. TBA reacts with the oxidative degradation products of

lipids in samples, yielding red complexes that absorb at 532 nm. Lipid peroxidation levels were expressed as percentage of absorbance at 532 nm of the sample under test, compared to the untreated sample. Three independent experiments were carried out, each one with three determinations.

3.2.14 Western blot analysis

HaCaT cells were seeded at a density of 3×10^5 cells/cm² in complete medium for 24 h and then treated with 50 µg/mL of lipophilic extract for different length of time. To analyze Nrf-2 expression levels, nuclear and cytosolic lysate were prepared as follow. Cells were detached by trypsin, centrifuged at 1000 g for 10 min. Pellets were resuspended in lysis buffer (0.5% Triton X-100 in PBS pH 7.4) containing protease and phosphate inhibitors. After 20 min incubation on ice, samples were centrifuged at 1200 g for 5 min at 4°C. The supernatants were removed and collected as cytosolic lysates. The residual pellets were washed in the same buffer and resuspended in RIPA buffer (50mM Tris-HCl pH 7.4, 1% NP-40, 0.25% Na deoxycholate, 150 mM NaCl, 1 mM EDTA) completed with protease and phosphatase inhibitors. After 20 min incubation on ice, vortexing every 5 min, samples were centrifuged at 14000 g for 30 min at 4 °C. The supernatants were collected as nuclear lysates. Concentration of samples was determined by the Bradford assay and the samples were analyzed by SDS-PAGE (sodium dodecyl sulfate–polyacrylamide gel electrophoresis) and western blot analysis. To normalize protein intensity levels, antibodies against GAPDH and B23 were used. The chemiluminescence detection system was from Bio-Rad (Hercules, CA, USA).

3.2.15 Statistical analysis

Experimental data results were analysed by ANOVA and means were compared by Tukey's HSD (SPSS statics V15 IBM, New York, United States), Value of $p \leq 0.05$ was considered statistically significant, figured by alphabetical letters along means in tables.

3.3 Results and Discussion

3.3.1 Optimization of phycocyanin purification

We recently set up a procedure to disrupt *G. phlegrea* biomass by using a conventional high-pressure procedure. PC was then easily recovered from the supernatant by a single purification step, i.e. the gel-

filtration (Imbimbo 2019). However, from an economic point of view, the size exclusion chromatography is not feasible, as it is difficult to be scaled-up. Thus, we optimized PC purification by using ultrafiltration and compared the results with those previously obtained. As shown in Table 1, both ultrafiltration technique and gel filtration let us to obtain a PC with a purity grade. It is known that a purity grade ≤ 0.7 is indicative of a food grade, between 0.7 and 3.9 is of reagent grade and ≥ 4.0 of analytical grade (Fernández-Rojas, Hernández-Juárez, & Pedraza-Chaverri 2014). As for the yield, about 80% PC was obtained with both techniques. However, the protein concentration was much higher when ultrafiltration was used, as 13 mg/mL of PC were obtained with respect to 0.19 mg/mL of gel-filtration.

Table 1. Comparison in PC recovery after gel-filtration and ultrafiltration. PC was determined spectrophotometrically. Data shown are means \pm S.D. of three independent experiments. a indicates $p < 0.05$ with respect to gel-filtration.

Technique used	Initial PC (mg/g biomass)	PC recovery (%)	PC concentration (mg/mL)	Purity grade (Abs ₆₂₀ /Abs ₂₈₀)
Gel-filtration	98 \pm 1.4	78 \pm 8	0.19 \pm 0.01	5 \pm 0.2
Ultrafiltration	98 \pm 1.4	80 \pm 7	13 \pm 1.4 ^a	5 \pm 1

3.3.2 Total carotenoids extraction

Starting from the residual wet biomass after PC extraction, carotenoids extraction was performed by using PLE technology. In order to compare the carotenoids extraction after PLE, a conventional acetone extraction was performed in parallel on dried raw biomass and on the dried residual biomass after PC extraction, as schematized in Figure 1. Usually, one of the mechanism used to break cell wall is freeze-drying the biomass, which is a high energy consuming treatment and causes rapid loss and degradation of carotenoids, thus affecting the bioactivity of the desired compounds (Mcmillan, Watson, Ali, & Jaafar 2013; Papaioannou, Roukas, & Liakopoulou-Kyriakides 2008).

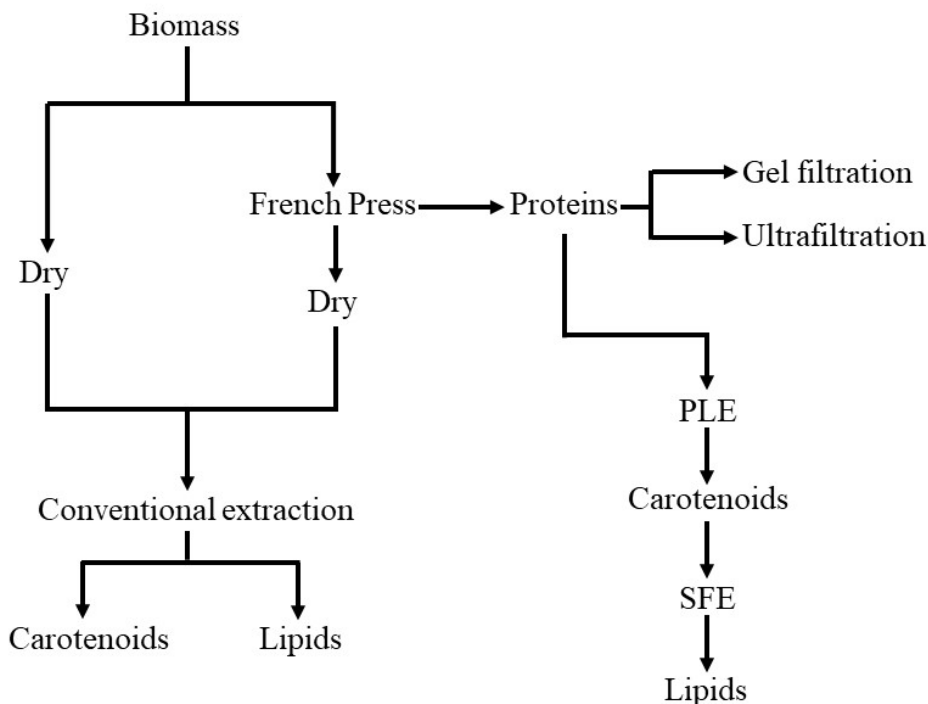


Figure 1. A schematic representation of the extraction strategy.

The results of the extractions are reported in Table 2. The carotenoid yield is expressed as mg of carotenoids extracted per g of dry biomass. It is interesting to notice that the conventional extraction allowed to obtain 62 mg of carotenoids from the raw biomass, whereas about 100 mg were recovered starting from the disrupted biomass. Thus, a significant increase ($p < 0.05$) in total carotenoids extraction was observed when the disrupted biomass was used. When PLE was employed on residual wet biomass, about 90 mg of carotenoids were obtained. Noteworthy, although the PLE did not increase the extraction yield with respect to the conventional method, the time needed to obtain carotenoids significantly decreased from 24 h to 30 min. In addition, no organic solvents were used, thus suggesting that this technology is green and very effective. In terms of total carotenoids content in the extract, the high-pressure procedure did not extract carotenoids, but allowed a further better extraction. In fact, as shown in Table 2, the conventional extraction allowed an increase in carotenoids content up

to 63% when the disrupted biomass was used instead of the raw one ($p<0.05$). Surprisingly, PLE allowed a further increase of 250% in total carotenoid content when compared to the conventional extraction technique on the disrupted biomass ($p<0.005$) and 400% on the raw biomass ($p<0.05$).

Table 2. Comparison between conventional extractions performed on raw biomass and biomass post French press extraction and PLE extraction after French press in terms of extracted carotenoids. Data shown are means \pm S.D. of three independent experiment. a indicates $p<0.05$ with respect to raw biomass, b indicates $p<0.005$ with respect to conventional extraction after PC recovery and c indicates $p<0.005$ with respect to raw biomass.

Sample	Carotenoids yield (mg/g biomass)	Carotenoids content (mg/g extract)	Zeaxanthin (mg/g extract)	β -carotene (mg/g extract)
Raw biomass (conventional extraction)	62 \pm 2	222 \pm 24	2.7 \pm 0.3	22 \pm 4
Post French press (conventional extraction)	100 \pm 5 ^a	362 \pm 24 ^a	33.4 \pm 3.7 ^a	320 \pm 76
Post French press (PLE)	89 \pm 6	911 \pm 23 ^{a,b}	48 \pm 5 ^a	436 \pm 60 ^c

3.3.3 Carotenoids characterization by HPLC-DAD-MS

Carotenoids obtained by PLE technique were analyzed by high-performance liquid chromatography coupled to diode array detector and mass spectrometry detector (HPLC-DAD-MS) in order to collect more information about the specific pigments (carotenoids and chlorophylls). When possible, a tentative identification was accomplished by combining the information provided by UV-vis spectra from DAD, $[M + H]^+$ and MS/MS fragmentation patterns from mass spectrometry detector and bibliographic search (Table 3).

Chromatographic profiles shown in Figure 2 revealed that the extract obtained by PLE with ethanol is the one with the highest number of pigments. Peaks number 4, 5 and 11 stood out as the most relevant ones and they could be tentatively identified as zeaxanthin, chlorophyll a and β -carotene respectively. These pigments were also present in the pressurized liquid extracts obtained with ethanol from other microalgae

(*Neochloris oleoabundans*) (Castro-Puyana 2013) and *Porphyridium cruentum* (Gallego, Martínez, Cifuentes, Ibáñez, & Herrero 2019). Protonated ions of these compounds were detected (m/z 569.6 $[M + H]^+$ for zeaxanthin, m/z 894.0 $[M + H]^+$ for chlorophyll a and m/z 537.7 $[M + H]^+$ for β -carotene), along with fragment ions of zeaxanthin and chlorophyll a produced by the loss of a water molecule (m/z 551.5 $[M + H - H_2O]^+$) or phytol group (m/z 615.4 $[M + H - C_{20}H_{38}]^+$) respectively. Furthermore, the identification of these three compounds was corroborated by the injection of commercial standards.

Other minor chlorophylls, peaks 2 and 9 were tentatively assigned as hydroxychlorophyll a (Castro-Puyana 2013) and pheophytin a (Gallego & Bueno 2019) due to their UV-vis UV and MS/MS spectra, showing the particular loss of a phytol group. Peaks number 6 and 10 have been tentatively identified as chlorophyll a' and pheophytin a' in concordance with their spectra, similar to those of chlorophyll a and pheophytin a, but presenting longer retention times. Peak number 3 presented the characteristic absorbance spectrum of chlorophylls, and therefore have been designed as chlorophyll-type.

The rest of the minor peaks in the chromatogram presented the characteristic absorbance spectrum of carotenoids. With the exception of peak number 7, that could not be detected in MS due to the lack of enough ionization efficiency, the rest of carotenoids were characterized in terms of $[M + H]^+$ and many fragments from MS/MS were detected. However, a tentative identification was not possible. On the other hand, it is not the first time that peak number 12 has been reported. This carotenoid with UV-vis spectrum with maximums at 446 and 472 nm was previously mentioned in gas expanded liquid (GXL) extracts obtained with 75% of ethanol from *Scenedesmus obliquus* microalga (Gilbert-López 2017). In conclusion, the pigment analysis revealed β -carotene and zeaxanthin as the two main carotenoids in all extracts in agreement with Marquardt (Marquardt 1998), but with a different microalgal strain (*G. sulphuraria*).

In addition, a method based on HPLC-DAD was employed to quantify the amount of zeaxanthin and β -carotene. To fit the calibration curves prepared with the commercial standards of both pigments, the samples analyzed were diluted in pure methanol at different concentrations: 10 mg/mL for the conventional extraction starting from raw biomass, and 1 mg/mL for the two extracts obtained after French press. Quantification results are reported in Table 2. As we expected, PLE improved the amount of both pigments. Nevertheless, the increase obtained was surprisingly interesting: up to 40% in comparison with the

ones obtained by conventional extraction and to about 2000 times with respect to the raw biomass.

Table 3. Pigments detected in *Galdieria phlegrea* extracts after PLE.

Peak	Identification	RT (min)	UV-Vis max, nm	[M + H] ⁺ m/z	MS/MS main fragments detected
1	Carotenoid	13.706	450, 475	664.3	607.5, 551.5, 495.4
2	Hydroxychlorophyll a	15.062	430, 663	910.1	893.0, 631.8, 614.5
3	Chlorophyll-type	15.696	426, 665	940.7	629.4, 661.4, 907.7, 852.7,
4	Zeaxanthin [#]	17.926	428, 450, 476	569.6	551.5
5	Chlorophyll a [#]	19.092	432, 664	894.0	615.4, 583.3
6	Chlorophyll a [']	20.523	430, 665	894.1	615.6
7	Carotenoid	21.453	445, 471	-	-
8	Carotenoid	24.772	450, 476	584.7	564.8
9	Pheophytin a	30.425	408, 666	872.1	594.0, 683.3, 535.5
10	Pheophytin a [']	31.681	408, 666	871.9	593.8
11	β-Carotene [#]	33.685	450, 475	537.7	-
12	Carotenoid	35.591	446, 472	592.8	533.4

[#]Identification corroborated by comparison with commercial standards; RT: retention time

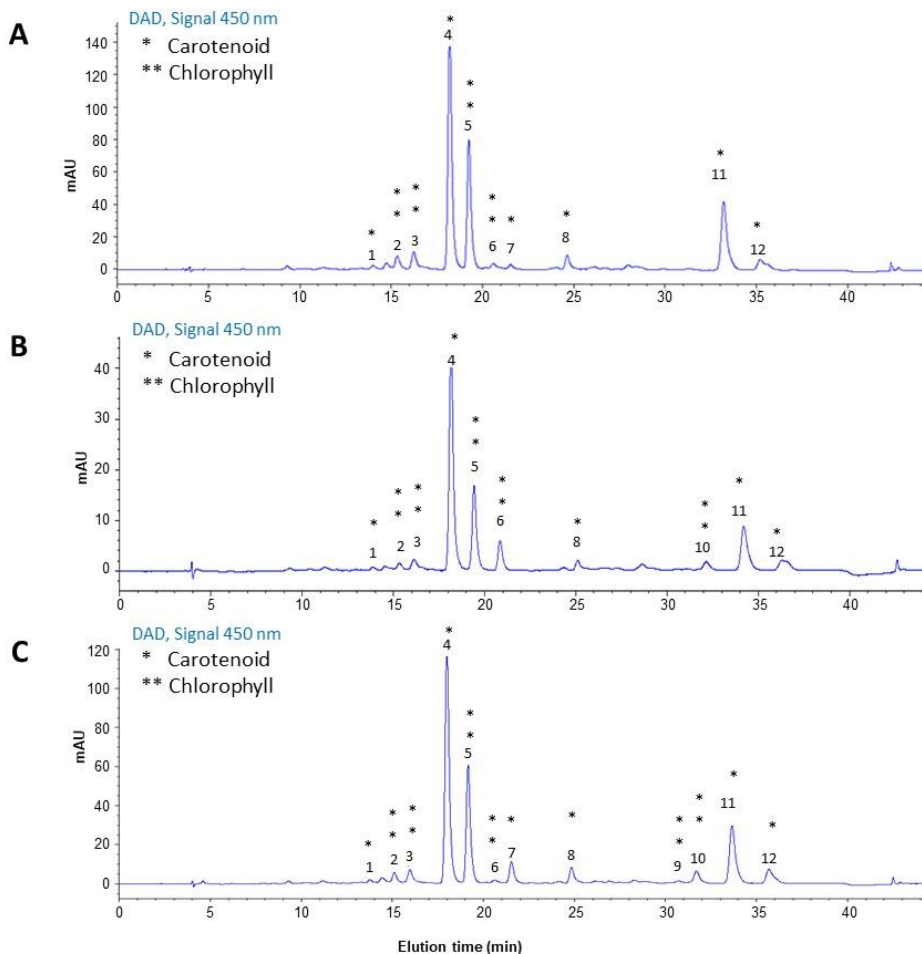


Figure 2. Representative HPLC-DAD chromatograms of carotenoids extracted from *G. phlegrea*. **A:** conventional extraction of raw biomass. **B:** conventional extraction of the residual biomass after PC extraction. **C:** PLE extraction of the residual biomass after PC extraction. * indicates carotenoids, ** indicates chlorophylls. Peak numbers and their identification are reported in Table 3

3.3.4 Total lipid extraction

To further improve the biorefinery design, after the PLE extraction a lipid extraction was carried out using supercritical CO₂ (ScCO₂). Noteworthy, both PLE and SFE were performed on the same apparatus, without the needing to recover the biomass from the extraction cell after carotenoids extraction. In particular, after PLE, CO₂ was injected in the extraction cell to push out ethanol containing

carotenoids. Afterwards, pressure was increased to the super critical point and lipids were extracted (Figure S1). As benchmark, conventional chloroform/methanol extraction was carried out on raw dried biomass and on the residual dried biomass after PC extraction. Results of the extractions are reported in Table 4. The ScCO₂ extraction allowed to obtain the same amount of lipids that were obtained by conventional extraction, avoiding the use of organic solvent. This result was quite surprising, as the lipids extracted are the third class of molecules obtained in a biorefinery approach. When compared with our previous results (Imbimbo 2019), we found a lower recovery in lipid yield, but this could be due to a different extraction method used.

Table 4. Comparison between conventional extractions performed on raw biomass and biomass post French press extraction and SFE extraction after French press in terms of extracted lipids. Data shown are means \pm S.D. of three independent experiment. a indicates $p < 0.05$

Sample	Lipid yield (mg/g biomass)
Raw biomass (Conventional extraction)	110 \pm 3
Post French press (Conventional extraction)	164 \pm 6
Post French press (SFE)	184 \pm 5

3.3.5 Evaluation of biocompatibility and antioxidant activity of lipophilic extract obtained by PLE extraction on eukaryotic cells

To verify if the carotenoids extracted by the PLE technique were biologically active and safe for humans, their in vitro antioxidant activity, along with their biocompatibility on eukaryotic cells, was tested. The results of the in vitro ABTS colorimetric assay are shown in Figure 3 and clearly indicate that the lipophilic extract is endowed with a

significant antioxidant activity. Its IC_{50} value, i.e. the concentration of the extract able to inhibit 50% of the radical, is 50 $\mu\text{g}/\text{mL}$. This result is much lower than those reported in literature, as the IC_{50} value here obtained is about 1600 times lower than others reported with different microalgae (Muthukumaran, Peraman 2019).

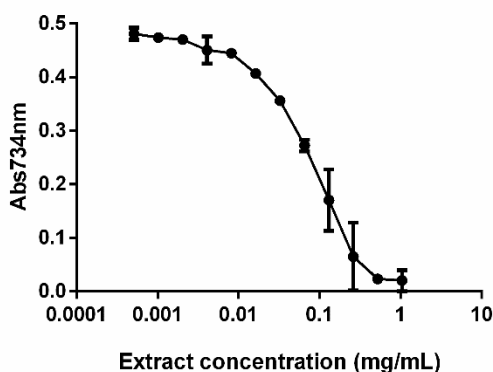


Figure 3. ABTS assay on carotenoids extracted from *G. phlegrea*. ABTS scavenging activity of different concentrations of lipophilic extract (mg/mL) obtained by PLE from *G. phlegrea*. Data shown are means \pm S.D. of three independent experiment.

The biocompatibility of the extract was tested by a time-course and dose-response test on immortalized murine fibroblasts (BALB/c 3T3) and immortalized human keratinocytes (HaCaT). Cell viability was assessed by the tetrazolium salt colorimetric (MTT) assay and cell survival was expressed as the percentage of viable cells in the presence of extract compared to that of control samples. As shown in Figure 4 A-B, after 48 h cell viability was not affected up to 50 $\mu\text{g}/\text{mL}$, while at the highest concentration tested (100 $\mu\text{g}/\text{mL}$) a 50% reduction of cell viability was observed.

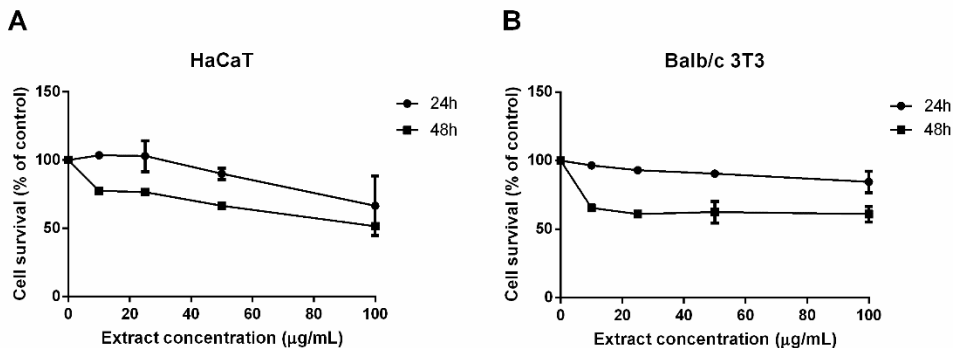


Figure 4: Effect of lipophilic extract on the viability of HaCaT and BALB/c 3T3 cells. Dose-response curves of HaCaT (A) and BALB/c 3T3 (B) cells after 24 h (black circles) and 48 h (black squares) incubation with increasing concentrations of lipophilic extracts obtained by PLE (10-100 µg/mL). Cell viability was assessed by the MTT assay and cell survival expressed as percentage of viable cells in the presence of the lipophilic extract under test, with respect to control cells grown in the absence of the extract. Data shown are means \pm S.D. of three independent experiment.

3.3.6 Protective effect of lipophilic extract against oxidative stress on HaCaT cells

As the lipophilic extract obtained by PLE contains antioxidants, the potential protective effect against oxidative stress was analyzed on a cell-based model. As cell system, we chose immortalized keratinocytes as they are normally present in the outermost layer of the skin, and UVA radiations as a source of stress. Cells were treated with 50 µg/mL extracts for different lengths of time (from 5 to 120 min), and then oxidative stress was induced by UVA irradiation (100 J/cm²). Immediately after irradiation, ROS levels were measured by using H₂DCF-DA as a probe. For each set of experiments, untreated cells were used as a control. Under physiological conditions (i.e. in the case of untreated cells) a physiological release of ROS is observed (100%). As shown in Figure 5A, no effect on ROS levels was observed when cells were incubated with the extract for 120 min (grey bars), whereas UVA treatment significantly increased DCF fluorescence intensity (black bars). Interestingly, pretreatment of cells with the lipophilic extract, prior to UVA exposure, resulted in an inhibition of ROS production, which was clear already after 5 min of pretreatment. We then performed a comparison between the antioxidant activity of the total lipophilic extract obtained by PLE and commercial β -carotene and

zeaxanthin, the two most abundant species identified in the extract. On the basis of the quantification data reported in Table 2, we calculated that, when the lipophilic extract was tested at 50 µg/mL, the amount of β-carotene corresponded to 24 µg/mL and that of zeaxanthin to 2.4 µg/mL. Thus, HaCaT cells were pre-incubated for 30 min with either: 50 µg/mL of lipophilic extract; 24 µg/mL of β-carotene; 2.4 µg/mL of zeaxanthin; a mixture of both carotenoids. At the end of incubation, oxidative stress was induced as previously mentioned. Alteration of ROS levels was measured by using H₂DCF-DA. As shown in Figure 5B, a significant increase in ROS production was observed when cells were incubated with commercial β-carotene (white bars) or zeaxanthin (black squared bars), also in the absence of any UVA exposure. Interestingly, only the mixture of both commercial carotenoids (dashed bars), as well as the lipophilic extract (grey bars), were able to counteract oxidative stress in a similar way. The protective effect of lipophilic extract was also confirmed by analyzing the lipid peroxidation levels. To this purpose, thiobarbituric acid reactive substances (TBARS) were measured and related to lipid peroxidation levels. A significant increase in lipid peroxidation levels was observed after UVA treatment but, noteworthy, this effect was abolished when cells were pretreated with the lipophilic extract, either after 15 or after 30 min pre-incubation (grey and white bars, respectively). Treatment of cells with lipophilic extract did not alter significantly lipid peroxidation levels (Figure 5C).

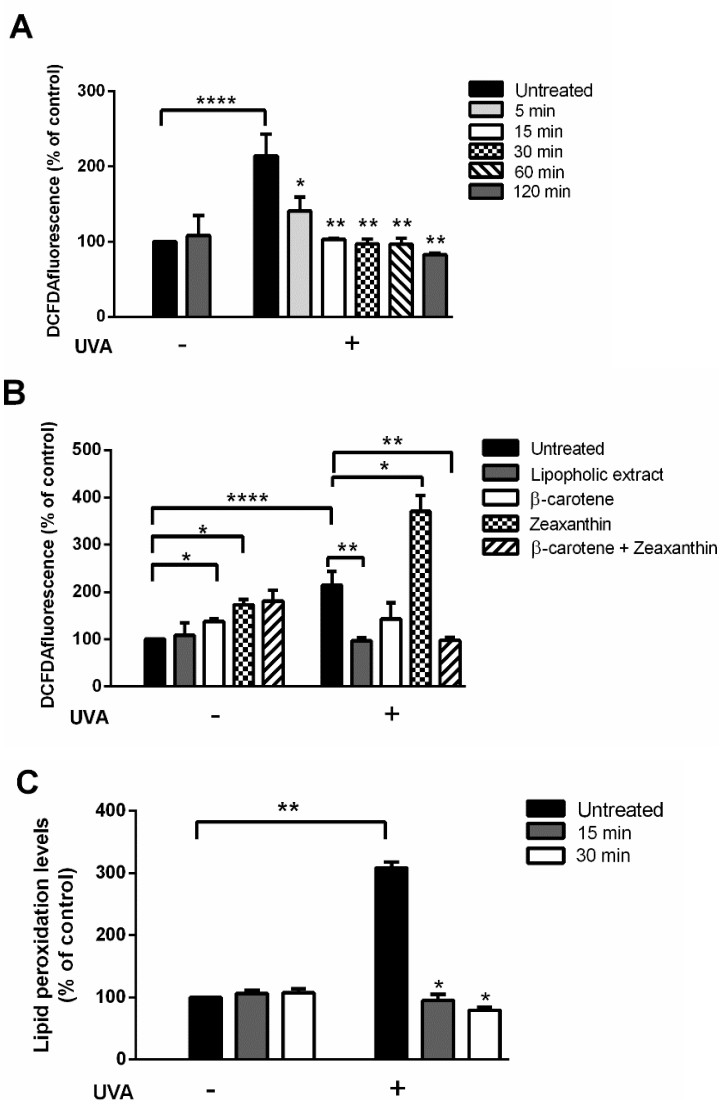


Figure 5: Antioxidant effect of the lipophilic extract from *G. phlegrea* on UVA-stressed HaCaT cells. Cells were pre-incubated in the presence of 50 $\mu\text{g}/\text{mL}$ lipophilic extract for different length of time, prior to be irradiated by UVA (100 J/cm^2). **A:** Determination of intracellular ROS levels by DCFDA assay. Cells were incubated for 5 min (light grey bars), 15 min (white bars), 30 min (black-squared bars), 60 min (dashed bars) or 120 min (dark grey bars) with the lipophilic extract in the absence (-) or in the presence (+) of UVA. Black bars are referred to untreated cells. For each experimental condition, ROS production was measured and a percentage of the ratio between ROS production in treated cells and ROS production in untreated cells was calculated and reported in the graph. **B:** Comparison of the protective effect of the lipophilic extract with commercial antioxidants by the DCFDA assay. Cells were

incubated for 30 min prior to UVA exposure. Black bars are referred to untreated cells in the absence (-) or in the presence (+) of UVA. Grey bars are referred to cells incubated with 50 µg/mL of lipophilic extract; white bars are referred to cells incubated with 24 µg/mL of β-carotene; black squared bars are referred to cells incubated with 2.4 µg/mL of zeaxanthin; white bars are referred to cells incubated with 24 µg/mL of β-carotene; dashed bars are referred to cells incubated with both β-carotene and zeaxanthin. **C**: Analysis of lipid peroxidation levels evaluated by TBARS assay. Cells were pre-incubated with the lipophilic extract for 15 (grey bars) or 30 min (white bars) before UVA irradiation. Values are expressed as % with respect to control (i.e. untreated) cells. For each experimental condition, lipid peroxidation levels were measured and a percentage of the ratio between lipid peroxidation levels in treated cells and lipid peroxidation levels in untreated cells was calculated and reported in the graph. Data shown are means ± S.D. of three independent experiment. * indicates $p < 0.05$, ** indicates $p < 0.005$, *** indicates $p < 0.0001$.

3.3.7 Nrf-2 regulates the antioxidant activity of lipophilic extract

To understand the molecular mechanism responsible for the protective effect of the lipophilic extract, the involvement of the transcription factor Nrf-2 was analyzed. Under normal physiological conditions, Nrf-2 is associated with Keap-1, which keeps Nrf-2 in the cytosol and directs it to the proteasomal degradation. Upon either oxidative stress induction and/or in the presence of antioxidants, Keap-1 dissociated from Nrf-2, which is translocated to the nucleus where it binds to antioxidant responsive elements (ARE) sequences and activates the transcription of several phase-II detoxifying enzymes (Ma 2013). Thus, we incubated HaCaT cells in presence of the lipophilic extract for different length of time (from 5 to 30 min) and lysates were analyzed by Western Blot analysis, using Nrf-2 antibody. As shown in Figure 6 A, an increase in nuclear Nrf-2 was observed after 15 min of incubation. The activation of Nrf-2 was further confirmed by analyzing the translation level of the heme oxygenase-1 (HO-1) by Western blot analysis. HO-1 is a ubiquitous and redox-sensitive inducible stress protein that degrades heme to CO, iron and biliverdin (Balogun 2003). The importance of this protein in physiological and pathological states is underlined by the versatility of HO-1 inducers and the protective effects attributed to heme oxygenase products in conditions that are associated with moderate or severe cellular stress. Thus, HaCaT cells were incubated for 30 min and 60 min and lysates were analyzed by Western Blot analysis, using a HO-1 antibody. As shown in Figure 6 B, an increase in HO-1 levels was observed after 30 min of incubation.

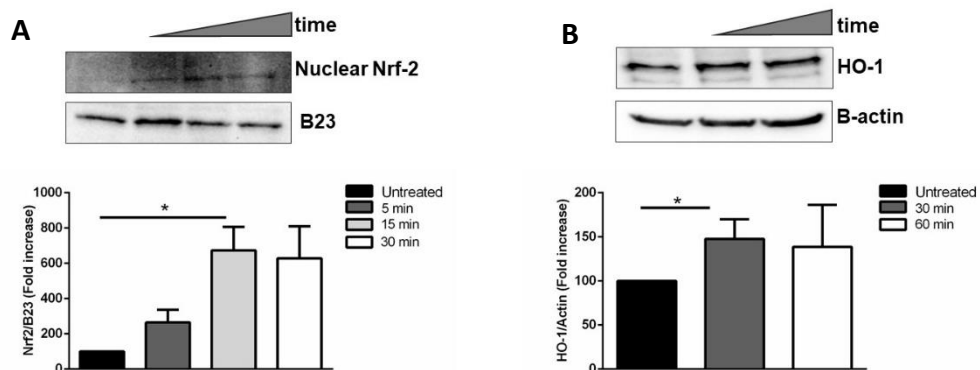


Figure 6: Effect of the lipophilic extract on Nrf-2 activation on HaCaT cells. Cells were incubated with 50 $\mu\text{g}/\text{mL}$ of lipophilic extract obtained by PLE technique for different length of time and then nuclear (A) or cytosolic (B) proteins were analyzed by Western blotting. **A:** Western blot analysis of nuclear Nrf-2 after 5 min (dark grey bar), 15 min (light grey bar) and 30 min (white bar) incubation. Nuclear Nrf-2 was normalized to B23 and quantified by densitometric analysis. The ratio between Nrf-2 and B23 of each treated sample was then related to the ratio Nrf-2/B23 of untreated cells, considered 100%. **B:** Western blot analysis of cytosolic HO-1 was performed after incubation with 50 $\mu\text{g}/\text{mL}$ of the extract for 30 min (dark grey bar), and 60 min (white bar). HO-1 and β -actin and were quantified by densitometric analysis and the ratio HO-1/ β -actin of each treated sample was then related to the ratio HO-1/ β -actin of untreated cells, considered as 100%. Data shown are means \pm S.D. of three independent experiment. * indicates $p < 0.05$ with respect to control cells.

3.4 Conclusions

One of the aims of green chemistry is to preserve the natural environment, promoting a better use of resources and limiting the negative influence of human involvement, such as the use of procedures that require the use of toxic solvents (Mustafa and Turner 2011). Compared to conventional extractions, this innovative green biorefinery approach is able to extract, in cascade, three different bioactive compounds from the microalga *Galdieria phlegrea*. In combination, the described process allows achieving higher yields of PC, carotenoids and lipids using GRAS (Generally Recognized As Safe) solvents, in shorter time and with less solvent consumption. Here, we demonstrated that PLE using ethanol has a high potential to extract carotenoids from *G. phlegrea*. Moreover, as *G. phlegrea* is an eukaryotic microalga, it possesses a robust cell wall, which prevents

the release of intracellular products. The idea of breaking the biomass by high pressure homogenization allowed to isolate PC and helped the subsequent release of carotenoids. Both final products, PC and carotenoids were biologically active in terms of antioxidant activity (Imbimbo 2019). These results will open the way to the idea of commercializing carotenoids from microalgae for cosmeceutical applications.

In conclusion, this work will help to achieve a complete valorization of the *G. phlegrea* microalga biomass. The results can then contribute to increase the revenue streams of the process, in order to compensate the large cultivation and downstream cost for biomass production and, finally, turn positive the economic balance of the microalgae biorefinery. Furthermore, they contribute to develop a green process which can also increase the social acceptance of industrial microalgal products.

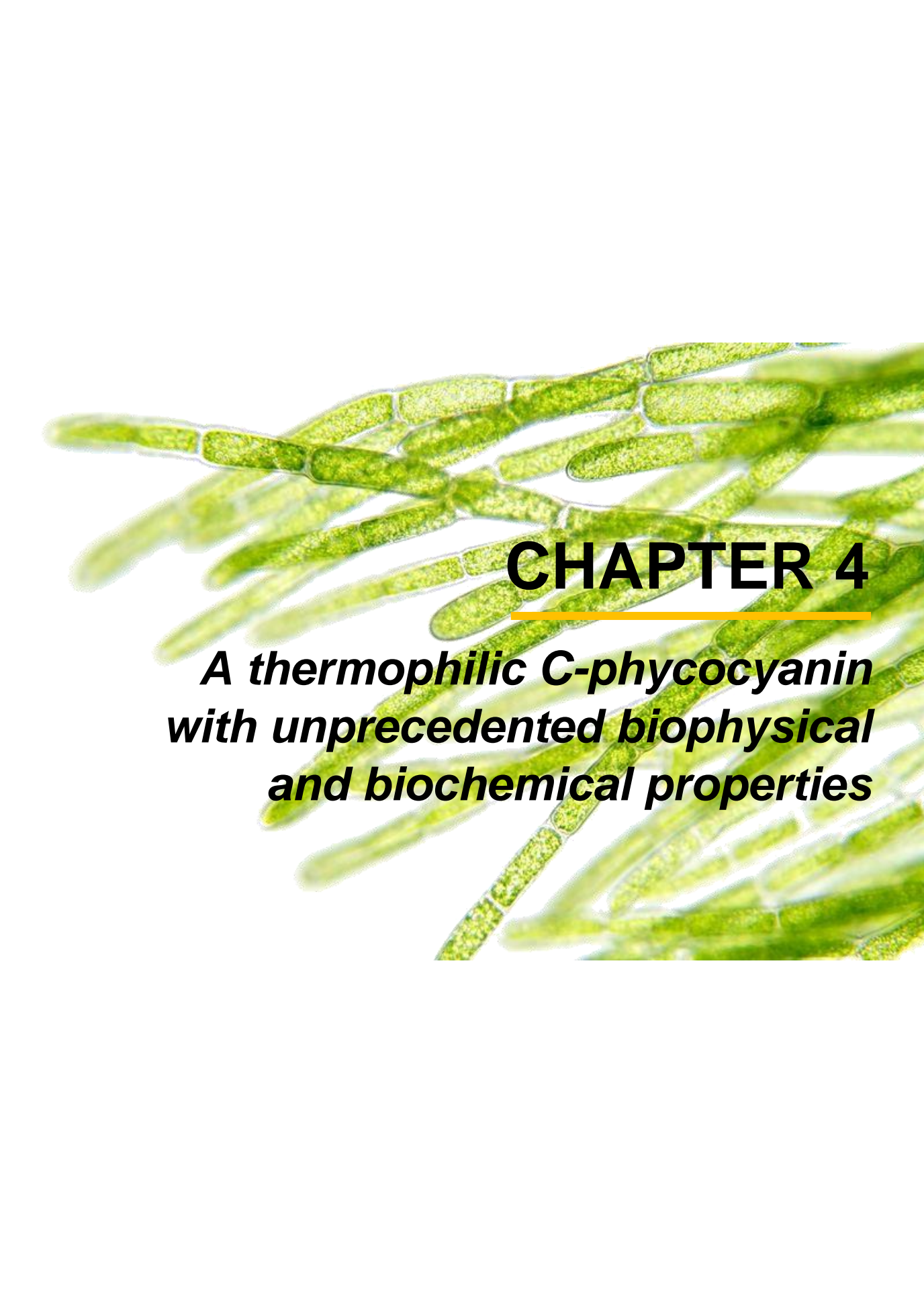
3.5 References

- Ambati, R. R., Gogisetty, D., Aswathanarayana, R. G., Ravi, S., Bikkina, P. N., Bo, L., & Yuepeng, S. (2019). Industrial potential of carotenoid pigments from microalgae: Current trends and future prospects. *Critical Reviews in Food Science and Nutrition*, 59(12), 1880–1902. <https://doi.org/10.1080/10408398.2018.1432561>.
- Arciello, A., De Marco, N., Del Giudice, R., Guglielmi, F., Pucci, P., Relini, A., Piccoli, R. (2011). Insights into the fate of the N-terminal amyloidogenic polypeptide of ApoA-I in cultured target cells. *Journal of Cellular and Molecular Medicine*, 15(12), 2652–2663. <https://doi.org/10.1111/j.1582-4934.2011.01271.x>
- Axelsson, M., & Gentili, F. (2014). A Single-Step Method for Rapid Extraction of Total Lipids from Green Microalgae. *PLoS one*. 9(2), 17–20. <https://doi.org/10.1371/journal.pone.0089643>.
- Balogun, E., Hoque, M., Gong, P., Killeen, E., Green, C. J., Foresti, R., Motterlini, R. (2003). Curcumin activates the haem oxygenase-1 gene via regulation of Nrf2 and the antioxidant-responsive element. *Biochemical Journal* 369, 887–895.
- Barsanti, L., & Gualtieri, P. (2018). Is exploitation of microalgae economically and energetically sustainable? *Algal Research*. 107–115. <https://doi.org/10.1016/j.algal.2018.02.001>
- Basha, O. M., Hafez, R. A., El-Ayouty, Y. M., Mahrous, K. F., Bareedy, M. H., & Salama, A. M. (2008). C-Phycocyanin inhibits cell proliferation and may induce apoptosis in human HepG2 cells. *The Egyptian Journal of Immunology*. 15(2), 161–167. <https://doi.org/10.1016/j.algal.2013.01.004>.

- Camel, V. (2001). Recent extraction techniques for solid matrices—supercritical fluid extraction, pressurized fluid extraction and microwave-assisted extraction: their potential and pitfalls. *Analyst*, 126(7), 1182-1193.
- Castro-Puyana, M., Herrero, M., Urreta, I., Mendiola, J. A., Cifuentes, A., Ibáñez, E., & Suárez-Alvarez, S. (2013). Optimization of clean extraction methods to isolate carotenoids from the microalga *Neochloris oleoabundans* and subsequent chemical characterization using liquid chromatography tandem mass spectrometry. *Analytical and Bioanalytical Chemistry*. 405(13), 4607–4616. <https://doi.org/10.1007/s00216-012-6687-y>
- Del Giudice, R., Petruk, G., Raiola, A., Barone, A., Monti, D. M., & Rigano, M. M. (2017). Carotenoids in fresh and processed tomato (*Solanum lycopersicum*) fruits protect cells from oxidative stress injury. *Journal of the Science of Food and Agriculture*. 97(5). <https://doi.org/10.1002/jsfa.7910>
- Fernández-Rojas, B., Hernández-Juárez, J., & Pedraza-Chaverri, J. (2014). Nutraceutical properties of phycocyanin. *Journal of Functional Foods*, Vol. 11, pp. 375–392. <https://doi.org/10.1016/j.jff.2014.10.011>
- Gallego, R., Bueno, M., & Herrero, M. (2019). Sub- and supercritical fluid extraction of bioactive compounds from plants, food-by-products, seaweeds and microalgae – An update. *Trends in Analytical Chemistry*. 116, 198– 213. <https://doi.org/10.1016/J.TRAC.2019.04.030>
- Gallego, R., Martínez, M., Cifuentes, A., Ibáñez, E., & Herrero, M. (2019). Development of a Green Downstream Process for the Valorization of *Porphyridium cruentum* biomass. *Molecules*. 24(8), 1564. <https://doi.org/10.3390/molecules24081564>
- Gilbert-López, B., Mendiola, J. A., Fontecha, J., Van Den Broek, L. A. M., Sijtsma, L., Cifuentes, A., Herrero, M., Ibáñez, E. (2015). Downstream processing of *Isochrysis galbana*: a step towards microalgal biorefinery. *Green Chemistry*. 17(9), 4599–4609. <https://doi.org/10.1039/c5gc01256b>
- Gilbert-López, B., Mendiola, J. A., van den Broek, L. A. M. Ambati, R. R., Gogisetty, D., Aswathanarayana, R. G., Ravi, S., Bikkina, P. N., Bo, L., & Yuepeng, S. (2019). Industrial potential of carotenoid pigments from microalgae: Current trends and future prospects. *Critical Reviews in Food Science and Nutrition*. 59(12), 1880–1902. <https://doi.org/10.1080/10408398.2018.1432561>
- Imbimbo, P., Romanucci, V., Pollio, A., Fontanarosa, C., Amoresano, A., Zarrelli, A., Monti, D. M. (2019). A cascade extraction of active phycocyanin and fatty acids from *Galdieria phlegrea*. *Applied Microbiology and Biotechnology*, 9455–9464. <https://doi.org/10.1007/s00253-019-10154-0>
- Jin, E. S., & Melis, A. (2003). Microalgal biotechnology: Carotenoid production by the green algae *Dunaliella salina*. *Biotechnology and Bioprocess Engineering*. 8(6), 331–337. <https://doi.org/10.1007/BF02949276>

- José, M., Reyes, F. A., Mendiola, J. A., & Iba, E. (2014). The Journal of Supercritical Fluids Astaxanthin extraction from *Haematococcus pluvialis* using CO₂ - expanded ethanol. *Journal of supercritical fluids*. 92, 75–83. <https://doi.org/10.1016/j.supflu.2014.05.013>
- Ma, Q. (2013). Role of nrf2 in oxidative stress and toxicity. *Annual review of pharmacology and toxicology*. 53, 401-426.
- Marquardt, J. (1998). Effects of carotenoid-depletion on the photosynthetic apparatus of a *Galdieria sulphuraria* (Rhodophyta) strain that retains its photosynthetic apparatus in the dark. *Journal of Plant Physiology*, 152(4–5), 372–380. [https://doi.org/10.1016/S0176-1617\(98\)80250-2](https://doi.org/10.1016/S0176-1617(98)80250-2).
- Mcmillan, J. R., Watson, I. A., Ali, M., & Jaafar, W. (2013). Evaluation and comparison of algal cell disruption methods : Microwave , waterbath , blender , ultrasonic and laser treatment. *Applied Energy*. 103, 128–134. <https://doi.org/10.1016/j.apenergy.2012.09.020>.
- Mubarak, M., Shaija, A., & Suchithra, T. V. (2015). A review on the extraction of lipid from microalgae for biodiesel production. *Algal Research*. 7, 117–123. <https://doi.org/10.1016/J.ALGAL.2014.10.008>.
- Mustafa, A., & Turner, C. (2011). Analytica Chimica Acta Pressurized liquid extraction as a green approach in food and herbal plants extraction : A review. *Analytica Chimica Acta*. 703(1), 8–18. <https://doi.org/10.1016/j.aca.2011.07.018>.
- Muthukumar Peraman, S. N. (2019). Identification and quantification of fucoxanthin in selected carotenoid-producing marine microalgae and evaluation for their chemotherapeutic potential. *Pharmacognosy Magazine*. 15(64), 243–249. https://doi.org/10.4103/pm.pm_64_19.
- Nagarajan, J., Ramanan, R. N., Raghunandan, M. E., Galanakis, C. M., & Krishnamurthy, N. P. (2017). Chapter 8. Carotenoids. In *Nutraceutical and Functional Food Components*. (2017): 259-296. <https://doi.org/10.1016/B978-0-12-805257-0.00008-9>.
- Papaioannou, E., Roukas, T., & Liakopoulou-Kyriakides, M. (2008). Effect of biomass pre-treatment and solvent extraction on β -carotene and lycopene recovery from *Blakeslea trispora* cells. *Preparative Biochemistry and Biotechnology*. 38(3), 246–256. <https://doi.org/10.1080/10826060802164942>.
- Petruk, G., Raiola, A., Del Giudice, R., Barone, A., Frusciantè, L., Rigano, M. M., & Monti, D. M. (2016). An ascorbic acid-enriched tomato genotype to fight UVA-induced oxidative stress in normal human keratinocytes. *Journal of Photochemistry and Photobiology B: Biology*. 163, 284-289.
- Pruvost, J., Van Vooren, G., Le Gouic, B., Couzinet-Mossion, A., & Legrand, J. (2011). Systematic investigation of biomass and lipid productivity by microalgae in photobioreactors for biodiesel application. *Bioresource Technology*. 102(1), 150–158. <https://doi.org/10.1016/j.biortech.2010.06.153>.

- Reyes, F. A., Mendiola, J. A., Suárez-Alvarez, S., Ibañez, E., & Del Valle, J. M. (2016). Adsorbent-assisted supercritical CO₂ extraction of carotenoids from *Neochloris oleoabundans* paste. *Journal of Supercritical Fluids*. 112, 7–13. <https://doi.org/10.1016/j.supflu.2016.02.005>.
- Santiago-Santos, M. C., Ponce-Noyola, T., Olvera-Ramírez, R., Ortega-López, J., & Cañizares-Villanueva, R. O. (2004). Extraction and purification of phycocyanin from *Calothrix* sp. *Process Biochemistry*. 39(12), 2047–2052. <https://doi.org/10.1016/j.procbio.2003.10.007>.
- Sathasivam, R., & Ki, J. S. (2018). A review of the biological activities of microalgal carotenoids and their potential use in healthcare and cosmetic industries. *Marine Drugs*. 16(1). <https://doi.org/10.3390/md16010026>.
- Spolaore, P., Joannis-Cassan, C., Duran, E., & Isambert, A. (2006). Commercial applications of microalgae. *Journal of Bioscience and Bioengineering*. 101(2), 87–96. <https://doi.org/10.1263/jbb.101.87>.
- Wu, H. L., Wang, G. H., Xiang, W. Z., Li, T., & He, H. (2016). Stability and Antioxidant Activity of Food-Grade Phycocyanin Isolated from *Spirulina platensis*. *International Journal of Food Properties*. 19(10), 2349–2362. <https://doi.org/10.1080/10942912.2015.1038564>

A microscopic view of green filamentous algae, showing multiple parallel chains of elongated, cylindrical cells. The cells are arranged in a regular, repeating pattern, and the overall structure is a dense, branching network of these filaments. The color is a vibrant green, and the individual cells are clearly visible, showing their internal structure and cell walls.

CHAPTER 4

***A thermophilic C-phycocyanin
with unprecedented biophysical
and biochemical properties***

International Journal of Biological Macromolecules

(2020) 150, 38-51

<https://doi.org/10.1016/j.ijbiomac>.**A thermophilic C-phycoyanin with unprecedented
biophysical and biochemical properties**

Giarita Ferraro^{a,^,§}, Paola Imbimbo^{a,^}, Angela Marseglia^a, Anna Illiano^a, Carolina Fontanarosa^a, Angela Amoresano^a, Giuseppe Olivieri^b, Antonino Pollio^c, Daria Maria Monti^{a,d}, and Antonello Merlino^{a,*}

^a Department of Chemical Sciences, University of Naples Federico II, Naples, Italy.

^b Bioprocess Engineering Group, Wageningen University and Research, Droevendaalsesteeg 1, 6700AA, Wageningen, the Netherlands.

^c Department of Biology, University of Naples Federico II, Naples, Italy.

^d Istituto Nazionale di Biostrutture e Biosistemi (INBB), Rome, Italy.

§ Present address: Department of Chemistry “Ugo Schiff”, University of Florence, Sesto Fiorentino, Italy.

^These authors equally contributed to this work**Abstract**

C-phycoyanins are abundant light-harvesting pigments which have an important role in the energy transfer cascade of photosystems in prokaryotic cyanobacteria and eukaryotic red algae. These proteins have important biotechnological applications, since they can be used in food, cosmetics, nutraceutical, pharmaceutical industries and in biomedical research. Here, C-phycoyanin from the extremophilic red alga *Galdieria phlegrea* (GpPC) has been purified and characterized from a biophysical point of view by SDS-PAGE, mass spectrometry, UV–Vis absorption spectroscopy, circular dichroism and intrinsic fluorescence. Stability against pH variations, addition of the oxidizing agent hydrogen peroxide and the effects of temperature have been also investigated, together with its in cell antioxidant potential and antitumor activity. GpPC is stable under different pHs and unfolds at a temperature higher than 80 °C within the pH range 5.0–7.0. Its fluorescence spectra present a maximum at 650 nm, when excited at

589 nm. The protein exerts interesting in cell antioxidant properties even after high temperature treatments, like the pasteurization process, and is cytotoxic for A431 and SVT2 cancer cells, whereas it is not toxic for non-malignant cells. Our results assist in the development of C-phycocyanin as a multitasking protein, to be used in the food industry, as antioxidant and anticancer agent.

4.1 Introduction

Phycobilisomes (PBSs) (Glazer 1985; MacColl 1998) are supramolecular protein complexes that absorb light and deliver energy to a reaction centre containing chlorophyll in prokaryotic cyanobacteria and eukaryotic red algae (Watanabe 2014). PBSs thus play a major role in photosynthesis energy absorption and transmission (Kirst 2014). These complexes contain a core and rods, which are constituted and organized by several phycobiliproteins (PBPs) and a small number of linker polypeptides that assemble in very large and intricate aggregates (MacColl 1998; Gingrich 1983). PBPs contain three classes of pigments, each with a specific spectral feature: phycoerythrins (PE; red, $\lambda_{\max} = 565$ nm), phycocyanins (PC; blue, $\lambda_{\max} = 617$ nm) and allophycocyanins (AP; bluish green, $\lambda_{\max} = 650$ nm) (MacColl 1998; Grossman 1993).

C-phycocyanins (C-PCs) were isolated, purified and characterized from many sources (Raposo 2013). They contain α - and β -chains (Adir 2003) forming a stable $\alpha\beta$ unit that then assembles into a multimeric structure $(\alpha\beta)_n$ ($n=1\sim 6$) (Storf 2001). C-PCs typically exist as $(\alpha\beta)_3$ trimer, shaped as a hollow disk, or as $[(\alpha\beta)_3]_2$ hexamer, shaped as a double disk. α - and β -chains share similar structures but have different sequences (identity between 25 and 40 %) and molecular weights (10-19 kDa for the α -chain and 14-21 kDa for the β -chain) (Glauer 1992). Each subunit binds from 1 to 4 chromophore molecules (phycocyanobilin, PCB) with a ring-opening tetrapyrrole structure. This results in specific absorption and emission spectra (O'Carra 1971; Bennet 1971).

Moreover, the tetrapyrrole ring is responsible for the excellent radical scavenging and antioxidant properties of the C-PCs (Piron 2019; Pleonsil 2013). C-PCs also exert anti-tumour (Jiang 2018; Jiang 2017) and anti-inflammatory activity (Zhu 2016). It has been also reported that they can decrease the progression of Alzheimer's disease (Penton-Rol 2016), probably by inhibiting the β -Secretase protein (Singh 2014), and that they can be used as fluorophores in diagnostics therapeutics or as food colorants (Kuddus 2013). In this respect, it is important to identify

and characterize C-PCs that are stable to high temperatures and extreme pH, so that they can be stable after/during the sterilization treatments. Here we report a complete biophysical characterization, including sequence determination and analysis, stability against temperature and pH variations of C-phycoyanin from *Galdieria phlegrea* (GpPC), a unicellular thermo-acidophilic red alga with optimal growth conditions of $T = 35\text{--}45\text{ }^{\circ}\text{C}$ at pH 1.5. The GpPC in cell antioxidant activity, before and after pasteurization, along with its cytotoxic activity have been also evaluated. Our results open the way to the use of GpPC as food colorant and preservative, as the protein fully retains its structure and antioxidant activity after high temperature treatments.

4.2 Materials and Methods

4.2.1 Protein purification and *in situ* digestion

Galdieria phlegrea (strain 009) was provided from the Algal Collection of the University Federico II (ACUF) and grown as described in Imbimbo et al. (Imbimbo 2019). The isolation of GpPC was carried out by ultrafiltration. Briefly, the total protein extract obtained by conventional high-pressure procedures was purified by using a 100 kDa molecular weight cutoff membrane. The permeate was discarded and the retentate was collected. The process was carried out at room temperature. The purity grade of GpPC was evaluated first by measuring the ratio $A_{620\text{nm}}/A_{280\text{nm}}$, and then by SDS- and native PAGE and mass spectrometry (Kuddus 2013). 15% SDS-PAGE was performed to evaluate GpPC purity. Native PAGE was carried out using 10% (w/v) polyacrylamide. Gels were stained with Coomassie brilliant blue purchased from BIO-Rad. For *in situ* digestion, following 12.5% polyacrylamide gel (0.1% SDS, 25 mM Tris-HCl, 192 mM glycine, pH 8.3) and Coomassie brilliant blue staining, the two bands corresponding to the predicted molecular weight of α and β -chains were excised from the gel and fully destained prior to further processing. Briefly, the gel pieces were washed with three cycles of 0.1 M NH_4HCO_3 pH 8.0 and acetonitrile (ACN), followed by reduction (10 mM dithiothreitol (DTT) in 100 mM NH_4HCO_3 45 min, $56\text{ }^{\circ}\text{C}$) and alkylation (55 mM iodoacetamide (IAM) in 100 mM NH_4HCO_3 , 30 min, room temperature). Then, the gel pieces were washed with three further cycles of 100 mM NH_4HCO_3 pH 8.0 and ACN. Finally, gel plugs were rehydrated and incubated overnight at $37\text{ }^{\circ}\text{C}$ with trypsin (10 ng/ μL trypsin; 10 mM NH_4HCO_3) and chymotrypsin (1 $\mu\text{g}/\mu\text{L}$). Peptides

mixture was eluted, vacuum-dried, and resuspended in 0.1% formic acid for LC-MS/MS analysis. The marker used was the prestained protein ladder-Broad molecular weight (10–245 kDa) from Abcam (ab116028; Cambridge, UK). Trypsin (proteomics grade) and chymotrypsin were from Sigma-Aldrich (Saint Louis, Mo, USA).

4.2.2 LC-MS/MS analysis

Peptide samples were loaded via an autosampler (Surveyor MS Pump Plus and Micro AS) onto a Michrom C18 Captrap and then were introduced directly into an Orbitrap LTQ-Velos MS (Thermo Fisher Scientific, Surrey, UK) via a fused silica C18 capillary column (Nikkyo Technos CO, Tokyo, Japan) and a nanoelectrospray ion source. The mobile phase comprised H₂O with 0.1% formic acid (buffer A) and 100% acetonitrile with 0.1% formic acid (buffer B). The gradient ranged from 5% to 30% buffer B in 95 min, followed by 30% to 60% B in 15 min and a step gradient to 85% B for 5 min with a flow of 0.42 μ L/min. Finally, the system returns to the initial conditions of 5% B. FTMS full scan mass spectra (from 450 to 1600 m/z) were acquired with a resolution of $r=60\,000$. This was followed by data dependent MS/MS fragmentation in centroid mode of the most intense ion from the survey scan using collision induced dissociation (CID) in the linear ion trap: normalized collision energy 35%; activation Q 0.25; electrospray voltage 1.5kV; capillary temperature 200°C; and isolation width 2.00. This MS/MS scan event was repeated for the top 20 peaks in the MS survey scan; the targeted ions were then dynamically excluded for 30s. Singly charged ions were excluded from the MS/MS analysis; Xcalibur software version 2.1.0 SP1 build 1160 (Thermo Fisher Scientific, U.K.) was used for data acquisition.

4.2.3 Mascot identification of phycocyanin sequences

The acquired MS/MS spectra were transformed in mzData (.XML) format and used for protein identification with a licensed version of MASCOT software (www.matrixscience.com) version 2.4. with 10 ppm MS tolerance and 0.6 Da MS/MS tolerance; peptide charge from +2 to +3. Carboxyamidomethylation of Cys as fixed modification was inserted, but possible oxidation of methionines and formation of pyroglutamic acid from glutamine residues at the N-terminal position of peptides, were considered as variable modifications to query SwissProt databases, without including taxonomy restrictions.

4.2.4 Sequence comparison

Primary structures of C-phycoyanin from *Pseudanabaena sp. Iw0831*, *Thermosynechococcus elongatus*, *Thermosynechococcus vulcanus*, *Leptolyngbya sp. N62DM*, *Synechocystis sp. PCC 6803*, *Synechococcus elongatus*, *Arthrospira platensis*, *Gracilaria chilensis*, *Polysiphonia urceolata*, *G. sulphuraria*, *C. caldarium* and *Microchaete diplosiphon* were obtained from the NCBI/BLAST server against the PDB database. ExPASy ProtParam tool was used to calculate the percentage amino acid composition (Wilkins 1999).

4.2.5 Spectrophotometric characterization

UV-Vis absorption spectra of GpPC were collected at different pHs (buffers: 10 mM sodium citrate pH 2.0 or pH 3.0, 10 mM sodium acetate pH 4.0 or pH 5.0, 10 mM bis-Tris, pH 6.0, 10 mM Tris-HCl pH 7.0 or 8.0, 10 mM bicine pH 9.0, 10 mM CAPS (N-cyclohexyl-3-aminopropanesulfonic acid pH 10.0 or 11.0) with a protein concentration of 0.2 mg/mL using a quartz cuvette of 1 cm path length. The protein was extensively dialysed against milliQ water using tubing cellulose membranes with a 35 kDa pore size before the 24 h incubation with the buffers. Spectra were collected at 25°C over 250-700 nm wavelength range using a Varian Cary 5000 UV-vis-NIR spectrophotometer and the following parameters: data pitch: 1 nm, scanning speed: 600 nm/min, band width: 2 nm. The UV-Vis absorption signal of GpPC was then followed titrating the protein (2.5 mL, concentration 0.2 mg/mL) with a 50% solution of hydrogen peroxide (added volumes between 10 and 100 μ L) to evaluate the phycoyanin response to oxidative stress.

GpPC intrinsic fluorescence was determined using a Fluoromax-4 spectrofluorometer from Horiba Scientific and a 1 cm optical path-length quartz cell, under controlled temperature conditions (Peltier control system) at 25°C using a cuvette of 500 μ L. Emission spectra were collected using a protein concentration of 0.2 mg/mL at the same pHs used to register UV-Vis absorption spectra. Data were registered between 295 and 450 nm upon excitation using excitation wavelength (λ_{ex})= 280 nm, between 310 and 450 nm upon excitation using λ_{ex} =295 nm, and between 600 and 800 nm upon excitation using λ_{ex} =589 nm.

Far-UV CD spectra of GpPC (0.2 mg/mL), at the same pH values used to register UV-Vis absorption spectra, were registered at 25°C using a Jasco J-810 spectropolarimeter equipped with a Peltier block arrangement (Model PTC-348WI) (Jasco, Easton, MD), a quartz

cuvette of 0.1 cm path length, and a spectral band pass of 2 nm. Raw ellipticity data were converted to mean residue ellipticity using the formula $[\theta] = [\theta_{\text{raw}} \times 100 \times \text{MRW}] / c \times l$, where MRW is GpPC mean residue weight, c is the concentration (mg/mL) and l is the path length (cm). Deconvolution of CD spectra for secondary structure amount was performed using BestSel (Table S1) (Micsonai 2018). Other experimental settings were: scan speed: 50 nm/min, resolution: 0.2 nm, sensitivity: 50 mdeg, response: 4 s.

4.2.6 Stability against temperature

The temperature stability of GpPC was determined by monitoring the changes in mean residue ellipticity (at 222 nm) and the change in the maximum emission wavelength as a function of temperature. For CD measurements, the temperature was raised to 95°C in 1°C every 60 s. The two-state unfolding model was used to calculate the melting temperature. Unfolding curves were registered at different pHs (10 mM sodium acetate, pH 5.0 or pH 5.5, 10 mM Tris-HCl, pH 7.0 or 10 mM CAPS, pH 10.0) with a protein concentration of 0.2 mg/mL. For fluorescence measurements, spectra were registered at different temperatures after 5 min equilibration in 10 mM sodium acetate, pH 5.0.

4.2.7 Antitumor activity

Human epidermoid A431 cells, murine fibroblasts BALB/c 3T3 and SVT2 cells were obtained from ATCC, whereas human epidermal keratinocytes HaCaT cells were from Innoprot (Biscay, Spain). All cells were cultured in Dulbecco's modified Eagle's medium (DMEM) (Sigma-Aldrich, St Louis, MO, USA), supplemented with 10% foetal bovine serum (HyClone), 2 mM L-glutamine and antibiotics, all from Sigma-Aldrich, under a 5% CO₂ humidified atmosphere at 37°C. For toxicity experiments, cells were seeded in 96-well plates at a density of 2.5×10^3 cells per well. 24 h after seeding, increasing concentrations of GpPC were added to the cells (0.5-10 µM). Cell viability was assessed by the MTT (3-(4,5-dimethylthiazol-2-yl)-2,5-diphenyltetrazolium bromide) assay after 72 h incubation, as previously described (Petruk 2016).

4.2.8 Thermal pasteurization

For thermal pasteurization, GpPC was heated at 75°C in a water bath. After 10 min incubation, the sample was transferred to a second water bath at 20°C. The sample was stored at 4°C until analysis.

4.2.9 Cellular reactive oxygen species (ROS) assay

The antioxidant activity of pure GpPC before and after pasteurization was determined by measuring intracellular ROS levels, according to the protocol previously reported (Petruk 2016), with some modification. HaCaT cells were pre-incubated for 2 h with 0.4 μ M GpPC or pasteurized GpPC. Cells were then exposed to UVA irradiation for 10 min (100 J/cm²). The fluorescence of the probe 2',7'-dichlorodihydrofluorescein diacetate (H₂-DCFDA) was detected at an emission wavelength of 525 nm and an excitation wavelength of 488 nm using a Perkin-Elmer LS50 spectrofluorometer (Shelton, CT, USA). Emission spectra were acquired at a scanning speed of 300 nm/min, with 5 nm slit width both for excitation and emission. ROS levels were expressed as percentage of fluorescence intensity of the sample under test, compared to untreated cells. Three independent experiments were carried out, each one with three determinations.

4.2.10 Statistical analyses

In all the experiments, samples were analyzed in triplicate. The results are presented as mean of results obtained after three independent experiments (mean \pm SD) and compared by one-way ANOVA according to the Bonferroni's method (post-hoc) using Graphpad Prism for Windows, version 6.01.

4.3 Results and Discussion

4.3.1 GpPC purification

It has been reported that a measure of the purity grade of C-PCs is the $A_{620\text{nm}}/A_{280\text{nm}}$ ratio. A value ≥ 4.0 indicates an analytical grade (Patel 2005; Fernandez-Rojas 2014). Some of us have recently optimized a simple purification procedure to obtain highly pure GpPC by a single ultrafiltration step (Imbimbo 2019) recovering a protein sample with a purity grade of 5 and a recovery yield of 80%. This $A_{620\text{nm}}/A_{280\text{nm}}$ ratio is much higher than that required for food applications (0.7) (Kuddus 2013; Patel 2005; Fernandez-Rojas 2014).

The purified protein was analyzed by SDS-PAGE and the results are shown in Figure 1A and by mass spectrometry. As expected, GpPC was characterized by two blue bands, in line with other C-PCs (Bennet 1971; Glazer 1971), suggesting that it is constituted by two chains which are able to bind the chromophore. The approximate molecular weights of the two subunits are 17 and 18 kDa, respectively. Pure

GpPC was then analysed by electrophoresis under non-denaturing conditions (Native-PAGE) at pH 8.8. The results, reported in Figure 1B, indicate that a single molecular species exists in our sample. Similar results have been obtained analysing a native gel carried out in a Bis-Tris-HEPES/MES-Acetic acid and Bis-Tris-Tricine PAGE system at pH 7.0 (data not shown). GpPC purity was further confirmed by in solution trypsin digestion, followed by LC-MS/MS tandem mass spectrometry. MASCOT analysis led to the identification of peptides occurring within PCs sequences. No different proteins were identified, thus confirming the purity of the protein (data not shown).

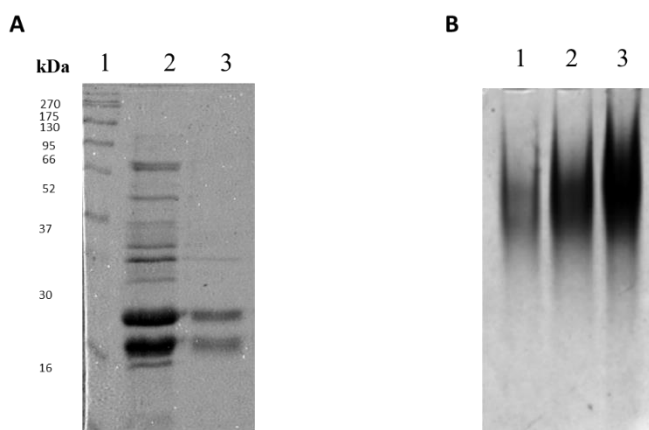


Figure 1. Electrophoretic analysis of GpPC samples after ultrafiltration. A: SDS-PAGE. Lane 1: molecular weight markers; lane 2: total protein extract (30 μ g); lane 3: 5 μ g of purified GpPC. **B:** Native-PAGE. Lanes 1-3: 10, 20, 40 μ g of pure GpPC. After electrophoresis, the two gels were stained with Coomassie-Blue.

4.3.2 Protein sequence analysis

The two bands corresponding to the α - (1) and β - (2) chains were excised from the gel and subjected to hydrolysis with trypsin and chymotrypsin in order to ensure the greatest possible sequence coverage for the two chains. The obtained peptide mixtures were analyzed by LC-MS/MS; the MASCOT in house software was used for protein identification. Table 1 reports the sequences obtained from MS-MS fragmentation spectra related to the α -chain after the treatment with chymotrypsin and trypsin and the scores associated with each one. Similar analyses were performed on protein bands corresponding to the β -chain. The results are summarized in Table 2. On the basis of mass spectral sequencing data and considering the high sequence identity

among C-phycocyanins from different sources, the sequences of the α and the β -chains of GpPC were determined.

Table 1. Peptides from GpPC α - chain (LC-MS/MS results).

End	Observed	Mr(expt)	ppm	Start	U	Peptide
1	17	903.4594	1804.904	2.97	99	U -.MKTPITEAIAATADSQGR.F + Oxidation (M)
1	17	895.4615	1788.908	2.5	112	U -.MKTPITEAIAATADSQGR.F
1	30	818.1502	3268.572	-3.03	23	U -.MKTPITEAIAATADSQGRFLSNTELQSCAGR.F + Oxidation (M)
1	17	602.6424	1804.905	3.59	56	U -.MKTPITEAIAATADSQGR.F + Oxidation (M)
1	17	597.3096	1788.907	1.67	64	U -.MKTPITEAIAATADSQGR.F
1	17	448.2353	1788.912	4.54	8	U -.MKTPITEAIAATADSQGR.F
2	17	829.9396	1657.865	0.7	80	U M.KTPITEAIAATADSQGR.F
2	17	553.6308	1657.871	4.27	12	U M.KTPITEAIAATADSQGR.F
3	30	998.8264	2993.457	2.05	34	U K.TPITEAIAATADSQGRFLSNTELQSCAGR.F
3	17	765.8943	1529.774	3.6	113	U K.TPITEAIAATADSQGR.F
3	30	749.37	2993.451	-0.12	11	U K.TPITEAIAATADSQGRFLSNTELQSCAGR.F
3	17	510.9315	1529.773	2.7	67	U K.TPITEAIAATADSQGR.F
18	33	957.47	1912.925	2.13	14	U R.FLSNTELQSCAGRFR.A
18	30	741.8561	1481.698	2.96	104	U R.FLSNTELQSCAGR.F
18	33	638.6494	1912.926	2.61	47	U R.FLSNTELQSCAGRFR.A
34	50	836.9449	1671.875	6.01	28	U R.AGASLDAARSLTANAQR.L
34	50	558.2959	1671.866	0.4	19	U R.AGASLDAARSLTANAQR.L
34	42	416.2206	830.4266	2.46	82	U R.AGASLDAAR.S
43	50	430.734	859.4534	2.67	48	U R.SLTANAQR.L
51	81	1099.541	3295.6	3.14	61	U R.LIDGAAQAVYSKFPYTTQMTGPCYASSAIGK.A
51	81	1104.874	3311.601	5.17	81	U R.LIDGAAQAVYSKFPYTTQMTGPCYASSAIGK.A + Oxidation (M)
51	83	878.6933	3510.744	7.91	18	U R.LIDGAAQAVYSKFPYTTQMTGPCYASSAIGKAK.C + Oxidation (M)
51	81	828.9073	3311.6	4.79	20	U R.LIDGAAQAVYSKFPYTTQMTGPCYASSAIGK.A + Oxidation (M)
51	81	824.9083	3295.604	4.48	27	U R.LIDGAAQAVYSKFPYTTQMTGPCYASSAIGK.A
51	62	618.3352	1234.656	0.095	90	U R.LIDGAAQAVYSK.F
63	81	1040.482	2078.95	2.93	89	U K.FPYTTQMTGPCYASSAIGK.A
63	81	1048.48	2094.945	3.04	99	U K.FPYTTQMTGPCYASSAIGK.A + Oxidation (M)
63	81	699.3214	2094.942	1.58	63	U K.FPYTTQMTGPCYASSAIGK.A + Oxidation (M)
63	81	693.9896	2078.947	1.36	70	U K.FPYTTQMTGPCYASSAIGK.A
66	91	968.1071	2901.3	19	1.2	U Y.TTQMTGPCYASSAIGKAKCSRDIGYY.L + Oxidation (M)
75	91	923.9559	1845.897	57	0	U Y.ASSAIGKAKCSRDIGYY.L
87	93	450.2352	898.4558	1.11	26	U R.DIGYYLR.M
94	120	997.4736	2989.399	3.96	33	U R.MVITYCLVAGGTGPMDEYL VAGLEEINR.T + 2 Oxidation (M)
121	137	1006.037	2010.059	6.59	63	U R.TFDLSPSWYVEALKNIK.A
121	134	828.4219	1654.829	3.01	84	R.TFDLSPSWYVEALK.N
121	137	671.0239	2010.05	1.82	21	U R.TFDLSPSWYVEALKNIK.A
121	134	552.615	1654.823	-0.66	20	R.TFDLSPSWYVEALK.N
135	162	936.4738	2806.4	3.94	49	U K.NIKASHGLSGAAASEANAYINYAINSL.S.-
138	162	1226.595	2451.176	3.71	98	U K.ASHGLSGAAASEANAYINYAINSL.S.-
138	162	818.0644	2451.171	1.96	90	U K.ASHGLSGAAASEANAYINYAINSL.S.-

Table 2. Peptides from GpPC β - chain (LC-MS/MS results).

End	Observed	Mr(expt)	ppm	Start	U	Peptide
1	18	652.3271	1953.96	-1.21	48	U -.MLDAFSKVVVAQADARGEFL
1	18	657.6605	1969.96	1.48	61	U -.MLDAFSKVVVAQADARGEFL + Oxidation (M)
1	19	690.0261	2067.057	5.12	21	U -.MLDAFSKVVVAQADARGEFL.S
1	19	695.3568	2083.049	3.72	33	U -.MLDAFSKVVVAQADARGEFL.S + Oxidation (M)
1	18	977.9863	1953.958	-1.94	56	U -.MLDAFSKVVVAQADARGEFL
1	18	985.9841	1969.954	-1.58	61	U -.MLDAFSKVVVAQADARGEFL + Oxidation (M)
1	19	1034.534	2067.054	4.04	66	U -.MLDAFSKVVVAQADARGEFL.S
1	19	1042.527	2083.039	-0.95	88	U -.MLDAFSKVVVAQADARGEFL.S + Oxidation (M)
3	18	570.9556	1709.845	4.49	3	U L.DAFSKVVVAQADARGEFL
3	18	855.9295	1709.844	4.18	70	U L.DAFSKVVVAQADARGEFL
3	19	912.4658	1822.917	-2.36	55	U L.DAFSKVVVAQADARGEFL.S
6	18	459.9062	1376.697	-5.85	39	U F.SKVVVAQADARGEFL
6	19	497.6017	1489.783	-3.76	42	U F.SKVVVAQADARGEFL.S
6	14	678.6898	2033.048	-3.24	14	U F.SKVVVAQADARGEFLSNTQLD
6	18	689.3541	1376.694	-8.11	63	U F.SKVVVAQADARGEFL
6	19	745.8997	1489.785	-2.71	77	U F.SKVVVAQADARGEFL.S
6	27	778.4056	2332.195	-3.13	34	U F.SKVVVAQADARGEFLSNTQLDAL.S
6	24	1017.534	2033.054	0.047	5	U F.SKVVVAQADARGEFLSNTQLD
19	27	487.7613	973.508	0.038	39	F.LSNTQLDAL.S
19	38	544.295	2173.151	-0.72	13	U F.LSNTQLDALSKMVADGNKRLD
19	38	725.3891	2173.146	-3.22	30	U F.LSNTQLDALSKMVADGNKRLD
19	38	730.7202	2189.139	-3.93	37	U F.LSNTQLDALSKMVADGNKRLD + Oxidation (M)
20	38	516.024	2060.067	-0.73	42	U L.SNTQLDALSKMVADGNKRLD
20	38	687.6966	2060.068	-0.21	48	U L.SNTQLDALSKMVADGNKRLD
20	38	693.024	2076.05	-6.34	15	U L.SNTQLDALSKMVADGNKRLD + Oxidation (M)
20	38	1039.042	2076.068	2.47	64	U L.SNTQLDALSKMVADGNKRLD + Oxidation (M)
25	38	511.9378	1532.792	-4.23	32	U L.DALSKMVADGNKRLD + Oxidation (M)
25	38	767.4005	1532.786	-7.57	60	U L.DALSKMVADGNKRLD + Oxidation (M)
28	38	412.2231	1233.648	-1.99	27	U L.SKMVADGNKRLD + Oxidation (M)
28	38	617.8314	1233.648	-1.37	38	U L.SKMVADGNKRLD + Oxidation (M)
39	60	717.0458	2148.116	-0.88	31	U L.DATAAISANAATIVTNAARSLF.S
39	66	944.4854	2830.434	-4.13	1	U L.DATAAISANAATIVTNAARSLFSEQPQLI
39	59	1001.532	2001.05	0.4	13	U L.DATAAISANAATIVTNAARSLF
39	60	1075.076	2148.137	9.02	48	U L.DATAAISANAATIVTNAARSLF.S
39	66	1416.234	2830.454	2.68	6	U L.DATAAISANAATIVTNAARSLFSEQPQLI
84	92	604.8251	1207.636	-2.19	15	L.RDMEILRY.V
84	92	612.821	1223.627	-4.71	14	L.RDMEILRY.V + Oxidation (M)
91	95	344.1762	686.3378	-1.33	20	L.RYVSY.A
91	105	801.4111	1600.808	-1.27	31	U L.RYVSYATIAGDSSVLD
93	110	971.4611	1940.908	-3.77	60	U Y.VSYATIAGDSSVLDLDRCLN

End	Observed	Mr(expt)	ppm	Start	U	Peptide
96	105	467.2466	932.4786	-3.03	70	U Y.ATIAGDSSVL.D
96	110	796.881	1591.747	-2.35	106	U Y.ATIAGDSSVLDDRCL.N
96	117	809.3878	2425.142	-5.27	14	U Y.ATIAGDSSVLDDRCLNGLRETY.Q
96	113	938.9567	1875.899	-0.42	75	U Y.ATIAGDSSVLDDRCLNGL.R
96	117	1213.584	2425.153	-0.62	24	U Y.ATIAGDSSVLDDRCLNGLRETY.Q
106	110	339.6461	677.2776	-3.88	15	L.DDRCL.N
106	113	481.7201	961.4256	-3.2	35	L.DDRCLNGL.R
106	117	504.5699	1510.688	2.94	28	L.DDRCLNGLRETY.Q
106	117	756.3509	1510.687	2.53	19	L.DDRCLNGLRETY.Q
111	117	426.7121	851.4096	-4.77	34	L.NGLRETY.Q
118	129	533.3024	1064.59	3.4	21	U Y.QALGVPGASVAL.A + Gln->pyro-Glu (N-term Q)
118	129	541.8118	1081.609	-3.8	57	U Y.QALGVPGASVAL.A
118	141	785.4294	2353.266	-2.19	9	U Y.QALGVPGASVALAVEKMKEAAIAF.A + Gln->pyro-Glu (N-term Q)
118	141	791.1036	2370.289	-3.84	10	U Y.QALGVPGASVALAVEKMKEAAIAF.A
118	141	796.4377	2386.291	-0.72	6	U Y.QALGVPGASVALAVEKMKEAAIAF.A + Oxidation (M)
118	141	1177.641	2353.267	-1.73	36	U Y.QALGVPGASVALAVEKMKEAAIAF.A + Gln->pyro-Glu (N-term Q)
118	141	1186.154	2370.294	-1.69	33	U Y.QALGVPGASVALAVEKMKEAAIAF.A
118	141	1194.155	2386.294	0.61	13	U Y.QALGVPGASVALAVEKMKEAAIAF.A + Oxidation (M)
121	129	385.7229	769.4312	-2.81	33	U L.GVPGASVAL.A
121	141	687.0444	2058.111	-3.37	6	U L.GVPGASVALAVEKMKEAAIAF.A
121	141	1030.062	2058.11	-3.92	9	U L.GVPGASVALAVEKMKEAAIAF.A
121	141	1038.063	2074.111	-1.25	39	U L.GVPGASVALAVEKMKEAAIAF.A + Oxidation (M)
130	141	436.5724	1306.695	-0.07	35	U L.AVEKMKEAAIAF.A
130	141	654.3525	1306.69	-3.84	31	U L.AVEKMKEAAIAF.A
130	141	662.3491	1322.684	-5.09	40	U L.AVEKMKEAAIAF.A + Oxidation (M)
142	164	1224.565	2447.115	-0.56	25	U F.ANDSSNVTIGDCSALISEIATYF.D
157	164	472.241	942.4674	-2.53	35	U L.ISEIATYF.D
164	172	326.1903	975.5491	-1.11	26	U Y.FDRAAKAVV.-
164	172	488.7806	975.5466	-3.6	29	U Y.FDRAAKAVV.-
165	172	415.2473	828.48	-2.04	22	U F.DRAAKAVV.-

Sequences of α - and β -chains of GpPC determined by proteolysis-based mass spectrometry experiments are reported in Figure 2 aligned with those of C-PCs of known structure with highest sequence identity. The alignments show that the degree of identity of the α and β -chains of GpPC with other C-PCs is very high, and that α and β -chains share 84% and 82% sequence identity, respectively, with the corresponding chains of the protein from *Cyanidium caldarium* (code 1PHN) (Stec 1999) and 83% and 84% sequence identity, respectively, with the α and β -chains of C-PC from *Galdieria sulphuraria* (code 3BRP). The amino acid composition, the isoelectric point and other analysis of GpPC sequence, together with the values obtained using sequences of the C-PCs from *Pseudanabaena* sp. *lw0831*, *Thermosynechococcus elongatus*, *Thermosynechococcus vulcanus*, *Leptolyngbya* sp. *N62DM*, *Synechocystis* sp. *PCC 6803*, *Synechococcus elongatus*, *Arthrospira platensis*, *Gracilaria chilensis*, *Polysiphonia urceolata*, *G. sulphuraria*, *C. caldarium*, *Microchaete diplosiphon*, are reported in Table 3. Alignment is unambiguous since there are no gaps.

Comparative sequence alignment shows that GpPC and the protein from *t* have higher pI of the α -chain when compared to the other C-PCs. The content of charged residues (R, K, D and E) of GpPC is comparable with that observed for thermophilic C-PCs, although a lower amount of negatively charged residues is found in the α -chain (Table 3). In the latter protein, there is a significantly lower number of glycine residues in the β -chain and a higher number of polar residues in the α -chain, when compared to that found in other C-PCs. Other sequence features are reported in Table S2.

Table 3. Amino acid composition and other sequence analyses of C-phycocyanins from different sources.

PDB code (Organism)	Growth temp, °C	pI		Amino acid composition, %																	
				Hydrophobic (A, L, I, V, P, F, Y, W, M)			Charged (D, E, R, K)			Polar (N, Q, S, T, C)			Gly			Negatively (D, E)			Positively (R, K)		
				α	β	all	α	β	all	α	β	all	α	β	all	α	β	all	α	β	All
(GpPC)	35-45	7.62	4.96	47.5	50.6	49.1	16.7	20.3	18.6	27.2	23.8	25.4	8.0	5.2	6.6	8.0	11.0	9.6	8.6	9.3	9.0
1PHN (<i>Cyanidium caldarium</i>)	55-60	5.81	4.96	50.0	48.8	49.4	16.7	20.3	18.6	25.3	23.8	24.5	7.4	7.0	7.2	8.6	11.0	9.9	8.0	9.3	8.7
1BBO (<i>Thermosynechococcus elongatus</i>)	57	5.36	5.12	50.0	51.7	50.9	17.3	19.8	18.6	24.7	22.1	23.3	7.4	6.4	6.9	9.3	10.5	9.9	8.0	9.3	8.7
3O18 (<i>Thermosynechococcus vulcanus</i>)	57	5.36	5.12	50.0	51.7	50.9	17.3	19.8	18.6	24.7	22.1	23.3	7.4	6.4	6.9	9.3	10.5	9.9	8.0	9.3	8.7
3KVS (<i>Galdieria sulphuraria</i>)	42	6.57	4.96	49.4	48.8	49.1	16.0	20.3	18.3	26.5	23.8	25.1	7.4	7.0	7.2	8.0	11.0	9.6	8.0	9.3	8.7
4H0M (<i>Synechococcus elongates</i>)	42	5.36	5.18	49.7	50.3	50.0	18.4	22.0	20.2	23.3	20.2	21.7	8.0	7.5	7.7	9.8	11.6	10.7	8.6	10.4	9.5
4F0T (<i>Synechocystis</i> sp. PCC 6803)	37	5.35	4.98	45.7	50.0	47.9	19.7	20.3	20.1	25.9	21.5	23.6	8.0	8.1	8.1	10.5	11.0	10.8	9.3	9.3	9.3
2BV8 (<i>Gracilaria chilensis</i>)	30-42	5.15	4.65	47.5	45.9	46.7	17.9	20.9	19.5	27.2	26.7	26.9	6.8	6.4	6.6	9.9	12.2	11.1	8.0	8.7	8.4
1HA7 (<i>Arthrospira platensis</i>)	35	5.83	4.96	48.1	50.0	49.1	20.4	19.2	19.8	22.8	24.4	23.6	8.0	6.4	7.2	10.5	10.5	10.5	9.9	8.7	9.3
4L1E (<i>Leptolyngbya</i> sp. N62DM)	30	5.83	4.8	48.8	50	49.4	20.4	18.6	19.5	22.2	25.0	23.6	8.0	6.4	7.2	10.5	10.5	10.5	9.9	8.1	9.0
1CPC (<i>Microchaete diplosiphon</i>)	24	6.56	5.10	48.1	50.6	49.4	17.3	19.8	18.6	25.9	21.5	23.6	8.0	8.1	8.1	8.6	10.5	9.6	8.6	9.3	9.0
5TOU (<i>Pseudanabaena sp. lw0831</i>)	10-15	5.79	5.40	46.9	52.3	49.7	17.9	19.1	18.6	26.5	20.9	23.6	8.0	7.5	7.8	9.2	9.9	9.6	8.6	9.3	9.0
1F99 (<i>Polysiphonia urceolata</i>)	10-15	5.81	4.92	48.1	53.5	50.9	17.9	19.2	18.6	25.9	21.5	23.6	7.4	5.8	6.6	9.3	10.5	9.9	8.6	8.7	8.7

Table S2. Amino acid composition and other sequence analyses of C-phycocyanins from different sources (Micsonai 2018).

Organism	N. Asn (N)			N. Gln (Q)			N. Met (M)			N. Cys (C)			(M+C+Q+N)			(G+K+Y+I)			(S+K+T+H)			[E+K]/[Q+H]			[D+E+K+R]/[H+Q+S+T]			[(V+Y)+W+R+E+L]		
	A	β	all	A	β	all	A	β	all	A	β	all	A	β	all	A	β	all	A	β	all									
<i>Galdieria phlegrea</i>	7	9	16	6	6	12	4	5	9	4	3	7	21	23	44	38	35	43	37	33	70	1.86	2.2	2.01	-13	-3	-16	53	59	112
<i>Thermosynechococcus elongates</i>	7	11	18	8	7	15	5	5	10	2	3	5	22	26	48	40	32	72	39	35	74	1.7	1.6	1.62	-10	-1	-11	54	58	112
<i>Thermosynechococcus vulcanus</i>	7	11	18	8	7	15	5	5	10	2	3	5	22	26	48	41	32	73	43	35	78	1.7	1.6	1.62	-10	-1	-11	54	58	112
<i>Cyanidium caldarium</i>	11	9	20	7	7	14	4	6	10	2	3	5	24	25	49	38	34	72	37	35	72	1.75	1.71	1.73	-12	-3	-15	59	61	120
<i>Galdieria sulphuraria</i>	11	9	20	8	7	15	4	6	10	2	3	5	25	25	50	37	32	69	37	35	72	1.4	1.7	1.56	-15	-3	-18	58	61	119
<i>Synechococcus elongates</i>	10	8	18	3	4	7	1	4	5	1	3	4	15	19	34	38	34	72	41	35	76	3.75	3	3.4	-7	6	-1	54	63	117
<i>Synechocystis</i> sp. PCC 6803	10	8	18	9	6	15	1	4	5	2	3	5	22	21	43	38	33	71	41	34	75	1.3	1.83	1.5	-8	1	-7	55	64	119
<i>Arthrospira platensis</i>	6	7	13	7	5	12	4	6	10	2	4	6	19	22	41	44	29	73	38	32	70	2.12	2.4	2.23	-2	-5	-7	55	60	115
<i>Gracilaria chilensis</i>	8	11	19	7	6	13	4	5	9	2	3	5	21	25	46	38	28	66	34	32	66	1.9	2.2	2	-13	-7	-20	59	59	118
<i>Leptolyngbya</i> sp. N62DM	6	7	13	7	5	12	4	6	10	2	4	6	19	22	41	43	29	72	37	33	70	2.12	2.4	2.23	-1	-7	-8	56	60	116
Microchaete diplosiphon	7	7	14	5	5	10	2	6	8	2	3	5	16	21	37	39	35	74	40	35	75	2.3	2.2	2.27	-12	0	-12	52	58	110
<i>Pseudonabaena</i> sp. Iw0831	6	7	13	4	3	7	4	6	10	3	3	6	17	19	36	38	39	77	40	32	72	3	3.7	3.25	-11	0	-11	52	58	110
<i>Polysiphonia urceolata</i>	12	9	21	3	6	9	4	5	9	2	3	5	21	23	44	40	29	69	44	34	78	3.75	1.83	2.6	-11	-1	-12	59	60	119

4.3.3 Effect of pH variations and H₂O₂ addition on the structure of GpPC

To investigate the effect of the pH change on the structure of GpPC, UV-Vis absorption, far-UV circular dichroism (CD) and intrinsic fluorescence spectra were collected under different pH values (Figures 3A-E). Both the UV-Vis and CD spectra are almost superimposable in the pH range 4.0-9.0, while they slightly change when pH is < 4.0 or > 10.0. In particular, UV-Vis spectra show the typical features of the absorption spectra of C-PCs (Edwards 1996), with a prominent peak at 620 nm (Figure 3A). The protein remains blue up to pH 10.0, whereas it loses the colour at pH \geq 10.0 (Figure 4).

CD spectra of GpPC show the minima at 208 and 222 nm, which are diagnostic of the presence of a high α -helical content (Figure 3B). The

calculated percentages of GpPC α -helix content as a function of pH, obtained using BestSel (Micsonai 2018), are listed in Table S1. At pH values between 2.0 and 9.0, the helical content is significantly higher than 70%. These values are in good agreement with those derived from the known structures of C-PCs deposited in the Protein Data Bank and higher than those estimated on the basis of CD spectra for the protein from the red microalga *C. caldarium* (47.5%) (Edwards 1997), from the cyanobacterium *P. luridum* (67.1%) (Eisele 2000) and from the thermophilic microalga *Synechococcus lividus* (54.7%) (Edwards 1997). Interestingly, GpPC retains its secondary structure at acid pH, contrarily to what observed in the case of other C-PCs that unfold, dissociate into monomers and precipitate at pH <4.5 (Patil 2006; Wu 2016). At pH > 10.0, GpPC loses helicity (estimated α -helical content between 50 and 60%), but minima at 208 and 222 nm are still present in CD spectra, even though with lower ellipticity values.

These data were further confirmed by intrinsic fluorescence experiments. Fluorescence emission was measured at 25°C upon excitation at 280 nm (Figure 3C), 295 nm (Figure 3D) and 589 nm (Figure 3E) to follow the effect of pH on the environment of the Tyr/Trp residues (280nm), of the only Trp present in the protein sequence (residue 128 in the α -chain) (295 nm) and of the chromophore (589 nm). Upon excitation at 280 nm, GpPC has an emission maximum at 333-334 nm, in line with the expectation for a well-folded protein. Upon excitation at 295 nm, GpPC has an emission maximum at 333-334 nm, suggesting that Trp128 α is buried in the protein hydrophobic core, while upon excitation at 589 nm GpPC has an emission maximum at 646-650 nm, in agreement with other PCs (Edwards 1997). At pH 10.0 and 11.0 the emission maximum upon excitation at 295 nm is red-shifted to 337-342 nm, while it is red-shifted to 344 nm at pH 2.0. These findings suggest that changes in the tertiary structures occur at extreme acid and basic pHs.

These conformational variations affect the α -chain structure and the solvent exposure of Trp128 α ; they take place to varying extents at different pHs. This is in line with the idea that the β -chain has a higher stability when compared to the α -chain (Su 2017). Interestingly, the fluorescence due to the chromophore is altered only at the highly basic pH 10.0 and 11.0, where the emission maximum is blue-shifted to 616-624 nm.

The emission intensity of the protein also decreases upon deviation from the native state due to the solvent quenching of the Trp fluorescence. These data agree with the results of far-UV CD spectra,

which show a loss of secondary structure content at highly acid or basic pHs.

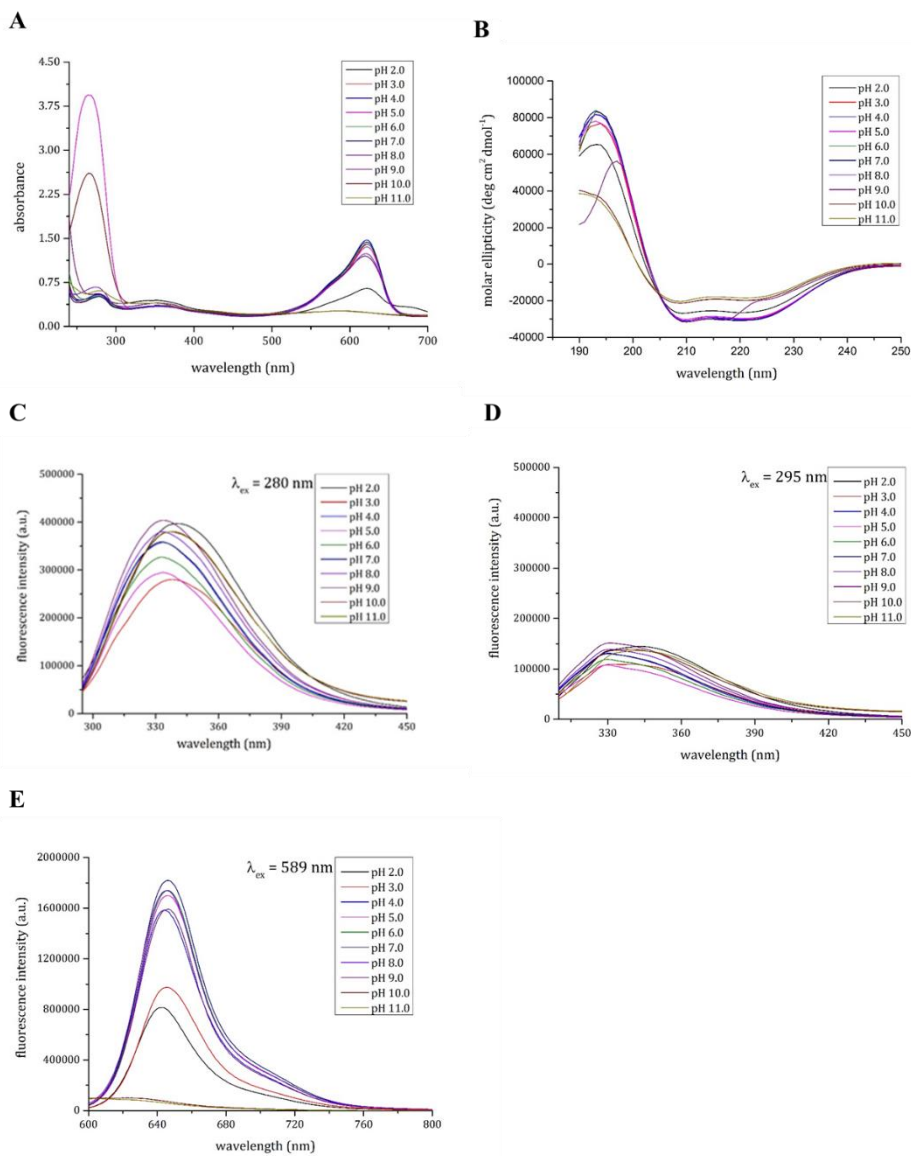


Figure 3. UV-Vis absorption spectra. A: far-UV CD spectra; **B:** intrinsic fluorescence spectra upon excitation at 280 nm; **C:** intrinsic fluorescence spectra upon excitation at 295 nm; **D:** intrinsic fluorescence spectra upon excitation at 589 nm; **E:** GpPC as a function of pH at 25°C. Protein concentration: 0.2 mg/mL.

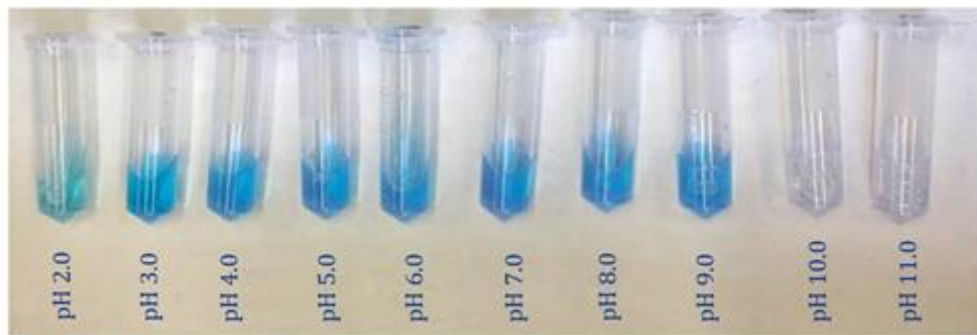


Figure 4. Images of GpPC solution at different pHs. The loss of colour of GpPC is due to the loss of the chromophore.

The effect of different concentrations of an oxidant agent on the structure of GpPC was then evaluated comparing the UV-Vis absorption spectra of the protein upon addition of different concentrations of H_2O_2 (Figure 5).

The presence of hydrogen peroxide induces oxidative stress via reactive oxygen species (ROS) production. Data show that the incubation of the protein with H_2O_2 leads to a slight decrease in the absorption capability of the protein at 620 nm, in agreement with results obtained with C-PCs from *Euhalothece sp.* (Mogany 2019) and *Geitlerinema sp. H8DM* (Patel 2018).

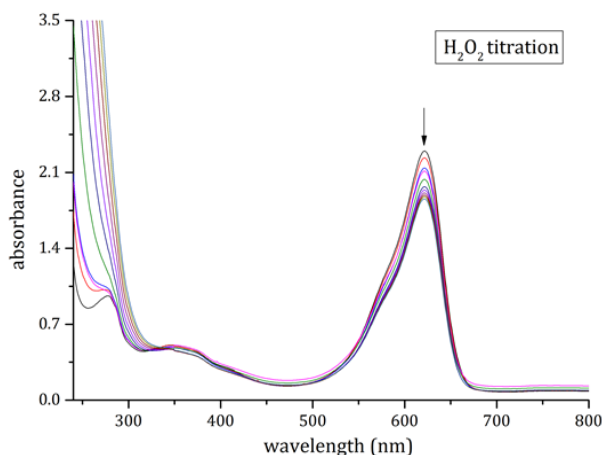


Figure 5. UV-Vis absorption spectra of GpPC upon addition of increasing amounts of H₂O₂. Spectra were collected at 25°C in 10 mM sodium acetate buffer, pH 5.0, using protein concentration 0.2 mg/mL.

4.3.4 Stability against temperature

The use of C-PCs as food colorant and in fluorescent applications is hampered by their sensitivity to high temperature. To enhance C-PC thermal stability, stabilizing agents like additives can be used; however, they are toxic for humans (Wu 2016). The stability of GpPC against temperature was analysed by following CD signal intensity at 222 nm at pH 5.0, 7.0 and 10.0 from 25°C to 95°C (Figure 6). Protein irreversibly denatures during thermal unfolding: spectra collected at 25°C after the thermal treatment indicate that the protein does not re-acquire the secondary structure that loses at high temperatures upon cooling. The inspection of the unfolding curves suggests that the thermal denaturation of the protein is a two-state process. At pH 5.0, the melting temperature (T_m) of the transition, i.e. the temperature at which 50% of GpPC is denatured, is $85\pm 1^\circ\text{C}$. T_m at pH 5.5 and at pH 7.0 is $87\pm 1^\circ\text{C}$. The thermostability is lower at pH 10.0, where T_m is $52\pm 1^\circ\text{C}$.

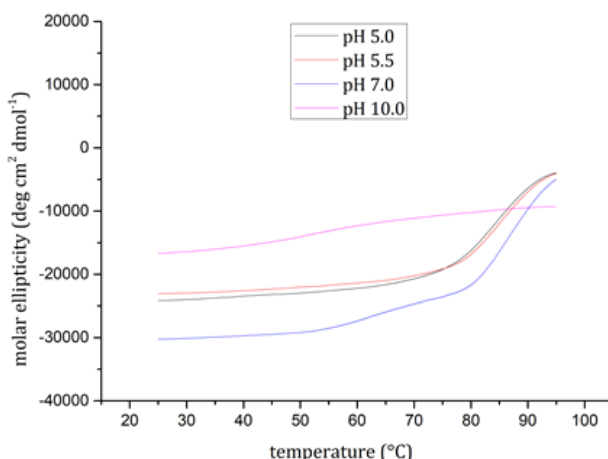


Figure 6. Thermal unfolding curves of GpPC as followed by molar ellipticity values at 222 nm. Heating rate was 1.0°C/min. Measurements were carried out in 10 mM sodium acetate buffer at pH 5.0, 10 mM Tris-HCl buffer at pH 7.0, 10 mM CAPS at pH 10.0, using protein concentration 0.2 mg/mL

This is in line to what happens with the protein from cyanobacterium *Spirulina platensis* (which shows T_m values of 61.8, 57.5 and 49.9°C at pH 5.0, 7.0 and 9.0, respectively) (Martelli 2014) and in agreement with the accepted idea that C-PCs have maximum stability between pH 5.0 and 7.0 (Chaiklahan 2012). Notably, at pH 5.0 and 7.0, the thermostability of the protein is sensibly higher than that observed for C-PCs from the mesophilic *Spirulina sp.* (47°C) (Chaiklahan 2012), from *Euhalothece sp.* (55°C) (Mogany 2019) and *Chroomonas sp.* (about 55°C) (Edwards 1997), from the psychrophilic source *Arctic cyanobacterium* (56°C) (Su 2007), from *C. caldarium* (65°C) (Eisele 2000) and *P. luridum* (about 62°C) (Edwards 1996; Edwards 1997), from *S. platensis* (72°C) (Su 2017), from the thermophilic sources *G. sulphuraria* (up to 60°C) (Moon 2014) and *S. lividus* (about 82°C) (Edwards 1996).

Tertiary structure loss of GpPC induced by temperature was then investigated by collecting intrinsic fluorescence spectra at different temperatures upon excitation at 295 nm at pH 5.0 (Figure 7A). When the temperature was increased, GpPC fluorescence spectra upon excitation at 295 nm showed a red-shift of the maximum emission wavelength and a decrease of the signal intensity. In particular, up to 75°C, the maximum emission wavelength of GpPC (333-334 nm) is close to that found at 20°C (333-334 nm), suggesting that the protein retains its tertiary structure up to this temperature.

At a temperature higher than 77.5°C, GpPC tertiary structure starts to unfold. The apparent melting temperature T_m of the protein tertiary structure is 87°C, in perfect agreement with data obtained by CD (Figure 8). This finding indicates a simultaneous collapse of the secondary and tertiary structure of the protein during thermal unfolding. To evaluate the effect of high temperature on the chromophore fluorescence, emission spectra were also collected as function of temperature upon excitation at 589 nm (Figure 7B). Interestingly, spectra do not show changes in the maximum emission wavelength at different temperatures, although a significant reduction of fluorescence intensity is observed. At temperature higher than 85°C, emission is no longer observed, suggesting loss of the chromophore. Overall, these features could be an advantage for the potential use of GpPC in the food industry. These results motivate us to perform further tests (that could be helpful for specific applications) that evaluated the protein resistance at high temperatures.

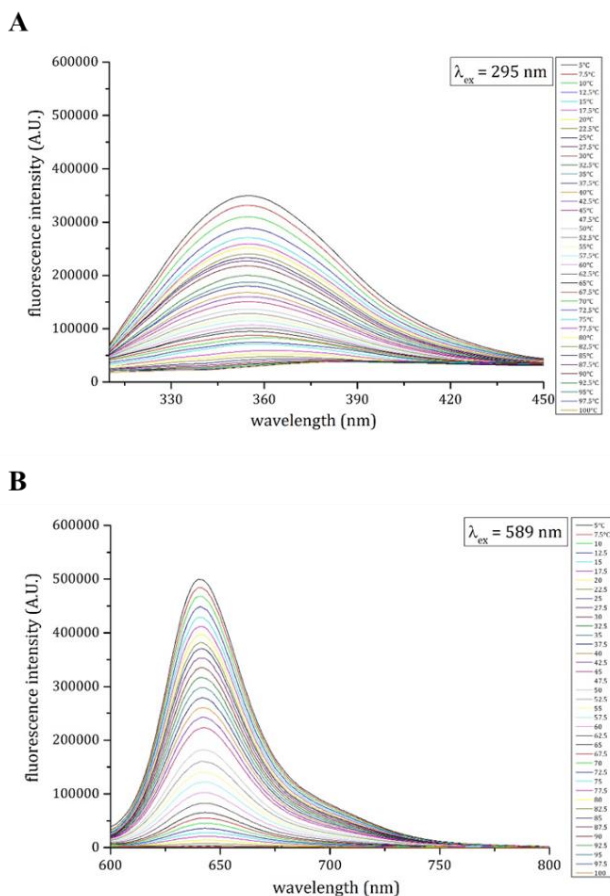


Figure 7. Fluorescence spectra of GpPC recorded at different temperatures at protein concentration 0.2 mg/mL in 10 mM sodium acetate pH 5.0, upon excitation using (A) $\lambda_{\text{ex}} = 295$ nm; (B) $\lambda_{\text{ex}} = 598$ nm.

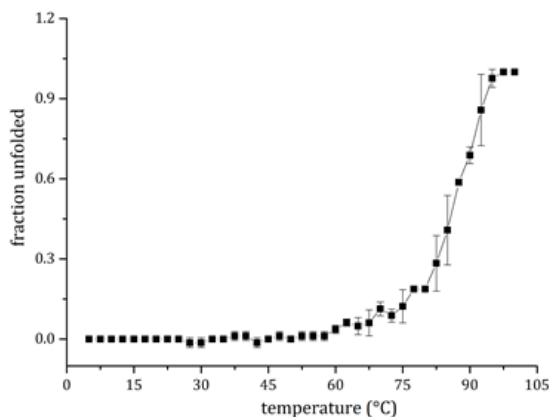


Figure 8. Fraction of protein unfolded shown as a function of temperature. Unfolding has been monitored by intrinsic tryptophan fluorescence. Spectra were collected in 10 mM sodium acetate buffer, pH 5.0, using protein concentration 0.2 mg/mL upon excitation at 295 nm.

To study the kinetics of GpPC denaturation process at pH 5.0 at high temperatures, CD spectra have been collected periodically at 75°C as a function of time (Figure 9). Surprisingly, GpPC shows CD spectra that are typical of a folded protein for more than 1 h at 75°C, although the prolonged exposure at this temperature results in fading of the blue colour with time. It is noteworthy that at this temperature, most of C-PCs undergo to rapid unfolding. For example, C-PC from *S.platensis* has a half-life ($t_{1/2}$) of 16 min at pH 7.0 and of 42 min at pH 5.0 at 75°C (Wu 2016), while, according to Chaiklahan, CP-C from *Spirulina sp.* precipitates at pH 5.0 and 6.0 after incubation at temperatures higher than 59°C for 15 min, and it precipitates at pH 7.0 after 30 min at 64°C (Chaiklahan 2012). Thus, GpPC appears much more resistant at high temperatures when compared to previously isolated C-PCs.

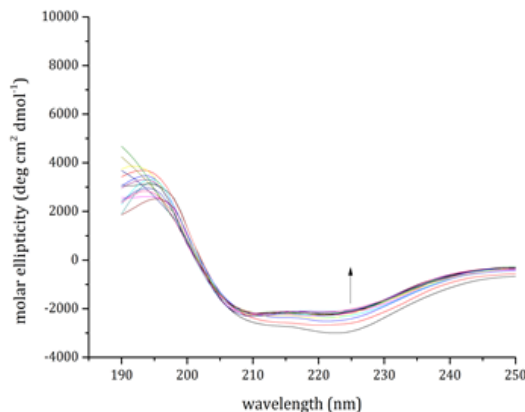


Figure 9. Far-UV CD spectra of GpPC at 75°C as a function of time. Spectra were collected in 10 mM sodium acetate buffer, pH 5.0, using protein concentration 0.2 mg/mL.

4.3.5 Antioxidant activity of GpPC

Recently, it has been reported that pure GpPC is an excellent antioxidant, as it is able to protect cells from UVA damages (Imbimbo 2019). To verify if high temperature treatments affect the bioactivity of GpPC, a comparison between the antioxidant activity of GpPC and that of pasteurized GpPC, which was heated at 75°C for 10 min, was performed. Cells were incubated for 2 h prior to UVA exposure with 0.4 μ M of either GpPC or GpPC after pasteurization. At the end of this experiment, ROS levels were measured by using 2',7'-dichlorodihydrofluorescein diacetate (H₂-DCFDA). As shown in Figure 10, no alteration in ROS levels was observed when cells were incubated with the two molecules (white and grey bars), whereas a significant increase in ROS levels was observed when cells were exposed to UVA irradiation (black bars).

Overall, these findings suggest that GpPC is commercially more competitive than the other C-PCs investigated up to now as it remains practically intact, both from physico-chemical and biological point of view, after high temperature treatments, like in the pasteurization process (Grant 2002).

These findings suggest a possible use of GpPC in food industry. C-PC contained in the extract from *Arthrospira platensis* (ApPC) has received the approval from FDA and EFSA and is currently used as food colorant (Code of Federal Regulation 2016, https://www.govregs.com/regulations/title21_chapterI_part73_subpart

A_section73.530), but this protein has a limited thermostability (denaturation above 60 °C) (Martelli 2014). The high thermostability of GpPC renders this protein an interesting alternative to ApPC.

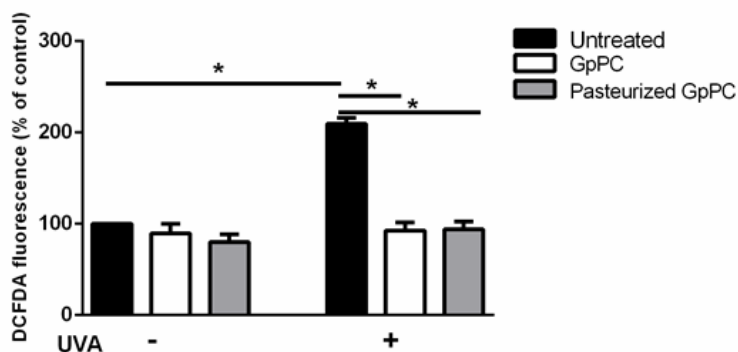


Figure 10. Comparison of antioxidant activity between GpPC and pasteurized GpPC on UVA-stressed HaCaT cells. Intracellular ROS levels were determined by DCFDA assay. Cells were pre-incubated in the presence of 0.4 μ M of GpPC (white bars) and 0.4 μ M of pasteurized GpPC (grey bars) for 2 h, prior UVA irradiation (100 J/cm²). Black bars refer to untreated cells in the absence (-) or in the presence (+) of UVA. Values are expressed as percentage with respect to control (i.e. untreated) cells. Data are shown as means \pm standard deviation (S.D.). Three independent measurements were carried out. * indicates $p < 0.05$.

4.3.6 Cytotoxic activity of GpPC

As it is known that antioxidants can potentially exert anticancer activity, the cytotoxicity of GpPC was evaluated on two cancer cell lines (A431 and SVT2 cells) and on two immortalized cell lines (Balb/c 3T3 and HaCaT cells). The cells were incubated for 72 h with increasing concentrations of GpPC and cell viability was evaluated by the MTT assay at the end of the experiment. The results are reported in Figure 11 and show typical dose–response curves for cancer cells and no significant toxicity on immortalized cells. Indeed, it was not possible to determine the IC₅₀ values, which correspond to the protein concentration able to inhibit cell growth by 50%, for non-cancer cells. As reported in Table 4, the IC₅₀ values determined for cancer cells are significantly lower than those reported in literature for other C-PCs (Safei 2019; Liu 2016; Ying 2016). C-PC isolated from *Limnothrix* sp. NS01 is toxic on MCF-7 cells, with an IC₅₀ of 4.52 μ g/ μ L (about 50 μ M) after 72h exposure, but not toxic against primary fibroblasts (Safei 2019), whereas C-PC isolated from *Spirulina pl.* shows IC₅₀ values

within the range 133.6-163.8 μM after 48 h exposure on human cancer SKOV-3 cells (Liu 2016; Ying 2016).

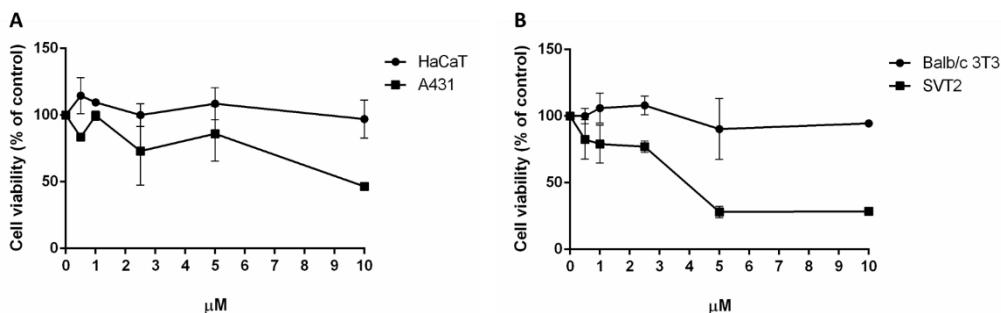


Figure 11. Dose-response curves of immortalized and cancer cell lines after 72 h incubation with increasing concentrations of GpPC (0.5 – 10 μM). A: HaCaT (black circles) and A431 (black squares). B: BALB/c 3T3 (black circles) and SVT2 (black squares) cells. Cell viability was assessed by the MTT assay and cell survival expressed as percentage of viable cells in the presence of the lipophilic extract under test, with respect to control cells grown in the absence of the extract. Data are shown as means \pm S.D. Three independent measurements were carried out.

Table 4. Cytotoxicity of GpPC expressed as the protein concentration (μM) able to inhibit cell growth by 50% (IC_{50} value), after 72h of incubation.

Cell line	IC_{50} (μM)
HaCaT	N.D.
A431	9.8 \pm 0.07
BALB/c 3T3	N.D.
SVT2	3.7 \pm 0.14

4.4 Conclusions

C-PCs have attracted the interest of the scientific community for several reasons. They can be used as food colorant and are able to exert numerous biological activities of interest for pharmaceutical and biomedical research. Here, a comprehensive biophysical study of C-phycoerythrin from the rare red microalga *Galdieria phlegrea*, including the determination of the primary sequence, a study on thermal stability

and of the antioxidant and cytotoxic activity of the protein, is reported. GpPC structure is not significantly influenced by the pH within the range 4.0-9.0, while it appears to be affected by highly acid or basic values. GpPC presents an intense absorption at 620 nm and emits at 646-650 nm, when excited at 589 nm at 25°C. Compared to its counterparts from mesophilic and even thermophilic sources (*G. sulphuraria* and *C. caldarium*), GpPC has a high thermal stability, with T_m values > 80°C at pH 5.0 and 7.0. The protein exhibits an interesting antioxidant activity even after pasteurization, as well as a high antitumor activity, selective for malignant cells. These unique features make GpPC a probable candidate for future applications in food and pharmaceutical industries.

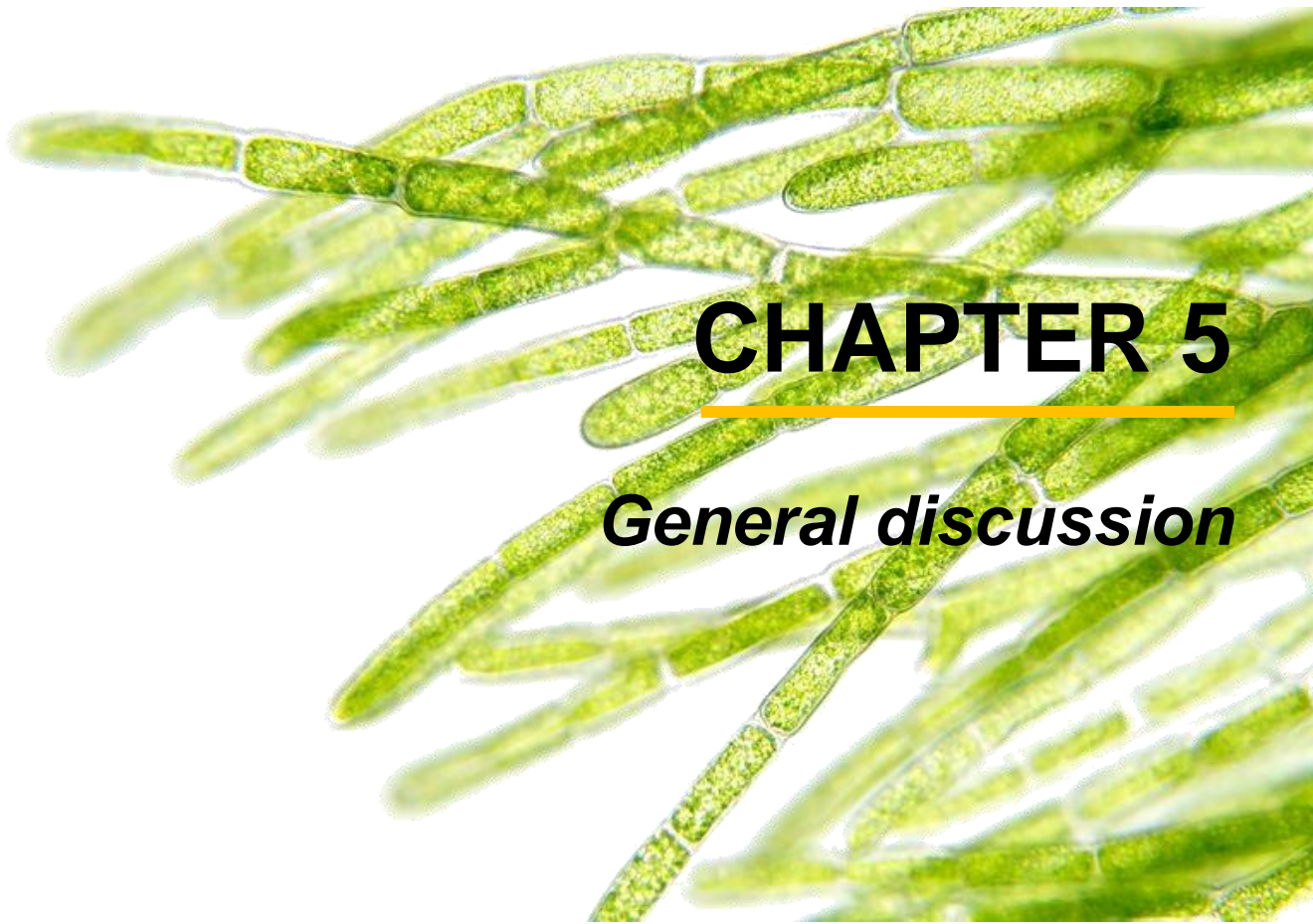
4.5 References

- Adir, N., & Lerner, N. (2003). The crystal structure of a novel unmethylated form of C-phycoyanin, a possible connector between cores and rods in phycobilisomes. *Journal of Biological Chemistry*, 278(28), 25926-25932.
- Bennett, A., & Bogorad, L. (1971). Properties of subunits and aggregates of blue-green algal biliproteins. *Biochemistry*, 10(19), 3625-3634.
- Chaiklahan, R., Chirasuwan, N., & Bunnag, B. (2012). Stability of phycoyanin extracted from *Spirulina* sp.: influence of temperature, pH and preservatives. *Process Biochemistry*, 47(4), 659-664.
- Edwards, M. R., MacColl, R., & Eisele, L. E. (1996). Some physical properties of an unusual C-phycoyanin isolated from a photosynthetic thermophile. *Biochimica et Biophysica Acta (BBA)-Bioenergetics*, 1276(1), 64-70.
- Edwards, M. R., Hauer, C., Stack, R. F., Eisele, L. E., & MacColl, R. (1997). Thermophilic C-phycoyanin: effect of temperature, monomer stability, and structure. *Biochimica et Biophysica Acta (BBA)-Bioenergetics*, 1321(2), 157-164.
- Eisele, L. E., Bakhru, S. H., Liu, X., MacColl, R., & Edwards, M. R. (2000). Studies on C-phycoyanin from *Cyanidium caldarium*, a eukaryote at the extremes of habitat. *Biochimica et Biophysica Acta (BBA)-Bioenergetics*, 1456(2-3), 99-107.
- Fernández-Rojas, B., Medina-Campos, O. N., Hernández-Pando, R., Negrette-Guzmán, M., Huerta-Yepez, S., & Pedraza-Chaverri, J. (2014). C-phycoyanin prevents cisplatin-induced nephrotoxicity through inhibition of oxidative stress. *Food & function*, 5(3), 480-490.
- Gasteiger, E., Hoogland, C., Gattiker, A., Wilkins, M. R., Appel, R. D., & Bairoch, A. (2005). Protein identification and analysis tools on the ExPASy server. In *The proteomics protocols handbook* (pp. 571-607). *Humana Press*.
- Gingrich, J. C., Lundell, D. J., & Glazer, A. N. (1983). Core substructure in cyanobacterial phycobilisomes. *Journal of Cellular Biochemistry*, 22(1), 1-14.

- Glauser, M., Stirewalt, V. L., Bryant, D. A., Sidler, W., Zuber, H. (1992). Structure of the genes encoding the rod-core linker polypeptides of *Mastigocladus laminus* phycobilisomes and functional aspects of the phycobiliprotein/linker-polypeptide interactions. *European Journal of Biochemistry*, 205(3), 927-937
- Glazer, A. N., & Cohen-Bazire, G. (1971). Subunit structure of the phycobiliproteins of blue-green algae. *Proceedings of the National Academy of Sciences*, 68(7), 1398-1401.
- Glazer, A. N. (1985). Light harvesting by phycobilisomes. *Annual Review of Biophysics and Biophysical Chemistry*, 14(1), 47-77.
- Grant, I. R., Hitchings, E. I., McCartney, A., Ferguson, F., & Rowe, M. T. (2002). Effect of commercial-scale high-temperature, short-time pasteurization on the viability of *Mycobacterium paratuberculosis* in naturally infected cows' milk. *Applied Environmental Microbiology*, 68(2), 602-607.
- Grossman, A. R., Schaefer, M. R., Chiang, G. G., & Collier, J. L. (1993). The phycobilisome, a light-harvesting complex responsive to environmental conditions. *Microbiology and Molecular Biology Reviews*, 57(3), 725-749.
- Imbimbo, P., Romanucci, V., Pollio, A., Fontanarosa, C., Amoresano, A., Zarrelli, A., Olivieri, G., Monti, D. M. (2019). A cascade extraction of active phycocyanin and fatty acids from *Galdieria phlegrea*. *Applied Microbiology and Biotechnology*, 103(23-24), 9455-9464.
- Jiang, L., Wang, Y., Liu, G., Liu, H., Zhu, F., Ji, H., & Li, B. (2018). C-Phycocyanin exerts anti-cancer effects via the MAPK signaling pathway in MDA-MB-231 cells. *Cancer Cell International*, 18(1), 12.
- Jiang, L., Wang, Y., Yin, Q., Liu, G., Liu, H., Huang, Y., & Li, B. (2017). Phycocyanin: A potential drug for cancer treatment. *Journal of Cancer*, 8(17), 3416.
- Kirst, H., Formighieri, C., & Melis, A. (2014). Maximizing photosynthetic efficiency and culture productivity in cyanobacteria upon minimizing the phycobilisome light-harvesting antenna size. *Biochimica et Biophysica Acta (BBA)-Bioenergetics*, 1837(10), 1653-1664.
- Kumar Singh, N., S Hasan, S., Kumar, J., Raj, I., A Pathan, A., Parmar, A., Shakil, S., Gourinath, S., Madamwar, D. (2014). Crystal structure and interaction of phycocyanin with β -secretase: A putative therapy for Alzheimer's disease. *CNS & Neurological Disorders-Drug Targets (Formerly Current Drug Targets-CNS & Neurological Disorders)*, 13(4), 691-698.
- Kuddus, M., Singh, P., Thomas, G., & Al-Hazimi, A. (2013). Recent developments in production and biotechnological applications of C-phycoyanin. *BioMed Research International*, 2013.
- Liu, Q., Huang, Y., Zhang, R., Cai, T., & Cai, Y. (2016). Medical application of *Spirulina platensis* derived C-phycoyanin. *Evidence-Based Complementary and Alternative Medicine*, 2016.

- MacColl, R. (1998). Cyanobacterial phycobilisomes. *Journal of Structural Biology*, 124(2-3), 311-334.
- Martelli, G., Folli, C., Visai, L., Daglia, M., & Ferrari, D. (2014). Thermal stability improvement of blue colorant C-Phycocyanin from *Spirulina platensis* for food industry applications. *Process Biochemistry*, 49(1), 154-159.
- Micsónai, A., Wien, F., Bulyáki, É., Kun, J., Moussong, É., Lee, Y. H., Goto, Y., Réfrégiers, M., Kardos, J. (2018). BeStSel: a web server for accurate protein secondary structure prediction and fold recognition from the circular dichroism spectra. *Nucleic Acids Research*, 46(W1), W315-W322.
- Mogany, T., Kumari, S., Swalaha, F. M., & Bux, F. (2019). Extraction and characterisation of analytical grade C-phycoerythrin from *Euhalothece sp.* *Journal of Applied Phycology*, 31(3), 1661-1674.
- Moon, M., Mishra, S. K., Kim, C. W., Suh, W. I., Park, M. S., & Yang, J. W. (2014). Isolation and characterization of thermostable phycocyanin from *Galdieria sulphuraria*. *Korean Journal of Chemical Engineering*, 31(3), 490-495.
- O'carra, P., & Killilea, S. D. (1971). Subunit structures of C-phycoerythrin and C-phycoerythrin. *Biochemical and biophysical research communications*, 45(5), 1192-1197.
- Patel, A., Mishra, S., Pawar, R., & Ghosh, P. K. (2005). Purification and characterization of C-Phycocyanin from cyanobacterial species of marine and freshwater habitat. *Protein Expression and Purification*, 40(2), 248-255.
- Patel, H. M., Rastogi, R. P., Trivedi, U., & Madamwar, D. (2018). Structural characterization and antioxidant potential of phycocyanin from the cyanobacterium *Geitlerinema sp.* H8DM. *Algal research*, 32, 372-383.
- Patil, G., Chethana, S., Sridevi, A. S., & Raghavarao, K. S. M. S. (2006). Method to obtain C-phycoerythrin of high purity. *Journal of Chromatography A*, 1127(1-2), 76-81.
- Pentón-Rol, G., Lagumersindez-Denis, N., Muzio, L., Bergami, A., Furlan, R., Fernández-Massó, J. R., Polentarutti, N. (2016). Comparative neuroregenerative effects of C-phycoerythrin and IFN-beta in a model of multiple sclerosis in mice. *Journal of Neuroimmune Pharmacology*, 11(1), 153-167.
- Petruk, G., Raiola, A., Del Giudice, R., Barone, A., Frusciante, L., Rigano, M. M., & Monti, D. M. (2016). An ascorbic acid-enriched tomato genotype to fight UVA-induced oxidative stress in normal human keratinocytes. *Journal of Photochemistry and Photobiology B: Biology*, 163, 284-289.
- Pleonsil, P., Soogarun, S., & Suwanwong, Y. (2013). Anti-oxidant activity of holo- and apo-c-phycoerythrin and their protective effects on human erythrocytes. *International Journal of Biological Macromolecules*, 60, 393-398.

- Piron, R., Bustamante, T., Barriga, A., & Lagos, N. (2019). Phycobilisome isolation and C-phycoyanin purification from the cyanobacterium *Aphanizomenon gracile*. *Photosynthetica*, 57(2), 491-499.
- Raposo de Jesus, M. F., de Morais, R. M. S. C., & de Morais, A. M. M. B. (2013). Health applications of bioactive compounds from marine microalgae. *Life Sciences*, 93(15), 479-486.
- Safaei, M., Maleki, H., Soleimanpour, H., Norouzy, A., Zahiri, H. S., Vali, H., & Noghabi, K. A. (2019). Development of a novel method for the purification of C-phycoyanin pigment from a local cyanobacterial strain *Limnothrix sp.* NS01 and evaluation of its anticancer properties. *Scientific Reports*, 9(1), 1-16.
- Stec, B., Troxler, R. F., & Teeter, M. M. (1999). Crystal structure of C-phycoyanin from *Cyanidium caldarium* provides a new perspective on phycobilisome assembly. *Biophysical Journal*, 76(6), 2912-2921.
- Storf, M., Parbel, A., Meyer, M., Strohmam, B., Scheer, H., Deng, M. G., Zheng, M., Zhou, M., Zhao, K. H. (2001). Chromophore attachment to biliproteins: Specificity of PecE/PecF, a lyase-isomerase for the photoactive 31-Cys- α 84- phycoviolobilin chromophore of phycoerythrocyanin. *Biochemistry*, 40(41), 12444-12456.
- Su, H. N., Wang, Q. M., Li, C. Y., Li, K., Luo, W., Chen, B., Zhang, X.Y., Qin, Q.L., Zhou, B.C., Chen, X.L., Zhang, Y.Z., Xie B.B. (2017). Structural insights into the cold adaptation of the photosynthetic pigment-protein C-phycoyanin from an Arctic cyanobacterium. *Biochimica et Biophysica Acta (BBA)-Bioenergetics*, 1858(4), 325-335.
- Watanabe, M., Semchonok, D. A., Webber-Birungi, M. T., Ehira, S., Kondo, K., Narikawa, R., Ohmori, M., Boekema, E.J., Ikeuchi, M. (2014). Attachment of phycobilisomes in an antenna-photosystem I supercomplex of cyanobacteria. *Proceedings of the National Academy of Sciences*, 111(7), 2512-2517.
- Wu, H. L., Wang, G. H., Xiang, W. Z., Li, T., & He, H. (2016). Stability and antioxidant activity of food-grade phycocyanin isolated from *Spirulina platensis*. *International Journal of Food Properties*, 19(10), 2349-2362.
- Ying, J., Wang, J., Ji, H., Lin, C., Pan, R., Zhou, L., Yulong, S., Zhang, E., Ren, P., Chen, J., Liu, Q., Xu, T., Yi, H., Li, J., Bao, Q., Hu, Y., Li, P. (2016). Transcriptome analysis of phycocyanin inhibitory effects on SKOV-3 cell proliferation. *Gene*, 585(1), 58-64.
- Zhu, C., Ling, Q., Cai, Z., Wang, Y., Zhang, Y., Hoffmann, P. R., Zheng, W., Zhou, T., Huang, Z. (2016). Selenium-containing phycocyanin from Se-enriched *Spirulina platensis* reduces inflammation in dextran sulfate sodium-induced colitis by inhibiting NF- κ B activation. *Journal of Agricultural and Food Chemistry*, 64(24), 5060-5070.



CHAPTER 5

General discussion

5.1 General discussion

The present PhD project was aimed at designing a biorefinery by using a red thermo-acidophilic microalgae, *Galdieria phlegrea* (strain 009). Three different high value bio-products, starting from the one with the highest market value, were extracted by developing a cascade extraction.

To this purpose, the attention was first focused on the design of a feasible process at lab-scale to obtain two different high-value molecules starting from the wet biomass of *Galdieria phlegrea*: phycocyanin (PC) and PUFAs. First, proteins were extracted in aqueous buffer by a high-pressure procedure and PC was isolated to a very high purity level by a single purification step. By this way, the antioxidant activity of PC was fully preserved as it was able to protect cells from UVA-induced damages. Then, the second step of the biorefinery was focused on lipids extraction starting from the residual biomass. Lipids were fractionated and PUFAs characterized. Interestingly, the amount of isolated PUFAs obtained from the broken biomass was higher than that obtained from the raw biomass, suggesting an efficient biorefinery.

To further valorize the algal biomass, the biorefinery design was integrated with the principles of green chemistry. The new set up of the green biorefinery consisted in three sequential steps, which combined a conventional extraction in aqueous medium and two innovative procedures:

1. High pressure extraction to recover PC;
2. Pressurized Liquid Extraction (PLE) to extract carotenoids;
3. Supercritical Fluid Extraction (SFE) to obtain lipids.

Compared to conventional organic solvents extractions performed on the same biomass, this combination allowed achieving higher yields of carotenoids and lipids by using GRAS (Generally Recognized As Safe) solvents, in shorter time and with less solvent consumption. The carotenoid fraction contained β -carotene and zeaxanthin, and the mixture extracted showed high antioxidant activity, the same observed by combining the two commercial antioxidants. This clearly indicates that PLE does not affect the biological activity of the extracted molecules. Interestingly, the carotenoids extracted were able to prevent the production of intracellular ROS after the induction of oxidative stress and to activate the Nrf-2 pathway, which is normally involved in the stress response.

Finally, a complete biophysical and biochemical characterization of PC from *G. phlegrea* was carried out. In particular, the primary sequence was determined, and the stability of the protein was analyzed. PC revealed to possess a very high stability up to 85°C and in a wide range of pH (4.0-9.0). Thus, it was not surprising to verify that PC retained its antioxidant activity also after thermal pasteurization. Finally, PC showed a high and selective antitumor activity for cancer cell lines.

The set up of the biorefinery machine allows valorizing many of the active molecules present in *G. phlegrea*. This approach could be easily scaled up at industrial level, as all the procedures are economic and compatible with industrial machines. Indeed, the obtained results could also contribute to increase the revenue streams of the process, thus compensating the large cultivation and downstream costs for biomass production. This could lead to a positive economic balance of the microalgae biorefinery. Furthermore, the development of a green process could also increase the social acceptance of industrial microalgal products.

Despite the achieved results are encouraging, there are still many issues that hinder the full exploitation of microalgae: (i) social impact; (ii) control of growth parameters; (iii) extraction techniques; (iv) the overall costs.

Social impact. The first problem to be overcome with microalgae is the social acceptance of microalgae products. To date, microalgae have been commercialized only as “functional food” (Nethravathy 2019). Currently, the microalgae market is dominated by *Spirulina* as dried whole alga or as supplement in food and beverage and by *Chlorella* as dried whole algae. *Dunaliella salina* is cultivated to extract carotenoids, *Haematococcus pluvialis* for the production of astaxanthin, *Cryptocodinium cohnii* and *Shizochytrium* for the production of DHA (Garcia 2017). According to Future Market Insights, in 2017 the market for Spirulina powder was estimated to be US\$ 220.5 million and is expected to increase over US\$ 380 million by the end of 2027, at a CAGR (Compound Annual Growth Rate) of 5.9%. Whereas, the growth prospect in food and beverage segment will be at a CAGR of 6.9%. The PC market is constantly growing and is expected to reflect 1.8 times increase in revenue growth from 2017 to 2025. In 2018, PC market was valued at US\$ 112.3 million and is predicted to be valued at US\$ 232.9 million with CAGR of 7.2% by 2025. The powder segment of PC will emerge as a global leader with US\$114 million market cap between 2018 and 2028. When compared to the global market of food and feed products derived from all the other sources, the market

portfolio of microalgae-based products is still smaller, but increasing steadily (Nethravathy 2019).

Control of growth parameters. Another bottleneck that inhibits microalgae exploitation at large-scale production is the control of the growth parameters and the problem of contaminations. At industrial scale, microalgal cultures are generally carried out in open ponds or photobioreactors (PBRs). PBRs are closed systems that allow controlling the cultivation parameters and obtaining higher productivity yields. Open ponds are uncontrolled outdoor systems that do not allow a good productivity. Despite PBRs result to be the most efficient cultivation method, to date, open pond systems are the most widely employed systems for industrial purpose. This is due to several reasons: (i) a low initial investment, (ii) a low power demand, (iii) low operating and maintenance costs (Gonzales 2011). In this context, extremophile microorganisms have gained much interest, since they have the ability to live and thrive stressful conditions, such as heavy metals concentration, acidic environments (pH 1.0-3.0) or high temperatures ($> 50^{\circ}\text{C}$) (Varshney 2015). Extremophile microalgae represent thus excellent candidates for large-scale production in open pond systems in which the risk of contaminations is very low (Sydney 2019).

Extraction techniques. The selection of the right extraction procedure to be employed is another important issue to be considered. In fact, the molecules obtained from the biomass have to be biologically active and dissolved in a fully biocompatible buffer. Currently, conventional extraction techniques are used, but they involve organic solvents, such as chloroform, acetone, methanol and diethyl ether (Saini and Keum 2018). The conventional solvent extraction usually requires large amounts of solvent, long extraction times and needs a dried biomass as a starting material. All these factors strongly increase the costs of the downstream processes.

Recently, the demand for greener, safer and natural products that do not require the involvement of toxic solvents, increased. Green chemistry is aimed at preserving the environment and human health by promoting the use and reuse of natural resources and by limiting or completely avoid the use of toxic organic solvents. The development of green extraction procedures to recover active compounds represents a significant advance, as no toxic solvents are needed, thus minimizing the environmental impact. Moreover, they allow to reduce the extraction time and to improve the extraction yields, without affecting the biological activity.

In this scenario, compressed fluid extractions are considered valuable green alternatives to conventional extractions. Compressed fluid extractions include Sub-critical Water Extraction (SWE), Pressurized Liquid Extraction (PLE), and Supercritical Fluid Extraction (SFE). SFE operates at temperature and pressure above the critical point of the solvent selected. These conditions allow increasing the diffusivity of the solvent, thus improving the penetration of the solvent into the matrix. On the other hand, the solvents involved in PLE and SWE are maintained at a temperature above the boiling point and at a pressure high enough to keep fluids in their liquid states. Besides the differences among these techniques, they all share a small amount of GRAS solvents to perform extractions, without affecting the bioactivity or the chemical structure (Herrero and Ibañez 2018). The main disadvantage of these procedures are the high costs to build the equipment.

Among innovative techniques, in the last years other promising approaches have been investigated. Microwave Assisted Extraction (MAE) is a technique for the extraction of pigments, lipids and other bioactive molecules which involves the use of microwaves to heat up the solvents in contact with the cell (Juin 2015). The heating is caused by two phenomena: dipole rotation and ionic conduction, which may happen individually or simultaneously (Tatke and Jaiswal 2011). MAE is generally performed in closed system to avoid the dissipation of the heat. By this way, the heating mechanism is targeted and selective, thus reducing the extraction time and improving the yield. However, the main limitation of this method is that the high temperature required may affect the bioactivity of the extracted molecules.

Ionic Liquids (ILs) are organic solution of salts that can melt at mild temperature (<100°C). They are typically composed of a large number of inorganic or organic cations. ILs are characterized by synthetic flexibility and thermal stability. Moreover, they are non-volatile and non-flammable (Harris 2018; Vekariya 2017). These features make them attractive as alternatives to volatile organic solvents. They are generally employed for lipid extraction, however, to date, only limited papers are available in literature (Motlagh 2019). One of the main drawbacks of ILs is the unrealistic application at industrial scale, due to their costs and the environmental impact (Zhang 2008). Many ILs have been proved to be not harmful for humans, however, their synthesis involves many steps that require expensive, toxic and volatile reagents (Harris 2018). Switchable Solvents (SSs) represent a second generation of ILs. First reported by Philipp Jessop (Jessop 2005), SSs are non-volatile liquids able to convert their characteristics from

hydrophobic to hydrophilic state and *vice-versa* in response to an external stimulus, such as a change in temperature or pH and/or the addition or removal of a gas (i.e. CO₂) (Yook 2019; Al-Ameri and Al-Zuhair 2019). This unique “switching” property allows performing cascade extractions of high value molecules and to recover and reuse the solvent. For this reason, SSs are considered economically competitive as their sustainability rely only in the low energy consumption (Clarke 2018; Pollet 2011). However, the solvent selection points out one of the main problems related to this procedure. The properties of SSs may be improved by incorporating functional groups into the structure during the chemical synthesis. Obviously, this makes the preparation difficult as well as it may affect the costs (Clarke 2018). For this reason, the solvents used in this kind of extraction are generally amines, whose synthesis is less expensive, but not environmentally friendly (Schuur 2019).

Overall costs. Despite the strategic relevance of bio-based products for many industries, numerous technological and strategic challenges still hamper the commercial industrialization of microalgae. Overall, many evidence of the effectiveness of individual steps of biorefinery are reported in literature, but very few attempts have been faced to set up entire processes. Furthermore, the companies should conform to the social and environmental needed to gain public acceptance. To date, conventional crop-biorefinery costs represent the 20-40% of the whole process costs. These costs can increase up to 60% for the algae-based biorefinery (Lam 2018; Caporgno and Mathys 2018).

To reduce costs, simple processes that require only few unit operations should be developed, keeping in mind that the technologies tailored for a single unit operation should always be followed by an evaluation of the impact on the overall process.

In conclusion, the complete valorization of microalgae biomass by a well-integrated platform would facilitate the transition from lab-scale to large-scale production, thus making green biorefineries a strong reality.

5.2 References

- Al-Ameri, M., Al-Zuhair, S. (2019). Using switchable solvents for enhanced, simultaneous microalgae oil extraction-reaction for biodiesel production. *Biochemical Engineering Journal*, 141, 217-224.
- Caporgno, M. P., Mathys, A. (2018). Trends in microalgae incorporation into innovative food products with potential health benefits. *Frontiers in Nutrition*, 5.
- Clarke, C. J., Tu, W. C., Levers, O., Bröhl, A., Hallett, J. P. (2018). Green and sustainable solvents in chemical processes. *Chemical Reviews*, 118(2), 747-800.
- García, J. L., de Vicente, M., Galán, B. (2017). Microalgae, old sustainable food and fashion nutraceuticals. *Microbial Biotechnology*, 10(5), 1017-1024.
- González-Delgado, Á. D., Kafarov, V. (2011). Microalgae based biorefinery: Issues to consider. *CT&F-Ciencia, Tecnología y Futuro*, 4(4), 5-22.
- Harris, J., Viner, K., Champagne, P., Jessop, P. G. (2018). Advances in microalgal lipid extraction for biofuel production: a review. *Biofuels, Bioproducts and Biorefining*, 12(6), 1118-1135.
- Jessop, P. G., Heldebrant, D. J., Li, X., Eckert, C. A., Liotta, C. L. (2005). Green chemistry: Reversible nonpolar-to-polar solvent. *Nature*, 436(7054), 1102.
- Juin, C., Chérouvrier, J. R., Thiéry, V., Gagez, A. L., Bérard, J. B., Joguey, N., Picot, L. (2015). Microwave-assisted extraction of phycobiliproteins from *Porphyridium purpureum*. *Applied Biochemistry and Biotechnology*, 175(1), 1-15.
- Vermuë, M. H., Eppink, M. H. M., Wijffels, R. H., Van Den Berg, C. (2018). Multi-product microalgae biorefineries: from concept towards reality. *Trends in Biotechnology*, 36(2), 216-227.
- Rezaei Motlagh, S., Harun, R., Biak, A., Radiah, D., Hussain, S. A., Wan Ab Karim Ghani, W. A., Elgharbawy, A. A. (2019). Screening of suitable ionic liquids as green Solvents for extraction of Eicosapentaenoic Acid (EPA) from microalgae biomass using COSMO-RS model. *Molecules*, 24(4), 713.
- MU, N., Mehar, J. G., Mudliar, S. N., Shekh, A. Y. (2019). Recent advances in microalgal bioactives for food, feed, and healthcare products: commercial potential, market space, and sustainability. *Comprehensive Reviews in Food Science and Food Safety*, 18(6), 1882-1897.
- Pollet, P., Eckert, C. A., Liotta, C. L. (2011). Switchable solvents. *Chemical Science*, 2(4), 609-614.
- Schuur, B., Brouwer, T., Smink, D., Sprakel, L. M. (2019). Green solvents for sustainable separation processes. *Current Opinion in Green and Sustainable Chemistry*.

- Tatke, P., Jaiswal, Y. (2011). An overview of microwave assisted extraction and its applications in herbal drug research. *Research Journal of Medicinal Plant*, 5(1), 21-31.
- Varshney, P., Mikulic, P., Vonshak, A., Beardall, J., Wangikar, P. P. (2015). Extremophilic micro-algae and their potential contribution in biotechnology. *Bioresource Technology*, 184, 363-372.
- Vekariya, R.L. (2017). A review of Ionic Liquids: applications towards catalytic organic transformations. *Journal of Molecular Liquids* 227: 44–60. <https://doi.org/10.1016/j.molliq.2016.11.123>.
- Do Yook, S., Kim, J., Woo, H. M., Um, Y., Lee, S. M. (2019). Efficient lipid extraction from the oleaginous yeast *Yarrowia lipolytica* using switchable solvents. *Renewable energy*, 132, 61-67.
- Zhang, Y., Bakshi, B. R., Demessie, E. S. (2008). Life cycle assessment of an ionic liquid versus molecular solvents and their applications. *Environmental Science & Technology*, 42(5), 1724-1730.

APPENDIX

List of scientific publication:

I- Petruk, G., Di Lorenzo, F., **Imbimbo, P.**, Silipo, A., Bonina, A., Rizza, L., Piccoli, R., Monti, D.M., Lanzetta, R.: *Protective effect of Opuntia ficus-indica L. cladodes against UVA-induced oxidative stress in normal human keratinocytes*. Bioorg Med Chem Lett. 2017 Dec 15;27(24):5485-5489. doi: 10.1016/j.bmcl.2017.10.043.

II- Boroja, T., Mihailović, V., Katanić, J., Pan, S. P., Nikles, S., **Imbimbo, P.**, & Bauer, R. (2018). *The biological activities of roots and aerial parts of Alchemilla vulgaris L.* South African Journal of Botany, 116, 175-184.

III- Ricciardelli, A., Casillo, A., Papa, R., Monti, D. M., **Imbimbo, P.**, Vrenna, G., Artini, M., Selan, L., Corsaro, M.M., Tutino, M.L., Parrilli, E. (2018). *Pentadecanal inspired molecules as new anti-biofilm agents against Staphylococcus epidermidis*. Biofouling, 34(10), 1110-1120.

IV- Katanić, J., Yousfi, F., Caruso, M. C., Matić, S., Monti, D. M., Loukili, E. H., Boroja, T., Mihailović, V., Galgano, F., **Imbimbo, P.**, Petruk, G., Bouhrim, M., Bnouham, M., Ramdani, M.. *Characterization of bioactivity and phytochemical composition with toxicity studies of different Opuntia dillenii extracts from Morocco*. Food Bioscience, 2019, 30, 100410.

V- Annunziata, A., Cucciolo, M. E., Esposito, R., **Imbimbo, P.**, Petruk, G., Ferraro, G., Pinto, V., Tuzi, A., Monti, D.M., Merlino, A., Ruffo, F.. *A highly efficient and selective antitumor agent based on a glucoconjugated carbene platinum (ii) complex*. Dalton Transactions. 2019, 48, 7794– 7800

VI- Sobeh, M., Petruk, G., Osman, S., El Raey, M. A., **Imbimbo, P.**, Monti, D. M., & Wink, M. (2019). *Isolation of Myricitrin and 3, 5-di-O-Methyl Gossypetin from Syzygium samarangense and Evaluation of their Involvement in Protecting Keratinocytes against Oxidative Stress via Activation of the Nrf-2 Pathway*. Molecules, 24(9), 1839.

VII- **Imbimbo, P.**, Romanucci, V., Pollio, A., Fontanarosa, C., Amoresano, A., Zarrelli, A., Olivieri, G., Monti, D. M.. *A cascade extraction of active phycocyanin and fatty acids from Galdieria phlegrea*. Applied microbiology and biotechnology, 2019, 103(23-24), 9455-9464. (Chapter 2)

VIII- Stanković, J. S. K., Srećković, N., Mišić, D., Gašić, U., **Imbimbo, P.**, Monti, D. M., Mihailović, V.. *Bioactivity, biocompatibility and phytochemical assessment of lilac sage, Salvia verticillata L.(Lamiaceae)-A plant rich in rosmarinic acid.* Industrial Crops and Products, 2019, 143, 111932.

IX- Mihailović, V., Stanković, J. S. K., Jurić, T., Srećković, N., Mišić, D., Šiler, B., Monti, D.M., **Imbimbo, P.**, Nikles, S., Pan, S., Bauer, R. (2019). *Blackstonia perfoliata (L.) Huds. (Gentianaceae): A promising source of useful bioactive compounds.* Industrial Crops and Products, 111974.

X- Del Giudice, R.^ **Imbimbo, P.** ^, Pietrocola, F., Maiuri, M.C., Monti, M.D. *Autophagy alteration in ApoA- related systemic amyloidosis.* **Submitted to Pharmacological Research.**

^These authors equally contributed to this work

XI- **Imbimbo, P.**, Bueno, M., D'Elia, L., Pollio, A., Ibañez, E., Olivieri, G., Monti, D.M. *Green compressed fluid technologies to extract antioxidants and lipids from Galdieria phlegrea in a biorefinery approach.* **Submitted to ACS Sustainable Chemistry & Engineering (Chapter 3)**

XII- Ferraro, G.^, **Imbimbo, P.** ^, Marseglia, A., Illiano, A., Fontanarosa, C., Amoresano, A., Olivieri, G., Pollio, A., Monti, D.M., Merlino, A.. *A thermophilic C-phycoyanin with unprecedented biophysical and biochemical properties.* **Minor revision - International Journal of Biological Macromolecules (Chapter 4)**

^These authors equally contributed to this work

XIII- Annunziata, A., Amoresano, A., Cucciolito, M.E., Esposito, R., Ferraro, G., **Imbimbo, P.**, Iacobucci, I., Lucignano, R., Monti, M., Scognamiglio, C., Tuzi, A., Monti, D.M., Merlino, A., Ruffo, F. *Pt(II) versus Pt(IV) in carbene glycoconjugates antitumor agents: minimal structural variations, great performance changes.* **Major revision- Inorganic Chemistry**

List of scientific communications:

- **Organizing committee** of the II Industrial Biotechnology Congress “*BioID&A: Biotechnology Identity and Application*”. (Naples, October 28, 2019)

- Petruk, G., Del Giudice, R., **Imbimbo, P.**, Di Lorenzo, F., Rigano, M.M., Lanzetta, R., Piccoli, R., Monti, D.M. “*Fighting UVA-induced oxidative stress with natural antioxidant*”. I° GIORNATA S.I.R.R. 2017-NAPOLI (Naples, May 31)

- Petruk, G., Del Giudice, R., **Imbimbo, P.**, Di Lorenzo, F., Rigano, M.M., Lanzetta, R., Piccoli, R., Monti, D.M. “*Natural products as a source of antiaging molecules*”. 59th Congress of the Italian Society of Biochemistry and Molecular Biology (SIB) (Caserta, September 20-22, 2017)

- Ricciardelli, A., Casillo, A. , Ziaco, M. , Lauro, C., Papa, R., Monti, D.M., **Imbimbo, P.**, Artini, M., Selan, L., Corsaro, M.M., Tutino, M.L. , Parrilli, E. “*Treatment of biofilm infections and development of biofilm resistance EUR-1162 Anti-Biofilm Activity Of Pentadecanal And Its Synthetic Derivatives*”. Eurobiofilms 2017 (Amsterdam, September 19-22, 2017)

- Petruk, G., Gifuni, I., Roxo, M., **Imbimbo, P.**, Olivieri, G., Marzocchella, A., Piccoli, R., Wink, M., Monti, M.D. “*Microalgae in circular economy: from waste to high value products*”. SIB 2017 - 59th Congress of the Italian Society of Biochemistry and Molecular Biology (SIB) (Caserta, September 20-22, 2017)

- **Imbimbo, P.**, Bueno, M., D’Elia, L., Olivieri, G., Pollio, A., Monti, M.D., Ibañez, E. “*Green compressed fluids technologies for downstream processing of *Galdiera phlegrea* in a biorefinery approach*”. IX reunion de expertos en tecnologías de fluidos supercriticos, 2018 (Madrid, June 13-15, 2018)

- Katanić, J., Srećković, N., Mišić, D., Gašić, U., **Imbimbo, P.**, Monti, D. M., Mihailović, V. *New insights into the phytochemical profile, antioxidant properties and biocompatibility of *Salvia verticillata* L. aerial parts methanol extract*. UNIFood Conference (Belgrade, October 5-6, 2018)

- **Imbimbo, P.**, Bueno, M., D'Elia, L., Pollio, A., Ibañez, E., Olivieri, G., Monti, M.D. *A green cascade approach for the downstream of high value bioproducts from Galdieria phlegrea*. Secondo Workshop BIO/10 - SIB (Naples, May 17, 2019)

- Mihailović, V., Stanković, J. S. K., Jurić, T., Srećković, N., Mišić, D., Šiler, B., **Imbimbo, P.**, Monti, D.M., Nikles, S., Pan, S., Bauer, R.. *Anti-inflammatory activity and cytotoxicity of Gentiana asclepiadea L. extracts*. Serbian Biochemical Society Ninth Conference (Belgrade, November 14-16, 2019)

Scientific activities in foreign laboratory: In 2018, from March 12th to June 12th in Foodomics Laboratory of Prof. Elena Ibañez, Bioactivity and Food Analysis Department, Food Research Institute (CIAL-CSIC), Madrid (Spain)



Contents lists available at ScienceDirect

Bioorganic & Medicinal Chemistry Letters

journal homepage: www.elsevier.com/locate/bmcl



Protective effect of *Opuntia ficus-indica* L. cladodes against UVA-induced oxidative stress in normal human keratinocytes



Ganna Petruk^{a,d}, Flaviana Di Lorenzo^{a,d}, Paola Imbimbo^a, Alba Silipo^a, Andrea Bonina^b, Luisa Rizza^b, Renata Piccoli^{a,c}, Daria Maria Monti^{a,c,*}, Rosa Lanzetta^{a,*}

^a Department of Chemical Sciences, University of Naples Federico II, Complesso Universitario Monte Sant'Angelo, via Cinthia 4, 80126 Naples, Italy

^b Bionap srl, R&D Contrada Furera, ZIO 950125 Piano Tavola, Belpasso, Italy

^c Istituto Nazionale di Biostrutture e Biosistemi (INBB), Rome, Italy

ARTICLE INFO

Article history:

Received 3 July 2017

Revised 5 October 2017

Accepted 19 October 2017

Available online 20 October 2017

Keywords:

Opuntia ficus-indica L.

Cladode water extracts

Antioxidants

UVA-induced oxidative stress

Eucomic acid

Piscidic acid

ABSTRACT

Opuntia ficus-indica L. is known for its beneficial effects on human health, but still little is known on cladodes as a potent source of antioxidants. Here, a direct, economic and safe method was set up to obtain water extracts from *Opuntia ficus-indica* cladodes rich in antioxidant compounds. When human keratinocytes were pre-treated with the extract before being exposed to UVA radiations, a clear protective effect against UVA-induced stress was evidenced, as indicated by the inhibition of stress-induced processes, such as free radicals production, lipid peroxidation and GSH depletion. Moreover, a clear protective effect against apoptosis in pre-treated irradiated cells was evidenced. We found that eucomic and piscidic acids were responsible for the anti-oxidative stress action of cladode extract. In conclusion, a bioactive, safe, low-cost and high value-added extract from *Opuntia* cladodes was obtained to be used for skin health/protection.

© 2017 Elsevier Ltd. All rights reserved.

Natural products are receiving a great deal of interest by scientists and pharmacologists for their use in the prevention of oxidative stress-related pathologies, which include obesity, atherosclerosis, diabetes, cancer, neurodegenerative diseases, and aging.¹

Opuntia is widely distributed in Mexico and in all American hemispheres, as well as in Africa and in the Mediterranean basin.² Among all the species, *Opuntia ficus-indica* (referred to here on as *Opuntia*) is the most widely distributed. The multiplicity of

health-promoting properties of *Opuntia* are well known. Indeed, in traditional medicine it has been recognized as a source of prebiotics and phytochemicals.³ Most of the studies report the protective effect of fruits and stems; for example, extracts from *Opuntia ficus-indica* var. *saboten* have been reported to protect against neuronal damage produced under oxidant conditions,⁴ or against renal and hepatic alterations caused by mycotoxins.⁵ On the other side, only few studies have been performed on the antioxidant, anti-inflammatory, wound healing, hypoglycemic and antimicrobial activities of *Opuntia* cladodes.^{6,7} Lee and colleagues showed that an ethanol extract of cladodes decreased the oxidation of linoleic acid and DNA.⁸ Recently, Avila demonstrated an increased antioxidant activity in plasma and blood in subjects consuming cladodes (300 g/day for 3 days).⁹

Given these premises, and taking into account the high annual productivity of biomass per hectare (10–40 tones dry weight), it is undeniable that *Opuntia* cladodes represent an economic and suitable substrate for isolation of antioxidants. However, it has to be considered that all the above studies have a common drawback, namely the use of organic solvents to extract bioactive compounds. Indeed, it was previously demonstrated that the extraction procedure, as well as the extraction solvent, notably affect the yield of natural products, their content as well as their antioxidant

Abbreviations: ABTS, 2,2-azino(3-ethylbenzothiazoline-6-sulfonic acid); CASP-3, caspase-3; CASP-7, caspase-7; DCF, 2,2'-dichlorofluorescein; DTNB, 5,5'-dithiobis-2-nitrobenzoic acid; HAA, hydrophilic antioxidant activity; H₂-DCFDA, 2,2'-dichlorodihydrofluorescein diacetate; MTT, 3-(4,5-dimethylthiazol-2-yl)-2,5-diphenyltetrazolium bromide; ORE, *Opuntia* raw extract; OSMF, *Opuntia* small molecular weight fraction; P-p38, phosphorylated p38 MAP kinase; P-MAPKAPK-2, phosphorylated MAP kinase-activated protein kinase; ROS, reactive oxygen species; SPF, sun protection factor; TEAC, Trolox equivalent antioxidant capacity; TBA, thiobarbituric acid; TBARS, TBA reactive substances; TNB, 5-thio-2-nitrobenzoic acid.

* Corresponding authors at: Department of Chemical Sciences, University of Naples Federico II, Complesso Universitario Monte Sant'Angelo, via Cinthia 4, 80126 Naples, Italy (R. Lanzetta, D.M. Monti).

E-mail addresses: mdmonti@unina.it (D.M. Monti), lanzetta@unina.it (R. Lanzetta).

^d These authors contributed equally to the paper.

<https://doi.org/10.1016/j.bmcl.2017.10.043>

0960-894X/© 2017 Elsevier Ltd. All rights reserved.

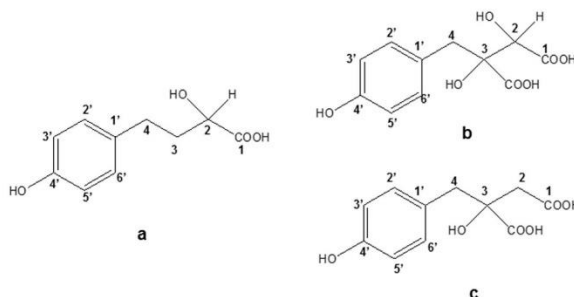


Fig. 1. Structure of 2-hydroxy-4-(4'-hydroxyphenyl)-butanoic acid (a) found in OSMF C, and of piscidic (b) and eucomic (c) acids found in OSMF D.

activity.¹⁰ Furthermore, the use of organic solvents has elevated costs with the risk of contamination of the extract by solvent residues.

We previously reported that *Opuntia* extracts can be obtained by simple mechanical press and that the *Opuntia* raw extract (ORE) was constituted by two main components: i) a high molecular weight constituent consisting in two polysaccharide entities: a linear β -(1 \rightarrow 4)-galactose polymer and a highly branched xyloarabinan; ii) a low molecular weight component consisting in lactic acid, D-mannitol and three phenolic derivatives, i.e. piscidic, eucomic and 2-hydroxy-4-(4'-hydroxyphenyl)-butanoic acids (Fig. 1).⁶

Phenolic compounds are used in several applications due to their proved antioxidant and potentially health-promoting properties.^{11–13} Importantly, the chemical structure of phenolic compounds, in terms of their reducing properties as electron or hydrogen-donating agents, determines their potential for action as antioxidants.¹⁴

In this context, we investigated whether ORE is able to protect human keratinocytes against UVA-induced oxidative stress. UVA radiations are known to increase reactive oxygen species (ROS) production, thus causing oxidative damage of proteins, lipids and nucleic acids. These damages result in different detrimental effects on the skin, such as inflammation, premature aging and development of cancer.^{15,16} Keratinocytes are essential components of skin and connective tissue, normally present in the outermost layer of the skin.¹⁷ This prompted us to select cultured human keratinocytes (HaCaT cell line) as an excellent experimental model to test the protective role of *Opuntia* extracts against UVA radiations.

We first tested the *in vitro* antioxidant activity of the whole ORE and of each isolated fraction (OSMF A–D), obtained following the procedure described in Di Lorenzo et al.⁶ and reported in Supplementary material.

By the ABTS colorimetric assay, we found that ORE is endowed with a significant antioxidant activity, as a low IC_{50} value was obtained (0.52 ± 0.01 mg/mL). Fraction OSMF A, namely the lactic acid component,⁶ showed the highest IC_{50} value (1.4 ± 0.01 mg/mL), in agreement with findings obtained in a different experimental system by Lampe, who reported that lactic acid is able to scavenge free radicals.¹⁸ The IC_{50} values of OSMF C (namely 2-hydroxy-4-(4'-hydroxyphenyl)butanoic acid, Fig. 1a) and D (namely piscidic and eucomic acids, Fig. 1b and c, respectively)⁶ were found to be much lower (0.09 ± 0.02 and 0.03 ± 0.01 , respectively) than those obtained for the whole extract and for OSMF B (D-mannitol,¹⁹) ($IC_{50} = 0.79 \pm 0.37$ mg/mL). These results were confirmed by the TEAC (Trolox equivalent antioxidant capacity) test, from which

Table 1
Opuntia raw extract (ORE) and its fractions (OSMF A–D) were tested for their *in vitro* antioxidant properties. The antioxidant activity is expressed as the concentration required to scavenge 50% of free radical ABTS[•] (IC_{50}), Trolox equivalent antioxidant capacity (TEAC), and the ability to counteract UV radiations, expressed as sun protecting factor (SPF). Values are normalized to the concentration of each sample.

Sample	IC_{50} (mg/mL)	TEAC (μ M/mg)	SPF
ORE	0.52 ± 0.01	43.2 ± 4.53	2.25 ± 0.5
OSMF A	1.4 ± 0.01	10.6 ± 3.39	1.4 ± 0.1
OSMF B	0.79 ± 0.37	24.08 ± 0.34	0.94 ± 0.11
OSMF C	0.09 ± 0.02	225.79 ± 15.85	0.2 ± 0.01
OSMF D	0.03 ± 0.01	749.65 ± 11.81	2.23 ± 0.41

much higher TEAC values were obtained for OSMF C and D, with respect to OSMF A and B, indicating a high content in antioxidants in the former two fractions (Table 1).

We also tested the UV-protective properties of ORE and its OSMF fractions by measuring their sun protection factor (SPF) *in vitro*, according to a spectrophotometric method.¹⁹ As shown in Table 1, while OSMF B and C did not show any significant protective effect, a value of about 2 was obtained when ORE or OSMF D

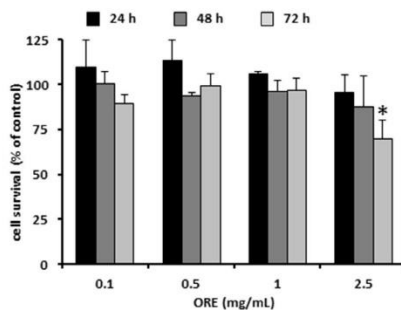


Fig. 2. Effect of ORE on the viability of human keratinocytes. Dose-response curve of HaCaT cells after 24 h (black bars), 48 h (dark grey bars) and 72 h (light grey bars) incubation in the presence of increasing concentrations of ORE. Cell viability was assessed by the MTT assay; the cell survival percentage was defined as described in Supplementary material. Values are given as means \pm S.D. ($n \geq 3$). * indicates $p < 0.05$ with respect to untreated cells.

was tested; this value has been reported to correspond to 50% UV blockage. Therefore, these samples can be considered as having good sunscreen activity.²⁰ OSMF A showed an *in vitro* SPF of 1.4, in agreement with the results obtained by Kornhauser, who reported that lactic acid is commonly used in cosmetics for the improvement of photoaged skin.²¹

The biocompatibility of ORE on HaCaT cells was tested by performing a dose-response experiment, in which cells were exposed for different lengths of time to the extract within the range 0.1–2.5 mg/mL. We found that cell viability was not affected up to 1 mg/

mL, even after 72 h incubation ($p > 0.05$) (Fig. 2), while after 72 h, at the highest concentration tested (2.5 mg/mL), about 30% cell death was observed. On the basis of these results and on previously reported data,⁹ further experiments were carried out at 1 mg/mL ORE concentration.

To test if ORE was able to protect keratinocytes from oxidative stress, we performed a time course experiment in which cells were pre-treated with ORE (1 mg/mL) for different lengths of time (from 5 min to 2 h) before inducing oxidative stress by UVA irradiation (100 J/cm²). Immediately after irradiation, intracellular GSH was evaluated by the DTNB assay (Fig. 3). As expected, UVA treatment significantly decreased intracellular GSH when compared to the non-irradiated samples (50% decrease), whereas ORE had no effect on intracellular GSH level. Interestingly, a pretreatment of cells with ORE, prior to UVA exposure, resulted in an inhibition of GSH oxidation in a time-dependent manner. In particular, we found that ORE was able to protect cells from GSH depletion after just 30 min incubation, and no difference was observed up to 2 h incubation. The efficacy of ORE at 1 mg/mL well correlates with the *in vitro* antioxidant assay (IC₅₀ 0.52 mg/mL).

In order to identify the low molecular weight fraction from *Opuntia* extract responsible for the antioxidant activity of the whole extract, each fraction was tested by DTNB and DCFDA assays. For a direct comparison between the whole extract and its fractions, a suitable volume of each fraction was tested to reach the concentration of the single component in the whole extract tested at 1 mg/mL.⁹ As shown in Fig. 4A, when cells were pre-incubated either with ORE or with the isolated fractions prior to be irradiated, ORE (dashed bars) and OSMF D (dotted bars) were found to be able to contrast the detrimental effects of UVA irradiation on GSH (GSH depletion), whereas the other fractions had no protective effect. In the absence of irradiation, instead, no effect on the intracellular GSH level was observed for any fraction. These results were also confirmed by the DCFDA assay (Fig. 4B), which showed no alteration in the redox state upon treatment with *Opuntia* samples. On the other hand, a significant increase in ROS production was observed when keratinocytes were irradiated by UVA (4-fold increase). Interestingly, the alteration in the redox state was fully counteracted when cells were pre-incubated either with ORE (dashed bars) or with OSMF D (dotted bars) prior to UVA

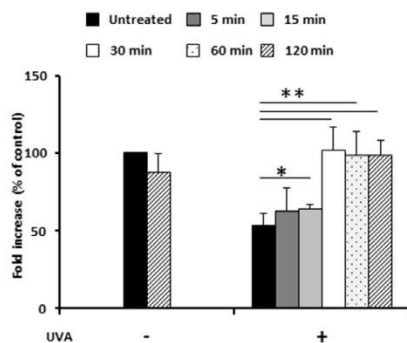


Fig. 3. GSH levels in HaCaT cells irradiated by UVA in the presence of ORE. Cells were pre-incubated in the presence of 1 mg/mL ORE (grey bars) for different lengths of time, irradiated by UVA (100 J/cm²) and intracellular GSH levels determined by DTNB assay. Control cells, black bars; cells pre-treated with ORE are indicated by: dark grey bars (5 min of pre-incubation), light grey bars (15 min of pre-incubation), white bars (30 min of pre-incubation), spotted bars (60 min of pre-incubation) and dashed bars (120 min of pre-incubation). Values are expressed as fold increase with respect to control (i.e. untreated) cells. Data shown are the means \pm S.D. of three independent experiments. * indicates $p < 0.05$; ** indicates $p < 0.001$.

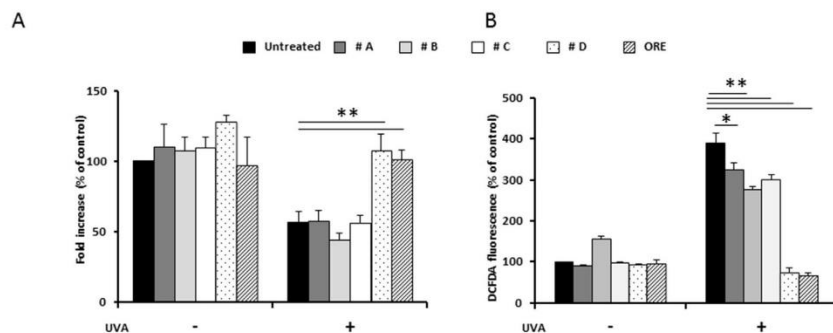


Fig. 4. GSH oxidation and ROS production in HaCaT cells irradiated by UVA in the presence of ORE and isolated fractions. A–B. Cells were pre-incubated in the presence of ORE (1 mg/mL) or equivalent amount of each *Opuntia* fraction for 30 min and then irradiated by UVA (100 J/cm²). A, changes in intracellular GSH levels of cells before (–) and after (+) UVA treatment; B, intracellular ROS levels determined by DCFDA assay. Black bars, untreated cells; dark grey bars, fraction A (OSMF A, # A); light grey bars, fraction B (OSMF B, # B); white bars, fraction C (OSMF C, # C); spotted bars, fraction D (OSMF D, # D); dashed bars, ORE. Values are expressed as fold increase with respect to control (i.e. untreated) cells. Data shown are the means \pm S.D. of three independent experiments. * indicates $p < 0.01$, ** indicates $p < 0.001$.

irradiation. A small, although significant, protective effect was observed with the other fractions. The slight antioxidant activity of lactic acid (present in OSMF A) is in line with Lampe and colleagues who found that lactic acid was effective in counteracting free radicals produced by a photoinitiator, but no effect was observed in the presence of hydrogen peroxide radicals, which are more reactive and able to enter the cell.¹⁸ As for OSMF C, it is well known that the antioxidant activity of a phenolic compound must be related to the amount, position and number of the hydroxyl groups in the molecule.²² In this context, piscidic and eucemic acids are richer in hydroxyl groups than 2-hydroxy-4-(4-hydroxyphenyl)-butanoic acid, the component of OSMF C (Fig. 1).

Based on these results, ORE and OSMF D were used to deeply analyze their antioxidant protective effect.

To this purpose, measurement of lipid peroxidation levels was performed (Fig. 5A).

We found that UVA treatment significantly increased lipid peroxidation levels when compared to a non-irradiated sample.

Noteworthy, a strong protective effect was observed when cells were pre-treated with ORE or OSMF D, since both values were comparable to those obtained in the absence of any treatment.

This result is in line with those obtained by Hfaiedh, who studied the effects of a water *Opuntia* extract in counteracting the negative effects of NiCl₂ in rats.²³

The protective effect of ORE and OSMF D was further confirmed by Western blot experiments, in which the phosphorylation levels of p38 and its direct target, MAPKAPK-2, were analyzed (Fig. 5B). These proteins are directly involved in signaling stress pathways induced by UVA.^{24,25} When cells were UVA irradiated, we observed a significant increase in the phosphorylation levels of the analyzed markers (Fig. 5B-C). On the contrary, when cells were exposed to ORE or OSMF D prior to UVA treatment, the phosphorylation levels of p38 and MAPKAPK-2 were similar to those observed in non-irradiated cells. These results are in agreement with those obtained by Zoungui and colleagues in mice using an ethanol:water extract.⁵

Furthermore, we verified whether ORE and OSMF D were able to protect cells against UVA-induced cell death. As shown in Fig. 6, a cell treatment with ORE did not induce apoptosis, since no cleavage of caspase-3 or caspase-7 was observed, while, as expected, upon UVA exposure, the activation of caspase-3 and -7 was remarkably increased, as indicated by the presence of the cleaved form of both proteins (Fig. 6, third lane). These results

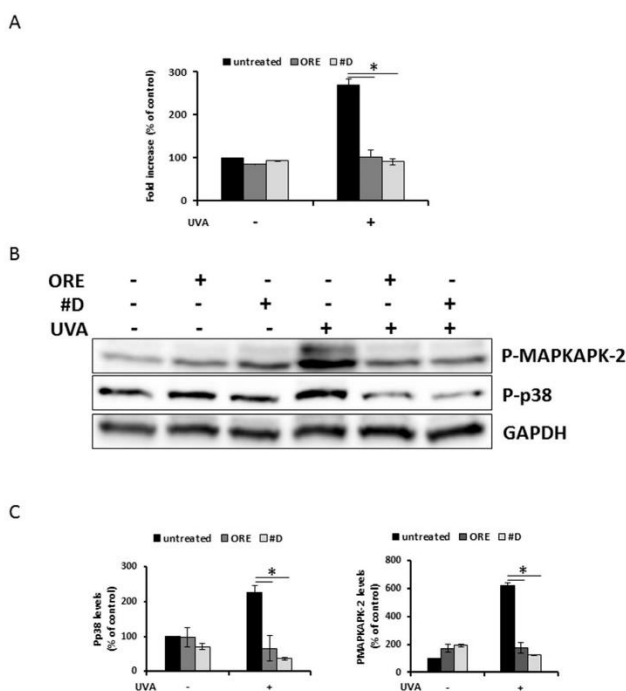


Fig. 5. Effect of ORE extract and OSMF D on UVA-induced oxidative stress markers in human keratinocytes. Cells were incubated with 1 mg/mL ORE or 0.15 mg/mL OSMF D for 30 min prior to UVA irradiation (100 J/cm²) and then incubated for 90 min. A, lipid peroxidation levels determined by TBARS assay; B, Western blots. In Western blots the phosphorylation level of P-p38 and P-MAPKAPK-2 is reported, with the relative densitometric analysis (C) in the absence (black bars) or in the presence of ORE (dark grey bars) or OSMF D (light grey bars). GAPDH was used as internal standard. Data shown are the means \pm S.D. of three independent experiments. * indicates $p < .005$.

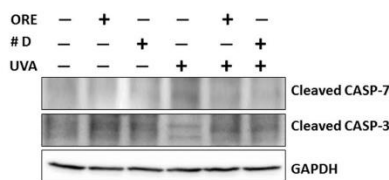


Fig. 6. ORE extract and OSMF D protect HaCaT cells from UVA-induced apoptosis. Cells were incubated with 1 mg/ml ORE or 0.15 mg/ml OSMF D for 30 min, irradiated with UVA (100 J/cm^2) and then grown for 24 h. Western blots were performed using anti-caspase-3 and -7, which recognize the activated forms of the proteins. GAPDH was used as loading control.

are in agreement with those reported by others, who demonstrated that many epidermal skin cells, including keratinocytes, undergo apoptosis following UVA exposure as a result of DNA strand breaks.^{24,25} When, instead, keratinocytes were pre-incubated in the presence of ORE or OSMF D, and then exposed to UVA, no caspase-3 and -7 activation was observed, thus indicating a protective role of piscidic and eucomic acids from UVA-induced cellular stress.

The beneficial properties of *Opuntia* mucilage in producing a physical barrier on the cutis, favoring cutaneous reparative processes, is historically well known. Nowadays, given the enormous potential benefits on health of natural bioactive compounds isolated from *Opuntia* cladode extracts, intensive investigation is ongoing attracting the interest of food scientists and clinical pharmacologists. Some of the beneficial effects of *Opuntia* extracts have been attributed to fibers and polyphenols isolated from cladodes. However, all the studies published so far have been performed on extracts treated with organic solvents, which may not be completely removed with a potential danger for human health.

Here, we report the discover of an additional and intriguing beneficial property of water extracts from cladodes, i.e. a protective effect against UVA-induced oxidative stress and apoptosis, which has never been investigated so far. Altogether, our results demonstrate that ORE water extract has strong antioxidant properties, being able to counteract the negative effects induced in human keratinocytes by UVA radiations, and to protect cells from this common and pernicious source of stress. We demonstrated that the anti-stress effect of cladode extracts has to be ascribed to eucomic and piscidic acids, as these phenolic compounds are the sole components of fraction OSMF D, which fully retains the antioxidant activity of the whole extract. As widely known, the antioxidant potency of phenolic acids strongly depends on their structural features. Indeed, it has been demonstrated that the main structural characteristic responsible for the antioxidant activity of phenol derivatives is the number and location of the hydroxyl groups present in the molecule.²⁷ Two main mechanisms by which antioxidants can play their protective role have been proposed. Due to the presence of such hydroxy functions, phenols are able to easily donate hydrogen atoms to the free radicals thus blocking the chain propagation step occurring in the oxidation process (H-atom-transfer mechanisms).^{14,28} Alternatively, the antioxidant can give an electron to the free radical becoming itself a radical cation (single-electron-transfer mechanisms). In addition, deprotonated carboxyl groups behave as electron-donating groups thus favoring the hydrogen atom transfer and electron-donating based radical scavenging.²⁹ Therefore, the potent antioxidant effect

observed for both the piscidic and eucomic acids is clearly reflected in their structural features which promote the hydrogen atoms transfer to free radicals. The slight structural differences, as example, between the piscidic and the 2-hydroxy-4-(4'-hydroxyphenyl)-butanoic acid, namely the absence, in the latter, of one hydroxyl and one carboxyl group, could be reflected in the lower antioxidative power observed for OSMF C.

In our opinion the present study, shedding light on bioactive compounds responsible for *Opuntia* cladode antioxidant activity, represents an important step towards the therapeutic values of *Opuntia* properties.

It is important to underline that aqueous *Opuntia* antioxidant extracts can be obtained by simple mechanical press of cladodes, thus avoiding the use of expensive materials and of organic solvents, responsible for environmental pollution and persistence of residues dangerous for human health. Therefore, we obtained a bioactive, safe, low-cost and high value-added extract to be used in pharmaceutical and/or cosmetics applications for skin health/protection.

Conflict of interest

The authors declare no competing financial interest.

A. Supplementary data

Supplementary data associated with this article can be found, in the online version, at <https://doi.org/10.1016/j.bmcl.2017.10.043>.

References

- Basaga H. *Biochem Cell Biol*. 1990;68:989–998.
- Zoungui L, Ayed-Boussema I, Ayed Y, Bacha H, Hassen W. *Food Chem Toxicol*. 2009;47:662–667.
- Coria Cayupán YS, Ochoa MJ, Nazareno MA. *Food Chem*. 2011;126:514–519.
- Dok-Go H, Lee KH, Kim HJ, et al. *Brain Res*. 2003;965:130–136.
- Zoungui L, Golli EEI, Bouaziz C, Bacha H, Hassen W. *Food Chem Toxicol*. 2008;46:1817–1824.
- Di Lorenzo F, Silipo A, Molinaro A, et al. *Carbohydr Polym*. 2017;157:128–136.
- El-Mostafa K, El Kharrassi Y, Badreddine A, et al. *Molecules*. 2014;19:14879–14901.
- Lee JC, Kim HR, Kim J, Jang YS. *J Agric Food Chem*. 2002;50:6490–6496.
- Avila-Nava A, Calderón-Oliver M, Medina-Campos ON, et al. *J Funct Foods*. 2014;10:13–24.
- Ammar I, Ennouri M, Attia H. *Intl Crops Prod*. 2015;64:97–104.
- Kähkönen MP, Hoppia AI, Vuorela HJ, et al. *J Agric Food Chem*. 1999;39:354–362.
- Rice-Evans CA, Miller NJ, Paganga G. *Free Radic Biol Med*. 1996;20:933–956.
- Dai J, Mumper RJ. *Molecules*. 2010;15:7313–7352.
- Rice-Evans CA, Miller NJ, Paganga G. *Trends Plant Sci*. 1997;2:152–159.
- Kulms D, Schwarz T. *Photodermatol Photoimmunol Photomed*. 2000;16:195–201.
- Hseu YC, Chou CW, Senthil Kumar KJ, et al. *Food Chem Toxicol*. 2012;50:1245–1255.
- Camera E, Mastrofrancesco A, Fabbri C, et al. *Exp Dermatol*. 2009;18:222–231.
- Lampe KJ, Namba RM, Silverman TR, Bjugstad KB. *Biotechnol Bioeng*. 2009;103:1214–1223.
- Mansur JS, Breder MNR, Mansur MCA, Azulay RD. *An Bras Dermatol, Rio Janeiro*. 1986;61:121–124.
- Kale S, Gaikwad M, Bhandare S. *Int J Res Pharm Biomed Sci*. 2011;2:1220–1224.
- Kornhauser A, Coelho SG, Hearing VJ. *Clin Cosmet Investig Dermatol*. 2010;3:135–142.
- Biskup I, Golonka I, Gamian A, Sroka Z. *Postep Hig Med Dosw*. 2013;67:958–963.
- Hfaiedh N, Allagui MS, Hfaiedh M, Feki AEI, Zoungui L, Croute F. *Food Chem Toxicol*. 2008;46:3759–3763.
- Petruk G, Raiola A, Del Giudice R, et al. *Photochem Photobiol B Biol*. 2016;163:284–289.
- Klotz L, Pellioux C, Briviba K, Pierlat C. *Eur J Biochem*. 1999;260:917–922.
- Ichihashi M, Ueda M, Budiyanto A, et al. *Toxicology*. 2003;189:21–39.
- Bendary E, Francis RR, Ali HMG, Sarwat MI, El Hady S. *Ann Agric Sci*. 2013;58:173–181.
- Wright JS, Johnson ER, Dilabio GA. *J Am Chem Soc*. 2001;123:1173–1183.
- Vetlika B, Kron I. *Free Radicals Antioxidants*. 2012;2:62–67.

Supplementary Material

Protective effect of *Opuntia ficus-indica* L. cladodes against UVA-induced oxidative stress in normal human keratinocytes

Ganna Petruk^{a§}, Flaviana Di Lorenzo^{a§}, Paola Imbimbo^a, Alba Silipo^a, Andrea Bonina^b, Luisa Rizza^b, Renata Piccoli^{a,c}, Daria Maria Monti^{a,c*}, Rosa Lanzetta^{a*}

^a Department of Chemical Sciences, University of Naples Federico II, Complesso Universitario Monte Sant'Angelo, via Cinthia 4, 80126, Naples, Italy

^b Bionap srl, R&D Contrada Fureria, ZIO 950125 Piano Tavola, Belpasso, Italy

^c Istituto Nazionale di Biostrutture e Biosistemi (INBB), Rome, Italy

[§] These authors contributed equally to the paper.

* Corresponding authors. D.M. Monti, Department of Chemical Sciences, University of Naples Federico II, Complesso Universitario Monte Sant'Angelo, via Cinthia 4, 80126, Naples, Italy. E-mail: mdmonti@unina.it; Tel: +39 081 679150; Fax: +39 081 674330; R. Lanzetta Department of Chemical Sciences, University of Naples Federico II, Complesso Universitario Monte Sant'Angelo, via Cinthia 4, 80126, Naples, Italy. E-mail: lanzetta@unina.it; Tel: +39 081 674148; Fax: +39 081 674330.

Experimental information

Opuntia extract preparation and isolation of Opuntia small molecular weight fractions (OSMF)

The *Opuntia* cladode extract (ORE) was supplied by BIONAP srl (OPUNTIA BIOCOMPLEX SH, Italy) following the procedure described by Di Lorenzo et al.¹. Briefly, the cladode juice was extracted by a mechanical press system and lyophilized. ORE was then dissolved in water (0.5% w/w) and its components separated by ultrafiltration using an apparatus equipped with a semi-permeable PES (polyethersulfone) membrane (KMS HFK™ - 131, Koch, USA) with a cut-off of 10 kDa. From this process two fractions were obtained containing small molecular weight components (OSMF) and high molecular weight polysaccharides (OPF), respectively. OSMF was then injected into a 1.5 x 120 cm Bio-Gel P-2. (Bio-Rad) and four main fractions (named OSMF A-D) were collected and lyophilized. The identification of the main components has been previously reported¹.

Antioxidant activity

HAA (hydrophilic antioxidant activity) was evaluated in the water-soluble fractions using the protocol previously described². Briefly, ORE and each OSMF fraction (OSMF A-D) were allowed to react with an ABTS^{•+} solution for 7 min, and then the absorbance was taken at 734 nm by a spectrophotometer. The standard curve obtained by using Trolox was found to be linear in the concentration range 0-40 μM. Values were expressed either as IC₅₀ (mg/mL), representing the concentration of extract required to scavenge 50% of free radical ABTS^{•+}, and as TEAC (Trolox equivalent antioxidant capacity), which indicates the scavenging activity of the extract on free radical ABTS^{•+} compared with a standard amount of Trolox. The TEAC value was then normalized to the concentration of each sample. In the case of ORE, the concentration was obtained by diluting 1 mg of the lyophilized sample in 1 mL of water. Thus, when ORE is tested at 1 mg/mL, the concentration of each fraction is: OSMF A 0.35 mg/mL, OSMF B 0.3 mg/mL, OSMF C 0.2 mg/mL, OSMF D 0.15 mg/mL. Three separate analyses were carried out with each sample.

In vitro determination of the sun protection factor (SPF)

The sun protection factor (SPF) was determined spectrophotometrically as described by Mansur et al.³ with some modifications. Briefly, *Opuntia* samples were diluted to obtain a hydroalcoholic solution (40% ethanol). The samples were scanned with a Jasco V-630 UV-VIS Spectrophotometer (Jasco, Gross-Umstadt, Germany) between 290 and 320 nm, at intervals of 5 nm, using a HELM 6040- UV quartz cuvette (Hellma, Müllheim, Germany). The SPF was calculated by the following equation:

$$SPF \text{ in vitro} = CF \sum_{320}^{290} EE(\lambda)I(\lambda)Abs(\lambda)$$

where CF is the correction factor (=10), and $EE(\lambda)$ and $Abs(\lambda)$ are the erythrogenic effect of radiation, and the absorbance value, respectively, at the selected wavelength λ . The $EE(\lambda)I$ values, previously determined⁴, are constants.

Cell culture and analysis of cell viability

Human normal keratinocytes (HaCaT, from ATCC) were cultured in Dulbecco's Modified Eagle's Medium (Sigma-Aldrich, St Louis, Mo, USA), supplemented with 10% foetal bovine serum (HyClone), 2 mM L-glutamine and antibiotics, all from Sigma-Aldrich, in a 5% CO₂ humidified atmosphere at 37 °C. Every 72 h HaCaT cells were sub-cultured by removing the culture medium, rinsing the cells with PBS and then detaching them with trypsin-EDTA. After centrifugation (5 min at 1000 g) cells were diluted in fresh complete growth medium.

Cells were seeded in 96-well plates (100 μ L/well) at a density of 2×10^3 /well. For dose-dependent cytotoxicity assays, 24 h after seeding, increasing volumes of ORE were added to the cells, to reach a final concentration ranging from 0.1 to 2.5 mg/mL. Cell viability was assessed by the MTT (3-(4,5-dimethylthiazol-2-yl)-2,5-diphenyltetrazolium bromide) assay, as previously described⁵. Cell survival was expressed as the percentage of viable cells in the presence of the extract compared to controls. Two groups of cells were used as control, i.e. cells untreated with the extract and cells supplemented with identical volumes of water. The average of the two control groups was used as 100%. Each sample was tested in three independent analyses, each carried out in triplicates.

Analysis of oxidative stress

To analyze oxidative stress, cells were plated at a density of 2×10^4 cells/cm². 24 h after seeding, cells were incubated for different lengths of time with 1 mg/mL of ORE, or equivalent amount of each isolated fraction (the amount of each compound in fractions was determined from the concentration of the compound in 1 mg/mL of ORE). Then media was removed from culture plates, cells were washed with PBS twice and then covered with a thin layer of PBS before irradiation for 10 min with UVA light (UVItec, Cambridge, UK; 4 x 9W lamps, λ_{max} , 365 nm, no detectable emission below 320 nm; UVA radiation dose: 100 J/cm²).

DCFDA assay

To estimate ROS production, the protocol described in Del Giudice et al.⁶ was followed. Briefly, immediately after UVA irradiation, cells were incubated with 2',7'-dichlorodihydrofluorescein diacetate (H₂-DCFDA, Sigma-Aldrich). Fluorescence intensity was measured by a Perkin-Elmer LS50 spectrofluorimeter (525 nm emission wavelength, 488 nm excitation wavelength, 300 nm/min scanning speed, 5 slit width for both excitation and emission). ROS production was expressed as percentage of DCF fluorescence intensity of the sample under test, with respect to the untreated sample. Each value was assessed by three independent experiments, each with three determinations.

DTNB assay

To estimate intracellular glutathione levels, a procedure previously described was followed⁷. Immediately after UVA irradiation, cells were detached by trypsin, lysed and protein concentration was determined by the Bradford assay. Then, 50 μ g of proteins were incubated with 3 mM EDTA, 144 μ M 5,5'-dithiobis-2-nitrobenzoic acid (DTNB) in 30 mM TrisHCl pH 8.2, centrifuged and the absorbance of the supernatant was measured at 412 nm by using a multiplate reader (Biorad). GSH levels were expressed as the percentage of TNB (5-thio-2-nitrobenzoic acid) absorbance in the sample under test with respect to the untreated sample. Values are the mean of three independent experiments, each with triplicate determinations.

Lipid peroxidation

The thiobarbituric acid reactive substances (TBARS) assay was performed as previously described⁶. Briefly, after irradiation with UVA, cells were kept for 90 min at 37 °C, then detached and suspended (5×10^4 cells) in 0.67% thiobarbituric acid (TBA) and 20% trichloroacetic acid (1:1 v/v). After heating and centrifugation, samples were read at 532 nm. Lipid peroxidation levels were expressed as percentage of absorbance at 532 nm of the sample under test, compared to that of untreated cells. Three independent experiments were carried out, each one with three determinations.

Western blot analyses

Cells were plated at a density of 2×10^4 cells/cm² in complete medium for 24 h and then treated as described above. Untreated and treated cells, after induction of oxidative stress, were incubated for 90

min (for the evaluation of the oxidative stress pathway) or 24 h (for the analysis of apoptosis) at 37 °C, and cell lysates analyzed by Western blotting performed as reported⁸. Antibodies for Pp38, PMAKAPK-2, and activated CASP-3 CASP-7 were purchased from Cell Signal Technology (Danvers, MA, USA). To normalize protein intensity levels, a specific antibody against GAPDH (Thermo Fisher, Rockford, IL, USA) was used. The chemiluminescence detection system (SuperSignal[®] West Pico) was from Thermo Fisher.

Statistical analyses

In all the experiments samples were analyzed in triplicate. Quantitative parameters were expressed as the mean value \pm SD. Significance was determined by Student's t-test at a significance level of 0.05.

1. Di Lorenzo, F.; Silipo, A.; Molinaro, A.; Parrilli, M.; Schiraldi, C.; D'Agostino, A.; Izzo, E.; Rizza, L.; Bonina, A.; Bonina, F.; Lanzetta, R. *Carbohydr. Polym.* **2017**, *157*, 128–136.
2. Del Giudice, R.; Raiola, A.; Tenore, G. C.; Frusciantè, L.; Barone, A.; Monti, D. M.; Rigano, M. M. *J. Funct. Foods* **2015**, *18*, 83–94.
3. Mansur, J. S.; Breder, M. N. R.; Mansur, M. C. A.; Azulay, R. D. *An. Bras. Dermatol., Rio Janeiro* **1986**, *61*, 121–124.
4. Sayre, R. M.; Agin, P. P.; Vee, G. J. Le; Marlowe, E. *Phytochem. Photobiol.* **1979**, *29*, 559–566.
5. Monti, D. M.; Guarnieri, D.; Napolitano, G.; Piccoli, R.; Netti, P.; Fusco, S.; Arciello, A. *J. Biotechnol.* **2015**, *193*, 3–10.
6. Del Giudice, R.; Petruk, G.; Raiola, A.; Barone, A.; Monti, D. M.; Rigano, M. M. *J. Sci. Food Agric.* **2017**, *97*, 1616–1623.
7. Petruk, G.; Raiola, A.; Del Giudice, R.; Barone, A.; Frusciantè, L.; Rigano, M. M.; Monti, D. M. *J. Photochem. Photobiol. B Biol.* **2016**, *163*, 284–289.
8. Galano, E.; Arciello, A.; Piccoli, R.; Monti, D. M.; Amoresano, A. *Metallomics* **2014**, *6*, 587–597.



Contents lists available at ScienceDirect

South African Journal of Botany

journal homepage: www.elsevier.com/locate/sajbThe biological activities of roots and aerial parts of *Alchemilla vulgaris* L.T. Boroja^{a,*}, V. Mihailović^a, J. Katanić^a, S.-P. Pan^b, S. Nikles^b, P. Imbimbo^c, D.M. Monti^c, N. Stanković^a, M.S. Stanković^d, R. Bauer^b^a Department of Chemistry, Faculty of Science, University of Kragujevac, Radoja Domanovića 12, 34000 Kragujevac, Serbia^b Institute of Pharmaceutical Sciences, Department of Pharmacognosy, University of Graz, Universitätsplatz 4/1, 8010 Graz, Austria^c Department of Chemical Sciences, University of Naples Federico II, Complesso Universitario Monte Sant'Angelo, via Cinthia 4, 80126 Naples, Italy^d Department of Biology and Ecology, Faculty of Science, University of Kragujevac, Radoja Domanovića 12, 34000 Kragujevac, Serbia

ARTICLE INFO

Article history:

Received 14 December 2017

Received in revised form 9 March 2018

Accepted 20 March 2018

Available online 13 April 2018

Edited by AO Aremu

Keywords:

Alchemilla vulgaris

Lady's mantle

Antioxidant activity

Antimicrobial activity

Biocompatibility

Anti-inflammatory activity

ABSTRACT

Medicinal plants are considered to be a major source of biologically active compounds, which provides unlimited opportunities for their use either as medical treatments or as novel drug formulations.

The focus of our study was on basic phytochemical analysis and *in vitro* examination of the biological activity of *Alchemilla vulgaris* L. Methanolic extracts of above ground parts and roots of *A. vulgaris* (AVA and AVR, respectively) were prepared by maceration for 72 h. Phytochemical profile of extracts was evaluated by spectrophotometric determinations of phenolic compounds and HPLC-PDA analysis. AVA and AVR were analysed for their antioxidant efficacy as total antioxidant capacity, metal chelation and reducing power ability, inhibition of lipid peroxidation as well as their potential to neutralise DPPH, ABTS, and OH radicals. Microdilution method was employed to investigate the antibacterial and antifungal activity of extracts against nine ATCC and isolates of bacteria and ten fungal strains from biological samples. Anti-inflammatory activity of the extracts was evaluated using cyclooxygenase-1 (COX-1) and cyclooxygenase-2 (COX-2) assays and the assay for determination of COX-2 gene expression, while biocompatibility of extracts was assessed by MIT assay.

Our results revealed the high amount of phenolic compounds in both extracts; especially they were rich in condensed tannins. Ellagic acid and catechin were tentatively identified in AVA and AVR, respectively. Full biocompatibility as well as remarkable bioactivity were observed for both extracts in all employed assays, so our further investigations will be focused on the identification of active constituents in *A. vulgaris* and the molecular mechanisms of their action.

© 2018 SAAB. Published by Elsevier B.V. All rights reserved.

1. Introduction

Several lines of evidence support the hypothesis that secondary metabolites from plants (e.g. flavonoids and phenolic acids) may play an antioxidant role and diminish the adverse effects of an imbalance between the production of enzymatic and non-enzymatic antioxidants and overproduction of free radicals in oxidative stress (Hussein and Khalifa, 2014). As a result of their antioxidant activity, either through their reducing capacity or through potential influences on intracellular redox processes, phenolic compounds manifest various beneficial

effects, including anti-inflammatory and anticarcinogenic activities (Han et al., 2007; Li et al., 2014).

Alchemilla vulgaris L. (Lady's mantle), an herbaceous perennial plant belonging to the Rosaceae family, is widely spread across Europe and Asia and commonly known in traditional medicine for treatment of ulcers, wounds, eczema, and digestive problems as well as a remedy for gynaecological disorders, such as heavy menstrual flow, menorrhagia and dysmenorrhoea (Jarić et al., 2015; Masullo et al., 2015; Ilić-Stojanović et al., 2017). *Alchemilla* species have been reported to exert a variety of biological activities, including antiviral, antioxidant, antiproliferative, and antibacterial activity as well as healing effects on cutaneous wounds in rats (Trouillas et al., 2003; Shrivastava and John, 2006; Filippova, 2017). Previous findings showed that aerial parts of *A. vulgaris* comprise mostly phenolic compounds – a large amount of tannins, phenolic acids (predominantly ellagic acid, gallic, and caffeic acids), flavonoids (quercetin), and flavonoid glycosides (isoquercetin, rutin, avicularin, and tiliroside) (Møller et al., 2009). To the extent of our knowledge, there is a scarce literature on phytochemical profile and biological activity of roots of *A. vulgaris*.

Abbreviations: AVA, *Alchemilla vulgaris* aerial parts methanolic extract; AVR, *Alchemilla vulgaris* roots methanolic extract; ROS, reactive oxygen species; COX-1, cyclooxygenase-1; COX-2, cyclooxygenase-2; PGE₂, prostaglandin H₂; NSAIDs, non-steroidal anti-inflammatory drugs; IL, interleukin; TNF- α , tumour necrosis factor α ; iNOS, inducible nitric oxide synthase; NF- κ B, the nuclear factor kappa-light-chain-enhancer of activated B cells; DEX, dexamethasone.

* Corresponding author.

E-mail address: tatjanaboroja@gmail.com. (T. Boroja).

Reactive oxygen species (ROS) encompass a broad range of reactive molecules triggering a multitude of ailments, such as rheumatoid arthritis, cardiovascular disorders, neurological disease, and cancer (Hitchon and El-Gabalawy, 2004; Valko et al., 2004; Melo et al., 2011). Increased ROS generation has been described as one of the key factors in the progression of inflammatory disorders (Mittal et al., 2014). Cyclooxygenases (COX-1 and COX-2) are enzymes involved in the inflammatory process and responsible for the conversion of arachidonic acid into pro-inflammatory mediators, like prostaglandin H₂ (PGH₂). COX-1 is a constitutive enzyme expressed in almost all cells providing homeostatic functions. Under normal conditions, COX-2 is unexpressed in most cells, but its expression can be induced by inflammatory stimuli. Hence, COX-2 is a major target for anti-inflammatory therapies. Since the use of non-selective COX inhibitors (non-steroidal anti-inflammatory drugs-NSAIDs) may lead to side effects, particularly evident in the gastrointestinal tract (Jones et al., 2008), novel COX-2-specific agents, with no or very little undesirable effects, are urgently needed.

The presented study was focused on assessment of biocompatibility, antioxidant, antimicrobial, and anti-inflammatory activities of methanolic extracts of aerial parts and roots of Lady's mantle (*A. vulgaris*) and their phytochemical profile as well.

2. Materials and methods

2.1. Chemicals and instruments

All spectrophotometric determinations were performed on UV–Vis double beam spectrophotometer Halo DB-20S (Dynamica GmbH, Dietikon, Switzerland). Ellagic acid, hyperoside, rutin and TRIS/HCl-buffer were obtained from Carl Roth (Karlruhe, Germany), trolox, epicatechin, catechin, gallic acid, vanillic acid, rutin, kaempferol, quercetin, DMSO (>99.98% purity), and formic acid from Sigma-Aldrich (Deisenhofen, Germany), caffeic acid and Na₂EDTA (Titriplex III) from Merck KGaA (Darmstadt, Germany), HPLC-grade acetonitrile, water, and trifluoroacetic acid were purchased from Merck (Darmstadt, Germany). Resazurin was purchased from Acros Organics (Geel, Belgium), while all other chemicals used in antimicrobial experiments were purchased from Torlak Institute of Virology, Vaccines, and Sera (Belgrade, Serbia). Reagents used in COX-1 and -2 assays: purified prostaglandin H synthase (PGHS)-1 from ram seminal vesicles, human recombinant PGHS-2, NS-398, and arachidonic acid were obtained from Cayman Chemical Co. (Ann Arbor, MI, USA), hematin (porcine) and indomethacin from ICN (Aurora, Ohio, USA), epinephrine hydrogen tartrate from Fluka (Buchs, Switzerland), and competitive PGE₂ EIA kit from Assay Designs Inc. (Ann Arbor, MI, USA). COX-2 gene expression kits, reagents and chemicals for this method: fetal bovine serum (FBS), N-2-hydroxyethylpiperazine-N-2-ethane sulfonic acid (HEPES), phosphate buffered saline (PBS), penicillin, and streptomycin human leukemic monocytic cell line THP-1 (European Collection of Cell Culture; Item No. 88081201), and RPMI1640 were obtained from Gibco® (NY, USA), phorbol 12-myristate 13-acetate (PMA), while dexamethasone, lipopolysaccharide (LPS) as well as GenElute™ Mammalian TotalRNA Miniprep Kit were from Sigma-Aldrich (MO, USA). High-Capacity cDNA Reverse Transcription Kit, Pre-developed TaqMan® Assay, COX-2 primers and COX-2 probe were from Applied Biosystems (NY, USA). BalbC-3 T3 fibroblasts (clone A31) were purchased from ATCC (Manassas, VA) and human epidermal keratinocytes (HaCaT) from Innoprot (Biscay, Spain).

2.2. Plant material and preparation of the extracts

The roots and aerial parts of *Alchemilla vulgaris* L. were collected in August 2014 at Goč Mountain (Central Serbia). Collection of plant material was carried out by the sampling of 20 representative individuals of the population in the full flowering period. The taxonomic and botanical identity was confirmed by Milan Stanković, Ph.D. A

voucher specimen (No. 120/015) is kept in the Herbarium of the Department of Biology and Ecology, Faculty of Science, University of Kragujevac, Kragujevac, Serbia. The collected plants were air-dried in darkness at ambient temperature. The dried aerial parts and roots separately from all individuals were cut up, mixed and powdered for extracts preparation.

Dried and powdered aerial parts (30.00 g) and roots (55.80 g) of *A. vulgaris* were macerated with methanol (150 and 280 mL, respectively) for 24 h three times, by continuous stirring at room temperature. Mass of the extracts was determined after filtration through Whatman No.1 filter paper and concentrating under reduced pressure at 45 °C. The obtained dry weights of the extracts were 3.70 g for *A. vulgaris* aerial parts (AVA) and 9.00 g for roots (AVR), (12% w/w and 16.13% w/w, respectively). The obtained extracts were kept at +4 °C until further use.

2.3. Chromatographic analysis

The identification of individual phenolic compounds in the extracts was performed using HPLC system (Shimadzu Prominence, Kyoto, Japan) as described previously (Mihalović et al., 2016). The detection wavelength of PDA was monitored at 260, 280, 325 and 330 nm. Methanolic solutions of ellagic acid, caffeic acid, gallic acid, vanillic acid, quercetin, rutin, kaempferol, (+)-catechin, and (–)-epicatechin were used as reference standards for the identification of compounds in the extracts, which was performed by comparing retention times and absorption spectra of the peaks with reference standards. The compounds identified in the extracts were confirmed by spiking the sample with the standard compound.

2.4. Phytochemical analysis

2.4.1. Total phenolics

The method developed by Singleton et al. (1998) was used to determine the total phenolic content. 0.5 mL aliquots of the extracts diluted in methanol were mixed with 2.5 mL of Folin-Ciocalteu solution (previously diluted ten-fold with water) and 2 mL of 7.5% aqueous NaHCO₃ solution. The reaction mixture was incubated for 15 min at 45 °C. The absorbance was read at 765 nm. Mass concentrations of total phenols in plant material were determined using the standard curve for gallic acid and results were calculated as gallic acid equivalents (mg GAE/g dry weight of extract).

2.4.2. Total flavonoids

The total flavonoid content was estimated by the method of Quettier-Delieu et al. (2000). The reaction mixture contained 0.5 mL 2% AlCl₃ in methanol and 0.5 mL of extracts solutions in methanol (1 mg/mL). The absorbance was measured at 415 nm after one hour of incubation at room temperature. Results were calculated as milligrammes of rutin equivalents per gram of dry weight of extract (mg RUE/g dry weight of extract).

2.4.3. Phenolic acids

Determination of the total phenolic acids content in plant extracts was performed according to the method described in the The Polish Pharmacopoeia VIII (2009), with slight modifications. Briefly, 1 mL of plant extracts solutions was added to 5 mL of distilled water, followed by addition of 1 mL of 0.1 M HCl, 1 mL of Arnov's reagent (10% Na-molybdate and 10% Na-nitrite), 1 mL of 1 M NaOH, and 1 mL of distilled water. The absorbance was read immediately at 490 nm. Results are presented as caffeic acid equivalents (mg CAE/g dry weight of extract).

2.4.4. Determination of tannins

The method suggested by Scalbert et al. (1989) was used to estimate the content of condensed tannins in plant extracts. In brief, the extracts were mixed with a certain amount of phloroglucinol (for each equivalent

of gallic acid in extracts 0.5 mol phloroglucinol was added). Subsequently, 1 mL of 4.8 M HCl solution and 1 mL of formaldehyde (13 mL of 37% formaldehyde diluted to 100 mL in water) were added. The reaction mixture was allowed to stand overnight at room temperature to precipitate the tannins. Total phenolics were determined in the solution above the precipitate using Folin–Ciocalteu method and this value was subtracted from the total phenolics' value to obtain the total tannin content, expressed as gallic acid equivalents (mg GAE/g dry weight of extract).

The gallotannin content was determined according to the procedure described by Haslam (1965). To 1.5 mL of a saturated KIO_3 solution, 3.5 mL of a methanol solution of the examined extracts were added. The absorbance of the red intermediate was spectrophotometrically determined at 550 nm until the maximum absorbance was reached. The gallotannin content was determined as gallic acid equivalents (mg GAE/g dry weight of extract).

2.4.5. Total anthocyanin content

Determination of total and monomeric anthocyanins was conducted using single pH and pH differential methods (Cheng and Breen, 1991), based on the ability of anthocyanins to change their structure depending on the pH. The specified volume of the sample was mixed with pH 1.0 KCl -buffer (0.025 M) and pH 4.5 sodium-acetate buffer (0.4 M), respectively. After 30 min incubation, the absorbance was measured spectrophotometrically at 520 and 700 nm. The concentrations of the total and monomeric anthocyanins were determined as cyanidin-3-glycoside equivalents according to the following equation: $c = (A \cdot M + F \cdot 1000) / (\epsilon \cdot l)$, where c - concentration of total or monomeric anthocyanins; A - absorbance of total and monomeric anthocyanins, which is calculated as $(A_{520} - A_{700})_{\text{pH } 1.0}$ and $(A_{520} - A_{700})_{\text{pH } 4.5}$, respectively; M - molar weight of cyanidin-3-glycoside (449.2 g/mol); F - dilution factor; ϵ - molar absorptivity (26 900 L/mol \cdot cm); l - cell length (1 cm).

2.5. Antioxidant activity

2.5.1. ABTS⁺ radical scavenging activity

Radical scavenging activity against ABTS radical cation (2,2'-azino-bis (3-ethylbenzothiazoline-6-sulphonic acid)) was measured spectrophotometrically following the procedure of Re et al. (1999). The percentage of ABTS⁺ decoloration is proportional to the ability of extract to neutralise radicals and has been calculated using the formula: % inhibition = $((A_c - A_s) \cdot 100) / A_c$, where: A_c - absorbance of the control (methanol instead of the sample); A_s - absorbance of the sample.

The concentration of samples providing 50% of radical scavenging activity (IC_{50}) was calculated using dose-response sigmoidal curve plotted the percentage of inhibition against extract concentration ($\mu\text{g/mL}$).

2.5.2. DPPH[•] radical scavenging activity

The ability of plant extracts to neutralise DPPH[•] radical was estimated according to Kumarasamy et al. (2007). The reaction mixture containing 1 mL of DPPH[•] solution in methanol (80 $\mu\text{g/mL}$) and 1 mL of each extract solution (serial dilutions in methanol, started from 0.25 mg/mL) was allowed to stand in the dark for 30 min. The absorbance was read spectrophotometrically at 517 nm and IC_{50} values were calculated.

2.5.3. Hydroxyl radical scavenging activity

OH radical scavenging activity of extracts was determined using the method performed by Kunchandy and Rao (1990). Briefly, 200 μL of the extract was mixed with 200 μL of 10 mM iron (III) chloride solution, followed by 100 μL of 1 mM ascorbic acid solution, 100 μL of 1 mM EDTA solution, 200 μL of 10 mM 2-deoxy-ribose solution, and 100 μL of 10 mM hydrogen-peroxide solution. The reaction mixture was incubated at 37 °C for 1 h. Subsequently, 1 mL of TCA-TBA solution (0.5% TBA in 10% TCA water solution) was added and the final mixture was incubated at 80 °C for 30 min and cooled to room temperature. The absorbance of the cooled reaction mixtures was measured at 535 nm.

On the basis of the obtained absorbance values, the percentage of inhibition and IC_{50} values were calculated.

2.5.4. Estimation of metal chelating ability

The assessment of ability of plant extracts to inhibit the formation of Fe^{2+} -ferrozine complex was carried out according to the method by Chew et al. (2009). One millilitre of 0.125 mM iron (II) sulphate solution and 1 mL of 0.3125 mM ferrozine water solution were added to 1 mL of serial dilutions of extracts dissolved in methanol. The reaction mixture then allows standing at room temperature for 10 min. The IC_{50} values were determined after reading the absorbance at 562 nm.

2.5.5. Reducing power

According to the method of Oyaizu (1986), to 2.5 mL of extracts solutions in methanol (0.5 mg/mL), 2.5 mL of sodium-phosphate buffer (0.2 M, pH 6.6) and 2.5 mL of 1% potassium ferricyanide were added. The reaction mixture was left to stand for 20 min at 50 °C, followed by addition of 2.5 mL of 10% TCA. In 5 mL of this solution, 1 mL of 1% iron (III) chloride solution was added and absorbance was read promptly at 700 nm. Trolox, as a referent antioxidant, was used for the construction of calibration curve and the results of reducing capacity of tested extracts were expressed as Trolox equivalents (mg TE/g dry weight of extract).

2.5.6. Total antioxidant activity

Prieto et al. (1999) developed a method for the determination of the total antioxidant activity of plant extracts. In brief, 0.3 mL of the extracts dissolved in methanol was mixed with 3 mL of reagent solution (0.6 M sulphuric acid, 28 mM sodium phosphate, 4 mM ammonium molybdate) and incubated for 90 min at 95 °C. Then, the reaction mixture was cooled to room temperature and the absorbance of the green-phosphate/Mo (V) complex was monitored at 695 nm. The results are expressed as mg ascorbic acid (AA) per gram of dry extract, using a standard curve for ascorbic acid.

2.5.7. Oil-in-water emulsion

Inhibitory activity of AVA and AVR towards lipid peroxidation was performed according to the procedure described by Hsu et al. (2008). To 0.5 mL of the serial dilutions of the extracts in methanol, 2.5 mL of linoleic acid emulsion (0.2804 g of linoleic acid and 0.2804 g of Tween-40 in 50 mL of 40 mM sodium phosphate buffer pH 7.0) was added. The emulsion was incubated for 72 h at 37 °C. Thereafter, 0.1 mL of this solution was mixed with 4.7 mL of ethanol, 0.1 mL of 30% ammonium thiocyanate solution, and 0.1 mL of 20 mM iron (II) chloride solution. Subsequently, the mixture was stirred for 3 min and afterwards the absorbance was read spectrophotometrically at 500 nm against the methanol (blank).

2.6. Antimicrobial activity

2.6.1. Test microorganisms

The antimicrobial properties of *A. vulgaris* were tested against nine bacterial and ten fungal strains. The employed bacteria were as follows: *Micrococcus lysodeikticus* (ATCC 4698), *Enterococcus faecalis* (ATCC 29212), *Escherichia coli* (ATCC 25922), *Klebsiella pneumoniae* (ATCC 70063), *Pseudomonas aeruginosa* (ATCC 10145), *Salmonella typhimurium* (ATCC 14028), *Bacillus subtilis* (ATCC 6633), and isolated strains from biological samples *Bacillus mycoides* (FSB 1) and *Azotobacter chroococcum* (FSB 14). Antifungal activity was evaluated against ATCC cultures of *Aspergillus brasiliensis* (ATCC 16404) and yeast *Candida albicans* (ATCC 10259), whereas following fungi were isolated from biological samples: *Phialophora fastigiata* (FSB 81), *Penicillium canescens* (FSB 24), *Trichoderma viride* (FSB 11), *Trichoderma longibrachiatum* (FSB 13), *Aspergillus glaucus* (FSB 32), *Fusarium oxysporum* (FSB 91), *Alternaria alternata* (FSB 51), and *Doratomyces stemonitis* (FSB 41). The isolates of the bacteria and fungi were obtained from the Laboratory for Microbiology, Faculty of Science, University of Kragujevac, Serbia.

The ATCC strains were provided from Institute of Public Health, Kragujevac, Serbia. The bacteria and fungi cultures were subcultured prior to testing; bacterial strains were cultured for 24 h at 37 °C on nutrient agar (NA), *C. albicans* was cultured on Sabouraud dextrose broth (SDB) for 24 h at 35 °C, whereas fungi were grown on potato glucose agar (PDA).

2.6.2. Microdilution method

Microdilution method described by Sarker et al. (2007) was employed to evaluate the antimicrobial activity of the samples, with some modifications. Briefly, overnight-cultured bacterial cultures were suspended in small amount of 5% DMSO than adjusted to the 0.5 McFarland turbidity standard using sterile normal saline and diluted to obtain inoculum concentration of 5×10^6 CFU/ml for broth microdilution MIC testing (CLSI, 2012). The analysed extracts (40 mg/mL), ellagic acid and catechin (1 mg/mL) and antibiotic erythromycin (40 µg/mL) were also dissolved in 5% DMSO. Determination of minimum inhibitory concentrations (MIC) of extracts for bacteria was performed in sterile 96 well plates (Spektar, Čačak, Serbia). 50 µL of two-fold serial diluted extracts in Muller-Hinton broth (MHB) was added to each well, followed by addition of 10 µL of resazurin (indicator), 30 µL of MHB, and 10 µL of bacteria suspension. The final bacterial concentration of in each well was 5×10^5 CFU/mL (CLSI, 2012). Each plate also included positive (erythromycin at a concentration range 20–0.156 µg/mL), growth (MHB, resazurin, and bacteria suspension) and sterility (MHB and resazurin, without bacteria suspension) controls. The microplates were incubated for 24 h at 37 °C. The lowest concentration of the extracts containing blue–purple indicator's colour was considered as MIC.

Fungal species were cultured on PDA at 28 °C from 48 h to 5 days. Obtained colonies covered with a small volume of 5% DMSO to obtain the suspension, and then a final concentration of inoculum suspension was adjusted with sterile normal saline to 5×10^8 CFU/mL in accordance with NCCLS recommendation (NCCLS, 2002a, 2002b). The concentration of the extracts was 40 mg/mL, 40 µg/mL for antimycotic nystatin, and 2 mg/mL for ellagic acid and catechin. MICs for fungal species were also determined in sterile 96 well plates (NCCLS, 2002a, 2002b). 50 µL of serially diluted extracts in SDB, 40 µL of SDB, and 10 µL of fungal suspension were added to each well, whereupon microplates were incubated at 28 °C for 48 h. MICs were determined as the lowest concentration of extracts without visible fungal growth.

2.7. Evaluation of anti-inflammatory activity

2.7.1. COX-1 and COX-2 *in vitro* assays

The inhibition of COX-1 and COX-2 enzymes were evaluated using *in vitro* assays in a 96-well plate with prostaglandin H synthase (PGHS)-1 from ram seminal vesicles for COX-1 and human recombinant PGHS-2 for COX-2 as previously described (Fiebich et al., 2005) with modifications published by Katanić et al. (2016). Briefly, 10 µL of extracts (50 µg/mL) dissolved in DMSO were added to the incubation mixture containing 180 µL of 0.1 M TRIS/HCl-buffer (pH 8.0), 5 µM hematin, 18 mM epinephrine hydrogen tartrate, 0.2 U enzyme preparation and 50 µM Na₂EDTA (only for COX-2 assay) and allowed to stand for 5 min. Positive controls, indomethacin (1.25 µM, for COX-1) and NS-398 (5 µM, for COX-2) were also dissolved in DMSO. To start the reaction, 10 µL of 5 µM arachidonic acid in ethanol was

added to the reaction mixture. After 20 min of incubation at 37 °C, the reaction was terminated by adding 10 µL of 10% formic acid.

The competitive PGE₂ EIA kit was applied for the determination of the PGE₂, the main arachidonic acid metabolite in this reaction. The microplate reader (Tecan Rainbow, Switzerland) was used for evaluation of EIA and the PGE₂ concentration was determined according to the method described by Fiebich et al. (2005). All experiments were performed in at least three independent experiments run in duplicate. Inhibition of COX refers to the reduction of PGE₂ formation in comparison to a blank without inhibitor.

2.7.2. COX-2 gene expression assay

COX-2 gene expression analysis was performed in accordance with the previously described method (Livak and Schmittgen, 2001) and with slight modifications described in Katanić et al. (2016). The differentiated human leukemic monocytic cell line THP-1 were treated with plant extracts (25 µg/mL) for 1 h and stimulated with 7.5 ng/mL final concentration LPS (lipopolysaccharide). Cells treated with DMSO (dimethylsulfoxide < 0.1%) were used as calibrator sample.

2.8. Biocompatibility of extracts

BalBc-3 T3 fibroblasts and human epidermal keratinocytes were cultured in Dulbecco's Modified Eagle's Medium, supplemented with 10% fetal bovine serum, 2 mM L-glutamine and antibiotics (streptomycin and penicillin) in a 5% CO₂ humidified atmosphere at 37 °C.

For biocompatibility experiments, cells were seeded in 96-well plates at a density of 2×10^3 /well (HaCaT cells) and 3×10^3 /well (BalBc-3 T3 cells). 24 h after seeding, increasing concentrations of the extracts (from 10 to 50 µg/mL) were added to the cells. After 48 and 72 h incubation, cell viability was assessed by the MTT (3-(4,5-dimethylthiazol-2-yl)-2,5-diphenyltetrazolium bromide) assay, as described by Del Giudice et al. (2015). Cell survival was expressed as the percentage of viable cells in the presence of the extract compared to controls. Two groups of cells were used as a control, i.e. cells untreated with the extract and cells supplemented with identical volumes of buffer. The average of the two control groups was used as 100%. Each sample was tested in three independent analyses, each carried out in triplicates.

2.9. Statistical analysis

The standard deviation was calculated using Microsoft Office Excel 2007 software and all results were expressed as mean values ± SD. Statistical analysis of the results was performed by one-way analysis of variance (ANOVA) using the OriginPro8 software package (OriginLab, Northampton, Massachusetts, USA) for Windows. The statistical significance was set at $p < 0.05$.

3. Results

3.1. Phytochemical results

We analysed the total phenolic compounds by spectrophotometry and HPLC-PDA to identify major phenolic components in the *A. vulgaris* extracts. Our results of the analysis of phenolic compounds in methanolic extracts of aerial parts and roots of *A. vulgaris* revealed a high content in

Table 1
Total phenolic compounds in methanolic extracts of aerial parts and roots of *A. vulgaris*.

Plant extracts	mg GAEs/g d.w.			mg RUEs/g	mg CAEs/g	mg C3Gs/g	
	Total phenolics	Condensed tannins	Gallotannins	Total flavonoids	Phenolic acids	Total anthocyanins	Monomeric anthocyanins
AVA	558.19 ± 4.83 ^a	386.70 ± 6.82 ^a	97.98 ± 0.01 ^a	13.30 ± 1.69 ^{ab}	33.43 ± 1.15 ^b	8.41 ± 0.17 ^{abc}	8.00 ± 0.18 ^d
AVR	442.32 ± 22.31 ^b	360.88 ± 2.17 ^a	n.d.	19.80 ± 0.35 ^a	57.36 ± 5.18 ^a	1.36 ± 0.06 ^c	0.95 ± 0.07 ^c

Results are expressed as mean values ± SD from three measurements; GAEs – gallic acid equivalents, RUEs – rutin equivalents, CAEs – caffeic acid equivalents, and C3Gs – cyanidine-3-glucoside equivalents per gram of dry weight of extract; n.d. – not detected; means with different symbol in superscript are significantly different at $p < 0.05$.

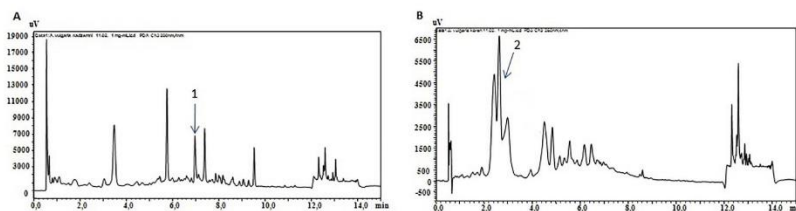


Fig. 1. HPLC-PDA chromatogram of *A. vulgare* methanolic extract of aerial parts (A) and roots (B) recorded at 280 nm with tentatively identified ellagic acid (1) and (+)-catechin (2).

both extracts. As can be seen from Table 1, spectrophotometrical determination demonstrated significantly higher ($p < 0.05$) amount of total phenolics in AVA (558.27 mg GAEs/g) in comparison with AVR (442.32 mg GAEs/g). The most dominant phenolics in AVA were condensed tannins (proanthocyanidins) and gallotannins (386.70 and 97.80 mg GAEs/g), while AVR contained a slightly lower amount of condensed tannins (360.88 mg GAEs/g) and no detectable amount of gallotannins. On the contrary, the concentration of hydroxycinnamic acids derivatives was found to be significantly higher in the roots of *A. vulgare*, while no significant difference in the content of flavonoids was observed. Anthocyanins content in the root extract was significantly lower ($p < 0.05$) when compared to all other examined classes of phenolic compounds. Fig. 1 presents HPLC-PDA chromatograms of AVA and AVR. Two of the peaks were tentatively identified as ellagic acid in the above ground parts and (+)-catechin in the roots extract by matching their retention times and comparing their UV-spectra at 260, 280, 325 and 330 nm. The identified compounds in the extracts were also confirmed by spiking the extracts with reference compounds.

3.2. Antioxidant activity

Because of the drawbacks of the individual use of any *in vitro* method for evaluation of antioxidant activity, several methods for screening the antioxidant potential of AVA and AVR have been employed and the results are reported in Table 2. The absorbance of green phosphate/Mo (V) complex formed at acidic pH was measured to evaluate the total antioxidant activity of the extracts. The obtained results showed that AVR exerts a higher total antioxidant activity than AVA (316.5 and 265.6 mg ascorbic acid/g, respectively). The potential ability of the extracts to neutralise free radicals was investigated using DPPH[•], ABTS^{•+}, and [•]OH assays. In these assays, AVA showed better antiradical activity with significantly lower ($p < 0.05$) IC₅₀ values than AVR. Considering the reference antioxidants, AVA and AVR could scavenge DPPH[•], ABTS^{•+}, and [•]OH radicals at significantly lower ($p < 0.05$) concentrations than the synthetic antioxidant butylated hydroxytoluene (BHT). Furthermore, there was no statistically significant difference in DPPH[•] radical scavenging activities between AVA and the well-known phenolic

Table 2
Antioxidant capacity of the *A. vulgare* aerial parts and roots methanolic extracts and standards: BHT, catechin, and ellagic acid.

Plant extracts and standards	IC ₅₀ value (μg/mL)			Inhibition of lipid peroxidation Oil-in-water system	Total antioxidant activity (mg AA/g of extract)	Reducing capacity (mg Trolox/g of extract)
	Radical scavenging activity DPPH [•]	ABTS ^{•+}	[•] OH			
AVA	5.96 ± 0.21 ^a	14.80 ± 2.15 ^a	13.06 ± 0.97 ^a	31.91 ± 3.12 ^a	265.62 ± 12.10	632.99 ± 10.26
AVR	11.86 ± 0.56 ^b	32.49 ± 1.95 ^b	18.44 ± 1.11 ^b	475.13 ± 11.41 ^b	316.47 ± 18.71	607.52 ± 10.01
BHT	26.25 ± 1.9 ^c	44.67 ± 3.00 ^c	21.93 ± 0.47 ^c	4.53 ± 0.07 ^c	n.t.	n.t.
Catechin	7.52 ± 0.04 ^a	5.97 ± 0.16 ^d	6.32 ± 0.33 ^a	6.63 ± 0.11 ^c	n.t.	n.t.
Ellagic acid	3.54 ± 0.13 ^d	8.14 ± 0.18 ^d	7.18 ± 0.89 ^a	10.87 ± 0.50 ^c	n.t.	n.t.

AA – ascorbic acid; means in the same column with different symbol in superscript are significantly different at $p < 0.05$.

Table 3
Antibacterial activity of methanolic extracts of aerial parts and roots of *A. vulgare*.

Bacterial species	MIC values ^a				
	AVA	AVR	Ellagic acid	Catechin	Erythromycin
<i>Micrococcus lysodeikticus</i> (ATCC 4698)	0.156	0.156	0.5	>1	20
<i>Salmonella typhimurium</i> (ATCC 14028)	0.625	0.625	0.5	0.5	20
<i>Bacillus subtilis</i> (ATCC 6633)	2.5	1.25	0.25	0.5	10
<i>Enterococcus faecalis</i> (ATCC 29212)	0.625	0.156	0.031	>1	1.25
<i>Escherichia coli</i> (ATCC 25922)	1.25	1.25	>1	>1	5
<i>Klebsiella pneumoniae</i> (ATCC 70063)	5	10	>1	>1	>20
<i>Pseudomonas aeruginosa</i> (ATCC 10145)	2.5	5	1	1	20
<i>Bacillus mycoloides</i> (FSB 1)	0.625	0.156	0.016	>1	1.25
<i>Azotobacter chroococcum</i> (FSB 14)	5	2.5	0.031	>1	20

^a MIC values, minimum inhibitory concentrations given as mg/mL for plant extracts, ellagic acid, and catechin, and as μg/mL for antibiotic erythromycin.

antioxidant catechin. The significant difference ($p < 0.05$) in antioxidant activity between the two extracts was also observed in an oil-in-water system, where AVR showed almost fifty times higher IC_{50} value than AVA (475.1 and 31.9 $\mu\text{g/mL}$, respectively). Quite similar results for AVA and AVR were obtained in the reducing power assay (633.0 and 607.5 mg Trolox/g, respectively).

The ferrous ion chelating test was employed to estimate the ability of the extracts to chelate transition metals and to avoid the iron-overload and generation of free radicals. All tested samples failed to chelate Fe^{2+} at concentration 1 mg/mL.

3.3. Antimicrobial activity

The results obtained for antimicrobial activity are shown in Tables 3 and 4. *Enterococcus faecalis*, *Salmonella typhimurium*, *Micrococcus lysodeikticus*, and *Bacillus mycoides* were the most sensitive examined bacterial species to the tested *A. vulgaris* extracts, with MICs between 0.156 and 0.625 mg/mL. On the contrary, *Klebsiella pneumoniae* was the most resistant bacteria in our study (MIC = 5 mg/mL for AVA and 10 mg/mL for AVR). MICs values above 1 mg/mL for AVA and AVR were also observed for *Pseudomonas aeruginosa*, *Bacillus subtilis*, *Azotobacter chroococcum*, and *Escherichia coli*. Ellagic acid and catechin were used as reference compounds. Catechin failed to inhibit the growth of all tested bacteria at concentrations lower than 0.5 mg/mL. We observed that ellagic acid has antibacterial potential against the same bacteria as the extracts, but MICs obtained for it were lower than those for the extracts for the majority of bacteria. The commercially available antibiotic erythromycin was more active against all tested bacteria than the investigated extracts, ellagic acid, and catechin, with MICs ranging from 1.25 to 20 $\mu\text{g/mL}$.

The investigated extracts showed similar activity against most of the tested fungi, with MICs from 2.5 to above 20 mg/mL (Table 4). AVA and AVR exhibited negligible antifungal activity against *Doratomyces stemonitis* (2.5 and 5 mg/mL, respectively) and *Aspergillus glaucus* (5 and 10 mg/mL, respectively). On the contrary, AVA failed to inhibit both *Trichoderma* species, while AVR did not show any antifungal effect against *Aspergillus brasiliensis* and *Alternaria alternata* at a concentration of 20 mg/mL. Moreover, both extracts did not inhibit the growth of *Candida albicans* at the highest tested concentration. Ellagic acid failed to inhibit the growth of the majority of the employed fungi at a concentration lower than 1 mg/mL, except for *P. canescens* (MIC = 0.25 mg/mL), while catechin did not exhibit any antifungal activity at the same concentration. Our results showed the lower activity of AVA, AVR, and reference compounds against all tested fungi in comparison with the antimycotic nystatin, which has demonstrated antifungal activity at concentrations from 0.078 up to 5 $\mu\text{g/mL}$.

Table 4
Antifungal activity of the methanolic extracts of aerial parts and roots of *A. vulgaris*.

Fungal species	MIC ^a values				
	AVA	AVR	Ellagic acid	Catechin	Nystatin
<i>Phialophora fastigiata</i> (FSB 81)	10	20	>1	>1	1.25
<i>Penicillium canescens</i> (FSB 24)	20	20	0.25	>1	2.5
<i>Trichoderma viride</i> (FSB 11)	>20	20	1	>1	0.078
<i>Trichoderma longibrachiatum</i> (FSB 13)	>20	20	>1	>1	0.078
<i>Aspergillus brasiliensis</i> (ATCC 16404)	20	>20	>1	>1	5
<i>Aspergillus glaucus</i> (FSB 32)	5	10	1	>1	5
<i>Fusarium oxysporum</i> (FSB 91)	10	20	1	>1	2.5
<i>Alternaria alternata</i> (FSB 51)	20	>20	>1	>1	0.625
<i>Doratomyces stemonitis</i> (FSB 41)	2.5	5	>1	>1	2.5
<i>Candida albicans</i> (ATCC 10259)	>20	>20	>1	>1	0.625

^a MIC values, minimum inhibitory concentrations given as mg/mL for plant extracts, ellagic acid, and catechin, and as $\mu\text{g/mL}$ for antimycotic nystatin.

3.4. Anti-inflammatory activity

Fig. 2. represents results of COX-1 and COX-2 inhibition assays as well as COX-2 gene expression. Our results revealed that at a concentration of 50 $\mu\text{g/mL}$, AVA was capable of inhibiting the activity of COX-1 enzyme by 44.4%, whereas the inhibition of COX-2 was higher (63.6%). Similar results were observed for AVR (44.1% for COX-1 and 40.4% for COX-2). The tested extracts at a concentration of 25 $\mu\text{g/mL}$ did not inhibit COX-2 gene expression.

3.5. Biocompatibility results

Finally, we analysed the biocompatibility of the extracts by performing a cell survival assay. The extracts were tested on immortalised murine Balb-C-3 T3 fibroblasts and human normal HaCaT keratinocytes in a dose- and time-response test. As shown in Fig. 3, no significant differences in cell survival between control group and groups treated with extracts were observed. Indeed, both extracts showed total biocompatibility with the two cell lines after 48 and 72 h.

4. Discussion

Notwithstanding that species from genus *Alchemilla* have been used for many years in traditional medicine and are widely spread across Europe, only a few reports have focused on their chemical composition analysis. We tentatively identified ellagic acid in AVA and (+)-catechin in AVR by HPLC-PDA analysis. Our results supported previously published research, which indicated that ellagic acid is the major phenolic component in the aerial parts of *A. vulgaris* (Møller et al., 2009; Neagu et al., 2015; Ilić-Stojanović et al., 2017). To the best of our knowledge, phytochemical screening of *A. vulgaris* underground parts was performed only by Geiger et al. (1994). They found condensed tannins as major components (50% of the total tannins) of the 80% methanolic extract of *A. vulgaris* roots and confirmed the presence of ellagitannins (agrimoniin, pedunculagin, and laevigatin F) in the fresh aerial and underground parts as well. By spectrophotometric determination, we observed a high amount of phenolic compounds in both extracts; the extracts were especially rich in condensed tannins. Maier et al. (2017) found that the Lady's mantle herb extract contains about 30% w/w of tannins, which is in agreement with our findings. Ellagic acid manifests a broad spectrum of biological activity (Khanduja et al., 1999; Beserra et al., 2011). With regard to the high amount of phenolic compounds with proven health benefits, *A. vulgaris* can be considered as a promising medicinal plant.

Free radicals and other oxidants are responsible for the emergence of a large number of diseases, such as Parkinson's disease, cancer, cardiovascular, and obesity-related diseases (Lobo et al., 2010). There is increasing evidence that phenolics and other natural antioxidants from plants in the human diet may prevent, postpone and control the development of degenerative diseases (Consolini and Sarubbio, 2002; Dastmalchi et al., 2012; Costa et al., 2013; Batista et al., 2014). The results we obtained for antioxidant activity of examined extracts through seven methods undoubtedly demonstrated the strong antioxidant potential of extracts, comparable with reference compound catechin and even better than synthetic preservative (BHT) in certain antioxidant assays. AVA showed significantly better ($p < 0.05$) antioxidant activities in all employed methods in our study, except for total antioxidant activity. Furthermore, AVA demonstrated particularly better antioxidant activity in the inhibition of lipid peroxidation than AVR. The lowest IC_{50} values for the extracts were recorded in DPPH assay. IC_{50} values for the extracts were lower in comparison with those for BHT and they are in common with the results reported by Ilić-Stojanović et al. (2017), while no statistically significant difference ($p < 0.05$) was observed between AVA and catechin. Since numerous plant phenolics have been found to be responsible for biological properties, it can be assumed that antioxidant activities of these extracts are

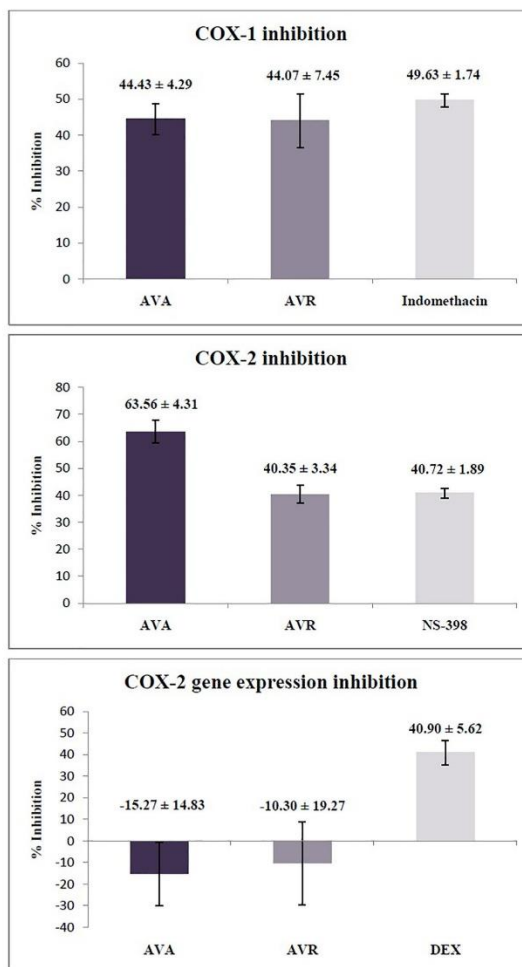


Fig. 2. COX-1 and COX-2 inhibitory activities and COX-2 gene expression on THP-1 of *A. vulgaris* extracts (50 and 25 µg/mL, respectively). Indomethacin, NS-398 and dexamethasone (DEX) were used as positive controls, according to Katančić et al. (2016). The graph represents compiled data (% inhibition) of two independent experiments (mean ± SD).

related to their phenolic profile. With respect to the high amount of polyphenols, strong antioxidant activity under *in vitro* and *in vivo* conditions was reported for other species from the Rosaceae family (Katančić et al., 2015; Jiménez-Aspée et al., 2016).

One of the main reasons to find novel natural sources of antioxidants is the fact that a large number of reactive oxygen species is produced during the inflammatory process (Conner and Grisham, 1996). Serious

side effects of existing anti-inflammatory drugs are burning pharmaceutical concern worldwide. Therefore, research goes on to find new highly effective and harmless anti-inflammatory remedies of natural origin which can be alternatives to NSAIDs. The undertaken study demonstrates, for the first time, the effects of *A. vulgaris* methanolic extracts on COX-1 and COX-2 enzymes inhibition, with the preferential COX-2 inhibitory activity of AVA with AVR approximately the same

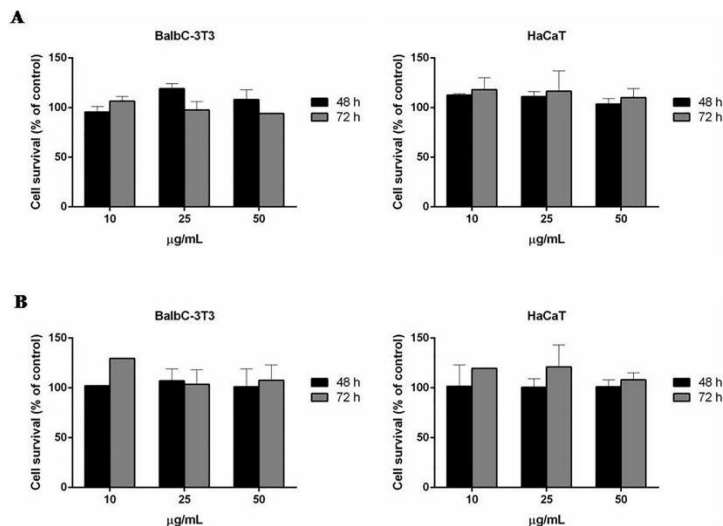


Fig. 3. Effects of *A. vulgaris* aboveground parts (A) and roots (B) methanol extracts on the viability of mouse immortalised BalbC-3T3 fibroblasts and human normal HaCaT keratinocytes. Dose- and time-response curves of cells after 48 h (black bars) and 72 h (grey bars) incubation in the presence of increasing concentrations of the extracts. Cell viability was assessed by the MTT assay; the cell survival percentage was defined as described in Materials and Methods section. Values are given as means \pm S.D. ($n \geq 3$).

inhibitory activity on both COX isoforms. Notwithstanding that AVR is not COX-2 specific, the relatively high percentage of the inhibition of COX enzymes is confirming the presence of anti-inflammatory compounds in this extract. Therefore, these results can be of great importance for further testing of Lady's mantle as a potential anti-inflammatory remedy. NF- κ B is a nuclear transcription factor regulating the expression of various genes, including IL-1 β , IL-6, TNF- α , and iNOS, which play critical roles in inflammation, apoptosis, and tumour genesis (Lawrence et al., 2001). Negative results obtained for NF- κ B production in our study indicate that neither AVA nor AVR exert their anti-inflammatory activity through the inhibition of NF- κ B. Anti-inflammatory activity of *A. vulgaris* has already been tested for the inhibition of 15-lipoxygenase activity (Trouillas et al., 2003), and the results provided a presumption that anti-inflammatory action of *A. vulgaris* may be related to the inhibitory activity of phenolic compounds on arachidonic acid metabolism through the lipoxygenase pathway. According to Şeker-Karatoprak et al. (2017), methanolic and water extracts of *A. mollis* decreased the nitrite as well as inhibited TNF- α production in LPS-induced macrophages. In support of the traditional use of *Alchemilla* species in wound treatment, Shrivastava et al. (2007) displayed acceleration in wound healing and a significant reduction in the size of dorsal skin lesions in rats by the second day of the treatment with 3% *A. vulgaris* in glycerine. Also, *A. vulgaris* enhanced proliferation of epithelial, liver and myofibroblasts cells as well. It is worth noting that no cytotoxic effect or any morphological changes were observed in the cells exposed to *A. vulgaris* extract in the above mentioned study. We obtained the same results in our study through biocompatibility assays on immortalised fibroblasts BalbC-3 T3 and normal epidermal HaCaT cells during 48 and 72 h. Fibroblasts and keratinocytes facilitate the protective role of normal skin and play a crucial role in cutaneous reparation process. When a wound occurs, then natural skin barrier is disrupted, which promotes the proliferation as well as the maturation

of fibroblasts and keratinocytes. They migrate into the wound site and communicate via certain signalling loops, which support the restoration and regeneration of tissue homeostasis after wounding (Wojtowicz et al., 2014). Biocompatibility of plant extracts may prevent differentiation, proliferation, and attaching of these skin cells. The results of our study indicate that the application of AVA and AVR at doses ranging from 10 to 50 μ g/mL provides good biocompatibility, with no toxic or injurious effects on the healthy cells.

According to Kuete (2010), an extract can be considered as a potent antibacterial agent with significant antibacterial activity with MICs below 0.1 mg/mL, while MICs between 0.1 and 0.625 mg/mL pointed to moderate activity against bacterial growth. MICs above 0.625 mg/mL referred to weak activity. The results in Table 3 revealed that Gram-positive bacteria are more susceptible in comparison with Gram (–) ones. These findings are not surprising, considering the fact that Gram (–) bacteria are more resistant than Gram (+) ones to plant extract treatment, because of the porins and lipopolysaccharides present in their outer membrane, which provides a protective barrier and prevents intracellular penetration of antibiotics, especially lipophilic ones (Apetrei et al., 2011). To the extent of our knowledge, this is the first study covering antimicrobial activity of *Alchemilla* roots. Additionally, there are no literature data related to the antifungal activity of *Alchemilla* species, while only a few scientific reports provide information about activities of the aboveground parts of *Alchemilla* species against bacteria and *C. albicans*. Our results displayed negligible antifungal activity of *A. vulgaris* with MICs from 2.5 to above 20 mg/mL. Our results are in accordance with the results published by Keskin et al. (2010), indicated that ethanol extract of *A. vulgaris* at a concentration of 4 mg/mL exhibited moderate antibacterial activity against ten bacterial species, whereby the most sensitive ones were Gram-positive bacteria, including *E. faecalis*. Krivokuća et al. (2015) reported that extracts of four *Alchemilla* species exerted anti-*Helicobacter pylori* effect with MICs

ranging from 4 to 256 µg/mL. The same pattern of antibacterial activity as for AVR and AVA has been observed for ellagic acid, where the most sensitive strains were Gram positive bacteria *M. lysodeikticus*, *E. faecalis*, and *B. mycoides* and Gram negative – *A. chroococcum*. Our results showed low susceptibility of tested bacteria to catechin. Antibacterial effects of *A. vulgare* may be attributed to the high content of tannins presented in the extracts (Djipa et al., 2000). With respect to the results of antibacterial activity of phenolic standards, our findings indicate that use of *A. vulgare* extracts may be more beneficial than the application of individual compounds, due to the possible synergistic effects of the other components of the extracts.

5. Conclusion

Our results have demonstrated that methanolic extracts of aerial parts and roots of *A. vulgare* are rich in phenolic compounds. Through the evaluation of antioxidant, antibacterial, antifungal, and anti-inflammatory activities, we observed the remarkable biological activity of the tested extracts, as well as their full biocompatibility with fibroblasts and keratinocytes. Taking into account promising biological activity and safety of *A. vulgare*, our further research will be aimed to investigate its biological activities under *in vivo* conditions. We hope to discover the potential mechanism of biological action and to elucidate whether the specific biological activity is a result of the activity of individual components or synergistic action of several constituents.

Conflict of interest

The authors declare no conflict of interest.

Acknowledgments

This research is financially supported by the Ministry of Education, Science and Technological Development of the Republic of Serbia (grant No. 43004).

References

- Apetrei, C.L., Tuchilus, C., Aprotosoia, A.C., Oprea, A., Malterud, K.E., Miron, A., 2011. Chemical, antioxidant and antimicrobial investigations of *Pinus cembra* L. bark and needles. *Molecules* 16, 7773–7788.
- Batista, A.G., Lenquist, S.A., Cazarin, C.B.B., da Silva, J.K., Luiz-Ferreira, A., Bogusz, S., Hantao, W.L., de Souza, R.N., Augusto, F., Prado, M.A., Marostica, M.R., 2014. Intake of jaboritoba peel attenuates oxidative stress in tissues and reduces circulating saturated lipids of rats with high-fat diet-induced obesity. *Journal of Functional Foods* 6, 450–461.
- Beserra, A.M.S.E.S., Calegari, P.I., Souza, M.D.C., Dos Santos, R.A.N., Lima, J.C.D.S., Silva, R.M., Balogun, S.O., Martins, D.T.D.O., 2011. Gastroprotective and ulcer-healing mechanisms of ellagic acid in experimental rats. *Journal of Agricultural and Food Chemistry* 59, 6957–6965.
- Cheng, G., Breen, P., 1991. Activity of phenylalanine ammonia-lyase (PAL) and concentrations of anthocyanins and phenolics in developing strawberry fruit. *Journal of the American Society for Horticultural Science* 116, 865–869.
- Chew, Y.L., Goh, J.K., Lim, Y.Y., 2009. Assessment of *in vitro* antioxidant capacity and polyphenolic composition of selected medicinal herbs from Leguminosae family in Peninsular Malaysia. *Food Chemistry* 116, 13–18.
- CLSI, 2012. Methods for Dilution Antimicrobial Susceptibility Tests for Bacteria that Grow Aerobically: Approved Standard—Ninth Edition. CLSI Document M07-A9. Clinical and Laboratory Standards Institute, Wayne, PA.
- Conner, E.M., Grisham, M.B., 1996. Inflammation, free radicals and antioxidants. *Nutrition* 12, 274–277.
- Consolini, A.E., Sarubbio, M.G., 2002. Pharmacological effects of *Eugenia uniflora* (Myrtaceae) aqueous crude extract on rat's heart. *Journal of Ethnopharmacology* 81, 57–63.
- Costa, A.C.V., Garcia-Diaz, D.F., Jimenez, P., Silva, P.I., 2013. Bioactive compounds and health benefits of exotic tropical red-black berries. *Journal of Functional Foods* 5, 539–549.
- Dastmalchi, K., Flores, G., Wu, S.B., Ma, C., Dabo, A.J., Whalen, K., Kennelly, E.J., 2012. Edible *Myricaria tozeri* fruits: bioactive phenolics for potential COPD therapy. *Bioorganic & Medicinal Chemistry* 20, 4549–4555.
- De Giudice, R., Raiola, A., Tenore, G.C., Frusciano, L., Barone, A., Monti, D.M., Rigano, M.M., 2015. Antioxidant bioactive compounds in tomato fruits at different ripening stages and their effects on normal and cancer cells. *Journal of Functional Foods* 18, 83–94.
- Djipa, C.D., Delmeé, M., Quetin-Leclercq, J., 2000. Antimicrobial activity of bark extracts of *Syzygium jambos* (L.) Alston (Myrtaceae). *Journal of Ethnopharmacology* 71, 307–313.
- Fiebig, B.L., Grozdova, M., Hess, S., Hill, M., Danesh, U., Bodensieck, A., Bauer, R., 2005. *Petasites hybridus* extracts *in vitro* inhibit COX-2 and PGE2 release by direct interaction with the enzyme and by preventing p42/44 MAP kinase activation in rat primary microglial cells. *Planta Medica* 71, 12–19.
- Filipova, E.I., 2017. Antiviral activity of Lady's mantle (*Alchemilla vulgaris* L.) extracts against orthopoxviruses. *Bulletin of Experimental Biology and Medicine* 163, 374–377.
- Geiger, C., Scholz, E., Rimpler, H., 1994. Ellagitannins from *Alchemilla xanthochlora* and *Potentilla erecta*. *Planta Medica* 60, 384–385.
- Han, X., Shen, T., Lou, H., 2007. Dietary polyphenols and their biological significance. *International Journal of Molecular Sciences* 8, 950–988.
- Haslam, E., 1968. Galloyl esters in the Aecaceae. *Phytochemistry* 4, 495–498.
- Hitchon, C.A., El-Gabalawy, H.S., 2004. Oxidation in rheumatoid arthritis. *Arthritis Research and Therapy* 6, 265.
- Hsu, C.K., Chiang, B.H., Chen, Y.S., Yang, J.H., Liu, C.T., 2008. Improving the antioxidant activity of buckwheat (*Fagopyrum tataricum* Gaertn.) sprout with trace element water. *Food Chemistry* 108, 633–641.
- Hussein, R.H., Khalifa, F.K., 2014. The protective role of ellagitannins flavonoids pretreatment against N-nitrosodietylamine induced hepatocellular carcinoma. *Saudi Journal of Biological Sciences* 21, 589–596.
- Ilić-Stojanović, S., Nikolić, V., Kundaković, T., Savić, I., Savić-Gajić, L., Jocić, E., Nikolić, L.J., 2017. Thermosensitive hydrogels for modified release of ellagic acid obtained from *Alchemilla vulgaris* L. extract. *International Journal of Polymeric Materials and Polymeric Biomaterials*. <https://doi.org/10.1080/00914037.2017.1354202> (Accepted Manuscript).
- Jarić, S., Mačkunović-Jocić, M., Djurdjević, L., Mitrović, M., Kostić, O., Karadžić, B., Pavlović, P., 2015. An ethnobotanical survey of traditionally used plants on Suva planina mountain (south-eastern Serbia). *Journal of Ethnopharmacology* 175, 93–108.
- Jiménez-Aspée, F., Theoduloz, C., Ávila, F., Thomas-Valdés, S., Mardones, C., Von Baer, D., Schmeda-Hirschman, C., 2016. The Chilean wild raspberry (*Rubus grossus* Sm.) increases intracellular GSH content and protects against H₂O₂ and methylglyoxal-induced damage in AGS cells. *Food Chemistry* 194, 908–919.
- Jones, R., Rubin, G., Berenbaum, F., Scheiman, J., 2008. Gastrointestinal and cardiovascular risks of nonsteroidal anti-inflammatory drugs. *American Journal of Medicine* 121, 464–474.
- Katančić, I., Mihalović, V., Matić, S., Stanković, V., Stanković, N., Boroja, T., Mihalović, M., 2015. The ameliorating effect of *Filipendula hexapetala* extracts on hepatorenal toxicity of cisplatin. *Journal of Functional Foods* 18, 198–212.
- Katančić, J., Boroja, T., Mihalović, V., Nikles, S., Pan, S.-P., Rosić, G., Selaković, D., Joksimović, J., Mitrović, S., Bauer, R., 2016. *In vitro* and *in vivo* assessment of meadowsweet (*Filipendula ulmaria*) as anti-inflammatory agent. *Journal of Ethnopharmacology* 193, 627–636.
- Keskin, D., Oskay, D., Oskay, M., 2010. Antimicrobial activity of selected plant spices marketed in the West Anatolia. *International Journal of Agriculture and Biology* 12, 916–920.
- Khanduja, K.L., Gandhi, R.K., Pathania, V., Syal, N., 1999. Prevention of N-nitrosodietylamine-induced lung tumorigenesis by ellagic acid and quercetin in mice. *Food and Chemical Toxicology* 37, 313–318.
- Krivošić, A., Nikolić, M., Milenković, M., Goljić, N., Masia, C., Scatrina, M.M., Kundaković, T., 2015. Anti-helicobacter pylori activity of four *Alchemilla* species (Rosaceae). *Natural Product Communications* 10, 1369–1371.
- Kuceta, V., 2010. Potential of Cameroonian plants and derived products against microbial infections: a review. *Planta Medica* 76, 1479–1491.
- Kumarasamy, Y., Byres, M., Cox, P.J., Jaspars, M., Nahar, L., Sarker, S.D., 2007. Screening seeds of some Scottish plants for free radical scavenging activity. *Phytotherapy Research* 21, 615–621.
- Kunehandy, E., Rao, M.N.A., 1990. Oxygen radical scavenging activity of curcumin. *International Journal of Pharmacology* 58, 237–240.
- Lawrence, T., Gilroy, D.W., Colville-Nash, P.R., Willoughby, D.A., 2001. Possible new role for NF- κ B in the resolution of inflammation. *Nature Medicine* 7, 1291–1297.
- Li, A.-N., Li, S., Zhang, Y.-J., Xu, X.-R., Chen, Y.-M., Li, H.-B., 2014. Resources and biological activities of natural polyphenols. *Nutrients* 6, 6020–6047.
- Livak, K.J., Schmittgen, T.D., 2001. Analysis of relative gene expression data using real-time quantitative PCR and the 2^{- $\Delta\Delta$ CT} method. *Methods* 25, 402–408.
- Lobo, V., Patil, A., Phatak, A., Chandra, N., 2010. Free radicals, antioxidants and functional foods: impact on human health. *Pharmacognosy Reviews* 4, 118.
- Maler, M., Oelbermann, A.-L., Renner, M., Weidne, E., 2017. Screening of European medicinal herbs on their tannin content—new potential tanning agents for the leather industry. *Industrial Crops and Products* 99, 19–26.
- Masullo, M., Montoro, P., Mari, A., Pizzi, C., Piacente, S., 2015. Medicinal plants in the treatment of women's disorders: analytical strategies to assure quality, safety and efficacy. *Journal of Pharmaceutical and Biomedical Analysis* 113, 189–211.
- Melo, A., Monteiro, L., Lima, R.M., Oliveira, D.M., Cerqueira, M.D., El-Bachá, R.S., 2011. Oxidative stress in neurodegenerative diseases: mechanisms and therapeutic perspectives. *Oxidative Medicine and Cellular Longevity* 2011, 1–14.
- Mihalović, V., Kreft, S., Tavčar Benkovič, E., Ivanović, N., Stanković, M.S., 2016. Chemical profile, antioxidant activity and stability in simulated gastrointestinal tract model system of three *Verbascum* species. *Industrial Crops and Products* 89, 141–151.
- Mittal, M., Siddiqui, M.R., Tran, K., Reddy, S.P., Malik, A.B., 2014. Reactive oxygen species in inflammation and tissue injury. *Antioxidants & Redox Signaling* 20, 1126–1167.
- Møller, C., Hansen, S.H., Cornett, C., 2009. Characterisation of tannin-containing herbal drugs by HPLC. *Phytochemical Analysis* 20, 231–239.
- NCCLS, 2002a. Reference Method for Broth Dilution Antifungal Susceptibility Testing of Filamentous Fungi: Approved Standard. NCCLS Document M28-A. [ISBN 1-56238-470-8]. NCCLS, 940 West Valley Road, Suite 1400, Wayne, Pennsylvania 19087–1898 USA.
- NCCLS, 2002b. Reference Method for Broth Dilution Antifungal Susceptibility Testing of Yeasts: Approved Standard—Second Edition. NCCLS Document M27-A2. [ISBN 1-56238-469-4]. NCCLS, 940 West Valley Road, Suite 1400, Wayne, Pennsylvania 19087–1898 USA.

- Neagu, E., Paun, G., Albu, C., Radu, G.L., 2015. Assessment of acetylcholinesterase and tyrosinase inhibitory and antioxidant activity of *Alchemilla vulgaris* and *Filipendula ulmaria* extracts. *Journal of the Taiwan Institute of Chemical Engineers* 52, 1–6.
- Oyaizu, M., 1986. Studies on products of browning reaction. Antioxidative activities of products of browning reaction prepared from glucosamine. *Japanese Journal of Nutrition* 44, 307–315.
- Prieto, P., Pineda, M., Aguilar, M., 1999. Spectrophotometric quantitation of antioxidant capacity through the formation of a phosphomolybdenum complex: specific application to the determination of vitamin E. *Analytical Biochemistry* 269, 337–341.
- Quettier-Deleu, C., Gressier, B., Vasseur, J., Dine, T., Brunet, C., Luyckx, M., Cazin, M., Cazin, J.C., Baillet, F., Trouin, F., 2000. Phenolic compounds and antioxidant activities of buckwheat (*Fagopyrum esculentum* Moench) hulls and flour. *Journal of Ethnopharmacology* 72, 35–42.
- Re, R., Pellegrini, N., Proteggente, A., Pannala, A., Yang, M., Rice-Evans, C., 1999. Antioxidant activity applying an improved ABTS radical cation decolorization assay. *Free Radical Biology and Medicine* 26, 1231–1237.
- Sarker, S.D., Nahar, L., Kumarasamy, Y., 2007. Microtitre plate-based antibacterial assay incorporating resazurin as an indicator of cell growth, and its application in the *in vitro* antibacterial screening of phytochemicals. *Methods* 42, 321–324.
- Scalbert, A., Monties, B., Janin, G., 1989. Tannin in wood: comparison of different estimation methods. *Journal of Agricultural and Food Chemistry* 37, 1324–1329.
- Şeker-Karatoprak, G., Ilgın, S., Koşar, M., 2017. Phenolic composition, anti-inflammatory, antioxidant, and antimicrobial activities of *Alchemilla mollis* (Buser) Rothm. *Chemistry & Biodiversity* 14.
- Shrivastava, R., John, G.W., 2006. Treatment of aphthous stomatitis with topical *Alchemilla vulgaris* in glycerine. *Clinical Drug Investigation* 26, 567–573.
- Shrivastava, R., Cuesat, N., John, G.W., 2007. Effects of *Alchemilla vulgaris* and glycerine on epithelial and myofibroblast cell growth and cutaneous lesion healing in rats. *Phytotherapy Research* 21, 369–373.
- Singleton, V.L., Orthofer, R., Lamuela-Raventós, R.M., 1998. Analysis of total phenols and other oxidation substrates and antioxidants by means of Folin-Ciocalteu reagent. *Methods in Enzymology* 299, 152–178.
- The Polish Pharmacopoeia VIII. P.T.Farm, Warszawa, Poland.
- Trouillas, P., Calliste, C., Allais, D., Simon, A., Marfak, A., Delage, C., Duroux, J., 2003. Antioxidant, anti-inflammatory and antiproliferative properties of sixteen water plant extracts used in the Limousin countryside as herbal teas. *Food Chemistry* 80, 399–407.
- Valle, M., Izakovic, M., Mazur, M., Rhodes, C.J., Telsler, J., 2004. Role of oxygen radicals in DNA damage and cancer incidence. *Molecular and Cellular Biochemistry* 266, 37–56.
- Wojtowicz, A.M., Oliveira, S., Carlson, M.W., Zawadzka, A., Rousseau, C.F., Baksh, D., 2014. The importance of both fibroblasts and keratinocytes in a bilayered living cellular construct used in wound healing. *Wound Repair and Regeneration* 22, 246–255.

Pentadecanal inspired molecules as new anti-biofilm agents against *Staphylococcus epidermidis*

Annarita Ricciardelli^a, Angela Casillo^a, Rosanna Papa^b, Daria Maria Monti^a, Paola Imbimbo^a, Gianluca Vrenna^b, Marco Artini^b, Laura Selan^b, Maria Michela Corsaro^a, Maria Luisa Tutino^a and Ermenegilda Parrilli^a

^aChemical Sciences, University of Naples "Federico II", Naples, Italy; ^bDepartment of Public Health and Infectious Diseases, Sapienza University, Rome, Italy

ABSTRACT

Staphylococcus epidermidis, a harmless human skin colonizer, is a significant nosocomial pathogen in predisposed hosts because of its capability to form a biofilm on indwelling medical devices. In a recent paper, the purification and identification of the pentadecanal produced by the Antarctic bacterium *Pseudoalteromonas haloplanktis* TAC125, able to impair *S. epidermidis* biofilm formation, were reported. Here the authors report on the chemical synthesis of pentadecanal derivatives, their anti-biofilm activity on *S. epidermidis*, and their action in combination with antibiotics. The results clearly indicate that the pentadecanal derivatives were able to prevent, to a different extent, biofilm formation and that pentadecanoic acid positively modulated the antimicrobial activity of the vancomycin. The cytotoxicity of these new anti-biofilm molecules was tested on two different immortalized eukaryotic cell lines in view of their potential applications.

ARTICLE HISTORY

Received 12 June 2018
Accepted 30 October 2018

KEYWORDS

Anti-biofilm; pentadecanal; *Pseudoalteromonas haloplanktis* TAC125; vancomycin; pentadecanoic acid; pentadecanoic acid methyl ester; 1,1-dimethoxypentadecane

Introduction

Although *Staphylococcus epidermidis* is a harmless human skin colonizer, it has emerged as an important opportunistic pathogen in infections associated with medical devices (such as urinary and intra-vascular catheters, orthopaedic implants), causing approximately 30–43% of joint prosthesis infections (Valour et al. 2013) and fracture fixation infections (Morgenstern et al. 2016). The capability of *S. epidermidis* to adhere on both eukaryotic cells and abiotic surfaces and to form biofilm is an essential virulence factor (Otto 2012) that contributes to the chronicization of infections caused by this bacterium as particularly difficult to eradicate. *S. epidermidis* can migrate from the skin along the surface of the device into the body, forming a highly organized bacterial community known as biofilm. A biofilm is a microbially derived sessile community, characterized by cells attached either to a substratum, or to an interface, or to each other, embedded in a self-produced matrix of extracellular polymeric substance, which exhibit an altered phenotype with regard to growth, gene expression and protein production (Donlan and Costerton 2002).

In a biofilm, cells are embedded and protected from external assaults and in this condition bacteria have been found to be more resistant to conventional antibiotic treatments, thus resulting in recalcitrant biofilm-associated infections (Koo et al. 2017). Biofilm resistance to antimicrobials is a complex phenomenon, not only correlated merely with the genetic resistance that arises from mutations, although the increased microbial cell density may help the transfer of resistance genes. Indeed, other mechanisms are involved, such as: (1) the low penetration of the antimicrobial agent due to the barrier function performed by the biofilm matrix; (2) the presence of persister cells exhibiting a high multidrug tolerance; and (3) a reduced susceptibility to antibiotics as a consequence of stress adaptive responses or changes in the chemical biofilm microenvironment (Satpathy et al. 2016). Accordingly, the strategies adopted to treat these challenging infections are rapidly changing, according to the increasing understanding of the structure and functions of the biofilm. Nonetheless, the prevention of biofilm formation and the treatment of existing biofilms is currently a difficult challenge

CONTACT Ermenegilda Parrilli  erparril@unina.it

 Supplemental data for this article can be accessed at <https://doi.org/10.1080/08927014.2018.1544246>.

© 2019 Informa UK Limited, trading as Taylor & Francis Group

and therefore the discovery of new multi-targeted or combinatorial therapies is increasingly urgent (Koo et al. 2017).

In recent years, several authors working in this field have focused their studies on the search for anti-biofilm molecules in extreme environments, such as Antarctica, since it has been reported that cold-adapted bacteria represent an unexploited source of chemical biodiversity, able to produce a wide range of high added-value compounds (Papaleo et al. 2013; De Santi et al. 2016; Sannino et al. 2017; Sannino et al. 2018), including anti-biofilm molecules (Papa et al. 2015).

In a recent paper, it was demonstrated that Antarctic bacterium *Pseudoalteromonas haloplanktis* TAC125 produces a long-chain fatty aldehyde, the pentadecanal (Casillo et al. 2017), endowed with a strong anti-biofilm activity against *S. epidermidis* (Papa et al. 2013; Parrilli et al. 2015). The pentadecanal interferes with the quorum sensing system of *S. epidermidis* and reduces biofilm formation without affecting bacterial viability (Casillo et al. 2017). It is interesting to note that the pentadecanal is also found in the essential oils of different plant species (Gao et al. 2017). This mechanism of action should prevent the development of escape mutants, making the pentadecanal a good candidate for combined therapies with conventional antibiotics. Moreover, the pentadecanal's capability of preventing biofilm formation could be exploited for the development of new materials, or surface coatings, which avoid the adhesion of viable bacteria. In the literature, the incorporation of an antibiotic or biocide within a 'reservoir' coating is being studied as a possible approach to inhibit bacterial adhesion and biofilm formation (Busscher et al. 2012). An ideal anti-biofilm molecule must be endowed with several characteristics described by Batoni et al. (2016); amongst the other things it should interfere with the bacterial cell communication machinery, penetrate the extracellular matrix and/or interfere with its production, and synergize with other conventional and unconventional antimicrobial compounds. Moreover, an anti-biofilm molecule, to have a concrete therapeutic application, should be active following its incorporation within a 'reservoir' coating and, in any case, the coating should not alter the biocompatibility of devices or delivery systems. However, as the pentadecanal is an aldehyde (a chemically reactive agent), it could easily undergo oxidation reactions, therefore it may not be suitable for all possible anti-biofilm strategies. One of the aims of this work was the design of some

pentadecanal derivatives to enrich the arsenal of weapons to fight biofilm development. With the purpose of obtaining new anti-biofilm molecules endowed with different physico-chemical properties, the dimethyl acetal of the pentadecanal, the pentadecanoic acid, and its methyl ester, were synthesized.

The capability of the pentadecanal derivatives to prevent biofilm formation by *S. epidermidis* and their possible use in combination with antibiotics was investigated. Finally, to explore the possible clinical applications, their biocompatibility on eukaryotic cells was analysed on two different immortalized cell lines.

Materials and methods

Bacterial strains and culture conditions

The bacterial strains used in this work were: *S. epidermidis* RP62A, a reference strain isolated from an infected catheter (ATCC collection no. 35984); and *S. epidermidis* O-47, a strong biofilm producer (Figure S1 in Supplemental material) *agr*-mutant, isolated from clinical septic arthritis and kindly provided by Prof. Gotz (Heilmann et al. 1996). Bacteria were grown in brain heart infusion broth (BHI, Oxoid Ltd./Thermo Fisher Scientific, Cambridge, United Kingdom). Biofilm formation was assessed in static conditions at 37 °C, whereas planktonic cultures were performed under vigorous agitation (180 rpm) at 37 °C. All strains were maintained at -80 °C in cryovials with 15% glycerol.

Derivatives design and synthesis and purification

To generate new anti-biofilm molecules endowed with physico-chemical properties different from those of pentadecanal, pentadecanoic acid (carboxylic acid), pentadecanoic acid methyl ester (ester), and 1,1-dimethoxypentadecane (acetal) were synthesized. The choice of these derivatives was mainly suggested by the well-known reactivity of an aldehyde, which is able to be oxidized by oxygen in the air, even in the presence of a catalytic amount of Fe³⁺ (Carey and Sundberg 2000; Farquhar 1961; Jiang et al. 2018).

Pentadecanoic acid was purchased from Sigma (Sigma-Aldrich, Inc., St. Louis, MO © 2018 Merck KGaA, Darmstadt, Germany).

The acetal was obtained by treating the pentadecanal (50 mg) by reaction with 6 ml of 1.25 M HCl/CH₃OH at 80 °C for 16 h. After overnight reaction, the reaction was quenched with anionic exchange resin (HCO₃⁻ form), and the product recovered with a yield of 98%.

To obtain the methyl ester, 50 mg of pentadecanoic acid were treated with 5 ml of 1.25 M HCl/CH₃OH at 80 °C for 16 h. The methanol layer was extracted three times with hexane to recover the methyl ester with a yield of 99%. The mixture was then treated with Dowex 1X8 resin (Sigma, HCO₃⁻ form) and dried under argon flow. As for the methyl ester, the recovery of the acetal was 98%.

All the synthesized compounds were characterized by ¹H-NMR spectroscopy and gas chromatography-mass spectrometry (GC-MS). Furthermore, the purity of the synthesized derivatives was confirmed by GC-MS analysis (Figure S2). All the compounds were analysed on an Agilent 7820 A GC System-5977B MSD spectrometer equipped with the automatic injector 7693A and a Zebtron ZB-5 capillary column (Phenomenex, Toornace, CA, USA; flow rate 1 ml min⁻¹; He as carrier gas), using the following temperature program: 150 °C for 3 min, 150 °C → 300 °C at 15 °C/min, 300 °C for 5 min. As for the ¹H NMR experiments, each sample was dissolved in 0.55 ml of dimethyl sulfoxide-d6 (DMSO-d6), and the spectra were recorded at 298 K using a Bruker Avance 600 MHz spectrometer equipped with a cryoprobe (Bruker Italia, Milano, Italy).

Biofilm formation by staphylococci

Static biofilm assay

The quantification of *in vitro* biofilm production was based on the method described by Christensen with slight modifications (Papa et al. 2013).

Briefly, the wells of a sterile 96-well flat-bottomed polystyrene plate (tissue culture treated by vacuum gas plasma, Falcon® Corning, Corning, NY) were filled with *S. epidermidis* RP62A or *S. epidermidis* O-47 cultures in exponential growth phase diluted in BHI with a final concentration of about 0.1 and 0.001 OD_{600nm} respectively. The derivatives were added at different concentrations and the final volume was 200 µl.

The first row contained the untreated bacterial cells, while each of the remaining rows contained different concentrations (from 12.5 µg ml⁻¹ to 100 µg ml⁻¹) of the derivatives samples. Dried derivatives were first re-solubilized in DMSO and a working solution of each derivative to be tested was diluted in BHI (0.8% DMSO final concentration at the maximal concentration used). From this stock solution, serial two-fold dilutions in BHI broth were carried out in 96-well plates over the concentration range 100–12.5 µg ml⁻¹. A control using BHI broth with

0.8% DMSO was also included in each experiment. The plates were incubated aerobically for 24 h at 37 °C. After the incubation, planktonic cells were gently removed; each well was washed three times with double-distilled water and patted dry with a piece of paper towel in an inverted position. To quantify the biofilm formation, each well was stained with 0.1% (w v⁻¹) crystal violet and incubated for 15 min at room temperature, rinsed twice with double-distilled water, and thoroughly dried. The dye bound to adherent cells was solubilized with 20% (v v⁻¹) glacial acetic acid and 80% (v v⁻¹) ethanol. After incubation at room temperature for 30 min, the OD was measured at 590 nm to quantify the total biomass of biofilm formed in each well. Each data point is composed of three independent experiments, each performed in six replicates. The data reported were statistically validated using the Student's *t*-test comparing the mean absorbance of treated and untreated samples. The significance of differences between the mean absorbance values was calculated using a two-tailed Student's *t*-test. A *p*-value of <0.05 was considered significant.

CLSM analysis and COMSTAT

For confocal microscope analysis, biofilms were formed on Nunc™ Lab-Tek® 8-well Chamber Slides (n° 177445; Thermo Scientific, Ottawa, Canada). Briefly, the wells of the chamber slide were filled with *S. epidermidis* RP62A or *S. epidermidis* O-47 cultures in exponential growth phase diluted in BHI at a final concentration of ~0.1 and 0.001 OD_{600nm} respectively and incubated in the presence of derivatives (100 µg ml⁻¹ – 0.8% DMSO). The final volume was 300 µl. The bacterial cultures were incubated at 37 °C for 20 h in the presence and absence of derivatives in order to assess their anti-biofilm activity and their influence on cell viability. The biofilm cell viability was determined by the FilmTracer™ LIVE/DEAD® Biofilm Viability Kit (Molecular Probes, Invitrogen, Carlsbad, CA, USA) following the manufacturer's instructions. After rinsing with filter-sterilized PBS, each well of the chamber slide was filled with 300 µl of a working solution of fluorescent stains, containing the SYTO® 9 green fluorescent nucleic acid stain (10 µM) and propidium iodide, and the red-fluorescent nucleic acid stain (60 µM), and incubated for 20–30 min at room temperature, protected from light. Excess stain was removed by gently rinsing with filter-sterilized PBS. All microscopic observations and image acquisitions were performed with a confocal

laser scanning microscope (CLSM; LSM700-Zeiss, Jena, Germany) equipped with an Ar laser (488 nm), and a He-Ne laser (555 nm). Images were obtained using a 20×/0.8 objective. The excitation/emission maxima for these dyes are ~480/500 nm for SYTO[®] 9 stain and 490/635 nm for propidium iodide. Z-stacks were obtained by driving the microscope to a point just out of focus on both the top and bottom of the biofilms. Images were recorded as a series of .tif files with a file-depth of 16 bits. A COMSTAT software package was used to determine biomasses (μm^3 μm^{-3}), average thicknesses (μm) and roughness coefficient (Ra^*). For each condition, two independent biofilm samples were used.

MIC and MBC of vancomycin determination

The conventional MIC of vancomycin was determined for *S. epidermidis* RP62A in duplicate, by two-fold serial dilution (Clinical & Laboratory Standards Institute (CLSI) 2017). Briefly, an overnight culture was diluted at 0.5 McFarland and 90 μl of this dilution were added to each well of a 96-well microtitre dish. Ten μl vancomycin previously diluted to the desired final concentration were added to the wells. Ten μl water were added for the control lane. The microtitre plate was incubated at 37°C for 24 h. After the incubation the MIC was determined. Furthermore, the minimal bactericidal concentration (MBC) of vancomycin was determined as reported. Using the replica plater for 96-well plate (Sigma Aldrich) ~3 μl of planktonic culture from each well of the microtitre plate were transferred to the surface of a BHI agar plate. Plates were incubated for 16 h at 37°C. The MBC was determined by identifying the cut off for bacterial growth.

MBIC and MBEC of vancomycin determinations

The minimum biofilm inhibitory concentration (MBIC) and the minimum biofilm eradication concentration (MBEC) of vancomycin for *S. epidermidis* RP62A were determined. Briefly, the wells of a sterile 96-well flat-bottomed polystyrene plate (Falcon) were filled with 100 μl of BHI with an appropriate dilution of overnight cultures of *S. epidermidis* RP62A (0.1 $\text{OD}_{600\text{nm}}$) and incubated overnight at 37°C without shaking, to allow bacterial attachment. Non-adherent cells were removed by gentle washing three times with sterile PBS. The plates were left to air dry for 15 min. Serial twofold dilutions of vancomycin (initial concentration 240 $\mu\text{g ml}^{-1}$) in cation-adjusted Mueller-

Hinton broth (CAMHB) were added to the microplates followed by incubation at 37°C for 24 h. The MBIC was defined as the minimal antimicrobial concentration at which there was no observable bacterial growth in wells containing adherent microcolonies, ie the minimal concentration that inhibited the release of planktonic bacteria from the biofilm (Reiter et al. 2013).

After MBIC measurement, the content of each well was spotted on an agar plate using a replica plater for 96-well plate (Sigma-Aldrich). The agar plate was incubated for 24 h at 37°C. The MBEC was defined as the minimal antimicrobial concentration at which bacteria fail to regrow after antimicrobial exposure, ie the minimal concentration required for eradicating the biofilm (Reiter et al. 2013). All the determinations were performed in duplicate.

Synergy testing by checkerboard assay

Synergism between the pentadecanoic acid or the pentadecanal and vancomycin was assessed by the so-called 'checkerboard' assay against *S. epidermidis* RP62A. Twofold serial dilutions of pentadecanoic acid or the pentadecanal and vancomycin were tested in combination. To do this, the pentadecanoic acid and the pentadecanal were tested at concentrations ranging from 250 to 31.25 $\mu\text{g ml}^{-1}$ and vancomycin at concentrations ranging from 240 to 7.5 $\mu\text{g ml}^{-1}$, respectively. All the determinations were performed in duplicate.

MBIC and MBEC experiments were performed as previously described.

Synergy testing by CLSM analysis

For synergy evaluation between the anti-biofilm molecules and vancomycin by confocal microscopy, biofilm formation was assessed as previously described. Briefly, an overnight culture of *S. epidermidis* RP62A grown in BHI was diluted and inoculated into each well of an eight-well chamber slide at an appropriate cell concentration, ~0.1 $\text{OD}_{600\text{nm}}$. The bacterial cultures were incubated at 37°C for 2 h in presence of 120 $\mu\text{g ml}^{-1}$ of vancomycin, with or without the anti-biofilm molecules, pentadecanal and pentadecanoic acid (250 $\mu\text{g ml}^{-1}$), in order to assess whether the anti-biofilm molecules were able to improve the antimicrobial activity of vancomycin. The biofilm cell viability was determined by the FilmTracer[™] LIVE/DEAD[®] Biofilm Viability Kit (Molecular Probes, Invitrogen) as previously described (Casillo et al. 2017).

Cytotoxicity assay

Immortalized human keratinocyte cells (HaCaT), and mouse fibroblasts (BALB/c3T3) were from ATCC. These cell lines are commonly used for biocompatibility and cytotoxicity assay, as reported by Wiegand and Hipler (2009), and are particularly appropriate cell lines for use in cytotoxicity and tolerance tests concerning the skin because they represent dermal fibroblasts and epidermal keratinocytes, both targets of *S. epidermidis*. Cells were cultured in Dulbecco's modified Eagle's medium (Sigma-Aldrich), supplemented with 10% foetal bovine serum (HyClone, Logan, UT, USA), 2 mM L-glutamine and antibiotics. Cells were grown in a 5% CO₂ humidified atmosphere at 37 °C. To test the biocompatibility of the molecules, cells were seeded in 96-well plates at a density of 2.5×10^3 well⁻¹. Twenty-four hours after seeding, cells were incubated with increasing amounts of the molecule under test (from 10 to 100 µg ml⁻¹) for 24, 48 and 72 h. At the end of incubation, cell viability was assessed by the MTT assay as previously described (Arciello et al. 2011). Cell survival was expressed as a percentage of viable cells in the presence of the analysed molecule, with respect to the control cells. Control cells were represented by cells grown in the absence of the molecule and by cells supplemented with identical volumes of DMSO. Two-way ANOVA was performed as a statistical analysis.

Results

Anti-biofilm activity of derivatives

To evaluate the anti-biofilm activity of pentadecanal derivatives, molecules were tested at different concentrations against the reference strain *S. epidermidis* RP62A and against *S. epidermidis* O-47, a strong biofilm producer *agr*-mutant (Heilmann et al. 1996). As shown in Figure 1, all the molecules reduced biofilm formation by the reference strain *S. epidermidis* RP62A and, surprisingly, the carboxylic acid, at low concentrations (25 µg ml⁻¹ and 12.5 µg ml⁻¹), was more active than the pentadecanal. Besides the pentadecanal, the most effective derivatives on *S. epidermidis* O-47 biofilm was the ester and then the acetal. It is interesting to note that the acid was not able to induce a significant reduction in the *S. epidermidis* O-47 biofilm, contrary to what found on *S. epidermidis* RP62A. The anti-biofilm activity of pentadecanal derivatives was further confirmed by CLSM. CLSM analysis of *S. epidermidis* O-47 and RP62A biofilms were performed after 24 h incubation in the presence

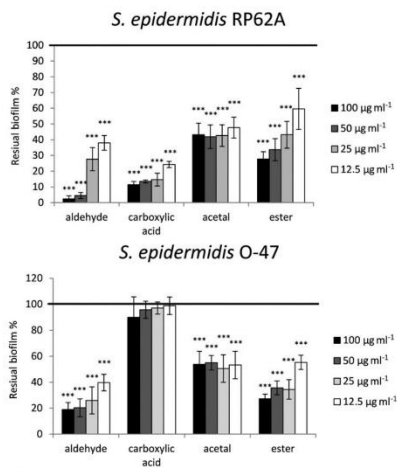


Figure 1. The anti-biofilm activity of pentadecanal and its derivatives on *S. epidermidis* biofilm formation. The anti-biofilm effect was evaluated on biofilm formation of *S. epidermidis* O-47 and *S. epidermidis* RP62A using different concentrations of the tested molecules. The data are reported as percentages of residual biofilm. Each data point represents the mean \pm the SD of three independent samples; the mean values were compared to the untreated control and considered significant when $p < 0.05$ (* $p < 0.05$, ** $p < 0.01$, *** $p < 0.001$) according to the Student *t*-test.

and absence of the derivatives, respectively. The LIVE/DEAD staining was used to analyse the biofilm structure and cell viability. As shown in Figure 2A, cells exposed to derivatives were alive (green indicates viable cells and red indicates dead cells), confirming that the new molecules, exactly like the pentadecanal (Casillo et al. 2017), had no bactericidal activity on either of the *S. epidermidis* bacterial strains living in the biofilm. To obtain more detailed information on the biofilm structure, the collected three-dimensional files were analysed using the COMSTAT image analysis software package (Heydorn et al. 2000). The results demonstrated that biofilms formed in the presence of the derivatives were characterized by a lower biomass (Figure 2B) and this effect was clearly evident in both the *S. epidermidis* strains using all the derivatives. It is interesting to note that the carboxylic acid by CLSM and COMSTAT analysis was active, contrary to what was demonstrated when its anti-biofilm activity was evaluated by crystal violet assay (Figure 1). As shown in Figure 2C and D, the

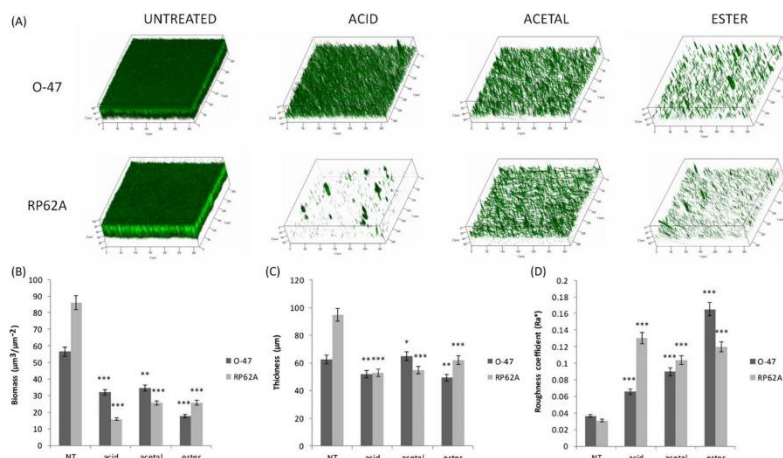


Figure 2. Analysis of the effect of pentadecanal derivatives on *S. epidermidis* O-47 and *S. epidermidis* RP62A biofilm structure. (A) CLSM analysis of *S. epidermidis* O-47 and *S. epidermidis* RP62A biofilms were performed after 24 h incubation at 37 °C in the presence and in absence of the derivatives. Three-dimensional biofilm structures were obtained using the LIVE/DEAD[®] Biofilm Viability Kit. COMSTAT quantitative analysis of (B) biomass, (C) average thickness and (D) roughness coefficient of *S. epidermidis* O-47 and *S. epidermidis* RP62A biofilms were performed for all the tested conditions.

biofilms obtained in the presence of the derivatives were quite similar in terms of thickness, but the roughness coefficient indicated significant differences. In particular, an increase in the roughness coefficient was observed. This dimensionless factor provides a measure of how much the thickness of a biofilm varies, and it is thus used as a direct indicator of biofilm heterogeneity. The same reported trend was observed also for biofilm obtained in presence of the pentadecanal (Figure S3).

The synergy of derivatives with vancomycin by checkerboard assay

The pentadecanal or its synthetic derivatives were tested in combination with an antibiotic on mature biofilm in order to assess whether the anti-biofilm activity could modulate the antibiotic activity by weakening the *S. epidermidis* biofilm structure, making it less compact and rougher, and thus allowing the penetration of the antimicrobial agent. These experiments were performed using vancomycin as antibiotic and *S. epidermidis* RP62A as the target strain.

To exclude any interference between the anti-biofilm molecules and the vancomycin, the MBC of this antibiotic on *S. epidermidis* RP62A was calculated

in the presence and in the absence of anti-biofilm compounds (up to 250 $\mu\text{g ml}^{-1}$). The MBC value was evaluated for the vancomycin on *S. epidermidis* RP62A planktonic cells according to CLSI (2017) (Table 1) and, in all the tested conditions, the vancomycin efficacy was not affected by the presence of the anti-biofilm molecules (data not shown). Measurement of the MBIC and of the MBEC was used to evaluate the vancomycin antimicrobial activity against the mature biofilms (Reiter et al. 2013). The *S. epidermidis* RP62A 24 h mature biofilm was subjected to antimicrobial exposure and, as expected, the MBEC and MBIC values were extremely high when compared to the MBC value. The MBIC and MBEC were equivalent and significantly higher than the value obtained for the MBC on planktonic growth (Table 1). The possible synergistic effect of anti-biofilm molecules and vancomycin was evaluated on 24 h mature biofilm using the pentadecanoic acid or the pentadecanal as only these two molecules showed a slight, but significant effect on mature *S. epidermidis* RP62A biofilm (data not shown). The synergy was evaluated by using the checkerboard method, as described in the Materials and methods section. The results are reported in Table 1. The addition of pentadecanal did not prompt a reduction

Table 1. Antimicrobial activities of vancomycin and vancomycin in the presence of pentadecanoic acid and pentadecanal against *S. epidermidis* RP62A in planktonic and biofilm growth.

	Vancomycin	Vancomycin + pentadecanoic acid 250 $\mu\text{g ml}^{-1}$	Vancomycin + pentadecanoic acid 125 $\mu\text{g ml}^{-1}$	Vancomycin + pentadecanal 250 $\mu\text{g ml}^{-1}$	Vancomycin + pentadecanal 125 $\mu\text{g ml}^{-1}$
MBC ($\mu\text{g ml}^{-1}$)	7.5	7.5	7.5	7.5	7.5
MBIC ($\mu\text{g ml}^{-1}$)	60	15	15	60	60
MBEC ($\mu\text{g ml}^{-1}$)	60	15	15	60	60

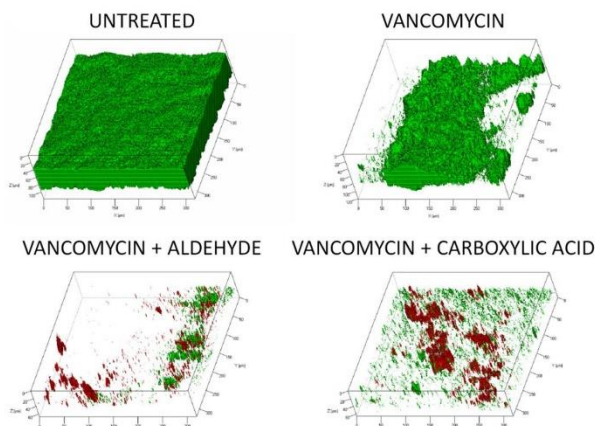


Figure 3. Analysis of the synergistic effect of derivatives with vancomycin on *S. epidermidis* RP62A biofilm structure. CLSM analysis of *S. epidermidis* RP62A biofilms was performed on mature biofilms after 2h incubation at 37 °C in the presence and absence of derivatives and vancomycin. Three-dimensional biofilm structures were obtained using the LIVE/DEAD[®] Biofilm Viability Kit.

in the MBIC or MBEC values of vancomycin on *S. epidermidis* RP62A. Conversely, the pentadecanoic acid modulated the antimicrobial activity of the vancomycin. In particular, the MBIC and MBEC values, obtained after 24 h incubation, were reduced twofold in combination with 125 $\mu\text{g ml}^{-1}$ and 250 $\mu\text{g ml}^{-1}$ of pentadecanoic acid, respectively.

In order to collect information on the mechanism of action of the pentadecanoic acid in combination with the vancomycin and to understand the reasons for the inefficiency of pentadecanal, a CLSM analysis of *S. epidermidis* RP62A mature biofilm treated with vancomycin in the absence or in the presence of either pentadecanal or pentadecanoic acid was performed.

In detail, 24 h mature biofilm of *S. epidermidis* RP62A was incubated for 2 h in the presence of 120 $\mu\text{g ml}^{-1}$ of vancomycin and in the presence or absence of 250 $\mu\text{g ml}^{-1}$ of the pentadecanal or the pentadecanoic acid.

As shown in Figure 3, the vancomycin led to a slight reduction in the biofilm biomass, but it was

not able to kill the cells embedded in the biofilm matrix. Whereas, when the vancomycin was combined with either the pentadecanal or the carboxylic acid, it was able to penetrate the biofilm structure, showing a substantial bactericidal activity even against the deepest cells in the biofilm structure (Figure 3, red signal).

Effect of pentadecanal derivatives on eukaryotic cell viability

The biocompatibility of the pentadecanal and its derivatives was investigated on keratinocytes and fibroblasts. These two cell lines were chosen as they represent the skin, in which keratinocytes are the outer part of the skin and cover the fibroblasts layer and are a target for *S. epidermidis* infections. As shown in Figure 4, after 24 h incubation, in the case of keratinocytes, all the analysed molecules were fully biocompatible, as no toxicity was

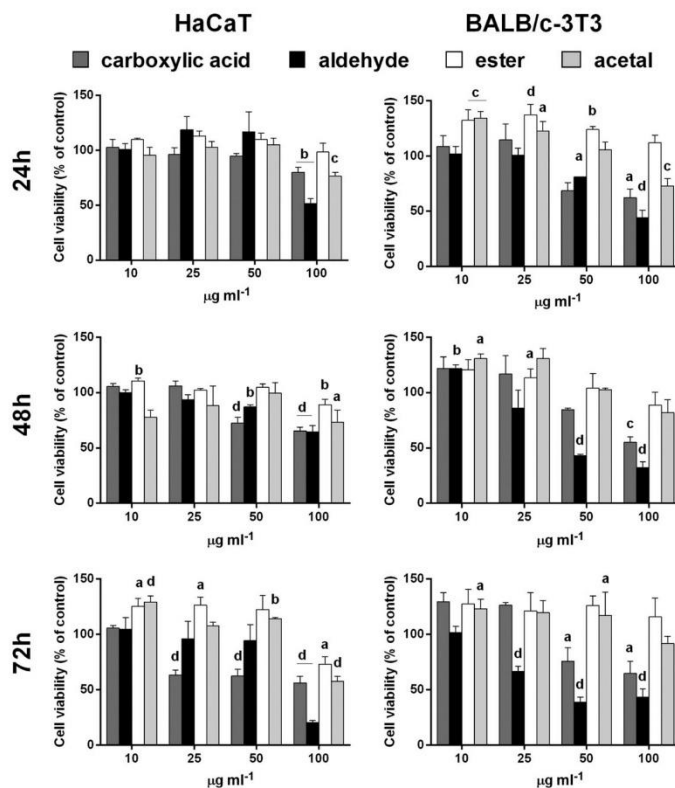


Figure 4. Effect of pentadecanal and its derivatives on immortalized cell lines. Dose-response plot of cells after 24, 48 and 72 h incubation with increasing concentrations ($10\text{--}100\ \mu\text{g ml}^{-1}$) of molecules. Cell viability was assessed by the MTT assay and expressed as described in the Materials and methods section. Values are given as means \pm SD ($n \geq 3$); a indicates $p < 0.05$, b indicates $p < 0.01$, c indicates $p < 0.005$, d indicates $p < 0.001$, with respect to control cells.

observed, except for the pentadecanal, which was biocompatible up to $50\ \mu\text{g ml}^{-1}$. After 48–72 h the ester and acetal were safe for HaCaT cells up to $50\ \mu\text{g ml}^{-1}$, whereas a toxicity was observed for the acid (after 72 h incubation). The pentadecanal was fully biocompatible when used at concentrations up to $50\ \mu\text{g ml}^{-1}$. These results were similar also in the case of BALB/c-3T3 cells.

Altogether, these data clearly indicate that the ester derivative is fully biocompatible, followed by acetal.

Discussion

Recently, the identification of the pentadecanal as a new anti-biofilm molecule against *S. epidermidis* was reported (Casillo et al. 2017). This molecule, produced by the Antarctic bacterium *P. haloplanktis* TAC125, is a very promising anti-biofilm molecule. Nonetheless, the pentadecanal is a chemically reactive agent which could easily undergo reactions of oxidation, polymerization, and/or hydration, and therefore it could be not chemically compatible with

all anti-biofilm strategies. Therefore, the aim of this work was to produce and characterize novel pentadecanal derivatives to be used in anti-biofilm applications.

In a previous paper, the specificity of the pentadecanal action on *S. epidermidis* biofilm was explored by testing chemical analogues differing either in the length of the aliphatic chain or in their functional group properties (Casillo et al. 2017). In particular, similar aldehydes and corresponding alcohols, characterized by different lengths of the aliphatic chain (C-14/C-20), were analysed, and the results demonstrated that both the length of the aliphatic chain and the functional group properties were important for the pentadecanal activity against *S. epidermidis* biofilm (Casillo et al. 2017). Since the hexadecanal and the tetradecanal did not show anti-biofilm activity (Casillo et al. 2017), whereas the pentadecanal showed a slight but significant activity, the new anti-biofilm molecules were designed preserving the length of the aliphatic chain and modifying the functional group.

The pentadecanal derivatives synthesized were: pentadecanoic acid, the pentadecanoic acid methyl ester and 1,1-dimethoxypentadecane. In particular, the acetal could offer the opportunity to generate the aldehyde when treated with an electrophilic agent. Therefore, the acetal could be a good choice in treating *in vivo* infections, especially those close to the implant surface, where the bacterial metabolic activity generates a local acidic pH (4–5) (Vroom et al. 1999; Wang et al. 2014). The ester and the carboxylic acid were selected since both are less reactive than aldehyde in oxidation and polymerization reactions.

All the synthesized molecules were tested for their anti-biofilm activity and, unexpectedly, all of them showed that they were able to prevent, to a different extent, biofilm formation by *S. epidermidis* RP62A. This result clearly demonstrates that the functional group has a key role in the anti-biofilm activity, even if they are not strictly related. Casillo et al. (2017) demonstrated that the pentadecanal interfered in the AI-2 quorum sensing system of *S. epidermidis*. It is interesting to note that the AI-2 quorum sensing molecular pathway in Gram-positive bacteria is not completely clarified, and a putative receptor for AI-2 molecules has not yet been identified (Ma et al. 2017). Thus, it is not clear how AI-2 signals are detected, or which functions are regulated by them in many luxS-containing bacteria. Moreover, in *S. epidermidis*, no potential AI-2 receptors have been found. Therefore, it is not possible to exclude the possibility that the pentadecanal and its derivatives cross the bacterial cell wall

by diffusion since their physico-chemical properties are compatible with this mechanism.

Moreover, the AI-2 mechanism of action in *S. epidermidis* has not yet been thoroughly characterized, and probably, this unexpected result will be clarified when all the details of the AI-2 quorum sensing molecular mechanism in *S. epidermidis* have been explained.

The efficacy of the pentadecanoic acid addition on *S. epidermidis* RP62A and *S. epidermidis* O-47 biofilm formation was different. Indeed, *S. epidermidis* O-47 biofilm formation was poorly affected by the carboxylic acid addition, compared to the strong effect shown on the reference strain.

S. epidermidis O-47 is a naturally occurring agr mutant (Vuong et al. 2003). As previously reported (Vuong et al. 2003; Kohler et al. 2014), the agr-negative genotype enhanced biofilm formation on polymer surfaces by increasing expression of the surface protein AtlE, a bifunctional adhesin/autolysin abundant in the cell wall of *S. epidermidis*. The amount of AtlE present in the cell envelope is one of the reported differences between the *S. epidermidis* RP62A and *S. epidermidis* O-47 (Vuong et al. 2003). It is possible to speculate that the overexpression of AtlE renders the *S. epidermidis* O-47 cell envelope less permeable, compared to RP62A, to a hypothetical diffusion of charged molecules, such as the pentadecanoic acid, the only charged molecule tested here. Moreover, AtlE induces significant changes in the hydrophobicity of the bacterial surface (Büttner et al. 2015); this effect could explain the inefficacy of the pentadecanoic acid, that is less hydrophobic compared to the pentadecanal. Nevertheless, the *S. epidermidis* O-47 genome sequence is not available, and this information will be instrumental in understanding the observed difference.

Although the detailed molecular mechanism that underpins the anti-biofilm activity of aldehyde derivatives is far from being elucidated, their effect on the *S. epidermidis* biofilm structure is quite evident, as the biofilm formed in their presence is strongly reduced and characterized by a porous structure containing many channels and voids. These results suggested exploring the use of the aldehyde and its derivatives in combination with antibiotics to treat biofilm infections. *S. epidermidis* RP62A is a strongly adherent, slime-producing pathogenic strain isolated from a patient with intravascular catheter-associated sepsis and, for this reason, it represents the ideal candidate for these experiments since it is a reference biofilm positive/ica-positive strain and methicillin-resistant (Qin et al. 2007). As for the antibiotic, the

glycopeptide vancomycin was chosen since it is considered one of the most reliable therapeutic agents against infections caused by multidrug-resistant staphylococci (Qin et al. 2007). Moreover, it is the primary antibiotic used to cure infections caused by coagulase-negative staphylococci and is used to treat prosthetic valve endocarditis caused by *S. epidermidis* (Nailor and Sobel 2009). On the other hand, vancomycin displays a reduced penetration into the biofilm matrix and a low microbicidal effect on *S. epidermidis* within the biofilm (Zhang et al. 2015).

To investigate a possible synergy between the pentadecanal or the pentadecanoic acid and vancomycin, the MBEC and the MBIC in the presence of the anti-biofilm molecules were evaluated, since these methodologies have been suggested as a laboratory assay to evaluate antimicrobial activity against mature biofilm (Reiter et al. 2013). The results demonstrated that the pentadecanoic acid modulated the antimicrobial activity of vancomycin, with a twofold reduction in MBIC and MBEC values at a concentration of anti-biofilm molecules of $125 \mu\text{g ml}^{-1}$, whereas no effect was detected using the aldehyde. As the MBIC and MBEC assays were usually performed on mature biofilm treated with the anti-biofilm and antibiotic for 24 h, this condition could not be optimal for a chemically reactive agent such as the pentadecanal. Therefore, CLSM analyses of mature biofilm of *S. epidermidis* RP62A treated with vancomycin and pentadecanal were performed, selecting experimental conditions which allowed the detection of a possible effect in a short incubation time. The results obtained revealed the capacity of the pentadecanal and the carboxylic acid to weaken the *S. epidermidis* biofilm structure, making it less compact and homogeneous, and thus allowing the penetration of the vancomycin into the structure of the biofilm, making cells deeply embedded into the matrix easier to reach. This could be a great advantage in the case of a possible therapeutic strategy providing an antibiotic/anti-biofilm combination.

To explore the clinical potential of pentadecanal and its derivatives, their biocompatibility was investigated on fibroblasts and keratinocytes, eukaryotic cell lines which represent the target of *S. epidermidis* infections. The data clearly indicate that the pentadecanal derivatives are biocompatible with all the cell lines analysed at all the concentrations tested, while the aldehyde is fully biocompatible when used at concentrations lower than $50 \mu\text{g ml}^{-1}$.

In conclusion, this work endorses pentadecanal and its derivatives as useful molecules for the development of innovative approaches mainly aimed at the

prevention of biofilm formation. Nevertheless, these molecules could also be useful to fight established infections in combination with an opportune antibiotic therapy, thus suggesting that the use of pentadecanoic acid in combination with vancomycin could improve the efficacy of therapy for the treatment of *S. epidermidis* biofilm-associated infections.

References

- Arciello A, De Marco N, Del Giudice R, Guglielmi F, Pucci P, Relini A, Monti DM, Piccoli R. 2011. Insights into the fate of the N-terminal amyloidogenic polypeptide of ApoA-I in cultured target cells. *J Cell Mol Med.* 15:2652–2663. doi: 10.1111/j.1582-4934.2011.01271.x
- Batoni G, Maisetta G, Esin S. 2016. Antimicrobial peptides and their interaction with biofilms of medically relevant bacteria. *Biochim Biophys Acta.* 1858:1044–1060. doi: 10.1016/j.bbame.2015.10.013
- Busscher HJ, van der Mei HC, Subbiahdoss G, Jutte PC, van den Dungen JJ, Zaat SA, Schultz MJ, Grainger DW. 2012. Biomaterial-associated infection: locating the finish line in the race for the surface. *Sci Transl Med.* 4:153rv10.
- Büttner H, Mack D, Rohde H. 2015. Structural basis of *Staphylococcus epidermidis* biofilm formation: mechanisms and molecular interactions. *Front Cell Infect Microbiol.* 5:14.
- Carey FA, Sundberg RJ. 2000. *Advanced organic chemistry. Part A* 4th ed. Berlin, Germany: Springer, Ch. 8.
- Casillo A, Papa R, Ricciardelli A, Sannino F, Ziaco M, Tilotta M, Selan L, Marino G, Corsaro MM, Tutino ML, et al. 2017. Anti-biofilm activity of a long-chain fatty aldehyde from Antarctic *Pseudoalteromonas haloplanktis* TAC125 against *Staphylococcus epidermidis* biofilm. *Front Cell Infect Microbiol.* 7:46.
- De Santi C, Altermark B, de Pascale D, Willassen NP. 2016. Bioprospecting around Arctic islands: marine bacteria as rich source of biocatalysts. *J Basic Microbiol.* 56:238–253. doi:10.1002/jobm.201500505
- Donlan RM, Costerton JW. 2002. Biofilms: survival mechanisms of clinically relevant microorganisms. *Clin Microbiol Rev.* 15:167–193. doi:10.1128/CMR.15.2.167-193.2002
- Farquhar JW. 1961. Identification and gas-liquid chromatographic behavior of plasmalogen aldehydes and their acetal, alcohol, and acetylated alcohol derivatives. *Journal of Lipid Research.* 1062:21–30.
- Gao Y, Rao H, Mao LJ, Ma QL. 2017. Chemical composition, antioxidant, antibacterial and cytotoxic activities of essential oil of *Leontopodium leontopodioides* (Willd.) Beauverd. *Nat Prod Res.* 17:1–4.
- Heilmann C, Schweitzer O, Gerke C, Vanittanakom N, Mack D, Götz F. 1996. Molecular basis of intercellular adhesion in the biofilm-forming *Staphylococcus epidermidis*. *Mol Microbiol.* 20:1083–1091. doi:10.1111/j.1365-2958.1996.tb02548.x
- Heydorn A, Nielsen AT, Hentzer M, Sternberg C, Givskov M, Ersbøll BK, Molin S. 2000. Quantification of biofilm structures by the novel computer program COMSTAT.

- Microbiology. 146:2395–2407. doi:10.1099/00221287-146-10-2395
- Jiang X, Zhai Y, Chen J, Han Y, Yang Z, Ma SC. 2018. Iron-catalyzed aerobic oxidation of aldehydes: single component catalyst and mechanistic studies. *Chin J Chem*. 36:15–19. doi:10.1002/cjoc.201700576
- Kohler T, Gisch N, Binsker U, Schlag M, Darm K, Völker U, Zähringer U, Hammerschmidt S. 2014. Repeating structures of the major staphylococcal autolysin are essential for the interaction with human thrombospondin 1 and vitronectin. *J Biol Chem*. 289:4070–4082. doi:10.1074/jbc.M113.521229
- Koo H, Allan RN, Howlin RP, Stoodley P, Hall-Stoodley L. 2017. Targeting microbial biofilms: current and prospective therapeutic strategies. *Nat Rev Microbiol*. 15:740–755. doi:10.1038/nrmicro.2017.99
- Ma R, Qiu S, Jiang Q, Sun H, Xue T, Cai G, Sun B. 2017. AI-2 quorum sensing negatively regulates rbf expression and biofilm formation in *Staphylococcus aureus*. *Int J Med Microbiol*. 307:257–267. doi:10.1016/j.ijmm.2017.03.003
- Morgenstern M, Post V, Erichsen C, Hungerer S, Bühren V, Militz M, Richards RG, Moriarty TF. 2016. Biofilm formation increases treatment failure in *Staphylococcus epidermidis* device-related osteomyelitis of the lower extremity in human patients. *J Orthop Res*. 34:1905–1913. doi:10.1002/jor.23218
- Nailor MD, Sobel JD. 2009. Antibiotics for gram-positive bacterial infections: vancomycin, teicoplanin, quinupristin/dalfopristin, oxazolidinones, daptomycin, dalbavancin, and telavancin. *Infect Dis Clin North Am*. 23:965–982. doi:10.1016/j.idc.2009.06.010
- Otto M. 2012. Molecular basis of *Staphylococcus epidermidis* infections. *Semin Immunopathol*. 34:201–214. doi:10.1007/s00281-011-0296-2
- Papa R, Parrilli E, Sannino F, Barbato G, Tutino ML, Artini M, Selan L. 2013. Anti-biofilm activity of the Antarctic marine bacterium *Pseudoalteromonas haloplanktis* TAC125. *Res Microbiol*. 164:450–456. doi:10.1016/j.resmic.2013.01.010
- Papa R, Selan L, Parrilli E, Tilotta M, Sannino F, Feller G, Tutino ML, Artini M. 2015. Anti-biofilm activities from marine cold adapted bacteria against staphylococci and *Pseudomonas aeruginosa*. *Front Microbiol*. 6:1333.
- Papaleo MC, Romoli R, Bartolucci G, Maida I, Perrin E, Fondi M, Orlandini V, Mengoni A, Emiliani G, Tutino ML, et al. 2013. Bioactive volatile organic compounds from Antarctic (sponges) bacteria. *N Biotechnol*. 30:824–838. doi:10.1016/j.nbt.2013.03.011
- Parrilli E, Papa R, Carrillo S, Tilotta M, Casillo A, Sannino F, Cellini A, Artini M, Selan L, Corsaro MM, Tutino ML. 2015. Anti-biofilm activity of *Pseudoalteromonas haloplanktis* TAC125 against *Staphylococcus epidermidis* biofilm: evidence of a signal molecule involvement? *Int J Immunopathol Pharmacol*. 28:104–113. doi:10.1177/0394632015572751
- Qin Z, Yang X, Yang L, Jiang J, Ou Y, Molin S, Qu D. 2007. Formation and properties of in vitro biofilms of ica-negative *Staphylococcus epidermidis* clinical isolates. *J Med Microbiol*. 56:83–93. doi:10.1099/jmm.0.46799-0
- Reiter KC, Villa B, Paim TG, de Oliveira CF, d'Azevedo PA. 2013. Inhibition of biofilm maturation by linezolid in methicillin-resistant *Staphylococcus epidermidis* clinical isolates: comparison with other drugs. *J Med Microbiol*. 62:394–399. doi:10.1099/jmm.0.048678-0
- Sannino F, Parrilli E, Apuzzo GA, de Pascale D, Tedesco P, Maida I, Perrin E, Fondi M, Fani R, Marino G, Tutino ML. 2017. *Pseudoalteromonas haloplanktis* produces methyamine, a volatile compound active against *Burkholderia cepacia* complex strains. *N Biotechnol*. 35:13–18. doi:10.1016/j.nbt.2016.10.009
- Sannino F, Sansone C, Galasso C, Kildgaard S, Tedesco P, Fani R, Marino G, de Pascale D, Ianora A, Parrilli E, et al. 2018. *Pseudoalteromonas haloplanktis* TAC125 produces 4-hydroxybenzoic acid that induces pyroptosis in human A459 lung adenocarcinoma cells. *Sci Rep*. 8:1190. doi:10.1038/s41598-018-19536-2
- Satpathy S, Sen SK, Pattanaik S, Raut S. 2016. Review on bacterial biofilm: an universal cause of contamination. *Biocatal Agric Biotechnol*. 7:56–66. doi:10.1016/j.bcab.2016.05.002
- Valour F, Trouillet-Assant S, Rasigade J, Lustig S, Chanard E, Meugnier H, Tigaud S, Vandenesch F, Etienne J, Ferry T, Laurent F. 2013. *Staphylococcus epidermidis* in orthopedic device infections: the role of bacterial internalization in human osteoblasts and biofilm formation. *PLoS One*. 8:e67240. doi:10.1371/journal.pone.0067240
- Vroom JM, De Grauw KJ, Gerritsen HC, Bradshaw DJ, Marsh PD, Watson GK, Birmingham JJ, Allison C. 1999. Depth penetration and detection of pH gradients in biofilms by two-photon excitation microscopy. *Appl Environ Microbiol*. 65:3502–3511.
- Vuong C, Gerke C, Somerville GA, Fischer ER, Otto M. 2003. Quorum-sensing control of biofilm factors in *Staphylococcus epidermidis*. *J Infect Dis*. 188:706–718. doi:10.1086/377239
- Wang F, Raval Y, Chen H, Tzeng TR, DesJardins JD, Anker JN. 2014. Development of luminescent pH sensor films for monitoring bacterial growth through tissue. *Adv Healthc Mater*. 3:197–204. doi:10.1002/adhm.201300101
- Wiegand C, Hippler UC. 2009. Evaluation of biocompatibility and cytotoxicity using keratinocyte and fibroblast cultures. *Skin Pharmacol Physiol*. 22:74–82. doi:10.1159/000178866
- Zhang Y, Fu Y, Yu J, Ai Q, Li J, Peng N, Song S, He Y, Wang Z. 2015. Synergy of ambroxol with vancomycin in elimination of catheter-related *Staphylococcus epidermidis* biofilm in vitro and in vivo. *J Infect Chemother*. 21:808–815. doi:10.1016/j.jiac.2015.08.017

**Pentadecanal inspired molecules as new anti-biofilm agents against
*Staphylococcus epidermidis***

Annarita Ricciardelli¹, Angela Casillo¹, Rosanna Papa², Daria Maria Monti¹, Paola Imbimbo¹, Gianluca Vrenna², Marco Artini², Laura Selan², Maria Michela Corsaro¹, Maria Luisa Tutino¹, Ermenegilda Parrilli^{1,*}

¹Chemical Sciences, University of Naples "Federico II", Naples, ²Department Of Public Health and Infectious Diseases, Sapienza University, Rome, Italy

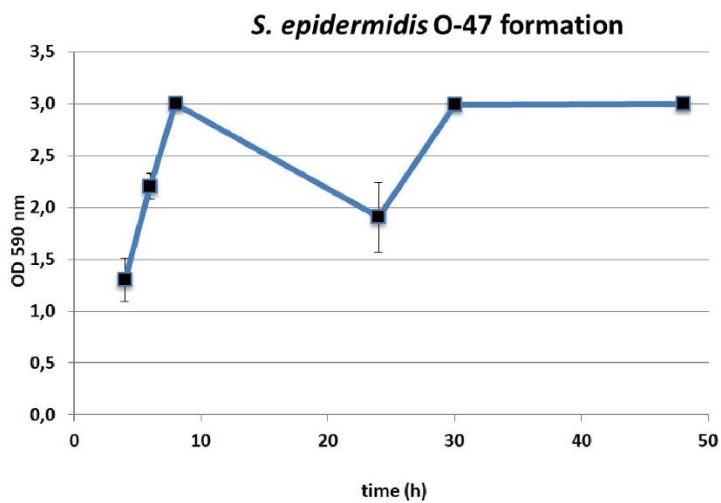


Figure S1 *S. epidermidis* O-47 biofilm formation curve in BHI.

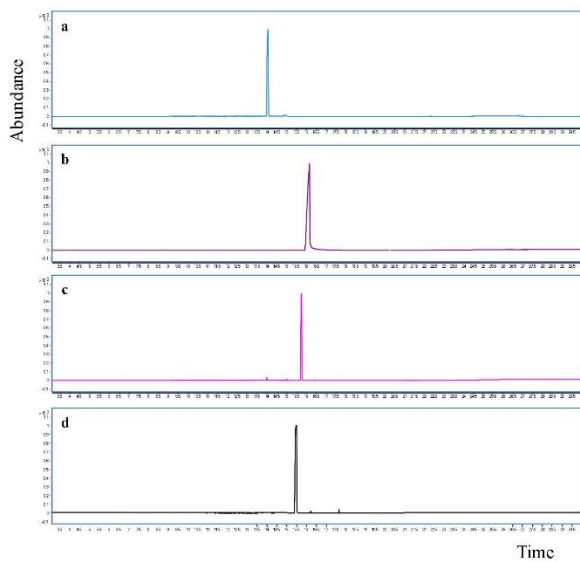


Figure S2: GC-MS chromatograms of: a) pentadecanal, b) pentadecanoic acid, c) 1,1-dimethoxypentadecane, d) pentadecanoic acid methyl ester.

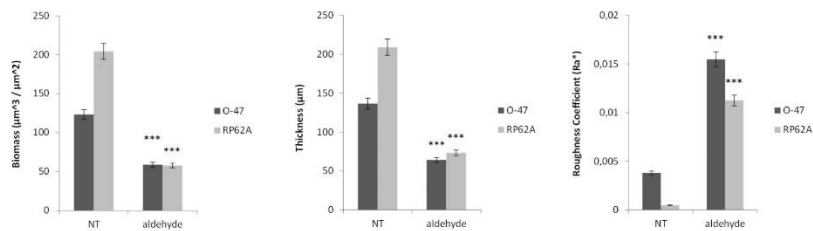


Figure S3: Analysis of *S. epidermidis* O-47 and *S. epidermidis* RP62A biofilm structure obtained adding the pentadecanal (12.5 µg/ml) during biofilm formation. COMSTAT quantitative analysis of biomass, average thickness and roughness coefficient of *S. epidermidis* O-47 and *S. epidermidis* RP62A biofilms were reported. Each data point represents the mean \pm the SD of two independent samples. The mean values of the treated samples were compared to the untreated control and considered significant when $p < 0.05$ (* $p < 0.05$, ** $p < 0.01$, *** $p < 0.001$) according to the Student t-test.



Contents lists available at ScienceDirect

Food Bioscience

journal homepage: www.elsevier.com/locate/fbio

Characterization of bioactivity and phytochemical composition with toxicity studies of different *Opuntia dillenii* extracts from Morocco

Jelena Katanić^{a,*}, Fatima Youfi^b, Marisa Carmela Caruso^c, Sanja Matić^d, Daria Maria Monti^e, El Hassania Loukili^b, Tatjana Boroja^{a,f}, Vladimir Mihailović^a, Fernanda Galgano^c, Paola Imbimbo^e, Ganna Petruk^e, Mohamed Bouhrim^g, Mohamed Brouham^g, Mohammed Ramdani^b

^a Department of Chemistry, Faculty of Science, University of Kragujevac, 34000, Kragujevac, Serbia

^b Laboratory of Applied Analytical Chemistry Materials and Environment, Faculty of Sciences, Mohammed First University, 60000, Oujda, Morocco

^c School of Agricultural, Forestry, Food and Environmental Sciences, University of Basilicata, 85100, Potenza, Italy

^d Department of Biology and Ecology, Faculty of Science, University of Kragujevac, 34000, Kragujevac, Serbia

^e Department of Chemical Sciences, University of Naples Federico II, 80126, Naples, Italy

^f University of Novi Sad, Faculty of Agriculture, 21000, Novi Sad, Serbia

^g Laboratory of Genetic Physiology and Ethnopharmacology, Faculty of Sciences, Mohammed First University, 60000, Oujda, Morocco



ARTICLE INFO

Keywords:

Opuntia dillenii
Prickly pear
Pear bush
Cactus
Polyphenols

ABSTRACT

The phytochemical composition, *in vitro* antioxidant and antimicrobial activities, cytotoxicity and anti-genotoxicity of fruit extracts of *Opuntia dillenii* were studied. The phytochemical composition was evaluated using HPLC, GC-MS and UV-Vis spectrophotometry. Spectrophotometric methods were used to estimate the antioxidant potential. Antimicrobial activity was determined using a microdilution method. The cytotoxic effects of the extracts were evaluated using the MTT assay. *In vitro* DNA-protective activity against hydroxyl radical-induced DNA damage was also determined. The results showed that polar extracts of *O. dillenii* had a significant amount of phenolic compounds, including flavonoids, whereas non-polar extracts had mostly terpenoids and fatty acid derivatives. Moreover, several extracts showed good antioxidant and antimicrobial activities, with low cytotoxicity and significant DNA-protective effects. These results showed that the extracts of *O. dillenii* have promising bioactivity and further studies on the potential application in different areas of food and health might be beneficial.

1. Introduction

Opuntia dillenii (Ker Gawl.) Haw., known as prickly pear or pear bush, is a perennial plant belonging to the genus *Opuntia* (family Cactaceae). It is able to grow in the desert and dry conditions in semi-desert regions in the tropics and subtropics (Ahmed, El Tanbouly, Islam, Sleem, & El Senousy, 2005). *O. dillenii* is reported to be native to America and India, nevertheless, it can be found in Asia, Australia and in the Mediterranean area (Betancourt, Cejudo-Bastante, Heredia, & Hurtado, 2017). The species of the genus *Opuntia*, including *O. dillenii*, have been used primarily as food (fruits), for their functional properties, for production of carminic acid, and other uses (Díaz Medina, Rodríguez Rodríguez, & Díaz Romero, 2007). The fruits of *O. dillenii* are characterized by an intense red color, an acidic taste, cladode spines, and a high content of seeds (Betancourt et al., 2017; Cejudo-Bastante,

Hurtado, & Heredia, 2015). Commonly, the fruits are consumed fresh or as juice, sweets, etc. (Feugang, Konarski, Zou, Stintzing, & Zou, 2006; Perez Mendez, Flores, Martín, Rodríguez Rodríguez, & Díaz Romero, 2015). *O. dillenii* fruits (prickly pears) are a good source of dietary fibers, but besides their use as natural colorants and functional food with a high nutritional value (Embaby, Gaballah, Hamed, & El-Samary, 2016), they have been used in traditional medicine in the treatment of inflammatory conditions, ophthalmia, gastric ulcers, intestinal spasm, hepatitis, diabetes, asthma, bronchial troubles, and whooping cough (Loro, Del Río, & Pérez-Santana, 1999; Siddiqui et al., 2016).

O. dillenii fruits have a wide range of bioactivities, such as anti-inflammatory, anti-nociceptive and analgesic effects (Loro et al., 1999; Siddiqui et al., 2016), anti-diabetic activity (Gao et al., 2015; Zhao, Lan, Huang, Ouyang, & Zeng, 2011), hypotensive (Saleem et al., 2005), anti-fertility (Bajaj & Gupta, 2012), antioxidant (Chang, Hsieh, & Yen, 2008;

* Corresponding author. Department of Chemistry, Faculty of Science, University of Kragujevac, Radoja Domanović 12, 34000, Kragujevac, Serbia.
E-mail address: jkatanic@kg.ac.rs (J. Katanić).

<https://doi.org/10.1016/j.fbio.2019.04.011>

Received 28 May 2018; Received in revised form 13 March 2019; Accepted 23 April 2019

Available online 26 April 2019

2212-4292/ © 2019 Elsevier Ltd. All rights reserved.

Ghazi et al., 2015; Moussa-Ayoub et al., 2016), antiproliferative (Pavithra, Sumanth, Manonmani, & Shashirekha, 2015), and antimicrobial properties (Ratnaweera, de Silva, Williams, & Andersen, 2015). Also, Saleem et al. (2005) showed that *O. dillenii* fruits protect neuronal cells in the treatment of Alzheimer's disease, Parkinson's disease, and heart stroke.

Several studies on *O. dillenii* fruits reported a complex chemical composition: phenolic compounds, mainly phenolic acids and flavonoids (e.g., gallic acid, catechin, epicatechin, quercetin and derivatives of kaempferol, isorhamnetin and quercetin) in different extracts of fruits and flowers, and a high content of ascorbic acid in peel and pulp (Ahmed et al., 2005; Betancourt et al., 2017; Chang et al., 2008; Diaz Medina et al., 2007; Embaby et al., 2016; Mata et al., 2016; Moussa-Ayoub et al., 2016). Moreover, fruit and juice of *Opuntia* spp., with special focus on the tested plant, are known for the presence of betalains (betacyanins and betaxanthins) (Betancourt et al., 2017; Cejudo-Bastante et al., 2015; Embaby et al., 2016; Fernández-López & Almela, 2001; Melgar et al., 2017). They are rich in polysaccharides (Gao et al., 2015; Han et al., 2016; Li, Yuan, Zhou, Zeng, & Lu, 2016), as well as fiber, amino acids, macroelements, and minerals (Ghazi et al., 2015; Stintzing, Schieber, & Carle, 2001).

The present study was done to evaluate the phytochemical composition of *O. dillenii* fruit extracts obtained using different solvents, i.e., ether, ethyl acetate, ethanol, and water. The extracts from skin, juice, and seeds, obtained from two different localities in Morocco (Nador and Essaouira), were analyzed using spectrophotometric methods, GC-MS and HPLC analyses. In addition, the antioxidant, antibacterial and antifungal activities, cytotoxicity and antigenotoxicity of the extracts were evaluated.

2. Materials and methods

2.1. Chemicals and reagents

Diethyl ether, ethyl acetate, and ethanol were purchased from Merck (Darmstadt, Germany). All other chemicals and solvents were of the highest analytical grade and used as supplied by Merck KGaA and Carl Roth GmbH (Karlsruhe, Germany).

All chemicals and reagents for determination of total phenolics and antioxidant activity were of analytical grade and were purchased from Sigma Chemical Co. (St. Louis, MO, USA), Aldrich Chemical Co. (Steinheim, Germany), and Alfa Aesar (Karlsruhe, Germany). All spectrophotometric measurements were done using a UV-Vis double beam spectrophotometer Halo DB-20S (Dynamica GmbH, Dietikon, Switzerland). Broths for the antimicrobial activity tests (nutrient agar - NA, Sabouraud dextrose agar - SDA, Müller-Hinton broth - MHB and Sabouraud dextrose broth - SDB) were purchased from Torlak Institute of Virology, Vaccines and Sera (Belgrade, Serbia). Human breast cancer cells (MCF-7), human colon cancer cells (LoVo) and human hepatocytes (HepG2) were from the American Type Culture Collection (ATCC, Manassas, VA, USA). Dulbecco's modified Eagle's medium, antibiotics, L-glutamine, and fetal bovine serum (HyClone) were purchased from Sigma-Aldrich. DNA from herring sperm was purchased from Carl Roth GmbH.

2.2. Sample collection and preparation

Plants of *O. dillenii* sprawled out and reached a height of about 50–200 cm. They showed 6–8 cm wide flowers that were finally lemon yellow in color. The purple-skinned fruits measured 4–7 cm in length and about 3 cm in diameter. The matured purple fruits of prickly pear (*O. dillenii*) were collected in February 2016 from Essaouira and Nador in Morocco. The plant species was identified by Prof. M. Bnouham (Faculty of Sciences, Mohammed First University, Oujda, Morocco). The sampled fruits were transported to the laboratory, washed with tap water, peeled, and mixed for 5 min using a Moulinex blender (Facile

glass LM310E, Groupe Seb, Mayerne, France) to separate seeds from the juice by passing through a sieve with a 2 mm screen. The juice was dehydrated by heating at 40 °C in the oven for 15 days, yielding 4.12% of juice powder. Seeds and skins were washed with distilled water, dried at room temperature (25 ± 1 °C), ground to a fine powder using a Moulinex coffee grinder (DPA241, Groupe Seb, Lourdes, France) and stored at –20 °C as well as the juice, for a maximum of 8 wk.

2.3. Preparation of *O. dillenii* fruit extracts

Ground seeds, skin, and juice of *O. dillenii* were macerated with diethyl ether as a non-polar solvent for removal of fatty acids. Each powder (50 g) was mixed with 110 ml of diethyl ether. The mixture was stirred at room temperature (18 °C) for 24 h and filtered through a glass filter crucible (50 ml, Porosity 4, Isolab, Wertheim, Germany) connected to a water aspirator. The extracts were concentrated on a rotary evaporator (Laborota 4000, Heidolph Instruments, Schwabach, Germany) under reduced pressure at 40 °C to obtain the corresponding powder. Then, three organic solvents were used successively: diethyl ether, ethyl acetate, and ethanol, to obtain the corresponding extracts by repeating the process of maceration, filtration and concentration under reduced pressure. The aqueous extracts were prepared using the recovered powder from the previous extraction (delipidation), which was mixed with 110 ml of water, stirred, filtered, and concentrated as described above. Aqueous extracts were dried by heating at 40 °C in the oven for a wk and all extracts were stored at 4 °C for a maximum of 8 wk.

2.4. Determination of total phenolics in *O. dillenii* extracts

2.4.1. Total phenolic compounds content

The total phenolics were estimated using the Folin-Ciocalteu method (Singleton, Orthofer, & Lamuela-Raventós, 1999). Plant extracts were diluted to 2 mg/ml, and aliquots of 0.5 ml were mixed with 2.5 ml of Folin-Ciocalteu reagent (previously diluted 10-fold with distilled water) and 2 ml of NaHCO₃ (7.5%). After 15 min of incubation at 45 °C, the absorbance was measured at 765 nm on the spectrophotometer versus a blank sample. Total phenolics were expressed as gallic acid equivalents (mg GAE/g dry extract) and were done in triplicate.

2.4.2. Total flavonoids content

The total flavonoid content was determined using AlCl₃ (Brighente, Dias, Verdi, & Pizzolatti, 2007). Aluminum chloride (0.5 ml, 2%) solution in methanol was mixed with the same volume of a methanol solution of plant extracts (1 mg/ml). After 1 h of incubation at room temperature (21 °C), the absorbances of the samples were measured at 415 nm. Total flavonoids were expressed as rutin equivalents (mg RUE/g dry extract) and were done in triplicate.

2.5. Flavonols analysis

Flavonols (quercetin, kaempferol, myricetin) were determined in the ethanolic extracts using HPLC. The dry residue was dissolved in methanol (10 mg/ml). The crude extract was filtered using a 0.22 µm RC membrane (Sartorius, Varedo MB, Italy) and injected into the HPLC system. Moreover, to determine flavonol aglycones, acidic hydrolysis of the extracts was done according to Caruso et al. (2015). Briefly, 200 µl of crude ethanolic extract was mixed with 400 µl of water and 100 µl of 37% HCl. Hydrolysis was done in a water bath at 100 °C for 30 min. After cooling, 300 µl of methanol was added and the sample was then filtered with a 0.22 µm RC membrane. Crude or hydrolyzed ethanolic extracts were analyzed using a Varian - Agilent (Milan, Italy) chromatographic system comprising a 9012 pump and a 1260 Infinity diode array detector at 360 nm. An aliquot of 20 µl of each extract was injected in a Gemini NX 5 µm C18 110 Å, 250 × 4.60 mm column

(Phenomenex, Bologna, Italy) equipped with a 4×3 mm C18 μ m cartridge pre-column (Phenomenex). During the entire analysis, the column was maintained at a constant temperature of 40 °C. The mobile phases used for the elution of the samples were: A) 90% water - 10% formic acid, B) 50% acetonitrile - 40% water - 10% formic acid; using a flow rate of 0.5 ml/min and with the following elution program: 0–0.6 min, 88% A; 0.6–20.5 min, 88–70% A; 20.5–22 min, 70–0% A; 22–25 min, 0–88% A; 25–35 min, 88% A.

Quantification was carried out using the external standard technique by verifying the response linearity of the detector for concentrations from 3.35 to 56 ppm using pure standards of quercetin, kaempferol, and myricetin (> 97%, Sigma Aldrich, Milan, Italy). Analyses were done in triplicates.

2.6. Gas chromatography-mass spectrometry analysis

The analysis of diethyl ether and ethyl acetate extracts was carried out on a GC/MS-QP2010 (Shimadzu, Kyoto, Japan). The volatile compounds were separated on a BPX25 capillary column of 30 m \times 0.25 mm i.d. and 0.25 μ m film thickness (Restek, Bellefonte, PA, USA). The carrier gas was helium, 3 ml/min, split ratio 70:0 and injector temperature 250 °C. The temperature program used for the column oven was 50 °C (held for 1 min), heated to 250 °C at 10 °C/min and held for 1 min. The ion-source temperature and interface temperature were set at 250 °C and the ionization of the sample components was done in the EI mode (70 eV). The mass range scanned was 40–300 m/z. All samples were analyzed in triplicate. The volatile compounds were identified by comparison of the mass spectra fragmentation patterns with those found in databases or libraries (Adams, 2007; Cornu & Massot, 1975; McLafferty & Stauffer, 1989). Post-run analysis software (Shimadzu, Kyoto, Japan) was used for compound identification. The highest similarity of the unknown spectrum compared to reference spectra registered in mass spectral libraries corresponded to the first choice. So among the three choices given, the first was accepted although there is no way to verify whether this is correct.

2.7. Antioxidant activity of *O. dillenii* extracts

2.7.1. Total antioxidant activity

The total antioxidant capacity of the *O. dillenii* extracts was measured using the phosphomolybdenum method described by Prieto, Pineda, and Aguilar (1999). The method is based on the reduction of Mo(VI) - Mo(V) by the antioxidant compounds and formation of a green phosphate/Mo (V) complex in acidic conditions. Sample extracts (0.3 ml) were combined with 3 ml of reagent solution (0.6 M sulfuric acid, 28 mM sodium phosphate and 4 mM ammonium molybdate). The reaction mixtures were incubated at 95 °C for 90 min. Thereafter, the absorbance of the solution was measured at 695 nm against a blank after cooling to room temperature. Ascorbic acid (AA) was used as the standard and the total antioxidant activity was expressed in ascorbic acid equivalents (mg AAE/g dry extract).

2.7.2. DPPH radical scavenging activity

For the determination of DPPH radical scavenging activity of *O. dillenii* extracts, the method of Kumarasamy et al. (2007) was adopted with suitable modifications (Katanić et al., 2015). Briefly, serial dilutions of the extracts in methanol (2 ml each) were mixed with 2 ml of purple DPPH \cdot solution (80 μ g/ml) and after 30 min the absorbance of the yellow product was measured at 517 nm. Ascorbic acid, ellagic acid, and quercetin were used as reference standards. The DPPH free-radical scavenging activity (%) was calculated using the following equation:

$$\% \text{ Inhibition} = (A_{\text{control}} - A_{\text{sample}}) / A_{\text{control}} \times 100$$

where A_{control} is the absorbance of the blank control (DPPH solution without a test sample) and A_{sample} is the absorbance of the test sample.

The results of *O. dillenii* antioxidant activity on DPPH radical were expressed as the IC₅₀ values, defined as the concentration of the tested sample that reduces 50% of the free-radical concentration, were calculated as μ g/ml using nonlinear regression analysis from the sigmoidal dose-response inhibition curve using OriginPro8 (OriginLab, Northampton, MA, USA) data analysis software.

2.7.3. ABTS radical cation scavenging activity

The ABTS radical cation scavenging activity of *O. dillenii* extracts was estimated using the procedure of Re et al. (1999). Briefly, ABTS \cdot^+ was obtained by reacting 7 mM ABTS stock solution with 2.45 mM potassium persulfate and the mixture was left to stand in the dark at room temperature for 16 h before use. The ABTS \cdot^+ solution (stable for 2 days) was diluted with 5 mM sodium phosphate-buffered saline (pH 7.4) to an absorbance at 734 nm of 0.70 ± 0.02 . After the addition of 100 μ l of sample to 900 μ l of the diluted ABTS \cdot^+ solution, the absorbance was measured at 734 nm after 30 min in the dark. Ascorbic acid, ellagic acid, and quercetin were used as reference antioxidants. A control sample was prepared to contain the same volume without test compounds or reference antioxidants. All samples were measured in triplicate. The ABTS \cdot^+ scavenging activity of the samples was expressed as:

$$\% \text{ Inhibition} = (A_{\text{control}} - A_{\text{sample}}) / A_{\text{control}} \times 100$$

where A_{control} is the absorbance of the blank control (ABTS \cdot^+ solution without a test sample) and A_{sample} is the absorbance of the test sample.

The results of *O. dillenii* antioxidant activity on ABTS \cdot^+ were expressed as IC₅₀ values (μ g/ml).

2.8. Determination of antimicrobial properties of *O. dillenii* extracts

2.8.1. Microorganisms and culture conditions

The antibacterial activity was tested using 6 bacterial species, namely: *Bacillus subtilis* (ATCC 6633), *Micrococcus lysodeikticus* (ATCC 4698), *Enterococcus faecalis* (ATCC 92912), *Klebsiella pneumoniae* (ATCC 70063), *Escherichia coli* (ATCC 25922), and *Pseudomonas fluorescens* (FSB 28). Antifungal activity of tested extracts was determined on the 6 fungal strains: *Trichoderma harzianum* (FSB 12), *Penicillium cyclopium* (FSB 23), *Aspergillus niger* (FSB 31), *Doratomyces stemonitis* (FSB 41), *Phialophora fastigiata* (FSB 81), *Fusarium oxysporum* (FSB 91); and a yeast *Candida albicans* (ATCC 10259). The ATCC and FSB strains and isolates of microorganisms were obtained from the Institute of Public Health, Kragujevac, Serbia and Laboratory for Microbiology, Department of Biology, Faculty of Science, University of Kragujevac (Kragujevac, Serbia), respectively. The bacteria and fungi cultures were stored at 4 °C and subcultured once a month. Bacterial strains were maintained on NA for 24 h at 37 °C, fungi were cultured on potato glucose agar (PDA) for 48 h at 28 °C, and *C. albicans* was maintained on SDA for 24 h at 35 °C.

2.8.2. Microdilution test

Minimum inhibitory concentrations (MIC) for antibacterial and antifungal activities of *O. dillenii* extracts were determined using the microdilution method in 96 well microtiter plates (CLSI, 2012; Sarker, Nahar, & Kumarasamy, 2007). MHB was used for all the tests with bacterial strains and tests with fungal strains were done on SDB. Chloramphenicol was used as a standard antibiotic for the bacteria; clotrimazole was used as the control for the fungi and nystatin was used as the control for *C. albicans*. Starting concentration of antibiotic and antimycotics was 20 μ g/ml. The microplates were incubated for 24 h at 37 °C for bacteria, 35 °C for yeast, and 48 h at 28 °C for fungi. For antibacterial activity, any color change of the indicator (resazurin) from purple to pink or colorless was measured as a positive and the lowest concentrations without visible growth of fungi were defined as MIC.

Table 1
The phenolic compound contents of *Opuntia dillenii* fruit extracts.^a

<i>O. dillenii</i> fruit	Extract	Extracts of <i>O. dillenii</i> from Water		Total phenolic compounds (mg GAE/g dry extract)		Total flavonoids content (mg RUE/g dry extract)		Extracts of <i>O. dillenii</i> from Essentia		Total phenolic compounds (mg GAE/g dry extract)		Total flavonoids content (mg RUE/g dry extract)																							
		E1	E2	E3	E4	E5	E6	E7	E8	E9	E10	E11	E12	E13	E14	E15	E16	E17	E18	E19	E20	E21	E22	E23	E24										
Skin	Diethyl ether	580 ± 30	318 ± 1	191 ± 5	120 ± 10	330 ± 60	810 ± 20	176 ± 0.5 (× 10 ²)	5.1	17.6 ± 0.5 (× 10 ²)	459 ± 10	840 ± 20	9.4 ± 0.2	31 ± 1	51 ± 1	398 ± 2	6.7 ± 0.2	2 ± 1	4 ± 1	20 ± 0.1	4.1 ± 0.2	459 ± 10	840 ± 20	9.4 ± 0.2	31 ± 1	51 ± 1	398 ± 2	6.7 ± 0.2	2 ± 1	4 ± 1	20 ± 0.1	4.1 ± 0.2	459 ± 10	840 ± 20	9.4 ± 0.2
	Ethyl acetate	318 ± 1	191 ± 5	120 ± 10	330 ± 60	810 ± 20	176 ± 0.5 (× 10 ²)	5.1	17.6 ± 0.5 (× 10 ²)	459 ± 10	840 ± 20	9.4 ± 0.2	31 ± 1	51 ± 1	398 ± 2	6.7 ± 0.2	2 ± 1	4 ± 1	20 ± 0.1	4.1 ± 0.2	459 ± 10	840 ± 20	9.4 ± 0.2	31 ± 1	51 ± 1	398 ± 2	6.7 ± 0.2	2 ± 1	4 ± 1	20 ± 0.1	4.1 ± 0.2	459 ± 10	840 ± 20	9.4 ± 0.2	
	Ethanol	191 ± 5	120 ± 10	330 ± 60	810 ± 20	176 ± 0.5 (× 10 ²)	5.1	17.6 ± 0.5 (× 10 ²)	459 ± 10	840 ± 20	9.4 ± 0.2	31 ± 1	51 ± 1	398 ± 2	6.7 ± 0.2	2 ± 1	4 ± 1	20 ± 0.1	4.1 ± 0.2	459 ± 10	840 ± 20	9.4 ± 0.2	31 ± 1	51 ± 1	398 ± 2	6.7 ± 0.2	2 ± 1	4 ± 1	20 ± 0.1	4.1 ± 0.2	459 ± 10	840 ± 20	9.4 ± 0.2		
	Water	120 ± 10	330 ± 60	810 ± 20	176 ± 0.5 (× 10 ²)	5.1	17.6 ± 0.5 (× 10 ²)	459 ± 10	840 ± 20	9.4 ± 0.2	31 ± 1	51 ± 1	398 ± 2	6.7 ± 0.2	2 ± 1	4 ± 1	20 ± 0.1	4.1 ± 0.2	459 ± 10	840 ± 20	9.4 ± 0.2	31 ± 1	51 ± 1	398 ± 2	6.7 ± 0.2	2 ± 1	4 ± 1	20 ± 0.1	4.1 ± 0.2	459 ± 10	840 ± 20	9.4 ± 0.2			
Seeds	Diethyl ether	50 ± 2	27 ± 1	18 ± 1	5.3 ± 0.2	1.1 ± 0.3	2.7 ± 0.1	9.8 ± 0.2	5.1	17.6 ± 0.5 (× 10 ²)	459 ± 10	840 ± 20	9.4 ± 0.2	31 ± 1	51 ± 1	398 ± 2	6.7 ± 0.2	2 ± 1	4 ± 1	20 ± 0.1	4.1 ± 0.2	459 ± 10	840 ± 20	9.4 ± 0.2	31 ± 1	51 ± 1	398 ± 2	6.7 ± 0.2	2 ± 1	4 ± 1	20 ± 0.1	4.1 ± 0.2	459 ± 10	840 ± 20	9.4 ± 0.2
	Ethyl acetate	50 ± 2	27 ± 1	18 ± 1	5.3 ± 0.2	1.1 ± 0.3	2.7 ± 0.1	9.8 ± 0.2	5.1	17.6 ± 0.5 (× 10 ²)	459 ± 10	840 ± 20	9.4 ± 0.2	31 ± 1	51 ± 1	398 ± 2	6.7 ± 0.2	2 ± 1	4 ± 1	20 ± 0.1	4.1 ± 0.2	459 ± 10	840 ± 20	9.4 ± 0.2	31 ± 1	51 ± 1	398 ± 2	6.7 ± 0.2	2 ± 1	4 ± 1	20 ± 0.1	4.1 ± 0.2	459 ± 10	840 ± 20	9.4 ± 0.2
	Ethanol	27 ± 1	18 ± 1	5.3 ± 0.2	1.1 ± 0.3	2.7 ± 0.1	9.8 ± 0.2	5.1	17.6 ± 0.5 (× 10 ²)	459 ± 10	840 ± 20	9.4 ± 0.2	31 ± 1	51 ± 1	398 ± 2	6.7 ± 0.2	2 ± 1	4 ± 1	20 ± 0.1	4.1 ± 0.2	459 ± 10	840 ± 20	9.4 ± 0.2	31 ± 1	51 ± 1	398 ± 2	6.7 ± 0.2	2 ± 1	4 ± 1	20 ± 0.1	4.1 ± 0.2	459 ± 10	840 ± 20	9.4 ± 0.2	
	Water	18 ± 1	5.3 ± 0.2	1.1 ± 0.3	2.7 ± 0.1	9.8 ± 0.2	5.1	17.6 ± 0.5 (× 10 ²)	459 ± 10	840 ± 20	9.4 ± 0.2	31 ± 1	51 ± 1	398 ± 2	6.7 ± 0.2	2 ± 1	4 ± 1	20 ± 0.1	4.1 ± 0.2	459 ± 10	840 ± 20	9.4 ± 0.2	31 ± 1	51 ± 1	398 ± 2	6.7 ± 0.2	2 ± 1	4 ± 1	20 ± 0.1	4.1 ± 0.2	459 ± 10	840 ± 20	9.4 ± 0.2		
Juice	Diethyl ether	50 ± 2	27 ± 1	18 ± 1	5.3 ± 0.2	1.1 ± 0.3	2.7 ± 0.1	9.8 ± 0.2	5.1	17.6 ± 0.5 (× 10 ²)	459 ± 10	840 ± 20	9.4 ± 0.2	31 ± 1	51 ± 1	398 ± 2	6.7 ± 0.2	2 ± 1	4 ± 1	20 ± 0.1	4.1 ± 0.2	459 ± 10	840 ± 20	9.4 ± 0.2	31 ± 1	51 ± 1	398 ± 2	6.7 ± 0.2	2 ± 1	4 ± 1	20 ± 0.1	4.1 ± 0.2	459 ± 10	840 ± 20	9.4 ± 0.2
	Ethyl acetate	50 ± 2	27 ± 1	18 ± 1	5.3 ± 0.2	1.1 ± 0.3	2.7 ± 0.1	9.8 ± 0.2	5.1	17.6 ± 0.5 (× 10 ²)	459 ± 10	840 ± 20	9.4 ± 0.2	31 ± 1	51 ± 1	398 ± 2	6.7 ± 0.2	2 ± 1	4 ± 1	20 ± 0.1	4.1 ± 0.2	459 ± 10	840 ± 20	9.4 ± 0.2	31 ± 1	51 ± 1	398 ± 2	6.7 ± 0.2	2 ± 1	4 ± 1	20 ± 0.1	4.1 ± 0.2	459 ± 10	840 ± 20	9.4 ± 0.2
	Ethanol	27 ± 1	18 ± 1	5.3 ± 0.2	1.1 ± 0.3	2.7 ± 0.1	9.8 ± 0.2	5.1	17.6 ± 0.5 (× 10 ²)	459 ± 10	840 ± 20	9.4 ± 0.2	31 ± 1	51 ± 1	398 ± 2	6.7 ± 0.2	2 ± 1	4 ± 1	20 ± 0.1	4.1 ± 0.2	459 ± 10	840 ± 20	9.4 ± 0.2	31 ± 1	51 ± 1	398 ± 2	6.7 ± 0.2	2 ± 1	4 ± 1	20 ± 0.1	4.1 ± 0.2	459 ± 10	840 ± 20	9.4 ± 0.2	
	Water	18 ± 1	5.3 ± 0.2	1.1 ± 0.3	2.7 ± 0.1	9.8 ± 0.2	5.1	17.6 ± 0.5 (× 10 ²)	459 ± 10	840 ± 20	9.4 ± 0.2	31 ± 1	51 ± 1	398 ± 2	6.7 ± 0.2	2 ± 1	4 ± 1	20 ± 0.1	4.1 ± 0.2	459 ± 10	840 ± 20	9.4 ± 0.2	31 ± 1	51 ± 1	398 ± 2	6.7 ± 0.2	2 ± 1	4 ± 1	20 ± 0.1	4.1 ± 0.2	459 ± 10	840 ± 20	9.4 ± 0.2		

^a Data are represented as means ± SD (n = 3). GAE – gallic acid equivalents; RUE – rutin equivalents.

2.9. Cell culture and MTT assay

Human breast cancer cells (MCF-7), human colon cancer cells (LoVo) and human hepatocytes (HepG2) were cultured in DMEM, in the presence of 10% fetal bovine serum, antibiotics (penicillin and streptomycin, 1x) and 2 mM L-glutamine, in a 5% CO₂ humidified atmosphere at 37 °C. Cells were seeded in 96-well plates at a density of 2×10^3 /well. Approximately 24 h after seeding, increasing concentrations of each extract (0.1, 0.25, and 0.5 mg/ml) were added to the cells. To determine cell viability, the tetrazolium salt colorimetric assay (MTT) was used, as described by Del Giudice et al. (2015). This reagent (3-(4,5-dimethylthiazol-2-yl)-2,5-diphenyltetrazolium bromide) is converted into formazan crystals by active mitochondria, therefore only in living cells. Briefly, the MTT reagent was dissolved in DMEM without phenol red and added to the cells to a final concentration of 0.5 mg/ml. After 4 h at 37 °C, the culture medium was removed and the resulting formazan salts were dissolved using 2-propanol containing 0.01 N HCl. Absorbance of blue formazan was determined at 570 nm using an automatic plate reader (Microbeta Wallac 1420, PerkinElmer, Basel, Switzerland). Cell survival was expressed as the percentage of viable cells in the presence of the specific extract compared to control cells (represented by the average obtained between untreated cells and cells supplemented with the highest concentration of buffer). Each sample was tested in three independent analyses, each carried out in triplicates.

2.10. Hydroxyl radical-induced DNA damage

The protective effect of *O. dillenii* extracts against hydroxyl radical-induced DNA damage was evaluated with herring sperm DNA (Lin, Wang, Chang, & Wu, 2008). The extracts were dissolved in methanol at 1 mg/ml and various concentrations (50, 100, 200, and 400 µg/ml) were separately taken into Eppendorf tube. After evaporating to dryness, 45 µl of sodium phosphate buffer (0.2 mol/l, pH 7.4), 5 µl of herring sperm DNA solution (10 mg/ml NaCl), 0.9 µl 180 µmol/l FeSO₄ and 3.6 µl 600 µmol/l H₂O₂ were added. After incubation at room temperature for 15 min, the reaction was terminated by adding 10 µl of 1 µmol/l EDTA. The blank was the herring sperm DNA solution, while quercetin (50 µM) was used as a standard drug (Poorna, Resmi, & Soniya, 2013). Each mixture (5 µl) was loaded onto a 1% agarose gel in 1x TEA buffer containing ethidium bromide (10 mg/ml) and were run at 100 V in an electrophoresis system (BlueMarine™ 100, Serva Electrophoresis GmbH, Heidelberg, Germany). The gels were visualized (UV transilluminator, Vilber Lourmat, France) at 365 nm, photographed and DNA bands intensity was estimated using ImageJ software (version 1.48 for Windows, Softonic International, Barcelona, Spain).

2.11. Statistical analysis

The data are shown as the mean ± standard deviation (SD). The correlations between total phenolics and antioxidant activity were calculated using Pearson's test where, besides $p < 0.05$, values of < 0.01 were considered statistically significant to indicate the greater significance of the differences (* and ** indicate the significance levels at 0.05, and 0.01, respectively). Data for cytotoxicity are expressed as means ± SD of 3 separate experiments all carried out in triplicate and differences between means were analyzed using Student's t-test. Although a $p < 0.05$ was generally used, the authors have also chosen to use 0.01, 0.001, and 0.0001 to indicate the greater significance of the differences from untreated cells, with letters a, b, c, and d indicating the significance levels at $p < 0.05$, 0.01, 0.001, and 0.0001, respectively. The data for genotoxicity are shown as means ± SD (n = 3). Differences between means were analyzed using one-way analysis of variance (ANOVA) using the IBM Statistical Package for the Social Sciences statistical software package (version 13 for Windows, IBM Corp., Armonk, NY, USA) (* and ** indicate significant differences between defined groups ($p < 0.05$)).

3. Results

3.1. Phytochemical analysis

3.1.1. Total phenolic content

The phenolic compounds contents of *O. dillenii* extracts are shown in Table 1. The content of total phenolics varied considerably, from 17.6×10^2 mg GAE/g in ethanolic extract of seeds from the Essaouira locality (E19) to the lowest amount of total phenolics in ethyl acetate extract of the juice from the Nador locality (88 mg GAE/g, E11). The ethanolic extracts of *O. dillenii* seeds (E7 and E19) had the highest content of phenolic compounds among all investigated extracts from both localities. Almost all extracts from Essaouira (except E13 and E17) had a similar or significantly higher content of phenolic compounds than the corresponding extract from Nador. Although the *O. dillenii* juice extracts from Nador showed the presence of a significant amount of phenolics (88–160 mg GAE/g), all of the homologous extracts from the other locality had several folds higher content of total phenolic compounds (from 450 to 840 mg GAE/g).

Total flavonoid contents in the *O. dillenii* extracts are shown in Table 1. The lowest amount of flavonoids was in the ether extracts of seeds from both localities (E5 and E17). Ether, ethyl acetate, and ethanolic extracts of the skin of *O. dillenii* from both localities, with the highest flavonoid content in E1 and E14 extracts, were the richest in flavonoids. Generally, the sum of the total content of flavonoids in all extracts from Essaouira was much higher than the extracts from Nador.

3.1.2. HPLC of some polar extracts of *O. dillenii*

Flavonols were analyzed using HPLC in crude and hydrolyzed ethanolic extract of skin, seeds, and juice of *O. dillenii* fruits. As expected, hydrolyzed samples showed a higher flavonol concentration (Table 2). However, for fruit extracts from both localities, flavonols, particularly quercetin and kaempferol, were present in quantifiable amounts only in skin extracts (Fig. 1). Free quercetin concentration in the E15 crude extract was higher than in E3. However, when the extracts were hydrolyzed, total quercetin amounts were similar. Kaempferol was the dominant flavonol in the fruit skins. The E15 crude extract had a higher content of kaempferol than E3 extract. However, after hydrolyzation, a higher content of kaempferol was measured in the E3 extract, indicating a presence of this flavonol as a glycoside derivative in this sample. In other tested extracts (seeds and juice), all monitored flavonoids were present only in trace amounts. Myricetin was also present in trace amounts in all extracts.

3.1.3. GC-MS analysis of diethyl ether and ethyl acetate extracts

The major compounds and yields of diethyl ether and ethyl acetate extracts are shown in Table 3. The results showed that, besides the high amount of fatty acid methyl esters in diethyl ether extracts of *O. dillenii* seeds from both localities, the extracts had a high content of α -limonene (1-methyl-4-(1-methylethenyl)cyclohexane). α -limonene was also

Table 2
The content of flavonols in *O. dillenii* ethanolic skin, seeds, and juice extracts (mg/g dry extract).^a

Sample		Quercetin (mg/g)		Kaempferol (mg/g)	
		Crude extract	Hydrolyzed extract	Crude extract	Hydrolyzed extract
Skin	E3	0.36 ± 0.01	0.8 ± 0.01	2.4 ± 0.1	4.5 ± 0.2
	E15	0.6 ± 0.1	0.83 ± 0.01	2.7 ± 0.05	3.9 ± 0.1
Seeds	E7	tr	tr	tr	tr
	E19	tr	tr	tr	tr
Juice	E12	tr	tr	tr	tr
	E24	tr	tr	tr	tr

^a Data are represented as means ± SD (n = 3). tr – trace amounts, myricetin – only trace amounts in all tested samples.

found in the ethyl acetate extract of *O. dillenii* juice from Nador, as well as in both tested extracts of *O. dillenii* skin from Essaouira. Further, ethyl acetate extracts of *O. dillenii* seeds showed the presence of a low quantity of piperidine and its derivative. Also, in diethyl ether and ethyl acetate juice extracts of *O. dillenii* from Essaouira a dibutyl ester of sebacic acid was detected.

3.2. Antioxidant activity

The results of total antioxidant activity of *O. dillenii* fruit extracts are shown in Table 4. The aqueous juice extract of *O. dillenii* from Essaouira (E21) had the highest total antioxidant capacity. Twofold lower values were obtained for E19 and E24 extracts from the same locality. All the other extracts had lower total antioxidant potential. The results of free radicals (DPPH[•] and ABTS^{•+}) scavenging are given in Table 4. Analysis of DPPH[•] scavenging activity showed that most of the extracts had IC₅₀ values ranging from 200 to 500 µg/ml, in some cases even higher than 1 mg/ml. The ethanolic seed extracts from both localities, E7 and E19, showed the best DPPH[•] scavenging potential. Compared to the reference compounds, ascorbic acid, ellagic acid, and quercetin, E7 and E19 extracts had significantly lower antioxidant potential towards DPPH radical. Regarding scavenging effects of the extracts on ABTS radical cation, extracts E7 and E19 again stood out. Also, similar ABTS scavenging capacity showed ethyl acetate and ethanolic extracts of the juice of *O. dillenii* from Essaouira (E23 and E24).

According to the Pearson's correlation between the content of total phenolics and antioxidant activity of *O. dillenii* extracts (Table 5), the highest correlation was found for DPPH and ABTS activity ($p < 0.01$).

3.3. Antimicrobial activity

The results of antimicrobial activity of *O. dillenii* fruit extracts (E1–E24), obtained by microdilution tests, are reported in Tables 6 and 7. The antibacterial activity of the tested extracts was evaluated on a panel of 6 bacterial strains, three Gram-positive (*B. subtilis*, *M. lysodeikticus*, and *E. faecalis*) and three Gram-negative (*K. pneumoniae*, *E. coli*, and *P. fluorescens*) strains. The MIC results (Table 6) mostly varied between 0.63 and 2.5 mg/ml. In the case of *B. subtilis*, the lowest MIC value of 0.31 mg/ml was measured for the aqueous seed extract of *O. dillenii* from Nador (E8). The same level of antibacterial activity was shown for the E19 extract in the treatment of *K. pneumoniae* and several extracts (E7, E10, E11, E21, and E22) on *P. fluorescens*. Compared to the MIC values of the antibacterial activity of *O. dillenii* extracts, standard antibiotic chloramphenicol showed significantly higher potential against all tested bacteria, with MIC values from 1.3 to 20 µg/ml.

The extracts of *O. dillenii* seeds from the Nador locality showed the lowest overall antifungal MIC values, in a range from 0.16 to 2.5 mg/ml (Table 7). Considering the seeds of the plant material from Essaouira, only ether and aqueous extracts were effective on 6 fungal species. The most resistant species in the evaluation of antifungal activity was yeast *C. albicans*, for which the antifungal effects for *O. dillenii* extracts were not obtained (MIC > 10 mg/ml), except for E1 extract which had positive activity with MIC value of 10 mg/ml. Moreover, almost all skin extracts, except aqueous extracts (E4 and E16), were inefficient at the highest concentration used (MIC > 10 mg/ml).

3.4. Effects of *Opuntia dillenii* extracts on cell viability

To test the cytotoxic potential of *Opuntia* extracts three human cancer cells derived from liver (HepG2), colon (LoVo), and breast (MCF-7) were used. Cells were treated for 72 h with increasing amount of each extract (from 0.1 to 0.5 mg/ml dry weight), and cell viability was tested using the MTT reduction assay, as an indicator of metabolically active cells (Fig. 2). The corresponding IC₅₀ values, summarized in Table 8, indicate that after 72 h incubation none of the extracts showed a significant toxicity against hepatic cancer cells (IC₅₀ values

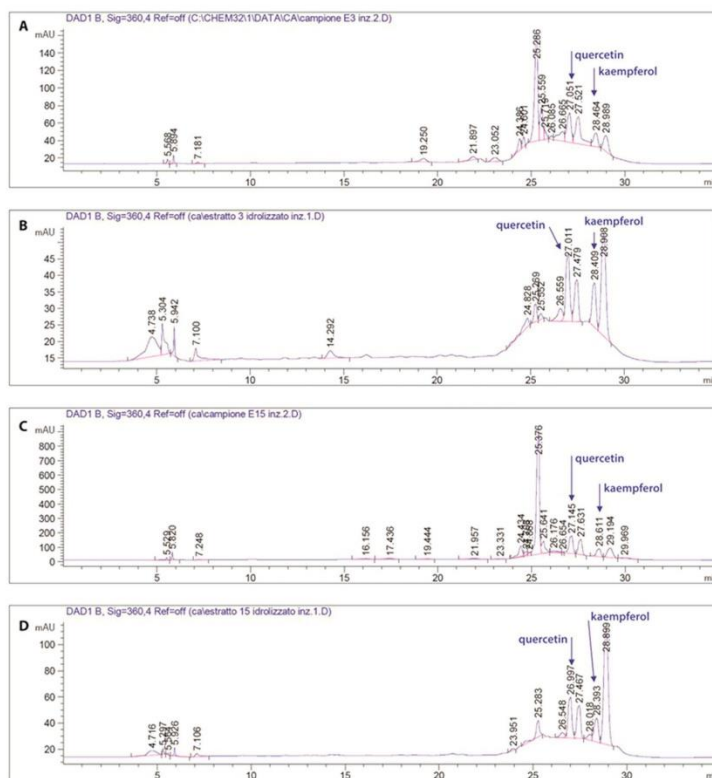


Fig. 1. HPLC chromatograms of flavonols in skin extracts of *O. dillenii*. A, B – sample E3, crude and hydrolyzed extract; C, D – sample E15, crude and hydrolyzed extract.

Table 3
GC-MS analysis of *O. dillenii* diethyl ether and ethyl acetate extracts (with percent of extracts yields and major compounds).

Locality	Plant organ	Diethyl ether extracts		Ethyl acetate extracts	
		Yield (%)	Major compounds (%)	Yield (%)	Major compounds (%)
Nador	Skin	0.3%	NI	0.47%	NI
	Seeds	3.47%	n-Limonene (40.2); 11,14-Octadecadienoic acid methyl ester (36.6); Imidazole, 2-amino-5-(2-carboxyvinyl) (21.5)	2.07%	1-Methylcaprolactam (8.3); Piperidine (6.23); n-Alanine (5.45)
	Juice	1.65%	NI	1.05%	p-Limonene (42.7)
Essouira	Skin	0.40%	p-Limonene (24.5); Methyl 3-alpha,12-alpha-dihydroxy-5-beta-cholan-24-oate (14.7)	0.86%	p-Limonene (30); 2H-Azepin-2-one, hexahydro-1-methyl- (9.8)
	Seeds	3.44%	11,14-Octadecadienoic acid, methyl ester (62.9); p-Limonene (17.2); Hexadecanoic acid, methyl ester (9.17)	1.2%	1,2-Benzenedicarboxylic acid, butyl octyl ester (13.5); 3,3-Dimethylpiperidine (12.6)
	Juice	0.9%	Tetradecane (50.1); Dibutylsebacate (15.4)	0.62%	Dibutylsebacate (56.3); 3-Methyl-3,5-(cyanoethyl) tetrahydro-4-thiapyranone (7.65)

NI: Not identified.

Table 4
Total antioxidant activity and IC₅₀ values of antioxidant effects of *O. dillenii* extracts on DPPH radical and ABTS radical cation.

Extract	Total antioxidant activity (mg AAE/g dry extract)	IC ₅₀ (µg/ml) ^a	
		DPPH [•] scavenging activity	ABTS ^{•+} scavenging activity
E1	190 ± 10	190 ± 10	550 ± 10
E2	130 ± 10	720 ± 10	536 ± 5
E3	150 ± 10	530 ± 10	736 ± 5
E4	82 ± 5	> 2 × 10 ³	970 ± 10
E5	95 ± 1	11.9 ± 0.4 (× 10 ³)	> 2 × 10 ³
E6	130 ± 10	220 ± 20	920 ± 10
E7	281 ± 5	63 ± 4	130 ± 10
E8	71 ± 2	> 2 × 10 ³	700 ± 10
E9	84 ± 2	690 ± 20	750 ± 20
E10	73 ± 3	13.4 ± 0.4 (× 10 ³)	> 2 × 10 ³
E11	53 ± 1	> 2 × 10 ³	> 2 × 10 ³
E12	64 ± 5	14.5 ± 0.3 (× 10 ³)	16.6 ± 0.3 (× 10 ³)
E13	140 ± 10	> 2 × 10 ³	570 ± 10
E14	190 ± 10	340 ± 10	307 ± 5
E15	240 ± 10	500 ± 20	460 ± 10
E16	77 ± 2	880 ± 10	820 ± 10
E17	92 ± 1	> 2 × 10 ³	> 2 × 10 ³
E18	129 ± 5	380 ± 10	857 ± 1
E19	410 ± 10	45 ± 3	88 ± 2
E20	110 ± 20	> 2 × 10 ³	380 ± 10
E21	830 ± 10	370 ± 10	213 ± 5
E22	230 ± 30	370 ± 10	190 ± 10
E23	220 ± 10	850 ± 10	95 ± 3
E24	420 ± 20	280 ± 10	100 ± 10
Reference compounds			
Ascorbic acid	–	2.8 ± 0.2	16 ± 1
Ellagic acid	–	0.9 ± 0.1	7.0 ± 0.4
Quercetin	–	2.4 ± 0.1	17 ± 1

AAE – ascorbic acid equivalents. IC₅₀ values were determined by nonlinear regression analysis.

^a Data are represented as means ± SD (n = 3).

higher than 0.5 mg/ml). However, in the case of extracts from seeds, the IC₅₀ value in LoVo and MCF-7 cells were determined only for E7 and E19 extracts, whose extraction was done in ethanol. The data suggested that *Opuntia dillenii* seeds extracts (E7, E19, and E18) showed a cytotoxic effect also on hepatic cells (about 60% cell survival when tested at 0.5 mg/ml), while E6, E8, and E20 showed a reduced viability of colon cancer cells (about 30% cell death when tested at 0.5 mg/ml).

In the case of skin extracts, the IC₅₀ value was obtained for E1 and E13 (extracted in diethyl ether) in the case of MCF-7 and LoVo cells, whereas in the case of HepG2 cells only 60% cell survival was obtained after treating the cells with the highest concentration tested. As for E2–E14 extracts, i.e., those obtained with ethyl acetate extraction, the IC₅₀ suggested a strong cytotoxic activity only on breast cancer cells, even if a 40% cell death (at 0.5 mg/ml) was observed for the other cell lines analyzed. The E15 extract showed only a 20–30% of cell inhibition when tested at the highest concentration.

In the case of extracts obtained from juice, only for E22 extract

(diethyl ether extraction), the IC₅₀ value showed significant cytotoxic activity on all the cell lines analyzed, whereas E10 was active only on breast cancer cells.

3.5. Antigenotoxic properties of *O. dillenii* extracts

To evaluate the ability of *O. dillenii* ether, ethyl acetate, ethanol, and water extracts to protect DNA from the harmful effect of hydroxyl radicals (OH), herring sperm DNA was treated with different concentrations of each extract and the results are shown in Fig. 3. DNA-protective activity among the *O. dillenii* skin extracts decreased in the following order: water > ethanol > ether > ethyl acetate from the Nador locality, and water > ethanol = ethyl acetate > ether from the Essaouira locality. Aqueous extracts of skin from both localities had good DNA protective activity in all tested concentrations. However, these effects were lower than the protection provided by the reference compound quercetin at a concentration of 50 µM. The decreasing order in the reduction of DNA damage among the extracts of *O. dillenii* seeds was found to be: ethanol > ethyl acetate > ether > water from Nador, and ether > ethanol > water > ethyl acetate from Essaouira. Even though all the extracts effectively protected the DNA from OH radicals, the ethanolic extract of seeds from Nador (E7) was found to be the most effective in the reduction of the DNA damage. Moreover, the DNA-protective effects of diethyl ether extract of seeds from Essaouira (E17) were equal to or greater than the protective effect of quercetin. Among the 4 tested extracts of *O. dillenii* juice, the diethyl ether extracts from both localities (E10 and E22) had the highest DNA protective activity, but only ether and ethanol extracts from Essaouira showed DNA protective activity in increasing order with the used concentration of the extracts. Diethyl ether extracts of juice from both localities were promising with the highest DNA-protective activity at 50 µg/ml for E10 and 400 µg/ml for E22, with relative density above the DNA control.

4. Discussion

The extracts from different parts of *O. dillenii* fruit, collected from two localities in Morocco, contained several classes of bioactive chemical compounds, mainly phenolic compounds in polar extracts and terpenoids with fatty acid derivatives in non-polar extracts. The ethanolic extracts of seeds from both localities had the highest content of total phenolic compounds. The results are in accordance with previously published data by several research groups. Chang et al. (2008) reported that, among all tested parts of *O. dillenii* fruits, seeds showed the highest amount of total phenolic compounds (213 mg/100 g fresh sample), compared with pulp and peel extracts. Recently, Betancourt et al. (2017) reported a high content of total phenolics in the crude extract of *O. dillenii* fruits (312 mg GAE/100 g fresh fruit) from Colombia, while Embaby et al. (2016) published a lower amount of phenolics (180 mg/100 g) in *O. dillenii* fruits from Egypt. The highest content of flavonoids in this study was measured, besides the already mentioned seed ethanolic extracts, in almost all skin extracts. HPLC analysis also confirmed the obtained results, which reflected in the contents of quercetin and kaempferol in crude ethanolic extracts of *O. dillenii* skin. The increased levels of quercetin and kaempferol after hydrolysis indicated the presence of derivatives of these two flavonoids

Table 5
Pearson's correlation between total phenolics and antioxidant activity of *O. dillenii* extracts.

	Total phenolic content	Total flavonoids content	Total antioxidant activity	DPPH activity	ABTS ^{•+} activity
Total phenolic content	1	0.29	0.53**	–0.59**	–0.56**
Total flavonoids content		1	0.19	–0.39	–0.44
Total antioxidant activity			1	–0.52**	–0.55**
DPPH activity				1	0.56**
ABTS ^{•+} activity					1

* and ** indicate the significance levels at 0.05 and 0.01, respectively.

Table 6
Antibacterial activity of *O. dillenii* extracts.

Extract/Bacterial strain	MIC value ^a					
	<i>Bacillus subtilis</i> (ATCC 6633)	<i>Micrococcus lysodeikticus</i> (ATCC 4698)	<i>Enterococcus faecalis</i> (ATCC 92912)	<i>Klebsiella pneumoniae</i> (ATCC 70063)	<i>Escherichia coli</i> (ATCC 25922)	<i>Pseudomonas fluorescens</i> (FSB 28)
E1	2.5	2.5	2.5	1.3	1.3	2.5
E2	2.5	1.3	2.5	1.3	1.3	1.3
E3	1.3	2.5	5.0	0.63	1.3	0.63
F4	1.3	1.3	2.5	0.31	2.5	0.63
E5	0.63	1.3	20	0.63	2.5	2.5
E6	0.63	2.5	20	0.63	2.5	0.63
E7	0.63	1.3	10	0.63	2.5	0.31
F8	0.31	1.3	10	0.63	5.0	0.63
F9	0.63	1.3	1.3	0.63	0.63	0.63
E10	0.63	0.63	0.63	0.63	0.63	0.31
E11	0.63	1.3	1.3	1.3	1.3	0.31
E12	0.63	1.3	1.3	1.3	1.3	0.63
E13	5.0	5.0	10	5.0	5.0	2.5
E14	0.63	0.63	2.5	2.5	2.5	1.3
E15	0.63	1.3	1.3	0.63	1.3	0.63
E16	0.63	0.63	2.5	0.63	2.5	0.63
E17	0.63	1.3	10	0.63	10	10
E18	0.63	0.63	2.5	0.63	2.5	1.3
E19	0.63	0.63	0.63	0.31	0.63	0.63
E20	0.63	0.63	0.63	0.63	0.63	1.3
E21	1.3	1.3	1.3	2.5	1.3	0.31
E22	2.5	2.5	10	2.5	2.5	0.31
E23	1.3	1.3	1.3	1.3	1.3	0.63
E24	1.3	1.3	1.3	1.3	1.3	0.63
Chloramphenicol	5.0	1.3	10	20	5.0	2.5

^a MIC – minimum inhibitory concentration values given as mg/ml and for antibiotic as µg/ml.

in the tested extracts. The presence of quercetin, along with some other phenolic compounds (e.g., catechin, epicatechin, gallic and ellagic acid), has been already reported in *O. dillenii* fruits, especially in seeds (Chang et al., 2008). According to Ahmed et al. (2005), the presence of kaempferol and isorhamnetin derivatives (kaempferol-3-O- α -arabinoside, isorhamnetin-3-O- β -D-glucopyranoside, and isorhamnetin-3-O- β -D-

rutinoside) was detected in the *O. dillenii*, and confirmed by Moussa-Ayoub et al. (2016). Sharma, Rani, Kumar, and Raj (2015) reported the identification by spectral analysis of quercetin, 3-O-methyl quercetin, and kaempferol from the stems of *O. dillenii*. It should also be noted that quercetin, isorhamnetin, kaempferol and their derivatives, were chromatographically detected in juices and peels of other *Opuntia*

Table 7
Antifungal activity of *O. dillenii* extracts.

Extract/Fungal strain	MIC value ^a						
	<i>Candida albicans</i> (ATCC 10259)	<i>Trichoderma harzianum</i> (FSB 12)	<i>Penicillium cyclopium</i> (FSB 23)	<i>Aspergillus niger</i> (FSB 31)	<i>Doratomyces stemonitis</i> (FSB 41)	<i>Phialophora fastigiata</i> (FSB 81)	<i>Fusarium oxysporum</i> (FSB 91)
E1	10	> 10	> 10	> 10	> 10	> 10	> 10
E2	> 10	> 10	> 10	> 10	> 10	> 10	> 10
E3	> 10	> 10	> 10	10	> 10	> 10	> 10
F4	> 10	0.16	0.16	1.3	0.31	0.16	0.16
E5	> 10	0.16	0.16	0.16	0.63	0.16	0.16
F6	> 10	0.16	0.16	0.16	0.31	0.16	0.16
E7	> 10	0.16	0.31	2.5	> 10	2.5	> 10
F8	> 10	0.16	0.16	1.3	0.16	0.16	0.16
E9	> 10	0.16	0.16	2.5	> 10	0.16	0.16
E10	> 10	> 10	> 10	> 10	> 10	10	> 10
E11	> 10	> 10	> 10	> 10	10	> 10	> 10
E12	> 10	0.16	0.16	0.63	5.0	0.63	0.16
E13	> 10	> 10	> 10	> 10	> 10	> 10	> 10
E14	> 10	> 10	> 10	> 10	> 10	> 10	> 10
E15	> 10	> 10	0.16	> 10	> 10	> 10	0.16
E16	> 10	0.16	0.16	0.16	0.63	0.16	0.16
E17	> 10	0.16	0.16	0.16	0.63	0.16	0.16
E18	> 10	> 10	> 10	> 10	> 10	> 10	> 10
E19	> 10	5.0	> 10	> 10	> 10	> 10	10
E20	> 10	0.16	0.16	0.16	0.31	0.16	0.16
E21	> 10	0.16	0.16	1.3	10	0.16	0.16
E22	> 10	> 10	> 10	> 10	> 10	0.16	> 10
E23	> 10	0.16	1.3	5.0	10	0.16	0.16
E24	> 10	0.16	0.16	0.16	0.31	0.16	0.16
Antimycotics	5.0	0.63	0.31	< 0.31	2.5	0.31	1.3

^a MIC – minimum inhibitory concentration values given as mg/ml and for antimycotics as µg/ml (nystatin for *C. albicans* and clotrimazole for the others).

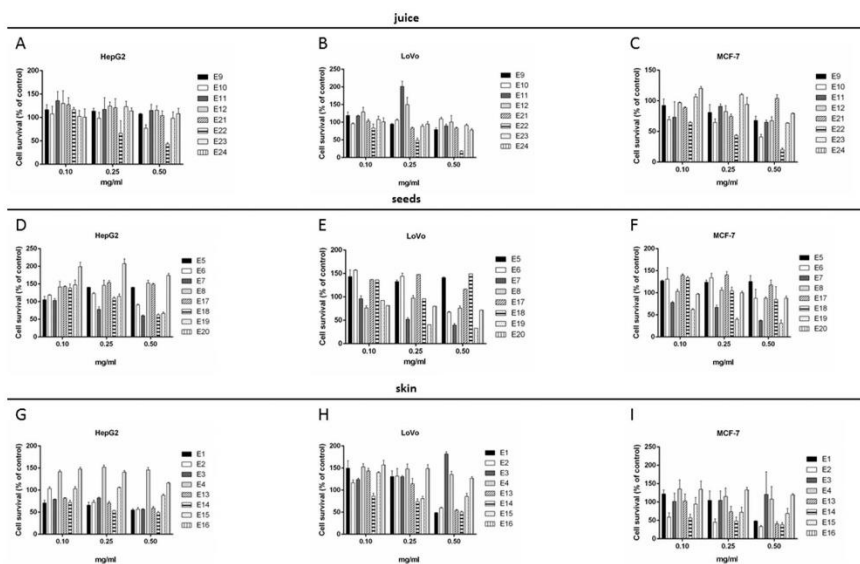


Fig. 2. Effect of *O. dillenii* extracts on the viability of cancer cells. Dose-response bar blot of human cancer cells after 72 h incubation in the presence of increasing concentrations of extracts (0.1–0.5 mg/ml). Cell viability was assessed using the MTT assay and cell survival percentage was defined as reported in the Methods section. Values are given as means \pm SD ($n \geq 3$). Differences between means with letters a, b, c, and d indicate $p < 0.05$, 0.01, 0.001, and 0.0001, respectively, with respect to untreated cells.

A-C, different juice extracts; D-F, different seed extracts; G-I, different skin extracts.

Table 8

Cytotoxic activity of the extracts. Cytotoxicity is expressed as IC_{50} values in mg/ml.

Extract	IC_{50} value (mg/ml)		
	MCF-7	LoVo	HepG2
E1	0.49 \pm 0.01	0.48 \pm 0.12	> 0.5
E2	0.11 \pm 0.04	> 0.5	> 0.5
E3	> 0.5	> 0.5	> 0.5
E4	> 0.5	> 0.5	> 0.5
E5	> 0.5	> 0.5	> 0.5
E6	> 0.5	> 0.5	> 0.5
E7	0.39 \pm 0.03	0.27	> 0.5
E8	> 0.5	> 0.5	> 0.5
E9	> 0.5	> 0.5	> 0.5
E10	0.4 \pm 0.1	> 0.5	> 0.5
E11	> 0.5	> 0.5	> 0.5
E12	> 0.5	> 0.5	> 0.5
E13	0.3 \pm 0.1	0.5	> 0.5
E14	0.1 \pm 0.1	0.5	0.5
E15	> 0.5	> 0.5	> 0.5
E16	> 0.5	> 0.5	> 0.5
E17	> 0.5	> 0.5	> 0.5
E18	> 0.5	> 0.5	> 0.5
E19	0.17 \pm 0.02	0.22	> 0.5
E20	> 0.5	> 0.5	> 0.5
E21	> 0.5	> 0.5	> 0.5
E22	0.18 \pm 0.01	0.25	0.42
E23	> 0.5	> 0.5	> 0.5
E24	> 0.5	> 0.5	> 0.5

species (Astello-García et al., 2015; Mata et al., 2016; Melgr et al., 2017). Moussa-Ayoub et al. (2016) detected only a flavonoid identified as isorhamnetin-3-*O*-rutinoside in the skin of *O. dillenii* fruit.

GC-MS analysis of non-polar extracts of *O. dillenii* showed the dominant presence of α -limonene, which was not reported so far. α -Limonene, known as a major constituent of several citrus, is a natural monoterpene with a lemon-like odor and can contribute to the aroma and taste of food, which can additionally promote the use of *O. dillenii* as a functional food with promising biological activity (Zahi, Liang, & Yuan, 2015).

The skin and seed extracts of *O. dillenii* had the similar total antioxidant capacity, irrespective of the site from which they were sampled. The differences were noticeable only in the case of ethanolic extracts of skin and seed, where the extracts from Essaouira had much stronger antioxidant capacity. This can be associated with total phenolics content in those extracts, as it is well known that phenolics compounds have extraordinary antioxidant activity (Del Rio et al., 2013; Leopoldini, Russo, & Toscano, 2011). Much higher total antioxidant capacity was shown in all juice extracts of *O. dillenii* from Essaouira, compared to those from Nador, which also corresponded to the total phenolic content in juice extracts. Moreover, the results of DPPH and ABTS scavenging capacity followed a similar trend. The antioxidant activity against those free radicals showed the advantage of the ethanolic seed extracts from both localities (E7 and E19) and all juice extracts from Essaouira (E21–24). The influence of phenolic compounds content was also confirmed using the Pearson's correlation between total phenolics and antioxidant activity of *O. dillenii* extracts. R values of the total phenolic and flavonoid contents and total antioxidant

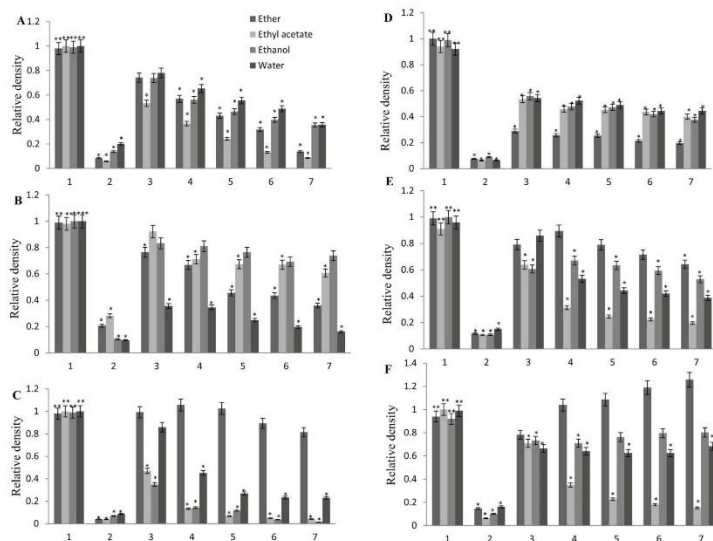


Fig. 3. Protecting effect of *O. dillenii* extracts against hydroxyl radical-induced DNA damage. *O. dillenii* extracts from two localities: Nador (A, skin; B, seeds; C, juice) and Essaouira (D, skin; E, seeds; F, juice). 1: DNA control; 2: DNA damage control; 3: standard compound quercetin (50 μ M); 4–7: extracts of *O. dillenii* at the concentrations of 50, 100, 200, and 400 μ g/ml. The data are shown as means \pm standard deviation ($n = 3$). Differences between means (* and **) indicate the significance levels at 0.05, compared with the negative and positive control groups, respectively.

activity ($R = 0.53$ and 0.19 , respectively) suggested that the amount of flavonoids did not significantly increase the total antioxidant activity level, as well as DPPH and ABTS scavenging activities, but other phenolic compounds had much more influence on antioxidant activity of *O. dillenii* extracts. Also, a similar correlation ($p < 0.01$) of tested extracts was observed between the total antioxidant activity and their ability to scavenge DPPH and ABTS free radicals. The observed negative correlation between the content of phenolic compounds and free radicals scavenging activity showed that phenolics in some of the *O. dillenii* fruit extracts are not the major contributors to their antioxidant activity. This indicates the presence of other nutrients with strong antioxidant capacity, such as vitamins, carotenes, ascorbate or glutathione, as shown for other *Opuntia* spp. by Astello-García et al. (2015).

Chang et al. (2008) also showed a significant antioxidant activity of *O. dillenii* fruit extracts in the term of LDL peroxidation inhibition, where phenolic compounds and betalains had a significant role. Betalains are water-soluble indole-derived pigments, present in most of the order of Caryophyllales, including the Cactaceae family and genus *Opuntia*, and they are responsible for red (betacyanins) and yellow (betaxanthins) color of the flowers and fruits of those plant species (Betancourt et al., 2017; Melgar et al., 2017; Montes-Lora, Hurtado, Mosquera, Heredia, & Cejudo-Bastante, 2016). It has been reported that the main betacyanins in *O. dillenii* fruits are betanin and isobetanin, while the principal detected betaxanthin is indicaxanthin (Böhm, 2008; Montes-Lora et al., 2016). Also, some publications reported the absence of betaxanthins in the fruits of *O. dillenii* (Chang et al., 2008; Moussa-Ayoub et al., 2016) or much higher content of betacyanins (Betancourt et al., 2017; Embaby et al., 2016). Furthermore, these betalain pigments were detected in juices and peels of other *Opuntia* species (e.g., *O. ficus-*

indica var *gialla* and var *sanguigna*, *O. engelmannii*, *O. stricta*, *O. undulata*, *O. robusta*) (Böhm, 2008; Mata et al., 2016; Melgar et al., 2017). On the other hand, the findings in this study suggest that, due to their sensitivity to temperature, time, pH values, etc. (Cejudo-Bastante et al., 2015), betalains were degraded during the preparation or storage of samples before analysis, probably due to an oxidative process (data not shown). Recently, a high antioxidant potential of *O. dillenii* fruit or its juice was reported (Betancourt et al., 2017; Montes-Lora et al., 2016; Moussa-Ayoub et al., 2016). Further, a high percentage of DPPH, peroxide, and hydroxyl free radicals scavenging activities of *O. dillenii* flowers extract were confirmed by Kumar, Ganesh, Peng, and Hyun Tae (2014).

The results of antimicrobial activity of *O. dillenii* extracts did not show a clear dependence on the solvent used or on the growth locality. The results are consistent with recently published data on the antimicrobial activity of peel extracts of selected *Opuntia* spp. (Melgar et al., 2017). Phenolic compounds, especially flavonoids, participate in the antimicrobial potential of *O. dillenii* based on their various modes of action (Cushnie & Lamb, 2011), but the presence of α -limonene, with well-known antimicrobial properties, certainly increased activity of non-polar extracts of *O. dillenii* (Gyawali & Ibrahim, 2014; Zahi et al., 2015).

It was found that the high phenolic and flavonoid content well correlated with cytotoxicity on some cancer cells, like skin and seed extracts obtained in diethyl ether and skin extracts obtained in ethyl acetate were more active on human breast cancer cells. Also, a parallel can be drawn between the cytotoxicity of the extracts from the different localities. This was reflected particularly in MCF-7 cytotoxicity results, where non-polar skin extracts (E1, E2, E13, E14), ethanolic seed

extracts (E7, E19), and diethyl ether juice extracts (E10, E22) are distinguished by their IC₅₀ values, generally lower in the extracts from Essaouira. From a general point of view, colon and hepatic cells were able to grow faster in the presence of low doses of the extracts. Since it is known that cancer cells are actively proliferating, the presence of nutrients in combination with low levels of antioxidants may have a positive effect on cell growth. Melgar et al. (2017) reported similar cytotoxicity of some *Opuntia* spp. on HepG2 cell line, along with beneficial antitumor activity on MCF-7 cells.

Hydroxyl radicals (OH[•]), as one of the most reactive oxygen species, are generated as a result of the Fenton reaction, and have the capacity to react with the purine and pyrimidine bases and the deoxyribose backbone in the DNA molecule, causing severe biological damage such as mutagenesis, cytotoxicity, and carcinogenesis (Ragu et al., 2007; Valko, Izakovic, Mazur, Rhodes, & Telsner, 2004). *O. dillenii* extracts were able to protect DNA from OH radical-induced damage with promising antigenotoxic activity. This is particularly observed in the case of aqueous and ethanolic extracts of skin, ethanolic seeds extracts, as well as ether and polar juice extracts, compared with the activity of the reference compound quercetin. So far, only the antigenotoxic effects of *O. ficus-indica* cactus juice and cladodes have been studied in vivo. Madrigal-Santillán et al. (2013) reported that juice extract of *O. ficus-indica* reduced the number of micronucleated polychromatic erythrocytes and in that sense had an anticlastogenic effect. Also, the antigenotoxic potential of *O. ficus-indica* cladodes extracts was confirmed in terms of effective protection from the clastogenic action and DNA damages of zearalenone (Zorgui, Ayed-Boussema, Ayed, Bacha, & Hassen, 2009). It is known that phenolic compounds, mainly flavonoids and phenolic acids, showed significant antigenotoxic effects (Mladenović et al., 2013), which was also confirmed in this study in the case of quercetin. This leads to the conclusion that most of the tested *O. dillenii* extracts can be used as efficient antigenotoxic agents based on their phytochemical composition and antioxidant potential.

5. Conclusion

The *in vitro* antioxidant, antimicrobial, cytotoxic and antigenotoxic potential of *O. dillenii* extracts were shown. They potentially have a very diverse phytochemical composition with different bioactive compounds, mainly phenolic compounds and terpenoids. The extracts of *O. dillenii* fruit from Essaouira showed distinctly better potential, compared to the corresponding extracts from Nador. Overall, the findings suggested a possible therapeutic potential of *O. dillenii* extracts, especially juice extracts, as well as their potential use as functional food ingredients. Of course, these results provide the basis for further research with *O. dillenii* and other *Opuntia* spp., in terms of showing the underlying mechanisms of action.

Conflicts of interest

There are no conflicts to declare.

Acknowledgments

The authors gratefully acknowledge the financial support for this study by the National Center for Scientific and Technical Research (CNRS) of Morocco (Project PPR2). One part of this research was supported by the Ministry of Education, Science and Technological Development of the Republic of Serbia (Project No. III 43004).

References

- Adams, R. P. (2007). *Identification of essential oil components by gas chromatography/mass spectrometry*. Carol Stream, IL, USA: Allured Publishing Corp.
- Ahmed, M. S., El Tanbouly, N. D., Islam, W. T., Sleem, A. A., & El Senousy, A. S. (2005). Antiinflammatory flavonoids from *Opuntia dillenii* (ker-Gawl) Haw. flowers growing

- in Egypt. *Phytotherapy Research*, 19, 807–809. <https://doi.org/10.1002/ptr.1708>.
- Astello-García, M. G., Cervantes, I., Nair, V., del Socorro Santos-Díaz, M., Reyes-Aguero, A., Guéraud, F., et al. (2015). Chemical composition and phenolic compounds profile of cladodes from *Opuntia* spp. cultivars with different domestication gradient. *Journal of Food Composition and Analysis*, 43, 119–130. <https://doi.org/10.1016/j.jfca.2015.04.016>.
- Bajaj, V. K., & Gupta, R. S. (2012). Fertility suppression in male albino rats by administration of methanolic extract of *Opuntia dillenii*. *Andrologia*, 44, 530–537. <https://doi.org/10.1111/j.1439-0272.2011.01220.x>.
- Betancourt, C., Cejudo-Bastante, M. J., Heredia, F. J., & Hurtado, N. (2017). Pigment composition and antioxidant capacity of betacyanins and betaxanthins fractions of *Opuntia dillenii* (Ker Gawl) Haw cactus fruit. *Food Research International*, 101, 173–179. <https://doi.org/10.1016/j.foodres.2017.05.007>.
- Böhni, H. (2008). *Opuntia dillenii* – an interesting and promising Cactaceae taxon. *Journal of the Professional Association for Cactus Development*, 10, 148–170. Retrieved from <http://www.jpacd.org/downloads/Vol10/V10P148-170.pdf>.
- Brighente, I. M. C., Dias, M., Verdi, L. G., & Pizzolatti, M. G. (2007). Antioxidant activity and total phenolic content of some Brazilian species. *Pharmaceutical Biology*, 45, 156–161. <https://doi.org/10.1089/15588220601113131>.
- Caruso, M. C., Galgano, F., Pecora, M., Tolve, R., Verrastro, M., & Favati, F. (2015). Improvement of analytical methods for the determination of polyphenolic bioactive compounds in berry fruits. *Journal of Chemistry*, 1–6. 2015 <https://doi.org/10.1155/2015/384051>.
- Cejudo-Bastante, M. J., Hurtado, N., & Heredia, F. J. (2015). Potential use of new Colombian cactaceae. Colorimetric study of red prickly pear (*Opuntia dillenii*) extracts under different technological conditions. *Food Research International*, 71, 91–99. <https://doi.org/10.1016/j.foodres.2015.02.011>.
- Chang, S. F., Hsieh, C. L., & Yen, G. C. (2008). The protective effect of *Opuntia dillenii* Haw fruit against low-density lipoprotein peroxidation and its active compounds. *Food Chemistry*, 106, 569–575. <https://doi.org/10.1016/j.foodchem.2007.06.017>.
- CLSI (2002). In (9th ed.). P. A. Wayne (Vol. Ed.), *Methods for dilution antimicrobial susceptibility tests for bacteria that grow aerobically: approved standard: Vol 32*. USA: Clinical and Laboratory Standards Institute (CLSI).
- Cornu, A., & Massot, R. (1975). *Compilation of mass spectral data*. London, UK: Heyden and Sons.
- Cushnie, T. P. T., & Lamb, A. J. (2011). Recent advances in understanding the antibacterial properties of flavonoids. *International Journal of Antimicrobial Agents*, 38, 93–107. <https://doi.org/10.1016/j.ijantimicag.2011.02.014>.
- Del Giudice, R., Raiola, A., Tenore, G. C., Frusciantone, L., Barone, A., Monti, D. M., et al. (2015). Antioxidant bioactive compounds in tomato fruits at different ripening stages and their effects on normal and cancer cells. *Journal of Functional Foods*, 18, 83–94. <https://doi.org/10.1016/j.jff.2015.06.068>.
- Del Rio, D., Rodríguez-Mateos, A., Spencer, J. P. E., Tognolini, M., Borges, G., & Crozier, A. (2013). Dietary (poly)phenolics in human health: Structures, bioavailability, and evidence of protective effects against chronic diseases. *Antioxidants and Redox Signaling*, 18, 1818–1892. <https://doi.org/10.1089/ars.2012.4581>.
- Díaz Medina, E. M., Rodríguez Rodríguez, E. M., & Díaz Romero, C. (2007). Chemical characterization of *Opuntia dillenii* and *Opuntia ficus-indica* fruits. *Food Chemistry*, 103, 38–45. <https://doi.org/10.1016/j.foodchem.2006.06.064>.
- Embaby, H. E., Gaballah, A. A., Hamed, Y. S., & El-Samahy, S. K. (2016). Physicochemical properties, bioactive compounds and sensory evaluation of *Opuntia dillenii* fruits mixtures. *Journal of Food and Nutrition Research*, 4, 528–534. <https://doi.org/10.13691/jfnr-4-8-2>.
- Fernández-López, J. A., & Almela, I. (2001). Application of high-performance liquid chromatography to the characterization of the betalain pigments in prickly pear fruits. *Journal of Chromatography A*, 913, 415–420. [https://doi.org/10.1016/S0021-9673\(00\)01224-3](https://doi.org/10.1016/S0021-9673(00)01224-3).
- Feuqiang, J. M., Komarski, P., Zou, D., Stintzing, F. C., & Zou, C. (2006). Nutritional and medicinal use of cactus pear (*Opuntia* spp.) cladodes and fruits. *Frontiers in Bioscience*, 11, 2574–2589.
- Gao, J., Han, Y. L., Jin, Z. Y., Xu, X. M., Zha, X. Q., Chen, H. Q., et al. (2015). Protective effect of polysaccharides from *Opuntia dillenii* Haw. fruits on streptozotocin-induced diabetic rats. *Carbohydrate Polymers*, 124, 25–34. <https://doi.org/10.1016/j.carbpol.2015.01.068>.
- Ghazi, Z., Roudani, M., Tahrir, M., Rami, R., Elmsellem, H., El Mahi, B., et al. (2015). Chemical composition and antioxidant activity of seeds oils and fruit juice of *Opuntia ficus indica* and *Opuntia dillenii* from Morocco. *Journal of Materials and Environmental Science*, 6, 2338–2345.
- Gyawali, R., & Ibrahim, S. A. (2014). Natural products as antimicrobial agents. *Food Control*, 46, 412–429. <https://doi.org/10.1016/j.foodcont.2014.05.047>.
- Han, Y. L., Gao, J., Yin, Y. Y., Jin, Z. Y., Xu, X. M., & Chen, H. Q. (2016). Extraction optimization by response surface methodology of mucilage polysaccharide from the peel of *Opuntia dillenii* haw. fruits and their physicochemical properties. *Carbohydrate Polymers*, 151, 381–391. <https://doi.org/10.1016/j.carbpol.2016.05.085>.
- Katanic, J., Mihalović, V., Stanković, N., Borjia, T., Mladenović, M., Solujić, S., et al. (2015). Drowpov (*Filipendula hexapetala* Glib.) Potential role as antioxidant and antimicrobial agent. *EXCLI Journal*, 14, 1–20. <https://doi.org/10.17179/excli2014-479>.
- Kumarasamy, Y., Byres, M., Cox, P. J., Jaspars, M., Nahar, I., & Sarker, S. D. (2007). Screening seeds of some Scottish plants for free radical scavenging activity. *Phytotherapy Research*, 21, 615–621. <https://doi.org/10.1002/ptr.2129>.
- Kumar, A. S., Ganeshi, M., Peng, M. M., & Hyun Tse, J. (2014). Phytochemical, antioxidant, antiviral and cytotoxic evaluation of *Opuntia dillenii* flowers. *Bangladesh Journal of Pharmacology*, 9, 351–355. <https://doi.org/10.3329/bjpp.v9i3.19489>.
- Leopoldini, M., Russo, N., & Toscano, M. (2011). The molecular basis of working mechanism of natural polyphenolic antioxidants. *Food Chemistry*, 125, 288–306. <https://doi.org/10.1016/j.foodchem.2010.11.044>.

- doi.org/10.1016/j.foodchem.2010.08.012.
- Lin, Y.-W., Wang, Y. T., Chang, H.-M., & Wu, J. S.-B. (2008). DNA protection and anti-tumor effect of water extract from residue of Jelly Fig (*Ficus anskoesang* Makino) achenes. *Journal of Food and Drug Analysis*, 16, 63–69.
- Li, H., Yuan, Q., Zhou, X., Zeng, F., & Lu, X. (2013). Extraction of *Opuntia dillenii* Haw. polysaccharides and their antioxidant activities. *Molecules*, 21, 1–14. [http://doi.org/10.3390/molecules21121612](https://doi.org/10.3390/molecules21121612).
- Loro, J. F., Del Rio, I., & Pérez-Santana, L. (1999). Preliminary studies of analgesic and anti-inflammatory properties of *Opuntia dillenii* aqueous extract. *Journal of Ethnopharmacology*, 67, 213–218. [http://doi.org/10.1016/S0378-8741\(99\)00027-6](https://doi.org/10.1016/S0378-8741(99)00027-6).
- Madrigal-Santillán, E., García-Melo, F., Morales-González, J. A., Vázquez-Alvarado, P., Muñoz-Juárez, S., Zúñiga-Pérez, C., et al. (2013). Antioxidant and anticlastogenic capacity of prickly pear juice. *Nutrients*, 5, 4145–4158. [http://doi.org/10.3390/nut5104145](https://doi.org/10.3390/nut5104145).
- Mata, A., Ferreira, J. P., Smedeo, C., Serra, T., Duarte, C. M. M., & Bronze, M. R. (2016). Contribution to the characterization of *Opuntia* spp. juices by LC-DAD-ESI-MS/MS. *Food Chemistry*, 210, 558–565. [http://doi.org/10.1016/j.foodchem.2016.04.033](https://doi.org/10.1016/j.foodchem.2016.04.033).
- McLafferty, F. W., & Stauffer, D. B. (1989). *Wiley/NBS registry of mass spectral data*. NY, USA: Wiley.
- Melgar, B., Diaz, M. I., Ciric, A., Sokovic, M., Garcia-Castello, E. M., Rodriguez-Lopez, A. D., et al. (2017). By-product recovery of *Opuntia* spp. peels: Betalainic and phenolic profiles and bioactive properties. *Industrial Crops and Products*, 107, 353–359. [http://doi.org/10.1016/j.indcrop.2017.06.011](https://doi.org/10.1016/j.indcrop.2017.06.011).
- Mladenović, M., Matić, S., Stanić, S., Solujić, S., Mihailović, V., Stanković, N., et al. (2013). Combining molecular docking and 3-D pharmacophore generation to enclose the *in vivo* antitumor activity of naturally occurring aromatic compounds: Myricetin, quercetin, rutin, and rosmarinic acid. *Biochemical Pharmacology*, 86, 1376–1396.
- Montes-Lora, S., Hurtado, N., Mosquera, N., Heredia, F. J., & Cejudo-Bastante, M. J. (2016). Effect of technological practices on individual betalains and antioxidant activity of Colombian betalains-rich raw materials. *International Journal of Food Science and Technology*, 51, 1041–1047. [http://doi.org/10.1111/ijfs.13056](https://doi.org/10.1111/ijfs.13056).
- Moussa-Ayoub, T. E., Jaeger, H., Yousef, K., Knorr, D., El-Samahy, S., Kroh, L. W., et al. (2016). Technological characteristics and selected bioactive compounds of *Opuntia dillenii* cactus fruit juice following the impact of pulsed electric field pre-treatment. *Food Chemistry*, 210, 249–261. [http://doi.org/10.1016/j.foodchem.2016.04.115](https://doi.org/10.1016/j.foodchem.2016.04.115).
- Pavithra, K., Samanthi, M. S., Manojmani, H. K., & Shashirekha, M. N. (2013). Pectin and isolated betalains from *Opuntia dillenii* (Ker-Gawl) Haw. fruit exerts antiproliferative activity by DNA damage induced apoptosis. *International Journal of Pharmacognosy and Phytochemical Research*, 7, 1101–1110.
- Perez Mendez, L., Flores, F. T., Martín, J. D., Rodríguez Rodríguez, E. M., & Diaz Romero, C. (2015). Phytochemical characterization of cactus pads from *Opuntia dillenii* and *Opuntia ficus indica*. *Food Chemistry*, 188, 392–398. [http://doi.org/10.1016/j.foodchem.2015.05.011](https://doi.org/10.1016/j.foodchem.2015.05.011).
- Poorna, C. A., Remi, M. S., & Soniya, E. V. (2013). *In vitro* antioxidant analysis and the DNA damage protective activity of leaf extract of the *Excoecaria agallocha* Linn mangrove plant. In M. Stoytcheva, & R. Zlatev (Eds.), *Agricultural chemistry* (pp. 155–166). London, UK: IntechOpen. [http://doi.org/10.5772/55416](https://doi.org/10.5772/55416).
- Prieto, P., Pineda, M., & Aguilar, M. (1999). Spectrophotometric quantitation of antioxidant capacity through the formation of a phosphomolybdenum complex: Specific application to the determination of vitamin E. *Analytical Biochemistry*, 269, 337–341. [http://doi.org/10.1006/abio.1999.4019](https://doi.org/10.1006/abio.1999.4019).
- Rago, S., Pave, O., Inquii, I., Mavret-Heneman, A., Kolodner, R. D., & Huang, M.-E. (2007). Oxygen metabolism and reactive oxygen species cause chromosomal rearrangements and cell death. *Proceedings of the National Academy of Sciences of the United States of America*, 104, 9747–9752. [http://doi.org/10.1073/pnas.0703192104](https://doi.org/10.1073/pnas.0703192104).
- Ratnavaveera, P. B., de Silva, E. D., Williams, D. F., & Andersen, R. J. (2015). Antimicrobial activities of endophytic fungi obtained from the arid zone invasive plant *Opuntia dillenii* and the isolation of equisetin, from endophytic *Fusarium* sp. *BMC Complementary and Alternative Medicine*, 15, 220. [http://doi.org/10.1186/s12906-015-0722-4](https://doi.org/10.1186/s12906-015-0722-4).
- Re, R., Pellegrini, N., Proteggente, A., Pannala, A., Yang, M., & Rice-Evans, C. (1999). Antioxidant activity applying an improved ABTS radical cation decolorization assay. *Free Radical Biology and Medicine*, 26, 1231–1237. [http://doi.org/10.1016/S0891-5849\(98\)00315-3](https://doi.org/10.1016/S0891-5849(98)00315-3).
- Saleem, R., Ahmad, M., Azmat, A., Ahmad, S. I., Faizi, Z., Abidi, L., et al. (2005). Hypotensive activity, toxicology and histopathology of opuntioside-I and methanolic extract of *Opuntia dillenii*. *Biological & Pharmaceutical Bulletin*, 28, 1844–1851. [http://doi.org/10.1248/bpb.28.1844](https://doi.org/10.1248/bpb.28.1844).
- Sarker, S. D., Nahar, L., & Kumarasamy, Y. (2007). Microtitre plate-based antibacterial assay incorporating resazurin as an indicator of cell growth, and its application in the *in vitro* antibacterial screening of phytochemicals. *Methods*, 42, 321–324. [http://doi.org/10.1016/j.jmth.2007.01.006](https://doi.org/10.1016/j.jmth.2007.01.006).
- Sharma, C., Rani, S., Kumar, B., Kumar, A., & Raj, V. (2015). Plant *Opuntia dillenii*: A review on its traditional uses, phytochemical and pharmacological properties. *BC Pharmaceutical Science*, 1(1), 29–43.
- Siddiqui, F., Naqvi, S., Abidi, L., Faizi, S., Lubna, Avesi, L., et al. (2016). *Opuntia dillenii* cladode: Opuntiol and opuntioside attenuated cytokines and eicosanoids mediated inflammation. *Journal of Ethnopharmacology*, 182, 221–234. [http://doi.org/10.1016/j.jep.2016.02.016](https://doi.org/10.1016/j.jep.2016.02.016).
- Singleton, V. L., Orthofer, R., & Lamuela-Raventós, R. M. (1999). Analysis of total phenols and other oxidation substrates and antioxidants by means of Folin-Ciocalteu reagent. *Methods in Enzymology*, 299, 152–178. [http://doi.org/10.1016/S0076-6879\(99\)99017-1](https://doi.org/10.1016/S0076-6879(99)99017-1).
- Stintzing, F. C., Schieber, A., & Carle, R. (2001). Phytochemical and nutritional significance of cactus pear. *European Food Research and Technology*, 212, 396–407. [http://doi.org/10.1007/s002170000219](https://doi.org/10.1007/s002170000219).
- Valko, M., Izakovic, M., Mazur, M., Rhodes, C. J., & Telsler, J. (2004). Role of oxygen radicals in DNA damage and cancer incidence. *Molecular and Cellular Biochemistry*, 266, 37–56. [http://doi.org/10.1023/B:MCBL.0000049134.69131.89](https://doi.org/10.1023/B:MCBL.0000049134.69131.89).
- Zahi, M. R., Liang, H., & Yuan, Q. (2015). Improving the antimicrobial activity of D-limonene using a novel organogel-based nanoemulsion. *Food Control*, 50, 554–559. [http://doi.org/10.1016/j.foodcont.2014.10.001](https://doi.org/10.1016/j.foodcont.2014.10.001).
- Zhao, L. Y., Lan, Q. J., Huang, Z. C., Ouyang, L. J., & Zeng, F. H. (2011). Antidiabetic effect of a newly identified component of *Opuntia dillenii* polysaccharides. *Phytomedicine*, 18, 661–668. [http://doi.org/10.1016/j.phymed.2011.01.001](https://doi.org/10.1016/j.phymed.2011.01.001).
- Zorqui, L., Ayed-Boussema, I., Ayed, Y., Bacha, H., & Hassen, W. (2009). The anti-genotoxic activities of cactus (*Opuntia ficus-indica*) cladodes against the mycotoxin zearalenone in Balb/c mice: Prevention of micronuclei, chromosome aberrations and DNA fragmentation. *Food and Chemical Toxicology*, 47, 662–667. [http://doi.org/10.1016/j.fct.2008.12.031](https://doi.org/10.1016/j.fct.2008.12.031).



Cite this: DOI: 10.1039/c9dt01614g

A highly efficient and selective antitumor agent based on a glucoconjugated carbene platinum(II) complex†

Alfonso Annunziata,^{a,b} Maria Elena Cucciolito,^{b,a,b} Roberto Esposito,^{b,a,b} Paola Imbimbo,^b Ganna Petruk,^b Giarita Ferraro,^b Valerio Pinto,^a Angela Tuzi,^b Daria Maria Monti,^b Antonello Merlino^b and Francesco Ruffo^b*

Received 16th April 2019.
Accepted 25th April 2019

DOI: 10.1039/c9dt01614g

rsc.li/dalton

New five-coordinate Pt(II) complexes containing a glycosylated carbene fragment were synthesized. A member of this class shows very high *in vitro* cytotoxicity and an exceptional selectivity toward malignant cells. The complex lacking the sugary portion fails in the recognition of cancer cells. The results support the use of glycosylation in the design of carbene Pt-based anticancer agents.

Introduction

It is well known that anticancer agents, such as cisplatin¹ and its derivatives, often exhibit common undesired effects and low selectivity towards tumoral cells.² Consequently, the design of drugs with enhanced performance and low collateral effects is urgent to open frontiers in the treatment of devastating diseases.³

New approaches have been proposed to overcome these problems, involving carrier systems, conjugation to bioactive molecules,^{4,5} or the use of saturated Pt(IV) complexes as 'pro-drugs' to improve stability in biological media.^{6,7}

It is also known that the hypoxic environment in tumoral cells causes a variation in their metabolic pathways, and, among these, glucose metabolism is deeply altered.⁸ Cancer cells respond to this reprogramming by increasing carbohydrate uptake and as a consequence, cells overexpress a family of glycosyl receptors, identified as GLUTs.⁹ This condition, known as the "Warburg effect", has inspired the design of glycoconjugate platinum complexes which exploit GLUT receptors as biological targets^{10–19} and may preferentially accumulate in cancer cells.²⁰

In recent years, N-heterocyclic carbene (NHC) ligands also captured the curiosity of the scientific community. The pro-

erties of these robust neutral ligands are generously tunable by appropriate modifications of the heterocyclic scaffold, generally derived from imidazole and 1,2,4-triazole type-structures.^{21,22} NHC ligands have been successfully explored in organometallic synthesis and catalysis,²³ and their unique features also encouraged their introduction in the structure of metal-based anticancer agents.^{24–29} This choice proved to be convincing, as many compounds have attracted attention and their study will certainly be deepened for applications in clinical trials.

Recently, our laboratory reported the synthesis of five-coordinate Pt(II) agents (A in Fig. 1) which combined the above-mentioned key structural aspects, such as the steady coordinative saturation, the biologically active oxidation state II, and the presence of a sugar based ligand.^{30,31} The complexes revealed to be active and fairly selective towards a number of cell lines. Herein, this scaffold has been used to obtain new Pt complexes bearing NHC carbene ligands incorporating a glucosyl (Glu) or a galactosyl (Gal) moiety (**1Pt-R** in Fig. 1).[‡] Remarkably, the complexes exhibit high cytotoxic activity, with **1Pt-Glu** which is 100-fold more active and 180-fold more selective than cisplatin considering the immortalized keratinocytes and human adenocarcinoma cells (HaCaT/A431). Notably, the structural analogue **1Pt-Et** (Scheme 1), lacking the sugary portion, fails in cellular recognition: this result is the clear-cut validation of the glycosylation strategy in the rational design of carbene-Pt-based anticancer agents.

^aDipartimento di Scienze Chimiche, Università di Napoli Federico II, Complesso Universitario di Monte S. Angelo, via Cintia 21, I-80126 Napoli, Italy.
E-mail: mdmonti@unina.it, antonello.merlino@unina.it, ruffo@unina.it

^bConsorzio Interuniversitario di Reattività Chimica e Catalisi, via Celso Ulpiani 27, I-70126 Bari, Italy

† Electronic supplementary information (ESI) available. CCDC 1904738. For ESI and crystallographic data in CIF or other electronic format see DOI: 10.1039/c9dt01614g

‡ A glucose substituted carbene ligand in a platinum agent has been reported, though its cytotoxic activity was not evaluated.²²

Paper

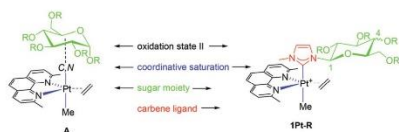
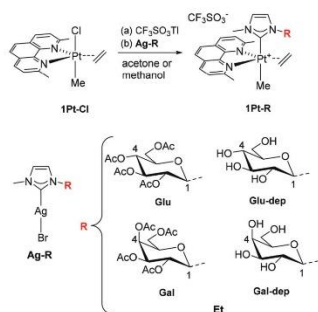


Fig. 1 Structure of the five-coordinate platinum(II) complexes.



Scheme 1 Synthesis and labelling of the here synthesized Pt complexes (Glu = glucose, Gal = galactose, dep = deprotected).

Results and discussion

The family of complexes **1Pt-R** was obtained through transmetalation between a cationic solvato species obtained from precursor **1Pt-Cl** and the appropriate silver carbene **Ag-R** derivative in acetone or in methanol (Scheme 1). In the latter case, the reaction led directly to the corresponding sugar deprotected complexes, probably through a silver-catalysed transesterification. The complexes were crystallised as white powders, and their structures were confirmed through LC/MS-QTOF analysis and NMR spectroscopy (Fig. S1–S5 in the ESI†). The carbene atom resonates at *ca.* 170 ppm in the carbon spectrum, with ^{195}Pt satellites. As expected, the signals of the coordinated ethylene were found at low frequencies, due to the high π -backdonation contribution in the metal–olefin bond.^{33,34}

The structure of **1Pt-R**, with R = **Glu**, was solved by X-ray crystallography (Fig. 2 and Fig. S6†). Details of the structural analysis and an additional figure describing crystal packing are reported in the ESI (Fig. S7 and Table S1).†

The X-ray diffraction study confirmed the identity of the compound as a cationic NHC carbene complex with CF_3SO_3^- as a counteranion. The compound crystallizes in the $P2_12_12_1$ space group with one cation and one anion in the independent unit. Both bond lengths and bond angles agree with the expectations. The Pt atom adopts a fairly regular trigonal bipyrami-

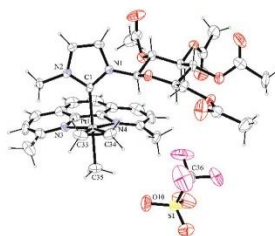


Fig. 2 ORTEP view of **1Pt-Glu** with thermal ellipsoids drawn at the 30% probability level. Selected bond lengths (Å) and angles (°): Pt1–C1 = 2.101(7), Pt1–N3 = 2.213(8), Pt1–N4 = 2.232(8), Pt1–C33 = 2.079(10), Pt1–C34 = 2.073(10), Pt–C35 = 2.070(9), C33–C34 = 1.444(16), Pt...O10 = 4.94(1), C1–Pt1–C35 = 177.1(4).

dal geometry with 2,9-dimethyl-1,10-phenanthroline (dmphen) and olefin ligands in the equatorial plane. The axial positions are occupied by the central carbon atom of the NHC ligand and by one methyl group. The encumbered pendant glucosyl group at N1 is in the usual chair conformation with all substituents in the equatorial positions. It assumes a flat shape and places far away from dmphen to allow favorable intermolecular interactions. A bowl-like distortion of dmphen is observed, due to steric interactions with the NHC ligand (dihedral angle between the mean planes of outer rings is $16.1(3)^\circ$) (Fig. S8†). The triflate anion places near Pt(II) in between the axial methyl group and the equatorial ethene ligand with the shortest distance Pt...O–S of 4.94(1) Å. The crystal packing is also stabilized by normal van der Waals and C–H...O weak interactions.³⁵

The stability of the compounds was evaluated collecting UV-Vis absorption spectra in DMSO and mixed DMSO/aqueous buffer solvents as a function of time. The spectra of **1Pt-R** with R = **Glu**, **Glu-dep** or **Et** are reported in Fig. S9–S11.† Data indicate that the compounds rapidly exchange a ligand with a solvent molecule in 100% DMSO, but they are very stable in mixed solvents, with a stability even higher than 7 days in 0.5% DMSO and 99.5% PBS at pH 7.4. ^1H NMR studies in DMSO- d_6 disclose that both 2,9-dimethyl-1,10-phenanthroline and ethene are displaced by the solvent, affording a square-planar species (Fig. S12†).

The selective cytotoxicity of **1Pt-Glu** and its derivatives was assessed by testing the drugs on two cancer cell lines, murine BALB/c-3T3 transformed with SV40 virus (SVT2) and human adenocarcinoma cells (A431), and two immortalized cell lines, murine fibroblasts (BALB/c-3T3) and human keratinocytes (HaCaT). Cells were incubated for 48 h with increasing concentrations of the Pt compounds, and then cell survival was evaluated by the MTT assay.³⁶ The IC_{50} values are reported in Table 1. Interestingly, **1Pt-Glu** is 100-times more cytotoxic than cisplatin toward A431. Furthermore, it is more toxic on A431 cancer cells than on HaCaT immortalized cells, with a selecti-

Table 1 IC₅₀ values (μM) obtained for Pt-compounds on HaCaT, A431, BALB/c-3T3 and SVT2 cells after 48 h incubation

Cell line	Cisplatin	1Pt-Glu	1Pt-Glu-dep	1Pt-Gal	1Pt-Gal-dep	1Pt-Et
HaCaT	6.6 ± 0.3	1.3 ± 1.7	66 ± 3	16 ± 3	92 ± 8	3.2 ± 0.7
A431	39 ± 12	0.40 ± 0.01	94 ± 8	94 ± 4	76 ± 16	15 ± 2
BALB/c-3T3	240 ± 47	6.3 ± 0.4	62 ± 4	37 ± 8	61.0 ± 0.9	5 ± 1.6
SVT2	195 ± 7	0.65 ± 0.07	4.8 ± 0.8	15 ± 2	52 ± 2	3 ± 1.3

viety index (SI = 32) which is more than 180-fold higher than that of cisplatin (SI = 0.17). It is noteworthy that the presence of the sugar moiety makes the drug more selective, as **1Pt-Et** is not able to discriminate between the normal and cancer cell lines and its toxicity is similar on all the analyzed cell lines. **1Pt-Glu** is also more toxic than **1Pt-Glu-dep**. It is not easy to establish the specific reason for the different behavior of these two molecules, since many factors contribute to the performance of these anticancer agents. A role could be played by the different polarity of the two molecules, which certainly affects their interaction with biological macromolecules (like proteins, that could be involved in the drug internalization and transport, or DNA, which is probably the final target of these potential drugs, see below).

We then studied the mechanism of action induced by **1Pt-Glu** on A431 cells, which are the most sensitive cells to the newly synthesized drug.

To this purpose, we measured intracellular ROS levels, as indicators of the redox state of the cells (Fig. 3A). When A431 cells were incubated with **1Pt-Glu**, 0.4 μM, for different times

(from 5 min to 48 h) we found a significant increase in the ROS levels after 6 h of incubation. The activation of the oxidative pathway was confirmed by western blot analysis (Fig. 3B). After 16 h incubation, a significant increase in the phosphorylation level of p38 was observed. Generally, the alteration in the redox state of the cell is translated in the depolarization of mitochondrial membrane ($\Delta\psi_m$), with consequent induction of apoptosis. As shown in Fig. 3C, a strong and significant depolarization level was observed in cells incubated with **1Pt-Glu** for 48 h. The activation of apoptosis was finally confirmed by the decrease in the levels of the survival factor Bcl-2 and of the inactivated forms of caspase-3, -7 and -9 (Fig. 3D and E).

We excluded that the increase in ROS could be associated with the capability of the Pt complexes to act as a photosensitizer, since preliminary results indicate that they are not able to produce singlet oxygen in cell-free experiments (data not shown).

To investigate the potential target of **1Pt-R**, with R = **Glu** or **Glu-dep**, DNA binding studies were carried out. In particular,

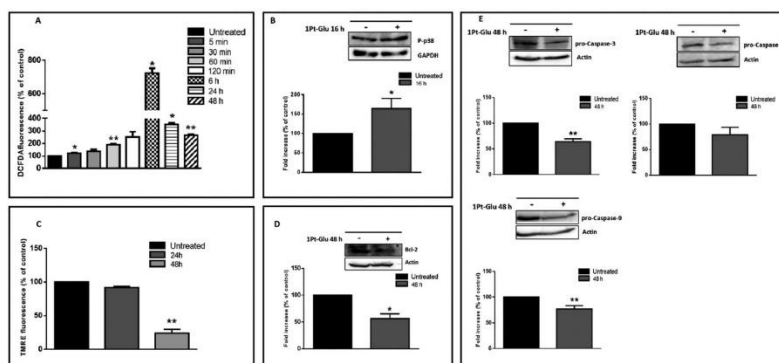


Fig. 3 **1Pt-Glu** mechanism of action on A431 cells. Cells were incubated with 0.4 μM of **1Pt-Glu** for different lengths of time. (A) Time-course experiment (5 min–48 h) to determine intracellular ROS levels. The fluorescence intensity of the probe is related to the intracellular ROS level and is reported as a percentage of untreated cells (%). (B) Analysis, by western blotting, of the phosphorylation level of p38 after 16 h of incubation with **1Pt-Glu**. Glyceraldehyde-3-phosphate dehydrogenase (GAPDH) was used as an internal standard. (C) Changes in the mitochondrial membrane potential ($\Delta\psi_m$) after 24 and 48 h incubation with **1Pt-Glu**. The fluorescence intensity of the probe, related to $\Delta\psi_m$, is reported as a percentage of the control (%). (D, E) Western blotting of cell extracts after 48 h incubation with **1Pt-Glu**. Western blotting experiments were performed using anti Bcl-2, pro-caspase-3, -7, -9; actin was used as the loading control. In B, D, E, the densitometric analysis is reported below each western blotting. Data shown are the means ± S.D. of three independent experiments and * indicates $p < 0.05$; ** indicates $p < 0.01$ with respect to untreated cells.

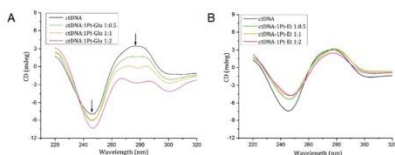


Fig. 4 CD spectra of ctDNA (200 μM in 0.01 M ammonium acetate buffer, pH 7.5) in the absence and in the presence of **1Pt-Glu** (A), and **1Pt-Et** (B) in 1:0.5 (green lines), 1:1 (orange lines) and 1:2 (purple lines) DNA to metal molar ratios. Spectra of ctDNA in the presence of **1Pt-Glu-dep** are reported in Fig. S12†

the binding of the two compounds toward calf-thymus DNA (ctDNA) was evaluated by fluorescence, through the ethidium bromide displacement assay, and circular dichroism spectroscopy. Interestingly, the CD spectra of **1Pt-Glu**, **1Pt-Glu-dep** and **1Pt-Et** suggest that the compounds could have a different effect on the structure of DNA, since the deprotected molecule and the sugar-free compound induce changes in the CD spectra of ctDNA that are significantly different from that obtained when the macromolecule is in the presence of **1Pt-Glu**.

The CD spectra of ctDNA consist of a positive band at 275 nm due to base stacking and a negative band at 245 nm due to helicity. These features are typical of DNA in the right-handed B form. When the DNA is incubated in the presence of **1Pt-Glu** the intensities of both positive and negative bands shift to lower ellipticity values, while when ctDNA is treated with **1Pt-Glu-dep** or **1Pt-Et** the intensity of negative bands increases (*i.e.* it shifts toward higher ellipticity values) and that of the positive band decreases without any changes in the wavelength (Fig. 4 and Fig. S13†). Notably, the interaction between the synthesized molecules and DNA is distinct when compared to cisplatin and the dmphen ligand, since both **1Pt-Glu** and **1Pt-Glu-dep** do not displace ethidium bromide from the ctDNA major groove (Fig. S14†). Similar results have been obtained in the case of **1Pt-Et**, thus indicating that the binding to DNA is not affected by the presence of the sugar, but rather by the NHC.

The different behaviour in DNA binding was further confirmed by the agarose gel mobility shift assay (Fig. S15†).

Altogether these data suggest that **1Pt-Glu** has a different mechanism of action when compared to canonical Pt-based drugs.

Experimental

Materials and general methods

All reagents and solvents were obtained from commercial sources and were used without any further purification. The ^1H and ^{13}C NMR spectra were recorded with a Bruker AVANCE 400. Referencing is relative to CD_2HOD (^1H) and $^{13}\text{CD}_3\text{OD}$ (^{13}C). **1Pt-Cl**³⁷ was described in the literature. **Ag-Gal** and **Ag-Et** were synthesized as described in the literature for **Ag-Glu**.³⁸

Ag-Gal: ^1H NMR (400 MHz, CDCl_3) δ 7.26 (d, 1H, H-4 Im), 7.01 (d, 1H, H-5 Im), 5.95 (d, $J_{\text{H11-H2}} = 9.0$ Hz, 1H, H-1), 5.53 (d, $J_{\text{H3-H4}} = 3.3$ Hz, 1H, H-4), 5.39 (t, $J_{\text{H2-H3}} = 9.0$ Hz, 1H, H-2), 5.28 (dd, 1H, H-3), 4.35 (t, 1H, $J_{\text{H5-H6}} = 6.5$ Hz, H-5), 4.15 (m, 2H, H-6 and H-6'), 3.86 (s, 3H, Me Im), 2.18 (s, 3H, OAc), 2.03 (s, 3H, OAc), 1.97 (s, 6H, OAc). **Ag-Et:** ^1H NMR (400 MHz, CDCl_3) δ 7.00 (d, 1H, H-4 Im), 6.97 (d, 1H, H-5 Im), 4.15 (q, 2H, $\text{CH}_2\text{Me Im}$), 3.83 (s, 3H, Me Im), 1.45 (t, 3H, $\text{CH}_2\text{Me Im}$).

Synthesis of 1Pt-Glu, 1Pt-Gal and 1Pt-Et

A solution of thallium triflate (0.170 g, 0.477 mmol) in acetone (2 mL) was added under stirring to a solution of the five-coordinate chloro-precursor **1Pt-Cl** (0.230 g, 0.477 mmol) in the same solvent (6 mL). After 10 minutes, thallium chloride was filtered off, and a solution of **Ag-R** (0.477 mmol) in acetone (2 mL) was added to the clear filtrate. The mixture was stirred at room temperature for 72 hours protected from light. The solid was filtered off and the solvent was removed under vacuum to obtain a yellow solid, which was recrystallized from dichloromethane/diethyl ether as a white powder (yield: 70–80%). **1Pt-Glu:** ^1H NMR (400 MHz, CD_3OD) δ 8.72 (d, 1H, H-4 or H-7 dmphen), 8.69 (d, 1H, H-7 or H-4 dmphen), 8.19 (d, 1H, H-3 or H-8 dmphen), 8.08 (br, 2H, H-5 and H-6 dmphen), 8.05 (d, 1H, H-8 or H-3 dmphen, partially hidden), 7.26 (d, 1H, H-4 Im), 6.93 (d, 1H, H-5 Im), 5.75 (d, $J_{\text{H11-H2}} = 9.6$ Hz, 1H, H-1), 5.44 (t, $J_{\text{H12-H3}} = 9.7$ Hz, 1H, H-2), 5.31 (t, $J_{\text{H13-H4}} = 9.6$ Hz, 1H, H-3), 5.20 (t, $J_{\text{H14-H5}} = 9.5$ Hz, 1H, H-4), 4.29–4.22 (m, 2H, H-5 and H-6), 4.17 (m, 1H, H-6'), 3.64 (s, 3H, Me Im), 3.53 (s, 3H, 2-Me or 9-Me dmphen), 3.47 (s, 3H, 9-Me or 2-Me dmphen), 2.79 (m, 1H, $J_{\text{Pt}} = 70.7$ Hz, ethene), 2.61–2.38 (m, 3H, ethene), 2.16 (s, 3H, OAc), 2.10 (s, 3H, OAc), 2.03 (s, 3H, OAc), 1.16 (s, 3H, OAc), 0.27 (s, 3H, $J_{\text{Pt}} = 50.6$ Hz, Pt-Me). ^{13}C NMR (100 MHz, CD_3OD) δ 174.8 ($J_{\text{Pt}} = 703$ Hz), 170.5, 169.8, 169.4, 168.2, 161.5, 159.5, 145.9, 139.3, 139.1, 138.7, 129.0, 127.2, 126.9, 126.4, 126.3, 125.0, 124.9, 120.8 (q, $J_{\text{C-F}} = 328$ Hz), 117.5, 84.4, 74.6, 71.9, 68.2, 68.1, 62.1, 37.8, 30.7 ($J_{\text{Pt}} = 352$ Hz), 29.6, 28.9, 28.8 ($J_{\text{Pt}} = 340$ Hz), 20.7, 20.6, 20.4, 19.9, –6.2 ($J_{\text{Pt}} = 467$ Hz). **1Pt-Gal:** ^1H NMR (400 MHz, CD_3OD) δ 8.71 (d, 1H, H-4 or H-7 dmphen), 8.69 (d, 1H, H-7 or H-4 dmphen), 8.13 (d, 1H, H-3 or H-8 dmphen), 8.09 (d, 1H, H-8 or H-3 dmphen, partially hidden), 8.07 (br, 2H, H-5 and H-6 dmphen), 7.13 (d, 1H, H-4 Im), 6.94 (d, 1H, H-5 Im), 5.72 (d, $J_{\text{H11-H2}} = 9.4$ Hz, 1H, H-1), 5.62 (d, $J_{\text{H13-H4}} = 2.9$ Hz, 1H, H-4), 5.44 (t, $J_{\text{H12-H3}} = 10.1$ Hz, 1H, H-2), 5.24 (dd, 1H, H-3), 4.44 (t, $J_{\text{H5-H6}} = 6.5$ Hz, 1H, H-5), 4.09 (m, 2H, H-6 and H-6'), 3.62 (s, 3H, Me Im), 3.54 (s, 3H, 2-Me or 9-Me dmphen), 3.49 (s, 3H, 9-Me or 2-Me dmphen), 2.80 (m, 1H, $J_{\text{Pt}} = 75.6$ Hz, ethene), 2.60 (m, 1H, $J_{\text{Pt}} = 79.8$ Hz, ethene), 2.56–2.43 (m, 2H, ethene), 2.19 (s, 3H, OAc), 2.13 (s, 3H, OAc), 2.00 (s, 3H, OAc), 1.25 (s, 3H, OAc), 0.25 (s, 3H, $J_{\text{Pt}} = 49.8$ Hz, Pt-Me). ^{13}C NMR (100 MHz, CD_3OD) δ 174.4 ($J_{\text{Pt}} = 691$ Hz), 170.6, 170.3, 169.7, 168.4, 161.6, 160.7, 145.7, 139.1, 138.9, 138.5, 129.1, 128.9, 126.7, 126.4, 126.2, 126.1, 124.2, 120.4 (q, $J_{\text{C-F}} = 329$ Hz), 118.1, 84.7, 73.4, 70.5, 67.4, 66.6, 61.2, 36.9, 29.7 ($J_{\text{Pt}} = 352$ Hz), 28.8 ($J_{\text{Pt}} = 348$ Hz), 28.3, 27.8, 19.3, 19.0 ($\times 2$), 18.7, –7.3 ($J_{\text{Pt}} = 463$ Hz). **1Pt-Et:** ^1H NMR (400 MHz, acetone- d_6) δ 8.75 (d, 2H,

H-4 and H-7 dmphen, 1H), 8.14 (d, 2H, H-3 and H-8 dmphen, partially hidden), 8.12 (s, 2H, H-5 and H-6 dmphen), 6.99 (d, 1H, H-4 Im), 6.92 (d, 1H, H-5 Im), 4.08 (q, 2H, CH₂Me Im), 3.53 (s, 3H, Me Im), 3.36 (s, 6H, 2-Me and 9-Me dmphen), 2.47 (s, $J_{\text{Pt}} = 76.8$ Hz, 4H, ethene), 0.71 (t, 3H, CH₂Me Im), 0.17 (s, $J_{\text{Pt}} = 49.2$ Hz, 3H, Pt-Me). ¹³C NMR (100 MHz, acetone-d₆) δ 169.5 ($J_{\text{Pt}} = 710$ Hz), 161.7 ($J_{\text{Pt}} = 32$ Hz), 145.7, 138.7, 128.7, 126.4, 124.6 (q, $J_{\text{C-F}} = 321$ Hz), 123.7, 119.8, 44.2, 36.6, 28.8 ($J_{\text{Pt}} = 360$ Hz), 27.9 ($J_{\text{Pt}} = 23$ Hz), 15.1, -7.4 ($J_{\text{Pt}} = 469$ Hz).

Synthesis of 1Pt-Glu-dep and 1Pt-Gal-dep

The complexes were obtained according to the procedure described above, but using methanol as the solvent. The compounds were re-crystallized from methanol/diethyl ether (yield: 70–80%). **1Pt-Glu-dep**: ¹H NMR (400 MHz, CD₃OD) δ 8.59 (d, 1H, H-4 or H-7 dmphen), 8.53 (d, 1H, H-7 or H-4 dmphen), 7.97 (d, 1H, H-3 or H-8 dmphen), 7.96 (s, 2H, H-5 and H-6 dmphen), 7.95 (d, 1H, H-8 or H-3 dmphen), 7.04 (d, 1H, H-4 Im), 6.83 (d, 1H, H-5 Im), 5.35 (d, $J_{\text{H1-H12}} = 9.0$ Hz, 1H, H-1), 3.64 (m, 2H), 3.48 (s, 3H, Me Im), 3.46 (s, 3H, 2-Me or 9-Me dmphen), 3.45–3.26 (m, 4H), 3.41 (s, 3H, 9-Me or 2-Me dmphen), 2.79 (m, 1H, $J_{\text{Pt}} = 79.2$ Hz, ethene), 2.68 (m, 1H, $J_{\text{Pt}} = 77.2$ Hz, ethene), 2.40 (m, 2H, $J_{\text{Pt}} = 76.5$ Hz, ethene), 0.15 (s, 3H, $J_{\text{Pt}} = 49.2$ Hz, Pt-Me). ¹³C NMR (100 MHz, CD₃OD) δ 173.3 ($J_{\text{Pt}} = 704$ Hz), 161.0, 160.8, 145.9, 145.7, 138.6, 128.9, 128.6, 126.4, 126.3, 125.8 ($\times 2$), 123.3, 120.6 (q, $J_{\text{C-F}} = 319$ Hz), 117.9, 87.2, 78.8, 76.6, 72.5, 69.1, 59.9, 36.6, 29.8 ($J_{\text{Pt}} = 350$ Hz), 28.9 ($J_{\text{Pt}} = 352$ Hz), 28.0, 27.7, -7.7 ($J_{\text{Pt}} = 464$ Hz). **1Pt-Gal-dep**: ¹H NMR (400 MHz, CD₃OD) δ 8.64 (d, 1H, H-4 or H-7 dmphen), 8.57 (d, 1H, H-7 or H-4 dmphen), 8.02 (d, 1H, H-3 or H-8 dmphen), 8.00 (s, 2H, H-5 and H-6 dmphen), 7.98 (d, 1H, H-8 or H-3 dmphen, partially hidden), 7.05 (d, 1H, H-4 Im), 6.86 (d, 2H, H-5 Im), 5.33 (d, $J_{\text{H1-H12}} = 8.9$ Hz, 1H, H-1), 4.02 (m, 1H), 3.70–3.60 (m, 4H), 3.51 (s, 3H, Me Im), 3.50 (s, 3H, 2-Me or 9-Me dmphen), 3.47 (m, 1H), 3.44 (s, 3H, 9-Me or 2-Me dmphen), 2.85 (m, 1H, $J_{\text{Pt}} = 80.6$ Hz, ethene), 2.72 (m, 1H, ethene), 2.44 (m, 2H, $J_{\text{Pt}} = 75.8$ Hz, ethene), 0.19 (s, 3H, $J_{\text{Pt}} = 49.1$ Hz, Pt-Me). ¹³C NMR (100 MHz, CD₃OD) δ 172.6 ($J_{\text{Pt}} = 709$ Hz), 161.0, 160.9, 145.9, 145.7, 138.6, 138.5, 129.0, 128.6, 126.3, 126.2, 125.7 ($\times 2$), 123.3, 120.4 (q, $J_{\text{C-F}} = 316$ Hz), 118.1, 87.5, 77.4, 73.6, 69.4, 68.4, 60.4, 36.6, 29.9 ($J_{\text{Pt}} = 352$ Hz), 29.0 ($J_{\text{Pt}} = 352$ Hz), 27.9, 27.7, -7.6 ($J_{\text{Pt}} = 468$ Hz).

Cell culture and the MTT assay

The cytotoxicity of **1Pt-Glu** and its derivatives was tested on different cell lines, *i.e.* human keratinocyte cells (HaCaT, Innoprot), human epidermoid carcinoma (A431, ATCC), murine BALB/c-3T3 and SVT2 fibroblasts (ATCC). All cell lines were cultured in Dulbecco's modified Eagle's medium (DMEM) (Sigma-Aldrich, St Louis, MO, USA), supplemented with 10% foetal bovine serum (HyClone), 2 mM L-glutamine and antibiotics, all from Sigma-Aldrich, under a 5% CO₂ humidified atmosphere at 37 °C. For the dose-response experiments, cells were seeded in 96-well plates at a density of 2.5×10^3 cells per well. 24 h after seeding, increasing concentrations of compounds were added to the cells (0.1–200 μM). Cell viabi-

lity was assessed by the MTT (3-(4,5-dimethylthiazol-2-yl)-2,5-diphenyltetrazolium bromide) assay after 48 h, as described by Ferraro *et al.*³⁶ Cell survival was expressed as the percentage of viable cells in the presence of the compound under test compared to the controls. Two groups of cells were used as the controls, *i.e.* untreated cells and cells supplemented with identical volumes of DMSO. Each sample was tested in three independent analyses, each carried out in triplicate.

Spectrophotometric measurements

The ethidium bromide (EtBr) displacement assay has been used to evaluate the DNA intercalation ability of the studied Pt compounds, following the variation of the fluorescence emission of EtBr upon excitation at 540 nm as a function of Pt concentration. This assay was performed using a HORIBA Fluoromax 4 spectrofluorometer equipped with a thermostat bath. Calf thymus DNA was incubated with EtBr in 0.05 M ammonium acetate at pH 7.5 at a DNA:EtBr molar ratio of 1:50 for 30 min in the dark at room temperature. Then, the fluorescence quenching of this complex was evaluated by adding to it increasing amounts of Pt compounds dissolved in DMSO (15×10^{-3} M, Fig. S14A and B[†]). Samples were equilibrated for 5 min before collecting each spectrum. Other experimental settings: 1.0 cm quartz cell, excitation/emission slit 5.0 nm, 560–750 nm range, 50 nm min⁻¹ scanning speed. Data have been obtained as the average of three independent measurements. Emission spectra of ethidium bromide bound to DNA in the presence of **1Pt-Et**, dmphen ligand and cisplatin are also reported as an internal control (Fig. S14C–E[†]).

The far-UV CD spectra of ctDNA in the presence of different amounts of **1Pt-Glu** (Fig. 4A), **1Pt-Et** (Fig. 4A and B) and **1Pt-Glu-dep** (Fig. S13[†]) have been collected in the 220–320 nm wavelength range. 200 μM DNA in pH 7.5 0.01 M ammonium acetate buffer was incubated for 24 h in different molar ratios with platinum (1:05, 1:1, 1:2 DNA to Pt). Then, the spectra were recorded using a Jasco J-810 spectropolarimeter equipped with a Peltier block arrangement and a quartz cuvette of a path length of 0.1 cm (25 °C temperature setting). Each spectrum was obtained averaging three scans and subtracting contributions from the corresponding references. Other experimental settings were: scanning speed 50 nm min⁻¹, bandwidth 2.0 nm, resolution 1.0 nm, sensitivity 50 mdeg, response 4 s.

UV-Vis spectra have been collected using a Varian Cary 5000 UV-vis-NIR spectrophotometer and the following parameters: wavelength range 240–450 nm, data pitch 1 nm, scanning speed 600 nm min⁻¹, quartz cuvette with 1 cm path length.

Analysis of the mechanism of action

To determine ROS levels a fluorescent probe 2',7'-dichlorodihydrofluorescein diacetate (DCFDA, Sigma-Aldrich) was used. The experiment was performed as reported by Petruk *et al.*³⁹ Briefly, after treatment with 0.4 μM of **1Pt-Glu** for different times (from 5 min to 48 h), cells were incubated with a cell-permeable DCFDA probe, whose fluorescence, upon oxidation

by ROS, was measured using a PerkinElmer LS50 spectrofluorometer (525 nm emission wavelength, 488 nm excitation wavelength, 300 nm min⁻¹ scanning speed and 5 nm slit width for both excitation and emission). ROS production was expressed as a percentage of DCF fluorescence intensity of the sample under test, with respect to the untreated sample. Each value was assessed by three independent experiments, each with three determinations. Significance was determined by the Student's *t*-test. The mitochondrial membrane potential ($\Delta\psi_m$) was measured as described by Monti *et al.*⁴⁰ Cells were plated at a density of 2×10^4 cells per well and after 24 h, they were treated as described above. At the end of the treatment, the cells were incubated with 200 nM of the cationic lipophilic dye tetramethylrhodamine ethyl ester (TMRE) for 20 min at 37 °C. Then, the cells were gently washed with 0.2% BSA in PBS three times and the fluorescence was measured in a microplate reader with a peak of $\lambda(\text{ex})/\lambda(\text{em}) = 549/575$ nm. Each value is the mean of three independent experiments, each with three determinations. Significance was determined by the Student's *t*-test. For western blotting analyses, cells were treated with 0.4 μM of **1Pt-Glu** and then incubated at 37 °C. Then, western blotting, performed as reported by Galano *et al.*,⁴¹ was used to determine the intracellular levels of phospho-p38 (after 16 h of incubation), pro-caspase-3, -7, -9 and Bcl-2 (after 48 h of incubation). All antibodies were purchased from Cell Signal Technology (Danvers, MA, USA). To normalize the protein intensity levels, a specific antibody against the internal standards was used, *i.e.* anti-GAPDH (Thermo Fisher, Rockford, IL, USA) or anti-actin (Sigma-Aldrich). The chemiluminescence detection system (SuperSignal® West Pico) was purchased from Thermo Fischer.

X-ray crystallography

Single crystals of **1Pt-Glu** suitable for X-ray diffraction studies were obtained under slow diffusion of diethyl ether into a methanol solution at room temperature. Data were obtained at room temperature using a Bruker-Nonius KappaCCD four-circle diffractometer equipped with a graphite monochromator (radiation Mo K $\alpha = 0.71073$ Å). Reduction of data and semiempirical absorption correction were done using the SADABS program.⁴² Structures were solved by direct methods (SIR97 program⁴³) and refined by the full-matrix least-squares method on F^2 using the SHELXL-2018/3 program⁴⁴ with the aid of the program WinGX.⁴⁵ Anisotropic parameters were used for non-H atoms. Ethylene hydrogen atoms were located in difference Fourier maps and refined as a riding model with the isotropic thermal parameter $U_{\text{iso}}(\text{H})$ equal to $1.2U_{\text{eq}}$ of the carrier atom. All the other H atoms were generated stereochemically and refined accordingly to the riding model with C–H distances in the range 0.93–0.98 Å and $U_{\text{iso}}(\text{H})$ equal to $1.2U_{\text{eq}}$ of the carrier atom ($1.5U_{\text{eq}}$ for C_{methyl}). Details on the crystal and refinement data are reported in Table S1.† The figures were generated using ORTEP-3⁴⁶ and Mercury CSD 3.9⁴⁷ programs. Crystallographic data for **1Pt-Glu** were deposited in the Cambridge Crystallographic Data Centre with the deposition number CCDC 1904738.†

Conclusion

In conclusion, here a new class of Pt complexes bearing a glycosylated carbene as the ligand has been synthesized and characterized. The crystal structure, solution behaviour, cytotoxicity and interaction with DNA model systems of the most promising member of this class, **1Pt-Glu**, were investigated. This molecule is 100-fold more cytotoxic than cisplatin on A431 and highly selective for cancer cells. It induces cancer cell death *via* ROS-mediated apoptosis and binds DNA with a different mode of binding when compared to cisplatin and other Pt-based drugs. The structural analogue lacking the sugar is not selective. These findings support the use of glycosylation as a strategy to improve the anticancer properties of metal carbene-based drugs.

Conflicts of interest

There are no conflicts to declare.

Acknowledgements

FR thanks MIUR for financial support (PRIN2015-Prot. 20154X9ATP). The authors thank Andrea Esposito for the Graphical Abstract.

Notes and references

- B. Rosenberg, L. Vancamp, J. E. Trosko and V. H. Mansour, *Nature*, 1969, **222**, 385–386.
- R. Oun, Y. E. Moussa and N. J. Wheate, *Dalton Trans.*, 2018, **47**, 6645–6653.
- P. Zhang and P. J. Sadler, *J. Organomet. Chem.*, 2017, **839**, 5–14.
- T. C. Johnstone, K. Suntharalingam and S. J. Lippard, *Chem. Rev.*, 2016, **116**, 3436–3486.
- R. G. Kenny and C. J. Marmion, *Chem. Rev.*, 2019, **119**, 1058–1137.
- R. G. Kenny, S. W. Chuah, A. Crawford and C. J. Marmion, *Eur. J. Inorg. Chem.*, 2017, 1596–1612.
- Z. Wang, Z. Deng and G. Zhu, *Dalton Trans.*, 2019, **48**, 2536–2544.
- A. Pettenuzzo, R. Pigot and L. Ronconi, *Metallo drugs*, 2016, **1**, 36–61.
- L. Szablewski, *Biochim. Biophys. Acta*, 2013, **1835**, 164–169.
- Y. Chen, M. J. Heeg, P. G. Braunschweiger, W. Xie and P. G. Wang, *Angew. Chem., Int. Ed.*, 1999, **38**, 1768–1769.
- M. Gottschaldt and U. Schubert, *Chem. – Eur. J.*, 2009, **15**, 1548–1557.
- J. Möker, U. Salge-Bartels and J. Thiem, *J. Carbohydr. Chem.*, 2012, **31**, 702–710.
- S. Yano, H. Ohi, M. Ashizaki, M. Obata, Y. Mikata, R. Tanaka, T. Nishioka, I. Kinoshit, Y. Sugai, I. Okura,

- S. Ogura, J. A. Czaplewski, M. Gottschaldt, U. S. Schubert, T. Funabiki, K. Morimoto and M. Nakai, *Chem. Biodiversity*, 2012, **9**, 1903–1915.
- 14 E. C. Calvaresi and P. J. Hergenrother, *Chem. Sci.*, 2013, **4**, 2319–2333.
- 15 P. Liu, Y. Lu, X. Gao, R. Liu, D. Zhang-Negrerie, Y. Shi, Y. Wang, S. Wang and Q. Gao, *Chem. Commun.*, 2013, **49**, 2421–2423.
- 16 Q. Wang, Z. Huang, J. Ma, X. Lu, L. Zhang, X. Wang and P. G. Wang, *Dalton Trans.*, 2016, **45**, 10366–10374.
- 17 J. Ma, Q. Wang, X. Yang, W. Hao, Z. Huang, J. Zhang, X. Wang and P. G. Wang, *Dalton Trans.*, 2016, **45**, 11830–11838.
- 18 M. Wu, H. Li, R. Liu, X. Gao, M. Zhang, P. Liu, Z. Fu, J. Yang, D. Zhang-Negrerie and Q. Gao, *Eur. J. Med. Chem.*, 2016, **110**, 32–42.
- 19 R. Liu, H. Li, X. Gao, Q. Mi, H. Zhao and Q. Gao, *Biochem. Biophys. Res. Commun.*, 2017, **487**, 34–40.
- 20 M. Patra, T. C. Johnstone, K. Suntharalingam and S. J. Lippard, *Angew. Chem., Int. Ed.*, 2016, **55**, 2550–2554.
- 21 H. V. Huynh, *Chem. Rev.*, 2018, **118**, 9457–9492.
- 22 K. Singh, A. Gangrade, A. Jana, B. B. Mandal and N. Das, *ACS Omega*, 2019, **4**, 835–841.
- 23 F. E. Hahn, *Chem. Rev.*, 2018, **118**, 9455–9456.
- 24 R. W. Y. Sun, A. L. F. Chow, X. H. Li, J. J. Yan, S. S. Y. Chui and C. M. Che, *Chem. Sci.*, 2011, **2**, 728–736.
- 25 W. Zhao, V. Ferro and M. V. Baker, *Coord. Chem. Rev.*, 2017, **339**, 1–16.
- 26 M. Bouché, A. Bonnefont, T. Achard and S. Bellemin-Laponnaz, *Dalton Trans.*, 2018, **47**, 11491–11502.
- 27 T. Zou, C. N. Lok, P. K. Wan, Z. F. Zhang, S. K. Fung and C. M. Che, *Curr. Opin. Chem. Biol.*, 2018, **43**, 30–36.
- 28 M. E. Cucciolito, M. Trinchillo, R. Iannitti, R. Palumbo, D. Tesaro, A. Tuzi, F. Ruffo and A. D'Amora, *Eur. J. Inorg. Chem.*, 2017, 4855–4961.
- 29 T. Rehm, M. Rothmund, A. Bär, T. Dietel, R. Kempe, H. Kostrohnova, V. Brabec, J. Kasparkova and R. Schobert, *Dalton Trans.*, 2018, **47**, 17367–17381.
- 30 M. E. Cucciolito, A. D'Amora, G. De Feo, G. Ferraro, A. Giorgio, G. Petruk, D. M. Monti, A. Merlino and F. Ruffo, *Inorg. Chem.*, 2018, **57**, 3133–3143.
- 31 M. E. Cucciolito, F. De Luca Bossa, R. Esposito, G. Ferraro, A. Iadonisi, G. Petruk, L. D'Elia, C. Romanetti, S. Traboni, A. Tuzi, D. M. Monti, A. Merlino and F. Ruffo, *Inorg. Chem. Front.*, 2018, **5**, 2921–2933.
- 32 M. Skander, P. Retailleau, B. Bourrié, L. Schio, P. Maillet and A. Marinetti, *J. Med. Chem.*, 2010, **53**, 2146–2154.
- 33 L. Calvanese, M. E. Cucciolito, A. d'Amora, G. D'Auria, A. Esposito, R. Esposito, L. Falcigno and F. Ruffo, *Eur. J. Inorg. Chem.*, 2015, 4068–4075.
- 34 R. Esposito, L. Calvanese, M. E. Cucciolito, G. D'Auria, L. Falcigno, V. Fiorini, P. Pezzella, G. Roviello, S. Stagni, G. Talarico and F. Ruffo, *Organometallics*, 2017, **36**, 384–390.
- 35 B. Panunzi, F. Borbone, A. Capobianco, S. Concilio, R. Diana, A. Peluso, S. Piotto, A. Tuzi, A. Velardo and U. Caruso, *Inorg. Chem. Commun.*, 2017, **84**, 103–108.
- 36 G. Ferraro, D. M. Monti, A. Amoresano, N. Pontillo, G. Petruk, F. Pane, M. A. Cinellu and A. Merlino, *Chem. Commun.*, 2016, **52**, 9518–9521.
- 37 L. Kelland, *Nat. Rev. Cancer*, 2007, **7**, 573–584.
- 38 M. E. Cucciolito, V. De Felice, A. Panunzi and A. Vitagliano, *Organometallics*, 1989, **8**, 1180–1187.
- 39 G. Petruk, A. Raiola, R. Del Giudice, A. Barone, L. Frusciantè, M. M. Rigano and D. M. Monti, *J. Photochem. Photobiol., B*, 2016, **163**, 284–289.
- 40 D. M. Monti, G. Ferraro, G. Petruk, L. Maiore, F. Pane, A. Amoresano, M. A. Cinellu and A. Merlino, *Dalton Trans.*, 2017, **46**, 15354–15362.
- 41 E. Galano, A. Arciello, R. Piccoli, D. M. Monti and A. Amoresano, *Metallomics*, 2014, **6**, 587–597.
- 42 Bruker-Nonius, *SADABS*, Delft, The Netherlands, 2002.
- 43 A. Altomare, M. C. Burla, M. Camalli, G. L. Casciarano, C. Giacovazzo, A. Guagliardi, A. G. Moliterni, G. Polidori and R. Spagna, *J. Appl. Crystallogr.*, 1999, **32**, 115–119.
- 44 G. M. Sheldrick, *Acta Crystallogr., Sect. C: Struct. Chem.*, 2015, **71**, 3–8.
- 45 L. J. Farrugia, *J. Appl. Crystallogr.*, 2012, **45**, 849–854.
- 46 L. J. Farrugia, *J. Appl. Crystallogr.*, 1997, **30**, 565–565.
- 47 C. F. Macrae, I. J. Bruno, J. A. Chisholm, P. R. Edgington, P. McCabe, E. Pidcock, L. Rodriguez-Monge, R. Taylor, J. v. Streek and P. A. Wood, *J. Appl. Crystallogr.*, 2008, **41**, 466–470.

Article

Isolation of Myricitrin and 3,5-di-O-Methyl Gossypetin from *Syzygium samarangense* and Evaluation of their Involvement in Protecting Keratinocytes against Oxidative Stress via Activation of the Nrf-2 Pathway

Mansour Sobeh ^{1,2,†,*}, Ganna Petruk ^{3,†}, Samir Osman ⁴, Mohamed A. El Raey ⁵, Paola Imbimbo ³, Daria Maria Monti ^{3,*} and Michael Wink ^{1,*}

- ¹ Institute of Pharmacy and Molecular Biotechnology, Heidelberg University, 69120 Heidelberg, Germany
² AgroBioSciences Research Division, Mohammed VI Polytechnic University, Lot 660–Hay Moulay Rachid, Ben-Guerir 43150, Morocco
³ Department of Chemical Sciences, University of Naples Federico II, Complesso Universitario Monte Sant'Angelo, via Cinthia 4, 80126 Naples, Italy; ganna.petruk@unina.it (G.P.); Paola.Imbimbo@unina.it (P.I.)
⁴ Department of Pharmacognosy, Faculty of Pharmacy, October 6 University, Giza 12585, Egypt; samirothman1965@yahoo.co.uk
⁵ Department of Phytochemistry and Plant Systematics, National Research Center, Dokki, Cairo 12622, Egypt; elraiy@gmail.com
 * Correspondence: sobeh@uni-heidelberg.de (M.S.); mdmonti@unina.it (D.M.M.); wink@uni-heidelberg.de (M.W.); Tel.: +496221544880 (M.W.)
 † The authors contributed equally to this work.

Received: 23 April 2019; Accepted: 10 May 2019; Published: 13 May 2019



Abstract: The wax apple (*Syzygium samarangense*) is traditionally employed as an antibacterial and immunostimulant drug in traditional medicine. This plant is rich in different flavonoids and tannins. In this study, we isolated two compounds from *S. samarangense* leaves: myricitrin and 3,5-di-O-methyl gossypetin. Then, we investigated the mechanisms of action of the two compounds against oxidative stress (induced by sodium arsenite) and inflammation (induced by UV light) on human keratinocytes. We could clearly demonstrate that the pre-treatment of cells with both compounds was able to mitigate the negative effects induced by oxidative stress, as no alteration in reactive oxygen species (ROS) production, glutathione (GSH) level, or protein oxidation was observed. Additionally, both compounds were able to modulate mitogen-activated protein kinase (MAPK) signaling pathways to counteract oxidative stress activation. Finally, we showed that 3,5-di-O-methyl gossypetin exerted its antioxidant activity through the nuclear transcription factor-2 (Nrf-2) pathway, stimulating the expression of antioxidant proteins, such as HO-1 and Mn-SOD-3.

Keywords: *Syzygium samarangense*; antioxidants; myricitrin; 3,5-di-O-methyl gossypetin; eukaryotic cells; sodium arsenite

1. Introduction

In the last 30 years, several lines of evidence demonstrate that oxidants play a crucial role in the etiology of aging. Reactive oxygen species (ROS) are considered responsible for the insurgence of many pathologies, such as malignancies, diabetes, inflammation, hypertension, atherosclerosis, cardiovascular diseases, liver diseases, and several types of bacterial and viral infections [1,2]. ROS

can oxidize the nuclear base guanosine to 8-oxoguanosine, which could lead to point mutations and, as a consequence, to genetically mediated health conditions (as mentioned before).

The respiratory burst, cytochrome P450, lipid metabolism, and mitochondria represent the main sites for the generation of ROS [2,3]; however, numerous environmental stimuli, such as hyperthermia, chemotherapy, ultraviolet radiation, and intense exercise are considered as external sources of ROS [3,4].

To neutralize the deleterious effects of ROS, most organisms including humans are endowed with an innate antioxidant defense system. The latter includes endogenous enzymes, alpha lipoic acid, glutathione, vitamins A, C and E, and minerals such as Se, Mn, Cu and Zn that help to maintain redox homeostasis. When the intracellular redox equilibrium is disrupted, the oxidative stress pathway is activated and additional exogenous antioxidants, such as natural ones in food, may help to inactivate ROS. Indeed, it is now well established that natural antioxidants of dietary origin, for instance flavonoids and other polyphenols, ascorbic acid, and carotenoids, scavenge ROS and can effectively slow ageing or delay the progression of age-related diseases [3,4].

Originating from the Greater Sunda Islands, Malay Peninsula, and Andaman and Nicobar Islands, the wax apple, *Syzygium samarangense*, has gained a reputation as an antibacterial and immunostimulant medicinal plant. We recently identified 92 compounds from the leaf extract, mainly flavonoids and condensed tannins [5]. The extract exhibited robust antioxidant activity in vitro on immortalized human keratinocytes (HaCaT cells), and in rats, in which a substantial hepatoprotective activity against CCl₄-intoxication was observed [5]. Recent research described five new triterpenoids, sysamarins A-D and sysamarin E (oleanane triterpenoid), in the leaf extract from plants grown in China [6].

In this study, we isolated two flavonoids, namely myricitrin and 3,5-di-O-methyl gossypetin (7,8,3',4'-tetrahydroxy-3,5-dimethoxyflavone), from *Syzygium samarangense* leaves. Then, we evaluated the antioxidant activity in vitro and in HaCaT cells stressed with sodium arsenite. Moreover, we analyzed their antioxidant and anti-inflammatory properties at the molecular level, including in the mitogen-activated protein kinase (MAPK) and nuclear transcription factor-2 (Nrf-2) pathways.

2. Results and Discussion

2.1. Compound Isolation

2.1.1. Myricitrin (Myricetin-3-O- α -rhamnoside) (Compound 1)

The pure yellow amorphous material of compound 1 exhibited chromatographic characteristics (a dark purple spot on paper chromatography (PC) under UV light, turning to reddish orange when fumed with ammonia vapor or sprayed with Naturstoff specific for flavonoids) and UV absorption maxima in MeOH at 252 and 360 nm, which were identical to those reported for flavonol-3-O-glycosides [7]. Compound 1 exhibited [M - H]⁻ at *m/z* = 463 (ESI), and a main daughter ion at *m/z* 317 which corresponded for myricetin aglycone, suggesting the structure to be myricetin rhamnoside.

¹H-NMR spectroscopic analysis was carried out to confirm the structure. The spectrum (MeOD-d₄) revealed, in the aromatic region, the characteristic pattern of myricetin proton resonances [8], and also revealed an anomeric proton resonance at δ ppm 5.23 (*J* = 1.5 Hz), assignable to the α -L-rhamnoside proton H-1''. Final confirmation of compound 1 was achieved through ¹³C-NMR spectroscopic analysis in (MeOD-d₄) and the data were consistent with those published before [9]. Therefore, the structure was assigned to myricitrin (myricetin-3-O- α -rhamnopyranoside, Figure 1) (¹H- and ¹³C-NMR data, Table 1).

Table 1. ^1H - (500 MHz) and ^{13}C -NMR (125 MHz) data in (MeOD- d_4) for myricetin-3- O - α -rhamnoside (compound 1) and 7,8,3',4'-tetrahydroxy-3,5-dimethoxyflavone (compound 2).

Position	Compound 1		Compound 2	
	δ_{H}	δ_{C}	δ_{H}	δ_{C}
2		159.56		155.61
3		136.44		141.29
4		179.80		176.64
5		163.36		154.64
6	6.20 (d, $J = 2.1$ Hz)	100.02	6.45 (s)	97.24
7		166.27		152.93
8	6.36 (d, $J = 2.1$ Hz)	94.88		127.47
8a		158.68		146.94
4a		105.95		108.79
3-OCH ₃			3.76 (s)	60.36
5-OCH ₃			3.83 (s)	56.56
1'		122.07		123.42
2'	6.95 (s)	109.70	7.70 (d, $J = 2.0$ Hz)	116.76
3'		147.01		146.39
4'		138.05		149.58
5'		147.01	6.89 (d, $J = 8.4$)	116.42
6'	6.95 (s)	109.70	7.61 (dd, $J = 8.4$ & 2.0 Hz)	122.45
1''	5.23 (d, $J = 1.5$ Hz)	103.78		
2''	4.22 (dd, $J = 1.5$ & 3.4 Hz)	72.04		
3''	3.79 (dd, $J = 9.5$ & 3.4 Hz)	72.19		
4''	3.35 (t, $J = 9.5$ Hz)	73.51		
5''	3.52 (dd, $J = 9.8$ & 6.2 Hz)	72.28		
CH ₃ -rh	0.98 (d, $J = 6.2$ Hz)	17.82		

2.1.2. 7,8,3',4'-Tetrahydroxy-3,5-dimethoxyflavone (3,5-di- O -Methyl Gossypetin) (Compound 2)

Compound (2) was obtained as a yellow amorphous powder. It showed a blue color under UV light (UV λ_{max} : 256, 270, and 353). The NaOAc shift reagent test showed a 19 nm bathochromic shift (free 7-OH), suggesting that the structure of compound (2) is a flavonol substituted at positions 3 and 5 [8]. In negative ESI/MS, it showed a molecular ion $[\text{M} - \text{H}]^-$ at m/z 345. ^1H -NMR showed two methoxyl groups resonating at δ ppm 3.76 and 3.83 and one singlet at δ ppm 6.45, suggesting the hydroxylation of one A-ring proton. It was also observed that there was an absence of signals from 11 to 14 ppm, suggesting that OH-5 is occupied. In addition, characteristic proton patterns of 3,4-dihydroxy substituted B-ring [10]. For the precise determination of the site of hydroxylation and methoxylation, APT, HSQC, HMBC, and 2D NOESY analyses were performed.

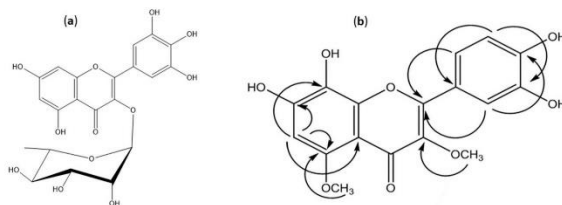


Figure 1. (a) Structure of compound 1. (b) HMBC correlations of compound 7,8,3',4'-tetrahydroxy-3,5-dimethoxyflavone (2).

In the HSQC spectrum of compound 2, δ ppm 3.76 correlated to δ ppm 60.36 and in the HMBC spectrum correlated to 141.29 (C-3); this proved the attachment of the methoxy group to C-3. The other

methoxy signal at δ ppm 3.83 will be then assigned to be 5-OCH₃ due to the absence of a 5-OH signal. Also, 3.83 correlated to δ ppm 56.56 (HSQC), so it is not at 8-OH which resonates at about 60 ppm [11]. Resonance at δ ppm 3.83 is also correlated to 154.64 (HMBC) and correlated to δ ppm 6.45 (H-6) through the 2D-NOESY experiment. Therefore, OCH₃ group (δ ppm 3.83) was assigned to be at C-5.

The APT experiment showed a signal at 127.47 assigned to C8-OH (about 133, if C6-OH) [11], thus, the site of hydroxylation was proved to be at C-8. Also, from the HMBC spectrum, δ ppm 6.45 resonance showed cross-peaks with signals at δ ppm 108.79 (C-4a), 154.64 (C-5), 152.93 (C-7) and 127.47 (C-8), which strongly supports that the signal is at H-6, rather than at H-7 or H-8. The signal at δ ppm 6.45 showed a cross-peak with the resonance at δ ppm 97.24 (HSQC) which is consistent with data published before [12], Figure 1. Therefore, the structure was identified as 7,8,3',4'-tetrahydroxy-3,5-dimethoxyflavone (3,5-di-O-methyl gossypetin) (¹H- and ¹³C-NMR data, Table 1).

2.2. In Vitro Antioxidant Activity

We first evaluated the in vitro antioxidant activity of the two isolated compounds using DPPH (2,2-diphenyl-1-picryl-hydrazyl-hydrate) and FRAP (radical scavenging and ferric reducing antioxidant power) assays. Both compounds exhibited substantial activities, as reported in Table 2. Similar activities were obtained from the total extract and positive controls [5].

Table 2. Antioxidant activities of myricetin-3-O- α -rhamnoside (compound 1) and 3,5-di-O-methyl gossypetin (compound 2). The EC₅₀ values for total extract, ascorbic acid and quercetin are reported for comparison.

Sample	DPPH	FRAP
	(EC ₅₀ μ g/mL)	(mM FeSO ₄ Equivalent/mg Sample)
Compound 1	3.21	22.9
Compound 2	3.89	21.08
Total extract [5]	5.80	10
Ascorbic acid	2.94	-
Quercetin	-	23.18

2.3. Antioxidant Activity in a Cell-Based Model

2.3.1. Biocompatibility in Human Keratinocytes

To verify that the isolated compounds were as nontoxic as the total extract [5], HaCaT cells were exposed to increasing amounts of compounds 1 and 2 (from 5 to 50 μ g/mL) for different lengths of time. At the end of incubation, the MTT (3-(4,5-dimethylthiazol-2-yl)-2,5-diphenyltetrazolium bromide) assay was performed and the results are reported in Figure 2A. We found that cell viability was not affected by compounds 1 and 2 up to 25 μ g/mL, independent of the length of the incubation (24 or 48 h). However, at a higher concentration (50 μ g/mL), both compounds became cytotoxic for keratinocytes, more evidently in the case of compound 2 after 48 h of incubation. This finding is in line with our previous result obtained for the whole extract [5]. Indeed, we found that the extract from *S. samarangense* was cytotoxic when tested at concentrations higher than 100 μ g/mL (after 48 h of incubation).

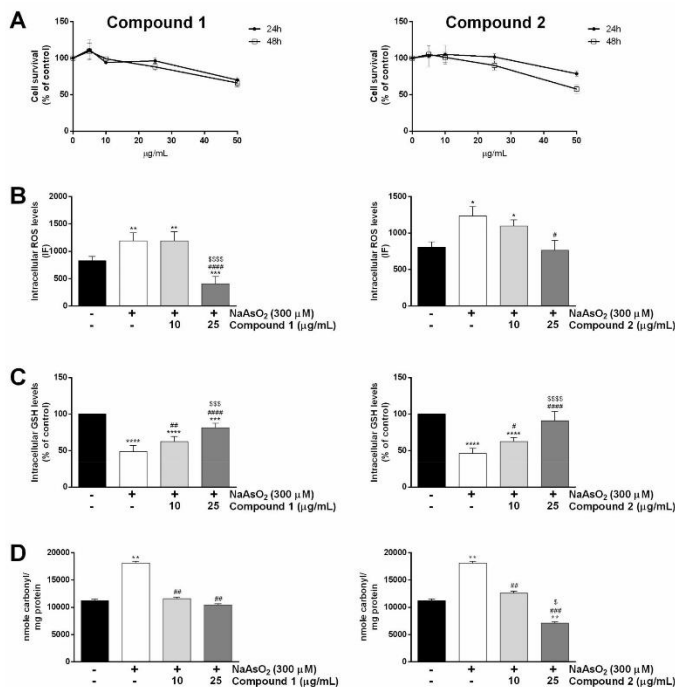


Figure 2. Effect of compounds 1 and 2 on human keratinocyte (HaCaT) cells. A: Dose–response curves of HaCaT cells after 24 h (black circles) and 48 h (empty squares) incubation in the presence of different concentrations of each compound. Cell survival rate was defined as in the Materials and Methods section. B–D: cells were pre-incubated in the presence of pure compounds (10 and 25 $\mu\text{g/mL}$) for 2 h and then exposed to 300 μM NaAsO₂ for 60 min. B: intracellular reactive oxygen species (ROS) levels; C: intracellular glutathione (GSH) levels; D: protein carbonylation levels. Black bars refer to untreated cells, white bars to NaAsO₂-treated cells, light grey bars to 10 $\mu\text{g/mL}$ -treated cells and dark grey bars to 25 $\mu\text{g/mL}$ -treated cells. Results are expressed as the means \pm S.D. of three independent experiments, each carried out in triplicate. * indicates $p < 0.05$, ** indicates $p < 0.01$, *** indicates $p < 0.001$, **** indicates $p < 0.0001$, with respect to control cells; # indicates $p < 0.05$, ## indicates $p < 0.01$, ### indicates $p < 0.001$, #### indicates $p < 0.0001$, with respect to NaAsO₂-treated cells; § indicates $p < 0.05$; §§ indicates $p < 0.01$, §§§ indicates $p < 0.001$, §§§§ indicates $p < 0.0001$ with respect to 10 $\mu\text{g/mL}$ -treated cells.

2.3.2. Antioxidative Effect of Compounds 1 and 2 in HaCaT Cells

To investigate whether the pure compounds were able to prevent ROS generation in stressed keratinocytes, the fluorescent probe 2',7'-Dichlorofluorescein diacetate (H₂-DCFDA) was used. Sodium arsenite (NaAsO₂) was used as a stress agent. Trivalent arsenic is one of the major contaminants of drinking water and air [13]. It acts as a prooxidant as it binds to critical thiol groups, which can inhibit important biochemical events thus leading to toxicity [14]. As shown in Figure 2B, ROS levels were significantly increased in cells after exposure to 300 μM NaAsO₂ for 1 h (Figure 2B, white bars),

whereas, when cells were pre-treated with 25 $\mu\text{g/mL}$ of each pure compound, no significant alteration in ROS production was observed in both cases (Figure 2B, dark grey bars), with compound 1 being the most active. No protective effect was observed at 10 $\mu\text{g/mL}$ (Figure 2B, light grey bars).

Subsequently, we analyzed the ability of the pure compounds to protect cells from NaAsO_2 -induced glutathione (GSH) depletion. GSH depletion is a direct consequence of ROS increase. We found that NaAsO_2 caused a 50% GSH reduction (Figure 2C, white bars). Interestingly, when cells were pre-treated with pure compounds and then stressed, a dose-dependent inhibition of GSH depletion was observed in both cases (Figure 2C, light and dark grey bars).

It is well documented that proteins are among ROS targets [15]. In particular, during protein oxidation, a stable carbonyl group is produced. Thus, carbonylation can be used as a marker of protein damage from prooxidants. Keratinocytes were treated as described above, and then carbonyl content was determined using 2,4-dinitrophenylhydrazine (DNPH). DNPH leads to the formation of stable dinitrophenyl (DNP) hydrazone adducts, which can be detected spectrophotometrically at 375 nm. The results obtained are reported in Figure 2D. As expected, exposure to NaAsO_2 induced a high production of carbonyls (Figure 2D, white bars), whereas both compounds were able to maintain unaltered carbonyl levels already at 10 $\mu\text{g/mL}$. Interestingly, compound 2, when tested at the highest concentration, significantly decreased carbonyl content with respect to untreated cells (Figure 2D, on the right, dark grey bar). These results agree with the data of Büchter et al. [16], who investigated the protective activities of the flavonoid myricetin in Hct116 human colon carcinoma cells against a lethal dose of H_2O_2 .

The protective effect exerted by both isolated compounds was further confirmed by analyzing the MAPK cascade pathway. The phosphorylation levels of p38 and of its direct target MAPKAPK-2 were analyzed in the presence of an increasing amount of each compound, and in the presence of oxidative stress [17]. As shown in Figure 3, both compounds protected human keratinocytes against NaAsO_2 , with compound 1 being the most active.

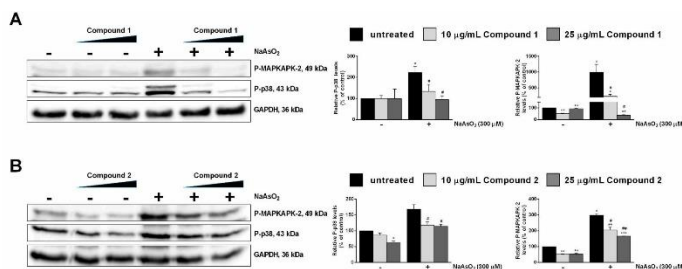


Figure 3. Effect of pure compounds on NaAsO_2 -induced mitogen-activated protein kinase (MAPK) cascade in HaCaT cells. Cells were pre-treated with compounds 1 (A) and 2 (B), as described in Materials and Methods, and Western blots were performed. The phosphorylation levels of MAPKAPK-2 (A, B, upper panel) and p38 (A, B, middle panel) are reported. Glyceraldehyde 3-phosphate dehydrogenase (GAPDH) was used as an internal standard. The relative densitometric analysis is reported. Black bars refer to control cells in the absence (–) or in the presence (+) of NaAsO_2 ; light grey bars refer to 10 $\mu\text{g/mL}$ -treated cells; and dark grey bars refer to 25 $\mu\text{g/mL}$ -treated cells. Data shown are the means \pm S.D. of three independent experiments. * indicates $p < 0.05$, ** indicates $p < 0.01$, *** indicates $p < 0.001$, with respect to control cells; # indicates $p < 0.05$, ## indicates $p < 0.01$ with respect to NaAsO_2 -treated cells.

Compound 2 Stimulates Nrf-2 Nuclear Translocation and Nrf2-ARE Transcriptional Activity

Flavonoids have been shown to exert their antioxidant activity by modulating one or more redox-sensitive transcription factors, such as nuclear factor (erythroid-derived 2)-like 2 (Nrf-2), fork-head box O (FoxOs) and/or peroxisome proliferator-activated receptor gamma (PPAR γ) [18]. Therefore, in order to analyze the mechanism of action of compounds **1** and **2**, the role of the Nrf-2 pathway was evaluated. Nrf-2 is a leucine zipper transcription factor which, under physiological conditions, is negatively regulated by its repressor, Kelch-like ECH-associated protein 1 (Keap-1), which directs Nrf-2 to proteasomal degradation [19]. Upon stimulation by prooxidants or small amounts of antioxidants [19,20], Nrf-2 dissociates from Keap-1 and translocates into the nucleus where it binds to antioxidant response elements (AREs), with the consequent transcription of many genes coding for antioxidant proteins, such as heme oxygenase-1 (HO-1), superoxide dismutase (SOD), NAD(P)H quinone oxidoreductase 1 (NQO1), and γ -glutamate-cysteine ligase (γ -GCLC) [21,22]. Thus, nuclear Nrf-2 levels were analyzed by Western blot after 5 and 15 min incubation with 25 μ g/mL of each compound, as these incubation times have been previously used to verify Nrf-2 nuclear translocation [23,24].

As shown in Figure 4A, no effect of compound **1** was observed on the nuclear translocation of Nrf-2, whereas compound **2** (Figure 4B) clearly induced the nuclear translocation of this transcription factor. This result is very interesting for compound **2** as this is the first report on the mechanism of action for this molecule. Moreover, the failure of compound **1** to activate the Nrf-2 pathway is not so surprising, as there is controversy in the literature regarding the pathways activated by flavonols [25,26]. In particular, the most studied flavonol, i.e., quercetin, has been reported to activate Nrf-2 and/or the cytosolic aryl hydrocarbon receptor (AhR). Indeed, recent studies have indicated that Nrf-2 can be activated either directly by flavonols, or downstream activated after AhR activation [26,27]. Moreover, longer exposure (1–48 h) to flavonols may be required to witness Nrf-2 activation [27,28]. Thus, it is conceivable that in our experimental system, the incubation time used was not long enough to activate Nrf-2 nuclear translocation. The effective activation of AREs by compounds **1** and **2** was next confirmed by analyzing the intracellular levels of HO-1 (Figure 4C,D, respectively) and Mn-SOD (Figure 4E, only for compound **2**). As expected, compound **2** was able to activate the expression of phase II detoxifying enzymes, whereas compound **1** failed.

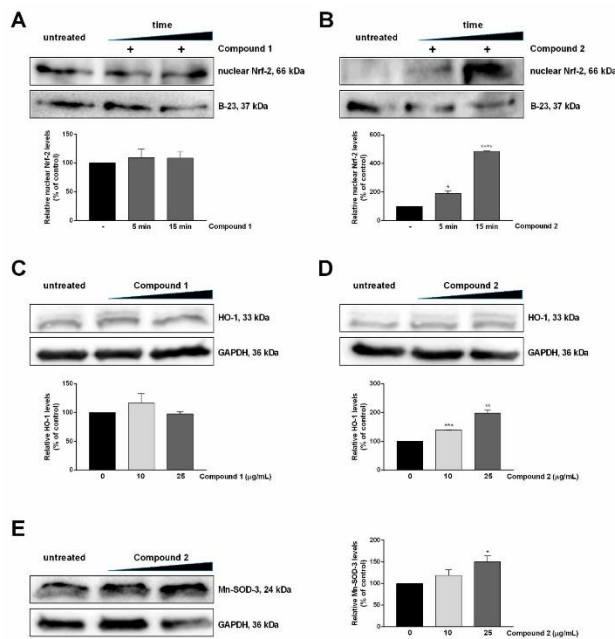


Figure 4. Mechanisms of action of isolated compounds. **A,B:** Nuclear transcription factor-2 (Nrf-2) levels were analyzed by Western blot. Keratinocytes were incubated with increasing concentrations of compound 1 (**A**) or compound 2 (**B**) for 5 min or 15 min and then lysed. The relative changes in Nrf-2 levels were quantified densitometrically; B-23 was used as a loading control. **C,D:** Western blot analysis for HO-1. **E:** Western blot analysis for Mn-SOD-3 of cells incubated with compound 1. HO-1 and Mn-SOD-3 levels were quantified by densitometric analysis and normalized to GAPDH. Data shown are the means \pm S.D. of three independent experiments. * indicates $p < 0.05$, ** indicates $p < 0.01$, *** indicates $p < 0.001$, **** indicates $p < 0.0001$, with respect to control cells.

2.4. Pure Compounds as a Shield against UVA-Mediated Inflammation

Finally, the ability of the two compounds to inhibit inflammation was analyzed. To this purpose, inflammation was induced on HaCaT cells by UVA irradiation, as it has been reported that UVA is able to activate the inflammation pathway [29]. Cells were treated with UVA in the presence or in the absence of each compound. Western blotting analyses, using a specific antibody against I κ B- α , were performed. I κ B- α is one of the key regulatory elements which plays a central role in NF- κ B regulation. Under physiological conditions, I κ B- α acts as a physical inhibitor of NF- κ B, whereas, upon inflammation stimuli, the two proteins dissociate, I κ B- α is degraded and NF- κ B translocates to the nucleus. As shown in Figure 5, a drastic decrease in I κ B- α level was observed only after UVA treatment, whereas the pre-treatment of cells with the pure compounds was able to inhibit I κ B- α degradation and consequent inflammation. These results are in agreement with the those reported in literature, in which different flavonols have been shown to inhibit inflammation [30].

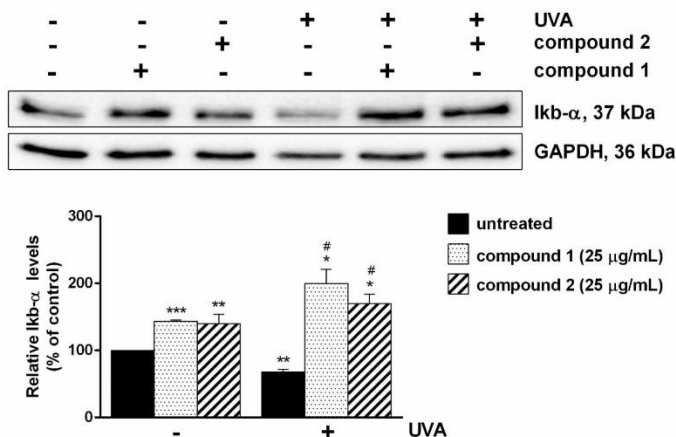


Figure 5. Effects of isolated compounds on inflammation. Cells were pre-treated with each compound (25 μg/mL) for 2 h. Then, cells were exposed to UVA (100 J/cm²) for 10 min and incubated at 37 °C for 30 min. Total lysates were resolved by 15% SDS-PAGE and the level of IκB-α was determined by Western blot analyses. All the values were normalized by using GAPDH as a loading control. The relative densitometric analysis, in the absence (black bars) or in the presence of each compound (dotted bars for compound 1 and diagonal lines bars for compound 2) is reported. Data shown are the means ± S.D. of three independent experiments. * indicates $p < 0.05$, ** indicates $p < 0.01$, *** indicates $p < 0.001$, with respect to control cells; # indicates $p < 0.05$, with respect to UVA-treated cells. In the graph, (-), is referred to not irradiated cells, whereas (+) is referred to cells irradiated by UVA.

3. Materials and Methods

3.1. Extraction and Isolation of Compounds

S. samarangense (Blume) Merr. & L. M. Perry (syn. *Eugenia javanica* L.) leaves were collected during the spring season in 2014. A plant sample is kept at the Pharmacognosy Department, Faculty of Pharmacy, Ain Shams University (Cairo, Egypt) under PHG-P-SS-182 [31]. Air-dried leaves (300 g) were ground and extracted using methanol (3×1 L). The combined extracts were filtered and consequently evaporated under a vacuum at 40 °C until dryness, yielding a semisolid extract. The latter was then subjected to lyophilization, yielding 40 g. The lyophilized extract was then defatted with n-hexane and finally subjected to sequential fractionation using ethyl acetate, yielding 4 g, and butanol, yielding 3 g.

A portion of the ethyl acetate fraction (900 mg) was applied to a medium-chromatography system (Puriflash 4100, Interchim, 03100 Montluçon, France) equipped with silica flash columns (PuriFlash column 30 Silica HP - 25.0 g, 22 bar). Elution was performed using a gradient of dichloromethane (A) and methanol (B). At 0 min, the ratio of B was 30% and reached 100% at 90 min. The flow rate was 15 mL/min and the UV detection was conducted at 254 and 365 nm. Three major fractions were obtained, which were further subjected to TLC screening, followed by purification on several Sephadex LH20 columns using methanol as eluent. Finally, two pure isolated compounds, namely myricetin-3-O-α-rhamnoside (myricitrin) (1) and 3,5-di-O-methyl gossypetin (7,8,3',4'-tetrahydroxy-3,5-dimethoxyflavone) (2) were obtained.

3.2. In Vitro Antioxidant Activity

2,2-Diphenyl-1-picryl-hydrazyl-hydrate (DPPH) radical scavenging and ferric reducing antioxidant power (FRAP) assays were used to determine the antioxidant properties of the isolated compounds, and were carried out as described earlier [32].

3.3. Cell Culture

The immortalized human skin keratinocyte cell line (HaCaT) was obtained from American Type Culture Collection (ATCC, Manassas, VA, USA) and was cultured in complete growth medium in a 5% CO₂ humidified atmosphere at 37 °C, as described before [17]. Subculture was carried out in a ratio of 1:4–1:5 every 48–72 h.

The biocompatibility of the compounds towards the cells was assessed by the MTT (3-(4,5-dimethylthiazol-2-yl)-2,5-diphenyltetrazolium bromide) assay, as described before [17]. In brief, HaCaT cells were plated at a density of 2×10^4 cells/cm². The next day, the medium from each well was aspirated and 100 µL of fresh growth medium containing increasing amounts of pure compounds (from 5 to 50 µg/mL) was added and left for 24 and 48 h. Two groups of cells were used as a control, i.e., untreated cells and cells supplemented with identical volumes of methanol. The biocompatibility of each compound was expressed as the percentage of viable cells in the presence of the compound under testing, compared to the average of the control cells. Each sample was tested in three independent analyses, each carried out in triplicate.

3.4. Induction of Oxidative Stress with Sodium Arsenite

To evaluate the protective effect of the pure compounds against oxidative stress, HaCaT cells were pre-treated with 10 and 25 µg/mL of the respective compound for 2 h. At the end of incubation, cells were exposed to 300 µM sodium arsenite (NaAsO₂) for 1 h. Immediately after oxidative stress induction, ROS production, GSH levels, protein carbonylation levels, and activation of mitogen-activated protein kinase (MAPK) cascade were determined by DCFDA assay, DTNB (5,5'-dithiobis-2-nitrobenzoic acid) assay, DNPH assay and Western blotting, respectively, as described below.

3.5. DCFDA Assay

To examine whether the pure compounds may interfere with free radical propagation, the accumulation of intracellular ROS levels was measured by DCFDA assay. In brief, 24 h after seeding, 10 and 25 µg/mL of each compound (dissolved in Dulbecco's Modified Eagle's Medium (DMEM) without phenol red) were added to the culture medium. After 2 h of incubation, cells were incubated with 25 µM 2',7'-dichlorodihydrofluorescein diacetate (H₂-DCFDA, Sigma-Aldrich) for 45 min at 37 °C in complete medium without phenol red. At the end of incubation, cells were incubated with 300 µM NaAsO₂ as described above. Cells were washed with warm PBS (phosphate buffer saline) supplemented with 1 mM CaCl₂, 0.5 mM MgCl₂, and 30 mM glucose (PBS plus) between each step. Then, the fluorescence intensity of the DCF probe was measured by using a Synergy™ HTX Multi-Mode Microplate Reader (excitation = 485 nm, emission = 535 nm, scanning speed = 300 nm/min and 5 slit widths for excitation and emission, BioTek Instruments, Inc., Winooski, VT, USA). ROS production was expressed as the DCF fluorescence intensity of the samples under testing. The results are given as the average of three independent experiments, each carried out in triplicate.

3.6. DTNB Assay

Total glutathione (GSH) content was determined by 5,5'-dithiobis-2-nitrobenzoic acid (DTNB) assay as described before [17]. The GSH content was expressed as the percentage of thio-2-nitrobenzoic acid (TNB) of the sample under testing, with respect to the untreated sample. The GSH content was extrapolated from absorbance values, obtained at 412 nm, based on the standard curve obtained by

incubating the DTNB reagent with GSH (1–500 μM). The results are given as the average of three independent experiments, each carried out in triplicate.

3.7. DNPH Assay

To analyze protein carbonyl content, cells were treated as described above and then 2,4-dinitrophenylhydrazine (DNPH) assay was performed by using the protocol of the protein carbonyl content assay kit (Sigma-Aldrich, St Louis, MO, USA).

The carbonyl content was calculated using the equations below:

$$\text{Carbonyl content} = \frac{\text{nmolecarbonyl}}{\text{mgprotein}} \quad (1)$$

$$\text{nmole carbonyl} = \frac{\text{Abs}_{375\text{nm}}}{6.364} \times 100 \quad (2)$$

where: 100 = total volume in well (μL); 6.364 = millimolar coefficient of extinction ($\epsilon^{\text{mM}} = 22 \text{ mM}^{-1} \text{ cm}^{-1}$) $\times 0.2893 \text{ cm}$ path length in a well; Abs 375 nm = absorption at 375 nm of DNPH, which is related to carbonyl content. Three independent experiments were carried out, each one with three determinations.

3.8. Induction of Inflammation by UVA Light Treatment

To evaluate the ability of each compound to counteract inflammation, HaCaT cells were plated as described above. After seeding, cells were pre-treated with 25 $\mu\text{g}/\text{mL}$ of the compounds for 2 h. At the end of incubation, the cells were washed with phosphate buffer saline (PBS) and then covered with a thin layer of PBS and exposed to UVA light (365 nm) for 10 min (100 J/cm^2). Then, cells were washed twice with PBS and incubated in complete medium for 30 min at 37 $^\circ\text{C}$. Inflammation was evaluated by Western blotting, as described below.

3.9. Western Blotting Analysis

To analyze MAPK cascade and inflammatory markers, cells were detached at the end of the treatment, and then lysed by re-suspending cell pellets in 50 μL of lysis buffer (300 mM NaCl, 0.5% NP40 in 100 mM Tris-HCl, at pH 7.4) supplemented with proteases and phosphatase inhibitors. To analyze nuclear transcription factor-2 (Nrf-2) activation, nuclear lysates were used. In the first step, cytosolic proteins were extracted by using PBS buffer containing 0.1% Triton and protease inhibitors. Then, the pellets, containing nuclear proteins, were resuspended in Radioimmunoprecipitation (RIPA) buffer (150 mM NaCl, 1% NP-40, 0.1% SDS, protease inhibitors in 50 mM Tris-HCl, at pH 8.0). For each condition, lysates (100 μg proteins) were analyzed by Western blotting performed as described before [33]. Specific antibodies against phosphorylated p38 and MAPKAPK-2, total Mn-SOD and Nrf-2 were purchased from Cell Signal Technology (Danvers, MA, USA). HO-1 antibody was from Bethyl (Montgomery, TX, USA). I κ B- α antibody was from Santa Cruz Biotechnology, Inc. (Santa Cruz, CA, USA). To normalize protein intensity levels, a specific antibody was used for total (anti-GAPDH, Thermo-Fisher, Rockford, IL, USA) and nuclear (anti B23, Thermo-Fisher) extracts. The chemiluminescence detection system (Super Signal[®] West Pico) was from Thermo-Fisher, Rockford, IL, USA.

3.10. Statistical Analyses

The results were expressed as the mean \pm standard deviation of the mean (SD) when data were combined. For statistical analyses, GraphPad Prism 6.01 software for Windows (GraphPad Software Inc., San Diego, CA, USA) was used: one-way analysis of variance (ANOVA) followed by Bonferroni's post-hoc test was used for all the experiments. Differences supported by $p < 0.05$ were considered statistically significant.

4. Conclusions

In this study, myricetin-3-O- α -rhamnoside and 7,8,3',4'-tetrahydroxy-3,5-dimethoxyflavone (3,5-di-O-methyl gossypetin) were isolated and identified from *S. samarangense* leaves. Both compounds show substantial antioxidant activities in vitro. In HaCaT cells, both compounds strongly reduced intracellular ROS accumulation and carbonyl content, and also protected the intercellular GSH levels in keratinocytes after exposure to the toxic agent sodium arsenite (NaAsO₂). Furthermore, we found that compound 2 exerts its antioxidant activity by stimulating translocation of the transcription factor Nrf-2 to the nucleus. Once in the nucleus, the transcription factor binds to ARE sequences and induces the expression of phase II detoxifying enzymes, i.e., HO-1 and Mn-SOD-3. Finally, we demonstrated that both compounds were able to inhibit I κ B- α degradation, thus protecting cells from UVA-induced inflammation. Both compounds may be useful to explore the antioxidant and anti-inflammatory potential of *S. samarangense*.

Author Contributions: M.S. performed extraction, fractionation and isolated the compounds, performed the antioxidant activities in vitro, wrote the manuscript and designed the project. G.P. performed the antioxidant activities in HaCaT cells and wrote the manuscript. S.O. performed fractionation and isolated the compounds. M.A.E.R. characterized the compounds and discussed them. P.I. performed the antioxidant activities in HaCaT cells. D.M.M. and M.W. supervision, revised the manuscript and designed the project.

Funding: The authors received financial support from the Deutsche Forschungsgemeinschaft and Ruprecht-Karls-Universität Heidelberg within the funding program Open Access Publishing.

Acknowledgments: The authors would like to thank Mrs. Therese Labib, Consultant of Plant Taxonomy at the Ministry of Agriculture and El-Orman Botanical Garden, Giza, Egypt, for morphological authentication of the plant.

Conflicts of Interest: The authors declare no conflict of interest.

Abbreviations

ARE, antioxidant response element; AhR, aryl hydrocarbon receptor; DCF, 2',7'-dichlorofluorescein; DMEM, Dulbecco's Modified Eagle's Medium; DNP, 2,4-dinitrophenol; DNPH, 2,4-dinitrophenylhydrazine; DPPH, 2,2-diphenyl-1-picryl-hydrazyl-hydrate; DTNB, 5,5'-dithiobis-2-nitrobenzoic acid; EDTA, ethylene diamine tetra acetic acid; FoxOs, fork-head box O; FRAP, radical scavenging and ferric reducing antioxidant power; HO-1, heme oxygenase-1; H₂-DCFDA, 2',7'-dichlorodihydrofluorescein diacetate; Keap-1, Kelch-like ECH-associated protein 1; Nrf-2, nuclear factor (erythroid-derived 2)-like 2; NQO1, NAD(P)H quinone oxidoreductase1; P-HSP-27, phosphorylated heat shock protein; P-MAPKAPK-2, phosphorylated MAP kinase-activated protein kinase; PPAR γ , peroxisome proliferator-activated receptor gamma; P-p38, phosphorylated p38 MAP kinase; ROS, reactive oxygen species; SOD, superoxide dismutase; TBA, thiobarbituric acid; TBARS, TBA reactive substances; TNB, 5-thio-2-nitrobenzoic acid; and γ -GCLC, γ -glutamate-cysteine ligase.

References

1. Beckman, K.B.; Ames, B.N. The free radical theory of aging matures. *Physiol. Rev.* **1998**, *78*, 547–581. [[CrossRef](#)]
2. Andreyev, A.Y.; Kushnareva, Y.E.; Starkov, A. Mitochondrial metabolism of reactive oxygen species. *Biochemistry* **2005**, *70*, 200–214. [[CrossRef](#)]
3. Van Wyk, B.-E.; Wink, M. *Phytochemicals, Herbal Drugs, and Poisons*; University of Chicago Press: Chicago, IL, USA, 2015.
4. Van Wyk, B.-E.; Wink, M. *Medicinal Plants of the World*; CABI: Wallingford, UK, 2017.
5. Sobeh, M.; Youssef, F.S.; Esmat, A.; Petruk, G.; El-Khatib, A.H.; Monti, D.M.; Ashour, M.L.; Wink, M. High resolution UPLC-MS/MS profiling of polyphenolics in the methanol extract of *Syzygium samarangense* leaves and its hepatoprotective activity in rats with CCl₄-induced hepatic damage. *Food Chem. Toxicol.* **2018**, *113*, 145–153. [[CrossRef](#)]
6. Hu, Y.-K.; Wang, L.; Li, Y.-Y.; Li, M.-J.; Xu, W.; Zhao, Y.; Li, F.; Zhao, Y. Five new triterpenoids from *Syzygium samarangense* (Bl.) Merr. et Perry. *Phytochem. Lett.* **2018**, *25*, 147–151. [[CrossRef](#)]
7. Mabry, T.; Markham, K.; Thomas, M. *The Systematic Identification of Flavonoids*; Springer Science and Business Media, Springer: New York, NY, USA, 1970.

8. Barakat, H.H.; El-Raey, M.; Nada, S.A.; Zeid, L.; Nawwar, M. Constitutive phenolics and hepatoprotective activity of *Eugenia supra-axillaris* leaves. *Egypt. J. Chem.* **2011**, *54*, 313–323.
9. El-Kashak, W.A.; Hamed, A.R.; El-Raey, M.; Elshamy, A.I.; Abd-Ellatef, G.E.F. Antiproliferative, antioxidant and antimicrobial activities of phenolic compounds from *Acrocarpus fraxinifolius*. *J. Chem. Pharmaceut. Res.* **2016**, *8*, 520–528.
10. Osman, S.M.; El Kashak, W.A.; Wink, M.; El Raey, M.A. New isorhamnetin derivatives from *Salsola imbricata* Forssk. leaves with distinct anti-inflammatory activity. *Pharmacog. Mag.* **2016**, *12*, S47.
11. Takemura, O.S.; Inuma, M.; Tosa, H.; Miguel, O.G.; Moreira, E.A.; Nozawa, Y. A flavone from leaves of *Arrabidaea chica* cuprea. *Phytochemistry* **1995**, *38*, 1299–1300. [[CrossRef](#)]
12. Hussein, S.A.; Hashem, A.N.; Seliem, M.A.; Lindequist, U.; Nawwar, M.A. Polyoxygenated flavonoids from *Eugenia edulis*. *Phytochemistry* **2003**, *64*, 883–889. [[CrossRef](#)]
13. Singh, N.; Kumar, D.; Sahu, A.P. Arsenic in the environment: Effects on human health and possible prevention. *J. Environ. Biol.* **2007**, *28*, 359. [[PubMed](#)]
14. Hughes, M.F. Arsenic toxicity and potential mechanisms of action. *Toxicol. Lett.* **2002**, *133*, 1–16. [[CrossRef](#)]
15. Dalle-Donne, I.; Rossi, R.; Giustarini, D.; Milzani, A.; Colombo, R. Protein carbonyl groups as biomarkers of oxidative stress. *Clin. Chim. Acta* **2003**, *329*, 23–38. [[CrossRef](#)]
16. Büchter, C.; Ackermann, D.; Havermann, S.; Honnen, S.; Chovolou, Y.; Fritz, G.; Kampkötter, A.; Wätjen, W. Myricetin-mediated lifespan extension in *Caenorhabditis elegans* is modulated by DAF-16. *Int. J. Molec. Sci.* **2013**, *14*, 11895. [[CrossRef](#)] [[PubMed](#)]
17. Petruk, G.; Raiola, A.; Del Giudice, R.; Barone, A.; Frusciantè, L.; Rigano, M.M.; Monti, D.M. An ascorbic acid-enriched tomato genotype to fight UVA-induced oxidative stress in normal human keratinocytes. *J. Photochem. Photobiol. B Biol.* **2016**, *163*, 284–289. [[CrossRef](#)] [[PubMed](#)]
18. Pallauf, K.; Duckstein, N.; Hasler, M.; Klotz, L.-O.; Rimbach, G. Flavonoids as putative inducers of the transcription factors Nrf2, FoxO, and PPAR γ . *Oxid. Med. Cell. Longev.* **2017**. [[CrossRef](#)] [[PubMed](#)]
19. Surh, Y.-J. Cancer chemoprevention with dietary phytochemicals. *Nat. Rev. Cancer* **2003**, *3*, 768. [[CrossRef](#)] [[PubMed](#)]
20. Hur, W.; Gray, N.S. Small molecule modulators of antioxidant response pathway. *Curr. Opin. Chem. Biol.* **2011**, *15*, 162–173. [[CrossRef](#)] [[PubMed](#)]
21. Hseu, Y.-C.; Tsai, Y.-C.; Huang, P.-J.; Ou, T.-T.; Korivi, M.; Hsu, L.-S.; Chang, S.-H.; Wu, C.-R.; Yang, H.-L. The dermato-protective effects of lucidone from *Lindera erythrocarpa* through the induction of Nrf2-mediated antioxidant genes in UVA-irradiated human skin keratinocytes. *J. Funct. Foods* **2015**, *12*, 303–318. [[CrossRef](#)]
22. Keum, Y.-S. Regulation of Nrf2-mediated phase II detoxification and anti-oxidant genes. *Biomolecul. Therapeut.* **2012**, *20*, 144. [[CrossRef](#)]
23. Jones, R.M.; Desai, C.; Darby, T.M.; Luo, L.; Wolfarth, A.A.; Scharer, C.D.; Ardita, C.S.; Reedy, A.R.; Keebaugh, E.S.; Neish, A.S. Lactobacilli modulate epithelial cytoprotection through the Nrf2 pathway. *Cell. Rep.* **2015**, *12*, 1217–1225. [[CrossRef](#)]
24. Hseu, Y.-C.; Lo, H.-W.; Korivi, M.; Tsai, Y.-C.; Tang, M.-J.; Yang, H.-L. Dermato-protective properties of ergothioneine through induction of Nrf2/ARE-mediated antioxidant genes in UVA-irradiated Human keratinocytes. *Free Rad. Biol. Med.* **2015**, *86*, 102–117. [[CrossRef](#)]
25. Zhang, H.; Tsao, R. Dietary polyphenols, oxidative stress and antioxidant and anti-inflammatory effects. *Curr. Opin. Food Sci.* **2016**, *8*, 33–42. [[CrossRef](#)]
26. Köhle, C.; Bock, K.W. Activation of coupled Ah receptor and Nrf2 gene batteries by dietary phytochemicals in relation to chemoprevention. *Biochem. Pharmacol.* **2006**, *72*, 795–805. [[CrossRef](#)]
27. Niestroy, J.; Barbara, A.; Herbst, K.; Rode, S.; van Liempt, M.; Roos, P.H. Single and concerted effects of benzo[a]pyrene and flavonoids on the AhR and Nrf2-pathway in the human colon carcinoma cell line Caco-2. *Toxicol. In Vitro* **2011**, *25*, 671–683. [[CrossRef](#)]
28. Schadich, E.; Hlaváč, J.; Volná, T.; Varanasi, L.; Hajdúch, M.; Džubák, P. Effects of ginger phenylpropanoids and quercetin on Nrf2-ARE pathway in human BJ fibroblasts and HaCaT keratinocytes. *BioMed Res. Int.* **2016**. [[CrossRef](#)]
29. Petruk, G.; Del Giudice, R.; Rigano, M.M.; Monti, D.M. Antioxidants from plants protect against skin photoaging. *Oxid. Med. Cell. Longev.* **2018**. [[CrossRef](#)] [[PubMed](#)]
30. Xie, J.; Zheng, Y. Myricetin protects keratinocyte damage induced by UV through I κ B/NF κ B signaling pathway. *J. Cosmet. Dermatol.* **2017**, *16*, 444–449. [[CrossRef](#)]

31. Sobeh, M.; Braun, M.S.; Krstin, S.; Youssef, F.S.; Ashour, M.L.; Wink, M. Chemical profiling of the essential oils of *Syzygium aqueum*, *Syzygium samarangense* and *Eugenia uniflora* and their discrimination using chemometric analysis. *Chem. Biodiv.* **2016**, *13*, 1537–1550. [CrossRef]
32. Ghareeb, M.A.; Mohamed, T.; Saad, A.M.; Refahy, L.A.-G.; Sobeh, M.; Wink, M. HPLC-DAD-ESI-MS/MS analysis of fruits from *Firmiana simplex* (L.) and evaluation of their antioxidant and antigenotoxic properties. *J. Pharm. Pharmacol.* **2017**. [CrossRef] [PubMed]
33. Petruk, G.; Donadio, G.; Lanzilli, M.; Isticato, R.; Monti, D.M. Alternative use of *Bacillus subtilis* spores: protection against environmental oxidative stress in human normal keratinocytes. *Sci. Rep.* **2018**, *8*, 1745. [CrossRef]

Sample Availability: Samples of the compounds are available from the authors.



© 2019 by the authors. Licensee MDPI, Basel, Switzerland. This article is an open access article distributed under the terms and conditions of the Creative Commons Attribution (CC BY) license (<http://creativecommons.org/licenses/by/4.0/>).



A cascade extraction of active phycocyanin and fatty acids from *Galdieria phlegrea*

Paola Imbimbo¹ · Valeria Romanucci¹ · Antonino Pollio² · Carolina Fontanarosa¹ · Angela Amoresano¹ · Armando Zarrelli¹ · Giuseppe Olivieri^{1,3} · Daria Maria Monti¹

Received: 4 June 2019 / Revised: 12 September 2019 / Accepted: 24 September 2019
© Springer-Verlag GmbH Germany, part of Springer Nature 2019

Abstract

The setup of an economic and sustainable method to increase the production and commercialization of products from microalgae, beyond niche markets, is a challenge. Here, a cascade approach has been designed to optimize the recovery of high valuable bioproducts starting from the wet biomass of *Galdieria phlegrea*. This unicellular thermo-acidophilic red alga can accumulate high-value compounds and can live under conditions considered hostile to most other species. Extractions were performed in two sequential steps: a conventional high-pressure procedure to recover phycocyanins and a solvent extraction to obtain fatty acids. Phycocyanins were purified to the highest purification grade reported so far and were active as antioxidants on a cell-based model. Fatty acids isolated from the residual biomass contained high amount of PUFAs, more than those recovered from the raw biomass. Thus, a simple, economic, and high effective procedure was set up to isolate phycocyanin at high purity levels and PUFAs.

Keywords *Galdieria phlegrea* · Phycocyanin · Lipids · Biorefinery approach

Introduction

Microalgae can be rich suppliers of proteins and carbohydrates and, under stress conditions, they can accumulate large quantities of lipids. Therefore, microalgae have been claimed to be potential feedstock for a number of different industrial applications, such as food commodities, biofuels, bio-based chemicals, fine organics, bioplastics, pigments, cosmetics, and pharmaceuticals (Moody et al. 2014; Posada et al. 2016;

Quinn and Davis 2015; Ruiz et al. 2016; Tredici et al. 2016). With respect to plants, microalgae possess several advantages: they do not need arable lands, they can grow on seawater and on residual nutrients from wastewater, and they possess higher areal productivity (Chauton et al. 2015).

However, the analysis of the large-scale production pointed out that the technologies proposed to obtain only one product are still not self-sustainable from an economic point of view (Leu and Boussiba 2014; Moody et al. 2014; Quinn and Davis 2015; Ruiz et al. 2016; Tredici et al. 2016). The reasons rely on the following: (1) high cultivation costs, especially for cooling in case of adopting close photobioreactor technology, and (2) low profit per unit of biomass coming from a single specific product, especially in case of bulk commodities (food, feed, or fuel), which are characterized by low prices that can hardly compensate the production cost. An intermediate step is first required to promote investments and foster the commercialization of algae-based products: the exploitation of some high-value products at production scale smaller than the large one needed for fuel and food (González-Delgado and Kafarov 2011). In that respect, among the cell components, hydrophilic antioxidants such as phycocyanins (PCs) (> 100 €/kg and > 100 ME/year) and lipids rich in polyunsaturated fatty acids (PUFAs) (> 10 €/kg and > 100 ME/year) are good candidates due to their high selling price (Ankush 2019; Ruiz et al. 2016). Moreover,

Electronic supplementary material The online version of this article (<https://doi.org/10.1007/s00253-019-10154-0>) contains supplementary material, which is available to authorized users.

✉ Giuseppe Olivieri
giuseppe.olivieri@wur.nl

✉ Daria Maria Monti
mdmonti@unina.it

¹ Department of Chemical Sciences, University of Naples Federico II, via Cinthia 4, 80126 Naples, Italy

² Department of Biology, University of Naples Federico II, via Cinthia 4, 80126 Naples, Italy

³ Bioprocess Engineering Group, Wageningen University and Research, Droevendaalsesteeg 1, 6700AA, Wageningen, the Netherlands

customers are frequently willing to pay a higher price for bio-based products than for chemical-based products.

Here, a cascade approach has been designed to get two classes of high-value molecules, starting from the same cultivation: phycocyanins and polyunsaturated fatty acids. PC is an antenna pigment which increases the photosynthetic efficiency by collecting light energy at wavelengths which chlorophylls do not absorb. PC is water soluble, very stable overtime at its physiological pH, and contains a chromophore prosthetic group. The latter is very fluorescent and is currently used in flow cytometry, immunological analysis, and in detection of reactive oxygen species. In addition, PC is a protein endowed with a strong antioxidant, hepato-protective, anti-inflammatory, neuro-protective, and anti-proliferative activity (Carfagna et al. 2015; Fernández-Rojas et al. 2014; Patel et al. 2018; Romay et al. 2003; Sonani et al. 2017). However, it has to be considered that the use of PC in industry is still limited because of its sensitivity to high temperature and extreme pH, which reduce PC yields or may cause dissociation phenomena, leading to the bleach of the blue color (Manirafasha et al. 2016; Mehta et al. 2018).

PUFAs are essential for human function, as they have anti-inflammatory, antioxidant, neuro-protective, and cardioprotective activities, but many of them (such as omega-3 and omega-6) have to be taken up through the diet (Cuellar-Bermudez et al. 2015; Zárate et al. 2017). Actually, they are obtained from fish oil (Salmonidae, Scombridae, and Clupeidae families), which is an unsustainable source both from an economic and environmental point of view (Patel et al. 2019). Moreover, pollution of marine ecosystems, and the possibility that fishes accumulate mercury, led to an increased interest in alternative sustainable sources (Spolaore et al. 2006). Marine microalgae are a source of commercial omega-3 PUFAs and they are the primary producers of basic fatty acids in marine food webs (Bergé and Bamathan 2005). PUFAs from algae also have the advantage of being suitable for vegetarian and vegan nutrition.

In this context, the microalga *Galdieria phlegrea*, a unicellular thermo-acidophilic red alga, has gained our attention since it is rich in pigments and PUFAs. Additionally, its optimal growth condition is at pH 1.5 and at temperatures in the range 35–45 °C (Carfagna et al. 2015). This represents a great advantage as it will dramatically reduce the risk of contaminations in open ponds systems as well as the cooling cost in case of closed photobioreactors (Sakurai et al. 2016).

Here, we set up the optimal autotrophic growth condition for *G. phlegrea* (strain 009) and extracted and purified active PC. Then, by using a cascade approach, we extracted and purified lipids from the residual biomass. Finally, PC antioxidant activity was validated in an applicative environment, with a cell-based model, using human immortalized keratinocytes. This contribution provides a clear validation of the feasibility of a multiproduct biorefinery applied to *G. phlegrea* at lab-scale.

Material and methods

Microalgal strain and culture conditions

Galdieria phlegrea (strain 009) was provided from the Algal Collection of the University Federico II (ACUF, <http://www.acuf.net>). Pre-cultures of 50 mL were inoculated in Allen medium (Allen 1968) with pH 1.5 in bubble column photobioreactors, with a starting concentration of 8 O.D./mL for autotrophic condition and 14 O.D./mL for the mixotrophic condition. Cultures were performed at 37 ± 1 °C under constant fluorescent light with an intensity of 200 PAR [$\mu\text{mol}/\text{m}^2/\text{s}$]. A gas mixing device provided the desired carbon dioxide (CO₂) concentration to the photobioreactors, by mixing air and pure carbon dioxide from a pressurized vessel at the final flow rate of 3 vvm. In autotrophy conditions, no organic carbon source was supplemented to the medium, whereas organic carbon with 3% glycerol (final concentration) was supplemented during mixotrophy conditions. The algal growth was monitored daily by measuring the absorbance at 730 nm, which is related to the biomass concentration and is indicated by optical density (O.D.).

Cell concentration

The biomass of *G. phlegrea* was measured as O.D. Analysis of the dry cell weight was carried out by weighing aliquots of culture. The O.D. values were converted into biomass concentration via an appropriate calibration between O.D. and dry cell weight. The conversion factor was 1 O.D./mL = 0.2 mg-biomass/mL for *G. phlegrea*.

Protein extraction and quantification

The biomass was harvested by centrifugation at 1200g for 30 min at room temperature and resuspended in 50 mM sodium acetate pH 5.5 (Wu et al. 2016). Cells were disrupted by two consecutive cycles of French Press (each at 2 kbar). After centrifugation at 5000g at 4 °C for 30 min, proteins were recovered in the supernatant, whereas the residual biomass was used to extract lipids (as described below). Proteins were assayed by BCA Protein Assay Kit (Thermo Scientific).

Phycocyanin quantification and purification

The absorbance of crude extracts was measured at 615 and 652 nm to obtain phycocyanin concentration, according to the Bennett and Bogorad equation (Bennett and Bogorad 1973):

$$C_{\text{PC}} \left(\frac{\text{mg}}{\text{mL}} \right) = \frac{[Abs_{615\text{nm}} - (0.474 \times Abs_{652\text{nm}})]}{5.34}$$

These wavelengths correspond to the maximum of absorption of phycocyanin (PC, 615 nm) and allophycocyanin

(APC, 652 nm), respectively. The grade of purity of phycocyanin was calculated by measuring the ratio $A_{620\text{nm}}/A_{280\text{nm}}$.

A single step purification was performed to recovery phycocyanin. A size-exclusion chromatography was performed by using a Sephadex G-75 fine equilibrated in 50 mM sodium acetate pH 5.5. Fractions were collected and the absorbance at 280 and 620 nm was measured.

Lipid extraction, purification, and analysis

The residual biomass (i.e., after protein extraction) was dried at 60 °C for 24 h. Lipids were selectively extracted by mixing CHCl_3 -MeOH (2:1 v/v) with a Soxhlet extractor for 8 h. Then, the solution was dried under nitrogen flux to recover and weigh lipids. One milligram was placed into a 16×125 mm screw-cap Pyrex tube and 1.0 mL of hexane and 1.0 mL of BF_3 in MeOH (14%, wt/vol) were added. The tube was incubated in a 50 °C water bath for 1 h with vigorous handshaking for 20 s every 30 min. Then, 1.0 mL of a saturated solution of NaHCO_3 and 2.0 mL of hexane were added and the tube was vortex-mixed. After centrifugation, the hexane layer containing the fatty acid methyl ester (FAME) was placed into a gas chromatography vial, capped, and stored at -20 °C until GC analysis.

The organic layer containing FAMEs was collected, dried, dissolved in an appropriate volume of hexane (100 μL), and analyzed using a Shimadzu 2010 series GC FID (Shimadzu, Milano, Italy). The gas chromatograph was equipped with an SP52-60 capillary column (100 m \times 0.25 mm i.d. \times 0.20 μm film thickness) with a non-bonded, poly(bis-cyanopropyl siloxane) phase (Sigma-Aldrich, St Louis, MO, USA) and nitrogen as the carrier gas. Samples (1.0 μL) were introduced into the injector using an AOC-20i auto sampler (Shimadzu, Milano, Italy) heated to 250 °C with a split ratio of 10:1. The initial temperature was 160 °C with a 2 min hold, followed by a 6 °C/min ramp to 200 °C with a 2 min hold and finally followed by a 6 °C/min ramp to 220 °C with a 25 min hold. The following parameters were set during the experiments: detector temperature, 275 °C; carrier gas: helium for chromatography at a pressure of 1.8 psi, auxiliary gas: hydrogen for chromatography at a pressure of 18 psi, air chromatography at a pressure of 22 psi; and sensitivity of the instrument, 4 to 16 times the minimum attenuation.

In situ digestion and mass spectrometry analyses

Sample aliquots (30 μg) were submitted to electrophoresis on a 10% polyacrylamide gel (0.1% SDS, 25 mM Tris-HCl, 192 mM glycine, pH 8.3). Gel was stained with Coomassie Brilliant blue, and the main gel lanes excised from the gel and destained prior to further processing. Briefly, gel slices were washed with three cycles of 0.1 M NH_4HCO_3 pH 8.0 and acetonitrile, followed by reduction (10 mM DTT; 100 mM NH_4HCO_3 45 min, 56 °C) and alkylation (55 mM IAM;

100 mM NH_4HCO_3 , 30 min, RT). Gel slices were washed with three further cycles of 100 mM NH_4HCO_3 pH 8.0 and acetonitrile. Finally, gel plugs were rehydrated in 40 mL sequencing grade modified trypsin (10 ng/ μL trypsin; 10 mM NH_4HCO_3) and incubated overnight at 37 °C. Peptides mixture was eluted, vacuum-dried, and resuspended in 0.1% formic acid for LC-MS/MS. Peptide samples were loaded onto a Michrom C18 Captrap to initially desalt samples and from there were introduced directly into a LTQ-Orbitrap MS (Thermo Fisher Scientific, Surrey, UK) via a fused silica C18 capillary column (Nikkyo Technos CO, Tokyo, Japan) and a nanoelectrospray ion source. The mobile phase comprised H_2O with 0.1% formic acid (buffer A) and 100% acetonitrile with 0.1% formic acid (buffer B). The gradient ranged from 5 to 30% buffer B in 95 min followed by 30 to 60% B in 15 min and a step gradient to 85% B for 5 min with a flow of 0.42 $\mu\text{L}/\text{min}$, finally a return to the initial conditions of 5% B. The FTMS full scan mass spectra (from 450 to 1600 m/z) were acquired with a resolution of $r = 60\,000$. This was followed by data-dependent MS/MS fragmentation in centroid mode of the most intense ion from the survey scan using collision-induced dissociation in the linear ion trap: normalized collision energy 35%; activation Q 0.25; electrospray voltage 1.5 kV; capillary temperature 200 °C; and isolation width 2.00. Singly charged ions were excluded from the MS/MS analysis and Xcalibur software version 2.1.0 SP1 build 1160 (Thermo Fisher Scientific, U.K.) was used for data acquisition.

Raw data files were processed using MaxQuant. MS/MS spectra were searched against human protein in Uniprot database. Proteins identified by in-gel digestion proteomics, carbamidomethylation on cysteine and oxidation of methionine with acetylation of protein N-terminal were considered as dynamic and static post-translational modifications, respectively.

Biological activity

Cell culture and MTT assay

Human immortalized keratinocytes (HaCaT) were from Innoprot and were cultured in 10% fetal bovine serum in Dulbecco's modified Eagle's medium, in the presence of 1% antibiotics and 2 mM L-glutamine, in a 5% CO_2 humidified atmosphere at 37 °C. Cells were seeded in 96-well plates at a density of $2 \times 10^3/\text{well}$. Approximately 24 h after seeding, increasing concentrations of the crude extract or pure PC (0.1–1 mg/mL) were added to the cells for different length of time. At the end of each experimental point, cell viability was measured by the tetrazolium salt colorimetric assay (MTT), as described by Arciello et al. (Arciello et al. 2011). Cell survival was expressed as the percentage of viable cells in the presence of the specific molecule compared with control

cells (represented by the average obtained between untreated cells and cells supplemented with the highest concentration of buffer). Each sample was tested in three independent analyses, each carried out in triplicates.

Determination of intracellular ROS levels

The protective effect of crude extract and of pure PC (0.1 or 0.25 mg/mL), against oxidative stress, was measured by determining the intracellular reactive oxygen species (ROS) levels. The protocol used by Del Giudice et al. was followed (Del Giudice et al. 2017), with some modifications. Briefly, cells were exposed for 2 h to the molecules under test and then irradiated by UVA light for 10 min (100 J/cm²). Fluorescence intensity of the fluorescent probe (2',7'-dichlorofluorescein, DCF) was measured at an emission wavelength of 525 nm and an excitation wavelength of 488 nm using a Perkin-Elmer LS50 spectrofluorimeter. Emission spectra were acquired at a scanning speed of 300 nm/min, with 5 slit width both for excitation and emission. ROS production was expressed as

percentage of DCF fluorescence intensity of the sample under test, compared with the untreated sample. Three independent experiments were carried out, each one with three determinations.

Statistical analyses

In all the experiments, samples were analyzed in triplicate. The results are presented as mean of results obtained after three independent experiments (mean \pm SD) and compared by one-way ANOVA according to the Bonferroni's method (post hoc) using Graphpad Prism for Windows, version 6.01.

Results

Effect of carbon dioxide

To establish *G. phlegrea* optimal growth conditions, different concentrations of carbon dioxide were tested: 2, 5, and 20%

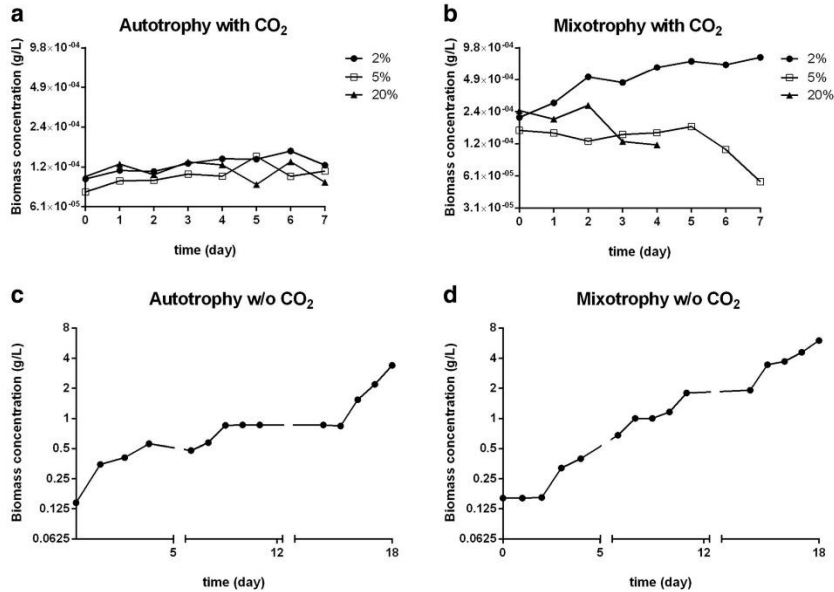
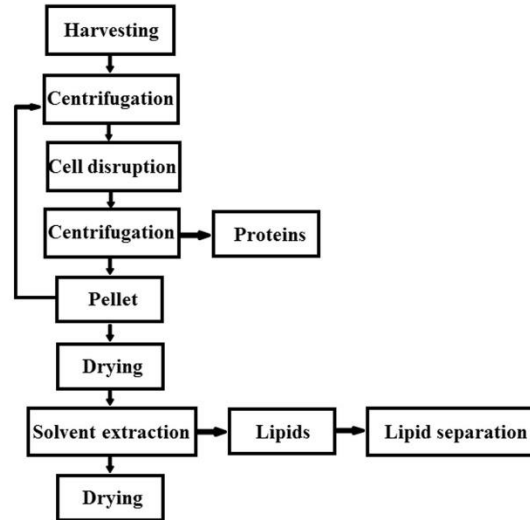


Fig. 1 Growth of *Galdieria phlegrea* in photobioreactors. Cells were grown in the presence on increasing amount of CO₂, and O.D. was measured every day. Growth is expressed as a function of time. **a, c** Cells grown in autotrophy. **b, d** Cells grown in mixotrophy. **a, b** Black

circles, cells grown in the presence of 2% CO₂; empty circles, cells grown in the presence of 5% CO₂; black triangles, cells grown in the presence of 20% CO₂. **c, d** *G. phlegrea* grown in the absence of CO₂, reported as biomass concentration

Fig. 2 A schematic representation of the biorefinery strategy designed



(v/v). As *Galdieria* is the only alga, among Cyanidiales, that can grow autotrophically as well as mixotrophically and heterotrophically, using over 27 kinds of sugars and sugar alcohols (Gross and Schnarrenberger 1995), we compared autotrophy and mixotrophy conditions overtime. Figure 1 a shows algal growth in autotrophic conditions, whereas Fig. 1 b is referred to mixotrophic conditions. CO₂ negatively affected

algal growth in both the experimental conditions analyzed, as an increase of the pH value was observed (pH 3) and a concomitant decrease in the total biomass concentration was found. Accordingly, in the absence of CO₂, a significant increase in the algal growth (up to 3.4 g/L for autotrophic growth and 6 g/L for mixotrophic growth) was observed (Fig. 1c, d). Thus, during mixotrophy (Fig. 1d), the reached

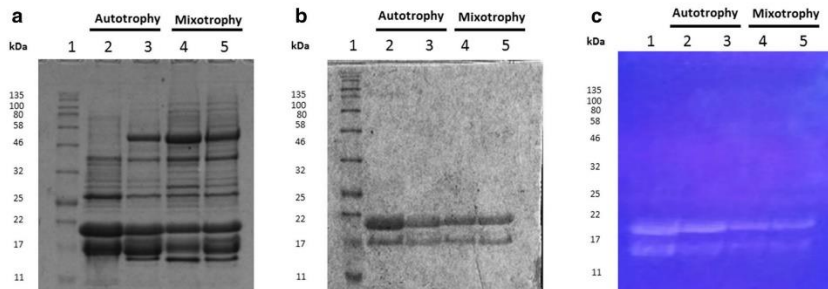


Fig. 3 PC extraction from *Galdieria phlegrea* grown in autotrophic and mixotrophic conditions. SDS-PAGE analysis of samples after French Press extraction. Lane 1: molecular weight markers; lanes 2-3: soluble proteins after the 1st and 2nd cycle of extraction by French Press of biomass grown in autotrophy; lanes 4-5: soluble proteins after the 1st

and 2nd cycle of extraction by French Press of biomass grown in mixotrophy. In all lanes, 30 μ g of total proteins was analyzed. a SDS-PAGE stained by Blue Coomassie. b Unstained gel. c Gel exposed to UV light

Table 1 Extraction yield of *Galdieria phlegrea* grown in autotrophic and mixotrophic conditions

	Total protein (mg)	Total PC (mg)	Protein yield (%)	PC yield (%)	PC/proteins (%)
Autotrophy	45 ± 5	28 ± 4	15 ± 3	9 ± 3	63
Mixotrophy	48 ± 4	31 ± 7	16 ± 2	10 ± 3	64

biomass concentration is almost two-fold higher than during autotrophy (Fig. 1c), suggesting mixotrophy as the best growth condition.

Biorefinery process design

In the context of using microalgae in a biorefinery approach, an efficient model for the recovery and isolation of high-value products was designed. The strategy (Fig. 2) was focused on the subsequent extraction of two class of molecules, phycocyanin and lipids, starting from phycocyanin, which has the highest market value.

Pigments extraction and purification

The harvested biomass was extracted by two cycles of French Press. Supernatants were analyzed by SDS-PAGE followed by Coomassie staining (Fig. 3a) and revealed the presence of two major protein species, whose molecular weight corresponded to those of α - and β -subunits of PC. As PC is a blue colored protein, it is visible also in the absence of any coloration (Fig. 3b), or after exposure to UV light (Fig. 3c), taking advantage of its fluorescent nature. These results suggested that the two major protein species were PC. As shown in Table 1, total proteins and PC extracted by the French Press were very similar in both the analyzed conditions. Interestingly, even though the protein yield was not high, the ratio between PCs and total proteins was higher than 60%, with a relative purity grade of 3. It has been reported that different purity grades indicate different applications of phycocyanin: (i) food grade if purity is ≤ 0.7 , (ii) reagent grade

Table 2 Concentration and purity grade of PC after purification

	PC concentration (mg/mL)	Purity grade (Abs_{620}/Abs_{278})
Autotrophy		
Crude extract	1.9 ± 0.1	3
Fraction 2	0.119 ± 0.003	5.02
Fraction 3	0.224 ± 0.04	5.28
Fraction 4	0.216 ± 0.09	5.01
Mixotrophy		
Crude extract	1.7 ± 0.8	1.9
Fraction 2	0.126 ± 0.03	2.8
Fraction 3	0.243 ± 0.02	2.97
Fraction 4	0.272 ± 0.08	2.76

when the ratio is between 0.7 and 3.9, and (iii) analytical grade if the ratio is ≥ 4.0 (Fernández-Rojas et al. 2014).

The isolation of phycocyanin was performed by a single step of purification, using a size-exclusion chromatography. SDS-PAGE analysis (Figure S1) showed the presence of few protein bands identified as phycocyanin by in situ digestion and mass spectrometry analyses, thus confirming the high purity level of the sample. Moreover, the purity grade reached was higher than 5 for autotrophy and higher than 2 for mixotrophy (Table 2). Thus, we decided to use the residual biomass from autotrophic growth to extract lipids.

The PC was recovered with a rate of 179 mg/g cell mass of *G. phlegrea* through this protocol.

Lipid extraction and purification

According to the circular economy strategy, we extracted lipids as the second class of molecules. The lipid extraction was performed on residual algal biomass after a drying step. In order to verify if lipids extraction could be affected by the previous French Press extraction, in a parallel experiment, lipids were extracted also from the raw dried biomass. As shown in Table 3, the yield of total lipids was 79% for the raw biomass and 21% for the disrupted biomass. The isolation of three different lipid classes was carried out by performing a solid phase extraction (SPE), and results are reported in Table 3. Then, a gas chromatography analysis was performed and the results are reported in Table 4. It is interesting to notice that polyunsaturated, monounsaturated, and saturated fatty acids were present, but a significant increase in PUFAs content was observed in the disrupted biomass, in comparison with the raw one, as reported in Fig. 4. In particular, in the raw material, oleic (MUFA) and linoleic (PUFA) acids (3.72 and 2.00%, respectively) were mainly present, whereas, in the disrupted biomass, ω -3 eicosapentaenoic acid (EPA, 6.81%), the two ω -6 linoleic (LA, 9.61%) and arachidonic acids (AA, 9.00%), and the monounsaturated oleic acid (OA, 4.00%)

Table 3 Yields of total lipids. Mean yields are expressed as a percentage of the algal sample dry weight

	Lipid yield (%)	Neutral lipids (%)	Fatty acids (%)	Phospholipids (%)
Before French press	79 ± 26	68 ± 23	16 ± 2	56 ± 28
Post-French press	21 ± 3	33 ± 2	17 ± 1	41 ± 3

Table 4 Gas chromatography analysis on samples before and after French Press. Polyunsaturated, monounsaturated, and saturated fatty acids are reported as relative percentages

PUFA		Before French press (%)	Post-French press (%)
Fatty acids			
18:3 (<i>n</i> -3)	α -Linoleic acid (ALA)	-	1.31 \pm 0.30
20:5 (<i>n</i> -3)	Eicosapentaenoic acid (EPA)	-	6.81 \pm 1.50
22:5 (<i>n</i> -3)	Docosapentaenoic-n3 acid (DPA)	0.17 \pm 0.04	0.41 \pm 0.10
18:2 (<i>n</i> -6)	Linoleic acid (LA)	2.00 \pm 0.24	9.61 \pm 1.11
18:3 (<i>n</i> -6)	γ -Linoleic acid (GLA)	-	3.30 \pm 0.40
20:3 (<i>n</i> -6)	Dihomo- γ -linoleic acid (DGLA)	0.23 \pm 0.05	2.40 \pm 10
20:4 (<i>n</i> -6)	Arachidonic acid (AA)	0.16 \pm 0.01	9.00 \pm 0.30
22:4 (<i>n</i> -6)	Docosatetraenoic acid (DTA)	-	0.20 \pm 0.01
MUFA			
16:1	Palmitoleic acid (POA)	0.42 \pm 0.01	1.20 \pm 0.20
18:1	Oleic acid (OA)	3.72 \pm 0.80	4.00 \pm 0.70
SFA			
16:0	Palmitic acid (PA)	69.0 \pm 3.3	45.1 \pm 3.0
18:0	Stearic acid (SA)	22.0 \pm 2.1	13.0 \pm 1.5

were present, along with lower percentages of α -linoleic (ALA), γ -linoleic (GLA), dihomogamma-linoleic (DGLA), and palmitoleic (POA) acids.

As for the saturated fatty acids, about 90% were present in the raw material and only 60% in the disrupted biomass, with palmitic and stearic acids as the main species, in the ratio of 3 to 1 in both materials.

Phycocyanin characterization

It is known that PC is endowed with many biological functions, among which the antioxidant activity. In order to verify that the extraction procedures did not affect PC biological activity, we analyzed its ability as an antioxidant agent. First, we analyzed its biocompatibility on immortalized human keratinocytes (HaCaT). Thus, cells were incubated in the

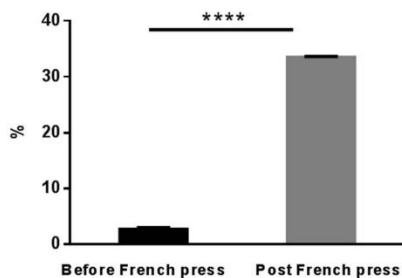


Fig. 4 Percentage of total polyunsaturated fatty acids. The black bar refers to PUFA extracted from the raw biomass and the grey bar to PUFA extracted from the residual biomass after PC extraction. **** p < 0.00005 between the samples

presence of increasing amount of PC (from 0.1 to 1 mg/mL) for different length of time (24–72 h). In a parallel experiment, the crude extract was analyzed as it is widely used to produce functional food or food additives (Chentir et al. 2018). At the end of each incubation, cell viability was assessed by the MTT assay, and cell survival was expressed as the percentage of viable cells in the presence of PC or of the crude extract compared with that of untreated cells. Interestingly, no cytotoxic effect was observed when cells were incubated with pure phycocyanin (Fig. 5a) under all the experimental conditions analyzed. On the other hand, when cells were incubated with the crude extract, a 50% reduction in cell viability was observed at the highest concentration after 72 h of incubation (Fig. 5b).

Once established the complete biocompatibility of purified PC, the protective effect on UVA-stressed HaCaT cells was evaluated. Keratinocytes were chosen as antioxidants should be able to protect the skin from UV-induced oxidative stress, as they are normally present in the outermost layer of the skin. As a source of stress, we used a UVA lamp, commonly used in the nail products industry. Cells were treated with 0.1 mg/mL and 0.25 mg/mL of PC or the crude extract for 2 h, and then oxidative stress was induced by UVA irradiation (100 J/cm²) for 10 min. At the end of the irradiation, H₂-DCFDA was added to measure intracellular ROS level. As shown in Fig. 5c, UVA induced a significant increase in intracellular ROS levels (200%) with respect to untreated cells. Interestingly, cells treated with 0.25 mg/mL of the crude extract showed an increase of intracellular ROS levels in the absence of any treatment, and no protection after UVA treatment, thus suggesting that the crude extract acts as a source of stress per se. Noteworthy, cells treated with 0.25 mg/mL of pure phycocyanin did not show any alteration in ROS level (Fig. 5d), and a significant protection against UVA-induced oxidative stress was observed when cells were treated with either 0.1 or 0.25 mg/mL of the purified PC.

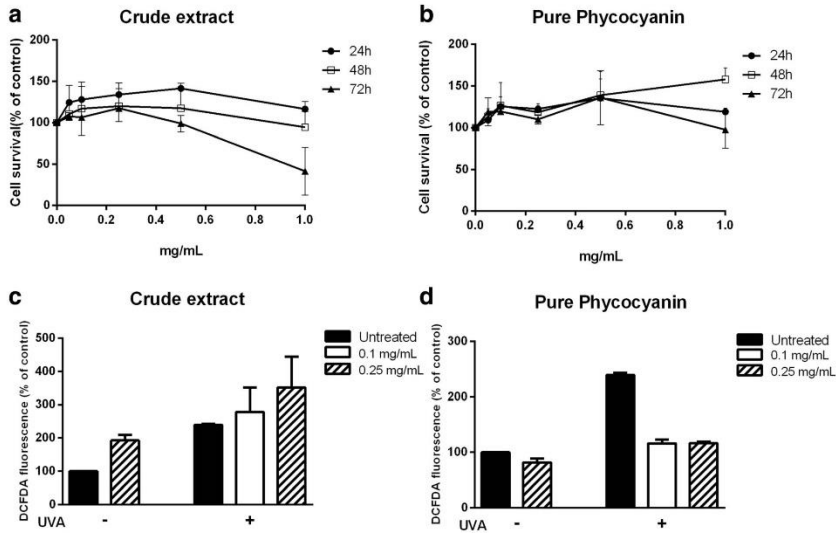


Fig. 5 Effect of crude extract and pure phycocyanin on HaCaT cells. **a, b** Dose-response curves of HaCaT cells after 24-h, 48-h, and 72-h incubation with increasing concentrations of crude extract (**a**) or pure PC (**b**) (0.1–1 mg/mL). Cell viability was assessed by the MTT assay and reported as a function of extract concentration. Data shown are means \pm S.D. of three independent experiments. **c, d** Cells were pre-incubated in the

presence of 0.1 mg/mL and 0.25 mg/mL crude extract (**c**) or pure PC (**d**) for 2 h and then irradiated by UVA (100 J/cm²). Intracellular ROS levels were evaluated by DCFDA assay. Values are expressed as fold increase with respect to control (i.e., untreated) cells. Data shown are means \pm S.D. of three independent experiments. ** p < 0.005, *** p < 0.0005 with respect to UVA-treated cells

Discussion

In this study, we have shown a feasible design to obtain different high-value molecules starting from the wet biomass of *Galdieria phlegrea*. We first extracted proteins and phycocyanin, with a ratio between total phycocyanin and total proteins higher than 60%. This ratio is much higher than that previously reported by Carfagna and colleagues, who found that PC content was about 10% (Carfagna et al. 2018). Moreover, the purity grade of PC in the raw extract was already 3, and became higher than 5 at the end of the single purification step. To the best of our knowledge, this is the first report on the purification of PC from *G. phlegrea* by a single step procedure and with such a high purity grade (Sonani 2016). It must be stressed out that the proposed procedure to isolate PC from *G. phlegrea* is an economical process, as it is obtained from wet biomass, in aqueous buffer and by using a size exclusion chromatography, which could be easily substituted by ultrafiltration in a scaling-up process. Thus, our procedure is economically sustainable and much “greener” than others, which usually use dried biomass or detergents and at least two

purification steps (Sonani 2016). Moreover, PC isolated by this procedure is active as antioxidant molecule when tested on a cell-based model. UV radiations were used to test the antioxidant potential of the purified PC. Indeed, it is well known that UV radiations are considered one of the most harmful exogenous factors for the human skin, as, in addition to the development of erythema, ROS are produced. Particularly, in the last few years, UVA radiations have been used in the nail industry more and more often. A recent paper reported that two healthy women, middle-aged, with no personal or family history of skin cancer, developed squamous cell carcinoma on the dorsum of their hands. Both women reported previous exposure to UVA radiation for cosmetic nail treatment (Diffey 2012). This has prompted some concerns about the safety of this procedure (Diffey 2012). Interestingly, PC was able to counteract the negative effects induced by UVA radiation. PC antioxidant activity at 0.1 mg/mL is in agreement with that one reported *in vivo* by Sonani and coworkers (Sonani et al. 2017) who purified PC from *Synechococcus*, but with a lower purity grade, 4. Even though PC is widely considered as an antioxidant protein, nothing is

reported in literature on its activity on stressed eukaryotic cells, but its activity is rather demonstrated only by in vitro assays, with some concerns from the scientific community (Charalampopoulos et al. 2018).

Moreover, starting from the residual biomass, we isolated polyunsaturated fatty acids. Interestingly, we found that the amount of isolated PUFAs from the broken biomass (34%) was higher than that obtained from the raw biomass (2.5%), suggesting that the biorefinery procedure here described could be a good alternative to obtain PUFAs without using fish oil (about 25% PUFAs) (Miyaguti et al. 2018). Among the several advantages of using PUFAs from microalgae, there is the absence of fishy taste, fishy smell, no risk of carcinogens accumulation, and the possibility to use “vegetarian,” “vegan,” or “organic” labels. Moreover, the world demand of PUFAs is increasing, as it is used for infants, nutritional supplements, and pharmaceuticals (Deschamps 2016). To date, microalgae are considered significant sources of PUFAs, as up to 30–70% of lipids in their cell dry weight is found (Breuer et al. 2013; Chisti 2007; Sun et al. 2018). It is well established that several factors can influence lipid accumulation, such as nitrogen and phosphorus starvation, pH, temperature, and light intensity (Hindersin et al. 2014), leading to a 20% increase (Ramesh Kumar et al. 2019). However, stress conditions imply extremely controlled systems and the possibility to obtain only lipids. In addition, stress conditions enhance the accumulation of intracellular triacylglycerol lipids which contain lower amount of PUFAs with respect to polar lipids, mainly located on the cell membrane (Breuer et al. 2013). By using our procedure, PC and lipids can be easily and economically obtained in a cascade approach.

Acknowledgments Authors would like to thank Dr. Davide Liberti for his work during his Master thesis.

Compliance with ethical standards

Conflict of interest The authors declare that they have no conflict of interest.

Ethical approval This article does not contain any study with human participants or animals.

References

- Allen MM (1968) Simple conditions for growth of unicellular blue-green algae on plates. *J. Phycol.* 4:1–4
- Ankush Nikam. 2019. Phycocyanin market growing at a value CAGR of 7.6% throughout the period of forecast 2018 – 2028 | Daily chronicle. March 7. URL <https://www.dailychronicle24.com/2019/03/07/phycoyanin-market-growing-at-a-value-cagr-of-7-6-throughout-the-period-of-forecast-2018-2028/>
- Arciello A, De Marco N, Del Giudice R, Guglielmi F, Pucci P, Relini A, Monti DM, Piccoli R (2011) Insights into the fate of the N-terminal amyloidogenic polypeptide of ApoA-I in cultured target cells. *J. Cell. Mol. Med.* 15:2652–2663
- Bennett A., Bogorad L., 1973. Complementary chromatic adaptation in a filamentous blue-green alga 58.
- Bergé J-P, Barnathan G (2005) Fatty acids from lipids of marine organisms: molecular biodiversity, roles as biomarkers, biologically active compounds, and economical aspects. *Adv. Biochem. Eng. Biotechnol.* 96:49–125
- Breuer, G., Evers, W.A.C., de Vree, J.H., Kleinegris, D.M.M., Martens, D.E., Wijffels, R.H., Lamers, P.P. 2013. Analysis of fatty acid content and composition in microalgae. *J. Vis. Exp.*
- Carfagna S, Napolitano G, Barone D, Pinto G, Pollio A, Venditti P (2015) Dietary supplementation with the microalga *Galdieria sulphuraria* (Rhodophyta) reduces prolonged exercise-induced oxidative stress in rat tissues. *Oxid. Med. Cell. Longev.* 2015:1–11
- Carfagna S, Landi V, Coraggio F, Salbitani G, Vona V, Pinto G, Pollio A, Ciniglia C (2018) Different characteristics of C-phycoyanin (C-PC) in two strains of the extremophilic *Galdieria phlegrea*. *Algal Res.* 31:406–412
- Charalampopoulos D, Ismail AB, Birch GG, Elmore S, Alasalvar C, Shahidi F, Kilmartin P, Pegg R, Finglas P, Wrostad R, Astley SB, van Camp J, Melton LD, Granato D, Zhou P, Miyashita K, Hidalgo FJ (2018) Antioxidant activity, total phenolics and flavonoids contents: should we ban in vitro screening methods? *Food Chem.* 264: 471–475
- Chauton MS, Reitan KI, Norsker NH, Tvetærås R, Kleivdal HT (2015) A techno-economic analysis of industrial production of marine microalgae as a source of EPA and DHA-rich raw material for aquafeed: research challenges and possibilities. *Aquaculture* 436: 95–103
- Chentir I, Hamdi M, Li S, Doumandji A, Markou G, Nasri M (2018) Stability, bio-functionality and bio-activity of crude phycocyanin from a two-phase cultured Saharian *Arthrospira* sp. strain. *Algal Res.* 35:395–406
- Chisti Y (2007) Biodiesel from microalgae. *Biotechnol. Adv.* 25:294–306
- Cuellar-Bermudez SP, Aguilar-Hernandez I, Cardenas-Chavez DL, Ornelas-Soto N, Romero-Ogawa MA, Parra-Saldivar R (2015) Extraction and purification of high-value metabolites from microalgae: essential lipids, astaxanthin and phycobiliproteins. *Microb. Biotechnol.* 8:190–209
- Del Giudice, R., Petruk, G., Raiola, A., Barone, A., Monti, D.M., Rigano, M.M., 2017. Carotenoids in fresh and processed tomato (*Solanum lycopersicum*) fruits protect cells from oxidative stress injury. *J. Sci. Food Agric.* 97.
- Deschamps, N., 2016. Nutritional supplements in the U.S., 7th Edition. URL <https://www.prnewswire.com/news-releases/nutritional-supplements-in-the-us-7th-edition-300469500.html>
- Diffey BL (2012) The risk of squamous cell carcinoma in women from exposure to UVA lamps used in cosmetic nail treatment. *Br. J. Dermatol.* 167:1175–1178
- Fernández-Rojas B, Hernández-Juárez J, Pedraza-Chaverri J (2014) Nutraceutical properties of phycocyanin. *J. Funct. Foods.*
- González-Delgado Á-D, Kafarov V (2011) Microalgae based biorefineries: issues to consider. *Ciencia, Tecnol. y Futur* 4:5–22
- Gross W, Schnarrenberger C (1995) Heterotrophic growth of two strains of the acidothermophilic red alga *Galdieria sulphuraria*. *Plant Cell Physiol.* 36:633–638
- Hindersin S, Leupold M, Kerner M, Hanelt D (2014) Key parameters for outdoor biomass production of *Scenedesmus obliquus* in solar tracked photobioreactors. *J. Appl. Phycol.* 26:2315–2325
- Leu S, Boussiba S (2014) Advances in the production of high-value products by microalgae. *Ind. Biotechnol.* 10:169–183
- Manirafasha, E., Ndikubwimana, T., Zeng, X., Lu, Y., Jing, K., 2016. Phycobiliprotein: potential microalgae derived pharmaceutical and biological reagent. *Biochem. Eng. J.*

- Mehta P, Singh D, Saxena R, Rani R, Gupta RP, Puri SK, Mathur AS (2018) High-value coproducts from algae—an innovational way to deal with advance algal industry. *Waste to Wealth*:343–363
- Miyaguti NADS, de Oliveira SCP, Gomes-Marcondes MCC (2018) Maternal nutritional supplementation with fish oil and/or leucine improves hepatic function and antioxidant defenses, and minimizes cachexia indexes in Walker-256 tumor-bearing rats offspring. *Nutr. Res.* 51:29–39
- Moody JW, McGinty CM, Quinn JC (2014) Global evaluation of biofuel potential from microalgae. *Proc. Natl. Acad. Sci. U. S. A.* 111:8691–8696
- Patel HM, Rastogi RP, Trivedi U, Madamwar D (2018) Structural characterization and antioxidant potential of phycocyanin from the cyanobacterium *Geitlerinema* sp. H8DM. *Algal Res.* 32:372–383
- Patel A, Matsakas L, Hružová K, Rova U, Christakopoulos P (2019) Biosynthesis of nutraceutical fatty acids by the oleaginous marine microalgae *Phaeodactylum tricoratum* utilizing hydrolysates from organosolv-pretreated birch and spruce biomass. *Mar. Drugs* 17:119
- Posada JA, Brentner LB, Ramirez A, Patel MK (2016) Conceptual design of sustainable integrated microalgae biorefineries: parametric analysis of energy use, greenhouse gas emissions and techno-economics. *Algal Res.* 17:113–131
- Quinn JC, Davis R (2015) The potentials and challenges of algae based biofuels: a review of the techno-economic, life cycle, and resource assessment modeling. *Bioresour. Technol.* 184:444–452
- Ramesh Kumar B, Deviram G, Mathimani T, Due PA, Pugazhendhi A (2019) Microalgae as rich source of polyunsaturated fatty acids. *Biocentral. Agric. Biotechnol.* 17:583–588
- Romay C, González R, Ledón N, Remírez D, Rimbau V (2003) C-phycocyanin: a biliprotein with antioxidant, anti-inflammatory and neuroprotective effects. *Curr. Protein Pept. Sci.* 4:207–216
- Rutz J, Olivier G, de Vree J, Bosma R, Willems P, Reith JH, Eppink MHM, Kleinegris DMM, Wijnfels R1, Barbosa MJ (2016) Towards industrial products from microalgae. *Energy Environ. Sci.* 9:3036–3043
- Sakurai T, Aoki M, Ju X, Ueda T, Nakamura Y, Fujiwara S, Umemura T, Tsuzuki M, Mimoda A (2016) Profiling of lipid and glycogen accumulations under different growth conditions in the sulfotolerant red alga *Galdieria sulphuraria*. *Bioresour. Technol.* 200:861–866
- Sonani RR (2016) Recent advances in production, purification and applications of phycobiliproteins. *World J. Biol. Chem.* 7:100
- Sonani RR, Patel S, Bhastana B, Jakharia K, Chaubey MG, Singh NK, Madamwar D (2017) Purification and antioxidant activity of phycocyanin from *Synechococcus* sp. R42DM isolated from industrially polluted site. *Bioresour. Technol.* 245:325–331
- Spolaore P, Joannis-Cassan C, Duran E, Isambert A (2006) Commercial applications of microalgae. *J. Biosci. Bioeng.* 101:87–96
- Sun XM, Geng LJ, Ren LJ, Ji XJ, Hao N, Chen KQ, Huang H (2018) Influence of oxygen on the biosynthesis of polyunsaturated fatty acids in microalgae. *Bioresour. Technol.*
- Tredici MR, Rodolfi L, Biondi N, Bassi N, Sampietro G (2016) Techno-economic analysis of microalgal biomass production in a 1-ha Green Wall Panel (GWP®) plant. *Algal Res.* 19:253–263
- Wu HL, Wang GH, Xiang WZ, Li T, He H (2016) Stability and antioxidant activity of food-grade phycocyanin isolated from *Spirulina platensis*. *Int. J. Food Prop.* 19:2349–2362
- Zárate R, el Jaber-Vazdekis N, Tejera N, Pérez JA, Rodríguez C (2017) Significance of long chain polyunsaturated fatty acids in human health. *Clin. Transl. Med.* 6

Publisher's note Springer Nature remains neutral with regard to jurisdictional claims in published maps and institutional affiliations.

Applied Microbiology and Biotechnology

A cascade extraction of active phycocyanin and fatty acids from *Galdieria phlegrea*

Paola Imbimbo^a, Valeria Romanucci^a, Antonino Pollio^b, Carolina Fontanarosa^a, Angela Amoresano^a, Armando Zarrelli^a, Giuseppe Olivieri^{a,c*}, Daria Maria Monti^{a*}

^a Department of Chemical Sciences, University of Naples Federico II, via Cinthia 4, 80126, Naples, Italy

^b Department of Biology, University of Naples Federico II, via Cinthia 4, 80126, Naples, Italy

^c Bioprocess Engineering Group, Wageningen University and Research, Droevendaalsesteeg 1, 6700AA, Wageningen, the Netherlands

*Corresponding Authors: G.O. giuseppe.olivieri@wur.nl; D.M.M. mdmonti@unina.it. Tel. +39 081-679150; Fax +39 081-674090.

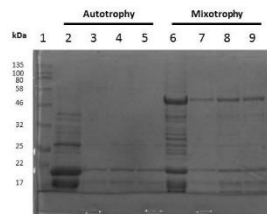


Figure S1. PC purification from *Galdieria phlegrea* extracts grown in autotrophic and mixotrophic conditions. SDS-PAGE analysis of samples after purification. Lane 1: molecular weight markers; lane 2: soluble proteins extracted by French Press grown in autotrophy (30 μg); lanes 3-5: samples eluted by the size-exclusion chromatography (5 μg); lane 6: soluble proteins extracted by French Press grown in mixotrophy (30 μg). lanes 7-9: samples eluted by the size-exclusion chromatography (5 μg).



Contents lists available at ScienceDirect

Industrial Crops & Products

journal homepage: www.elsevier.com/locate/indcrop

Bioactivity, biocompatibility and phytochemical assessment of lilac sage, *Salvia verticillata* L. (Lamiaceae) - A plant rich in rosmarinic acid

Jelena S. Katanić Stanković^{a,*}, Nikola Srećković^b, Danijela Mišić^c, Uroš Gašić^{c,d}, Paola Imbimbo^e, Daria Maria Monti^c, Vladimir Mihailović^b

^a Institute for Information Technologies Kragujevac, Department of Science, University of Kragujevac, Jovana Cvijića bb, 34000 Kragujevac, Serbia

^b Department of Chemistry, Faculty of Science, University of Kragujevac, Radoja Domanovića 12, 34000 Kragujevac, Serbia

^c Institute for Biological Research "Siniša Stanković" - National Institute of Republic of Serbia, University of Belgrade, Bulevar despota Stefana 142, 11060 Belgrade, Serbia

^d University of Belgrade, Faculty of Chemistry, P. O. Box 51, 11158 Belgrade, Serbia

^e Department of Chemical Sciences, University of Naples Federico II, Complesso Universitario Monte Sant'Angelo, via Cinthia 4, 80126 Naples, Italy

ARTICLE INFO

Keywords:

Salvia verticillata L.
Lilac sage
Antioxidant
Antimicrobial
Biocompatibility
Phytochemical analysis

ABSTRACT

The plants from genus *Salvia*, as one of the largest genus in Lamiaceae family, are frequently in use for various purposes, as foods, in cosmetic industry, or in traditional and official medicine. *Salvia verticillata* L. (lilac sage) is one of sidelined sage species with potential bioactivity, reported in traditional medicine. The aim of this study was to acquire a phytochemical profile of the methanol extract obtained from *S. verticillata* aerial parts and to evaluate its antioxidant, antimicrobial, and biocompatibility potential. Characteristic compounds of the genus *Salvia*, such as rosmarinic and caffeic acids, along with their derivatives (e.g. salvianolic and yunaneic acids isomers) and flavonoids, have been identified by ultrahigh-performance Orbitrap metabolomic fingerprinting as the main phenolic metabolites in *S. verticillata*. The extract displayed moderate antimicrobial properties and significant antioxidant potential, with the half maximal inhibitory concentration values (IC₅₀) ranging from 33 to 73 µg/mL. Importantly, full biocompatibility of the extract with eukaryotic cell lines was observed up to 72 h. The obtained results revealed the presence of polyphenolic bioactive compounds in *S. verticillata* extract with promising antioxidant potential and significant biocompatibility. In this regard, *S. verticillata* can find new perspectives of application as a food ingredient, in cosmetic and pharmaceutical industries, as it represents a valuable source of compounds with prominent health properties, with a special focus on rosmarinic acid.

1. Introduction

The genus *Salvia*, the largest genus in the Lamiaceae family, consists of over a thousand plant species distributed worldwide (Lu and Yeap Foo, 2002; Walker et al., 2004). The name of the genus was derived from the Latin word "salvare", which means "to heal/to save" (Topçu, 2006). The *Salvia* species are aromatic plants used as food spices and culinary herbs, as tea, in cosmetic industries, and in traditional medicine because of their bioactive properties (Ghorbani and Esmailizadeh, 2017). Since ancient times, the most known and most used *Salvia* spp. is a common sage (*Salvia officinalis* L.). This sage is used as a spice in food products, in traditional medicine for different ailments such as hemorrhage, menstrual disorders like dysmenorrhea, against tuberculosis, as well as in the treatment of numerous inflammatory diseases, dyspepsia, diarrhea, age-related cognitive disorders, tremor, excessive sweating, and hyperglycemia (EMA, 2016; Ghorbani and

Esmailizadeh, 2017; Sharifi-Rad et al., 2018; Topçu, 2006). Besides *S. officinalis*, many other plants from genus *Salvia* are in use due to their biological benefits. For example, roots of red sage (*Salvia miltiorrhiza* Bunge) are highly respected and widely utilized in the treatment of cardiovascular and cerebrovascular diseases (Chen and Chen, 2018; Zhang et al., 2016). Also, chia seeds (*Salvia hispanica* L.) are used worldwide for their multifunctional properties and benefits to human health (Parker et al., 2018). One *Salvia* spp. that is marginalized from the use in modern pharmacological and functional food formulations is *Salvia verticillata* L.

Salvia verticillata L., called "lilac sage" or even "purple rain", is a herbaceous perennial herb with tiny lilac-blue flowers which grow tightly packed in whorls (Forouzin et al., 2015). This plant has been employed in the cheese-making process to obtain specific taste and for the preservation of meat products and cheese (Topçu, 2006). In Serbia, this herb is known by the name "sjeruša" that indicates its use for

* Corresponding author.

E-mail address: jkatanic@kg.ac.rs (J.S. Katanić Stanković).

<https://doi.org/10.1016/j.indcrop.2019.111932>

Received 13 May 2019; Received in revised form 31 October 2019; Accepted 31 October 2019

Available online 13 November 2019

0926-6690/ © 2019 Elsevier B.V. All rights reserved.

flavoring in cheese production. In traditional Serbian medicine, *S. verticillata* tea, made from its aerial parts, has been used as an expectorant, for disinfection of the oral cavity and as cataplasm for healing wounds (Jarić et al., 2015).

The chemical composition of *Salvia* plants is mostly comprised of several groups of secondary metabolites: terpenes (mono-, di-, and tri-terpenes), phenolic compounds (flavonoids and phenolic acids), and saccharides (Ghorbani and Esmailzadeh, 2017; Lu and Yeap Foo, 2002; Topçu, 2006; Xu et al., 2018). Moreover, a wide range of terpenoid compounds (e.g., tanshinones, camphor, caryophyllene, borneol, α - and β -thujone) and polyphenolics (with characteristic high content of rosmarinic acid, caffeic acid and its metabolites salvianolic and yunnanic acids) detected in *Salvia* spp. were found to endow a vast array of recorded bioactivities (Ghorbani and Esmailzadeh, 2017; Jassbi et al., 2016; Lu and Yeap Foo, 2002; Sharifi-Rad et al., 2018; Topçu, 2006; Wu et al., 2012; Xu et al., 2018).

In this respect, the aim of the presented study was to thoroughly investigate the phytochemical profile of methanol extract obtained from *S. verticillata* aerial parts (herein denoted as SV), to quantify targeted compounds, to evaluate its antioxidant and antimicrobial properties (antibacterial and antifungal), as well as its cytotoxicity on different cancer and immortalized cell lines.

2. Materials and methods

2.1. Chemicals

The reagents and chemicals used in the assays for evaluation of total phenolic compounds, antioxidant and antimicrobial activities were purchased from Sigma Aldrich (Steinheim, Germany) and Alfa Aesar (Karlsruhe, Germany). Nutrient agar (NA), Sabouraud dextrose agar (SDA), Müller-Hinton broth (MHB), and Sabouraud dextrose broth (SDB) were purchased from Torlak Institute of Virology, Vaccines and Sera (Belgrade, Serbia). Standards of 5-O-caffeoylquinic acid (chlorogenic acid), caffeic acid, quercetin 3-O-rutinoside (rutin), quercetin 3-O-rhamnoside (quercitrin), rosmarinic acid, salvianolic acid B, apigenin-7-O-glucoside (apigenitrin), apigenin, carnosol, and carnosic acid were purchased from Sigma Aldrich (Steinheim, Germany).

2.2. Plant material and extract preparation

The aerial parts of *Salvia verticillata* L. (Lamiaceae) were collected in July 2016 during flowering season in the area of village Prijedor (43°55'19.3"N 20°15'14.5"E), near the Ovčar-Kablar Gorge (Western Serbia) by J. S. Katančić Stanković. A voucher specimen (No. 125/016) was deposited in the Herbarium of the Department of Biology and Ecology, Faculty of Science, University of Kragujevac (Kragujevac, Serbia). Taxonomic and botanical identification was confirmed by Dr. Milan S. Stanković. The air-dried *S. verticillata* aerial parts (130 g) were finely powdered and macerated with methanol at the room temperature for 24 h three times (500 mL each). The extract was filtered and the solvent was entirely removed using the rotary evaporator (RV 10 basic, IKA, Staufen, Germany) under low pressure to obtain the dry extract. The final weight of *S. verticillata* dry extract (SV) was 16.8 g. The percentage yield of SV was found to be 12.92% (w/w). The concentrations used in the experiments were based on the dry weight of the extract.

2.3. Determination of phenolic compounds

2.3.1. Total phenolic content (TPC)

The total phenolic content was estimated according to Singleton et al. (1999). Concisely, in 0.5 mL of SV extract (0.5 mg/mL) 2.5 mL of Folin-Ciocalteu reagent (diluted 10-fold) and 2 mL of NaHCO₃ (7.5%) were added. The absorbance was measured at 765 nm on UV-Vis double beam spectrophotometer Halo DB-20S (Dynamica GmbH, Dietikon, Switzerland) with temperature control after 15 min of

incubation. TPC value was expressed as gallic acid equivalents (mg GA/g dry extract).

2.3.2. Total flavonoids content

The total flavonoid content was determined using the AlCl₃-method according to Brighente et al. (2007). The aluminum trichloride solution (0.5 mL, 2% AlCl₃) and the same volume of a methanol solution of SV (0.5 mg/mL) were incubated for 1 h at room temperature and the absorbance was measured at 415 nm. The total flavonoid content was expressed as rutin equivalents (mg RU/g extract).

2.3.3. Total flavonols content

Total flavonols content in the extract was evaluated by the method of Yermakov et al. (1987). The SV extract (1 mL, 1 mg/mL) was mixed with AlCl₃ (1 mL, 2%) and sodium acetate (3 mL, 50 mg/mL). The absorbance was read after 2.5 h at 440 nm. The content of flavonols was calculated as rutin equivalents and expressed as mg RU/g extract.

2.3.4. Total phenolic acids content

Total phenolic (hydroxycinnamic) acids content was adopted from Polish Pharmacopoeia as reported by Matkowski et al. (2008). Distilled water (5 mL) was added to SV (1 mL, 1 mg/mL). Thereafter, the mixture of HCl (1 mL, 0.1 M), Arnow reagent (1 mL, 10% w/v of sodium molybdate and 10% w/v sodium nitrite) and NaOH (1 mL, 1 M) was added and filled up to 10 mL. The absorbance was read immediately at 490 nm. The result was expressed as caffeic acid equivalents (mg CA/g extract).

2.4. UHPLC/MS-MS orbitrap analysis

Separations of compounds of interest were performed using an ultrahigh-performance liquid chromatography (UHPLC) system consisting of a quaternary Accela 600 pump and Accela autosampler (ThermoFisher Scientific, Bremen, Germany). A Syncronis C18 column (100 × 2.1 mm, 1.7 μ m particle size), thermostated at 40°C, was used for compounds separation. The flow rate was set to 300 μ L/min and the mobile phase consisted of 0.1% acetic acid in water (A) and acetonitrile (B). The injection volumes were 5 μ L and the linear gradient program was previously described (Božunović et al., 2018).

The UHPLC system was coupled to a linear ion trap - orbitrap mass spectrometer (LTQ Orbitrap MS) equipped with heated electrospray ionization probe (HESI-II, ThermoFisher Scientific, Bremen, Germany) operating in negative ionization mode. Parameters of the ion source were as in the literature (Božunović et al., 2018). The MS spectra were acquired by full-range acquisition covering 100-1000 *m/z*. The resolution was set to 30,000 for full scan analysis. The data-dependent MS/MS events were always performed on the most intense ions detected in the full scan MS. The ions of interest were isolated in the ion trap with an isolation width of 3 ppm and activated with 35% collision energy levels.

Xcalibur software (version 2.1) was used for the instrument control, data acquisition, and analysis. The identification of unknown compounds was done by exact mass search of their deprotonated molecule ($[M - H]^-$) and its MSⁿ fragmentation, as well as by literature search of available chromatographic and MS data.

2.5. UHPLC-DAD/(-)HESI-MS/MS analysis

Targeted phenolic compounds were quantified using Dionex Ultimate 3000 UHPLC system (Thermo Fisher Scientific, Bremen, Germany) configured with a triple-quadrupole mass spectrometer (TSQ Quantum Access Max, Thermo Fisher Scientific, Basel, Switzerland) with a heated electrospray ionization (HESI) source. Phenolics in the methanol extract of *S. verticillata* were chromatographically separated on Hypersil gold C18 column (50 × 2.1 mm) with 1.9 μ m particle size (Thermo Fisher Scientific, USA), thermostated at 30°C. The mobile

phase, applied with a flow rate of 0.4 mL/min, consisted of 0.02% acetic acid in water (A) and LC-MS grade acetonitrile (B). Elution was performed according to Mišić et al. (2015), while the settings of the mass spectrometer were as described in Boroja et al. (2018): vaporizer temperature 350°C, spray voltage 3510 V, sheath gas (N₂) pressure 28 AU, ion sweep gas pressure 0 AU and auxiliary gas pressure at 4 AU, capillary temperature at 270°C, capillary offset 35 V, and skimmer offset 0 V. Targeted compounds were quantified in a selected reaction monitoring (SRM) mode of the mass spectrometer operated in the negative ionization mode. Collision-induced fragmentation was achieved using argon as the collision gas and collision energy was set to 30 eV.

Compounds were quantified by the external standard quantification procedure. Salvianolic acid C, rosmarinic acid hexoside, and methylrosmarinic acid were quantified relatively, based on the calibration curve of rosmarinic acid, while dicaffeoylquinic acid was quantified using the calibration curve of caffeic acid. Stock standard solutions were prepared by dissolving 1 mg of a pure compound in 1 mL methanol, and working standard solution was further prepared by mixing the stock solutions of pure compounds in methanol to obtain the concentration of 100 µg/mL. Calibration levels in the concentration range from 20 to 0.002 µg/mL were obtained by diluting the working solution with methanol. Determination of the limit of detection (LOD), limit of quantitation (LOQ), linearity, repeatability, and sensitivity of the developed UHPLC-DAD/(-)HESI-MS/MS method was performed. The LOD and LOQ were determined as peak-to-peak values by the signal-to-noise ratios (S/N), with S/N > 3 for LOD and S/N > 10 for LOQ. Five replicates of each calibration level were run for LOD and LOQ testing. Regressions of calibration curves showed good linearity with correlation coefficients between $r = 0.990$ and 0.999 , $p < 0.001$. The amounts of targeted compounds in the sample were expressed as µg per 100 mg of dry extract (µg/100 mg d.e.).

2.6. Antimicrobial activity

2.6.1. Tested microorganisms

The bacterial and fungal cultures (ATCC cultures and the clinically isolated strains) were used to evaluate the antimicrobial activity of *S. verticillata* extract. Sixteen microorganisms were tested, eight bacterial and eight fungal strains. In particular, the bacterial strain tested were: *Micrococcus lysodeikticus* ATCC 4698, *Enterococcus faecalis* ATCC 29212, *Escherichia coli* ATCC 25922, *Klebsiella pneumoniae* ATCC 70063, *Pseudomonas aeruginosa* ATCC 10145, *Bacillus cereus* ATCC 10876, *Bacillus mycoides* FSB 1, and *Azobacter chroococcum* FSB 14; and the eight fungal strains were: *Candida albicans* ATCC 10259, *Aspergillus brasiliensis* ATCC 16404, *Fusarium oxysporum* FSB 91, *Alternaria alternata* FSB 51, *Aureobasidium pullulans* FSB 61, *Trichoderma harzianum* FSB 12, *Penicillium canescens* FSB 24, and *Doratomyces stemonitis* FSB 41. All microbial strains were obtained from the Institute of Public Health Kragujevac, University of Kragujevac, Serbia and Laboratory for Microbiology, Department of Biology, Faculty of Science, University of Kragujevac, Kragujevac, Serbia. The bacteria and fungi cultures were stored at 4°C and subcultured once a month. Bacterial strains were cultured overnight at 37°C in nutrient agar (NA) and fungi were cultured on Sabouraud dextrose agar (SDA) and potato glucose agar (PDA) at 28°C for 3 days.

2.6.2. Antibacterial activity tests

The minimum inhibitory concentration (MIC) of SV extract against tested microorganisms was determined based on the microdilution method in 96 multi-well microtiter plates (Sarker et al., 2007), with some modifications. All tests were performed in Müller–Hinton broth (MHB). Briefly, a fresh overnight culture of bacteria was suspended in sterile 0.85% saline (8.5 g/L NaCl) and adjusted by the colorimeter to a concentration of 5×10^8 CFU/mL (colony-forming units per milliliter) (CLSI, 2012). Different solvent dilutions of plant extract were dissolved in 5% dimethyl sulfoxide (DMSO) in sterile water and added to over the

wells containing 50 µL of MHB; then, 10 µL of resazurin indicator solution (6.25 mg/mL in sterile distilled water) and 30 µL of MHB were added to each well. Finally, 10 µL of bacterial colony suspension was added to all the wells. The final bacterial concentration of in each well was 5×10^5 CFU/mL (CLSI, 2012). For each strain, the growth conditions and the sterility of the medium were checked. Standard antibiotic chloramphenicol was used to control the sensitivity of the tested bacteria. The microplates were incubated for 24 h at 37°C. Any color change of the indicator from purple to pink or colorless was recorded as positive. The lowest concentration that produced a significant inhibition of the growth of the bacteria in comparison with the positive control was identified as the MIC.

2.6.3. Antifungal activity tests

The fungal colonies were washed from the surface of agar plates with sterile 0.85% saline and the inoculum suspension was adjusted to a concentration of 5×10^4 CFU/mL according to NCCLS recommendation (NCCLS, 2002a,b). Identically, the 2-fold serial microdilution method was used for determination of MIC. The test was performed on Sabouraud dextrose broth (SDB). The SV extract (50 µL) was dissolved in sterile water to obtain a concentration of 40 mg/mL, added into the first row of the plate and double dilutions were made in all the other rows that were filled with 50 µL of SDB. Thereafter, 10 µL of SDB was added in all wells followed by addition of fungal inoculum suspension. For each strain, the growth conditions and the sterility of the medium were checked. Nystatin was used as the control against the tested fungi. Plates were placed in an incubator at 28°C for 48 h. The lowest concentrations without visible growth of fungi were defined as MICs.

2.7. Antioxidant activity

2.7.1. Total antioxidant capacity

The total antioxidant capacity of SV (Prieto et al., 1999) was monitored by the formation of a green phosphate/Mo (V) complex at acid pH. In 0.3 mL of extract solution (0.5 mg/mL) was added 3 mL of reagent solution (0.6 M sulfuric acid, 28 mM sodium phosphate and 4 mM ammonium molybdate). Then, the mixtures were incubated at 95°C for 90 min. After cooling to room temperature, the absorbance of the solution was measured at 695 nm. The total antioxidant capacity is expressed as ascorbic acid equivalents (mg AA/g).

2.7.2. 2,2-Diphenyl-1-picrylhydrazyl (DPPH) free-radical scavenging activity

To determine scavenging DPPH radical activity different concentrations of SV in methanol (2 mL, eight double dilutions from 2 mg/mL) were mixed with the same volume of DPPH solution (80 µg/mL) (Kumarasamy et al., 2007). After 30 min of incubation at room temperature, the absorbance was measured at 517 nm. Ascorbic acid (AA) and butylated hydroxytoluene (BHT) were used as reference standards. The DPPH free-radical scavenging activity (%) was calculated with the following equation [Eq. 1]:

$$(1) \% \text{ radical scavenging activity} = [(A_{\text{control}} - A_{\text{sample}}) / A_{\text{control}}] \times 100$$

where A_{control} is the absorbance of the DPPH radical in methanol and A_{sample} is the absorbance of the samples. The IC₅₀ value, which is the concentration of the test material that reduces 50% of the free-radical concentration, was calculated as µg/mL through a sigmoidal dose-response curve.

2.7.3. 2,2'-Azinobis-(3-ethylbenzothiazoline-6-sulfonic acid) diammonium (ABTS) radical-cation scavenging activity

The ABTS radical cation scavenging activity was estimated by the method described by Re et al. (1999). The radical cation (ABTS⁺) was generated by reacting 7 mM stock solution of ABTS (2,2'-azinobis(3-

ethylbenzothiazoline-6-sulfonic acid) diammonium salt) with 2.45 mM potassium persulfate and the mixture was left to stand in the dark at room temperature for 16 h before use. The ABTS⁺ solution was diluted with 5 mM phosphate-buffered saline (pH 7.4) to rich the absorbance of 0.70 ± 0.02 at 734 nm. After 30 min from the addition of 100 μ L of sample to 900 μ L of ABTS⁺ solution, the absorbance was measured at 734 nm. Two compounds, AA and BHT, were used as reference antioxidants. A control sample was prepared to contain the same volume without test compounds or reference antioxidants. The percent of ABTS⁺ scavenging activity of the samples was calculated using a previous equation [Eq. 1] and IC₅₀ values were expressed as previous using a sigmoidal dose-response curve.

2.7.4. Nitric oxide radical scavenging activity

Nitric oxide radical (NO) scavenging capacity was measured using the Griess reaction, according to the method described by Green et al. (1982). The samples (0.5 mL of SV or reference antioxidants AA and BHT) at different concentrations were mixed with the same volume of 5 mM sodium nitroprusside dissolved in 0.01 M phosphate-buffered saline (NaCl 0.138 M; KCl 0.0027 M, pH 7.4). Incubation was performed at 25°C for 2.5 h, and after that 1 mL of Griess reagent (1% sulphani-lamide, 2% orthophosphoric acid, and 0.1% N-(1-naphthyl)ethylene-diamine dihydrochloride) was added to the mixture. After an additional incubation at 25°C for 30 min, the absorbance of the solution was measured at 546 nm. The results of nitric oxide radical scavenging activity were expressed as IC₅₀.

2.7.5. Determination of the inhibitory activity toward lipid peroxidation

The thiocyanate method (Hsu et al., 2008) was used to determine the antioxidant activity of SV extract in an oil-in-water emulsion. The extract or reference compounds (0.5 mL; SV, AA, and BHT) were added to linoleic acid emulsion (2.5 mL; 0.2804 g linoleic acid, 0.2804 g Tween-80 as an emulsifier in 50 mL 40 mM phosphate buffer, pH 7.0) and the mixture was homogenized. The final volume was adjusted to 5 mL with phosphate buffer (40 mM, pH 7.0). After incubation at 37°C in the dark for 72 h, a 0.1 mL aliquot of the reaction solution was mixed with methanol (4.7 mL, 75%), FeSO₄ (0.1 mL, 20 mM), and ammonium thiocyanate (0.1 mL, 30%). The absorbance of this mixture was measured at 500 nm, after 3 min of stirring. Inhibition percent of linoleic acid peroxidation was calculated using the following equation [Eq. 2]:

$$\% \text{ inhibition} = [(A_{\text{control}} - A_{\text{sample}}) / A_{\text{control}}] \times 100 \quad (2)$$

where A_{control} is the absorbance of the control and A_{sample} is the absorbance of the samples. The IC₅₀ values were calculated as μ g/mL through a sigmoidal dose-response curve.

2.7.6. Measurement of ferrous ion chelating ability

The ferrous ion chelating activity of SV extract was measured by the decrease in absorbance at 562 nm of the iron (II)-ferrozine complex (Yan et al., 2006). Iron (II) sulfate (1 mL, 0.125 mM FeSO₄) was added to 1 mL sample (with different dilutions), followed by ferrozine (1 mL, 0.3125 mM). After 10 min the absorbances of the mixtures were measured. AA and BHT were used as standards. The ability of the sample to chelate ferrous ion was calculated relative to the control (consisting of iron and ferrozine only) using the equation [Eq. 3]:

$$\% \text{ chelating effect} [(A_{\text{control}} - A_{\text{sample}}) / A_{\text{control}}] \times 100 \quad (3)$$

where A_{control} is the absorbance of the control and A_{sample} is the

absorbance of the samples. The IC₅₀ values were calculated as previous using a sigmoidal dose-response curve.

2.8. Biocompatibility analysis

Murine BALBC-3T3 (fibroblasts), human A431 (epidermoid carcinoma), HepG2 (hepatic carcinoma), and LoVo (colorectal adenocarcinoma) cells were obtained from ATCC, whereas HaCaT (primary epidermal keratinocyte) cells were from AddexBio (San Diego, CA, USA). All cells were cultured in Dulbecco's modified Eagle's medium (DMEM) (Sigma-Aldrich, St Louis, MO, USA), supplemented with 10% fetal bovine serum (HyClone), 2 mM L-glutamine and antibiotics, all from Sigma-Aldrich, under a 5% CO₂ humidified atmosphere at 37°C. For toxicity experiments, cells were seeded in 96-well plates at a density of 2.5×10^3 cells per well. Twenty-four hours after seeding, increasing concentrations of SV extract were added to the cells (5–50 μ g/mL). Cell viability was assessed by the MTT (3-(4,5-dimethylthiazol-2-yl)-2,5-diphenyltetrazolium bromide) assay after 48–72 h, as described by Petruk et al. (2016).

2.9. Statistical analysis

The data are expressed as the mean \pm standard deviation (SD). The IC₅₀ for *in vitro* antioxidant potential was calculated using nonlinear regression analysis from the sigmoidal dose-response inhibition curve using OriginPro 8 Software. For statistical analyses of the data, the analysis of variance (ANOVA) was applied and the group means were compared with the least significant difference test (LSD). The results were considered statistically significant at $p < 0.05$.

3. Results

3.1. Phytochemical composition of *S. verticillata* extract

The spectrophotometrically measured contents of total phenolic compounds, along with total flavonoids, flavonols, and phenolic acids in SV extract are shown in Table 1. Data indicated a high content in total phenolics in aerial parts of *S. verticillata*, with flavonoids (244.4 mg QU/g d.e.) and phenolic acids (41.9 mg CA/g d.e.) as the most abundant phytochemicals.

The qualitative evaluation of phenolic compounds in methanol extract of *S. verticillata* aerial parts was performed using high resolution mass spectrometry (HRMS) in combination with MS⁴ fragmentation. The obtained UHPLC-MS³ Orbitrap metabolic fingerprinting data of SV extract resulted in the detection of totally 29 phenolic compounds (Table 2) and the corresponding base peak chromatogram is depicted in Fig. 1. The identified compounds can be divided into two structurally different groups: 1) phenolic acids and their derivatives (21 compounds) and 2) flavonoids and their derivatives (8 compounds). Among all identified compounds, eight were confirmed using available standards, while the others were identified using HRMS technique (exact mass search of their deprotonated molecule [M-H]⁻) and MS², MS³, and MS⁴ fragmentation behavior, as well as the comparison with the available literature. The peak numbers, retention times (t_R , min), compound names, molecular formulas, calculated and exact masses ([M-H]⁻, m/z), mean mass accuracy errors (ppm), as well as major MS², MS³ and MS⁴ fragment ions of phenolics founds in SV extracts are summarized in Table 2.

Table 1
Total phenolic compounds, flavonoids, flavonols, and phenolic acids in *S. verticillata* aerial part extract (SV).

Extract	Total phenolic compounds (mg GA/g d.e.)	Total flavonoids (mg QU/g d.e.)	Total flavonols (mg RU/g d.e.)	Total phenolic acids (mg CA/g d.e.)
SV	175.6 \pm 16.3	244.4 \pm 4.7	16.9 \pm 0.8	41.9 \pm 5.4

GA – gallic acid equivalents, QU – quercetin equivalents, RU – rutin equivalents, CA – caffeic acid equivalents, d.e. – dry weight of the extract.

Table 2
UHPLC-MSⁿ Orbitrap metabolic fingerprinting (negative ionization mode) of *Salvia verticillata* L. aerial part extract.

No ^a	t _r , min	Compound name	Molecular formula, [M-H]	Calculated mass, [M-H]	Exact mass, [M-H]	Δ ppm	MS ¹ Fragments, (% Base Peak)	MS ² Fragments, (% Base Peak)	MS ⁿ Fragments, (% Base Peak)
<i>Phenolic acids</i>									
1 ^a	3.90	Danshensu	C ₁₅ H ₁₀ O ₅ ⁻	197.04555	197.04539	0.81	179(100), 151(15), 135(10)	135(100)	107(100), 79(60)
2	5.16	Caffeic acid hexoside	C ₁₇ H ₁₆ O ₇ ⁻	341.08781	341.08781	2.17	179(100), 135(10)	135(100)	91(100)
3	5.20	5-O-Caffeoylquinic acid ^b	C ₁₉ H ₁₈ O ₇ ⁻	353.08781	353.08719	1.76	191(100), 179(5)	179(100), 111(40), 93(60), 85(90)	109(40), 99(50), 85(100)
4	5.28	Coumaric acid hexoside	C ₁₇ H ₁₆ O ₆ ⁻	325.09289	325.09241	1.48	168(100), 119(10)	135(100), 119(10)	107(100)
5	5.75	Caffeic acid ^c	C ₉ H ₈ O ₄ ⁻	179.03498	179.03491	0.39	135(100)	135(100)	107(100)
6	5.85	Salvianolic acid C	C ₁₄ H ₁₂ O ₅ ⁻	377.08781	377.08789	-0.21	359(100)	161(100), 133(10)	133(100)
7	6.10	Yunnanic acid E isomer 1	C ₂₀ H ₂₂ O ₄ ⁻	571.10933	571.10876	1.00	553(60), 527(100), 509(80), 483(40), 439(90)	347(40), 329(50), 285(100)	285(100)
8	6.28	Yunnanic acid E isomer 2	C ₂₀ H ₂₂ O ₄ ⁻	571.10933	571.10895	0.67	553(60), 527(100), 509(80), 359(20), 285(20)	509(100), 347(100), 329(20), 331(30), 285(70)	285(100)
9	6.38	Rosmarinic acid hexoside isomer 1	C ₂₄ H ₂₆ O ₇ ⁻	521.13006	521.12970	0.69	359(100)	161(100), 133(10)	133(100)
10	6.70	Rosmarinic acid hexoside isomer 2	C ₂₄ H ₂₆ O ₇ ⁻	521.13006	521.12976	0.58	359(100)	161(100), 133(10)	133(100)
11	6.88	Methyl yunnanic acid E	C ₂₀ H ₂₂ O ₄ ⁻	585.12498	585.12439	1.01	553(100), 541(10), 509(20)	533(20), 509(100), 355(40)	465(10), 329(20), 311(100), 285(10), 267(30)
12	7.02	Sagerinic acid isomer 1	C ₁₆ H ₁₄ O ₆ ⁻	719.16176	719.16119	0.79	673(15), 539(30), 521(20), 359(100), 341(25)	223(15), 197(20), 179(20), 161(100), 133(5)	143(10), 133(100)
13	7.04	Methylsalvianolic acid C	C ₁₄ H ₁₂ O ₅ ⁻	391.10346	391.10324	0.56	359(100)	161(100), 133(10)	133(100)
14	7.12	Decafoylquinic acid	C ₂₂ H ₂₂ O ₇ ⁻	515.11950	515.11957	-0.14	359(100), 335(5), 191(5)	191(100), 179(20), 135(10)	173(70), 171(30), 127(100), 117(50), 83(90)
15	7.20	Salvianolic acid B isomer 1	C ₁₆ H ₁₄ O ₆ ⁻	717.14611	717.14545	0.92	555(100), 519(10), 357(30), 313(20), 253(20)	357(40), 331(5), 313(100), 289(5), 267(30)	285(100), 267(30), 161(5), 133(100)
16	7.50	Sagerinic acid isomer 2	C ₁₆ H ₁₄ O ₆ ⁻	719.16176	719.16339	-2.27	359(100)	161(100), 133(5)	161(5), 133(100)
17	7.50	Hydroxyrosmarinic acid	C ₁₇ H ₁₄ O ₇ ⁻	375.07216	375.07196	0.53	179(100)	135(100)	105(100)
18	7.50	Rosmarinic acid ^b	C ₁₇ H ₁₄ O ₆ ⁻	359.07724	359.07736	-0.33	223(10), 197(30), 179(40), 161(100), 133(10)	161(100), 133(10)	105(100)
19	7.80	Salvianolic acid B isomer 2	C ₁₆ H ₁₄ O ₆ ⁻	717.14611	717.14539	1.00	577(5), 519(100), 321(10)	339(20), 321(100), 295(5), 279(5), 185(5)	303(10), 293(30), 279(100), 277(60), 249(5)
20	8.02	Methylcaffeate	C ₁₃ H ₁₀ O ₄ ⁻	193.05063	193.05045	0.93	178(100), 161(40), 147(100), 144(20)	135(100)	105(100)
21	8.92	Methylrosmarinate	C ₁₇ H ₁₆ O ₆ ⁻	373.09289	373.09268	0.56	261(10), 179(100), 135(50)	135(100)	105(100)
22	6.44	Quercetin 3-O-rutinoside ^b	C ₂₉ H ₃₀ O ₆ ⁻	609.14611	609.14594	0.28	343(5), 301(100), 300(30), 271(10), 253(5)	273(25), 257(20), 179(100), 151(75)	241(5), 226(15), 213(30), 197(100)
23	6.73	Luteolin 7-O-glucoside ^b	C ₂₁ H ₂₀ O ₁₁ ⁻	447.09329	447.09454	-2.80	285(100)	199(85), 175(95)	177(100)
24	6.75	Luteolin 7-O-hexuronide	C ₂₃ H ₂₀ O ₁₂ ⁻	461.07200	461.07275	-1.63	285(100), 175(5)	267(70), 257(20), 241(90)	151(100)
25	7.22	Quercetin 3-O-hammeside ^b	C ₂₃ H ₂₀ O ₁₁ ⁻	447.09329	447.09290	0.87	301(100), 300(30)	233(30), 273(20), 257(10)	197(100)
26	7.25	Apigenin 7-O-glucoside ^b	C ₂₁ H ₂₀ O ₁₀ ⁻	431.09837	431.09772	1.51	311(5), 269(100)	269(30), 255(100), 197(45)	210(10), 197(100), 181(50), 169(40)
27	7.31	Apigenin 7-O-hexuronide	C ₂₃ H ₂₀ O ₁₁ ⁻	445.07763	445.07803	-0.90	269(100), 175(15)	225(100), 201(20), 183(15), 151(15), 149(40)	151(100)
28	9.51	Apigenin ^b	C ₁₅ H ₁₀ O ₅ ⁻	269.04554	269.04544	0.37	269(60), 225(10), 201(30), 151(70), 149(50)	183(40), 181(100)	151(100)

(continued on next page)

Table 2 (continued)

No ^a	t _R , min	Compound name	Molecular formula, [M-H] ⁻	Calculated mass, [M-H] ⁻	Exact mass, [M-H] ⁻	Δ ppm	MS ¹ Fragments, (% Base Peak)	MS ² Fragments, (% Base Peak)	MS ³ Fragments, (% Base Peak)
29	10.92	Cisimarinin	C ₁₇ H ₁₄ O ₆ ⁻	313.07176	313.07141	1.12	298 (100), 283(5)	283 (100), 269(30), 150(10)	255(100), 239(5), 227(10), 21(5), 163(5)

^a Peak number of compounds corresponding to Fig. S1. ^bConfirmed using available standards, all the other compounds were identified based on MS data. ^cpeaks that were further fragmented in MS² and MS³ experiment are marked **bold** in table.

The examination of mass spectra of phenolic acids and their derivatives revealed various caffeic acid derivatives, which were expected (Li et al., 2015). More specifically, from phenolic acids group, only one identified compound is not a caffeic acid derivative and it is a coumaric acid hexoside (compound 4). This compound eluting at 5.28 min and showing ([M-H]⁻) at *m/z* 325, gave MS² base peak at *m/z* 163 (mass of deprotonated coumaric acid) and secondary MS² peak at 119 *m/z* which was obtained by further loss of CO₂ group (44 Da). As for the other phenolic acid derivatives, they all showed specific fragments of residues of caffeic acid. For example, compound 14(dicaffeoylquinic acid, eluting at 7.12 min and showing [M-H]⁻ at *m/z* 515) showed MS² base peak at *m/z* 353 (loss of caffeoyl moiety) and MS³ base peak at *m/z* 191 which corresponds to deprotonated quinic acid (Table 2).

Eight compounds from the group of flavonoids (quercetin 3-*O*-rutinoside, luteolin 7-*O*-glucoside, quercetin 3-*O*-rhamnoside, apigenin 7-*O*-glucoside, and apigenin) were identified in the SV extract and presence of five of them was confirmed by comparison with appropriate standards. Luteolin 7-*O*-hexuronide (compound 24) and apigenin 7-*O*-hexuronide (compound 27) were identified by a specific fragment at 175 *m/z*, which corresponds to deprotonated hexuronic acid. Presence of luteolin and apigenin as aglycones was confirmed by specific MS³ fragmentation in both cases. These two hexuronyl derivatives were already identified in some *Salvia* species (Šuljić et al., 2017). Girsamarinin (compound 29), known to be present in *S. verticillata* (Ulubeien and Topcu, 1984) was visible as pseudomolecular ion [M-H]⁻ at *m/z* 313 and was eluted at 10.92 min. It produced the MS² base peak at *m/z* 298 (generated by the loss of CH₃ group – 15 Da) and MS³ base peak at *m/z* 269 (loss of second CH₃ group). The MS³ base peak resulting from a further loss of CO group (28 Da) was identified at *m/z* 255. Proposed fragmentation pathway of this compound is depicted in Fig. S1.

UHPLC-DAD/(-)HESI-MS/MS analysis was targeted towards totally 14 compounds belonging to the phenolics (12 compounds) and phenolic diterpenes (2 compounds). The quantitative data of targeted phenolic compounds in SV extract (expressed in µg per 100 mg of dry extract) are presented in Table 3. The most abundant compound in SV was rosmarinic acid (235 mg/g d.e.), along with salvianolic acid C (1.1 mg/g d.e.). Their concentration in the extract was approximately more than a dozen times higher than those of the other quantified polyphenolics. Also, a high concentration of several rosmarinic acid derivatives, i.e., rosmarinic acid hexoside and methyrosmarinate (3.6 and 1.07 mg/g d.e., respectively) was found in SV extract. Salvianolic acid B was present in SV in much lower amount (470 µg/g d.e.) compared with salvianolic acid C. The aerial parts of *S. verticillata* had moderate amounts of caffeic acid and its' derivatives with quinic acid. Flavonoids (quercetin, rutin, quercitrin, apigenin, and apigenin-7-*O*-glucoside) and characteristic diterpenes (carnosol and carnosic acid) were also present in SV in lower concentrations.

3.2. Biocompatibility and cytotoxicity of *S. verticillata* extract

The biocompatibility of *S. verticillata* aerial part extract was first assessed by using a cell survival assay. SV extract was tested on a panel of eukaryotic cell lines, from immortalized murine BalbC-3T3 fibroblasts and human normal HaCaT keratinocytes to human cancer cells: epidermoid carcinoma (A431), liver cancer (HepG2), and colon carcinoma (LoVo). Cells were treated for 48 and 72 h with an increasing amount of SV extract (from 5 to 50 µg/mL) and cell viability was assessed by the MTT assay. As shown in Fig. 2, no toxicity of SV extract was observed on any cell line analyzed after 48 h incubation. After 72 h incubation, the extract did not affect cell viability on immortalized cells, however a very slight, but significant, decrease in the viability of LoVo cancer cells was found after 72 h incubation only at the highest concentration used. These results indicate that SV extract is full biocompatible with eukaryotic cells.

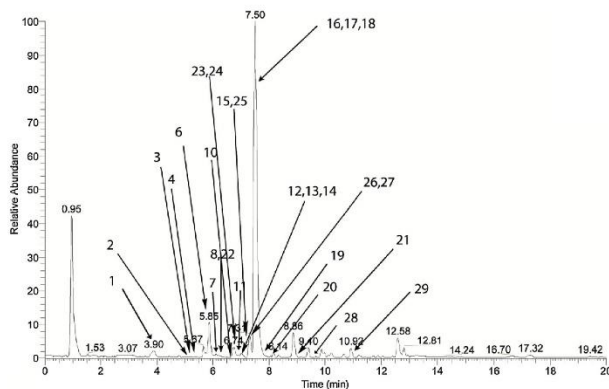


Fig. 1. UHPLC-MS⁴ Orbitrap chromatogram (negative ionization mode) of *S. verticillata* aerial part extract. Peak numbers are as indicated in Table 2.

3.3. Bioactivity of *S. verticillata* extract

To explore the possibility to use SV extract as a source of the bioactive molecule(s), the extract was tested for its antibacterial and antifungal effects, as well as for its antioxidant activity *in vitro*. The antibacterial potential of SV, reported in Table 4, clearly indicated that this extract was very active on *B. cereus*, as it was able to inhibit the growth of this strain at a concentration of 1.25 mg/mL. On the other hand, the extract was less active on the other bacterial species tested (as indicated by higher MIC values). As for antifungal activity, the lowest MIC value was found on *P. canescens* (5 mg/mL), then *C. albicans* and *F. oxysporum* (10 and 20 mg/mL, respectively), while the extract had no antifungal potential on other treated fungal species (MIC > 20 mg/mL). Compared with the positive control used, *i.e.*, the commercial antibiotic chloramphenicol and the antimycotic nystatin, SV extract had moderate activity.

Then, the antioxidant activity of SV extract was evaluated, by using six different *in vitro* assays. The results of the experiments are shown in Table 5. SV extract exerted a very good antioxidant activity, in some cases comparable with the reference antioxidants used (ascorbic acid and BHT). The total antioxidant capacity of 1 g SV was in the range of 255 mg of ascorbic acid activity. The scavenging potential of SV

towards DPPH radicals (IC₅₀ 33.04 µg/mL) was much lower than ascorbic acid, but comparable with that of BHT (IC₅₀ 26.11 µg/mL, $p < 0.05$). The ABTS⁺ scavenging results indicated that SV extract had a pronounced activity (IC₅₀ 67.01 µg/mL), but around three and two times lower, compared with ascorbic acid and BHT (15.43 and 37.18 µg/mL, respectively). NO radical scavenging potential of SV was comparable with ascorbic acid activity (IC₅₀ 73.12 and 50.56 µg/mL, respectively), given that BHT was not active at the highest concentration tested. BHT was able to markedly inhibit lipid peroxidation in linoleic acid emulsion (IC₅₀ value 3.82 µg/mL), while SV had moderate activity (IC₅₀ 58.07 µg/mL) and ascorbic acid had no effects at the highest concentration applied. All tested samples did not exert metal chelating effects.

4. Discussion

In very few previous studies addressing the phytochemical characterization of *S. verticillata* extracts, caffeic acid and its derivatives were the main identified compounds (Fig. 3), with rosmarinic acid being the most abundant bioactive metabolite (Öztürk et al., 2011; Šulnitić et al., 2017; Tepe et al., 2007), according to our results. Caffeic acid has an essential role in the biosynthesis of secondary metabolites of

Table 3

UHPLC/(–)HESI-MS/MS quantitative data of targeted phenolic compounds in *S. verticillata* aerial part methanol extract. Concentration is presented as µg per 100 mg of dry extract [µg/100 mg d.e.]. Values are means of three replicates ± SD.

No.	Rt (min)	Compounds	[M–H] [–]	Diagnostic MS ² fragments [M–H] [–]	Concentration [µg/100 mg d.e.]
1	1.80	5- <i>O</i> -Caffeoylquinic acid ^a	353	127; 191	145.303 ± 22.461
2	2.45	Caffeic acid ^a	179	134; 135	9.539 ± 2.054
3	3.17	Salvianolic acid C	377	161; 359	1115.486 ± 19.941
4	3.92	Quercetin 3- <i>O</i> -rutinoside ^b	609	301; 179	0.262 ± 0.031
5	4.14	Rosmarinic acid hexoside	521	161; 359	359.519 ± 20.830
6	4.38	Dicaffeoylquinic acid	515	135; 191	35.981 ± 1.062
7	4.55	Quercetin 3- <i>O</i> -rhamnoside ^b	447	201; 300	0.013 ± 0.007
8	4.55	Apigenin-7- <i>O</i> -glucoside ^b	431	269; 311	7.964 ± 0.274
9	4.58	Rosmarinic acid ^a	359	133; 161	23458.624 ± 521.508
10	5.10	Salvianolic acid B ^a	717	321; 519	46.980 ± 1.055
11	5.72	Methylrosmarinat	373	135; 179	107.425 ± 2.690
12	5.88	Apigenin ^a	269	117; 149	0.676 ± 0.032
13	7.70	Carnosol ^a	329	201; 285	0.257 ± 0.002
14	9.86	Carnosic acid ^a	331	244; 287	0.169 ± 0.011

^a Identified according to the standards.

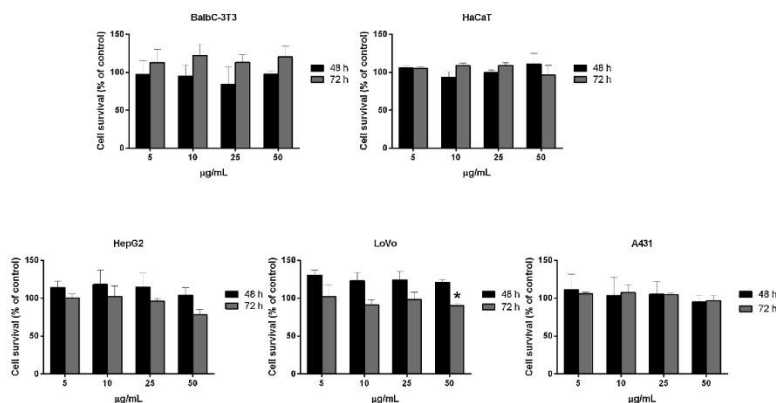


Fig. 2. Biocompatibility of the *S. verticillata* extract (SV) on BalbC-3T3, HaCaT, A431, HepG2, and LoVo cell lines. Dose- and time-response curves of cells after 48 and 72 h of incubation in the presence of 5, 10, 25, and 50 µg/mL of the extract. Values are given as means \pm SD ($n \geq 3$). * indicated $p < 0.05$ with respect to untreated cells.

Table 4
Antibacterial and antifungal activity of *S. verticillata* methanolic extract.

Bacterial species		MIC*	
		<i>S. verticillata</i>	Chloramphenicol
<i>Micrococcus lysodeikticus</i>	ATCC 4698	10	1.25
<i>Enterococcus faecalis</i>	ATCC 29212	20	10
<i>Escherichia coli</i>	ATCC 25922	20	2.5
<i>Klebsiella pneumoniae</i>	ATCC 70063	20	2.5
<i>Pseudomonas aeruginosa</i>	ATCC 10145	20	40
<i>Bacillus cereus</i>	ATCC 10876	1.25	2.5
<i>Bacillus mycoides</i>	FSB 1	10	10
<i>Azobacter chroococcum</i>	FSB 14	10	10
Fungal species		MIC	
		<i>S. verticillata</i>	Nystatin
<i>Candida albicans</i>	ATCC 10259	10	5
<i>Aspergillus brasiliensis</i>	ATCC 16404	> 20	40
<i>Fusarium oxysporum</i>	FSB 91	> 20	20
<i>Alternaria alternata</i>	FSB 51	> 20	40
<i>Aureobasidium pullulans</i>	FSB 61	> 20	> 40
<i>Trichoderma harzianum</i>	FSB 12	> 20	> 40
<i>Penicillium canescens</i>	FSB 24	5	10
<i>Doratomyces stemonitis</i>	FSB 41	> 20	> 40

* MIC - minimum inhibitory concentration values given as mg/mL for plant extracts and as µg/mL for antibiotic (Chloramphenicol) and antimycotic (Nystatin).

Table 5
Antioxidant activity of *S. verticillata* methanolic extract.

Sample and standards	Total antioxidant activity (mg AA/g)	IC ₅₀ values* (µg/mL)				
		DPPH radical scavenging activity	ABTS radical-cation scavenging activity	NO radical scavenging activity	Inhibitory activity toward lipid peroxidation	Metal chelating activity
<i>S. verticillata</i>	254.55 \pm 17.75	33.04 \pm 5.83 ^a	67.01 \pm 13.62 ^a	73.12 \pm 19.04	58.07 \pm 9.72	> 4000
Ascorbic acid	-	5.69 \pm 0.82 ^b	15.43 \pm 2.65 ^b	50.56 \pm 20.69	> 100	> 100
BHT	-	26.11 \pm 2.58 ^a	37.18 \pm 4.92 ^c	> 1000	3.82 \pm 0.42	> 100

* IC₅₀ values were determined by nonlinear regression analysis. Results are mean values \pm SD from three independent experiments; -, not tested; AA - ascorbic acid equivalents; DPPH - 2,2-diphenyl-1-picrylhydrazyl; ABTS - 2,2'-azino-bis(3-ethylbenzothiazoline-6-sulphonic acid); NO - nitric oxide; BHT - butylated hydroxytoluene. Means in the same column with different letters as superscripts are significantly different at $p < 0.05$.

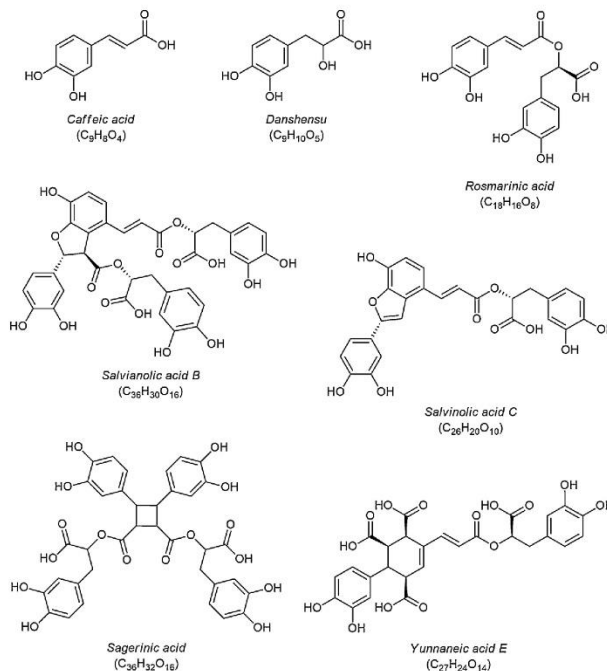


Fig. 3. Chemical structures of caffeic acid and its derivatives (mono-, di-, tri-, and tetramers) identified in the *S. verticillata* aerial part extract (SV).

that the amount of rosmarinic acid in SV (67 mg/g) is higher than the usual amounts found in other *Salvia* species. However, in this study, the concentration of rosmarinic acid in SV was much higher (ca. 235 mg/g), consistently with the results of Tepe et al. (2007) who quantified similar levels of rosmarinic acid in methanol extracts of both subspecies of *S. verticillata* (subsp. *verticillata* and subsp. *amasiaca*). Besides polyphenolic compounds, characteristic *Salvia* diterpenes, including carnosic acid and carnosol (phenolic diterpene), were detected and quantified in this study. Carnosic acid was also detected in this plant by Šulnūte et al. (2017), but with no traces of carnosol. Generally, the aerial parts of *Salvia* spp. contain flavonoids, triterpenoids, and monoterpenes, mainly in the leaves and flowers, while the roots are rich in diterpenoids (Topçu, 2006). Moreover, Matkowski et al. (2008) reported that the levels of total phenolic content (TPC) in *S. verticillata* leaf and root extracts are quite similar, while Šulnūte et al. (2016) showed that ethanolic extract of *S. verticillata* aerial parts was considerably richer in total phenolics than water extract. Our results also confirmed high TPC in SV extract, where flavonoids and phenolic acids were mostly present.

Salvia species are well-known for their broad spectrum of biological activities. One of the most prominent properties of the Lamiaceae family and, in particular, *Salvia* plants, is the antimicrobial activity. Besides *S. officinalis* (Gericke et al., 2018; Ghorbani and Esmailizadeh, 2017), many other members of this genus showed remarkable antimicrobial potential, for instance *S. potentillifolia*, *S. verbenaca*, *S.*

chorassanica, *S. veneris*, etc., as it was recently very well summarized by Sharifi-Rad et al. (2018). The same authors reported that *Salvia* spp. showed significant bactericidal and bacteriostatic activities against both Gram-positive and Gram-negative bacteria, mostly *Bacillus*, *Klebsiella*, *Pseudomonas*, and *Salmonella* species, as well as microorganisms from *Candida* and *Aspergillus* spp. Therefore, *Salvia* antimicrobial properties are directed, to the highest point, against food spoilage and foodborne pathogens, in order to be used as a natural preservative in food applications (Sharifi-Rad et al., 2018; Tajkarimi et al., 2010). The antimicrobial potential of *S. verticillata* was not tested previously, so the results of this study showed, for the first time, the antimicrobial properties of *S. verticillata* extract, which were consistent with previously published data on *Salvias'* effects. SV showed antibacterial activity towards all tested bacterial strains, whereby the effects on Gram-positive strain *B. cereus* was particularly noteworthy, followed by *B. mycoides*, *M. lysodeketicus*, and Gram-negative *A. chroococcum*. The antifungal activity of SV was less notable, except for *P. canescens* and *C. albicans*. This potential is ascribed to the chemical composition of the extracts, mainly to the phenolic compounds presented in *Salvia* species. First and foremost compound, presented in high content in SV, is certainly rosmarinic acid, endowed with high antimicrobial potential towards a wide range of microbes, with minimal inhibitory concentration values (MIC) starting from 0.01 mg/mL (Abedini et al., 2013; Amoah et al., 2016). Also, many other phenolics detected in SV, e.g. phenolic acids, apigenin, luteolin, and quercetin derivatives (Cushnie and Lamb, 2005),

and diterpenoids like camosol and carnosic acid (Ghorbani and Esmailizadeh, 2017), exert antibacterial and antifungal potential due to the high presence of –OH groups which play an important role in the antimicrobial activity (through the interaction with the cell membrane, delocalization of electrons, binding the active site of enzymes, and leading to the microorganisms growth restriction) (Gyawali and Ibrahim, 2014). Although the extracts of *Salvia* species generally have good antimicrobial properties, *Salvia* essential oils are mostly used due to the high content of volatile antimicrobial compounds like α -thujene, α - and β -pinene, myrcene, limonene, etc., which were also identified in *S. verticillata* essential oil (Giuliani et al., 2018; Pitarokili et al., 2006; Rzepa et al., 2009). As SV extract had moderate antimicrobial activity, perhaps the more justified use of SV in this sense would be in the form of essential oil.

Besides antimicrobial activity, phenolic compounds are recognized for their prominent antioxidant effects. Their hydrogen atom donating potential render them exceptionally efficacious antioxidants, with different mechanisms of action counteracting oxidative stress in materials and organisms (Brewer, 2011). They can interfere with the process of free radical generation in phases of initiation or propagation, and sometimes even as metal chelators, they have the ability to activate antioxidant enzymes and modification of prooxidant properties of low molecular antioxidants (Procházková et al., 2011; Shahidi and Ambigaipalan, 2015). Many of them are in use in the food industry as food additives for preventing lipid oxidation and therefore extending the shelf-life of food products without any influence on the food nutritional quality and sensory properties (Shahidi and Ambigaipalan, 2015). Regarding Lamiaceae plants, numerous members of this family and one of their main phenolic compounds, rosmarinic acid, are used in industrial applications for cosmetic and food products, because of significant antioxidant activity (Trivellini et al., 2016). Since the tested *S. verticillata* aerial part extract contains a high content of phenolic compounds, known to act as antioxidants, it is not surprising that SV extract exerts good total antioxidant capacity and scavenging potential towards different free radicals. Sulhiüt et al. (2016) reported good ABTS⁺ scavenging activity and high ORAC values of different *S. verticillata* aerial part extracts, while Matkowski et al. (2008) showed that the root extract had better ABTS⁺ scavenging activity than its leaves, but lower reducing power and DPPH antioxidant potential. Moreover, in a study from Tepe et al. (2007), it was shown that both *S. verticillata* subspecies (subsp. *verticillata* and *amasiaca*) exerted similar free radical-scavenging capacities and the inhibition ratio of linoleic acid oxidation, comparable to the effects of rosmarinic acid. Several other studies described the antioxidant activity of *S. verticillata* subsp. *amasiaca* against free radicals, as well as chelating and reducing potential (Orhan et al., 2007, 2013; Zengin et al., 2018). Thus, the traditional use of *S. verticillata* in preparing cheese and meat products is supported by these results, since its antioxidant capacity helps to prevent food quality deterioration. Like many other members of the Lamiaceae family (rosemary, sage, basil, oregano, marjoram, savory, and thyme), rich in rosmarinic acid and other proven antioxidant compounds (Brewer, 2011), *S. verticillata* extract may also be included in the food industry for different purposes. In that sense, the biocompatibility of the extract is very important for its implementation in the human diet and incorporation in human-used products.

Taking into account the content of diverse phenolic compounds with proven bioactivity, it is surprising that there is no literature data related to the influence of *S. verticillata* extract on eukaryotic cell lines. Our results showed, for the first time, that SV was not toxic towards murine immortalized fibroblasts (BalbC-3T3) and human immortalized epidermal keratinocytes (HaCaT) in all tested concentrations. Moreover, there were no significant cytotoxic effects on three cancer cell lines (A431, HepG2, and LoVo), except at the highest concentration of SV. Zengin et al. (2018) confirmed the absence of antiproliferative activity of *S. verticillata* subsp. *amasiaca* on human alveolar lung epithelial carcinoma (A549) and human breast adenocarcinoma (MCF-7),

as well as its influence on inhibition of some key enzymes (cholinesterases, tyrosinase, glucosidase, amylase, lipase, and elastase) in different illnesses of modern age, such as Alzheimer's disease, diabetes mellitus, and obesity.

5. Conclusion

The results showed that a methanol extract from *S. verticillata* aerial parts is quite rich in phenolic compounds, particularly rosmarinic acid and its derivatives. The extract exerted good antimicrobial activity against some of the selected bacteria and fungi species. Also, SV extract exhibited prominent antioxidant properties and antiradical potential, comparable to referent antioxidants. Its action on normal and cancer cell lines indicates high biocompatibility and absence of cytotoxicity. The observed results suggested that *S. verticillata* should not be considered just like a weed plant, but rather as a rich source of compounds with prominent bioactive properties and as a potential additive in food or cosmetic industries, with further exploration of concrete possibilities of use and extract standardization.

Declaration of Competing Interest

The authors declare no conflict of interest.

Acknowledgment

This research was supported by the Ministry of Education, Science and Technological Development of the Republic of Serbia (project Nos. III 43004, OI172017, and OI173024).

Appendix A. Supplementary data

Supplementary material related to this article can be found, in the online version, at doi:<https://doi.org/10.1016/j.indcrop.2019.111932>.

References

- Abedini, A., Roumy, V., Mahieux, S., Biabiani, M., Standaert-Vitse, A., Rivière, C., Shpaz, S., Baillou, F., Neut, C., Hennebelle, T., 2013. Rosmarinic acid and its methyl ester as antimicrobial components of the hydromethanolic extract of *Hyptis arvensis* Poit. (Lamiaceae). *Evid. Complement. Alternat. Med.* 2013, 604536. <https://doi.org/10.1155/2013/604536>.
- Amoah, S.K.S., Sandjo, L.P., Kratz, J.M., Biavatti, M.W., 2016. Rosmarinic acid - pharmaceutical and clinical aspects. *Planta Med.* 82, 388–406. <https://doi.org/10.1055/s-0035-1568274>.
- Boroja, T., Katančić, J., Rosić, G., Selaković, D., Joksimović, J., Mišić, D., Stanković, V., Jovičić, N., Mihalović, V., 2018. Summer savory (*Satureja hortensis* L.) extract: phytochemical profile and modulation of cisplatin-induced liver, renal and testicular toxicity. *Food Chem. Toxicol.* 118, 252–263. <https://doi.org/10.1016/j.fct.2018.05.001>.
- Božanović, J., Živković, S., Gašić, U., Glamočlija, J., Čirić, A., Matekalo, D., Šiler, B., Soković, M., Tešić, Ž., Mišić, D., 2018. *In vitro* and *in vivo* transformations of *Centaureum erythraea* secoiridoid glucosides alternate their antioxidant and antimicrobial capacity. *Ind. Crops Prod.* 111, 705–721. <https://doi.org/10.1016/j.indcrop.2017.11.040>.
- Brewer, M.S., 2011. Natural antioxidants: sources, compounds, mechanisms of action, and potential applications. *Compr. Rev. Food Sci. Food Saf.* 10, 221–247. <https://doi.org/10.1111/j.1541-4337.2011.00156.x>.
- Brighente, I.M.C., Dias, M., Verdi, L.G., Pizzolatti, M.G., 2007. Antioxidant activity and total phenolic content of some Brazilian species. *Pharm. Biol.* 45, 156–161. <https://doi.org/10.1080/13880200601131313>.
- Chen, W., Chen, G., 2018. Danshen (*Salvia miltiorrhiza* Bunge): a prospective healing sage for cardiovascular diseases. *Curr. Pharm. Des.* 23. <https://doi.org/10.2174/1381612825666170822101112>.
- CLSI, 2012. Methods for Dilution Antimicrobial Susceptibility Tests for Bacteria That Grow Aerobically; Approved Standard - Ninth Edition, vol. 32 Clinical and Laboratory Standards Institute (CLSI), Wayne, PA, USA.
- Cushnie, T.P.T., Lamb, A.J., 2005. Antimicrobial activity of flavonoids. *Int. J. Antimicrob. Agents* 26, 343–356. <https://doi.org/10.1016/j.ijantimicag.2005.09.002>.
- European Medicines Agency, 2016. European Union Herbal Monograph on *Salvia officinalis* L., folium. Accessed: 06.05.2019. .
- Forouzain, F., Jamei, R., Heidari, R., 2015. Compositional analysis and antioxidant activity of volatile components of two *Salvia* spp. *Trop. J. Pharm. Res.* 14, 2009–2013. <https://doi.org/10.4314/tjpr.v14i11.9>.

- Gericke, S., Lübken, T., Wolf, D., Kaiser, M., Hannig, C., Speer, K., 2018. Identification of new compounds from sage flowers (*Salvia officinalis* L.) as markers for quality control and the influence of the manufacturing technology on the chemical composition and antibacterial activity of sage flower extracts. *J. Agric. Food Chem.* **66**, 1843–1853. <https://doi.org/10.1021/acs.jafc.8b00581>.
- Ghorbani, A., Esmailzadeh, M., 2017. Pharmacological properties of *Salvia officinalis* and its components. *J. Tradit. Complement. Med.* **7**, 433–440. <https://doi.org/10.1016/j.jtcme.2016.12.014>.
- Giuliani, C., Acerizi, R., Lupi, D., Tassera, G., Santagostini, L., Giovanetti, M., Flamin, G., Fico, G., 2018. *Salvia verticillata*: linking glandular trichomes, volatiles and pollinators. *Phytochemistry* **155**, 53–60. <https://doi.org/10.1016/j.phytochem.2018.07.016>.
- Green, L.C., Wagner, D.A., Glogowski, J., Skippner, P.L., Wishnok, J.S., Tannenbaum, S.R., 1992. Analysis of nitrate, nitrite, and [N]nitrate in biological fluids. *Anal. Biochem.* **126**, 131–138. [https://doi.org/10.1016/0003-2697\(92\)90118-X](https://doi.org/10.1016/0003-2697(92)90118-X).
- Gyawali, R., Ibrahim, S.A., 2014. Natural products as antimicrobial agents. *Food Control* **46**, 412–429. <https://doi.org/10.1016/j.foodcont.2014.05.047>.
- Hsu, C.-K., Chiang, B.-H., Chen, Y.-S., Yang, J.-H., Liu, C.-L., 2008. Improving the antioxidant activity of buckwheat (*Fagopyrum tataricum* Gaertn.) sprout with trace element water. *Food Chem.* **108**, 633–641. <https://doi.org/10.1016/j.foodchem.2007.11.028>.
- Jarić, S., Maćuković-Jokić, M., Đurđević, L., Mitrović, M., Kostić, O., Karadžić, B., Pavlović, P., 2015. An ethnobotanical survey of traditionally used plants on Suva planina mountain (south-eastern Serbia). *J. Ethnopharmacol.* **175**, 93–108. <https://doi.org/10.1016/j.jep.2015.09.002>.
- Jasbi, A.R., Zare, S., Finzi, A., Xiao, J., 2016. Bioactive phytochemicals from shoots and roots of *Salvia* species. *Phytochem. Rev.* **15**, 829–867. <https://doi.org/10.1007/s11101-015-9427-z>.
- Kumarasamy, V., Byres, M., Cox, P.J., Jaspars, M., Nahar, L., Sarker, S.D., 2007. Screening seeds of some Scottish plants for free radical scavenging activity. *Phyther. Res.* **21**, 615–621. <https://doi.org/10.1002/ptr.2129>.
- Li, M., Wang, F., Huang, Y., Du, F., Zhong, C., Olatoye, O.E., Jia, W., Li, Y., Xu, F., Dong, J., Li, J., Lin, J.B.R., Zhao, B., Jia, L., Li, L., Li, C., 2015. Systemic exposure to and disposition of catechols derived from *Salvia miltiorrhiza* roots (Danshen) after intravenous dosing danhong injection in human subjects, rats, and dogs. *Drug Metab. Dispos.* **43**, 679–690. <https://doi.org/10.1124/dmd.114.061473>.
- Lu, Y., Teap Foo, L., 2002. Polyphenolics of *Salvia* - a review. *Phytochemistry* **59**, 117–140. [https://doi.org/10.1016/S0031-9320\(01\)00415-0](https://doi.org/10.1016/S0031-9320(01)00415-0).
- Matkowski, A., Zielińska, S., Ozmiński, J., Lamer-Zarawska, E., 2008. Antioxidant activity of extracts from leaves and roots of *Salvia miltiorrhiza* Bunge, *S. przewalskii* Maxim., and *S. verticillata* L. *Bioresour. Technol.* **99**, 7892–7896. <https://doi.org/10.1016/j.biortech.2008.02.013>.
- Mišić, D., Šiler, B., Gašić, U., Avramov, S., Živković, S., Nestorović Živković, J., Milutinović, M., Tešić, Ž., 2015. Simultaneous UHPLC/DAD/(+/-)HESI-MS/MS analysis of phenolic acids and nepetalactones in methanol extracts of *Nepeta* species: A possible application in chemotaxonomic studies. *Phytochem. Anal.* **26**, 72–85. <https://doi.org/10.1002/pca.2538>.
- NCCLS, 2002a. Reference Method for Broth Dilution Antifungal Susceptibility Testing of Filamentous Fungi; Approved Standard. NCCLS Document M38-A. [ISBN 1-56238-470-8]. NCCLS, 940 West Valley Road, Suite 1400, Wayne, Pennsylvania 19087-1898 USA.
- NCCLS, 2002b. Reference Method for Broth Dilution Antifungal Susceptibility Testing of Yeasts; Approved Standard - Second Edition. NCCLS Document M27-A2. [ISBN 1-56238-469-4]. NCCLS, 940 West Valley Road, Suite 1400, Wayne, Pennsylvania 19087-1898 USA.
- Orhan, I., Kartal, M., Naz, O., Ejaz, A., Yilmaz, G., Kan, Y., Konuklugil, B., Şener, B., Işal Choudhary, M., 2007. Antioxidant and anticholinesterase evaluation of selected Turkish *Salvia* species. *Food Chem.* **103**, 1247–1254. <https://doi.org/10.1016/j.foodchem.2006.10.030>.
- Orhan, I.E., Senol, F.S., Ercetin, T., Kahraman, A., Celop, F., Akaydin, G., Şener, B., Dogan, M., 2013. Assessment of anticholinesterase and antioxidant properties of selected sage (*Salvia*) species with their total phenol and flavonoid contents. *Ind. Crops Prod.* **41**, 21–30. <https://doi.org/10.1016/j.indcrop.2012.04.002>.
- Öztürk, N., Tunçel, M., Uysal, U.D., Öncü-Kaya, E.M., Koyuncu, O., 2011. Determination of rosmarinic acid by high-performance liquid chromatography and its application to certain *Salvia* species and rosemary. *Food Anal. Methods* **4**, 300–306. <https://doi.org/10.1007/s12161-010-9164-2>.
- Parker, J., Schellenberger, A.N., Roe, A.L., Oketch-Rabah, H., Calderón, A.J., 2018. Therapeutic perspectives on chia seed and its oil: a review. *Planta Med.* **84**, 606–612. <https://doi.org/10.1055/a-0586-4711>.
- Petrak, G., Raiola, A., Del Giudice, R., Barone, A., Fruscante, L., Rigano, M.M., Monti, D.M., 2016. An ascorbic acid-enriched tomato genotype to fight UVA-induced oxidative stress in normal human keratinocytes. *J. Photochem. Photobiol. B Biol.* **163**, 284–289. <https://doi.org/10.1016/j.jphotobiol.2016.08.047>.
- Pitarokili, D., Tzakou, O., Loukis, A., 2006. Essential oil composition of *Salvia verticillata*, *S. verbenaca*, *S. glutinosa* and *S. candidissima* growing wild in Greece. *Flavour Fragr. J.* **21**, 670–673. <https://doi.org/10.1002/ffj.1647>.
- Prieto, P., Pincha, M., Aguilar, M., 1999. Spectrophotometric quantitation of antioxidant capacity through the formation of a phosphomolybdenum complex: specific application to the determination of vitamin E. *Anal. Biochem.* **269**, 337–341. <https://doi.org/10.1006/abio.1999.0018>.
- Procházková, D., Boušková, L., Wilhelmová, N., 2011. Antioxidant and prooxidant properties of flavonoids. *Fitoterapia* **82**, 513–523. <https://doi.org/10.1016/j.fitote.2011.01.018>.
- Re, R., Pellegrini, N., Proteggente, A., Pannala, A., Yang, M., Rice-Evans, C., 1999. Antioxidant activity applying an improved ABTS radical cation decolorization assay. *Free Radic. Biol. Med.* **26**, 1231–1237. [https://doi.org/10.1016/S0891-5849\(98\)00315-3](https://doi.org/10.1016/S0891-5849(98)00315-3).
- Rzepa, J., Wojtal, L., Staszek, D., Grygierczyk, G., Labe, K., Hajnos, M., Kowalska, T., Waksmundzka-Hajnos, M., 2009. Fingerprint of selected *Salvia* species by HS-GCMS analysis of their volatile fraction. *J. Chromatogr. Sci.* **47**, 575–580. <https://doi.org/10.1093/chromsci/47.7.575>.
- Sarker, S.D., Nahar, L., Kumarasamy, Y., 2007. Microtitre plate-based antibacterial assay incorporating resazurin as an indicator of cell growth, and its application in the *in vitro* antibacterial screening of phytochemicals. *Methods* **42**, 321–324. <https://doi.org/10.1016/j.jymeth.2007.01.006>.
- Shahidi, F., Ambigaipalan, P., 2015. Phenolics and polyphenolics in foods, beverages and spices: antioxidant activity and health effects - a review. *J. Funct. Foods* **18**, 820–897. <https://doi.org/10.1016/j.jff.2015.06.018>.
- Sharif-Rad, M., Ozelik, B., Altun, G., Daşgaya-Dikmen, C., Martorell, M., Ramírez-Alarcón, K., Alarcón-Zapata, P., Morais-Braga, M.F.B., Carneiro, J.N.P., Borges, Alves, Leal, A.L., Coutinho, H.D.M., Gyawali, R., Tuberghero, N., Ibrahim, S.A., Sahriř-Rad, R., Sharopov, F., Salehi, B., del Mar Contreras, M., Segura-Carretero, A., Sen, S., Adachi, A., Shariř-Rad, J., 2018. *Salvia* spp. Plants from farm to food applications and phytopharmacotherapy. *Trends Food Sci. Technol.* <https://doi.org/10.1016/j.tifs.2018.08.008>.
- Singleton, V.L., Orthofer, R., Lamuela-Raventós, R.M., 1999. Analysis of total phenols and other oxidation substrates and antioxidants by means of Folin-Ciocalteu reagent. *Methods Enzymol.* **299**, 152–178. [https://doi.org/10.1016/S0076-6875\(99\)99017-1](https://doi.org/10.1016/S0076-6875(99)99017-1).
- Sulinić, V., Pakulski, A., Venkutsionis, P.R., 2017. Phytochemical composition of fractions isolated from ten *Salvia* species by supercritical carbon dioxide and pressurized liquid extraction methods. *Food Chem.* **224**, 37–47. <https://doi.org/10.1016/j.foodchem.2016.12.047>.
- Sulinić, V., Ragažinskić, O., Venkutsionis, P.R., 2016. Comprehensive evaluation of antioxidant potential of 10 *Salvia* species using high pressure methods for the isolation of lipophilic and hydrophilic plant fractions. *Plant Food Hum. Nutr.* **71**, 64–71. <https://doi.org/10.1007/s11130-015-0526-1>.
- Tajkari, M.M., Ibrahim, S.A., Cliver, D.O., 2010. Antimicrobial herbs and spice compounds in food. *Food Control* **21**, 1199–1218. <https://doi.org/10.1016/j.foodcont.2010.02.003>.
- Tepe, B., Eminoglu, O., Akpulat, H.A., Aydin, E., 2007. Antioxidant potentials and rosmarinic acid levels of the methanolic extracts of *Salvia verticillata* (L.) subsp. *verticillata* and *S. verticillata* (L.) subsp. *amasiaca* (Frey & Borm.) Borm. *Food Chem.* **100**, 985–989. <https://doi.org/10.1016/j.foodchem.2005.10.062>.
- Topcu, G., 2006. Bioactive terpenoids from *Salvia* species. *J. Nat. Prod.* **69**, 482–487. <https://doi.org/10.1021/np060040z>.
- Trivellia, A., Iacchetti, M., Maggini, R., Mossedeh, H., Villamarin, T.S.S., Vernieri, P., Mensual-Sodi, A., Pardossi, A., 2016. Lamiaceae phenols as multifaceted compounds: bioactivity, industrial prospects and role of "positivestress". *Ind. Crops Prod.* <https://doi.org/10.1016/j.indcrop.2015.12.039>.
- Urbelen, A., Topcu, G., 1984. Flavonoids and terpenoids from *Salvia verticillata* and *Salvia pinnata*. *J. Nat. Prod.* **47**, 1068.
- Walker, J.B., Sytan, K.J., Treutlein, J., Wink, M., 2004. *Salvia* (Lamiaceae) is not monophyletic: implications for the systematics, radiation, and ecological specializations of *Salvia* and tribe Menthaeae. *Am. J. Bot.* **91**, 1115–1125. <https://doi.org/10.3732/ajb.91.7.1115>.
- Wu, Y., Ni, Z., Shi, Q., Dong, M., Kiyota, H., Gu, Y., Cong, B., 2012. Constituents from *Salvia* species and their biological activities. *Chem. Rev.* **112**, 5967–6026. <https://doi.org/10.1021/cr2005058>.
- Xu, J., Wei, K., Zhang, G., Lei, L., Yang, D., Wang, W., Han, Q., Xia, Y., Bi, Y., Yang, M., Li, M., 2018. Ethnopharmacology, phytochemistry, and pharmacology of Chinese *Salvia* species: a review. *J. Ethnopharmacol.* **225**, 18–30. <https://doi.org/10.1016/j.jep.2018.06.029>.
- Yan, L., Teng, L., Jhi, T., 2006. Antioxidant properties of guava fruits: comparison with some local fruits. *Sunw. Acad. J.* **3**, 9–20.
- Yermakov, A.I., Arasimov, V.V., Yarosh, N.P., 1987. *Methods of Biochemical Analysis of Plants*. Agropromizdat, Leningrad.
- Zengin, G., Llorent-Martínez, E.J., Córdova, M.L.Fde, Bahadori, M.B., Mocan, A., Locatelli, M., Aktumsek, A., 2018. Chemical composition and biological activities of extracts from three *Salvia* species: *S. hyperborealis*, *S. euphratica* var. *italocalydia*, and *S. verticillata* subsp. *amasiaca*. *Ind. Crops Prod.* **111**, 11–21. <https://doi.org/10.1016/j.indcrop.2017.09.065>.
- Zhang, Q., Yang, H., An, J., Zhang, R., Chen, B., Hao, D.-J., 2016. Therapeutic effects of Traditional Chinese medicine on spinal cord injury: a promising supplementary treatment in future. *Evid. Complement. Alternat. Med.* **2016**, 1–18. <https://doi.org/10.1155/2016/8958721>.



Contents lists available at ScienceDirect

Industrial Crops & Products

journal homepage: www.elsevier.com/locate/indcrop

Blackstonia perfoliata (L.) Huds. (Gentianaceae): A promising source of useful bioactive compounds

Vladimir Mihailović^{a,*}, Jelena S. Katanić Stanković^b, Tatjana Jurić^{b,c}, Nikola Srećković^a, Danijela Mišić^d, Branislav Šiler^d, Daria Maria Monti^e, Paola Imbimbo^e, Stefanie Nikles^f, San-Po Pan^f, Rudolf Bauer^f

^a University of Kragujevac, Faculty of Science, Department of Chemistry, Radoja Domanovića 12, 34000, Kragujevac, Serbia

^b University of Kragujevac, Institute for Information Technologies Kragujevac, Department of Science, Jovana Cvijića bb, 34000 Kragujevac, Serbia

^c University of Novi Sad, Faculty of Agriculture, Trg Dositeja Obradovića 8, 21000 Novi Sad, Serbia

^d Institute for Biological Research "Siniša Stanković" - National Institute of Republic of Serbia, University of Belgrade, Bulevar despota Stefana 142, 11060 Belgrade, Serbia

^e Department of Chemical Sciences, University of Naples Federico II, Complesso Universitario Monte Sant'Angelo, via Cinthia 4, 80126, Naples, Italy

^f Institute of Pharmaceutical Sciences, Department of Pharmacognosy, University of Graz, Universitätsplatz 4, 8010, Graz, Austria

ARTICLE INFO

Keywords

Blackstonia perfoliata
Secoiridoid glycosides
Phenolics
Antimicrobial activity
Antioxidant activity
Anti-inflammatory effect

ABSTRACT

Blackstonia perfoliata (L.) Huds. is known as a highly bitter secoiridoid glycosides-containing plant and as a possible substitute for some Gentianaceae plants in herbal preparations. Nevertheless, its bioactive properties are still unknown. The present study aimed to characterize both, secoiridoid glycosides and phenolic constituents, and to investigate antioxidant, antimicrobial, anti-inflammatory, and cytotoxic activities of *B. perfoliata* methanolic extract. The secoiridoid glycosides swertiamarin, gentiopirrin, and sweroside were found to be the dominant compounds of the extract, while 23 phenolic compounds were identified in much lower concentrations. Among phenolics, flavanols were the most abundant, which represents a unique feature among Gentianaceae species. The extract showed moderate to weak antioxidant activity with better performance in inhibition of lipid peroxidation than in free radical scavenging activities. The extract showed generally better antifungal properties compared with its antibacterial potential. Also, *B. perfoliata* demonstrated *in vitro* anti-inflammatory activity, the extract (50 µg/mL) showed inhibition of cyclooxygenases, COX-1 and COX-2, activities (19.65 and 48.02%, respectively). It also displayed biocompatibility on the immortalized and cancer cells, as no cytotoxic effect was observed. For the first time, the bioactive potential of this species was demonstrated, justifying its usage in pharmaceutical and food products as an alternative for some overexploited and endangered species from the Gentianaceae family.

1. Introduction

Blackstonia perfoliata (L.) Huds. (yellow wort) is a 10–60 cm high annual plant mainly found in the Mediterranean, central and Western European regions (Tutin, 1972; van der Sluis, 1985; Brys et al., 2013). According to Euro + Med PlantBase (<http://www2.bgbm.org/EuroPlusMed>) (Euro + Med, 2016), *Blackstonia* is a monotypic genus containing only *B. perfoliata*, which further includes five subspecies. *Blackstonia perfoliata* belongs to the Gentianaceae family, which comprises many species widely used in traditional medicine as constituents of bitters and related herbal preparations (Jensen and Schripsema, 2002). *Centaurea herba* (dried flowering aerial parts of *Centaureum erythraea*) and *Gentiana radix* (the dried root of *Gentiana lutea*), have a

long tradition of use in Europe as medicines for mild dyspeptic/gastrointestinal disorders, and for the temporary loss of appetite (European Medicines Agency, 2016; 2018), which has been reported in many European medicinal handbooks and Pharmacopoeias (European Pharmacopoeia, 2010). Their pharmacological activity is mainly attributed to the presence of secoiridoid glycosides ('bitters') with swertiamarin, gentiopirrin, and sweroside being the most common. Moreover, xanthenes, phenolic acids, and other compounds may contribute to their pharmacological activity (European Medicines Agency, 2016; 2018). Aerial parts of *B. perfoliata* have been proposed as a possible substitute for *Centaurea herba* and *Gentiana radix* in medicinal preparations (Bijelović et al., 2004; Sabovljević et al., 2006).

Iridoids, xanthone-C-glycosides, and flavone-C-glycosides were

* Corresponding author.

E-mail address: vladimir.mihailovic@pmf.kg.ac.rs (V. Mihailović).

<https://doi.org/10.1016/j.indcrop.2019.111974>

Received 25 April 2019; Received in revised form 31 October 2019; Accepted 8 November 2019
0926-6690/ © 2019 Elsevier B.V. All rights reserved.

reported as the main classes of compounds in Gentianeaceae (Jensen and Schripsema, 2002). Swertiamarin and/or gentiopiricin are the major secoiridoid glycosides and bioactive ingredients of Gentianeaceae plants. Their pharmacological effects, including attenuation of gastrointestinal disorders (Niibo et al., 2006; Ruan et al., 2015), hepatoprotective (Kondarasamy et al., 1994; Lian et al., 2010), antibacterial, antifungal (Kumarasamy et al., 2003a,b; Šiler et al., 2010, 2014), anti-inflammatory (He et al., 2015; Berkan et al., 1991), antioxidant (Đorđević et al., 2017), and gastroprotective effects (Tuluze et al., 2011), are well documented. However, there are only a few studies about the chemical composition of *B. perfoliata* (Nishikawa et al., 1998; Kaoudji, 1990; Kaoudji et al., 1990; Sabovljević et al., 2006; Skrzypczak et al., 1992). Secoiridoid glycosides, especially gentiopiricin (1.6–7.4%, depending on the sources and methods of extraction), are reported as the major constituents of *B. perfoliata* shoots (Nishikawa et al., 1998; van der Sluis, 1985). Swertiamarin, sweroside, and amarogentin have also been identified in *B. perfoliata*, but in much lower quantities (Skrzypczak et al., 1992; Nishikawa et al., 1998; Sabovljević et al., 2006). Van der Sluis (1985), consequently, compares the aerial parts of *B. perfoliata* with *Gentiana radix* rather than *Centaurei herba*. Among flavonoids, apigenin, kaempferol, quercetin, isorhamnetin, and their di- and triglycosides have been identified in *B. perfoliata* (Kaoudji, 1990; Kaoudji et al., 1990; Nishikawa et al., 1998). Other phenolic compounds, such as gentsin (Nishikawa et al., 1998) and various xanthones (van der Sluis, 1985) have been reported. Therefore, determination of the chemical composition and the therapeutic benefits of *B. perfoliata* is necessary to make evidence-based decisions about the safe use of *B. perfoliata* in pharmacology and medicine as a substitute for *Centaurei herba* and *Gentiana radix*.

In this study, a more detailed chemical profiling of the constituents of *B. perfoliata* and, for the first time, a comprehensive study on its biological activities have been performed. UHPLC-DAD/± HESI-MS/MS analysis was used to identify and quantify the secondary metabolites of the methanol extract of *B. perfoliata* aerial parts. Moreover, the antioxidant, antibacterial, antifungal, anti-inflammatory and biocompatibility properties of the extract were evaluated *in vitro*.

2. Material and methods

2.1. Chemicals and instruments

All chemicals and reagents used in antioxidant assays and for quantification of phenolic compounds were purchased from Sigma-Aldrich (Steinheim, Germany). Solvents for HPLC analyses (acetonitrile and formic acid, LC-MS grade) were obtained from Fisher Scientific (Loughborough, UK), while methanol (HPLC grade) was purchased from AppliChem (Cheshire, CT, USA). Ultrapure water was generated by deionisation (Millipore, Billerica, MA, USA). Standards of phenolic compounds (protocatechuic, gallic, gentsin, *p*-hydroxybenzoic, caffeoylquinic, caffeic, *p*-coumaric, rosmarinic, and ferulic acids, aesculin, apigenin, quercetin, kaempferol, myricetin, naringin, rutin, gallic acid, epigallocatechin, catechin, epicatechin, gallic acid gallate, catechin-3-gallate, and epigallocatechin gallate) were purchased from Sigma-Aldrich (Steinheim, Germany). Standards of swertiamarin, sweroside, and gentiopiricin (all of 98% purity) were purchased from Oskar Tropiczsch (Marktredwitz, Germany). UV/Vis double beam spectrophotometer Halo DB-20S (Dynamica GmbH, Dietikon, Switzerland) was used for spectrophotometric measurements.

2.2. Plant material and preparation of the extract

Seeds of *Blackstonia perfoliata* (L.) Huds. (collected at Majdan, Serbia, 46°09'25" N, 19°36'31" E) were sown on wet sandy soil in a greenhouse of the Institute for Biological Research "S. Stanković", Serbia. After three months, the plants were harvested while in the flowering stage. Above ground parts were air-dried at room

temperature in the dark and ground using a cutter mill. The powdered material (46.2 g) was macerated in methanol (1:10, w/v), for 24 h at room temperature in the dark, and the extract finally paper-filtered. This procedure was repeated two times with the same plant material. The extracts were combined and methanol was evaporated at 30–45°C under reduced pressure by a rotary evaporator (IKA RV 10, Staufen, Germany). The yield of the obtained semisolid extract was 23% (w/w). The concentrations used in the experiments were based on the dry weight of the extracts (d.e.).

2.3. Quantification of phenolic contents

Spectrophotometric determination of phenolic compounds in *B. perfoliata* methanol extract (BPE) was performed according to the previously published procedures (Mihalović et al., 2015). All methods for quantification of phenolic compounds in BPE were performed in three replications and results presented as the mean ± standard deviation. The total phenolic content in BPE was determined by the Folin-Ciocalteu method and expressed as milligrams of gallic acid equivalents per gram of dry extract (mg GAE/g d.e.). The total flavonoids content was measured using a spectrophotometric method with aluminium chloride and expressed as milligrams of rutin equivalents per gram of dry extract (mg RUE/g d.e.). Total phenolic (hydroxycinnamic) acids content in the extract was expressed as caffeic acid equivalents (mg CAE/g d.e.). For determination of condensed tannin content, a method using formaldehyde for precipitation of proanthocyanidins was employed. The condensed tannins content was expressed as the difference between total phenolic content and unprecipitated phenols as gallic acid equivalents (mg GAE/g d.e.). The content of gallotannins was determined in reaction with potassium iodate and expressed as gallic acid equivalents (mg GAE/g d.e.). The spectrophotometric pH differential method was used for determination of monomeric and total (monomeric plus polymerized) anthocyanins in the extract and expressed as cyanidin-3-glycoside equivalents (mg CGE/g d.e.).

2.4. Chromatographic analyses

Phenolics and secoiridoid glycosides in BPE were identified, separated and quantified using Dionex Ultimate 3000 UHPLC system (Thermo Fisher Scientific, Bremen, Germany) configured with a triple quadrupole mass spectrometer equipped with heated electrospray ionization (HESI) source (TSQ Quantum Access Max, Thermo Fisher Scientific, Basel, Switzerland).

Secoiridoid glycosides were chromatographically separated on a Hypersil gold C18 column (50 × 2.1 mm) with 1.9 mm particle size (Thermo Fisher Scientific, Waltham, USA), thermostated at 30°C. The mobile phase, consisting of 0.2% acetic acid in water (A) and LC-MS grade acetonitrile (B), was eluted with a flow rate of 0.4 mL/min, according to Mišić et al. (2015). The injection volume was 10 µL. Settings of the mass spectrometer were as follows: vaporizer temperature 300°C, spray voltage 4500 V, sheath gas (N₂) pressure 40 AU, ion sweep gas pressure 1 AU, auxiliary gas pressure 10 AU, capillary temperature 270°C, skimmer offset 0 V. Mass spectrometry data were acquired in the positive ionization mode, while collision-induced fragmentation in a single reaction monitoring (SRM) experiment used for the quantification of compounds in samples, was performed using argon as the collision gas. The collision energy was set to 20 eV.

A Syneris C18 column (100 × 2.1 mm, 1.7 mm particle size; Thermo Fisher Scientific, Waltham, USA), thermostated at 40°C, was used for the separation of phenolics. The mobile phase, eluted with the flow rate of 0.3 mL/min, consisted of (A) 0.1% formic acid in the water, and (B) acetonitrile. The gradient elution program was previously reported by Gašić et al. (2015). The injection volume was 5 µL. Mass spectrometer was operated with the vaporizer temperature kept at 200°C and the following ion source settings: spray voltage 5000 V, sheath gas (N₂) pressure 40 AU, ion sweep gas pressure 1 AU and

auxiliary gas (N₂) pressure 8 AU, capillary temperature 300 °C, and skimmer offset 0 V. The mass spectrometry data were acquired in the negative ionization mode, in the *m/z* range from 100 to 1000. Multiple mass spectrometric scanning modes, including full scanning (FS) and product ion scanning (PIS), were conducted for the qualitative analysis of the targeted compounds. The collision-induced fragmentation experiments were performed using argon as the collision gas. The collision energy varied depending on the compound (Table 3). The time-selected reaction monitoring (SRM) experiments for quantitative analysis were performed using two MS² fragments for each compound that were previously defined as dominant in PIS experiments.

All compounds were identified by comparing their MS² fragmentation patterns with the chromatographic and MS data available in the literature and by using available reference standards. Compounds were quantified by the external standard quantification procedure. Stock standard solutions (1 mg of a pure compound in 1 mL methanol) were mixed and dissolved in methanol to obtain working standard solutions (100 mg/mL). Calibration mixtures were obtained by diluting the working solution with methanol (100 mg/mL to 0.001 mg/mL). Regressions were calculated for each calibration curve. They showed good linearity with correlation coefficients between $r = 0.990$ and 0.999 , $p < 0.001$. The total amount of each targeted compound was calculated from its peak area. The content of phenolics was expressed as μg per g of dry extract ($\mu\text{g/g}$ d.e.) and the content of secoiridoid glycosides as mg per g of dry extract (mg/g d.e.).

2.5. Antioxidant activity evaluation

The antioxidant potential of BPE was determined using different methods including ABTS^{•+}, DPPH[•] and NO[•] scavenging activities, the ferrous ion chelating ability, reducing power, and inhibitory activity toward lipid peroxidation assays as described in our previous studies (Nikićforović et al., 2010; Mihailović et al., 2016). All experiments for the determination of antioxidant activities were performed in three replications and results presented as the mean \pm standard deviation.

2.6. Antimicrobial activity

2.6.1. Tested microorganisms

Blackstonia perfoliata methanol extract was tested against five Gram-positive (*Enterococcus faecalis* ATCC 29212, *Bacillus subtilis* ATCC 6633, *Bacillus cereus* ATCC 10876, *Micrococcus lysodeikticus*, and *Staphylococcus aureus* ATCC 25923), and four Gram-negative (*Escherichia coli* ATCC 25922, *Klebsiella pneumoniae* ATCC 70063, *Pseudomonas aeruginosa* ATCC 10145, and *Salmonella enteritidis* ATCC 13076) bacterial strains, the yeast *Candida albicans* ATCC 10231, and mould *Aspergillus brasiliensis* 16404, which were obtained from the Institute of Public Health, Kragujevac, Serbia. It was also tested against nine fungal isolates including *Trichoderma harzianum* FSB 12, *Trichoderma longibrachiatum* FSB 13, *Penicillium cyclopium* FSB 23, *Penicillium canescens* FSB 24, *Aspergillus glaucus* FSB 32, *Doratomyces stemonitis* FSB 41, *Alternaria alternata* FSB 51, *Phialophora fastigiata* FSB 81, and *Fusarium oxysporum* FSB 91 obtained from Laboratory for Microbiology, Department of Biology and Ecology, Faculty of Science, University of Kragujevac, Serbia. The bacterial species were cultivated on Nutrient agar at 37°C for 24 h. *C. albicans* was grown on Sabouraud dextrose agar at 28°C for 48 h, while fungi were cultured on potato glucose agar at 28°C for 3–7 days before testing.

2.6.2. Determination of minimal inhibitory concentration (MIC)

Determinations of MICs values for BPE were performed in accordance with the Clinical and Laboratory Standards Institute recommendations (CLSI, 2012). The microdilution antibacterial assay

was performed in sterile 96 well microplates, using Mueller–Hinton broth (MHB) for bacterial strains, and Sabouraud dextrose broth (SDB) for fungi. Two-fold serial dilutions of dissolved extract in 5% (v/v) DMSO (from 10 to 0.078 mg/mL) and a standard antibiotic/antimicrobial (from 40 to 0.3125 $\mu\text{g/mL}$) were performed in corresponding columns of 96 well plates. All wells in microplate were sequentially filled with resazurin solution, nutrient broth, and the cell suspension of a test microorganism (Sarker et al., 2007). In the tests with fungal species, SDB was used instead of the resazurin solution. The added inoculums were previously adjusted to a concentration of approximately 5.0×10^5 CFU/mL for bacteria (CLSI, 2012) and 5.0×10^4 CFU/mL for fungi (CLSI, 2008a, 2008b). The final volume in wells was 100 μL . Either ciprofloxacin, or nystatin was considered as positive controls. The experiments were performed in three repetitions. The minimal inhibitory concentration value corresponded to the lowest concentration of the extract that inhibited bacterial growth after 24 h at 37°C or fungal growth after 48 h at 28°C. The colour change of resazurin was assessed visually as an indicator of bacterial growth, while the visible growth of fungi was checked.

2.7. Anti-inflammatory activity

2.7.1. Cyclooxygenase-1 and -2 assays

For the cyclooxygenases (COX-1 and COX-2) inhibition assays purified prostaglandin H synthase (PGHS)-1 from ram seminal vesicles for COX-1 and human recombinant PGHS-2 for COX-2 (both Cayman Chemical Co., Ann Arbor, MI, USA) were used. The assays were performed in a 96-well plate format as described by Fiebič et al. (2005) and previously reported in Katanić et al. (2016). Assays for COX-1 and COX-2 inhibition were performed in two independent experiments in two replications (four replications in total, $n = 4$). The tested extract (50 $\mu\text{g/mL}$) and positive controls, indomethacin (1.25 μM , ICN, Aurora, OH, USA) and NS-398 (5 μM , Cayman Chemical Co., Ann Arbor, MI, USA), were dissolved in DMSO (> 99.98% purity, Sigma-Aldrich, St. Louis, MO, USA).

A competitive PGE₂ enzyme immunoassay (EIA) kit (Enzo Life Sciences Inc., Farmingdale, NY, USA) was used for the determination of the concentration of PGE₂, the main arachidonic acid metabolite in this assay. The enzyme immunoassay was evaluated by a microplate reader (Tecan, Männedorf, Switzerland), and the PGE₂ concentration was determined as described by Fiebič et al., 2005.

2.7.2. COX-2 gene expression assay

Cell culture and reagents: Human leukemic monocytic cell line THP-1 (European Collection of Cell Culture; Item No. 88081201) was maintained as described in Katanić et al. (2016). Briefly, after the initiation and monocyte-macrophage differentiation, cells were treated with plant extracts (25 $\mu\text{g/mL}$) for 1 h and stimulated with 7.5 ng/mL final concentration LPS (lipopolysaccharide, Sigma-Aldrich, St. Louis, MO, USA). Cells treated with DMSO (dimethylsulfoxide $\leq 0.1\%$) were used as calibrator sample. Before RNA extraction, cells were washed 3 times with cold PBS (phosphate buffered saline, Gibco®, Waltham, MA, USA) to remove non-attached cells. In this assay, two independent experiments in two replications ($n = 4$) were performed.

RNA extraction and RT-PCR: Total RNA was extracted using GenElute™ Mammalian Total RNA Miniprep Kit (Sigma Sigma-Aldrich, St. Louis, MO, USA) and reverse transcribed to cDNA using High-Capacity cDNA Reverse Transcription Kit (Applied Biosystems, Waltham, MA, USA) according to the manufacturer's manual. The thermal cycling conditions were set to 25°C for 25 min, 37°C for 120 min and 85°C for 5 s.

Real-time PCR: COX-2 gene expression analysis was performed on ABI-7300 Real-Time PCR System (Applied Biosystems, Waltham, MA,

USA) using Pre-developed TaqMan® Assay (Applied Biosystems, Waltham, MA, USA) as previously reported in Katanić et al. (2016), briefly target cDNA was amplified using COX-2 primers: forward 5'-GAA-TCA-TTC-ACCAGG-CAA-ATT-G-3', reverse 5'-TCT-GTA-CTGCGG-GTG-GAA-CA-3' and COX-2 probe: FAM-5'-TCC-TAC-CACCAG-CAA-CCC-TGC-CA-3'-TAMRA with cycling conditions: 50°C for 2 min, 95°C for 10 min, followed by 40 PCR cycles of 95°C for 15 s and 60°C for 1 min. After amplification of cDNA, target genes were normalized to glyceraldehyde-3-phosphate dehydrogenase (GAPDH) and relative quantified using the 2^{-ΔΔCT} method (Livak and Schmittgen, 2001).

2.8. Biocompatibility

BalBC-3T3 fibroblasts (clone A31), human hepatocellular carcinoma (HepG2), human colon cancer (LoVo), and human squamous carcinoma (A431) cells were purchased from ATCC (Manassas, VA, USA), while human epidermal keratinocytes (HaCaT) were purchased from Innoprot, Biscay, Spain. Cells were cultured in Dulbecco's Modified Eagle's Medium, supplemented with 10% fetal bovine serum, 2 mM L-glutamine and antibiotics in 5% CO₂ humidified atmosphere at 37°C. To test the biocompatibility of the extract, cells were seeded in 96-well plates at a density of 2 × 10⁵/well for 24 h. The different amounts of the extracts (from 10 to 200 µg/mL) were added to the cells. After 72 h incubation, cell viability was assessed by the MTT (3-(4,5-dimethylthiazol-2-yl)-2,5-diphenyltetrazolium bromide) assay, as described by Guglielmi et al., 2009. To determine cell survival, the percentage of viable cells in the presence of the extract was compared to that of the control cells. Untreated cells and cells incubated with the maximum volume of buffer were used as controls. The average of the two controls was considered as 100%. Each sample was tested in three independent analyses, each carried out in triplicates.

2.9. Statistical analysis

The concentration of the extract that reduces 50% of the free-radical concentration (IC₅₀) were determined using OriginPro8 software (OriginLab, Northampton, MA, USA), while for the calculation of the IC₅₀ values in the cytotoxicity assay, SigmaPlot 13.0 (Systat Software Inc., Erkrath, Germany; four parameters logistic curve) was used. The data were expressed as the mean of three experiments ± standard deviation.

3. Results and discussion

3.1. Phytochemical profile of *B. perfoliata* methanol extract

The results of phenolic compounds content (Table 1) showed that in each gram of BPE there was 65.07 mg of total phenolic compounds, expressed as GAE. Flavonoids and phenolic acids represented only a small part of the total phenolic compounds in the extract, while the condensed tannins content in 1 g of extract was equivalent to 41.17 mg of gallic acid, which presents the largest group of

spectrophotometrically identified phenolic compounds in the extract. Gallotannins and anthocyanins were found in very low quantities in the extract.

Detailed MS² fragmentation behaviour of sweroside, swertiamarin, and gentiopiricin in the positive ionization mode of the UHPLC/(+) HESI – MS² was previously described (Božunović et al., 2018). Within the present study, secoiridoids were quantified in an SRM experiment. Swertiamarin, with pseudomolecular ion [M+H]⁺ at *m/z* 375 at *t*_R = 2.66 min, was identified based on two diagnostic MS² fragments [M – C₆H₁₀O₅ – 2H₂O + H]⁺ at *m/z* 177 and [M + H – C₆H₁₀O₅ – 2H₂O – CO]⁺ at *m/z* 149 (Table 2 and Fig. 1A). Gentiopiricin, visible in the SRM chromatogram as a peak at *t*_R = 3.00 min (Fig. 1A), exhibited a pseudomolecular ion [M+H]⁺ at *m/z* 357, and diagnostic MS² fragments [M+H – C₆H₁₀O₅ – H₂O]⁺ at *m/z* 177 and [M + H – C₆H₁₀O₅ – H₂O – 2CO]⁺ at *m/z* 121. Pseudomolecular ion [M + H]⁺ at *m/z* 359, visible at *t*_R = 3.11 min (Fig. 1A), was assigned to sweroside, and MS² fragments [M + H – C₆H₁₂O₅ – H₂O]⁺ at *m/z* 179 and [M + H – RDA fragment]⁺ at *m/z* 127, were utilized in an SRM experiment. Secoiridoid glycosides were found to be the main class of secondary metabolites with much higher quantities compared with other compounds identified in the extract. Generally, their concentrations were more than a thousand times higher than individual concentrations of each of the phenolic compounds identified (Tables 2 and 3). Results show (Table 2) that gentiopiricin (278.49 mg/g d. e.) is the most dominant compound among secoiridoids, followed by sweroside (175.60 mg/g d. e.) and swertiamarin (21.38 mg/g d. e.), which is in agreement to the previous studies (van der Sluis, 1985; Skrzypczak et al., 1996; Nishikawa et al., 1998; Sabovljević et al., 2006). Previous studies revealed gentiopiricin as the major secoiridoid compound in *Gentiana radix* (Aberham et al., 2011), which is the official herbal drug from *Gentiana lutea*. On the other hand, aerial parts of *Sweetgum erythraea* (*Centaurea herba*) are characterized by the prevalence of swertiamarin over the gentiopiricin and sweroside content (Šiler et al., 2012, 2014; Banjanac et al., 2017; Đorđević et al., 2017; Božunović et al., 2018; Matekalo et al., 2018). Thus, according to these findings, aerial parts of *B. perfoliata* may be used as a substitute for *Gentiana radix*, as proposed earlier by van der Sluis (1985).

A total of 23 phenolic compounds were identified in BPE by UHPLC/(–)HESI – MS² metabolic profiling approach (Fig. 1B), 10 of which representing phenolic acids, and 13 flavonoids. All compounds were identified by using reference standards (Table 3). The identified compounds, together with their retention times, masses, and MS² molecular fragments are presented in Table 3. Among phenolic acids, hydroxybenzoic acids (protocatechuic, gallic, gentisic, and *p*-hydroxybenzoic acids) and hydroxycinnamic acids derivatives (asculin, caffeoylquinic, caffeic, *p*-coumaric, rosmarinic, and ferulic acids) were detected. From the group of flavonoids, flavones (apigenin), flavonols (rutin, myricetin, quercetin, and kaempferol), flavanols (gallocatechin, epigallocatechin, catechin, epicatechin, gallocatechin gallate, catechin 3-gallate, and epigallocatechin gallate), and flavanones (naringin) were found. Interestingly, *B. perfoliata* is characterized by a relatively high content and diversity of flavanols (catechins) in comparison to other species of the

Table 1
Quantification of phenolic compounds (mg/g of dry extract) in methanol extracts of *B. perfoliata*.

Extract	mg GAE/g		mg RUE/g	mg CAE/g	mg CGE/g	
	Total phenolics	Gallotannins	Condensed tannins	Total flavonoids	Phenolic acids	Monomeric anthocyanins
<i>B. perfoliata</i>	61.07 ± 4.04	3.87 ± 0.21	41.17 ± 1.35	12.76 ± 0.75	7.81 ± 0.51	3.76 ± 0.64
						1.11 ± 0.39

GAE – gallic acid equivalents; RUE – rutin equivalents; CAE – caffeic acid equivalents; CGE – cyanidin-3-O-glucoside equivalents.

ARTICLE IN PRESS

V. Mihailović, et al.

Industrial Crops & Products xxx (xxxx) xxx

Table 2List of identified secoiridoid glycosides in *B. perfoliata* extract with peak labels, retention times (t_R), parent ions $[M+H]^+$ m/z , and MS^2 fragments used in SRM experiment for the quantification of compounds by UHPLC/ \pm HESI-MS/MS analysis.

Peak	Assignment	t_R (min)	$[M+H]^+$ m/z	MS^2 fragments m/z (Collision Energy, eV)	Content [mg/g d. e.]
Secoiridoid glycosides					
A	Swertiamarin ^{S,R}	2.71	375	177 (30), 147 (30)	21.38
B	Gentiopicroin ^{S,R}	3.05	357	177 (30), 121 (30)	278.50
C	Sweroside ^{S,R}	3.14	359	179 (30), 127 (30)	175.60

d.e., dry extract.

^S Confirmed by standard.^R Confirmed by reference.**Table 3**List of identified phenolics in *B. perfoliata* extract with peak numbers, retention times (t_R), parent ions $[M-H]^-$ m/z , and MS^2 fragments used in SRM experiment for the quantification of compounds by UHPLC/ \pm HESI-MS/MS analysis.

Peak No.	Assignment	t_R (min)	$[M-H]^-$ m/z	MS^2 fragments m/z (Collision Energy, eV)	Content [μ g/g d. e.]
Phenolic acids and their derivatives					
Hydroxybenzoic acids					
1.	Protocatechuic acid ^{S,R}	4.58	153	108.09 (23); 109.10 (14)	20.85
2.	Gallic acid	2.48	169	79.11 (31); 125.04 (16)	4.09
3.	Genistic acid	3.38	153	108.09 (23); 109.10 (14)	0.86
4	<i>p</i> -Hydroxybenzoic acid	4.58	137	93.19 (19); 108.33 (22)	16.48
Hydroxycinnamic acids					
5.	Aesculin ^{S,R}	4.39	339	133.090 (44); 177.060 (25)	12.16
6.	Caffeoylquinic acid 1 ^R	4.73	353	191.28 (25)	5.92
7.	Caffeic acid ^{S,R}	5.01	179	134.00 (13); 135.00 (16)	17.21
8.	<i>p</i> -Coumaric acid	5.65	163	93.12 (39); 119.09 (16)	26.10
9.	Rosmarinic acid ^{S,R}	6.20	359	133.00 (43); 161.00 (21)	16.87
10.	Ferulic acid ^{S,R}	6.05	193	134.00 (18); 178.00 (15)	89.21
Flavonoids and their derivatives					
Flavones					
11.	Apigenin ^{S,R}	7.60	269	117.24 (43); 149.00 (24)	0.47
Flavonols					
12.	Rutin ^{S,R}	5.54	609	299.98 (42); 301.20 (32)	76.75
13.	Myricetin	6.44	317	109.31 (45); 150.97 (27)	2.40
14.	Quercetin ^{S,R}	7.08	301	151.01 (22); 179.00 (20)	1.48
15.	Kaempferol ^{S,R}	7.69	285	211.00 (32); 227.00 (32)	2.20
Flavanols					
16.	Gallocatechin ^S	3.37	305	125.22 (27); 179.19 (17)	14.21
17.	Epigallocatechin ^S	4.57	305	125.22 (27); 179.19 (17)	129.94
18.	Catechin ^S	4.75	289	203.00 (23); 245.03 (31)	15.00
19.	Epicatechin ^S	5.15	289	203.00 (23); 245.03 (31)	11.75
20.	Gallocatechin gallate ^S	5.32	457	161.08 (25); 359.23 (16)	273.98
21.	Catechin 3-gallate ^S	5.75	441	289.15 (20)	2.08
22.	Epigallocatechin gallate ^S	6.31	457	161.08 (25); 359.23 (16)	94.96
Flavanones					
23.	Naringin ^S	5.94	579	151.42 (43); 217.36 (33)	28.58

d.e., dry extract.

^S Confirmed by standard.^R Confirmed by reference.

Gentianaceae family. The flavanols, gallocatechin gallate, epigallocatechin, and epigallocatechin gallate quantities of 273.98, 129.94, and 94.96 μ g/g of d. e., respectively, were present in higher concentrations in comparison to other identified phenolics in the extract. Flavanols are only scarcely reported from Gentianaceae species, like in *Ericostemma littorale* (Natarajan and Prasad, 1972; Ambikapathy et al., 2011.) and *Gentiana spicata* (Handoussa et al., 2009), for which four flavanols: epicatechin, catechin, epigallocatechin gallate, and gallocatechin gallate have been isolated. Based on available literature data, gallocatechin, epigallocatechin, and catechin 3-gallate have not been previously identified in Gentianaceae species. Phytochemical analysis revealed that BPE also contained ferulic acid (89.21 μ g/g d. e.) and

rutin (76.75 μ g/g d. e.) in significant concentrations. Other identified phenolic acids and flavonoids were present at concentrations less than 30 μ g/g d. e. Quercetin and kaempferol, as well as their diglycosides and triglycosides, have been previously identified in *B. perfoliata* (Kaouadji, 1990; Kaouadji et al., 1990; Skrzypczak et al., 1992), and were confirmed within the present study. Thus, this species offers an interesting and unique composition of phenolics and secoiridoids with promising bioactive potential. Flavanols present in *B. perfoliata*, well known for their bioactive properties (Erlund, 2004; Crozier et al., 2009), could significantly add to the bioactive potential of this species. Therefore, BPE was further analysed in a series of biological tests.

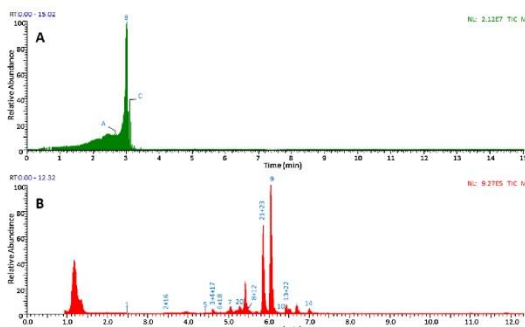


Fig. 1. Metabolic profiling of *B. perfoliata* methanol extract: (A) UHPLC/(+)HESI-MS² total ion chromatogram (TIC) representing targeted secoiridoid glycosides. For compound labels (A–C) please refer to Table 2; (B) UHPLC/(–)HESI-MS² TIC of targeted phenolic compounds. For peak assignment, please refer to Table 3.

3.2. Antioxidant activities of *B. perfoliata* methanol extract

Antioxidant activities of BPE were estimated using seven different methods: total antioxidant capacity, ABTS^{•+}, DPPH[•], and NO[•] radical scavenging activities, reducing power, metal chelating activity, and inhibitory activity toward lipid peroxidation. The results are presented in Table 4. The total antioxidant capacity assay showed a potential of BPE to reduce Mo(VI) to (V), and results showed that 1 g of the extract had total antioxidant potential as if it contained 161.25 mg of ascorbic acid (161.25 mg AA/g of d. e.). This result indicates that BPE possessed approximately 16% of the antioxidant capacity of ascorbic acid. The rate of free radical scavenging activities of the extract was assessed using DPPH and ABTS assays. Obtained IC₅₀ values of the extract in the DPPH assay were found to be higher (1346.82 µg/mL) than that observed in the ABTS assay (781.90 µg/mL). Free radicals (i.e. ABTS^{•+} and DPPH[•]) may be neutralized either by direct reduction via electron transfers or by radical quenching via H atom transfer. However, the major difference between the two methods is, that DPPH assay is characterized by better access of small molecules to the radical site, which leads to higher antioxidant activity. This disadvantage is not observed in the ABTS assay (Prior et al., 2005). Better radical scavenging activity of the extract in ABTS than in DPPH assay showed that it may contain antioxidants inert to DPPH due to steric inaccessibility. According to previous studies, secoiridoid glycosides identified as the most abundant compounds in *Centaureum erythraea* extract possessed a lower affinity to scavenge DPPH than ABTS radical (Božunović et al., 2018). Free radical scavenging activity of BPE was also determined by an *in vitro* assay which uses biologically relevant NO radicals. It was shown that BPN in concentration up to 4 mg/mL did not have the antioxidant potential to neutralize 50% of NO[•]. According to Kachmar et al. (2019), the IC₅₀ value of the aqueous extract of *C. erythraea* aerial parts for NO[•] scavenging activity was 251.29 µg/mL. Considering IC₅₀ values of DPPH, ABTS, and NO radical scavenging activities of BPE and reference antioxidants (Trolox, quercetin, and BHT), it can be summarized that the extract possessed only weak potential in the neutralization of free radicals. Antioxidant properties of plants with a high content of secoiridoid glycosides have been previously reported. It has been reported that *G. algida*, *G. decumbens*, *G. macrophylla*, and *G. triflora* decoctions have been shown IC₅₀ values between 287.91 and 89.22 µg/mL in DPPH and ABTS assays (Olennikov et al., 2015). Different extracts of *G. asclepiadea* aerial part were previously shown to have IC₅₀ values between 131 and 614.3 µg/mL in DPPH assay (Nićiforović et al., 2010; Stefanović et al., 2018). Balijagić et al. (2012)

found that methanol leaves extracts of *G. lutea* with high amounts swertiamarin and gentiopicrine possessed IC₅₀ for DPPH[•] scavenging activity between 0.45–2.02 mg/mL. In previous studies, secoiridoid rich methanol extracts of *G. cruciata* and *C. erythraea* possessed stronger antioxidant activity in ABTS assay than in DPPH assay, which is in accordance with results obtained in this study (Mihailović et al., 2015; Božunović et al., 2018). The radical scavenging activity of BPE was similar or lower compared with some examined plants from Gentianeae, but, the extraction conditions and methods for determination of antioxidant activity, used by other authors, were not the same.

The antioxidant activity of BPE was also measured in a heterogeneous (emulsion) lipid system to determine the inhibition of spontaneous peroxidation of linoleic acid during 72 h at 37°C. In this assay, BPE at a concentration of 120.41 µg/mL exhibited 50% peroxidation inhibition of linoleic acid. It showed better antioxidant potential with a lower IC₅₀ value in the inhibition of lipid peroxidation compared with its radical scavenging activities, suggesting that the extract contains also less polar antioxidant compounds which have higher partition into the lipid phase and thus are more effective antioxidants in lipid systems. Similar trends in the antioxidant activity of extracts containing higher amounts of secoiridoids than phenolic compounds were observed in previous studies (Mihailović et al., 2013, 2015). These results showed that gentiopicrin-rich extracts possessed better inhibitory effects on lipid peroxidation than radical scavenging activities. Moreover, DPPH radicals do not have similarity with highly reactive and transient peroxy radicals involved in lipid peroxidation, so antioxidants in the extract that react with peroxy radicals may react slowly or may even be inert to DPPH (Prior et al., 2005). The reference antioxidant BHT had much lower IC₅₀ value (13.03 µg/mL) than the extract.

The ability of BPE to act as an electron donor and potential reductant of oxidants (free radicals) was measured using reduction of Fe³⁺, in ferricyanide complex, to Fe²⁺. As can be seen in Table 4, the reducing power of the extract was 54.51 mg TE/g d.e., which represents approximately 5.5% of the reducing power of the well-known antioxidant Trolox. The antioxidant potential of BPE was also determined using metal chelating activity assay, a method which reflects the capacity of antioxidants to bind the pro-oxidant metal and prevent the formation of hydroxyl radicals (Valko et al., 2007). The results showed that BPE, at a concentration of 3.17 mg/mL, chelated 50% of Fe²⁺, as did EDTA at 15.06 µg/mL. These results indicate that BPE contains some chelators but in very low concentrations. Among identified compounds in the extract, the most powerful chelating compounds are flavonoids and their derivatives (Craft et al., 2012), but they represent

Table 4
Antioxidant activity of *B. perfoliata* methanol extract.

Extract/standards	Total antioxidant capacity (mg AAE/g of d.e.)	Reducing power (mg TE/g of d.e.)	IC ₅₀ (µg/mL)				Metal chelating ability
			ABTS ^{•+} scavenging activity	DPPH [•] scavenging activity	NO [•] scavenging activity	Inhibitory activity toward lipid peroxidation	
<i>B. perfoliata</i>	161.25 ± 3.70	54.51 ± 8.04	781.90 ± 61.40	1346.82 ± 48.71	> 1000	129.41 ± 9.65	3165.5 ± 135.27
Trolox	–	–	23.84 ± 0.94	15.59 ± 0.75	30.74 ± 6.37	–	–
Quercetin	–	–	15.32 ± 0.68	6.70 ± 0.26	13.01 ± 0.78	–	–
AA	–	–	5.58 ± 0.33	19.65 ± 0.81	72.91 ± 1.07	> 1000	–
BHT	–	–	29.26 ± 1.14	28.52 ± 1.26	–	13.03 ± 1.17	–
EDTA	–	–	–	–	–	–	15.06 ± 0.45

IC₅₀ values were determined by nonlinear regression analysis. Results are mean values ± SD from three experiments; d.e., dry extract; AAE, ascorbic acid equivalents; TE, Trolox equivalents; ABTS, 2,2'-azino-bis(3-ethylbenzothiazoline-6-sulphonic acid); DPPH, 2,2-diphenyl-1-picrylhydrazyl; NO, nitric oxide; AA, ascorbic acid; BHT, butylated hydroxytoluene; EDTA, ethylenediaminetetraacetic acid; –, Not tested.

only about 1.3% of the extract, according to the spectrophotometric measurement, while flavonoids identified by HPLC analysis contributed approximately 0.05% to the extract weight.

A number of *in vitro* studies have shown that the phenolic compounds identified and quantified in BPE are powerful antioxidants (Senanayake, 2013; Gullon et al., 2017). Flavanols monomers, known as catechins, including gallo catechin gallate, epigallocatechin, and epigallocatechin gallate, were found to be most abundant among all identified phenolic compounds in the extract. They are well known as very active natural antioxidants. These catechins have been reported as highly potent in scavenging physiologically relevant reactive oxygen species *in vitro* as exceptional electron donors, as well as chelating redox-active transition metal ions, and inhibiting lipid peroxidation (Senanayake, 2013). Among the other compounds, ferulic acid and rutin were also highly abundant, but at lower concentrations than catechins. Rutin and its aglycone quercetin have been reported to possess powerful antioxidant capacity, both *in vitro* and *in vivo* antioxidant systems (Gullon et al., 2017). Unlike phenolic compounds, known as powerful antioxidants, which were found in BPE in rather low concentrations, the dominant compounds, secoiridoid glycosides (about 50% w/w of d. e.) are known for their weak antioxidant activity (Şiler et al., 2014). Oleonikovic et al. (2015) have characterized the antioxidant potential of some plant extracts with high concentrations of secoiridoids using a DPPH-HPLC technique and have shown that swertiamarin, sweroside, and gentiopicrin have been inactive in DPPH radical scavenging. Other studies support these findings (Kumarasamy et al., 2003a; Şiler et al., 2014; Božunović et al., 2018). This suggests that phenolic compounds present in the extract in lower concentration than secoiridoids are the essential compounds for the observed antioxidant activities of the extract.

3.3. Antimicrobial activity

The antibacterial and antifungal activities of BPE against twenty microorganisms are presented in Table 5. The extract showed the antibacterial activity against most of the tested bacterial species, except for highly resistant *P. aeruginosa* (MIC > 10 mg/mL), which was previously noticed by Belfadel et al. (2016) in the study with different extracts of *B. grandiflora*. The most sensitive bacteria to BPE were two Gram-positive *Bacillus* species, *B. cereus* and *B. subtilis*, with MIC values 2.5 and 5 mg/mL, respectively. The extract had moderate potential to inhibit the growth of other tested bacterial strains, with MICs of 10 mg/mL. Antibacterial activity of ciprofloxacin was in the range of MIC from < 0.3125 to 40 µg/mL.

Antifungal activity of BPE (Table 5) was found to be more pronounced than its antibacterial activity. The extract was the most active against *P. fastigiata* inhibiting fungal growth at MIC concentrations of 0.625 mg/mL and 1.25 mg/mL in the cases of *A. glaucus* and *A. alternata*. The extract's activity against the remaining fungi ranged from 2.5

to 10 mg/mL, with the exception of *T. harzianum*, which was resistant to the extract even at the highest concentration (MIC > 10 mg/mL). The commercial antimycotic Nystatin, which was used as a positive control, was active in concentrations from less than 0.3 and up to 10 µg/mL. Generally speaking, BPE displayed much better antifungal than antibacterial properties.

This is the first thorough report on the antimicrobial activity of *B. perfoliata*, earlier initiated by Belfadel et al. (2016). However, recent findings suggest the effectiveness of various plant species from Gentianaceae family on a wide range of microorganisms (Božunović et al., 2018; Oleonikovic et al., 2015; Şiler et al., 2014). A high number of natural compounds is known for their exquisite antimicrobial potential. It mainly refers to phenolic acids, polyphenolic compounds and their derivatives (Daglia, 2012; Cushnie and Lamb, 2005). The qualitative phytochemical analysis of BPE revealed several groups of polyphenolics. Detected phenolic acids, e.g. *p*-hydroxybenzoic, caffeic, protocatechuic, ferulic, *p*-coumaric, and rosmarinic acids, have been previously accounted for their antibacterial and antifungal properties (Heleno et al., 2015). The presence of flavonoids and their derivatives, i.e. naringin, myricetin, kaempferol, quercetin, and its derivative rutin, may also contribute to the antimicrobial activity of BPE (Cushnie and Lamb, 2005). Moreover, significant amounts of flavanols

Table 5
Antimicrobial activity of *B. perfoliata* methanol extract.

			MIC (mg/mL)	
			<i>B. perfoliata</i>	Ciprofloxacin Nystatin
Bacteria				
<i>E. faecalis</i>	ATCC 29212	G+	10	40
<i>B. subtilis</i>	ATCC 6633	G+	5	< 0.3125
<i>B. cereus</i>	ATCC 10876	G+	2.5	1.25
<i>S. aureus</i>	ATCC 25923	G+	10	< 0.3125
<i>M. lysodeikticus</i>	ATCC 4698	G+	10	< 0.3125
<i>K. pneumoniae</i>	ATCC 70063	G-	10	< 0.3125
<i>P. aeruginosa</i>	ATCC 10145	G-	> 10	< 0.3125
<i>S. enteritidis</i>	ATCC 13076	G-	10	< 0.3125
<i>E. coli</i>	ATCC 25922	G-	10	< 0.3125
Fungi				
<i>Caldicoccus</i>	ATCC 10231		5	–
<i>A. brasiliensis</i>	ATCC 16404		2.5	–
<i>A. glaucus</i>	FSB 32		1.25	–
<i>T. harzianum</i>	FSB 12		> 10	–
<i>T. longibrachiatum</i>	FSB 13		5	–
<i>P. cycloptum</i>	FSB 23		10	–
<i>P. canescens</i>	FSB 24		2.5	–
<i>D. strombolii</i>	FSB 41		2.5	–
<i>A. alternata</i>	FSB 51		1.25	–
<i>P. fastigiata</i>	FSB 81		0.625	–
<i>F. oxysporum</i>	FSB 91		5	–

MIC, minimal inhibitory concentration.

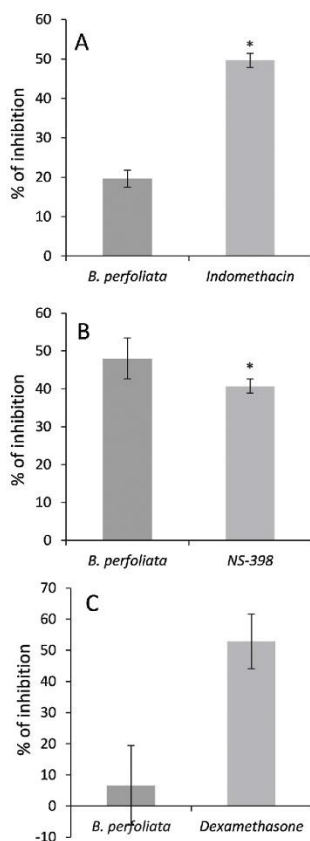


Fig. 2. Inhibitory effects of *B. perfoliata* methanol extract on COX-1 (A) and COX-2 activities (B), and inhibition of COX-2 gene expression in THP-1 macrophages (C) (mean \pm SD, $n = 4$). The applied concentration of the extract for the assays A and B - 50 $\mu\text{g/mL}$, and for C - 25 $\mu\text{g/mL}$. Indomethacin (1.25 μM), NS-398 (5 μM), and dexamethasone (2.5 nM) were used as positive controls. * - results for positive controls (indomethacin and NS-398) are from the same study as in Katančić et al. (2016).

epigallocatechin, gallic acid, and epigallocatechin gallate, which are known for their prominent activity against a panel of different microorganisms (Daglia, 2012), can considerably contribute to antimicrobial efficacy of BPE. Species from Gentianaceae family containing high amounts of secoiridoid glycosides, probably their most significant secondary metabolites, undoubtedly owe notable antimicrobial potential to these compounds. Gentiopiricin, sweroside, and swertiamarin displayed similar antimicrobial potential against a set of bacterial and fungal species with slightly stronger activity against fungal species (Kumarasamy et al., 2003b; Šiler et al., 2010; Božunović

et al., 2018). Generally, it is most likely that the combination of the compounds identified in BPE contributes to the overall antimicrobial potential of *B. perfoliata*.

3.4. Anti-inflammatory activity *in vitro*

The results of *in vitro* analysis of the anti-inflammatory activity of BPE are given in Fig. 2. The extract, applied at a concentration of 50 $\mu\text{g/mL}$, was unable to significantly inhibit COX-1 enzymatic activity showing only 19.65% of inhibition (Fig. 2A). Indomethacin, as a reference COX-1 inhibitor, according to Katančić et al. (2016), was able to reduce the activity of this enzyme to the value of 49.63% at a concentration of 1.25 μM (0.45 $\mu\text{g/mL}$). On the other hand, BPE was much more efficient in COX-2 inhibition. At a concentration of 50 $\mu\text{g/mL}$, BPE exhibited 48.02% inhibition of COX-2 activity (Fig. 2B). A selective inhibitor of COX-2, NS-398, used at a concentration of 5 μM (1.57 $\mu\text{g/mL}$), showed similar results with 40.72% of COX-2 activity inhibition (Katančić et al., 2016). The results of the COX-2 gene expression assay in THP-1 macrophages (Fig. 2C) clearly showed that BPE, at a concentration of 25 $\mu\text{g/mL}$, had no significant influence on COX-2 gene expression. On the other hand, the reference standard dexamethasone (2.5 nM; 0.098 $\mu\text{g/mL}$) exerted remarkable 52.82% inhibition of COX-2 gene expression.

The demonstrated anti-inflammatory activity of *B. perfoliata* can be associated with its phytochemical composition. Several phenolic compounds, identified in its methanol extract, have been appraised as potent anti-inflammatory agents *in vitro* or *in vivo*. Specifically, ferulic acid detected in BPE has been reported to be associated with COX-2 inhibition (Mancuso and Santangelo, 2014). Moreover, the anti-inflammatory potential of rutin, the most prominent flavonoid in the tested extract, was proven in several *in vitro* and *in vivo* chronic and acute inflammation models (García-Lafuente et al., 2009). Also, numerous studies reported the anti-inflammatory effects of epigallocatechin, epigallocatechin gallate, and other similar galloylated flavonols. Such activities might include the inhibition of LPS-induced microglial activation, NO and TNF- α production, as well as COX-1/COX-2 inhibitory activity (Pan et al., 2010; Santangelo et al., 2007). Secoiridoid glycosides (gentiopiricin, sweroside, and swertiamarin), were also examined as anti-inflammatory substances in earlier studies. Gentiopiricin, as the most dominant secoiridoid in the tested extract, failed to show significant *in vitro* anti-inflammatory activity on COX-1 and -2 activities, TNF- α and NO production (Park et al., 2010). But in the *in vivo* study by Olenikov et al. (2015), gentiopiricin succeeded to reduce the formation of carrageenan-induced paw oedema in rats. Much earlier, Kondo et al. (1994) have shown the suppressive effect of gentiopiricin on serum TNF levels in LPS treated mice. Also, Chen et al. (2008) reported that gentiopiricin produced significant analgesic effects against persistent inflammatory pain stimuli in mice. Sweroside and swertiamarin were reported to have inhibitory activity on IL-6 production in RAW264 cells (He et al., 2015), while hydrolysed swertiamarin inhibited thromboxane-B2 (TBX2) (Park et al., 2010). In another *in vivo* study, Saravanan et al. (2014) reported that swertiamarin attenuates inflammation mediators in adjuvant-induced arthritis. Based on the presented results, it can be concluded, that displayed anti-inflammatory activity of *B. perfoliata* could depend on its chemical composition and the synergistic action of a variety of anti-inflammatory compounds contained. These results suggest that further investigation should be done to identify the exact compounds responsible for these bioactive properties, but also to confirm these results in *in vivo* tests. The course of our work is to examine whether metabolic changes of the compounds present in the extract may have an influence on the activities under *in vivo* conditions.

3.5. Biocompatibility

Finally, the biocompatibility of the extract was analysed by

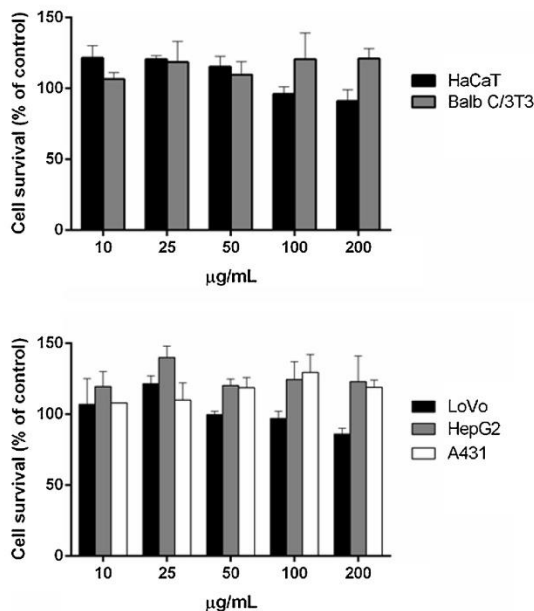


Fig. 3. Effects of *B. perfoliata* methanol extract on the viability of eukaryotic cells. Dose-response curves of viable cells after 72 h incubation in the presence of different concentrations of the extract (from 10 to 200 µg/mL). (A) – effect on normal cells, (B) – effect on human cancer cells. Values are given as means \pm S.D. ($n \geq 3$).

performing a cell survival assay on a panel of cell lines. Biocompatibility of BPE was tested on two immortalized (murine BalbC-3T3 fibroblasts and human HaCaT keratinocytes) and three human cancer cell lines (HepG2 hepatic cells, colon cancer cells, LoVo, and squamous carcinoma, A431) in a dose-response test. As shown in Fig. 3, no significant differences in cell survival between control groups and cells treated with BPE were observed. Indeed, BPE showed full biocompatibility after 72 h incubation in concentrations up to 200 µg/mL ($p > 0.05$). To the best of our knowledge, there are only a few reports regarding the cytotoxic activity of the compounds found in high concentrations in the BPE (Baljagić et al., 2012; Sun et al., 2013; Wu et al., 2017), and this is undoubtedly the first report on the biocompatibility of BPE. Previous studies have shown that gentiopiricin has failed to exhibit cytotoxicity against either human malignant cell MCF7 (human breast cancer), PC3 (human prostate cancer), or LS174 (human colon carcinoma) lines, with IC_{50} values higher than 200 µg/mL, while displaying strong activity against HeLa (human cervix adenocarcinoma) cells (IC_{50} 5.7 µg/mL) (Baljagić et al., 2012). In the study by Wu et al. (2017), gentiopiricin also showed no cytotoxicity to Madin-Darby Canine Kidney (MDCK) cells at a concentration of 50 mM. Sweroside was reported to have no toxic effect neither on the human osteosarcoma cell line MG-63, nor on rat osteoblast cells, causing even a marked increase in cell proliferation (Sun et al., 2013). Obtained results for BPE biocompatibility in this study are in agreement with these studies reporting low cytotoxic effects of secoiridoid glycosides. Also, BPE at the doses ranging from 10 to 200 µg/mL provides good biocompatibility, without

toxic effects on healthy cells (fibroblasts and keratinocytes).

4. Conclusions

The high content of bitter, secoiridoid glycosides, quantified in *B. perfoliata* extract, supports our hypothesis that this plant could be an adequate substitute for widely used Gentianaceae bitter herbs. *Blackstonia perfoliata* may be a good alternative in pharmaceutical and food products for *Gentiana lutea*, which natural populations are decreasing as a result of overexploitation and habitat degradation. Indeed, *B. perfoliata* methanol extract revealed a considerable amount of various phenolic compounds and a certain extent of antioxidant and antimicrobial activities. In addition to the bioactivity of well-known secoiridoid glycosides present in *B. perfoliata*, formulations containing BPE would be enriched with a variety of phenolic acids, flavonoids and their derivatives. Flavanones are found to be especially abundant in this species, and this chemical characteristic distinguishes the genus *Blackstonia* from other genera within the Gentianaceae family. Also, *B. perfoliata* extract could attract attention for finding new anti-inflammatory agents, considering the high potential of COX-2 enzyme inhibition recorded within the present study.

Declaration of Competing Interest

The authors declare that they have no known competing financial interests or personal relationships that could have appeared to

influence the work reported in this paper.

Acknowledgements

This study was conducted within the projects No. III43004 and No. OI173024 funded by the Ministry of Education, Science and Technological Development of the Republic of Serbia.

References

- Aberham, A., Pieri, V., Croom, J.E.M., Elmiger, E., Stuppner, H., 2011. Analysis of iridoids, secoiridoids and xanthones in *Centaureum erythraea*, *Prasera carolinensis* and *Gentiana lutea* using LC-MS and RP-HPLC. *J. Pharm. Biomed. Anal.* 54, 517–525. <https://doi.org/10.1016/j.jpba.2010.09.030>.
- Ambikapathy, V., Mahalingam, R., Panneerselvam, A., 2011. GC-MS determination of bioactive compounds of *Epicostema littorale* (Blume). *Asian J. Plant. Sci. Res.* 1, 56–60.
- Baljić, J., Janković, T., Zdunić, G., Bošković, J., Šavkin, K., Godevac, D., Stanjoković, T., Jovančević, M., Menković, M., 2012. Chemical profile, radical scavenging and cytotoxic activity of yellow gentian leaves (*Gentiana lutea* folium) grown in northern regions of Montenegro. *Nat. Prod. Commun.* 7, 1487–1490.
- Banjanac, T., Dragičević, M., Šiler, B., Gašić, U., Bohane, B., Nestorović, Ž., Trifunović, S., Mišić, D., 2017. Chemodiversity of two closely related tetraploid *Centaureum* species and their hexaploid hybrid: metabolomic search for high-resolution taxonomic classifiers. *Phytochemistry* 140, 27–44. <https://doi.org/10.1016/j.phytochem.2017.04.005>.
- Belfield, F.Z., Millet, A., Medjroub, K., Akkal, S., Seguin, E., Chaoche, N.K., 2016. Phytochemical and biological study of aerial parts extracts of *Blackstonia grandiflora* (Viv.) Maire. *Der Pharma Chemica* 8, 243–248.
- Berkan, T., Ustunes, L., Lermiöglu, F., Ozer, A., 1991. Antiinflammatory, analgesic, and antipyretic effects of an aqueous extract of *Erythraea centaureium*. *Planta Med.* 57, 34–37. <https://doi.org/10.1055/s-2006-960011>.
- Bijelović, A., Rosić, N., Mijuš-Džukić, J., Ninković, S., Grubišić, D., 2004. *In vitro* regeneration and transformation of *Blackstonia perfoliata*. *Biol. Plantarum* 48, 333–338.
- Božunović, J., Živković, S., Gašić, U., Glamočlija, J., Čirić, A., Matekalo, D., Šiler, B., Soković, M., Tešić, Z., Mišić, D., 2018. *In vitro* and *in vivo* transformations of *Centaureum erythraea* secoiridoid glycosides alternate their antioxidant and antimicrobial capacity. *Ind. Crop. Prod.* 111, 705–721. <https://doi.org/10.1016/j.indcrop.2017.11.040>.
- Bryx, R., Geens, B., Beckman, T., Jacquemyn, H., 2013. Differences in dichogamy and herkogamy contribute to higher selfing in contrasting environments in the annual *Blackstonia perfoliata* (Gentianeaceae). *Ann. Bot.* 111, 651–661. <https://doi.org/10.1093/aob/mct021>.
- Chen, L., Liu, J.-C., Zhang, X.-N., Guo, Y.-Y., Xu, Z.-H., Cao, W., Sun, X.-L., Sun, W.-L., Zhao, M.-G., 2008. Down-regulation of NR2B receptors partially contributes to analgesic effects of gentiopicroside in persistent inflammatory pain. *Neuropharmacology* 54, 1175–1181. <https://doi.org/10.1016/j.neuropharm.2008.03.007>.
- Clinical and Laboratory Standards Institute, 2012. ninth ed. Methods for Dilution Antimicrobial Susceptibility Tests for Bacteria That Grow Aerobically [Approved Standard]. Document M07. CLSI M07-A9 Clinical and Laboratory Standards Institute, Wayne, PA.
- Clinical and Laboratory Standards Institute, 2008a. third ed. Reference Method for Broth Dilution Antifungal Susceptibility Testing of Yeasts [Approved Standard]. Document M27. CLSI M27-A3 Clinical and Laboratory Standards Institute, Wayne, PA.
- Clinical and Laboratory Standards Institute, 2008b. second ed. Reference Method for Broth Dilution Antifungal Susceptibility Testing of Filamentous Fungi [Approved Standard]. Document M38. CLSI M38-A2 Clinical and Laboratory Standards Institute, Wayne, PA.
- Craft, B.D., Kerrhard, A.L., Amarovicz, R., Pegg, R.B., 2012. Phenol-based antioxidants and the *in vitro* methods used for their assessment. *Compr. Rev. Food Sci. Food Saf.* 11, 148–173. <https://doi.org/10.1111/j.1541-4337.2011.00173.x>.
- Crozier, A., Jaganath, I.B., Clifford, M.N., 2009. Dietary phenolics: chemistry, bioavailability and effects on health. *Nat. Prod. Rep.* 26, 1001–1043. <https://doi.org/10.1039/b802662a>.
- Cushnie, T.P., Lamb, A.J., 2005. Antimicrobial activity of flavonoids. *Int. J. Antimicrob. Agents* 26, 343–356. <https://doi.org/10.1016/j.ijantimicag.2005.09.002>.
- Daglia, M., 2012. Polyphenols as antimicrobial agents. *Curr. Opin. Biotechnol.* 23, 174–181. <https://doi.org/10.1016/j.copbio.2011.08.007>.
- Dordević, M., Mihalović, M., Arambašić Jovanović, J., Grdović, N., Uskoković, A., Tolić, A., Sinadinović, M., Rajić, J., Mišić, D., Šiler, B., Poznanović, G., Vidaković, M., Dinić, S., 2017. *Centaureum erythraea* methanol extract protects red blood cells from oxidative damage in streptozotocin-induced diabetic rats. *J. Ethnopharmacol.* 202, 172–183. <https://doi.org/10.1016/j.jep.2017.03.016>.
- Erlund, L., 2004. Review of the flavonoids quercetin, hesperetin, and naringenin. Dietary sources, bioactivities, bioavailability, and epidemiology. *Nutr. Res.* 24, 851–874. <https://doi.org/10.1016/j.jmtr.2004.07.005>.
- Euro + Med, 2016. Euro + Med PlantBase. The Information Resource for Euro-mediterranean Plant Diversity. Available from: <http://www.2.bghn.org/EuroPlusMed/> (Accessed 9 November 2018).
- European Medicines Agency (EMA), 2016. Assessment Report on *Centaureum erythraea* Rafn. s.l., Herba. (Doc. Ref.: EMA/HMPC/277491/2015). Committee on Herbal Medicinal Products, London, UK. https://www.ema.europa.eu/documents/herbal-report/assessment-report-centaureum-erythraea-rafn-sl-herba_en.pdf.
- European Medicines Agency (EMA), 2018. Draft Assessment Report on *Gentiana lutea* L., Radix – Revision 1. (Doc. Ref.: EMA/607863/2017). Committee on Herbal Medicinal Products, London, UK. https://www.ema.europa.eu/documents/herbal-report/draft-assessment-report-gentiana-lutea-l-radix-revision-1_en.pdf.
- European Pharmacopoeia, 2010. The European Directorate for the Quality of Medicines & HealthCare (EDQM). Strasbourg seventh ed.
- Fiebig, B.L., Grozdeva, M., Hess, S., Hill, M., Danesch, U., Bodensieck, A., Bauer, R., 2005. *Petasites hybridus* extracts *in vitro* inhibit COX-2 and PGE2 release by direct interaction with the enzyme and by preventing p42/44 MAP kinase activation in rat primary microglial cells. *Planta Med.* 71, 12–19. <https://doi.org/10.1055/s-2005-837744>.
- García-Lafuente, A., Guillamón, E., Villares, A., Rostagno, M.A., Martínez, J.A., 2009. Flavonoids as anti-inflammatory agents: implications in cancer and cardiovascular disease. *Inflamm. Res.* 58, 537–552. <https://doi.org/10.1007/s00011-009-0037-3>.
- Gašić, U., Natić, M., Mišić, D., Lusić, D., Milošević-Opsencica, D., Tešić, Ž., Lusić, D., 2015. Chemical markers for the authentication of unifloral *Salvia officinalis* L. honey. *J. Food Anal.* 44, 128–138. <https://doi.org/10.1016/j.jfa.2015.08.008>.
- Guglielmi, F., Monti, D.M., Ancillotto, A., Torrasa, S., Cozzolino, F., Pucci, P., Relini, A., Piccoli, R., 2009. Enzymatically active fibrils generated by the self-assembly of the ApoA-I fibrillogenesis domain functionalized with a catalytic moiety. *Biomaterials* 30, 829–835. <https://doi.org/10.1016/j.biomaterials.2008.10.036>.
- Gullon, B., Li-Chau, T.A., Moreira, M.T., Lema, J.M., Elbes, G., 2017. Rutin: a review on extraction, identification and purification methods, biological activities and approaches to enhance its bioavailability. *Trends Food Sci. Technol.* 67, 220–235. <https://doi.org/10.1016/j.tifs.2017.07.008>.
- Handoussa, H., Osmanova, N., Ayoub, N., Mahran, L., 2009. Spicatic acid: a 4-carboxy-gentisic acid from *Gentiana spicata* extract with potential hepatoprotective activity. *Drug Discov. Ther.* 3, 278–286.
- He, Y.M., Zhu, S., Ge, Y.W., Kazuma, K., Zou, K., Cai, S.Q., Komatsu, K., 2015. The anti-inflammatory secoiridoid glycosides from *Gentiana scabra* radix: the root and rhizome of *Gentiana scabra*. *J. Nat. Med.* 69, 303–312. <https://doi.org/10.1007/s11418-015-0894-8>.
- Heleno, S.A., Martins, A., Queiroz, M.J., Ferreira, I.C., 2015. Bioactivity of phenolic acids: metabolites versus parent compounds: a review. *Food Chem.* 173, 501–513. <https://doi.org/10.1016/j.foodchem.2014.10.057>.
- Jensen, S.R., Schripsema, J., 2002. Chemotaxonomy and pharmacology of Gentianeaceae. In: Struwe, L., Albert, V. (Eds.), *Gentianeaceae – Systematics and Natural History*. Cambridge University Press, pp. 573–631.
- Kachmar, M.R., Oliveira, A.P., Valentão, P., Gil-Izquierdo, A., Dominguez-Perles, R., Ouabli, A., Badioui, K.E., Andrade, P.B., Ferreres, F., 2019. HPLC-MS/MS phenolic profile and *in vitro* biological potential of *Centaureum erythraea* Rafn aqueous extract. *Food Chem.* 278, 424–433. <https://doi.org/10.1016/j.foodchem.2018.11.082>.
- Kaouadji, M., 1990. Flavonol diglycosides from *Blackstonia perfoliata*. *Phytochemistry* 29, 1345–1347. [https://doi.org/10.1016/0031-9422\(90\)85465-8](https://doi.org/10.1016/0031-9422(90)85465-8).
- Kaouadji, M., Doucoure, A., Mariotte, M., Chulia, A.J., Thomasson, F., 1990. Flavonol triglycosides from *Blackstonia perfoliata*. *Phytochemistry* 29, 1283–1286. [https://doi.org/10.1016/0031-9422\(90\)85443-3](https://doi.org/10.1016/0031-9422(90)85443-3).
- Katanić, J., Borja, T., Mihalović, V., Nikles, S., Pan, S.-P., Rosić, G., Selaković, D., Joksimović, J., Mitrović, S., Bauer, R., 2016. *In vitro* and *in vivo* assessment of meadowsweet (*Filipendula ulmaria*) as anti-inflammatory agent. *J. Ethnopharmacol.* 193, 627–636. <https://doi.org/10.1016/j.jep.2016.10.015>.
- Kondo, Y., Takano, F., Hojo, H., 1994. Suppression of chemically and immunologically induced hepatic injuries by gentiopicroside in mice. *Planta Med.* 60, 414–416. <https://doi.org/10.1055/s-2006-959521>.
- Kumarasamy, Y., Nahar, L., Cox, P.J., Jaspars, M., Sarker, S.D., 2003a. Bioactivity of secoiridoid glycosides from *Centaureum erythraea*. *Phytomedicine* 10, 344–347. <https://doi.org/10.1078/0944710032004857>.
- Kumarasamy, Y., Nahar, L., Sarker, S.D., 2003b. Bioactivity of gentiopicroside from the aerial parts of *Centaureum erythraea*. *Fitoterapia* 151–154. [https://doi.org/10.1016/S0367-326X\(02\)00319-2](https://doi.org/10.1016/S0367-326X(02)00319-2).
- Lian, L.H., Wu, Y.L., Wan, Y., Li, X., Xie, W.X., Nan, J.X., 2010. Anti-apoptotic activity of gentiopicroside in D-galactosamine/lipopolysaccharide-induced murine fulminant hepatic failure. *Chem. Biol. Interact.* 188, 127–133. <https://doi.org/10.1016/j.cbi.2010.06.004>.
- Livak, K.J., Schmittgen, T.D., 2001. Analysis of relative gene expression data using real-time quantitative PCR and the 2^{-ΔΔCt} method. *Methods* 25, 402–408. <https://doi.org/10.1006/meth.2001.1262>.
- Mancuso, C., Santangelo, R., 2014. Ferulic acid: pharmacological and toxicological aspects. *Food Chem. Toxicol.* 65, 185–195. <https://doi.org/10.1016/j.fct.2013.12.024>.
- Matekalo, D., Skorić, M., Nikolić, T., Novaković, L., Lukić, M., Božunović, J., Aničić, N., Filipović, B., Mišić, D., 2018. Organ-specific and genotype-dependent constitutive biosynthesis of secoiridoid glycosides in *Centaureum erythraea* Rafn, and its elicitation with methyl jasmonate. *Phytochemistry* 155, 69–82. <https://doi.org/10.1016/j.phytochem.2018.07.015>.
- Mihalović, V., Krefl, S., Tavčar Benković, E., Ivanović, N., Stanković, M.S., 2016. Chemical profile, antioxidant activity and stability in simulated gastrointestinal tract model system of three *Verbascum* species. *Ind. Crop. Prod.* 89, 141–151. <https://doi.org/10.1016/j.indcrop.2016.04.075>.
- Mihalović, V., Mišić, D., Matić, S., Mihalović, M., Stanić, S., Vrvčić, M.M., Katanić, J., Mladenović, M., Stanković, N., Borja, T., Stanković, M.S., 2015. Comparative phytochemical analysis of *Gentiana cruccata* L. roots and aerial parts, and their biological activities. *Ind. Crop. Prod.* 73, 49–62. <https://doi.org/10.1016/j.indcrop.2015.04.013>.
- Mihalović, V., Matić, S., Mišić, D., Solujić, S., Stanić, S., Katanić, J., Mladenović, M.,

- Stanković, N., 2013. Chemical composition, antioxidant and antigenotoxic activities of different fractions of *Gentiana asclepiadea* L. roots extract. *Excli J.* 12, 807–823.
- Mišić, D., Šiler, B., Gašić, U., Avramov, S., Živković, S., Nestorović Živković, J., Mihutinović, M., Tešić, Ž., 2015. Simultaneous UHPLC/DAD/(+/-)HESI-MS/MS analysis of phenolic acids and nepetalactones in methanol extracts of *Nepeta* species: a possible application in chemotaxonomic studies. *Phytochem. Anal.* 26, 72–85. <https://doi.org/10.1002/pca.2538>.
- Natarajan, P.N., Prasad, S., 1972. Chemical investigations of *Encostemma litoreale*. *Planta Med.* 22, 42–46. <https://doi.org/10.1055/s-0028-1099580>.
- Niho, Y., Yamazaki, T., Nakajima, Y., Yamamoto, T., Ando, H., Hirai, Y., Torizuka, K., Iida, Y., 2006. Gastroprotective effects of bitter principles isolated from Gentian root and Swertia herb on experimentally-induced gastric lesions in rats. *J. Nat. Med.* 60, 82–88. <https://doi.org/10.1007/s11418-005-0014-2>.
- Nishikawa, K., Nishida, M., Shimomura, K., Ishimaru, K., 1998. Secondary metabolites in tissue cultures of *Blackstonia perfoliata* and three *Gentiana* plants. *Nat. Med.* 52, 536–540.
- Ničiforović, N., Mihailović, V., Mašković, P., Solujić, S., Stojković, A., Pavlović Muratspahić, D., 2010. Antioxidant activity of selected plant species; potential new sources of natural antioxidants. *Food Chem. Toxicol.* 48, 3125–3130. <https://doi.org/10.1016/j.foodtox.2010.08.007>.
- Olemlkov, D.N., Kashchenko, N.I., Chirikova, N.K., Koryakina, L.P., Vladimirov, L.N., 2015. Bitter gentian teas: nutritional and phytochemical profiles, polysaccharide characterisation and bioactivity. *Molecules* 20, 20014–20030. <https://doi.org/10.3390/molecules201119674>.
- Pan, M.H., Tai, C.S., Ho, C.T., 2010. Anti-inflammatory activity of natural dietary flavonoids. *Food Funct.* 1, 15–31. <https://doi.org/10.1039/C9FO00103A>.
- Park, K.S., Kim, B.H., Chang, I.-M., 2010. Inhibitory potencies of several iridoidson cyclooxygenase-1, cyclooxygenase-2 enzymes activities, tumor necrosis factor- α and nitric oxide production in vitro. *Evid-Based Compl. Alt.* 7, 41–45. <https://doi.org/10.1093/ecom/nem129>.
- Prior, R.L., Wu, X., Schaich, K., 2005. Standardized methods for the determination of antioxidant capacity and phenolics in foods and dietary supplements. *J. Agr. Food Chem.* 53, 4290–4302. <https://doi.org/10.1021/jf0502698>.
- Ruan, M., Yu, B., Xu, L., Zhang, L., Long, J., Shen, X., 2015. Attenuation of stress-induced gastrointestinal motility disorder by gentiopicroside, from *Gentiana macrophylla* Pall. *Fitoterapia* 103, 265–276. <https://doi.org/10.1016/j.fitote.2015.04.015>.
- Saborjević, A., Rošić, N., Janković, T., Grubišić, D., 2006. Secoiridoid content of *Blackstonia perfoliata* in vivo and in vitro. *In Vitro Cell. Dev.-Pl.* 42, 427–431. <https://doi.org/10.1079/IVP2006759>.
- Santangelo, C., Vari, R., Scuzzocchio, B., Di Benedetto, R., Filesi, C., Masella, R., 2007. Polyphenols, intracellular signalling and inflammation. *Ann. Ist. Super. Sanita* 43, 394–405.
- Sarker, S.D., Nahar, L., Kumarasamy, Y., 2007. Microtitre plate-based antibacterial assay incorporating resazurin as an indicator of cell growth, and its application in the *in vitro* antibacterial screening of phytochemicals. *Methods* 42, 321–324. <https://doi.org/10.1016/j.ymeth.2007.01.006>.
- Saravanan, S., Islam, V.L.H., Babu, N.P., Pandikumar, P., Thirugnanasambantham, K., Chellappandian, M., Raj, C.S.D., Paolraj, M.G., Ignicimuthu, S., 2014. Swertiainarin attenuates inflammation mediators via modulating NF- κ B/1 κ B and JAK2/STAT3 transcription factors in adjuvant induced arthritis. *Eur. J. Pharm. Sci.* 2, 70–86. <https://doi.org/10.1016/j.ejps.2014.02.005>.
- Senanayake, N.S.P.J., 2013. Green tea extract: chemistry, antioxidant properties and food applications – a review. *J. Funct. Foods* 5, 1529–1541. <https://doi.org/10.1016/j.jff.2013.08.011>.
- Skrzypczak, L., Wesolowska, M., Thiem, B., Budzianowski, J., 1996. *Blackstonia perfoliata* (L.) Hudson (Yellow Wiert): *in vitro* culture and the production of gentiopicroside and other secondary metabolites. In: Bajaj, Y.P.S. (Ed.), *Biotechnology in Agriculture and Forestry*, Vol. 37 Medicinal and Aromatic Plants IX. Springer-Verlag, Berlin Heidelberg, pp. 64–75.
- Skrzypczak, L., Wesolowska, M., Krupiška, A., Thiem, B., 1992. *In vitro* cultures of *Blackstonia perfoliata* (L.) Hudson and an assay of the secoiridoid content. *Acta Soc. Bot. Pol.* 61, 359–368. <https://doi.org/10.5586/asbp.1992.031>.
- Stefanović, O., Ličina, B., Vasić, S., Radojević, I., Comić, I.J., 2018. Bioactive extracts of *Gentiana asclepiadea*: antioxidant, antimicrobial, and antibiofilm activity. *Bot. Serbica* 42, 223–229. <https://doi.org/10.5281/zenodo.1468319>.
- Sun, H., Li, L., Zhang, A., Zhang, N., Lv, H., Sun, W., Wang, X., 2013. Protective effects of sweroside on human MG-63 cells and rat osteoblasts. *Fitoterapia* 84, 174–179. <https://doi.org/10.1016/j.fitote.2012.11.010>.
- Šiler, B., Avramov, S., Banjanac, T., Cvetković, J., Nestorović Živković, J., Patenković, A., Mišić, D., 2012. Secoiridoid glycosides as a marker system in chemical variability estimation and chemotype assignment of *Centaureum erythraea* Rafn from the Balkan Peninsula. *Ind. Crops Prod.* 40, 336–344. <https://doi.org/10.1016/j.indcrop.2012.03.026>.
- Šiler, B., Mišić, D., Nestorović, J., Banjanac, T., Glamočlija, J., Soković, M., Čirić, A., 2010. Antibacterial and antifungal screening of *Centaureum pulchellum* crude extracts and main secoiridoid compounds. *Nat. Prod. Commun.* 5, 1525–1530.
- Šiler, B., Živković, S., Banjanac, T., Cvetković, J., Nestorović Živković, J., Čirić, A., Soković, M., Mišić, D., 2014. Centauries as underestimated food additives: antioxidant and antimicrobial potential. *Food Chem.* 147, 367–376. <https://doi.org/10.1016/j.foodchem.2013.10.007>.
- Tuluć, V., Ozkol, H., Koyuncu, I., Ine, H., 2011. Gastroprotective effect of small centaury (*Centaureum erythraea* L.) on aspirin-induced gastric damage in rats. *Toxicol. Ind. Health* 27, 760–768. <https://doi.org/10.1177/0748233710397421>.
- Tutin, T.G., 1972. Gentianales. In: Tutin, T.G., Heywood, V.H., Burges, N.A., Moore, D.A., Valiente, D.H., Walters, S.M., Webb, D.A. (Eds.), *Flora Europaea*, vol. 3. Cambridge University Press, Cambridge, pp. 56.
- Wu, S., Yang, L., Sun, W., Si, L., Xiao, S., Wang, Q., Dechoux, L., Thorimbert, S., Sollogoub, M., Zhou, D., Zhang, Y., 2017. Design, synthesis and biological evaluation of gentiopicroside derivatives as potential antiviral inhibitors. *Eur. J. Med. Chem.* 130, 308–319. <https://doi.org/10.1016/j.ejmech.2017.02.028>.
- Valko, M., Leibfritz, D., Moncol, J., Cronin, M.T.D., Mazur, M., Telser, J., 2007. Free radicals and antioxidants in normal physiological functions and human disease. *Int. J. Biochem. Cell.* B 39, 44–84. <https://doi.org/10.1016/j.biocel.2006.07.001>.
- Van der Sluis, W.G., 1985. Chemotaxonomical investigations of the genera *Blackstonia* and *Centaureum* (Gentianaceae). *Plant Syst. Evol.* 149, 253–286.